

# Percutaneous Penetration Enhancers Drug Penetration Into/Through the Skin

Methodology and  
General Considerations

Nina Dragicevic  
Howard I. Maibach  
*Editors*

 Springer

---

# Percutaneous Penetration Enhancers Drug Penetration Into/Through the Skin

---

Nina Dragicevic • Howard I. Maibach  
Editors

Percutaneous  
Penetration Enhancers  
Drug Penetration  
Into/Through the Skin

Methodology and General  
Considerations

 Springer

*Editors*

Nina Dragicevic  
Apoteka "Beograd"  
Belgrade  
Serbia

Howard I. Maibach  
San Francisco  
California  
USA

ISBN 978-3-662-53268-3      ISBN 978-3-662-53270-6 (eBook)  
DOI 10.1007/978-3-662-53270-6

Library of Congress Control Number: 2017937381

© Springer-Verlag Berlin Heidelberg 2017

This work is subject to copyright. All rights are reserved by the Publisher, whether the whole or part of the material is concerned, specifically the rights of translation, reprinting, reuse of illustrations, recitation, broadcasting, reproduction on microfilms or in any other physical way, and transmission or information storage and retrieval, electronic adaptation, computer software, or by similar or dissimilar methodology now known or hereafter developed.

The use of general descriptive names, registered names, trademarks, service marks, etc. in this publication does not imply, even in the absence of a specific statement, that such names are exempt from the relevant protective laws and regulations and therefore free for general use.

The publisher, the authors and the editors are safe to assume that the advice and information in this book are believed to be true and accurate at the date of publication. Neither the publisher nor the authors or the editors give a warranty, express or implied, with respect to the material contained herein or for any errors or omissions that may have been made. The publisher remains neutral with regard to jurisdictional claims in published maps and institutional affiliations.

Printed on acid-free paper

This Springer imprint is published by Springer Nature  
The registered company is Springer-Verlag GmbH Germany  
The registered company address is: Heidelberger Platz 3, 14197 Berlin, Germany

---

## Preface

The main function of skin is the protection of the body from the external environment by preventing loss of water and the ingress of exogenous substances. This implies that the skin acts as a barrier for the diffusion of substances into the underlying tissue. Despite this role, the skin has become recognized as an important drug delivery route which can be reached directly. It is an ideal site for the application of drugs for achieving local (topical) and systemic (transdermal) drug effects. Local or topical drug delivery assumes treating various skin diseases, while transdermal delivery aims to achieve systemically active drug levels in order to treat systemic diseases. Drugs have been applied to the skin to achieve also regional drug delivery which involves drug application to the skin to treat or alleviate disease symptoms in deep tissues beneath the skin (such as in musculature, etc.). Topical and transdermal drug delivery offer a number of advantages compared to other conventional routes, and hence they are of great interest to pharmaceutical research, which explains the increasing interest in skin as a site of drug application.

However, skin represents a formidable barrier for percutaneous drug absorption, being of crucial importance for achieving topical and transdermal effects of drugs. Significant efforts have been devoted to developing strategies to overcome the impermeability of intact human skin. There are many ways for circumventing the stratum corneum, which provides the main barrier to drug penetration. These methods can be divided into chemical and physical penetration enhancement methods, i.e., percutaneous penetration enhancers (as well as the skin structure are described in the other volumes in this book series).

The aim of this book is to provide to readers working in academia and industry, including young researchers, an up-to-date comprehensive work describing all the important topics required to understand the principles of enhancing transdermal and dermal drug delivery. We have divided this book into five volumes.

Volume 1 begins with a description of the skin, as understanding of its structure, function, and especially its penetration pathways is fundamental to understanding how topical and transdermal dosage forms work and how different methods may be employed and work to enhance percutaneous drug penetration as well as how they work. The first parts devoted to skin and the stratum corneum, representing its uppermost layer being responsible for its protection, discuss their structure, the importance of the lipid organization in the stratum corneum, the different penetration pathways through the skin

with a focus on the increasing importance of the follicular route, as well as the influence of different excipients on the skin. The first volume of this book focuses on the chemical methods used to overcome the impermeability of intact skin, such as different drug manipulation strategies (drug or prodrug selection, chemical potential control, eutectic systems, complexes with cyclodextrins, etc.) and influences of formulation/vehicle effects (influences of emulsions, nanoemulsions, Pickering emulsions, microemulsions, emulsifiers, emollients, liquid crystalline structures, gels, etc.) on the penetration enhancement of drugs.

Volume 2 describes, similarly to Volume 1, the chemical methods used in penetration enhancement of drugs. However, this volume is devoted to the application of different kinds of nanocarriers and represents an attempt to familiarize the readers with the importance of nanocarriers used to enhance the percutaneous penetration of drugs as they have numerous advantages in comparison to conventional drug formulations. More recently, different types of nanocarriers have been designed by researchers which allow controlled and targeted drug delivery (dermal or transdermal drug delivery), improved therapeutic effectiveness, and reduced side effects of drugs. As carriers they can be classified into lipid-based vesicles (e.g., liposomes, transfersomes, invasomes, etc.), surfactant-based vesicles (e.g., niosomes, novasomes, and others), lipid-based particulate carriers (e.g., solid lipid nanoparticles, nanostructured lipid carriers, and lipid nanocapsules), polymer-based particulate carriers (e.g., polymeric nano- and microparticles, polymeric nanocapsules, polymeric micelles, dendrimers, dendritic core-multishell nanocarriers, etc.), nanocrystals, and others. This volume therefore focuses on the different nanocarriers and gives a comprehensive review of their use as promising drug delivery systems. It also considers the use of nanocarriers for cutaneous immunization offering the important advantage of being painless and having a stronger immune response compared to the intramuscular injection of vaccines. In addition, the volume provides insights on the safety of the topical use of nanoparticles.

Volume 3, similarly to Volumes 1 and 2, describes the chemical methods used in penetration enhancement of drugs with an emphasis on the enhancing methods used to modify the stratum corneum. It starts with the classification of penetration enhancers and their mode of action and provides insights on the structure–activity relationship of chemical penetration enhancers. The focus of this volume is on the most commonly used classes of skin penetration enhancers being investigated in scientific literature and used in commercial topical and transdermal formulations, and their representatives are discussed in more detail, including their mechanism of action, where known. The following penetration enhancers are considered in this volume: alcohols (e.g., ethanol), glycols (e.g., propylene glycol), amides (1-dodecylazacycloheptan-2-one or laurocapram (Azone<sup>®</sup>)), fatty acids (e.g., oleic acid, etc.), fatty acid esters (e.g., isopropyl myristate, etc.), ether alcohols (e.g., diethylene glycol monoethyl ether (Transcutol<sup>®</sup>)), pyrrolidones (N-methyl-2-pyrrolidone), sulphoxides (e.g., dimethyl sulphoxide, etc.), surfactants (e.g., polysorbates, etc.), terpenes (e.g., L-menthol, etc.), peptides

and new classes of enhancers, such as iminosulfuranes, transcarbams, dimethylamino acid esters, and dicarboxylic acid esters. In addition, synergistic effects of different chemical penetration enhancers have been discussed in this book as an important feature of chemical penetration enhancers. Furthermore, the safety profile of chemical penetration enhancers is considered.

Volume 4 considers the current status and possible future directions in the emerging area of physical methods being used as potent enhancers for the percutaneous penetration of drugs. It gives a comprehensive overview of the most used methods of enhancing dermal and transdermal drug delivery. It covers sonophoresis, iontophoresis, electroporation, magnetophoresis, microneedles, needle-free jet injectors, ablation methods (electrical, thermal, or laser skin ablation), and others. The numerous advantages of these methods have opened new frontiers in the penetration enhancement of drugs for dermal and transdermal drug delivery. Cutaneous vaccination and gene delivery by physical methods have been also discussed in this volume. Consideration was given to new methods, too, such as a novel electrochemical device for penetration enhancement, different waves (e.g., photoacoustic waves, microwaves, etc.), natural submicron injectors, moxibustion, and others. Furthermore, the combined use of different physical methods or of physical methods and passive enhancement methods (chemical penetration enhancement methods) are discussed as they provide, due to their synergistic effects, higher percutaneous drug penetration when used together.

Volume 5 provides fundamental principles of the drug penetration into/through the skin, from covering basic mathematics involved in skin permeation of drugs, influences of drug application conditions and other factors on drug penetration, mechanistic studies of penetration enhancers, influences of the type of skin used (human native or reconstructed skin) to different methods utilized to assess the drug penetration into/through the skin and to determine the amount of permeated drug (such as tape-stripping of the stratum corneum, electron spin resonance, Raman spectroscopy, attenuated total reflection, confocal laser scanning microscopy, single and multiphoton microscopy). Retardation strategies are also discussed as being important for some classes of drugs, such as sunscreens. The safety of applied penetration enhancers as well as the research ethics in the investigation of dermal and transdermal drug delivery are addressed in this volume. This volume discusses the current status and future perspectives of passive/chemical and active/physical penetration enhancement methods as they are gaining extensive interest as promising tools to enable an efficient dermal or transdermal drug delivery.

We are very thankful to all authors who contributed chapters to the book series *Percutaneous Penetration Enhancers*, as they found time to work on the chapters despite having busy schedules and commitments. All the authors are eminent experts in the scientific field which was the subject of their chapter, and hence their contribution raised the value of this book. We also sincerely thank our publishing, developmental, and production editors Portia F. Wong, Ellen Blasig, Sverre Klemp, Andre Tournois, Grant Weston, and

others from Springer, for their dedicated work which was necessary to achieve such a high standard of publication. We highly appreciate readers' comments, suggestions, and criticisms to improve the next edition of this book.

Belgrade, Serbia  
San Francisco, CA, USA

Nina Dragicevic  
Howard I. Maibach



---

# Contents

## Part I Factors Influencing Percutaneous Drug Penetration

<b>1 Basic Mathematics in Skin Absorption</b> . . . . .	3
Dominik Selzer, Ulrich F. Schaefer, Claus-Michael Lehr and Steffi Hansen	
<b>2 Occlusive Versus Nonocclusive Application in Transdermal Drug Delivery</b> . . . . .	27
Gamal M. El Maghraby	
<b>3 Finite and Infinite Dosing</b> . . . . .	35
Wing Man Lau and Keng Wooi Ng	
<b>4 Non-formulation Parameters That Affect Penetrant-Skin- Vehicle Interactions and Percutaneous Absorption</b> . . . . .	45
Jeffrey E. Grice, Hamid R. Moghimi, Elizabeth Ryan, Qian Zhang, Isha Haridass, Yousuf Mohammed, and Michael S. Roberts	
<b>5 The Influence of Emollients on Dermal and Transdermal Drug Delivery</b> . . . . .	77
V.R. Leite-Silva, Jeffrey E. Grice, Yousuf Mohammed, Hamid R. Moghimi, and Michael S. Roberts	
<b>6 The Effects of Vehicle Mixtures on Transdermal Absorption: Thermodynamics, Mechanisms, Assessment, and Prediction</b> . . . . .	95
Jason T. Chittenden and Jim E. Riviere	
<b>7 Mechanistic Studies of Permeation Enhancers</b> . . . . .	119
S. Kevin Li and William I. Higuchi	
<b>8 High Throughput Screening of Transdermal Penetration Enhancers: Opportunities, Methods, and Applications</b> . . . . .	137
Amit Jain, Pankaj Karande, and Samir Mitragotri	

**Part II Methods for Measuring the Percutaneous Drug Penetration**

- 9 Models, Methods, and Measurements in Transdermal Drug Delivery** . . . . . 153  
Donald M. Cropek and Pankaj Karande
- 10 Human Native and Reconstructed Skin Preparations for In Vitro Penetration and Permeation Studies** . . . . . 185  
Ulrich F. Schaefer, D. Selzer, S. Hansen, and Claus-Michael Lehr
- 11 Stripping Procedures for Penetration Measurements of Topically Applied Substances** . . . . . 205  
Jürgen Lademann, Sabine Schanzer, Heike Richter, Martina C. Meinke, Hans-Jürgen Weigmann, and Alexa Patzelt
- 12 Application of EPR-spin Probes to Evaluate Penetration Efficiency, Storage Capacity of Nanotransporters, and Drug Release** . . . . . 215  
Stefan F. Haag, Jürgen Lademann, and Martina C. Meinke
- 13 Confocal Raman Spectroscopy as a Tool to Investigate the Action of Penetration Enhancers Inside the Skin** . . . . . 229  
Stéphanie Briçon, Marie-Alexandrine Bolzinger, and Yves Chevalier
- 14 ATR-FTIR Spectroscopy and the Skin Barrier: Evaluation of Penetration-Enhancement Effects** . . . . . 247  
Julia Covi-Schwarz, Victoria Klang, and Claudia Valenta
- 15 Confocal Microscopy for Visualization of Skin Penetration** . . . . . 255  
Mukul A. Ashtikar, Daya D. Verma, and Alfred Fahr
- 16 Clinical Cutaneous Drug Delivery Assessment Using Single and Multiphoton Microscopy** . . . . . 283  
Anthony P. Raphael and Tarl W. Prow
- 17 Corneoxenometry: A Bioassay Exploring Skin Barrier Breaching** . . . . . 303  
Claudine Piérard-Franchimont, Trinh Hermanns-Lê, and Gérard E. Piérard

**Part III The Retardation of Percutaneous Drug Penetration**

- 18 Retardation Strategies for Sunscreen Agents** . . . . . 311  
Katharina Bohnenblust-Woertz and Christian Surber
- 19 Retardation of Dermal Release by Film Forming Emulsions** . . . . . 321  
Dominique Jasmin Lunter and Rolf Daniels

**Part IV Current Status of Dermal and Transdermal Drug Delivery**

- 20 Penetration-Enhancement Strategies for Dermal and Transdermal Drug Delivery: An Overview of Recent Research Studies and Patents** . . . . . 337  
Syed Sarim Imam and Mohammed Aqil
- 21 Perspectives on Dermal Delivery of Macromolecular Drugs** . . . . . 355  
Marianna Foldvari and P. Kumar
- 22 Active Enhancement Methods in Transdermal Drug Delivery: Current Status and Future Perspectives** . . . . . 359  
Ryan F. Donnelly

**Part V Safety Issues and Ethics in Studies on Dermal and Transdermal Delivery**

- 23 Efficacy, Safety and Targets in Topical and Transdermal Active and Excipient Delivery** . . . . . 369  
Yousuf H. Mohammed, Hamid R. Moghimi, Shereen A. Yousef, Navin C. Chandrasekaran, Césa R. Bibi, Sinduja C. Sukumar, Jeffrey E. Grice, Wedad Sakran, and Michael S. Roberts
- 24 Ethical Considerations in Research Involving Dermal and Transdermal Drug Delivery** . . . . . 393  
Dusanka Krajinovic and Nina Dragicevic
- Index** . . . . . 405

---

## Contributors

**Mohammed Aqil** Department of Pharmaceutics, Faculty of Pharmacy, Hamdard University, New Delhi, India

**Mukul A. Ashtikar** Lehrstuhl für Pharmazeutische Technologie, Friedrich-Schiller-Universität Jena, Jena, Germany

**Césa R. Bibi** Therapeutics Research Centre, School of Medicine, University of Queensland, Princess Alexandra Hospital, Woolloongabba, QLD, Australia

**Katharina Bohnenblust-Woertz** Galderma Spirig, Egerkingen, Switzerland

**Marie-Alexandrine Bolzinger** University of Lyon, Laboratoire d'Automatique et de Génie des Procédés (LAGEP), CNRS UMR 5007, Université Claude Bernard Lyon 1, Villeurbanne, France

**Stéphanie Briançon** University of Lyon, Laboratoire d'Automatique et de Génie des Procédés (LAGEP), CNRS UMR 5007, Université Claude Bernard Lyon 1, Villeurbanne, France

**Navin C. Chandrasekaran** Therapeutics Research Centre, School of Medicine, University of Queensland, Princess Alexandra Hospital, Woolloongabba, QLD, Australia

**Yves Chevalier** University of Lyon, Laboratoire d'Automatique et de Génie des Procédés (LAGEP), CNRS UMR 5007, Université Claude Bernard Lyon 1, Villeurbanne, France

**Jason T. Chittenden** Department of Biomathematics, North Carolina State University, Raleigh, NC, USA

Product Development, Pharsight Corporation, Cary, NC, USA

**Donald M. Cropek** Environmental Chemistry Laboratory, U.S. Army Corps of Engineers, Engineering Research and Development Center, Construction Engineering Research Laboratory, Champaign, IL, USA

**Rolf Daniels** Department of Pharmaceutical Technology, Eberhard Karls University, Tuebingen, Germany

**Ryan F. Donnelly** School of Pharmacy, Queens University Belfast, Medical Biology Centre, Belfast, Northern Ireland, UK

**Dusanka Krajinovic** Department for Social Pharmacy and Pharmaceutical Legislation, University of Belgrade Faculty of Pharmacy, Belgrade, Serbia

University of Belgrade – Center for the study of Bioethics, Belgrade, Serbia

**Gamal M. El Maghraby** Department of Pharmaceutical Technology, College of Pharmacy, University of Tanta, Tanta, Egypt

**Alfred Fahr** Lehrstuhl für Pharmazeutische Technologie, Friedrich-Schiller-Universität Jena, Jena, Germany

**M. Foldvari** School of Pharmacy, University of Waterloo, Waterloo, ON, Canada

**Jeffrey E. Grice** Therapeutics Research Centre, School of Medicine, University of Queensland, Princess Alexandra Hospital, Woolloongabba, QLD, Australia

**Stefan F. Haag** Department of Dermatology, Venereology and Allergy, Charité – Universitätsmedizin Berlin, Center of Experimental and Applied Cutaneous Physiology, Berlin, Germany

**Steffi Hansen** Biopharmaceutics and Pharmaceutical Technology, Saarland University, Saarbrücken; Department of Drug Delivery, Helmholtz Institute for Pharmaceutical Research Saarland, Saarbrücken, Germany

**Isha Haridass** Therapeutics Research Centre, School of Medicine, University of Queensland, Princess Alexandra Hospital, Woolloongabba, QLD, Australia

**Trinh Hermanns-Lê** Laboratory of Skin Bioengineering and Imaging, Liège University, Liège, Belgium

**William I. Higuchi** Pharmaceutics and Pharmaceutical Chemistry, College of Pharmacy, University of Utah, Salt Lake City, UT, USA

**Syed Sarim Imam** Department of Pharmaceutics, School of Pharmacy, The Global University, Saharanpur, Uttar Pradesh, India

**Amit Jain** Department of Chemical Engineering, University of California – Santa Barbara, Santa Barbara, CA, USA

**Pankaj Karande** Howard Isermann Department of Chemical and Biological Engineering, Center for Biotechnology and Interdisciplinary Sciences, Rensselaer Polytechnic Institute, Troy, NY, USA

**Victoria Klang** University of Vienna, Department of Pharm. Technology and Biopharmaceutics, Vienna, Austria

**P. Kumar** Helix BioPharma Inc., Saskatoon, SK, Canada

**Jürgen Lademann** Charité – Universitätsmedizin Berlin, Department of Dermatology, Venereology and Allergy, Center of Experimental and Applied Cutaneous Physiology, Berlin, Germany

**Wing Man Lau** School of Pharmacy, University of Reading, Reading, UK

**Claus-Michal Lehr** Biopharmaceutics and Pharmaceutical Technology, Saarland University, Saarbrücken, Germany

Department of Drug Delivery, Helmholtz Institute for Pharmaceutical Research Saarland, Saarbrücken, Germany

**V.R. Leite-Silva** Universidade Federal de São Paulo, Instituto de Ciências Ambientais Químicas e Farmacêuticas, Diadema, SP, Brazil

**S. Kevin Li** Division of Pharmaceutical Sciences, College of Pharmacy, University of Cincinnati, Cincinnati, OH, USA

**Dominique Jasmin Lunter** Department of Pharmaceutical Technology, Eberhard Karls University, Tuebingen, Germany

**Martina C. Meinke** Charité – Universitätsmedizin Berlin, Department of Dermatology, Venereology and Allergy, Center of Experimental and Applied Cutaneous Physiology, Berlin, Germany

**Samir Mitragotri** Department of Chemical Engineering, University of California – Santa Barbara, Santa Barbara, CA, USA

**Hamid R. Moghimi** Therapeutics Research Centre, School of Pharmacy and Medical Sciences, University of South Australia, Adelaide, SA, Australia  
School of Pharmacy, Shahid Beheshti University of Medical Sciences, Tehran, Iran

**Yousuf H. Mohammed** Therapeutics Research Centre, School of Medicine, University of Queensland, Princess Alexandra Hospital, Woolloongabba, QLD, Australia

**Keng Wooi Ng** School of Pharmacy, University of Reading, Reading, UK

**Alexa Patzelt** Charité – Universitätsmedizin Berlin, Department of Dermatology, Venereology and Allergy, Center of Experimental and Applied Cutaneous Physiology, Berlin, Germany

**Gérald E. Piérard** Laboratory of Skin Bioengineering and Imaging, Liège University, Liège, Belgium

**Claudine Piérard-Franchimont** Laboratory of Skin Bioengineering and Imaging, Liège University, Liège, Belgium

**Tarl W. Prow** Dermatology Research Centre, School of Medicine, The University of Queensland, Princess Alexandra Hospital, Translational Research Institute, Brisbane, QLD, Australia

**Anthony P. Raphael** Dermatology Research Centre, School of Medicine, The University of Queensland, Princess Alexandra Hospital, Translational Research Institute, Brisbane, QLD, Australia

**Heike Richter** Charité – Universitätsmedizin Berlin, Department of Dermatology, Venereology and Allergy, Center of Experimental and Applied Cutaneous Physiology, Berlin, Germany

**Jim E. Riviere** Institute of Computational Comparative Medicine, College of Veterinary Medicine, Department of Anatomy and Physiology, Kansas State University, Manhattan, KS, USA

**Michael S. Roberts** Therapeutics Research Centre, School of Medicine, University of Queensland, Princess Alexandra Hospital, Woolloongabba, QLD, Australia

Therapeutics Research Centre, School of Pharmacy and Medical Sciences, University of South Australia, Adelaide, SA, Australia

**Elizabeth Ryan** Therapeutics Research Centre, School of Medicine, University of Queensland, Princess Alexandra Hospital, Woolloongabba, QLD, Australia

**Wedad Sakran** School of Pharmacy, Helwan University, Helwan, Egypt

**Ulrich F. Schaefer** Biopharmaceutics and Pharmaceutical Technology, Saarland University, Saarbrücken, Germany

**Sabine Schanzer** Charité – Universitätsmedizin Berlin, Department of Dermatology, Venereology and Allergy, Center of Experimental and Applied Cutaneous Physiology, Berlin, Germany

**Julia C. Schwarz** University of Vienna, Research Platform ‘Characterisation of Drug Delivery Systems on Skin and Investigation of Involved Mechanisms’, Vienna, Austria

**Dominik Selzer** Biopharmaceutics and Pharmaceutical Technology, Saarland University, Saarbrücken, Germany

**Sinduja C. Sukumar** Therapeutics Research Centre, School of Medicine, University of Queensland, Princess Alexandra Hospital, Woolloongabba, QLD, Australia

**Christian Surber** University Hospital Zürich, Department of Dermatology, Zürich, Switzerland

University Hospital Basel, Department of Dermatology, Basel, Switzerland

**Claudia Valenta** University of Vienna, Research Platform ‘Characterisation of Drug Delivery Systems on Skin and Investigation of Involved Mechanisms’, Vienna, Austria

University of Vienna, Department of Pharm. Technology and Biopharmaceutics, Vienna, Austria

**Daya D. Verma** Novartis Pharmaceutical Corp., East Hanover, NJ, USA

**Hans-Jürgen Weigmann** Charité – Universitätsmedizin Berlin, Department of Dermatology, Venereology and Allergy, Center of Experimental and Applied Cutaneous Physiology, Berlin, Germany

**Shereen A. Yousef** Therapeutics Research Centre, School of Medicine, University of Queensland, Princess Alexandra Hospital, Woolloongabba, QLD, Australia

**Qian Zhang** Therapeutics Research Centre, School of Pharmacy and Medical Sciences, University of South Australia, Adelaide, SA, Australia

---

**Part I**

**Factors Influencing Percutaneous Drug  
Penetration**



# Basic Mathematics in Skin Absorption

1

Dominik Selzer, Ulrich F. Schaefer,  
Claus-Michael Lehr, and Steffi Hansen

## Contents

1.1	<b>Mathematical Background of Analyzing Skin Absorption Processes</b> .....	4
1.2	<b>Analysis of Skin Permeation</b> .....	6
1.2.1	Dealing with Infinite Dose Skin Permeation ...	8
1.2.2	Dealing with Finite Dose Skin Permeation ...	10
1.3	<b>Analysis of Skin Penetration</b> .....	12
1.3.1	Skin-Concentration Depth Profiles .....	12
1.3.2	Skin Compartmental Approaches .....	15
1.4	<b>Advanced Mathematical Approaches for Studying Skin Absorption</b> .....	16
1.4.1	Laplace Domain Solutions .....	16
1.4.2	Numerical Diffusion Models.....	17
1.5	<b>In Vitro–In Vivo Correlation (IVIVC)</b> .....	19
1.6	<b>Tips and Tricks</b> .....	21
1.6.1	Infinite Sums in Analytical Solutions .....	21
1.6.2	Fitting of Experimental Data.....	21
	<b>Conclusion</b> .....	22
	<b>References</b> .....	22

## Table of Abbreviations

Symbol	Generic units	Description
$A$	$m^2$	Area of application
AUC	$kg/m^3$	Area under the curve
$c$	$kg/m^3$	Concentration
$c_{ss}$	$kg/m^3$	Steady-state concentration
$C_0$	$kg/m^3$	Initial concentration at $t = 0$
$Cl$	$m^3/h$	Systemic clearance
$D$	$m^2/s$	Diffusion coefficient
$h_v$	M	Height of applied formulation
$J$	$\frac{mol}{m^2 s}$	Diffusion flux
$J_{max}$	$\frac{mol}{m^2 s}$	Maximum diffusion flux
$J_{peak}$	$\frac{mol}{m^2 s}$	Peak flux
$k$	J/K	Boltzmann's constant
$K$	–	Partition coefficient
$K_{o/w}$	–	Octanol–water partition coefficient
$k_p$	m/s	Permeability coefficient
$k_t$	$\frac{\% \text{ applied}}{s}$	Transfer coefficient
$l$	m	(Macroscopic) thickness
$m$	kg	Mass
$M$	kg	Mass per area
$M_{ss}$	kg	Steady-state amount of solute in the membrane

D. Selzer • U.F. Schaefer  
Biopharmaceutics and Pharmaceutical Technology,  
Saarland University, Saarbrücken, Germany  
e-mail: [d.selzer@mx.uni-saarland.de](mailto:d.selzer@mx.uni-saarland.de);  
[ufs@mx.uni-saarland.de](mailto:ufs@mx.uni-saarland.de)

C.-M. Lehr • S. Hansen (✉)  
Biopharmaceutics and Pharmaceutical Technology,  
Saarland University, Saarbrücken, Germany

Department of Drug Delivery, Helmholtz Institute  
for Pharmaceutical Research Saarland,  
Saarbrücken, Germany  
e-mail: [lehr@mx.uni-saarland.de](mailto:lehr@mx.uni-saarland.de);  
[st.hansen@mx.uni-saarland.de](mailto:st.hansen@mx.uni-saarland.de)

Symbol	Generic units	Description
$M_\infty$	kg	Applied mass
MW	kg	Molecular weight
ODE	–	Ordinary differential equation
PK	–	Pharmacokinetic
$r$	m	Radius
$S$	s	Saturation concentration
$t$	s	Time
$t_{lag}$	s	Lag time
$t_{peak}$	s	Time to peak flux
$T$	K	Temperature
$V$	m <sup>3</sup>	Volume
$x$	m	Space
$\eta$	Pa s	Viscosity
$\varphi$	$\frac{J}{\text{mol K}}$	Chemical potential

## 1.1 Mathematical Background of Analyzing Skin Absorption Processes

It is usually assumed that the travel of molecules through the skin membrane is governed simply by passive diffusion due to the absence of active transporters. From an atomistic point of view, diffusion is based on Brownian motion of particles in virtue of their thermal energy. From an empirical and more macroscopic understanding, the driving force of molecular movement is a concentration gradient of the diffusant in a medium and can be mathematically described by laws derived by Adolf Fick in 1855.

Fick's first law (Eq. 1.1) relates the diffusion flux  $J$  (e.g., in mol/m<sup>2</sup> s) to the concentration gradient. Here,  $D$ , the diffusion coefficient, is a proportionality constant usually given in m<sup>2</sup>/s, and  $c$  the concentration at point  $x$  in space and time  $t$ .

$$J(x,t) = -D \nabla c(x,t) \quad (1.1)$$

Assuming conservation of mass, one can derive Fick's second law of diffusion (Eq. 1.2):

$$\frac{\partial c(x,t)}{\partial t} = \nabla (D \nabla c(x,t)) \quad (1.2)$$

In this general equation, the diffusion coefficient may vary in dependence of location and/or concentration. Additional terms can be included to address, for example, binding phenomena (Frasch et al. 2011), enzymatic reactions (Guy et al. 1987), corneocyte desquamation (Reddy et al. 2000a, b), or general convective transport to model elimination or clearance of molecules into the systematic circulation (Dancik et al. 2012). For the one-dimensional case and a homogenous medium (constant diffusivity), (Eq. 1.2) simplifies to Eq. 1.3

$$\frac{\delta c(x,t)}{\delta t} = D \frac{\delta^2 c(x,t)}{\delta x^2} \quad (1.3)$$

Homogeneity is often a strong simplification but a typical assumption for easy analytical models to describe transdermal drug transport. Solutions of these parabolic partial differential equations can be solved analytically for various initial and boundary conditions and are presented in Sect. 1.3. As mentioned earlier, these conditions often denote simplifications and are only true for the description of a specific experimental setup (e.g., infinite dose or finite dose conditions with certain initial conditions). This is a fundamental issue and must be always kept in mind when applying mathematical models in general. We will shortly discuss more flexible but complex models in Sect. 1.5 that allow the application to a wider range of scenarios.

For the inhomogeneous and more general case, the diffusion flux at a cross section  $x$  at time  $t$  is directed from sites of higher chemical potential to sites of lower chemical potential ((Eq. 1.4 (Crank 1975); Anissimov and Roberts 2004)). Inhomogenous media transitions change the classical diffusion problem to a diffusion-partition problem.

$$J(x,t) = -\frac{D}{kT} c(x,t) \frac{\delta \varphi(x,t)}{\delta x} \quad (1.4)$$

Here,  $\varphi(x, t)$  is the chemical potential of the substance,  $T$  is the temperature, and  $k$  is Boltzman's constant. For the homogeneous case with  $\varphi(x, t) = kT \ln(c(x, t))$  and a constant diffusivity, Eq. 1.4 simplifies to the standard diffusion equation as stated in Eq. 1.3.

The general case equation that describes the diffusion-partition problem with the chemical potential defined as  $\varphi(x, t) = kT \ln\left(\frac{c(x, t)}{K(x)}\right)$ , and the position-dependent partition coefficient  $K$  is given by Eq. 1.5 (Anissimov and Roberts 2004):

$$\frac{\delta c(x, t)}{\delta t} = \frac{\delta}{\delta x} \left( D(x) \frac{\delta}{\delta x} c(x, t) - D(x) c(x, t) \frac{\delta}{\delta x} \ln K(x) \right) \quad (1.5)$$

Besides studies with variable partition and/or diffusion coefficients inside a certain skin layer (Anissimov and Roberts 2004), it is more common (especially for more complex multilayer models) to assign specific diffusion coefficients to the different layers and specific partition coefficients to the interfaces of two adjacent layers. In this chapter, the presented solutions of the diffusion equation and determination of distinctive parameters almost exclusively depend on predicted, fitted, or experimentally determined diffusivities and partition coefficients. Therefore, at least a basic understanding of the relationship between molecular properties and the aforementioned parameters is essential when it comes to the preparation, setup, and evaluation of transdermal skin transport.

For spherical particles in a continuous fluid, the diffusion coefficient can be calculated by using the well-known Stokes–Einstein relation (Eq. 1.6), with viscosity of the solvent  $\eta$  and particle radius  $r$ :

$$D = \frac{kT}{6\pi\eta r} \quad (1.6)$$

For diffusion in polymers, it could be found empirically that for a small particle the following relationship holds (Eq. 1.7) (Anderson and Raykar 1989):

$$D_m = D_m^0 MW^{-n} \quad (1.7)$$

Here,  $MW$  is the solute molecular weight, and  $n$  and  $D_m^0$  are constants, the characteristics of the membrane at a specific temperature. Other theories derived from polymer research have also been applied successfully to the field of describing diffusivities in the skin domain. For deeper insight, the interested reader is kindly referred to Hansen et al. (2013).

Where the diffusivity  $D$  denotes the speed of a diffusant through a membrane and is inversely related to the weight of the solute, the partition coefficient  $K$  accounts for jumps in concentrations at the interface of two adjacent skin layers and is often related to a measure of solute lipophilicity, most commonly the logarithmic octanol–water partition coefficient.  $K$  is a thermodynamic parameter reflecting the relative affinity of a solute for a certain phase over another phase. Hence, the partition coefficient between layer  $m_2$  and layer  $m_1$  can be defined as Eq. 1.8

$$K_{m_2/m_1} = \frac{C_{m_2}^{\text{eq}}}{C_{m_1}^{\text{eq}}} \quad (1.8)$$

with  $C_{m_2}^{\text{eq}}$  and  $C_{m_1}^{\text{eq}}$  being the respective solute concentrations at the interface of the two adjacent phases at equilibrium. In general, the partition coefficient is concentration-dependent, but if the solubilities in the two phases are relatively low (which holds true for many cases), this effect can be neglected, and the partition coefficient can be defined by using the saturation concentrations  $S_{m_1}$  and  $S_{m_2}$  in the different layers (Anissimov et al. 2013), with Eq. 1.9

$$K_{m_2/m_1} = \frac{S_{m_2}}{S_{m_1}} \quad (1.9)$$

A typical strategy is to establish a relationship between an easy-to-observe parameter that mimics the membrane properties and the parameter of interest. A prominent example is the octanol/water partition coefficient  $K_{o/w}$  that could be related to the stratum corneum lipid phase/water partition coefficient  $K_{\text{lip}}$ , with the help of a linear free-energy relationship (Eq. 1.10) (Anderson et al. 1988)

$$K_{\text{lip}} = aK_{o/w}^b \quad (1.10)$$

Here, the constants  $a$  and  $b$  correspond to the characteristics of the relationship between aqueous vehicle and lipid phase of the stratum corneum. It is obvious that this relationship strongly depends on the physicochemical properties of the layers at the interface (e.g., donor/SC or viable epidermis/stratum corneum). We again refer the interested reader to Hansen et al. (2013) for an extensive overview about the determination of diffusion model input parameters.

It must be noted that representation of diffusivity and partition coefficient in certain skin layers by a single number basically averages several transport mechanisms (e.g., several different routes through the stratum corneum or implicit binding phenomena) of the diffusant. This important fact must be kept in mind when developing and applying mathematical models as well as when trying to generalize basic relationships, such as Eqs. (1.7) and (1.10). Since literally all mathematical models heavily oversimplify the underlying physics, parameters derived from mathematical concepts might obfuscate the governing mechanics.

## 1.2 Analysis of Skin Permeation

Permeation experiments are usually performed to measure the amount permeated through the barrier over time in relation to the diffusion area. For an *in vitro* setup, this relates to the accumulated mass in an acceptor compartment. This is an important measure, especially for systemic and regional drug delivery through the skin (e.g., for achieving therapeutic drug levels systemically or treatment of tissue beneath the site of application).

Permeation experiments are typically applied using diffusion cells yielding in a general separation of the diffusion domain in different compartments, namely donor, barrier, and acceptor compartments. Frequently used diffusion cells are static cells, like the well-known vertical Franz

diffusion cell (Franz 1975) and horizontal Bronaugh cell (Bronaugh and Stewart 1985) as well as flow through cells (for further details, see Sect. 3.3 of Chapter 10). Typical barrier membranes for investigation consist of excised human or animal skin in its various fashions, bioengineered skin or artificial skin surrogates (for a detailed overview, we kindly refer to Sect. 2 of Chap. 16).

When it comes to application scenarios, one can distinguish between infinite dose and finite dose experiments. In the case of infinite dosing, the applied dose is assumed to be so large that evaporation or diffusion through the barrier does only negligibly change the concentration in the donor compartment. Therefore, mathematically the dose is assumed to be infinite (Brain et al. 2002). For the finite dose case, according to the Organisation for Economic Cooperation and Development (OECD), finite dose experiments are defined by an application of a limited volume of formulation ( $\leq 10 \mu\text{l}/\text{cm}^2$  of a liquid formulation) (OECD 2004a, b). For semisolid and solid formulations, these values range from 1 to 10 mg/cm<sup>2</sup>.

Typical concentration/mass/flux versus time profiles for the infinite, semi-infinite (volume  $> 10 \mu\text{l}/\text{cm}^2$ , but with a depletion of the donor which is already perceptible), and finite dose cases are depicted in Fig. 1.1. These theoretical calculations were performed using the DSkin<sup>®</sup> software.<sup>1</sup> An aqueous donor/acceptor with a drug diffusion coefficient of  $6.33\text{E-}5 \text{ cm}^2/\text{s}$ , stratum corneum lipid channel diffusion coefficient of  $1.87\text{E-}8 \text{ cm}^2/\text{s}$ , and partition coefficient of 6.56 was used for simulations. The initial donor concentration was set to 1 mg/ml, and the donor volume for the semi-infinite dose and finite dose scenario was set as 2  $\mu\text{l}$  and 20  $\mu\text{l}$ , respectively for an area of diffusion of 1.767 cm<sup>2</sup>. A tortuous stratum corneum lipid path length of 180  $\mu\text{m}$  was assumed, which corresponds to a swollen membrane for an *in vitro* setup (Talreja et al. 2001). Perfect sink conditions of the acceptor compartment are assumed.

<sup>1</sup>DSkin<sup>®</sup> <http://www.scientific-consilience.com>

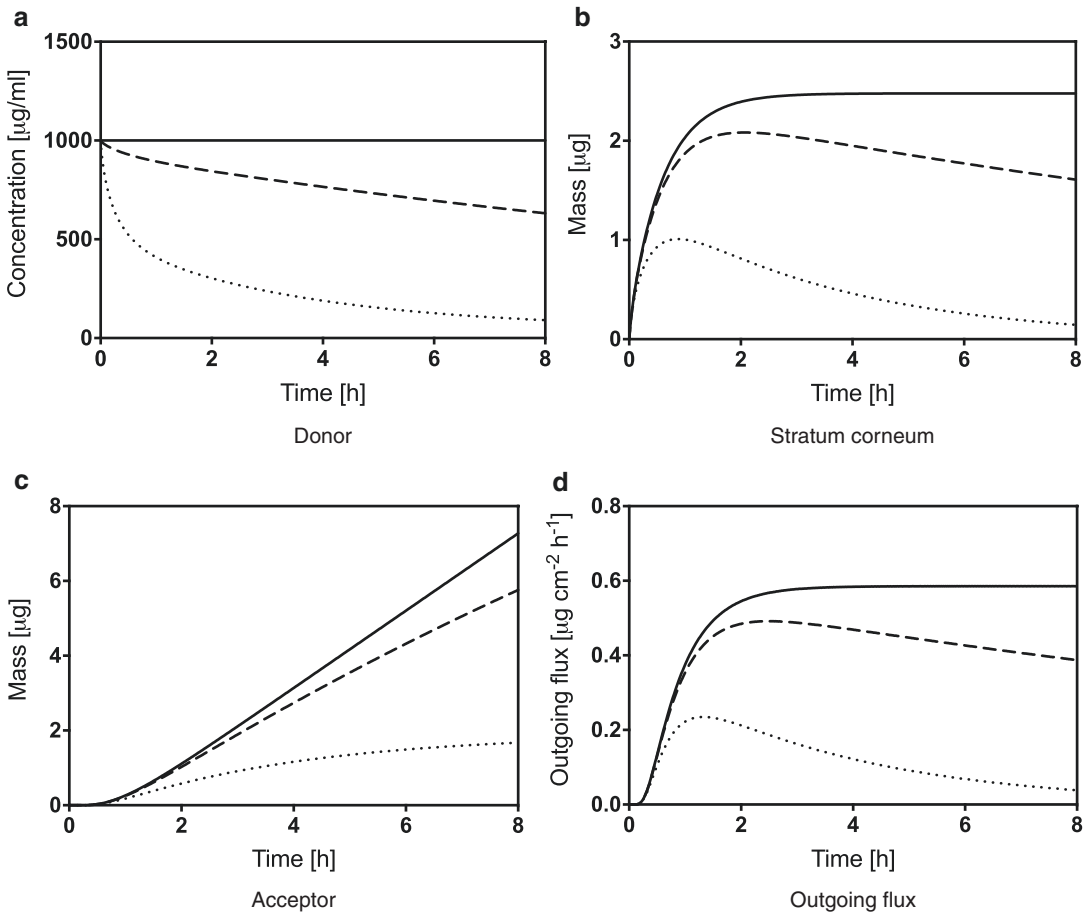


**Fig. 1.1** Theoretical change of concentration in the donor compartment over time (a), change of mass inside the stratum corneum (b), accumulated mass inside the acceptor compartment (c), and change of stratum corneum

outgoing flux (d) for infinite (solid line), semi-infinite (dashed line), and finite dosing (dotted line). Simulations were performed using the DSKin® software

The chosen values correspond to a model compound of approximately 300 Da with a  $\log K_{OW}$  of 2 in an aqueous vehicle, and model parameters were estimated by DSKin. The concentration-over-time profile depicted in Fig. 1.1a shows the characteristic depletion of the donor for the finite dose case and less pronounced for the semi-infinite case. The barrier mass-over-time curve for an infinite dose setup does reach a plateau as soon as the steady state is reached (Fig. 1.1b). As opposed to this, the mass of the finite dose case decreases after reaching a maximum (Fig. 1.1b). In case of the infinite dose setup, the accumulated mass inside the acceptor compartment reaches the typical straight steady-state line (Fig. 1.1c). This

corresponds to a plateau of the flux-over-time profile (Fig. 1.1d). In contrast, the finite dose scenario will reach a theoretical mass plateau in the acceptor compartment if all substance has traveled through the membrane. Obviously, the flux reaches a maximum and subsequently decreases with time. For the simulation of the semi-infinite dose case shown in Fig. 1.1d, the applied volume per area was set slightly higher than the finite dose threshold defined by the OECD. This shows clearly that the assumption of an infinite dose (no significant depletion) does not automatically hold by applying fixed volume-based rules. This is crucial when applying the mathematical concepts presented in the next subsections, since choosing

faulty assumptions can lead to serious misinterpretation of experimental data. It has to be kept in mind that even if small volumes of highly concentrated solutions are applied and the permeation is low, the system might behave like an infinite dose case due to the fact that significant donor depletion only occurs at very long experimental time periods in relation to the permeated solute amount in the acceptor compartment.

Investigation of infinite and finite dose experiments typically differ concerning their parameters of interest and application of mathematical concepts (e.g., analytical solutions of the diffusion equation are always tailored to certain boundary and initial conditions). In the next two sections, analytical solutions of the diffusion equation and mathematical concepts for the most typical experimental settings are presented. For an exhaustive compilation of solutions regarding the diffusion equation for various boundary and initial conditions, the reader is kindly referred to the excellent book *The Mathematics of Diffusion* by J. Crank (Crank 1975).

### 1.2.1 Dealing with Infinite Dose Skin Permeation

Analysis of infinite dose in vitro skin permeation is typically done by measuring the cumulative amount of substance inside the acceptor compartment over time. For short times, the amount increases exponentially until reaching a steady line (the steady state) with constant flux  $J_{SS}$

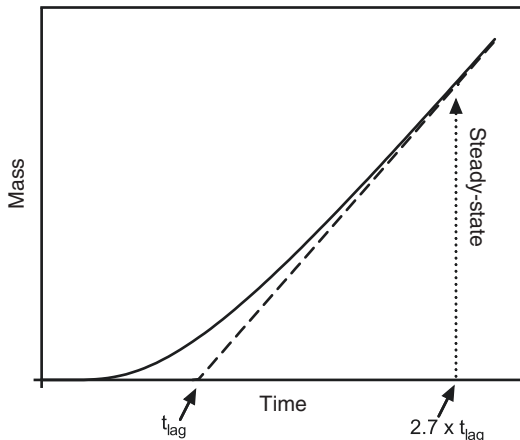


**Fig. 1.2** Accumulated mass over time in the acceptor compartment of an infinite dose experiment (solid line) and linear part of the steady-state phase (dashed line). The intersection of the linearized steady-state phase and time axis denotes the lag time

(see Fig. 1.2). From a mathematical point of view, a few assumptions must be made to derive an analytical solution for the diffusion equation by defining initial and boundary conditions. In this case, we assume a constant and steady concentration in the donor compartment, perfect sink conditions (zero concentration in the acceptor at all times), and that no compound of interest is located inside the barrier at time  $t = 0$ .

By incorporating these rules for a homogeneous membrane, the absorption curve can be described by an analytical solution of Fick's second law of diffusion (Scheuplein 1967; Crank 1975), with

$$m(t) = A \times K \times l \times C_0 \left[ K \times l \times t - \frac{1}{6} - \frac{2}{\pi^2} \sum_{n=1}^{\infty} \frac{(-1)^n}{n^2} \exp\left(-\frac{Dn^2\pi^2t}{l^2}\right) \right] \quad (1.11)$$

Here,  $A$  denotes the area of application,  $K$  is the partition coefficient between donor and barrier,  $C_0$  is the concentration of applied formulation in the donor which is assumed not to change significantly during experimental time periods,  $D$  is the macroscopic diffusion coefficient,  $l$  is the macroscopic thickness of the barrier, and  $t$  is the time after application. It is obvious that with  $t$  leaning toward infinity (and hence reaching the

steadystate), the solution simplifies to the linear part of the steady state (Fig. 1.2), with

$$m(t) = A \frac{DK}{l} C_0 \left( t - \frac{l^2}{6D} \right) \quad (1.12)$$

From Eq. 1.12, we can examine important parameters when it comes to analysis of infinite dose experiments. The first parameter is the

so-called apparent permeability coefficient,  $k_p$ , which is often given in units of cm/h and is defined as

$$k_p = \frac{DK}{l} \quad (1.13)$$

It is independent of the area of application and initial concentration, and hence a direct parameter for the strength of permeation for a compound through a certain barrier from a specific vehicle under infinite dose and perfect sink conditions. Mathematically, it denotes a normalization of steady-state flux  $J_{SS}$  with

$$k_p = \frac{J_{SS}}{C_0} \quad (1.14)$$

Such a parameter might heavily depend on experimental conditions. Hence, this has to be kept in mind when comparing parameters (interlaboratory and intralaboratory). Although  $k_p$  may be a useful and popular parameter when it comes to examination of permeation experiments, it can be sometimes misleading when comparing the permeation of several compounds (Michaels et al. 1975; Anissimov et al. 2013). The apparent permeability coefficient  $k_p$  describes an intrinsic property of a solute to permeate across a specific medium (e.g., the skin) which is independent of the dose but influenced by the applied vehicle. Therefore, comparisons are only possible between compounds which are applied in identical vehicles. In 2006, Sloan et al. introduced a change of paradigm when it comes to explaining experimental data (Sloan et al. 2006). They suggested to use the more expressive parameter  $J_{max}$  which denotes the maximum possible flux of a solute through a barrier for comparing permeability (Eq. 1.15). By using  $J_{max}$ , it is possible to overcome the limitations addressed before

$$J_{max} = k_p \times S_v = D \times \frac{S_m}{l} \quad (1.15)$$

Here,  $S_v$  is the saturated permeant concentration in the vehicle and  $S_m$  is the solubility of the solute within the barrier. In other words, by removing the influence of the partition coefficient between the skin and vehicle,  $J_{max}$  should be independent of the vehicle applied. Thus, it describes an

intrinsic permeability of a solute in a certain medium, making it an ideal parameter to compare permeability of different solutes. Obviously, this is the case, as long as the vehicle does not affect the transport kinetics in the barrier (Zhang et al. 2011).

In contrast to epidermal  $k_p$  which is optimally correlated to the molecular weight and lipophilicity of a compound (Fiserova-Bergerova et al. 1990; Potts and Guy 1992; McKone and Howd 1992), Magnusson et al. (2004) could show that molecular weight is the main determinant when it comes to predicting solute maximum flux.

A further parameter to characterize infinite dose absorption is the so-called lag time  $t_{lag}$  given by

$$t_{lag} = \frac{l^2}{6D} \quad (1.16)$$

It is a measure that relates to the time it takes for a compound to travel through the barrier and establish a steady state. A word of caution is necessary concerning the meaning of  $t_{lag}$ .  $t_{lag}$  does not directly represent the time when the steady state is achieved (see Fig. 1.2); however, it can be approximated by multiplying  $t_{lag}$  with 2.7 (Crank showed that steady state is achieved when  $\frac{Dt}{l^2} = 0.45$  approximately (Crank 1975)).

From a practical point of view, determination of permeability coefficient and lag time can generally be accomplished in two fashions:

1. The easiest approach utilizes the linearization of the steady state (see Fig. 1.2) which intersects the time axis at  $t_{lag}$ . This can be accomplished graphically by manual interpolation of the last data points that contribute to the steady state or mathematically more soundly by a linear fit (Schäfer-Korting et al. 2008). It is important to mention that the occurrence of physically untenable negative lag times often indicates experimental problems such as donor depletion (Barbero and Frascch 2009) or insufficient sink conditions (Anissimov and Roberts 1999). The permeability coefficient can be determined by dividing the slope of the linear part by the initial concentration  $C_0$  and

application area  $A$  or simply by using the two steady-state data points with

$$k_p = \frac{m_1 - m_2}{AC_0(t_1 - t_2)} \quad (1.17)$$

If the slope of the curve decreases after reaching steady state, a general strategy is to employ the steepest part of the curve for evaluation (Buist et al. 2010). The clear advantage is the simplicity in calculations, but several problems arise using this approach that makes it extremely prone to errors – from an experimental and evaluation point of view:

- (a) This approach cannot be applied if the steady state was not clearly reached at the end of the experiment.
- (b) It is often difficult to identify which data points contribute to the steady state and which do not. Often, a frequent sampling and stepwise addition of data points from  $t_{\text{end}}$  (last data point) toward  $t_0$  (first data point) and analyzing the linear interpolations can overcome this problem.
- (c) Using only a limited amount of data points generally ignores information. Carelessly

discarding data often yields wrong results and can produce a high variability, depending on which points are chosen for evaluation. This is an obvious but often neglected problem in processing experimental data.

2. A more sophisticated approach is the use of the mathematical representation of the entire curve (Eq. 1.11). In 2009, Henning et al. performed an in-depth analysis of problems that arise in data evaluation of infinite dose permeation experiments and showed the superiority of this procedure over the manual approach (Henning et al. 2009). A huge advantage is the ability to deliver sound results even if only a partial representation of the steady state is available. Often, the macroscopic thickness of the swollen skin is not exactly known. By defining partition parameter  $P_1$  and diffusion parameter  $P_2$  with

$$P_1 = K \cdot l \quad (1.18)$$

$$P_2 = \frac{D}{l^2} \quad (1.19)$$

and reformulating Eq. 1.11 yields (Díez-Sales et al. 1991; Kubota et al. 1993)

$$m(t) = A \cdot P_1 \cdot C_0 \cdot \left[ P_2 \cdot t - \frac{1}{6} - \frac{2}{\pi^2} \sum_{n=1}^{\infty} \frac{(-1)^n}{n^2} \exp(-P_2 n^2 \pi^2 t) \right] \quad (1.20)$$

This reduces the number of unknown parameters.

Hence,  $P_1$  and  $P_2$  can be easily fitted to experimental data using a nonlinear least squares approach. Permeability and lag time can be subsequently computed by

$$k_p = P_1 \cdot P_2 \quad (1.21)$$

$$t_{\text{lag}} = \frac{1}{6P_2} \quad (1.22)$$

### 1.2.2 Dealing with Finite Dose Skin Permeation

In contrast to the infinite dose exposure scenario, a typical finite dose absorption profile does not

reach a steady state, but builds a mass plateau inside the acceptor compartment at late time points (see Fig. 1.1c). Finite dose experiments also show a characteristic depletion of donor concentration (Fig. 1.1a) and increase in flux until reaching the so-called peak flux  $J_{\text{peak}}$  at time  $t_{\text{peak}}$  (Fig. 1.3).

As opposed to the infinite dose case, deduction and application of an analytical solution for the description of absorption curves require a more sound mathematical foundation. Based on the theory of heat flow by Carslaw and Jaeger, a description of the flux of the compound leaving the barrier at time  $t$  is given by Eq. 1.23 (Carslaw and Jaeger 1959; Cooper and Berner 1985):

$$J(t) = 2 \cdot A \cdot M_{\infty} \cdot \beta \cdot \frac{D}{l^2} \sum_{i=1}^{\infty} \frac{\alpha_i^2}{\cos \alpha_i (\beta + \beta^2 + \alpha_i^2)} \exp\left(-\frac{\alpha_i^2 D t}{l^2}\right), \quad (1.23)$$



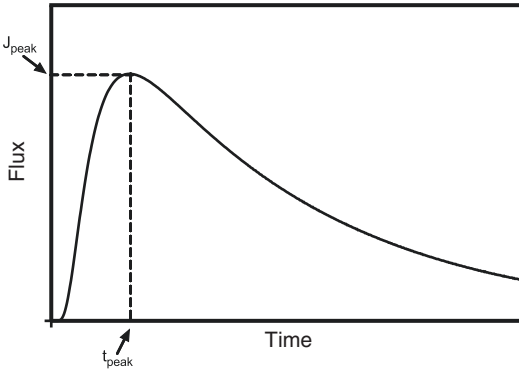


**Fig. 1.3** Sketch of outgoing flux across the barrier-acceptor interface over time of a finite dose experiment (solid line). The maximum of the curve denotes the peak flux  $J_{\max}$  at time to peak flux  $t_{\max}$

with

$$\beta = K \frac{l}{h_v}, \quad (1.24)$$

and the roots of the transcendental equation,  $\alpha_i$ , given by

$$\alpha_i \tan \alpha_i = \beta \quad (1.25)$$

Here,  $M_\infty$  denotes the applied mass, and  $h_v$  is the height of the formulation in the donor compartment. The remaining parameters keep their meaning as introduced above.

Integrating Eq. 1.23 yields the accumulated mass per area (Kasting 2001) with

$$\frac{M(t)}{M_\infty} = 1 - 2\beta \sum_{i=1}^{\infty} \frac{1}{\cos \alpha_i (\beta + \beta^2 + \alpha_i^2)} \exp\left(-\frac{\alpha_i^2 Dt}{l^2}\right) \quad (1.26)$$

In comparison to Eq. 1.11 for the infinite dose case, solving Eq. 1.26 requires a more skillful evaluation, since Eq. 1.25 must be solved for arbitrary values of  $i$ . A basic strategy to solve the transcendental equation is to use logistic regression to tabulated values of the first roots (see Fig. 1.4). To find further roots a subsequent linear extrapolation from previous roots ( $\text{root}_n = 2 \times \text{root}_{n-1} - \text{root}_{n-2}$ ) followed by a refinement step (root-finding with, e.g., Newton's method) (Kasting 2001) is key. To reduce the number of unknowns, the same approach that

worked for the infinite dose case (Eqs. 1.18 and 1.19) can be applied.

Equation 1.26 can be fitted to experimental data by a nonlinear least squares approach and yields values for  $\beta$ , diffusivity  $D$ , and macroscopic path length  $l$ .

Important parameters for evaluation of finite dose permeation experiments are the peak flux  $J_{\text{peak}}$  and time to peak flux  $t_{\text{peak}}$ .

A general strategy to easily find  $J_{\text{peak}}$  and  $t_{\text{peak}}$  is finding the root of the first derivative of  $J(t)$  and hence solving the following equation for  $t_{\text{peak}}$ :

$$2 \cdot M_\infty \cdot \beta \cdot \frac{D}{l^2} \sum_{i=1}^{\infty} \frac{\alpha_i^2}{\cos \alpha_i (\beta + \beta^2 + \alpha_i^2)} \exp\left(-\frac{\alpha_i^2 Dt_{\text{peak}}}{l^2}\right) \frac{\alpha_i^2 D}{l^2} = 0 \quad (1.27)$$

A reliable solution for the root-finding problem is, for example, Brent's method (Brent 1973).

For small doses ( $\beta < \sim 0.1$ ),  $J_{\text{peak}}$  and  $t_{\text{peak}}$  can be calculated by the following simple equations (Kasting 2001; Scheuplein and Ross 1974):

$$J_{\text{peak}} = 1.85 M_\infty \frac{D}{l^2}, \quad (1.28)$$

$$t_{\text{peak}} = \frac{(l^2 - h_v^2)}{6D} \quad (1.29)$$

If the thickness of the applied formulation is reasonably small in comparison to the macroscopic diffusion path length, it can be neglected, and Eq. 1.29 simplifies to the familiar expression:

$$t_{\text{peak}} = \frac{l^2}{6D} \quad (1.30)$$

In contrast to fitting solutions of the diffusion equation to experimental data, some researchers use the steepest linear part of the absorption curve

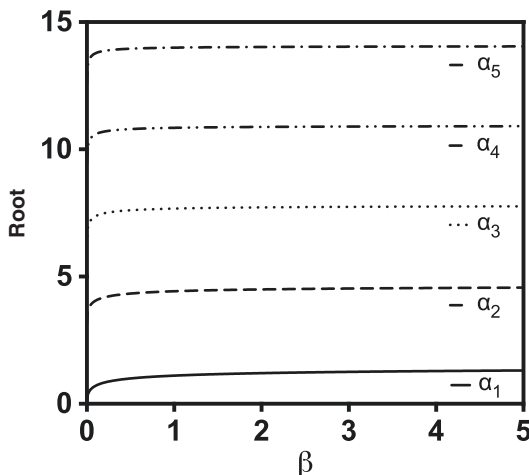


**Fig. 1.4** First five roots of the transcendal Eq. 1.25 for continuous values of  $\beta$  from 0 to 5. Values fitted by logistic regression to tableted values from Crank (1975)

and the time to the steepest part to determine peak flux and time to peak flux (van de Sandt et al. 2004; Wilkinson et al. 2006). Obviously, as for the manual method for the infinite dose case, this approach is prone to errors. Especially for long sampling intervals, a fitting of the right kinetic representation can overcome ambiguities and imprecisions of the manual method.

For the finite dose case, finding a parameter related to the permeability coefficient is obviously not possible, since the flux changes with time. However, in 1974, Scheuplein defined the so-called transfer coefficient  $k_t$  with units of percentage of dose per time (Eq. 1.31) (Scheuplein and Ross 1974):

$$k_t = \frac{\text{flux} \times 100}{\text{specific dose}} \quad (1.31)$$

He used the early flux of the linear part of the curve to estimate the fraction of absorbed dose after a certain time by multiplying  $k_t$  by  $t$ . Besides the fact that this parameter depends on the applied dose, the amount will be heavily overestimated when the flux drops and leans toward zero. These two major drawbacks tremendously limit the usefulness of this parameter.

It has to be kept in mind that finite dose kinetics are also prone to variability of drug distribution in

the donor, as shown by Hahn et al. (2012), and drug distribution to the nonincubated lateral parts in a Franz diffusion-cell setup (Selzer et al. 2013b) yielding a high variability in fitted parameters.

## 1.3 Analysis of Skin Penetration

### 1.3.1 Skin-Concentration Depth Profiles

Besides permeation profiles (accumulated mass over time) which provide valuable information about the absorption process and the transport to the blood circulation and deeper tissue, skin-concentration depth profiles supply precious data about the distribution of solute inside the barrier over time.

One of the most prominent experimental techniques to obtain skin-concentration depth profiles is tape-stripping (Stinchcomb et al. 1999; Wagner et al. 2000; Melero et al. 2011). Tape-stripping is a fast and relatively noninvasive technique to obtain absorption data for the in vitro and in vivo scenarios. For a description of the procedure, we kindly refer to Chapter 10, Sect. 3.11, and references (Escobar-Chavez et al. 2008; Lademann et al. 2009).

As for permeation experiments, the kinetics clearly differ for different exposure scenarios. Figure 1.5 shows theoretical skin-concentration depth profiles for the infinite dose case (Fig. 1.5a), semi-infinite dose case (Fig. 1.5b), and finite dose case (Fig. 1.5c). These curves were produced with the help of the DSkin software and show the change of concentration over time and space in the stratum corneum. The used input parameters correspond to the simulation parameters used to produce the permeation curves in Sect. 1.3.

The infinite dose curves show the typical exponential decay for short exposure times and transition into a straight line when steady state is reached (Fig. 1.5a). The semi-infinite case shows comparable kinetics at short times, reaches a pseudo steady state with a straight line that will drop due to the depletion of the donor over time (Fig. 1.5b). For the finite dose scenario, a straight

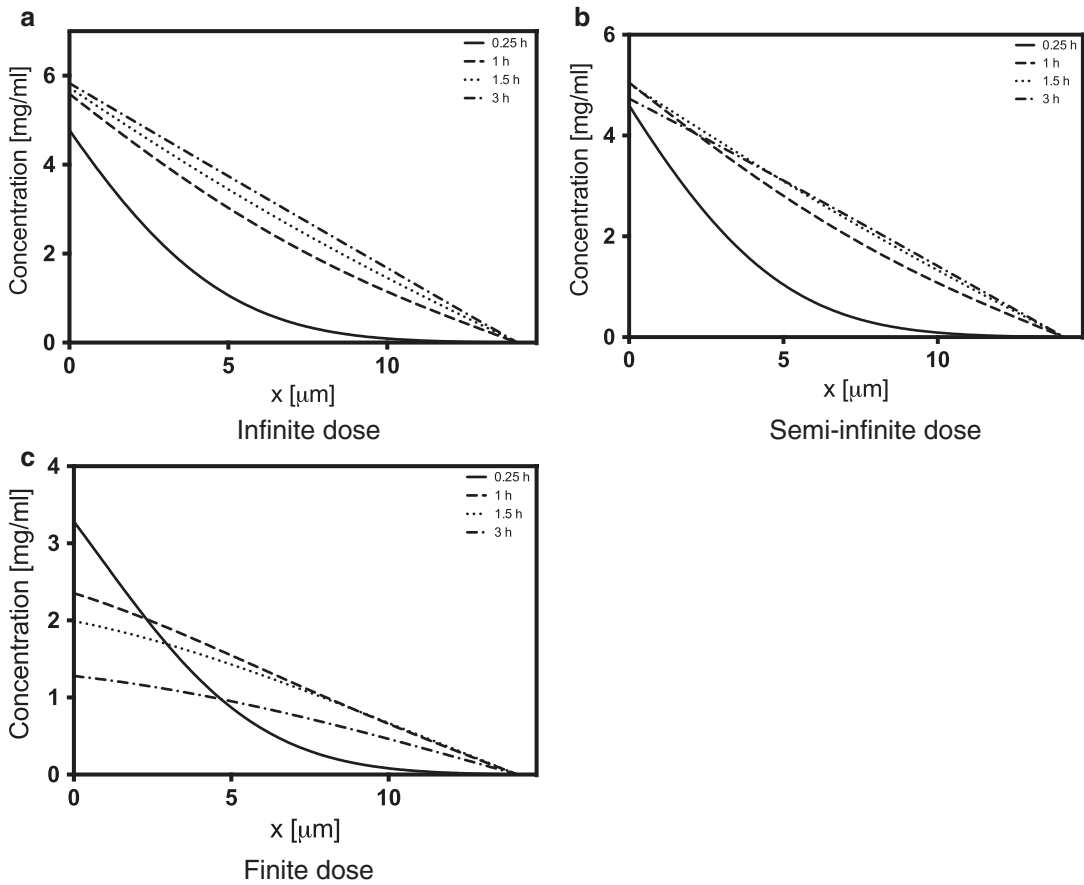


**Fig. 1.5** Theoretical change of concentration in the barrier over time for the infinite dose (a), semi-infinite dose (b), and finite dose (c) cases. Simulations were performed using the DSkin software

line in the concentration over space kinetics is typically not reached, and a significant drop can be recognized over time (Fig. 1.5c).

As for permeation experiments, analytical solutions for the diffusion equation can be obtained to describe the change of concentration

over time and space by using the appropriate initial and boundary conditions together with Eq. 1.3. For the infinite dose case, assuming a homogeneous membrane, one can calculate the concentration inside the barrier at point  $x$  and time  $t$  (Crank 1975; Hansen et al. 2008), with

$$c(x,t) = K \times C_0 \times \left( \left( 1 - \frac{x}{l} \right) - \frac{2}{\pi} \sum_{n=1}^{\infty} \frac{1}{n} \sin\left(\frac{n\pi x}{l}\right) \exp\left(-\frac{Dn^2\pi^2 t}{l^2}\right) \right) \quad (1.32)$$

As for the permeation case (Eq. 1.11),  $K$  denotes the barrier/vehicle partition coefficient,  $C_0$  the initial concentration in the vehicle,  $D$  the apparent diffusivity, and  $l$  the macroscopic thickness of the barrier membrane with  $0 \leq x \leq l$ . The equation can only be applied if the donor does not

deplete over time (typical infinite dose assumption), the receptor compartment is kept at a theoretical zero concentration (perfect sink conditions), and no solute is present inside the barrier at  $t = 0$ . Obviously, only the passive diffusion process is modeled. Hence, permeation

enhancement, binding phenomena, and convection effects are not part of the model.

Eq. 1.32 can be of great benefit to estimate the values for partition coefficient ( $K$ ) and diffusion coefficient ( $\frac{D}{l^2}$ ) and extrapolate the skin-concentration depth profile for later time points (Naegel et al. 2008) or even other exposure scenarios (Selzer et al. 2013a, b; Naegel et al. 2011).

For late times, the skin-concentration depth profile will reach steady state, and Eq. 1.32 simplifies to

$$c_{ss}(x) = K \times C_0 \left(1 - \frac{x}{l}\right) \quad (1.33)$$

Obviously, information about diffusivity can only be obtained before the steady state is reached. Hence, in order to obtain kinetic parameters, fitting Eq. 1.32 to experimental data should focus on short incubation times.

If experimental data that account for the depth profile at a certain time cannot be obtained immediately at the end of an experiment (e.g., due to a long tape-stripping procedure), the obtained values have to be adjusted according to the time delay (Reddy et al. 2000b), and the skin-concentration depth profile can be described with

$$c(x, t) = K \times C_0 \sum_{n=0}^{\infty} \frac{8}{(2n+1)\pi} \cos\left(\frac{(2n+1)\pi x}{2l}\right) \exp\left(-\frac{(2n+1)^2 \pi^2 t_d}{24 t_{lag}}\right) \quad (1.34)$$

Here,  $t_{lag}$  is the lag time with  $t_{lag} = \frac{l^2}{6D}$ , and  $t_d$  is the period of delay before the stratum corneum is stripped with  $t_d = t - t_{exp}$ .  $t_{exp}$  denotes the duration of exposure. Integration of Eq. 1.32 across the

membrane thickness provides the area under skin-concentration depth profile curve (AUC, Eq. 1.35). The AUC equals the total amount of drug present in the membrane at time  $t$  divided by the volume of this compartment (Herkenne et al. 2006):

$$AUC = K \times C_0 \left( \frac{1}{2} - \frac{4}{\pi^2} \sum_{n=0}^{\infty} \frac{1}{(2n+1)^2} \exp\left(-\frac{(2n+1)^2 \pi^2 Dt}{l^2}\right) \right) \quad (1.35)$$

In 1998, the Food and Drug Administration released a draft guidance on dermatopharmacokinetics for the evaluation of topically applied compounds (Shah et al. 1998). Besides the maximum amount in the outermost skin layer (stratum corneum) and the time to reach the maximum amount, the AUC was defined as a parameter of interest. Hence, Eq. 1.35 can be useful to predict the AUC as a function of time after obtaining  $K$  and  $\frac{D}{l^2}$  from parameter fits (Herkenne et al. 2007).

For the steady state, the amount of solute in the membrane can be easily calculated from a simplified formulation of Eq. 1.35:

$$M_{ss} = A \times l \times \frac{K \times C_0}{2} \quad (1.36)$$

For the finite dose case, an analytical solution for the diffusion equation can be obtained with  $\alpha$  and  $\beta$  (as defined earlier in Eqs. 1.25 and 1.24) (Kasting 2001):

$$c(x, t) = 2 \times K \times C_0 \times \sum_{n=1}^{\infty} \frac{\beta \cos(\alpha_n x / h) - \alpha_n \sin(\alpha_n x / h)}{\beta + \beta^2 + \alpha_n^2} \exp\left(-\frac{\alpha_n^2 Dt}{l^2}\right) \quad (1.37)$$

As for the infinite dose case, the same limitations hold (e.g., perfect sink conditions and no solute in the barrier at  $t = 0$ ).

### 1.3.2 Skin Compartmental Approaches

Compartmental or pharmacokinetic models (PK) are used since the early beginnings of mathematical description to study the fate of a substance that was applied in the systemic circulation and are also part of the history of describing transdermal drug absorption. They treat the body as a series of well-stirred compartments. The basic idea is the elimination of space dependence of the partial differential diffusion equation (Eq. 1.2) to obtain a series of ordinary differential equations (ODEs) that describe the change of amount of solute in different compartments over time.

For the family of PK models, a set of first-order rate constant can be assigned to denote the transfer of a compound from one compartment to another. Figure 1.6 shows two examples of skin compartment models: a one-compartment skin model and a two-compartment skin model.

The corresponding first-order ODE of the one-compartment model can be expressed by Eq. 1.38:

$$V_2 \frac{dC_2}{dt} = k_1 C_1 - k_{-1} C_2 + k_{-2} C_3 - k_2 C_2 \quad (1.38)$$

For the two-compartment model, Eqs. 1.39 and 1.40 hold, respectively:

$$V_2 \frac{dC_2}{dt} = k_1 C_1 - k_{-1} C_2 + k_{-2} C_3 - k_2 C_2, \quad (1.39)$$

$$V_3 \frac{dC_3}{dt} = k_2 C_2 - k_{-2} C_3 + k_{-3} C_4 - k_3 C_3 \quad (1.40)$$

The separation of the skin in a lipophilic part (the stratum corneum) and hydrophilic part (viable epidermis) is common practice to mimic the heterogeneity of the skin (McCarley and Bunge 2001; Seta et al. 1992). The underlying ODEs can be solved either analytically (for the most part, only for easy equations) or numerically. Numerical solvers for nonstiff equations are, for example, Euler’s method or the famous fourth-order Runge–Kutta method (widely known as RK4). For stiff equations, the backward differentiation formula (BDF) is a well-known algorithm. Commercial and free mathematical software package usually provide various possibilities for the convenient solving of these kinds of equations.

In comparison to solutions of the diffusion equation, using compartmental models can have some advantages.

A. Obviously, the solution of a set of ODEs can often be derived with little hassle in comparison to complex multicompartmental

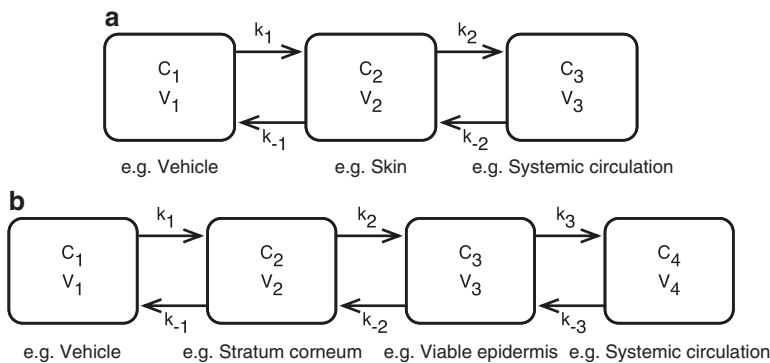


**Fig. 1.6** Exemplary sketch of a one-compartment (a) and two-compartment (b) skin model. Here, the number denotes the number of compartments used to describe the skin barrier, rather than the number of overall compartments.

$C$  denotes the average concentration in the compartment, assuming simplified well-stirred conditions, and  $V$  is the volume of the compartment that is accessible for the solute distribution

diffusion models which are more cumbersome mathematically. For simple models, even analytical solutions can be derived with ease.

- B. Complicated exposure scenarios with, for example, periodic application or evaporation can be implemented very easily in comparison to complex diffusion models.
- C. Adding systemic PK models to a skin PK model can be achieved with little overhead.
- D. Even numerical integration of the ODE is typically much faster than solving the diffusion equation numerically.

One big drawback comes with the oversimplification of having well-stirred compartments that obviously does not reflect reality. Certain kinetics, such as the transition of first-order to zero-order characteristics can only be described unsatisfactorily. PK models were typically used in the past to analyze *in vivo* data (Kubota 1991; Guy et al. 1982). A lot of effort was spent to relate rate constants to physicochemical parameters of the diffusant and fit experimental plasma curves or *in vitro* permeation profiles to PK models (Wallace and Barnett 1978; Guy and Hadgraft 1985), generally with less success than that for the class of diffusion models (Hansen et al. 2013).

Despite a growing trend toward numerical diffusion models, the class of PK models recently regained attention by the work of Davies et al. (2011). They showed that an efficient skin compartmental model can be achieved by a two-layer approach. For excellent overviews on PK models, the interested reader is kindly referred to references (McCarley and Bunge 2001; Reddy et al. 2000a; McCarley and Bunge 2000).

Besides PK models, in 1992, Seta et al. (1992) presented another compartmental approach and successfully studied the transport of radiolabeled hydrocortisone through hairless guinea-pig skin using three skin layers (stratum corneum, viable epidermis, and dermis). They divided each compartment into several hypothetical thin elements and calculated the flux between each element. This approach can be numbered among compartmental models, but rather trends toward numerical finite difference approaches which we will present briefly in Sect. 1.5.

## 1.4 Advanced Mathematical Approaches for Studying Skin Absorption

Previously, we presented basic mathematical concepts to analyze skin permeation and penetration experiments. These models typically relied on analytical solutions of the diffusion equation in the time and/or space domain (see Sects. 1.3 and 1.4.1) or used simple compartmental simplifications to represent the skin (see Sect. 1.4.2). In this section, we will briefly discuss more advanced models that are capable of describing more complex exposure scenarios on a macroscopic and microscopic scale. Statistical models (such as QSAR models (Potts and Guy 1992; Wilschut et al. 1995) or statistical learning approaches (Neumann et al. 2005; Agatonovic-Kustrin et al. 2001; Chen et al. 2007)) that are typically restricted to making predictions are beyond the scope of this chapter. The interested reader is referred to references (Patel et al. 2002; Fitzpatrick et al. 2004; Neumann 2008)

### 1.4.1 Laplace Domain Solutions

Another popular approach to solve the diffusion equation for various scenarios is the application of the Laplace transform to an objective function (Hadgraft 1979, 1980; Guy and Hadgraft 1982). Generically, for a concentration function  $C(x, t)$ , the Laplace transform  $L$  is defined as

$$\hat{C}(x, s) = L(C(x, t)) = \int_0^{\infty} C(x, t) \exp(-st) dt \quad (1.41)$$

The huge advantage of solving partial differential equations (PDE) with the help of Laplace transforms is the reduction of a PDE to an ordinary differential equation (ODE) which can be solved much more easily. In comparison to analytical solutions in the time domain, Laplace solutions of the diffusion equation typically lack infinite sums and can be expressed for various exposure conditions with relatively simple adaptations. A drawback is the need of (numerical) inversion to the time domain, but most mathematical or

scientific software packages are capable of performing this task easily and in a convenient manner. Some important parameters, such as steady-state flux and lag time can even be extracted from the Laplace solution without inversion (Anissimov and Roberts 1999).

Solutions for special cases of variable partition and/or diffusion coefficients inside the stratum corneum are available in the Laplace space (Anissimov and Roberts 2004). Finite dosing and finite receptor and variable receptor clearance for the infinite dose scenario could be successfully modeled by Anissimov and Roberts (1999, 2001). Frasch fruitfully applied a Laplace domain solution from Anissimov and Roberts to simulate the permeation of theophylline through the stratum corneum incorporating slow binding phenomena (Anissimov and Roberts 2009; Frasch et al. 2011). Even the effect of desquamation could be investigated, and Simon et al. delivered Laplace domain solutions for different epidermal turnover rates (Simon and Goyal 2009).

For further reading, Anissimov et al. compiled a large amount of Laplace domain solutions of the diffusion equation for different scenarios in reference (Anissimov et al. 2013).

### 1.4.2 Numerical Diffusion Models

Numerical methods for solving the diffusion equation for various initial and boundary conditions are important techniques and allow a more flexible construction of advanced skin models (e.g., incorporation of binding effects (George 2005)), iontophoretic transdermal delivery (Wearley et al. 1990), repeated applications (Kubota et al. 2002), controlled release vehicles (Kurnik and Potts (1997), and in vitro lateral transport (Selzer et al. 2013a, b)). In comparison with classical PK skin compartment models, it is typically much more convenient to relate the necessary input parameters (for the simple diffusion problem, only diffusivities and partition coefficients are needed) to physicochemical parameters of the diffusant (Hansen et al. 2013). These models can be used for descriptive and predictive tasks as well as for the theoretical investigation of

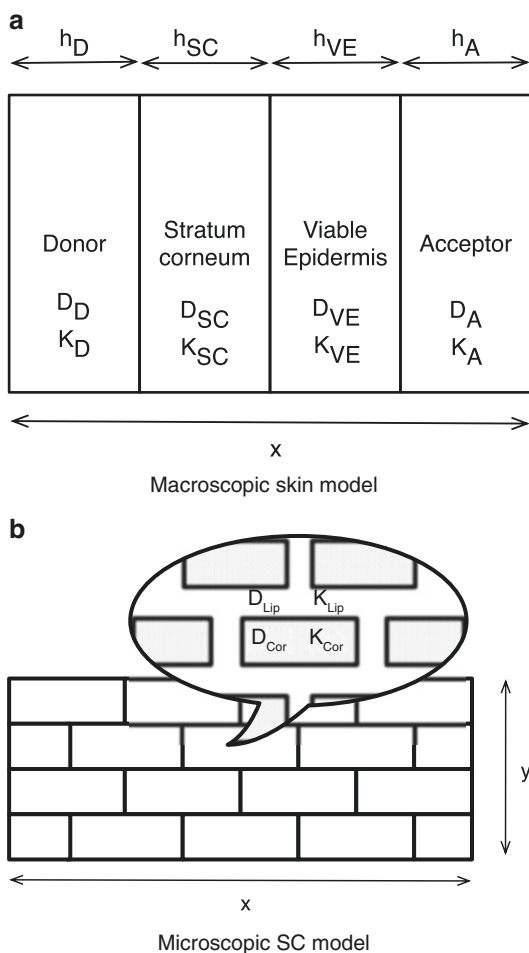


**Fig. 1.7** Simplified depiction of a macroscopic diffusion model with effective diffusivities and partition coefficients (a), and a microscopic representation of the brick-and-mortar structure (Elias 1983) of the stratum corneum (SC) with diffusivities and partition parameters for the lipid and the corneocyte phase (b). Figures are not drawn to scale

the interplay among input parameters. The basic idea consists of the discretization of time and space domain (gridding) and a numerical approximation of the partial differential diffusion equation (e.g., for the most trivial form, see Eq. 1.2). The discretization allows the construction of coarse-grained macroscopic and fine-grained microscopic models (a basic example is depicted in Fig. 1.7).

Macroscopic models do neglect the heterogeneity of different skin layers and use effective kinetic parameters of a diffusant for each layer to

describe the transport process. Usually, these kinds of models are only needed for solving the underlying diffusion equation for the one-dimensional case and hence treat the skin as a series of multilayered slabs (Fig. 1.7a).

Microscopic models allow a heterogeneous representation of the stratum corneum (Hansen et al. 2009) (lipid phase and protein phase, see Fig. 1.7b) and hence yield a more in-depth analysis of the underlying transport processes. In this case, the absorption kinetics do not only rely on the definition of diffusion parameters but also on the definition of spatial geometry. Due to the high spatial resolution, these models typically require much higher computational costs in comparison to coarse-grained macroscopic models. By mathematical homogenization, it is possible to reduce a microscopic model to a macroscopic one with preservation of model properties (e.g., anisotropic diffusivity in the stratum corneum) (Muha et al. 2010; Selzer et al. 2013b).

From a numerical perspective, several techniques exist to approximate the solution of the diffusion equation. For the one-dimensional case, probably the most prominent method is the finite differences approach. Assuming a constant diffusivity, Eq. 1.2 can be approximated by

$$\frac{C_i^{t+1} - C_i^t}{\Delta t} = D \frac{C_{i-1}^t - 2C_i^t + C_{i+1}^t}{(\Delta x)^2} \quad (1.42)$$

The left-hand side of equation is approximated by first-order forward differences and the right-hand side by second-order central differences that both arise from Taylor series expansions. As for every numerical method, the time and space domain is discretized. In this case,  $C_i^t$  denotes the concentration at point  $i \times \Delta x$  for time  $t \times \Delta t$ ,

with a system of constant space step size  $\Delta x$  and time step size  $\Delta t$ . Obviously, the above-mentioned equation can be easily generalized to problems in 2D and 3D space. Reformulation of Eq. 1.42 yields

$$C_i^{t+1} = MC_{i-1}^t + (1-2M)C_i^t + MC_{i+1}^t \quad (1.43)$$

with

$$M = D \frac{\Delta t}{(\Delta x)^2} \quad (1.44)$$

Because of the fact that every point of a certain layer only depends on points from the past, there is no functional relationship between different points of one time layer (it is a so-called *uncoupled problem*). This leads to the problem of numerical instabilities that depend on the value of  $M$  (Eq. 1.44) and hence on the choice of  $\Delta t$  for a given spatial resolution  $\Delta x$ . It can be shown that this explicit method is only stable for values of  $M \leq 0.5$  (for the one-dimensional case). A violation of this recommendation can produce noise which may result (empirically, it always does for the diffusion equation) in nonsmoothable rounding errors. For small diffusion coefficients (e.g., in the stratum corneum), this restriction can lead to extremely small time steps and therefore to high computational runtimes.

An elegant way to overcome this problem is by the use of implicit methods that rely not only on data from the last time point. Undoubtedly, the most widely used approach is the so-called Crank-Nicolson method (Crank 1975) (Eq. 1.45) that is unconditionally stable and provides a better overall error than the explicit approach:

$$\frac{C_i^{t+1} - C_i^t}{\Delta t} = \frac{D}{2} \left( \frac{C_{i-1}^{t+1} - 2C_i^{t+1} + C_{i+1}^{t+1}}{(\Delta x)^2} + \frac{C_{i-1}^t - 2C_i^t + C_{i+1}^t}{(\Delta x)^2} \right) \quad (1.45)$$

This equation yields a system of linear equations (tridiagonal matrix) that can be efficiently solved by, for example, the Thomas algorithm (an optimized form of Gaussian elimination that

can solve tridiagonal systems of equations). Using this implicit method, it is possible to choose larger time steps, which decrease the number of computational steps in spite of the



fact that the solving of the system of linear equations is computationally more complex compared to the explicit method. Various works on modeling transdermal transport that are based on finite differences exist (Kurnik and Potts 1997; Kubota et al. 2002; George 2005; Nitsche and Frasch 2011).

Finite differences are not the only mesh-based technique to find approximate solutions to partial differential equations, as the diffusion equations. The method of finite elements that is widely used in the field of mechanical engineering and finite volume approaches that can efficiently handle unstructured grids and is often applied in the field of computational fluid dynamics are known to successfully model transdermal transport (Barbero and Frasch 2005; Heisig et al. 1996; Naegel et al. 2008, 2011; Selzer et al. 2013b). For excellent overviews about numerical models, the interested reader is kindly referred to references (Frasch and Barbero 2013; Naegel et al. 2013).

---

## 1.5 In Vitro–In Vivo Correlation (IVIVC)

In vitro–in vivo correlations (IVIVC) address the question of the significance of in vitro data for predicting the situation in the living being. In vitro data are often compared to in vivo data from studies obtained under different experimental circumstances, and exact information on relevant experimental conditions is frequently lacking (ECETOC 1993). Factors which are known to influence transdermal absorption include among others the exposure conditions (such as dose, vehicle, humidity, temperature, and exposure duration), the skin type, and anatomical site of application (for more information, the interested reader is referred to Chapter 10 in this book). Therefore, only data which were obtained using harmonized protocols should be compared. The type of data obtained in in vitro and in vivo studies is usually quite different mostly due to experimental, physiological, and ethical constraints. Several different endpoints can be used to relate in vitro to in vivo skin absorption data. This paragraph should give an overview on which kind of

data can be used for the purpose of establishing IVIVC.

The topic of IVIVC is especially relevant for estimating bioavailability (BA) and for bioequivalence (BE) testing of topically applied dosage forms. For systemically acting drugs, BE is generally demonstrated based on a pharmacokinetic study comparing the plasma levels of test and reference product, following the idea that the pharmacokinetics are correlated to the pharmacological effect. Similarly, it is possible for transdermal patches which act systemically to demonstrate BE based on plasma levels or excretion data. In particular, a transdermal patch provides an infinite source and controls the invasion rate into the blood similar to an i.v. infusion. Consequently, in this case, the transdermal absorption rates which are measured in vitro can be correlated with the plasma concentrations (Chien et al. 1989; Franz et al. 2009).

Finite dosing is of course more relevant to the real exposure to chemicals or actives, and consequently also for demonstrating IVIVC (Bronaugh and Maibach 1985). At the same time, accurately detecting the low systemically absorbed and excreted amounts of solutes which are applied to the skin as a finite dose requires sensitive and selective analysis in complex biological media (blood, urine). Data which were obtained during the 1960s–1980s therefore often report radioactivity labeling as a technique to obtain pharmacokinetic data, for example, from excretion to the urine in human volunteers (Feldmann and Maibach 1969; Bartek et al. 1972; Feldmann and Maibach 1974; Wester and Maibach 1976). Indeed, if skin penetration is the rate-limiting step, the rate at which the compound appears in the urine will represent the rate at which it penetrates the skin. For solutes which are also fecally excreted, a correction for the proportion of urinary to fecal excretion is required. Results are calculated as percent of the applied doses which are excreted over time and corrected for application area and incomplete urinary excretion; division by time gives the absorption rate (Feldmann and Maibach 1969, 1974).

Likewise, if one assumes that the steady-state flux through skin in vitro ( $J_{ss}$  [ $\mu$  g/cm<sup>2</sup>/h]) is

equivalent to the rate of input to the systemic circulation in vivo, then in vitro percutaneous absorption data can be used, for example, during formulation development for formulation optimization based on known clinical data:

$$J_{ss} \times A = C_{ss} \times Cl \quad (1.46)$$

Here,  $A$  [ $\text{cm}^2$ ]=area of skin,  $C_{ss}$  [ $\mu\text{g/l}$ ]=steady-state blood concentration, and  $Cl$  [ $\text{l/h}$ ]=systemic clearance. With  $C_{ss}$  and  $Cl$  being known, for example, from i.v. application, a target flux can be calculated which needs to be achieved with a developed dosage form to obtain plasma levels accordingly (Franz et al. 2009).

Cnubben et al. further used linear systems dynamics (Opdam 1991; Vaughan and Dennis 1978; Fisher et al. 1985) to calculate an in vivo percutaneous absorption rate ( $\mu\text{g cm}^{-2}\text{h}^{-1}$ ) based on the plasma concentration–time profile of solutes after dermal application and after a reference i.v. administration (Cnubben et al. 2002). From this, they derived in vivo permeability coefficients and lag times and compared these to values obtained in vitro.

Difficulties arise for topically (i.e., on or in the skin) or regionally (i.e., in nearby tissues, such as the joints, muscle, or cartilage) acting drugs for which the plasma concentration is neither quantifiable nor relevant for their local activity. For those drugs, measuring the drug concentration at the site of action, or dermatopharmacokinetics (DPK), will be more relevant. Unfortunately, a draft guidance document recommending tape-stripping for demonstrating BE of topically acting drugs was withdrawn in 2002, due to issues arising from poorly defined experimental standardization. Currently, tape-stripping is only recommended by the FDA for BE testing for certain classes of drugs, such as for antifungals that target the stratum corneum itself (Narkar 2010). This results in the unfortunate situation that the in vivo skin blanching or vasoconstriction assay (only for corticosteroids) is currently the only FDA-recommended assay for demonstrating BE of generics which does not rely on clinical studies (with known problems such as poor sensitivity, requirement for high number of test persons, and consequently high costs). Franz et al. have

collected substantial evidence that in vitro skin absorption testing may be used as a surrogate method for in vivo BA or BE testing (Franz et al. 2009). In particular, two types of measurements are being discussed for this purpose. First, these are the already mentioned tape-stripping DPK measurements which can be performed in vivo as well as in vitro (for more details, the interested reader is referred to references (Herkenne et al. 2008; Russell and Guy 2009)). Second, these are also permeability measurements which are performed in vitro.

In fact, Franz et al. reported that the in vitro method was able to discriminate between different vehicles, a finding which was also supported by differences in clinical efficacy, while this difference was not picked up by the vasoconstriction assay (Franz et al. 2009). Importantly, Franz et al. as well as others demonstrated excellent IVIVC, provided that the study protocols between in vitro and in vivo studies were harmonized (Franz et al. 2009; Lehman et al. 2011). The latter aspect is certainly very important to ensure comparability between in vitro and in vivo results. Treffel and Gabard as well as Chatelain et al., later in a follow-up study, noticed that differences between several sun protection products which were obvious in tape-stripping experiments as well as sun protection factor (SPF) measurements in human volunteers as early as 30 min after application could in vitro not be detected until later time points, that is, 6 h (Treffel and Gabard 1996; Chatelain et al. 2003). In vivo and in vitro protocols differed in terms of the applied dose ( $2\text{ mg/cm}^2$  vs.  $3\text{ mg/cm}^2$ ). The differences may be also explained by artifacts from nonphysiological swelling of the skin inside the Franz diffusion cell obscuring early effects.

Comparing the skin penetration of the nonsteroidal anti-inflammatory drug flufenamic acid in vitro and in vivo by tape-stripping, Wagner et al. observed that the in vivo levels were consistently lower than the in vitro levels which they found inside the stratum corneum after different incubation times (Wagner et al. 2000). The reasons for these differences can be manifold, such as interindividual differences, regional variances, different pressures applied during tape-stripping

to name but a few. Nonetheless, correlating the amounts found after different incubation times, they demonstrated an excellent IVIVC (Wagner et al. 2000). To exclude interindividual differences in a follow-up study, Wagner et al. designed a special workflow, where they used abdominal skin from the same exact individual before and after undergoing abdominal reduction surgery (Wagner et al. 2002). Unfortunately, the results obtained from tape-stripping were not usable due to the disinfectant wipe which was necessary for the surgery and which significantly changed the drug levels inside the upper skin layers. However, they could show excellent agreement of the drug levels inside the deeper skin layers (Wagner et al. 2002). This collection of reports shows that obtaining a good IVIVC is possible. However, the parameters which should be correlated need to be carefully selected, and the conditions under which these parameters are obtained are most critical.

---

## 1.6 Tips and Tricks

This section supplies information about common difficulties when computing analytical solutions of the diffusion equation and fitting these solutions to experimental data. It should work as a guide when conducting mathematical analysis of experimental data.

### 1.6.1 Infinite Sums in Analytical Solutions

Many analytical solutions presented in this chapter include an infinite sum of form

$$F(x) = a \sum_i^{\infty} H_i(x) + b, \quad (1.47)$$

with  $H_i(x)$  going to zero for  $i$  going to infinity. These are typical examples of solutions of the diffusion equation for various scenarios. Being able to deal with this kind of equations is a key requirement for a sound evaluation of skin transport experiments. Hence, we will give a few hints for the solid handling.

From a practical point of view, the infinite sum has to be truncated at some point. Some researchers only use <10 summations, for example, for the infinite dose solution presented in Sect. 1.3.1, since the subsequent terms do not significantly contribute to the overall result (Frasch and Barbero 2008). To achieve maximal accuracy, a more precise way to truncate the sum is to incorporate a relative threshold, like the so-called machine epsilon of the computer – a relative error due to rounding in floating point arithmetic (Hansen et al. 2008). The machine epsilon  $\varepsilon_0$  is defined as the smallest number, such that  $1 + \varepsilon_0 > 1$  holds for a certain machine.

Nowadays, implementing more complex functions and fitting to experimental data can be achieved easily using commercial or free data analysis and statistical software packages or free scripting languages. For example, the authors used the popular scripting language *Python*<sup>2</sup> in combination with the *SciPy* package (scientific python) (Jones et al. 2001) to compute various equations presented for the finite dose case. These kinds of packages provide predefined functionalities for root-finding, fitting, and plotting.

### 1.6.2 Fitting of Experimental Data

As reported here, fitting of experimental data to analytical solutions of the diffusion equation is an excellent way of analysis. To gain confidence, experiments are typically conducted in a recurrent manner. For data evaluation, researchers can fit the objective function to either each individual dataset (of every single experiment) or a combination of experimental data (e.g., mean accumulated mass over time).

It is strongly recommended to report the evaluation of single experiments (OECD 2004b), and the authors support the approach of individual evaluation of experiments and averaging of individual determined parameters. Despite this fact, many researchers prefer to handle arithmetic means of combined experiments (Schäfer-

---

<sup>2</sup>Python: <http://www.python.org>

Korting et al. 2008). Fitting is typically done by applying a linear or nonlinear least-squares approach. The basic idea is to minimize the sum of squared residual errors (e.g., minimization of the so-called weighted root mean square function displayed in Eq. 1.48):

$$\text{RMS} = \sqrt{\frac{1}{n} \sum_{i=1}^n w_i (d_i^{\text{exp}} - d_i^{\text{calc}})^2} \quad (1.48)$$

Here,  $n$  is the number of data points,  $d_i^{\text{exp}}$  is the  $i$ th data point,  $d_i^{\text{calc}}$  is the quantity that is being modeled (e.g., concentration in the membrane at time  $t$  and point  $x$  or cumulative amount of substance in the acceptor compartment), and  $w_i$  are optional weights for every  $d_i$  pair. These weights are capable of emphasizing or de-emphasizing certain data points. If no weighting is applied,  $w_i$  is 1 for every  $i$ .

To emphasize experimental uncertainties, a typical choice of weights is  $w_i = \frac{1}{\sigma^2}$  (Henning et al. 2009). This requires knowledge about the kind of underlying error or variation. Using the standard deviation is not the only option to weight data. Krüse et al. suggested a weighting scheme with  $w_i = \frac{1}{|t_i|}$  to de-emphasize later time points (Krüse et al. 2007). This can be helpful for example, for fitting accumulated mass versus time data for the infinite dose case, since it is well known that the standard errors of later time points are additive in nature (Selzer et al. 2013a).

Fitting finite dose permeation data can be prone to variabilities in the unknowns (especially the partition coefficient). A stabilization can be achieved by either fixing an unknown to a constant value and/or fit data from several doses at once (Kasting 2001).

## Conclusion

We hold powerful mathematical tools in our hands which allow us to interpret experimental data, predict relevant endpoints, and improve our understanding of skin absorption. They find their applications in various fields, including toxicology, drug delivery, or regulatory affairs. Key to the useful application of

such mathematical tools is a fundamental understanding of the underlying physical and biological mechanistic but also of experimental and model constraints. These were highlighted in this chapter.

## References

- Agatonovic-Kustrin S, Beresford R, Yusuf APM (2001) ANN modeling of the penetration across a polydimethylsiloxane membrane from theoretically derived molecular descriptors. *J Pharm Biomed Anal* 26(2): 241–254
- Anderson BD, Raykar PV (1989) Solute structure–permeability relationships in human stratum corneum. *J Invest Dermatol* 93(2):280–286
- Anderson BD, Higuchi WI, Raykar PV (1988) Heterogeneity effects on permeability–partition coefficient relationships in human stratum corneum. *Pharm Res* 5(9):566–573
- Anissimov YG, Roberts MS (1999) Diffusion modeling of percutaneous absorption kinetics. 1. Effects of flow rate, receptor sampling rate, and viable epidermal resistance for a constant donor concentration. *J Pharm Sci* 88(11):1201–1209
- Anissimov YG, Roberts MS (2001) Diffusion modeling of percutaneous absorption kinetics: 2. Finite vehicle volume and solvent deposited solids. *J Pharm Sci* 90(4):504–520
- Anissimov YG, Roberts MS (2004) Diffusion modeling of percutaneous absorption kinetics: 3. Variable diffusion and partition coefficients, consequences for stratum corneum depth profiles and desorption kinetics. *J Pharm Sci* 93(2):470–487
- Anissimov YG, Roberts MS (2009) Diffusion modelling of percutaneous absorption kinetics: 4. Effects of a slow equilibration process within stratum corneum on absorption and desorption kinetics. *J Pharm Sci* 98(2):772–781
- Anissimov YG, Jepps OG, Dancik Y, Roberts MS (2013) Mathematical and pharmacokinetic modelling of epidermal and dermal transport processes. *Adv Drug Deliv Rev* 65(2):169–190
- Barbero AM, Frasch F (2009) Pig and guinea pig skin as surrogates for human in vitro penetration studies: a quantitative review. *Toxicol In Vitro* 23(1):1–13
- Barbero AM, Frasch HF (2005) Modeling of diffusion with partitioning in stratum corneum using a finite element model. *Ann Biomed Eng* 33(9):1281–1292
- Bartek MJ, LaBudde JA, Maibach HI (1972) Skin permeability in vivo: comparison in rat, rabbit, pig and man. *J Invest Dermatol* 58(3):114–123
- Brain KR, Walters KA, Watkinson AC (2002) Methods for studying percutaneous absorption. In: Walters KA (ed) *Dermatological and transdermal formulations*. Marcel Dekker AG, New York, pp 197–270

- Brent RP (1973) Algorithms for minimization without derivatives. Prentice-Hall, Englewood Cliffs, chap 3–4
- Bronaugh RL, Maibach HI (1985) Percutaneous absorption of nitroaromatic compounds: in vivo and in vitro studies in the human and monkey. *J Invest Dermatol* 84(3):180–183
- Bronaugh RL, Stewart RF (1985) Methods for in vitro percutaneous absorption studies. iv: the flow-through diffusion cell. *J Pharm Sci* 74(1):64–67
- Buist HE, van Burgsteden JA, Freidig AP, Maas WJM, van de Sandt JJM (2010) New in vitro dermal absorption database and the prediction of dermal absorption under finite conditions for risk assessment purposes. *Regul Toxicol Pharmacol* 57(2–3):200–209
- Carlsaw H, Jaeger J (1959) Conduction of heat in solids. Clarendon, Oxford, chap 128
- Chatelain E, Gabard B, Surber C (2003) Skin penetration and sun protection factor of five uv filters: effect of the vehicle. *Skin Pharmacol Appl Skin Physiol* 16:28–35
- Chen LJ, Lian GP, Han LJ (2007) Prediction of human skin permeability using artificial neural network (ANN) modeling. *Acta Pharmacol Sin* 28(4):591–600
- Chien YW, Chien TY, Bagdon RE, Huang YC, Bierman RH (1989) Transdermal dual-controlled delivery of contraceptive drugs: formulation development, in vitro and in vivo evaluations, and clinical performance. *Pharm Res* 6:1000–1010
- Cnubben NH, Elliott GR, Hakkert BC, Meuling WJ, van de Sandt JJ (2002) Comparative in vitro-in vivo percutaneous penetration of the fungicide ortho-phenylphenol. *Regul Toxicol Pharmacol* 35(2):198–208
- Cooper ER, Berner B (1985) Finite dose pharmacokinetics of skin penetration. *J Pharm Sci* 74(10):1100–1102
- Crank J (1975) The mathematics of diffusion, 2nd edn. Oxford University Press, London
- Dancik Y, Anissimov YG, Jepps OG (2012) Convective transport of highly plasma protein bound drugs facilitates direct penetration into deep tissues after topical application. *Br J Clin Pharmacol* 73(4):564–578
- Davies M, Pendlington RU, Page L, Roper CS, Sanders DJ, Bourner C, Pease CK, MacKay C (2011) Determining epidermal disposition kinetics for use in an integrated nonanimal approach to skin sensitization risk assessment. *Toxicol Sci* 119(2):308–318
- Díez-Sales O, Copoví A, Casabó VG, Herráez H (1991) A modelistic approach showing the importance of the stagnant aqueous layers in in vitro diffusion studies, and in vitro-in vivo correlations. *Int J Pharm* 77(1):1–11
- ECETOC (1993) Monograph 20, percutaneous absorption. European Centre for Ecotoxicology and Toxicology of Chemicals, Brussels
- Elias PM (1983) Epidermal lipids, barrier function, and desquamation. *J Invest Dermatol* 80(Suppl):44s–49s
- Escobar-Chavez JJ, Merino-Sanjuán V, López-Cervantes M, Urban-Morlan Z, Piñón Segundo E, Quintanar-Guerrero D, Ganem-Quintanar A (2008) The tape-stripping technique as a method for drug quantification in skin. *J Pharm Pharm Sci* 11(1):104–130
- Feldmann RJ, Maibach HI (1969) Percutaneous penetration of steroids in man. *J Invest Dermatol* 52(1):89–94
- Feldmann RJ, Maibach HI (1974) Percutaneous penetration of some pesticides and herbicides in man. *Toxicol Appl Pharmacol* 28(1):126–132
- Fiserova-Bergerova V, Pierce JT, Droz PO (1990) Dermal absorption potential of industrial chemicals: criteria for skin notation. *Am J Ind Med* 17(5):617–635
- Fisher HL, Most B, Hall LL (1985) Dermal absorption of pesticides calculated by deconvolution. *J Appl Toxicol* 5(3):163–177
- Fitzpatrick D, Corish J, Hayes B (2004) Modelling skin permeability in risk assessment – the future. *Chemosphere* 55(10):1309–1314
- Franz TJ, Lehman PA, Raney SG (2009) Use of excised human skin to assess the bioequivalence of topical products. *Skin Pharmacol Physiol* 22(5):276–286
- Franz TJ (1975) Percutaneous absorption. On the relevance of in vitro data. *J Invest Dermatol* 64(3):190–195
- Frasch F, Barbero AM (2013) Application of numerical methods for diffusion-based modeling of skin permeation. *Adv Drug Deliv Rev* 65(2):208–220
- Frasch HF, Barbero AM (2008) The transient dermal exposure: theory and experimental examples using skin and silicone membranes. *J Pharm Sci* 97(4):1578–1592
- Frasch HF, Barbero AM, Hettick JM, Nitsche JM (2011) Tissue binding affects the kinetics of theophylline diffusion through the stratum corneum barrier layer of skin. *J Pharm Sci* 100(7):2989–2995
- George K (2005) A two-dimensional mathematical model of non-linear dual-sorption of percutaneous drug absorption. *Biomed Eng Online* 4:40
- Guy RH, Hadgraft J (1982) Percutaneous metabolism with saturable enzyme kinetics. *Int J Pharm* 11(3):187–197
- Guy RH, Hadgraft J (1985) Transdermal drug delivery: a simplified pharmacokinetic approach. *Int J Pharm* 24(2–3):267–274
- Guy RH, Hadgraft J, Bucks DAW (1987) Transdermal drug delivery and cutaneous metabolism. *Xenobiotica* 17(3):325–343
- Guy R, Hadgraft J, Maibach H (1982) A pharmacokinetic model for percutaneous absorption. *Int J Pharm* 11(2):119–129
- Hadgraft J (1979) The epidermal reservoir; a theoretical approach. *Int J Pharm* 2(5–6):265–274
- Hadgraft J (1980) Theoretical aspects of metabolism in the epidermis. *Int J Pharm* 4(3):229–239
- Hahn T, Selzer D, Neumann D, Kostka KH, Lehr CM, Schaefer UF (2012) Influence of the application area on finite dose permeation in relation to drug type applied. *Exp Dermatol* 21(3):233–235
- Hansen S, Henning A, Naegel A, Heisig M, Wittum G, Neumann D, Kostka KH, Zbytovska J, Lehr CM, Schaefer UF (2008) In-silico model of skin penetration based on experimentally determined input parameters. Part i: experimental determination of partition and diffusion coefficients. *Eur J Pharm Biopharm* 68(2):352–367
- Hansen S, Naegel A, Heisig M, Wittum G, Neumann D, Kostka KH, Meiers P, Lehr CM, Schaefer U (2009)

- The role of corneocytes in skin transport revised – a combined computational and experimental approach. *Pharm Res* 26:1379–1397
- Hansen S, Lehr CM, Schaefer UF (2013) Improved input parameters for diffusion models of skin absorption. *Adv Drug Deliv Rev* 65(2):251–264
- Heisig M, Lieckfeldt R, Wittum G, Mazurkevich G, Lee G (1996) Non steady-state descriptions of drug permeation through stratum corneum. i. The biphasic brick-and-mortar model. *Pharm Res* 13(3):421–426
- Henning A, Schaefer UF, Neumann D (2009) Potential pitfalls in skin permeation experiments: influence of experimental factors and subsequent data evaluation. *Eur J Pharm Biopharm* 72(2):324–331
- Herkenne C, Naik A, Kalia YN, Hadgraft J, Guy RH (2006) Ibuprofen transport into and through skin from topical formulations: in vitro–in vivo comparison. *J Invest Dermatol* 127(1):135–142
- Herkenne C, Naik A, Kalia YN, Hadgraft J, Guy RH (2007) Dermatopharmacokinetic prediction of topical drug bioavailability in vivo. *J Invest Dermatol* 127(4):887–894
- Herkenne C, Alberti I, Naik A, Kalia YN, Mathy FX, Pr at V, Guy RH (2008) In vivo methods for the assessment of topical drug bioavailability. *Pharm Res* 25(1):87–103
- Jones E, Oliphant T, Peterson P (2001) Scipy: open source scientific tools for python
- Kasting GB (2001) Kinetics of finite dose absorption through skin 1. Vanillylnonanamide. *J Pharm Sci* 90(2):202–212
- Kr use J, Golden D, Wilkinson S, Williams F, Kezic S, Corish J (2007) Analysis, interpretation, and extrapolation of dermal permeation data using diffusion-based mathematical models. *J Pharm Sci* 96(3):682–703
- Kubota K, Koyama E, Twizell EH (1993) Dual sorption model for the nonlinear percutaneous kinetics of timolol. *J Pharm Sci* 82(12):1205–1208
- Kubota K, Dey F, Matar SA, Twizell EH (2002) A repeated-dose model of percutaneous drug absorption. *Appl Math Model* 26(4):529–544
- Kubota K (1991) A compartment model for percutaneous drug absorption. *J Pharm Sci* 80(5):502–504
- Kurnik RT, Potts RO (1997) Modeling of diffusion and crystal dissolution in controlled release systems. *J Control Release* 45(3):257–264
- Lademann J, Jacobi U, Surber C, Weigmann HJ, Fluhr JW (2009) The tape stripping procedure – evaluation of some critical parameters. *Eur J Pharm Biopharm* 72(2):317–323
- Lehman PA, Raney SG, Franz TJ (2011) Percutaneous absorption in man: in vitro-in vivo correlation. *Skin Pharmacol Physiol* 24(4):224–230
- Magnusson BM, Anissimov YG, Cross SE, Roberts MS (2004) Molecular size as the main determinant of solute maximum flux across the skin. *J Invest Dermatol* 122(4):993–999
- McCarley KD, Bunge AL (2001) Pharmacokinetic models of dermal absorption. *J Pharm Sci* 90(11):1699–1719
- McCarley K, Bunge A (2000) Physiologically relevant two-compartment pharmacokinetic models for skin. *J Pharm Sci* 89(9):1212–1235
- McKone TE, Howd RA (1992) Estimating dermal uptake of nonionic organic chemicals from water and soil: I. Unified fugacity-based models for risk assessments. *Risk Anal* 12(4):543–557
- Melero A, Hahn T, Schaefer U, Schneider M (2011) In vitro human skin segmentation and drug concentration-skin depth profiles. In: Turksen K (ed) *Permeability barrier, methods in molecular biology*, vol 763. Humana Press, New York City, USA, pp 33–50
- Michaels AS, Chandrasekaran SK, Shaw JE (1975) Drug permeation through human skin: theory and invitro experimental measurement. *AIChE J* 21(5):985–996
- Muha I, Naegel A, Stichel S, Grillo A, Heisig M, Wittum G (2010) Effective diffusivity in membranes with tetra-kaidekahedral cells and implications for the permeability of human stratum corneum. *J Membr Sci* 368(1–2):18–25
- Naegel A, Hansen S, Neumann D, Lehr CM, Schaefer UF, Wittum G, Heisig M (2008) In-silico model of skin penetration based on experimentally determined input parameters. Part ii: mathematical modelling of in-vitro diffusion experiments. Identification of critical input parameters. *Eur J Pharm Biopharm* 68(2):368–379
- Naegel A, Hahn T, Schaefer U, Lehr CM, Heisig M, Wittum G (2011) Finite dose skin penetration: a comparison of concentration–depth profiles from experiment and simulation. *Comput Vis Sci* 14(7):327–339
- Naegel A, Heisig M, Wittum G (2013) Detailed modeling of skin penetration – an overview. *Adv Drug Deliv Rev* 65(2):191–207
- Narkar Y (2010) Bioequivalence for topical products – an update. *Pharm Res* 27:2590–2601
- Neumann D, Kohlbacher O, Merkwirth C, Lengauer T (2005) A fully computational model for predicting percutaneous drug absorption. *J Chem Inf Model* 46(1):424–429
- Neumann D (2008) Modeling transdermal absorption. In: Ehrhardt C, Kim KJ (eds) *Drug absorption studies, biotechnology: pharmaceutical aspects*, vol VII. Springer, US, chap 20, pp 459–485
- Nitsche JM, Frasch HF (2011) Dynamics of diffusion with reversible binding in microscopically heterogeneous membranes: general theory and applications to dermal penetration. *Chem Eng Sci* 66(10):2019–2041
- OECD (2004a) Guidance document for the conduct of skin absorption studies. OECD Series on Testing and Assessment 28
- OECD (2004b) Test guideline 428: skin absorption: in vitro method
- Opdam JGG (1991) Linear systems dynamics in toxicokinetic studies. *Ann Occup Hyg* 35(6):633–649
- Patel H, Berge W, Cronin MTD (2002) Quantitative structure-activity relationships (QSARs) for the prediction of skin permeation of exogenous chemicals. *Chemosphere* 48(6):603–613
- Potts RO, Guy RH (1992) Predicting skin permeability. *Pharm Res* 9(5):663–669

- Reddy MB, Guy RH, Bunge AL (2000a) Does epidermal turnover reduce percutaneous penetration? *Pharm Res* 17(11):1414–1419
- Reddy M, McCarley K, Bunge A (2000b) Physiologically relevant one-compartment pharmacokinetic models for skin. 2. Comparison of models when combined with a systemic pharmacokinetic model. *J Pharm Sci* 87(4):482–490
- Russell L, Guy R (2009) Measurement and prediction of the rate and extent of drug delivery into and through the skin. *Expert Opin Drug Deliv* 6(4):355–369
- van de Sandt JJM, van Burgsteden JA, Cage S, Carmichael PL, Dick I, Kenyon S, Korinth G, Laresse F, Limasset JC, Maas WJM, Montomoli L, Nielsen JB, Payan JP, Robinson E, Sartorelli P, Schaller KH, Wilkinson SC, Williams FM (2004) In vitro predictions of skin absorption of caffeine, testosterone, and benzoic acid: a multi-centre comparison study. *Regul Toxicol Pharmacol* 39(3):271–281
- Schäfer-Korting M, Bock U, Diembeck W, Düsing HJ, Gamer A, Haltner-Ukomadu E, Hoffmann C, Kaca M, Kamp H, Kersen S, Kietzmann M, Korting HC, Krächter HU, Lehr CM, Liebsch M, Mehling A, Müller-Goymann C, Netzlaff F, Niedorf F, Rübhelke MK, Schaefer U, Schmidt E, Schreiber S, Spielmann H, Vuia A, Weimer M (2008) The use of reconstructed human epidermis for skin absorption testing: results of the validation study. *ATLA Altern Lab Anim* 36(2):161–187
- Scheuplein RJ, Ross LW (1974) Mechanism of percutaneous absorption. v. Percutaneous absorption of solvent deposited solids. *J Invest Dermatol* 62(4):353–360
- Scheuplein RJ (1967) Mechanism of percutaneous absorption. ii. Transient diffusion and the relative importance of various routes of skin penetration. *J Invest Dermatol* 48(1):79–88
- Selzer D, Abdel-Mottaleb M, Hahn T, Schaefer UF, Neumann D (2013a) Finite and infinite dosing: difficulties in measurements, evaluations and predictions. *Adv Drug Deliv Rev* 65(2):278–294
- Selzer D, Hahn T, Naegel A, Heisig M, Kostka KH, Lehr CM, Neumann D, Schaefer UF, Wittum G (2013b) Finite dose skin mass balance including the lateral part: comparison between experiment, pharmacokinetic modeling and diffusion models. *J Control Release* 165(2):119–128
- Seta Y, Ghanem AH, Higuchi WI, Borsadia S, Behl CR, Malick AW (1992) Physical model approach to understanding finite dose transport and uptake of hydrocortisone in hairless guinea-pig skin. *Int J Pharm* 81(1):89–99
- Shah VP, Flynn GL, Yacobi A, Maibach HI, Bon C, Fleischer NM, Franz TJ, Kaplan SA, Kawamoto J, Lesko LJ, Marty JP, Pershing LK, Schaefer H, Sequeira JA, Shrivastava SP, Wilkin J, Williams RL (1998) AAPS/FDA Workshop report: bioequivalence of topical dermatological dosage forms: methods of evaluation of bioequivalence, vol 22. Advanstar Communications, Duluth
- Simon L, Goyal A (2009) Dynamics and control of percutaneous drug absorption in the presence of epidermal turnover. *J Pharm Sci* 98(1):187–204
- Sloan KB, Wasdo SC, Rautio J (2006) Design for optimized topical delivery: prodrugs and a paradigm change. *Pharm Res* 23(12):2729–2747
- Stinchcomb AL, Pirot F, Touraille GD, Bunge AL (1999) Chemical uptake into human stratum corneum in vivo from volatile and non-volatile solvents. *Pharm Res* 16(8):1288–1293
- Talreja PS, Kasting GB, Kleene NK, Pickens WL, Wang TF (2001) Visualization of the lipid barrier and measurement of lipid pathlength in human stratum corneum. *AAPS PharmSci* 3(2):48–56
- Treffel P, Gabard B (1996) Skin penetration and sun protection factor of ultra-violet filters from two vehicles. *Pharm Res* 13:770–774
- Vaughan DP, Dennis M (1978) Mathematical basis of point-area deconvolution method for determining in vivo input functions. *J Pharm Sci* 67(5):663–665
- Wagner H, Kostka KH, Lehr CM, Schaefer UF (2000) Drug distribution in human skin using two different in vitro test systems: comparison with in vivo data. *Pharm Res* 17(12):1475–1481
- Wagner H, Kostka KH, Lehr CM, Schaefer UF (2002) Human skin penetration of flufenamic acid: in vivo/in vitro correlation (deeper skin layers) for skin samples from the same subject. *J Invest Dermatol* 118(3):540–544
- Wallace SM, Barnett G (1978) Pharmacokinetic analysis of percutaneous absorption: evidence of parallel penetration pathways for methotrexate. *J Pharmacokin Biopharm* 6(4):315–325
- Wearley LL, Tojo K, Chien YW (1990) A numerical approach to study the effect of binding on the lonthoretic transport of a series of amino acids. *J Pharm Sci* 79(11):992–998
- Wester RC, Maibach HI (1976) Relationship of topical dose and percutaneous absorption in rhesus monkey and man. *J Invest Dermatol* 67(4):518–520
- Wilkinson SC, Maas WJM, Nielsen JB, Greaves LC, Sandt JJM, Williams FM (2006) Interactions of skin thickness and physicochemical properties of test compounds in percutaneous penetration studies. *Int Arch Occup Environ Health* 79(5):405–413
- Wilschut A, ten Berge WF, Robinson PJ, McKone TE (1995) Estimating skin permeation. The validation of five mathematical skin permeation models. *Chemosphere* 30(7):1275–1296
- Zhang Q, Li P, Roberts MS (2011) Maximum transepidermal flux for similar size phenolic compounds is enhanced by solvent uptake into the skin. *J Control Release* 154(1):50–57

---

# Occlusive Versus Nonocclusive Application in Transdermal Drug Delivery

Gamal M. El Maghraby

## Contents

2.1	Introduction.....	27
2.2	Permeability Barrier of Human Skin.....	28
2.3	Enhancing Effect of Occlusion on Transdermal Delivery.....	28
2.4	Delivery Systems Utilizing the Method of Application.....	29
2.4.1	Transfersomes™.....	29
2.4.2	Supersaturable Transdermal Delivery Systems.....	30
	Conclusion.....	32
	References.....	32

---

## 2.1 Introduction

Dermal and transdermal drug delivery can be achieved after occlusive or nonocclusive (open) application with the former being traditionally considered as the standard application technique. Occlusion can be achieved by covering the skin by impermeable films or others, such as tape, gloves, diapers, textiles garments, wound dressings, or transdermal therapeutic systems (Zhai and Maibach 2002). Occlusion can be obtained from the occlusive nature of the formulation itself. For example, oleaginous formulation will have strong occlusive nature (Berardesca and Maibach 1988). Occlusion can increase the water content of the skin. Taking into consideration the fact that water acts as skin penetration enhancer, occlusion can enhance percutaneous absorption of drugs (Barry 1987). However, occlusion cannot be taken as the only tool to enhance transdermal drug delivery. This is due to the complex nature of percutaneous drug absorption and its enhancement which depends on many factors including the nature of the drug and the transdermal drug delivery system. With respect to the nature of the drug, occlusion was shown to enhance the permeation of lipophilic drugs, with lower efficacy on polar drugs (Cross and Roberts 2000; Treffel et al. 1992). With regard to the nature of the delivery system, the efficacy of some systems such as Transfersomes was linked with open application (Cevc and Blume 1992). The following sections will provide a brief over-

---

G.M. El Maghraby  
Department of Pharmaceutical Technology, College  
of Pharmacy, University of Tanta,  
El-Geish Street, 31111 Tanta, Egypt  
e-mail: [gmmelmag@yahoo.com](mailto:gmmelmag@yahoo.com)



view on the occlusive versus nonocclusive application and how it can alter the transdermal drug delivery.

---

## 2.2 Permeability Barrier of Human Skin

The advancement in research methods resulted in clear and detailed identification of skin structure and its barrier function (Scheuplein and Blank 1971; Elias 1981; Orland 1983; Barry 1983). The studies were extended to cover the barrier function of the skin in the healthy and diseased state. This has been reviewed and documented (Bouwstra and Ponac 2006). It is now accepted that the stratum corneum (SC) is the main barrier for transdermal drug delivery. Two pathways of drug permeation have been identified as the transepidermal and the transappendageal pathways (Scheuplein 1965). The former is considered as the main route with the latter playing only minor role in transdermal drug delivery (Scheuplein 1967). In the transepidermal pathway, drugs pass through the intact SC. This major pathway contains two routes: the intercellular route, which is a continuous but tortuous way through the intercellular lipids, and the transcellular route through the keratinocytes and across the intercellular lipids. Passing through these routes, drugs will face many defense lines which hinder their progress into and through the skin. These lines of defense are shown in Fig. 2.1, which considered both the intercellular and the transcellular pathways (Barry 1987). The diagram represents the keratin in the cells which contains hydrogen-bonding sites that can sequester drugs providing the first difficulty in their penetration through the transcellular pathway. The second defense line is the closely packed hydrocarbon chains of the intercellular lipid lamellae. This line provides the main barrier in both the intercellular and transcellular routes. In addition to this, the SC contains minimum amount of water which is provided by the hydrophilic domains in the diagram (Fig. 2.1; Barry 1987).

The integrity of human skin is also linked to its water content which varies across skin strata

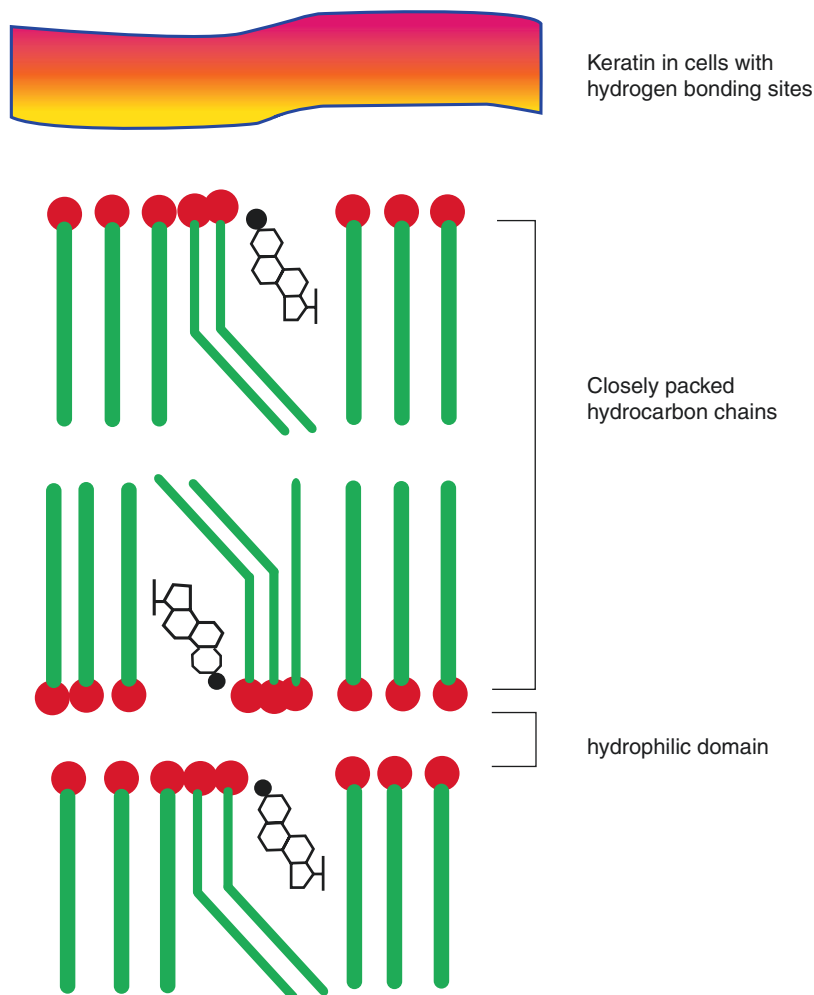
with the concentration of water increasing as we move from the skin surface to deep strata. At the SC, the water concentration is less than 15 %, but increases deeper into the skin where it reaches a five times higher value at the basal skin layers (Warner et al. 1988). This creates a transdermal hydration gradient which is characteristic for normal skin (Cevc and Blume 1992).

---

## 2.3 Enhancing Effect of Occlusion on Transdermal Delivery

Skin occlusion can inhibit the continuous water loss from skin surface. This can result in over-hydration of the SC with subsequent reduction in the barrier nature of the SC (Bucks et al. 1991). The penetration-enhancing effect of water can be explained on the basis that water forms hydration shells around the head groups of the SC lipids. This leads to the disruption of the closely packed hydrocarbon chains resulting in a loose organization of SC lipids. In addition, excess water can extend the hydrophilic domains of the lamellar structure of the SC lipids providing room for drug permeation (Barry 1987). However, occlusion does not increase percutaneous absorption of all types of drugs. For example, occlusion increased the permeation of ciprofloxacin (lipophilic compound) 1.6 times, but the transdermal flux of caffeine (amphiphilic compound) was the same under occlusive or open application (Treffel et al. 1992). In a more recent study, the effect of occlusion was shown to depend on the vehicle. In this study, the authors evaluated the penetration of a mixture of paraben ester preservatives from a commercially available test ointment and two commonly employed solvent vehicles (acetone and ethanol), together with the effect of occlusion on the rate of delivery of the preservatives from these systems. Occlusion was achieved by the placement of a piece of high-density polyethylene on the application site immediately after dosing. There was a significant difference in the epidermal flux of parabens provided by the different vehicles applied

**Fig. 2.1** Simplified diagram showing a model for the stratum corneum with various defense lines against penetration of xenobiotics (Modified from Barry 1987)



under occlusion. Whereas increased flux was observed from acetone and ethanol used as vehicles, a decreased flux was seen upon the occlusive application of the ointment formulation (Cross and Roberts 2000). These results can be explained on the basis that occlusion increased the contact time between the skin and the volatile solvents (ethanol and acetone) which possess the penetration-enhancing ability. In contrast, open application of these solvents will lead to their rapid evaporation and hence shorter contact time with the skin and lower penetration-enhancing effect. Open application of these solvents will thus provide a less damaging effect on the skin compared to the occlusive application of the same solvents.

## 2.4 Delivery Systems Utilizing the Method of Application

### 2.4.1 Transfersomes™

While most of the application studies employ mainly occlusive application with no attention paid to the possible effect of the application method, Cevc and Blume (1992) highlighted the importance of the application method on the transdermal delivery of drugs from the highly deformable lipid vesicles, *Transfersomes™*. They indicated that these vesicles can penetrate into and through intact skin, carrying therapeutic amounts of drugs if applied under nonocclusive conditions. The ability of such carriers to pene-

trate intact skin was attributed to their xerophobia (tendency to avoid dry surrounding), which causes the vesicles to resist dehydration at the skin surface by moving into the skin along with the local transdermal hydration gradient (Cevc and Blume 1992; Cevc et al. 1995). Vesicles' deformation ability was considered as another essential property which made the transdermal hydration gradient to provide sufficient driving force for vesicle penetration through the skin. The vesicles were thus given the name "ultradeformable vesicles" (El Maghraby et al. 2000, 2001a, b; Cevc et al. 2002). Based on this hypothesis, ultradeformable vesicles need to be applied under nonocclusive conditions, as occlusion is believed to abolish the driving force for the skin penetration of vesicles (Cevc and Blume 1992). The same group applied the local anesthetic lidocaine entrapped in *Transfersomes*<sup>TM</sup> under occlusion using a watertight wrapping for 25 min over the applied formulation (Planas et al. 1992). The results showed the superiority of *Transfersomes*<sup>TM</sup> compared to traditional formulations.

The above hypothesis was not accepted easily by researchers in the field of dermal and transdermal drug delivery. To test this hypothesis, it was important to test occlusive versus nonocclusive application of liposomes. On doing so, it was important to maintain the hydration gradient even in the in vitro experiments. To verify this, El Maghraby and coworkers developed an in vitro experiment which preserves the transepidermal hydration gradient (El Maghraby et al. 1999). This was achieved by the developed open hydration protocol in which the epidermal membrane was hydrated from viable epidermal side with the stratum corneal surface being left open to the atmosphere, to mimic the in vivo conditions. This protocol was employed to study the transdermal delivery of estradiol from ultradeformable liposomes after their occlusive and nonocclusive application (El Maghraby et al. 2001b). Occlusion resulted in a significant reduction of the transdermal flux of the drug which confirms the importance of the application protocol for the transdermal drug delivery from ultradeformable vesicles.

#### 2.4.2 Supersaturable Transdermal Delivery Systems

Supersaturation is the process of creation of a transient, metastable, supersaturated state in which the thermodynamic activity of the drug is increased above unity. This can increase the driving force for transdermal drug delivery. Alternative methods have been adopted to obtain drug supersaturation leading to increased chemical potential and enhanced transdermal drug delivery. The first method was based on mixing of cosolvents for a certain drug, with the rapid addition of a nonsolvent thereby creating a solution in which the drug concentration exceeds its equilibrium solubility (Megrab et al. 1995). In the second method, supersaturation can be achieved by the uptake of water diffusing passively out of the skin into the formulation, in which case water can act as the nonsolvent. This can represent a special case of the first method and can gain the benefit of occlusive application in which the formulation can mix with skin secretion. This process was used to explain the enhanced pharmacodynamic effect of bupranolol after dermal administration using microemulsion (ME) (Kemken et al. 1992). Taking this process into consideration, a self-microemulsifying drug delivery system (SMEDDS) of ethyl oleate, polyoxyethylene 20 sorbitan monooleate (Tween80) and sorbitan monolaurate (Span20), was developed and used to enhance the transdermal delivery of indomethacin compared to the corresponding ME formulation containing increasing concentration of water (El Maghraby 2010). The results indicated the superiority of SMEDDS compared to the tested ME as indicated from the recorded transdermal drug flux values which revealed greater transdermal drug delivery from SMEDDS compared to that obtained from ME. This superiority was attributed to possible supersaturation of the drug after dilution of the SMEDDS with the hydroalcoholic receptor which will diffuse from the receptor upward through the skin, acting as nonsolvent. The

author supported this claim by comparing the transdermal delivery of indomethacin from SMEDDS with that obtained from supersaturated microemulsion system which was prepared by diluting saturated drug solution in SMEDDS with water which acts as the nonsolvent, creating supersaturated system before occlusive application to the skin. The results revealed similar flux from the SMEDDS and the prepared supersaturated system.

The third method for obtaining supersaturated systems employs rapid evaporation of one or more volatile vehicle components upon application to the skin, leaving the drug at a concentration much greater than its equilibrium solubility in the remaining nonvolatile part of the formulation (Leichtnam et al. 2007). This process is graphically illustrated in Fig. 2.2 and requires open application of the formulation to the skin surface. Another important requirement of such process is that the drug must have higher solubility in the volatile solvent than in the nonvolatile components of the formulation. In this case, increasing the concentration of the volatile solvent in the formulation usually leads to exponential increase in drug solubility in the formulation. Evaporation of the volatile component after open application will be associated with linear reduction in the solubility creating transient supersaturation state (Fig. 2.2). The challenge here is to maintain the supersaturation for long time. This method was utilized to enhance the transdermal delivery of a lipophilic model drug (lavendustin), with supersaturation shown to be a promising strategy (Moser et al. 2001). Later, the same method was utilized to formulate a testosterone spray (Leichtnam et al. 2007). This study revealed enhanced transdermal delivery of testosterone from the spray.

In a more recent study, the transdermal delivery of progesterone from ME was studied under occlusive and open application (El Maghraby 2012). This study tested a ME formulation containing oleic acid, Tween<sup>TM</sup> 80, propylene glycol, and water. The ME system was used neat or with ethanol as a volatile cosurfactant. Results of this study (Fig. 2.3) indicated that ME formulations

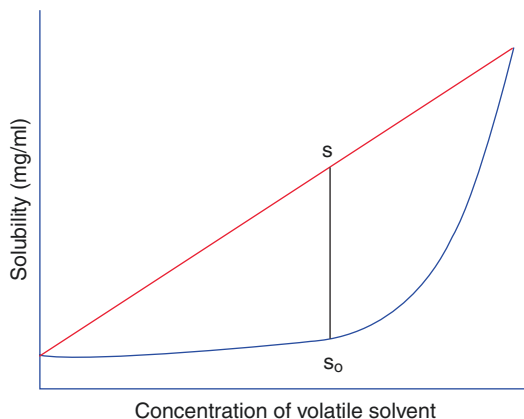
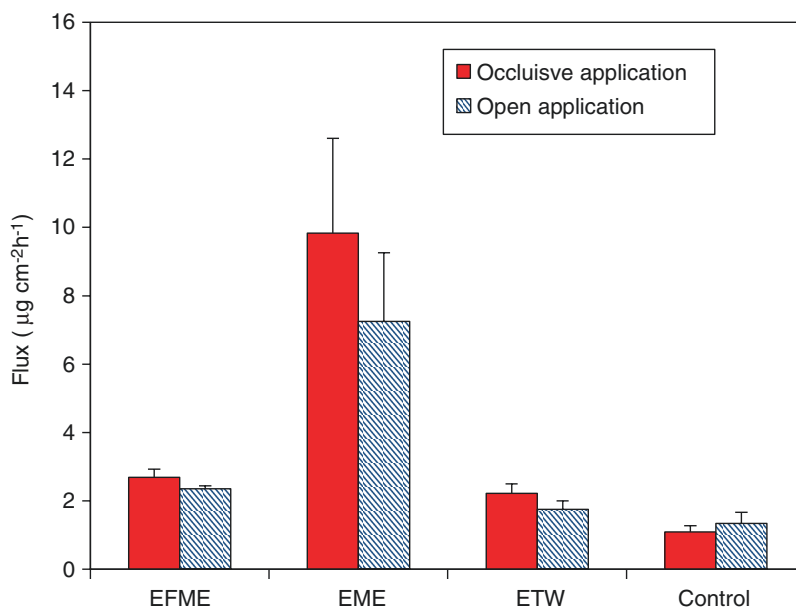


**Fig. 2.2** Exponential solubility profile of a given drug in the presence of increasing concentrations of volatile solvent. The linear plot indicates the theoretical solubility of the drug in a supersaturated system created by evaporation of the volatile solvent after open application. Dividing  $S$  by  $S_0$  produces the degree of supersaturation

enhanced progesterone transdermal flux compared to the saturated drug solution in 14% aqueous propylene glycol (control). Ethanol-containing ME (EME) was shown to be more effective than the ethanol-free system (EFME). Open application of EFME produced a minor change in drug flux compared to occlusive application (Fig. 2.3). For EME, open application reduced the flux by 26–28% compared to occlusive application of the same formulation, but the flux remained significantly higher than that obtained with EFME. This suggests a role for supersaturation with a contribution of ethanol in the recorded skin penetration enhancement. To verify this, the authors evaluated the transdermal delivery of progesterone from 40% ethanol in water (ETW). The sum of fluxes obtained from ETW and EFME was lower than that obtained from EME. It was thus concluded that the penetration enhancement induced by supersaturation played an important role in enhanced transdermal drug delivery. However, this cannot be considered as the only mechanism. The authors introduced ME formulations containing volatile components as candidates for the formulation of sprays for dermal application.

**Fig. 2.3** Transdermal delivery of progesterone after occlusive and open application of microemulsion. EFME is ethanol-free microemulsion, EME is ethanol-containing microemulsion, ETW is 40% ethanol in water, and control is 14% propylene glycol in water (This figure was produced using data published by El Maghraby 2012)



### Conclusion

This overview highlighted the importance of the method of application of drug formulations in dermal and transdermal delivery of drugs. The formulators should consider the application technique as a factor parallel to the formulation factors (composition) in developing dermal and transdermal drug delivery systems.

### References

- Barry BW (1983) Dermatological formulations: percutaneous absorption. Marcel Dekker, New York/Basel
- Barry BW (1987) Mode of action of penetration enhancers in human skin. *J Control Rel* 6:85–97
- Berardesca E, Maibach HI (1988) Skin occlusion: treatment or drug-like device? *Skin Pharmacol* 1:207–215
- Bouwstra JA, Ponc M (2006) The skin barrier in healthy and diseased state. *Biochim Biophys Acta* 1758:2080–2095
- Bucks D, Guy R, Maibach HI (1991) Effects of occlusion. In: Bronaugh RL, Maibach HI (eds) *Vitro percutaneous absorption: principles, fundamentals and applications*. CRC Press, Boca Raton, pp 85–114
- Cevc G, Blume G (1992) Lipid vesicles penetrate into intact skin owing to the transdermal osmotic gradients and hydration force. *Biochim Biophys Acta* 1104:226–232
- Cevc G, Schätzlein A, Blume G (1995) Transdermal drug carriers: basic properties, optimization and transfer efficiency in the case of epicutaneously applied peptides. *J Control Rel* 36:3–16
- Cevc G, Schätzlein A, Richardsen H (2002) Ultradeflexible lipid vesicles can penetrate skin and other semi-permeable membrane barriers unfragmented. Evidence from double label CLSM experiments and direct size measurement. *Biochim Biophys Acta* 1564:21–30
- Cross SE, Roberts MS (2000) The effect of occlusion on epidermal penetration of parabens from a commercial allergy test ointment, acetone and ethanol vehicles. *J Invest Dermatol* 115:914–918
- El Maghraby GM (2010) Self microemulsifying and microemulsion systems for transdermal delivery of indomethacin: Effect of phase transition. *Colloids Surf B Biointerfaces* 75:595–600
- El Maghraby GM (2012) Occlusive and non-occlusive application of microemulsion for transdermal delivery of progesterone: mechanistic studies. *Scintia Pharmaceutica* 80:765–778
- El Maghraby GM, Williams AC, Barry BW (1999) Skin delivery of oestradiol from deformable and traditional liposomes: mechanistic studies. *J Pharm Pharmacol* 51:1123–1134
- El Maghraby GM, Williams AC, Barry BW (2000) Oestradiol skin delivery from ultradeflexible liposomes: refinement of surfactant concentration. *Int J Pharm* 196:63–74
- El Maghraby GM, Williams AC, Barry BW (2001a) Skin delivery of 5-fluorouracil from ultradeflexible and standard liposomes in vitro. *J Pharm Pharmacol* 53:1069–1077

- El Maghraby GM, Williams AC, Barry BW (2001b) Skin hydration and possible shunt route penetration in controlled skin delivery of estradiol from ultradeformable and standard liposomes in vitro. *J Pharm Pharmacol* 53:1311–1322
- Elias PM (1981) Epidermal lipids; membranes and keratinization. *Int J Dermatol* 20:1–9
- Kemken J, Ziegler A, Muller BW (1992) Influence of supersaturation on the pharmacodynamic effect of bupranolol after dermal administration using microemulsion as vehicle. *Pharm Res* 9:554–558
- Leichtnam ML, Rolland H, Wüthrich P, Guy RH (2007) Impact of antinucleants on transdermal delivery of testosterone from a spray. *J Pharm Sci* 96:84–92
- Megrab NA, Williams AC, Barry BW (1995) Oestradiol permeation across human skin and silastic membranes: effects of propylene glycol and supersaturation. *J Control Rel* 36:277–294
- Moser K, Kriwet K, Kalia YN, Guy RH (2001) Enhanced skin permeation of a lipophilic drug using supersaturated formulations. *J Control Rel* 73:245–253
- Orland GF (1983) Structure of the skin. In: Goldsmith LA (ed) *Biochemistry and physiology of the skin*, vol 1. Oxford University Press, New York, pp 3–63
- Planas ME, Gonzalez P, Rodriguez L, Sanchez S, Cevc G (1992) Noninvasive percutaneous induction of topical analgesia by a new type of drug carrier, and prolongation of local pain insensitivity by anesthetic liposomes. *Anesth Analg* 75:615–621
- Scheuplein RJ (1965) Mechanisms of percutaneous absorption. I. Routes of penetration and the influence of solubility. *J Invest Dermatol* 45:334–346
- Scheuplein RJ (1967) Mechanisms of percutaneous absorption. II. Transient diffusion and the relative importance of various routes of skin penetration. *J Invest Dermatol* 48:79–88
- Scheuplein RJ, Blank IH (1971) Permeability of the skin. *Physiol Rev* 51:702–747
- Treffel P, Muret P, Muret-D’Aniello P, Coumes-Marquet S, Agache P (1992) Effect of occlusion on in vitro percutaneous absorption of two compounds with different physicochemical properties. *Skin Pharmacol* 5:108–113
- Warner RR, Myers MC, Taylor DA (1988) Electron probe analysis of human skin: determination of the water concentration profile. *J Invest Dermatol* 90:218–224
- Zhai H, Maibach HI (2002) Occlusion vs. skin barrier function. *Skin Res Technol* 8:1–6

Wing Man Lau and Keng Wooi Ng

**Contents**

3.1	<b>Introduction</b> .....	35
3.2	<b>Skin Absorption Kinetics</b> .....	36
3.2.1	Permeation Kinetics .....	36
3.2.2	Penetration Kinetics .....	41
	<b>Conclusion</b> .....	42
	<b>References</b> .....	42

**3.1 Introduction**

The aim of permeation studies is to determine how much of a preparation should be applied to the skin surface in order to achieve the desired bioavailability. In practice, many topical preparations are applied to the skin as a finite dose, often in the form of a cream, gel or ointment. However, when examining the fundamental permeation behaviour of a substance or when investigating the effects of penetration enhancers on percutaneous absorption, infinite dosing is usually employed to maintain a constant rate of absorption of the test compound through the skin, that is, the so-called steady-state flux.

With infinite dosing, it is generally assumed that there is no change in permeant concentration within the formulation throughout the experiment. When using Franz diffusion cells, this corresponds to a constant permeant concentration (or, more accurately, no change in thermodynamic activity of the permeant) in the donor phase. In practice, this can be achieved by regularly replenishing the donor solution or, more usually, by the addition of a small excess of solid permeant to a saturated donor solution; assuming that dissolution of the solid is not rate-limiting, then as the permeant leaves the donor solution, it is replaced by molecules entering the solution from the solid excess (Megrab et al. 1995). Alternatively, infinite dosing is commonly assumed by administering an amount of the

---

W.M. Lau (✉)  
School of Pharmacy, University of Reading,  
Whiteknights, PO Box 226, Reading RG6 6AP, UK  
e-mail: [w.lau@reading.ac.uk](mailto:w.lau@reading.ac.uk)

K.W. Ng (✉)  
School of Pharmacy and Biomolecular Sciences,  
University of Brighton, Huxley Building, Lewes  
Road, Brighton BN2 4GJ, UK  
e-mail: [K.Ng@brighton.ac.uk](mailto:K.Ng@brighton.ac.uk)

formulation large enough to preclude any ‘significant’ reduction in the test compound or any other component in the donor phase during the course of the experiment (Franz et al. 1993). In these cases, a ‘significant reduction’ usually occurs when the permeant concentration in the donor phase declines by more than 10% of the initial value (Kielhorn et al. 2006).

Under finite dose conditions, permeant concentration in the formulation changes during the experiment, due to penetration of the permeant into and permeation through the skin barrier, or due to evaporation. Generally, the experimental conditions should mimic as closely as possible the *in vivo* situation in order to provide suitable data. The amount and concentration of permeant formulation to be applied to the skin surface, as well as the duration and procedure of the protocols, depend on the study aims. For example, a small amount of permeant formulation may be applied in order to mimic *in vivo* application of an ointment. According to the Organisation for Economic Co-operation and Development (OECD), the application of  $\leq 10 \mu\text{l cm}^{-2}$  of a liquid or 1–5 mg  $\text{cm}^{-2}$  of a solid formulation should be used for finite dose studies (OECD 2004a). For infinite dose, amounts of  $>100 \mu\text{l cm}^{-2}$  or  $>10 \text{mg cm}^{-2}$  are required.

## 3.2 Skin Absorption Kinetics

Kinetically, the absorption of a substance into or through the skin is regarded as a passive diffusion process. It is also assumed that the skin is a pseudohomogeneous membrane providing a single transport route. Thus, both infinite dose and finite dose experiments can be described by Fick’s laws of diffusion.

Typically, the parameters describing the absorption of a substance through the skin barrier (such as the permeability coefficient and lag time) are obtained by evaluating the time-dependency of its cumulative permeated amount. An important parameter is the flux,  $J$ , which is proportional to the concentration gradient according to Fick’s first law of diffusion (Eq. 3.1).  $J$  can be estimated from the cumulative amount of

permeant passing through a unit area of membrane at time  $t$  (Crank 1975):

$$J = -D \frac{\delta c}{\delta x} \quad (3.1)$$

where  $J$  is the flux of the permeant (mass per  $\text{cm}^2$ ),  $D$  is the diffusion coefficient and  $\delta c/\delta x$  is the concentration gradient. To determine how diffusion affects the permeant concentration with time, Fick’s second law of diffusion (Eq. 3.2), which is derived from Fick’s first law of diffusion and the differential mass balance, can be employed:

$$\frac{\delta c}{\delta t} = D \frac{\delta^2 c}{\delta x^2} \quad (3.2)$$

This equation assumes that the permeant does not bind, nor is it metabolised. It is also assumed that the diffusion coefficient does not vary with the position or composition of the permeant, and that the barrier properties of the skin remain constant over time (Crank 1975).

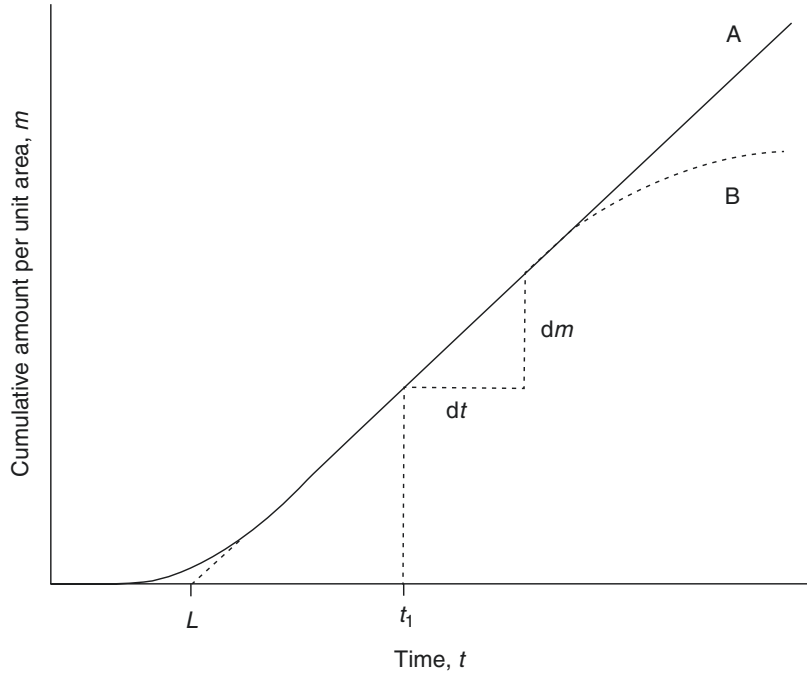
### 3.2.1 Permeation Kinetics

#### 3.2.1.1 Infinite-Dose Permeation

A typical infinite dosing regimen will produce a permeation profile of cumulative amount permeated across a unit area of membrane versus time, as shown in Fig. 3.1. Initially, when a permeant is applied to the skin, molecules penetrate into and diffuse through the stratum corneum. Depending on the permeants’ physical and chemical properties (e.g. lipophilicity, hydrogen bond acceptor or donor potential), it may penetrate and diffuse rapidly or may bind to stratum corneum components. A lag phase is seen where the amount of permeant in the receptor compartment increases exponentially due to binding and the increasing concentration of permeant in the stratum corneum. After a sufficient time (again dependent on the nature of the permeant, typically shorter for lipophilic non-bound molecules, longer for hydrophilic molecules), binding sites become fully occupied (or at steady-state equilibrium), and a steady-state concentration gradient of the permeant develops across the membrane. Under these conditions, the flux profile becomes essen-



**Fig. 3.1** Graph A (solid line) represents a typical permeation profile for an infinite dose regimen. The intercept on the horizontal axis,  $L$ , gives the lag time. The steady-state flux ( $J_{ss}$ ) is obtained from the gradient ( $dm/dt$ ) of the linear portion of the graph, from  $t=t_1$ , where  $t_1 \geq 2.7 L$ . Graph B shows an alternate situation where a plateau is reached following prolonged incubation, indicating deviation from infinite dose conditions, due possibly to donor depletion or non-sink conditions



tially constant, and the curve approaches a straight line. The linear portion of the graph represents the steady-state flux ( $J_{ss}$ ) and can be determined by simple linear regression of the linear portion of the graph (Crank 1975; Scheuplein and Blank 1971).

Typically, the steady-state flux is assessed from an in vitro experiment under infinite dose conditions, with ‘perfect’ sink conditions where the receptor compartment is at zero concentration throughout.  $J_{ss}$  can also be estimated by

$$J_{ss} = \frac{DC_0}{h} \quad (3.3)$$

where  $C_0$  is the concentration in the outermost first layer of the skin and  $h$  is the membrane thickness. Practically, it is very difficult to measure  $C_0$ . However, the concentration of the permeant in the donor vehicle,  $C_v$ , is easily obtainable or is usually known. Since  $C_0$  and  $C_v$  are related to the partition coefficient between donor and membrane ( $K_m$ ), where

$$C_0 = K_m C_v \quad (3.4)$$

then substitution of Eq. 3.4 into Eq. 3.3 gives Eq. 3.5, which is the most widely applied

mathematical model in examining skin permeation data:

$$J_{ss} = \frac{DK_m C_v}{h} \quad (3.5)$$

The lag time can be obtained by extrapolating the steady-state (linear) portion of the permeation graph to the intercept on the horizontal axis. Crank (1975) showed that the lag time,  $L$ , can be determined mathematically by

$$L = \frac{h^2}{6D} \quad (3.6)$$

It has been estimated that the time required for most permeants to achieve steady-state flux is about 2.7 times the lag time (Barry 1983).

Permeant transport across the skin is sometimes described in terms of the permeability coefficient ( $K_p$ ), essentially a measure for the speed of transport across a membrane (often as cm/h):

$$K_p = \frac{K_m D}{h} = \frac{J_{ss}}{C_v} \quad (3.7)$$

Typically, the steady-state flux  $J_{ss}$  and the permeability coefficient  $K_p$  are obtained from an in vitro

infinite dose experiment. As described above,  $J_{ss}$  is obtained from the gradient of the linear portion of the permeation profile, and therefore, if the concentration of the permeant in the applied vehicle ( $C_v$ ) is known, then  $K_p$  can be determined.  $K_p$  is often used to characterise the skin permeation of permeants, as calculations for other parameters such as  $D$  and  $K_m$  can be problematic as the membrane thickness ( $h$ ), or the diffusional path length, is often unknown.

Estimates of steady-state flux and permeability coefficients should only be derived from data points beyond 2.7 times the lag time when (pseudo-) steady-state conditions are established (Kielhorn et al. 2006); using data before steady state is established leads to false estimates of permeability coefficients (Shah et al. 1994). It has been recommended that infinite dose permeation experiments should last for at least 24 h (OECD 2004a). However, an increase in exposure time may alter the integrity of the skin barrier (Kleszczyński and Fischer 2012). Typically, experiments are performed for 24–48 h (Boonen et al. 2012; Karadzovska et al. 2012; Fasano et al. 2012; Brain et al. 2005; Walters et al. 1997), although shorter durations have also been reported (Chen et al. 2011). It has been suggested that 72 h or even longer may be needed in some cases for an infinite dose to establish steady-state flux, especially for permeants that have very low fluxes or present difficulties for detection (Franz et al. 1993; Howes et al. 1996).

Although Eqs. 3.5, 3.6 and 3.7 are commonly used to evaluate infinite dose experiments, it is assumed that the skin membrane acts as a homogeneous membrane and that permeation through the stratum corneum is the rate-limiting factor for transdermal transport. This assumption is usually valid for most permeants, but for highly viscous vehicles, highly lipophilic or highly hydrophilic molecules, partitioning behaviour may become the limiting factor (Cross et al. 2001). Also, the equations assume perfect sink conditions throughout the experiment in order to ensure drug permeation is not affected by solubility in the receptor phase. For *in vitro* studies, flow-through diffusion cells maintain sink conditions by constant replenishment of the receptor fluid,

but this may lead to dilution of the penetrant below the detection limit. For static diffusion cells, it is commonly regarded that sink conditions are maintained when the receptor fluid does not contain more than 10% of the saturated concentration of the penetrant (Ng et al. 2010; Skelly et al. 1987). The most widely used receptor fluid is isotonic buffered saline, pH 7.4. However, for highly lipophilic compounds, the solubility in the receptor fluid may become the rate-determining step in skin absorption and may have a significant effect on the total flux measured. When solubility is a concern, the receptor phase can include lipophilic solvents which do not affect the skin barrier or a solubilising agent (e.g. 50% ethanol, 6% polyethylene glycol, 20% oleyl ether or 5% bovine serum albumin) (Skelly et al. 1987; OECD 2004a).

In reality, even under infinite dose conditions, depletion of the donor phase, non-sink receptor conditions and deterioration of the skin can occur with time. These factors may result in inaccuracies in steady-state flux and lag time estimations (Moody 2000). Therefore, particular caution has to be exercised in experiments where prolonged incubation times are necessary.

### 3.2.1.2 Finite-Dose Permeation

*In vitro* percutaneous absorption studies often utilise an infinite dose regimen to define a permeant's properties, that is, steady-state flux, permeability coefficient and lag time. However, a major limitation of infinite dosing is its failure to mimic the application of topical drug formulations in common clinical situations, where a relatively small amount (i.e. a finite dose) of the formulation is used. Under these circumstances, steady-state permeation seldom occurs and, therefore, the permeability coefficient cannot be determined. Most *in vivo* experiments are based on finite dosing, although in some cases, infinite dose conditions may result when finite doses are applied repeatedly.

In contrast to the infinite-dose permeation profile, finite-dose application may result in a 'pseudo steady-state' condition, where the amount permeated may be transiently linear but then reaches a plateau, beyond which the amount

**Fig. 3.2** A typical permeation profile for a finite-dose regimen. Depletion of the donor phase gives the characteristic plateau in region A. The maximum flux ( $J_{\max}$ ) is obtained from the gradient ( $dm/dt$ ) of the near-linear portion of the curve in region B. Given that steady-state flux may not be obtained before donor depletion becomes significant, the maximum flux may not represent steady-state flux

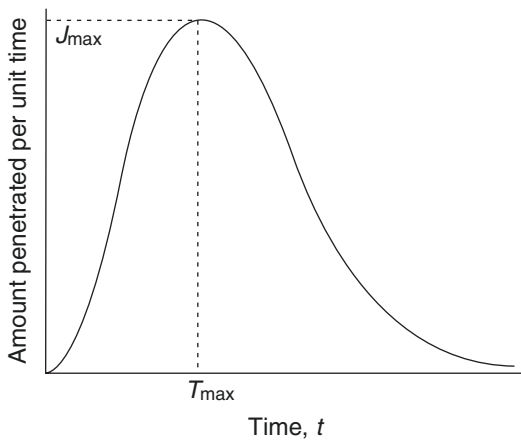
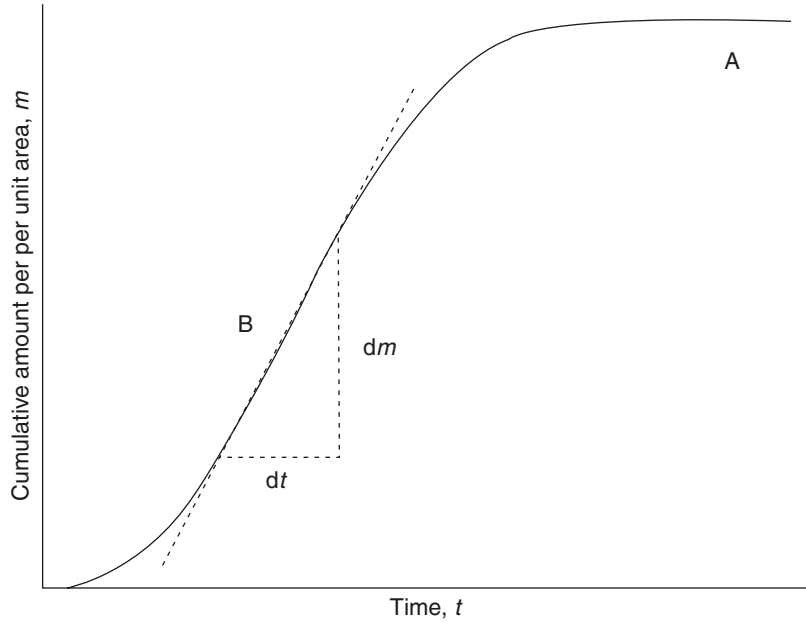


**Fig. 3.3** Estimation of maximum flux ( $J_{\max}$ ) from a graph of amount penetrated per unit time (assuming constant permeation area) versus time. In this case, the vertical axis represents instantaneous flux. The time taken to reach maximum flux is referred to as  $T_{\max}$

permeated remains constant due to donor depletion (Fig. 3.2).

Alternatively, by plotting the amount penetrated between the time points (i.e. instantaneous flux) against time (Figs. 3.3 and 3.4), a peak is observed which corresponds to the maximum flux before appreciable donor depletion (Franz 1983; Kasting 2001). The maximum flux ( $J_{\max}$ )

and the time to maximum flux ( $T_{\max}$ ) are the most commonly reported parameters in finite dosing. These can be represented by (Scheuplein and Ross 1974; Crank 1975; Kasting 2001)

$$J_{\max} = \frac{1.85DC_0\delta}{h^2} \quad (3.8)$$

$$T_{\max} = \frac{h^2 - \delta^2}{6D} \quad (3.9)$$

Here,  $D$  is the apparent diffusion coefficient,  $C_0$  is the concentration of the permeant in the first layer of the stratum corneum,  $h$  is the thickness of the stratum corneum and  $\delta$  is the thickness of the finite dose layer on the skin surface. For a finite dose, since  $\delta$  is considerably smaller in comparison with  $h$ ,  $\delta$  can be neglected, leading to

$$T_{\max} = \frac{h^2}{6D} \quad (3.10)$$

Thus, it is possible to estimate the apparent diffusion coefficient ( $D$ ), if the values of  $J_{\max}$  and  $T_{\max}$  are known. In addition to this mathematical model,  $J_{\max}$  and  $T_{\max}$  are sometimes obtained graphically from experimental data (Figs. 3.2 and 3.3) (van de Sandt et al. 2004; Wilkinson et al. 2006).

Due to the nature of finite dosing, experimental problems can ensue, since applying a small

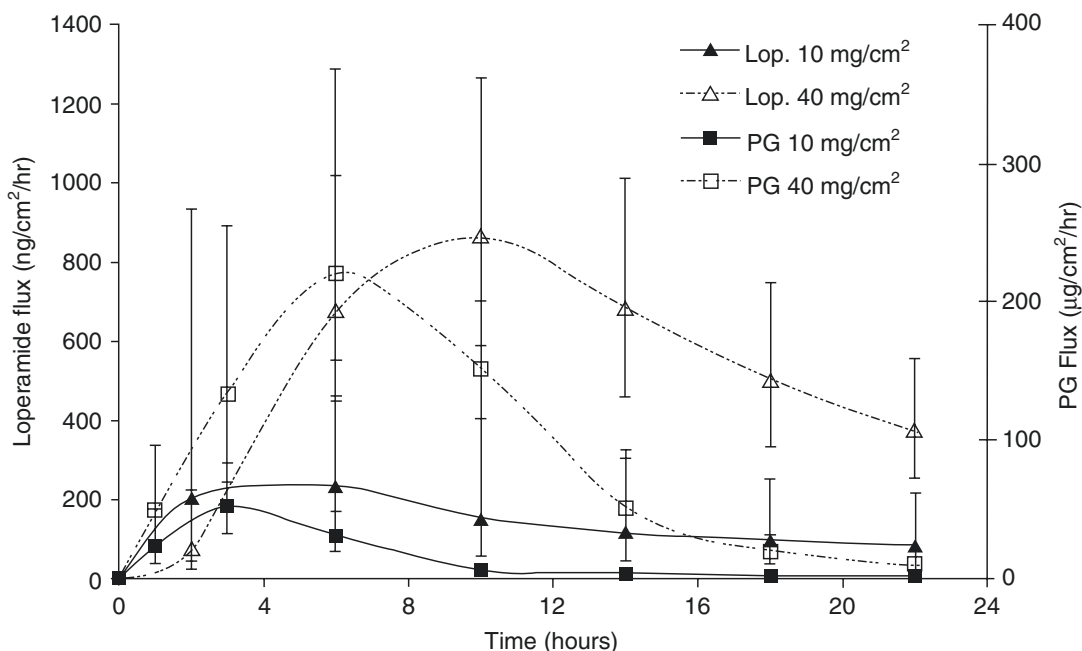


**Fig. 3.4** Exemplar data showing instantaneous flux of finite doses of loperamide and propylene glycol (PG) through human skin over time (Data are from Trottet et al.

(2004). Figure copyright (2012) reprinted with permission from Elsevier)

finite dose formulation evenly across a membrane *in vitro* can be difficult. Since the bioavailability of drugs applied to the skin in finite doses depends on the amount of drug applied per unit area (Wester and Maibach 1976; Franz et al. 1993), a homogenous drug distribution over the whole donor area is needed to minimise variation within and between experiments.

Applying semisolid formulations homogeneously poses more complications than liquid dosing. Semisolids are usually applied manually, using a mechanical device such as a glass rod (Hadgraft et al. 2003; Franz et al. 1993; Brain et al. 1995; Gupta et al. 1999) or spatula (Dreher et al. 2002; Trottet et al. 2004; Youenang Piemi et al. 1998) to help distribute the formulation evenly on the skin surface. In this case, it is important that the application device is also analysed in order to determine the actual dose applied to the skin. This is commonly done by extraction (Gupta et al. 1999) of the remaining drug from the application device, or by weight difference (Walters et al. 1997; Brain et al. 1995; Vallet et al. 2007). Sometimes, the permeant is dissolved in a volatile medium to allow easy application and

homogenous distribution (Kasting and Miller 2006; Southwell and Barry 1984). The volatile solvent evaporates, leaving a thin film of the drug on the skin surface. However, the volatile solvent may extract some lipids from the stratum corneum, affecting the integrity of the skin membrane. Another method used for uniform dose distribution is by massaging the formulation onto the skin surface, but this mechanical stress may influence the absorption rate in some cases (Amidouche et al. 1994; Lademann et al. 2007, 2009). To date, a very limited number of publications have investigated drug formulation distribution over the incubation area (Lademann et al. 2008); homogenous distribution is generally assumed in many reports.

The degree of occlusion of diffusion cells during experiments can affect skin hydration and, consequently, drug permeation (Akhter and Barry 1985; Zhai and Maibach 2001; Sarpotdar and Zatz 1986). Some researchers recommend that the skin be exposed to ambient conditions to simulate the *in-use* conditions of topically applied formulations (Wilkinson and Williams 2002; Grégoire et al. 2009). However, evaporation of

the vehicle and/or permeant can occur in non-occluded experiments which can impact significantly permeant absorption (Frasch et al. 2011). Moreover, the skin may become dry, and its barrier function can thus be affected (Selzer et al. 2013). Occlusion is also used during finite dosing to avoid drying of the skin surface due to application of small amounts of formulation, or to prevent evaporation, which could lead to a change in permeant concentration (van de Sandt et al. 2004; Koyama et al. 1994). However, care is required to avoid damage to skin integrity caused by excessive stratum corneum hydration (Zhai and Maibach 2002).

For finite dose studies, exposure times usually reflect ‘in-use’ scenarios to allow quantification of permeant absorption over a realistic period of time that relates to potential human exposure (OECD 2004a). Exposure times of up to 48 h are commonly used (Hadgraft et al. 2003; Gupta et al. 1999; Walters et al. 1998), but may be shorter to mimic exposure to rinse-off products (Brain et al. 1995, 2005; Okuda et al. 2011), or in studies on occupational exposure to hazardous materials (Howes et al. 1996; Moody et al. 2007). In such cases, data collection commonly continues for at least 24 h. On the other hand, if the drug formulation is for a once-a-week product, for example, the experiment design should mimic the application exposure period and thus should be performed over 7 days (Williams 2003).

Due to the limited amount of test substance used in finite dose studies, it is important that a mass balance is performed on completion of the experiment to ensure the total amount of applied permeant could be recovered. The OECD guidelines state that the mean recovery of the permeant and metabolites should be in the range of  $100 \pm 10\%$ , and reason must be sought if this is not met (OECD 2004a, b). However, under certain circumstances, the test of a volatile substance that had to be trapped in a filter, recovery can be broadened to  $100 \pm 20\%$  (OECD 2004a; European Commission 2006). The mass balance

should include permeant remaining in the donor phase, that within the skin and all equipment in contact with the test substance (e.g. the donor and receptor chambers of the diffusion cell). In some cases, the recommended total recovery may not be achieved, for example, due to the limits of analytical detection or difficulties with simple extraction methods. Degradation of the permeant could also aggravate the accuracy of total recovery. For example, skin esterase has been shown to degrade permeants in situ (Lau et al. 2010, 2012). Chemical degradation could also have a significant impact on permeant stability (Kubota et al. 1995; Müller et al. 2003). The degradation products are likely to have lower permeation rates than the test compound. Thus, failure to detect degradation products using suitable analytical methods may confound experimental results.

### 3.2.2 Penetration Kinetics

#### 3.2.2.1 Infinite-Dose Penetration

Although skin permeation data allow the transport parameters across skin to be determined, constructing a drug concentration/depth profile can be valuable. The tape-stripping technique is most commonly used to assess the change in permeant concentration throughout the stratum corneum (Lau et al. 2010; Thomas and Heard 2007; Weerheim and Ponc 2001; Pellett et al. 1997; Mohammed et al. 2012; Stinchcomb et al. 1999; Dreher et al. 1998). This is a method, whereby the stratum corneum is progressively removed by adhesive tape and the drug within each tape is then extracted and determined to calculate the diffusivity and solubility of the drug within the stratum corneum.

Under infinite dosing, it is possible to predict the concentration of the penetrant ( $c_{(x,t)}$ ) as a function of position and time within the stratum corneum, using the appropriate solution of Fick’s second law of diffusion (Anissimov et al. 2012; Moser et al. 2001; Selzer et al. 2013):

$$c_{(x,t)} = KC_0 \left[ \left( 1 - \frac{x}{h} \right) - \frac{2}{\pi} \sum_{n=1}^{\infty} \frac{1}{n} \sin \left( \frac{n\pi x}{h} \right) \exp \left( \frac{-Dn^2\pi^2 t}{h^2} \right) \right] \quad (3.11)$$

In Eq. 3.11,  $K$  is the partition coefficient between the stratum corneum and the formulation vehicle,  $x$  is the vertical position within the stratum corneum (where  $0 \leq x \leq h$ ),  $t$  is the time at which the permeant concentration is to be determined and  $D/h^2$  gives the characteristic diffusion parameter. If the concentration of the permeant in the stratum corneum is obtained experimentally, the experimental concentration profiles can be fitted into Eq. 3.11 to determine  $K$  and  $D/h^2$  (Pirrot et al. 1997). Again, it is assumed that the skin is a homogenous membrane and that the permeant transports across the stratum corneum by passive

diffusion. In addition, the formulation should not alter the membrane integrity or act as a carrier for the test permeant. It is also assumed that the experiment is maintained under sink conditions, and the stratum corneum is the rate-limiting barrier.

### 3.2.2.2 Finite-Dose Penetration

Similarly, with finite dosing, it is possible to predict permeant concentration at a given position inside the stratum corneum and at a given time, using Eq. 3.12 (Kasting 2001; Selzer et al. 2013):

$$c_{(x,t)} = 2KC_{v0} \sum_{n=1}^{\infty} \frac{\beta \cos(\alpha_n x/h) - \alpha_n \sin(\alpha_n x/h)}{\beta + \beta^2 + \alpha_n^2} \exp\left(-\frac{\alpha_n^2 Dt}{h^2}\right) \quad (3.12)$$

where  $C_{v0}$  is the initial concentration of the permeant in the donor compartment,  $\beta = K(h/h_v)$ ,  $h_v$  being the theoretical height of the volume of donor formulation and  $\alpha_n$  is related to  $\beta$  such that  $\alpha_n \tan \alpha_n = \beta$ . However, very few studies have made use of this mathematical model.

### Conclusion

Finite and infinite dose regimens have different applications in transdermal delivery. Each approach presents its own advantages and challenges. Mathematical models allow us to predict, characterise and compare the skin absorption kinetics relating to finite or infinite dosing. In this respect, they are an invaluable tool for transdermal delivery. However, in applying these models, it is important to appreciate the underlying assumptions and limitations of the models.

### References

- Akhter SA, Barry BW (1985) Absorption through human skin of ibuprofen and flurbiprofen; effect of dose variation, deposited drug films, occlusion and the penetration enhancer N-methyl-2-pyrrolidone. *J Pharm Pharmacol* 37:27–37
- Amidouche D, Montassier P, Poelman M-C, Duchene D (1994) Evaluation by laser Doppler velocimetry of the attenuation of tretinoin induced skin irritation by  $\beta$ -cyclodextrin complexation. *Int J Pharm* 111:111–116
- Anissimov YG, Jepps OG, Dancik Y, Roberts MS (2012) Mathematical and pharmacokinetic modelling of epidermal and dermal transport processes. *Adv Drug Deliv Rev* 65(2):169–190
- Barry B (1983) *Dermatological formulations: percutaneous absorption*. Marcel Dekker, New York
- Boonen J, Malysheva SV, Taevernier L, Diana di Mavungu J, De Saeger S, De Spiegeleer B (2012) Human skin penetration of selected model mycotoxins. *Toxicology* 301:21–32
- Brain KR, Walters KA, James VJ, Dressler WE, Howes D, Kelling CK, Moloney SJ, Gettings SD (1995) Percutaneous penetration of dimethylnitrosamine through human skin in vitro: application from cosmetic vehicles. *Food Chem Toxicol* 33:315–322
- Brain KR, Walters KA, Green DM, Brain S, Loretz LJ, Sharma RK, Dressler WE (2005) Percutaneous penetration of diethanolamine through human skin in vitro: application from cosmetic vehicles. *Food Chem Toxicol* 43:681–690
- Chen M, Liu X, Fahr A (2011) Skin penetration and deposition of carboxyfluorescein and temoporfin from different lipid vesicular systems: in vitro study with finite and infinite dosage application. *Int J Pharm* 408:223–234
- Crank J (1975) *The mathematics of diffusion*. Oxford University Press, Oxford
- Cross SE, Jiang R, Benson HAE, Roberts MS (2001) Can increasing the viscosity of formulations be used to reduce the human skin penetration of the sunscreen oxybenzone? *J Invest Dermatol* 117:147–150
- Dreher F, Arens A, Hostynek JJ, Mudumba S, Ademola J, Maibach HI (1998) Colorimetric method for quantifying human Stratum corneum removed by adhesive-tape stripping. *Acta Derm Venereol* 78:186–189

- Dreher F, Fouchard F, Patouillet C, Andrian M, Simonnet JT, Benech-Kieffer F (2002) Comparison of cutaneous bioavailability of cosmetic preparations containing caffeine or alpha-tocopherol applied on human skin models or human skin *ex vivo* at finite doses. *Skin Pharmacol Appl Skin Physiol* 15(Suppl 1):40–58
- European Commission (2006) Basic criteria for the *in vitro* assessment of dermal absorption of cosmetic ingredients, SCCP/0970/06. Health & Consumer Protection Directorate – General. [http://ec.europa.eu/health/ph\\_risk/committees/04\\_sccp/docs/sccp\\_s\\_03.pdf](http://ec.europa.eu/health/ph_risk/committees/04_sccp/docs/sccp_s_03.pdf)
- Fasano WJ, Ten Berge WF, Banton MI, Heneweer M, Moore NP (2012) Dermal penetration of propylene glycols: Measured absorption across human abdominal skin *in vitro* and comparison with a QSAR model. *Toxicol In Vitro* 25:1664–1670
- Franz TJ (1983) Kinetics of cutaneous drug penetration. *Int J Dermatol* 22:499–505
- Franz TJ, Lehman PA, Franz SF, North-Root H, Demetruilas JL, Kelling CK, Moloney SJ, Gettings SD (1993) Percutaneous penetration of N-nitrosodiethanolamine through human skin (*in vitro*): comparison of finite and infinite dose applications from cosmetic vehicles. *Fundam Appl Toxicol* 21:213–221
- Frasch HF, Dotson GS, Barbero AM (2011) *In vitro* human epidermal penetration of 1-bromopropane. *J Toxicol Environ Health A* 74:1249–1260
- Grégoire S, Ribaud C, Benech F, Meunier JR, Garrigues-Mazet A, Guy RH (2009) Prediction of chemical absorption into and through the skin from cosmetic and dermatological formulations. *Br J Dermatol* 160:80–91
- Gupta VK, Zatz JL, Rerek M (1999) Percutaneous absorption of sunscreens through micro-yucatan pig skin *in vitro*. *Pharm Res* 16:1602–1607
- Hadgraft J, Whitefield M, Rosher PH (2003) Skin penetration of topical formulations of ibuprofen 5%: an *in vitro* comparative study. *Skin Pharmacol Appl Skin Physiol* 16:137–142
- Howes D, Guy RH, Hadgraft J, Heylings J, Hoeck U, Kemper F, Maibach HI, Marty J-P, Merk H, Parra J, Rekkas D, Rondelli I, Schaefer H, Tauber U, Verbiest N (1996) Methods for assessing percutaneous absorption, ECVAM Workshop Report 13. *ATLA* 24:81–106
- Karadzovska D, Brooks JD, Riviere JE (2012) Experimental factors affecting *in vitro* absorption of six model compounds across porcine skin. *Toxicol In Vitro* 26:1191–1198
- Kasting GB (2001) Kinetics of finite dose absorption through skin 1. Vanillylnonanamide. *J Pharm Sci* 90:202–212
- Kasting GB, Miller MA (2006) Kinetics of finite dose absorption through skin 2: volatile compounds. *J Pharm Sci* 95:268–280
- Kielhorn J, Melching-Kollmu B, Mangelsdorf I (2006). Environmental Health Criteria 235 dermal absorption. World Health Organization, Geneva European Commission
- Kleszczyński K, Fischer T (2012) Development of a short-term human full-thickness skin organ culture model *in vitro* under serum-free conditions. *Arch Dermatol Res* 304:579–587
- Koyama Y, Bando H, Yamashita F, Takakura Y, Sezaki H, Hashida M (1994) Comparative analysis of percutaneous absorption enhancement by d-limonene and oleic acid based on a skin diffusion model. *Pharm Res* 11:377–383
- Kubota K, Ademola J, Maibach HI (1995) Simultaneous diffusion and metabolism of betamethasone 17-valerate in the living skin equivalent. *J Pharm Sci* 84:1478–1481
- Lademann J, Richter H, Teichmann A, Otberg N, Blume-Peytavi U, Luengo J, Weiäy B, Schaefer UF, Lehr C-M, Wepf R, Sterry W (2007) Nanoparticles – an efficient carrier for drug delivery into the hair follicles. *Eur J Pharm Biopharm* 66:159–164
- Lademann J, Richter H, Golz K, Zastrow L, Sterry W, Patzelt A (2008) Influence of microparticles on the homogeneity of distribution of topically applied substances. *Skin Pharmacol Physiol* 21:274–282
- Lademann J, Patzelt A, Richter H, Antoniou C, Sterry W, Knorr F (2009) Determination of the cuticula thickness of human and porcine hairs and their potential influence on the penetration of nanoparticles into the hair follicles. *J Biomed Opt* 14:021014
- Lau W, White A, Heard C (2010) Topical delivery of a naproxen-dithranol co-drug: *in vitro* skin penetration, permeation, and staining. *Pharm Res* 27:2734–2742
- Lau WM, Ng KW, Sakenyte K, Heard CM (2012) Distribution of esterase activity in porcine ear skin, and the effects of freezing and heat separation. *Int J Pharm* 433:10–15
- Megrab NA, Williams AC, Barry BW (1995) Oestradiol permeation through human skin and silastic membrane: effects of propylene glycol and supersaturation. *J Control Release* 36:277–294
- Mohammed D, Yang Q, Guy RH, Matts PJ, Hadgraft J, Lane ME (2012) Comparison of gravimetric and spectroscopic approaches to quantify stratum corneum removed by tape-stripping. *Eur J Pharm Biopharm* 82:171–174
- Moody RP (2000) Automated *In Vitro* Dermal Absorption (AIVDA): predicting skin permeation of atrazine with finite and infinite (swimming/bathing) exposure models. *Toxicol In Vitro* 14:467–474
- Moody RP, Akram M, Dickson E, Chu I (2007) *In vitro* dermal absorption of methyl salicylate, ethyl parathion, and malathion: first responder safety. *J Toxicol Environ Health A* 70:985–999
- Moser K, Kriwet K, Naik A, Kalia YN, Guy RH (2001) Passive skin penetration enhancement and its quantification *in vitro*. *Eur J Pharm Biopharm* 52:103–112
- Müller B, Kasper M, Surber C, Imanidis G (2003) Permeation, metabolism and site of action concentration of nicotinic acid derivatives in human skin: correlation with topical pharmacological effect. *Eur J Pharm Sci* 20:181–195
- Ng SF, Rouse JJ, Sanderson FD, Eccleston GM (2010) Validation of a static Franz diffusion cell system for *in vitro* permeation studies. *AAPS PharmSciTech* 11:1432–1441

- OECD (2004a) Guidance document for the conduct of skin absorption studies, no. 28. OECD, Paris
- OECD (2004b) OECD guideline for the testing of chemicals 428, skin absorption: in vitro method. OECD, Paris
- Okuda M, Donahue DA, Kaufman LE, Avalos J, Simion FA, Story DC, Sakaguchi H, Fautz R, Fuchs A (2011) Negligible penetration of incidental amounts of alpha-hydroxy acid from rinse-off personal care products in human skin using an in vitro static diffusion cell model. *Toxicol In Vitro* 25:2041–2047
- Pellett MA, Roberts MS, Hadgraft J (1997) Supersaturated solutions evaluated with an in vitro stratum corneum tape stripping technique. *Int J Pharm* 151:91–98
- Pirot F, Kalia YN, Stinchcomb AL, Keating G, Bunge A, Guy RH (1997) Characterization of the permeability barrier of human skin in vivo. *Proc Natl Acad Sci* 94:1562–1567
- Sarpotdar PP, Zatz JL (1986) Evaluation of penetration enhancement of lidocaine by nonionic surfactants through hairless mouse skin in vitro. *J Pharm Sci* 75:176–181
- Scheuplein RJ, Blank IH (1971) Permeability of the skin. *Physiol Rev* 51:702–747
- Scheuplein RJ, Ross LW (1974) Mechanism of percutaneous absorption. V. Percutaneous absorption of solvent deposited solids. *J Invest Dermatol* 62:353–360
- Selzer D, Abdel-Mottaleb MMA, Hahn T, Schaefer UF, Neumann D (2013) Finite and infinite dosing: difficulties in measurements, evaluations and predictions. *Adv Drug Deliv Rev* 65(2):278–294
- Shah JC, Kaka I, Tenjarla S, Lau SWJ, Chow D (1994) Analysis of percutaneous permeation data: II. Evaluation of the lag time method. *Int J Pharm* 109:283–290
- Skelly JP, Shah VP, Maibach HI, Guy RH, Wester RC, Flynn G, Yacobi A (1987) FDA and AAPS report of the workshop on principles and practices of in vitro percutaneous penetration studies: relevance to bioavailability and bioequivalence. *Pharm Res* 4: 256–257
- Southwell D, Barry BW (1984) Penetration enhancement in human skin; effect of 2-pyrrolidone, dimethylformamide and increased hydration on finite dose permeation of aspirin and caffeine. *Int J Pharm* 22:291–298
- Stinchcomb AL, Pirot F, Touraille GD, Bunge AL, Guy RH (1999) Chemical uptake into human stratum corneum in vivo from volatile and non-volatile solvents. *Pharm Res* 16:1288–1293
- Thomas CP, Heard CM (2007) Probing the skin permeation of eicosapentaenoic acid and ketoprofen 2. Comparative depth profiling and metabolism of eicosapentaenoic acid. *Eur J Pharm Biopharm* 67:156–165
- Trottet L, Merly C, Mirza M, Hadgraft J, Davis AF (2004) Effect of finite doses of propylene glycol on enhancement of in vitro percutaneous permeation of loperamide hydrochloride. *Int J Pharm* 274:213–219
- Vallet V, Cruz C, Josse D, Bazire A, Lallement G, Boudry I (2007) In vitro percutaneous penetration of organophosphorus compounds using full-thickness and split-thickness pig and human skin. *Toxicol In Vitro* 21:1182–1190
- van de Sandt JJM, van Burgsteden JA, Cage S, Carmichael PL, Dick I, Kenyon S, Korinth G, Larese F, Limasset JC, Maas WJM, Montomoli L, Nielsen JB, Payan JP, Robinson E, Sartorelli P, Schaller KH, Wilkinson SC, Williams FM (2004) In vitro predictions of skin absorption of caffeine, testosterone, and benzoic acid: a multi-centre comparison study. *Regul Toxicol Pharmacol* 39:271–281
- Walters KA, Brain KR, Howes D, James VJ, Kraus AL, Teetsel NM, Toulon M, Watkinson AC, Gettings SD (1997) Percutaneous penetration of octyl salicylate from representative sunscreen formulations through human skin in vitro. *Food Chem Toxicol* 35:1219–1225
- Walters KA, Watkinson AC, Brain KR (1998) In vitro skin permeation evaluation: the only realistic option. *Int J Cosmet Sci* 20:307–316
- Weerheim A, Ponc M (2001) Determination of stratum corneum lipid profile by tape stripping in combination with high-performance thin-layer chromatography. *Arch Dermatol Res* 293:191–199
- Wester RC, Maibach HI (1976) Relationship of topical dose and percutaneous absorption in rhesus monkey and man. *J Invest Dermatol* 67:518–520
- Wilkinson S, Williams F (2002) Effects of experimental conditions on absorption of glycol ethers through human skin in vitro. *Int Arch Occup Environ Health* 75:519–527
- Wilkinson S, Maas W, Nielsen J, Greaves L, van de Sandt J, Williams F (2006) Interactions of skin thickness and physicochemical properties of test compounds in percutaneous penetration studies. *Int Arch Occup Environ Health* 79:405–413
- Williams A (2003) Transdermal and topical drug delivery from theory to clinical practice. Pharmaceutical Press, London
- Youenang Piemi MP, de Luca M, Grossiord J-L, Seiller M, Marty J-P (1998) Transdermal delivery of glucose through hairless rat skin in vitro: effect of multiple and simple emulsions. *Int J Pharm* 171:207–215
- Zhai H, Maibach HI (2001) Effects of skin occlusion on percutaneous absorption: an overview. *Skin Pharmacol Appl Skin Physiol* 14:1–10
- Zhai H, Maibach HI (2002) Occlusion vs. skin barrier function. *Skin Res Technol* 8:1–6



# Non-formulation Parameters That Affect Penetrant-Skin-Vehicle Interactions and Percutaneous Absorption

# 4

Jeffrey E. Grice, Hamid R. Moghimi,  
Elizabeth Ryan, Qian Zhang, Isha Haridass,  
Yousuf Mohammed, and Michael S. Roberts

## Contents

<b>4.1</b>	<b>Introduction</b> .....	46	<b>4.10</b>	<b>Gender-Related Skin Barrier Performance</b> .....	64
<b>4.2</b>	<b>Skin Responsiveness as It Applies to Targets for Drugs and Cosmetics</b> .....	46	<b>4.11</b>	<b>Barrier Performance in Cosmetically Treated Skin</b> .....	65
<b>4.3</b>	<b>Structure-Permeation Relationship in Percutaneous Absorption</b> .....	48	4.11.1	Insect Repellents .....	65
<b>4.4</b>	<b>Permeation Through Intact Epidermis</b> ....	49	4.11.2	Chemical Depilatories.....	66
<b>4.5</b>	<b>Physicochemical Properties That Favour Appendageal Permeation</b> ....	53	4.11.3	Peeling Agents .....	66
<b>4.6</b>	<b>Physicochemical Properties That Favour Direct Subcutaneous and Deeper Tissue Permeation</b> .....	56	4.11.4	Other Cosmetic Products .....	67
<b>4.7</b>	<b>Skin Hydration and Percutaneous Absorption</b> .....	56	<b>4.12</b>	<b>Compromised Barrier Performance</b> .....	67
<b>4.8</b>	<b>Age-Related Skin Barrier Performance</b> ...	60	4.12.1	Intrinsic Barrier Defects.....	67
<b>4.9</b>	<b>Site-Related Skin Barrier Performance</b> ...	62	4.12.2	Thermally Damaged Skin and Its Manipulation.....	67
			<b>4.13</b>	<b>Prevention of Percutaneous Permeation: A Possibility and a Necessity</b> .....	68
			<b>Conclusion</b> .....		69
			<b>References</b> .....		69

J.E. Grice • E. Ryan • I. Haridass • Y. Mohammed  
Therapeutics Research Centre, School of Medicine,  
University of Queensland, Translational Research  
Institute, Woolloongabba,  
QLD 4102, Australia

H.R. Moghimi  
Therapeutics Research Centre, School of Pharmacy  
and Medical Sciences, University of South Australia,  
GPO Box 2471, Adelaide,  
SA 5000, Australia

School of Pharmacy, Shahid Beheshti University  
of Medical Sciences, Tehran, Iran

Q. Zhang  
Therapeutics Research Centre, School of Pharmacy  
and Medical Sciences, University of South Australia,  
GPO Box 2471, Adelaide, SA 5000, Australia

M.S. Roberts (✉)  
Therapeutics Research Centre, School of Medicine,  
University of Queensland, Translational Research  
Institute, Woolloongabba, QLD 4102, Australia

Therapeutics Research Centre, School of Pharmacy  
and Medical Sciences, University of South Australia,  
GPO Box 2471, Adelaide, SA 5000, Australia  
e-mail: [m.roberts@uq.edu.au](mailto:m.roberts@uq.edu.au)

## 4.1 Introduction

The skin is a site of non-invasive delivery for drugs, cosmetics and diagnostic agents. In addition, the skin is exposed to a wide variety of unwanted substances each day – from the environment (such as exposure to pesticides and allergens), the workplace and the home, as well as from the deliberate use of topical products for therapeutic (e.g. anti-inflammatory creams) and cosmetic purposes (such as to slow down skin ageing) and for local protection (such as the insect repellent, N,N-diethyl-meta-toluamide (DEET) and barrier creams). Whilst most of these products are relatively innocuous, some may be irritants and others toxicants. The advancement of skin science has resulted in an in-depth characterisation of the skin barrier performance and an understanding of the different factors that can impact on this barrier. There are two separate needs that a topical product fulfils: its cosmetic properties, including its sensorial feel arising from its emollient and hydrating effects (see Chap. 5) and the selective delivery of the active ingredient for a local or systemic therapeutic effect. In order to achieve the latter with minimal penetration of an excipient through the skin, a range of strategies can be employed. These can include the use of different types of formulations (paste, ointment, gel, cream, lotion, powder, patch, etc.), manipulating the thermodynamic activity of the active and excipients by manipulating formulation (vehicle) properties (such as pH, active concentration and the formulation components that these interact with) and by modifying skin permeability through the use of occlusion and the presence of penetration enhancers, etc.

However, skin varies enormously in its biology between and within individuals as well as between species. This variability, as it applies to this chapter, is reflected in a range of skin permeabilities and skin responsiveness. The variation arises not only from biological differences in skin composition between sites on the body, gender, age or the presence of particular skin conditions (e.g. dry skin or psoriasis) but is also determined by environmental conditions (e.g.

temperature and humidity), the prior application of topical products, burn injuries and some penetrant physicochemical properties that can affect skin-penetrant-vehicle interaction and percutaneous absorption. As these various sources of skin variability can greatly impact on the rate and extent of skin permeation for both active and excipients, we discuss in this chapter the required molecular properties for optimum permeation through intact stratum corneum (SC) and skin appendages, the effects of hydration and related conditions on percutaneous absorption, permeation through thermally damaged skin, skin absorption retardation, cosmetic-induced alteration of skin barrier and various biological variables.

---

## 4.2 Skin Responsiveness as It Applies to Targets for Drugs and Cosmetics

Drugs are applied to skin for local action, systemic delivery or regional effects. In systemic delivery, a drug is targeted to remote areas through systemic circulation, e.g. nicotine for smoking cessation and nitroglycerin for angina pectoris (Fig. 4.1). In this type of drug delivery, the delivery system and skin conditions should be optimised for higher percutaneous absorption and minimal skin retention. In contrast to this is local or dermal delivery, where the effect is limited to the skin itself and different parts of skin are the targets. In this case, minimal systemic absorption is desirable. Skin targets for local delivery include the skin surface (sunscreens, insect repellents, cleaning agents), hair follicles (depilatories or hair growth stimulators), sebaceous glands (anti-acne drugs), sweat ducts and sweat glands (antiperspirants and deodorants), the stratum corneum (hydratants and keratolytic agents) and the epidermis (anti-inflammatory drugs) (Fig. 4.1). Finally, the regional application of drugs aims to target areas beneath the site of application, such as joints and muscles. In such cases, minimal systemic absorption is desirable, although not always achievable (Fig. 4.1).

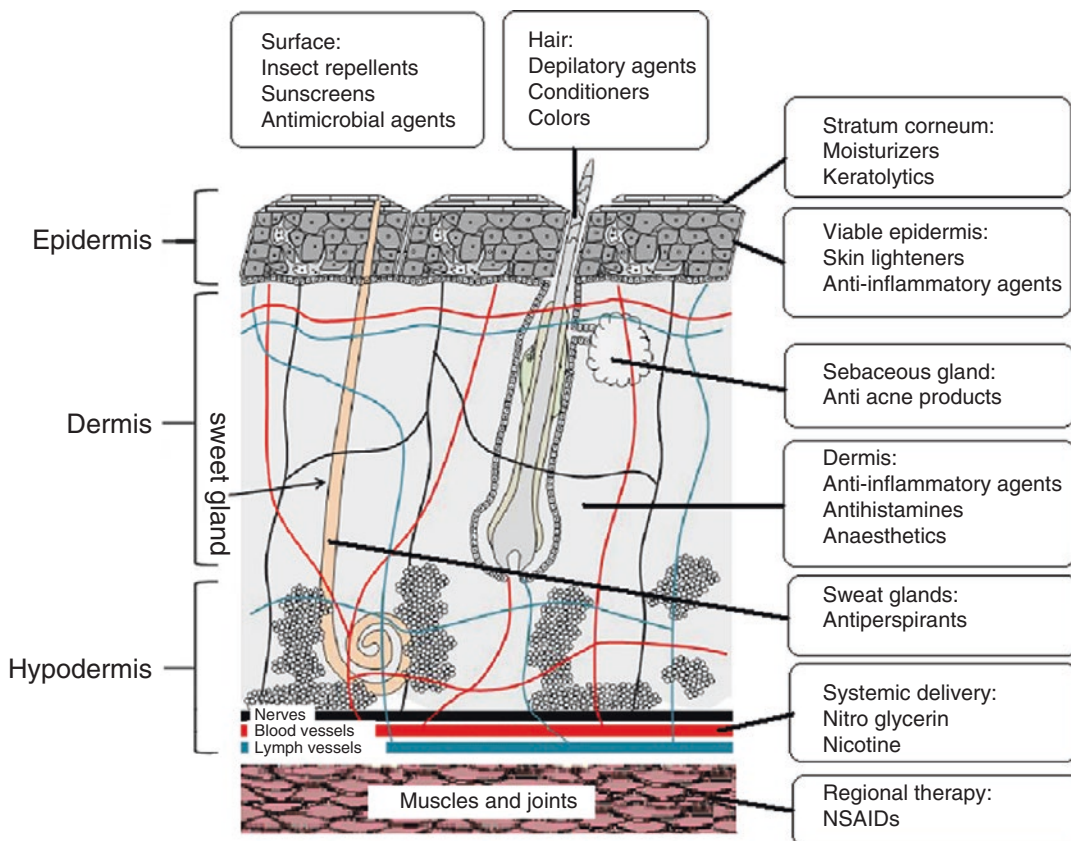


**Fig. 4.1** Schematic illustration of skin (showing epidermis, dermis, hypodermis and skin appendages) and underlying muscles and joints, showing targets of drugs and cosmetics applied to skin for local, systemic or regional action

Chemicals are targeted to the aforementioned regions for therapeutic, cosmetic or diagnostic purposes, but unwanted contact of the skin with toxic and hazardous material can also occur. A good understanding of the skin barrier and the conditions that affect its barrier performance is essential for the development of therapeutic, cosmetic and diagnostic delivery systems and for minimising any unwanted effects.

Sources for skin responsiveness in addition to variations in skin permeability include the actions of metabolising enzymes and transporters in the various skin regions and the variation in target receptor populations in the various skin types. As shown in our recent review of the range and location of various metabolising enzymes and transporters in the skin (Dancik et al. 2010), many of the enzymes have either hydrolysis or oxidative type activities and include aryl hydrocarbon

hydroxylase; 7-ethoxycoumarin O-deethylase; epoxide hydrolase; Cytochrome P450; esterases; aminopeptidases and peptidases. Hotchkiss (Hotchkiss 1998) suggests that the activities of cutaneous metabolising enzymes for Phase 1 metabolism (oxidation, reduction and hydrolysis) and for Phase 2 (conjugation) are 0.1–28% and 0.6–50% of those for the same enzymes in the liver. She also summarises the species and location variations for the various metabolising enzymes. As one illustration, the activity of cutaneous CYP1A1, a member of the Cytochrome P450 superfamily of enzymes, associated with the metabolism of benzo(a)pyrene and phenanthrene, is in the order SENCAR mouse > hairless guinea pig > human. The importance of location is illustrated in the work of Coomes et al. (1983), in which it is shown that for 7-ethoxycoumarin O-deethylase, benzo(a)pyrene hydroxylase (BPH),

uridine 5'-diphospho- glucuronosyltransferase (UGT) and glutathione S-transferase (GST), the relative sebaceous cell to epidermal basal activities were: 6.0, 3.2, 2.9 and 3.5, respectively.

Importantly, as reviewed by Hotchkiss, the activity of all enzymes may be induced, inhibited or destroyed by various agents and processes (Hotchkiss 1998). For instance, Coomes et al. also showed that topical treatment of the skin with beta-naphthoflavone induced 7-ethoxycoumarin O-deethylase by more than tenfold for both sebaceous and basal cells, with much lesser effects on the other enzymes studied (Coomes et al. 1983). Finnen et al. reported variable induction of cutaneous 7-ethoxycoumarin O-deethylase by various corticosteroids (Finnen et al. 1984), while Lockley et al. have pointed out that the dermal exposure to glycol ethers can lead to skin sensitisation and irritancy as well as systemic toxicity as a result of their oxidation by cytosolic alcohol and aldehyde dehydrogenase (Lockley et al. 2005). Low concentrations (5  $\mu\text{M}$ ) of disulfiram inhibited skin cytosolic aldehyde dehydrogenase 1 (ALDH1)-oxidation of aldehydes from ethanol and glycol ether, whereas high concentrations (500  $\mu\text{M}$ ) led to complete inhibition. Ethanol, a penetration enhancer for the transport of beta-estradiol across the epidermis, is also an inhibitor of its cutaneous metabolism to estrone in the viable epidermis (Liu et al. 1991). In addition, the treatment of psoriasis and ectopic dermatitis patients' skin with coal tar, a long-standing dermatologic treatment, for 24 h led to a two- to fivefold induction of aryl hydrocarbon hydroxylase (AHH) activity. Similar AHH induction was seen in excised normal human breast skin incubated with coal tar for 24 h (Bickers and Kappas 1978). Heating of full-thickness human skin at 60 °C for 2 min to separate the epidermis resulted in a 35% reduction in phosphatase activity responsible for the hydrolysis of diisopropyl fluorophosphate (Loden 1985), while both freezing and heat separation led to a 40–50% reduction in esterase hydrolysis of acetylsalicylic acid (Aspirin<sup>®</sup>, Bayer) in porcine skin (Lau et al. 2012). Cross et al. (1998) found that both full-thickness and separated epidermal membranes had methyl salicylate esterase activity that was about 25% of the in vivo activity.

The effect of the metabolic activity on epidermal flux can be expressed as a first pass effect, whereby the flux of a solute entering the body after topical application is modified by the skin bioavailability ( $F$ ), i.e. the fraction of solute entering the body intact after topical application, calculated as the ratio of area under the plasma intact solute concentration-time profiles ( $AUC$ ) after topical and intravenous dosing:  $F = AUC(\text{topical}) / AUC(\text{iv})$ . Wester et al. found the % bioavailability for nitroglycerin in rhesus monkeys to be  $56.6 \pm 5.8\%$  (Wester et al. 1983), while in healthy humans, it was estimated to be 75% from Nitroderm<sup>®</sup> TTS patches manufactured by Novartis (Imhof et al. 1984) and 68–76% from a transdermal ointment (Nakashima et al. 1987). As well as skin metabolism, the loss of nitroglycerin is due to retention in the skin and tissue binding (Imhof et al. 1984).

In the event of the complete loss of metabolic activity in in vitro skin, the steady state skin flux  $J_s$  (= amount penetrated/time period) in vivo is related to that in vitro by Eq. 4.1 (Dancik et al. 2008):

$$J_{ss, \text{in vivo}} = F \cdot J_{ss, \text{in vitro}} \quad (4.1)$$

### 4.3 Structure-Permeation Relationship in Percutaneous Absorption

Even though the advantages of transdermal delivery have been recognised for a long time, the drug candidates for application via this route are very few. The nature of the penetrant, in particular its physicochemical properties, always plays an important role in its passive delivery through the skin. Based on our knowledge of transdermal penetration and skin structure, it is generally accepted that the optimal molecular properties a drug candidate should possess for transdermal delivery are a low molecular size, a moderate lipophilicity, a low melting point and relatively few hydrogen bonding groups. Such requirements are discussed in more detail below. However, as we know, skin is not a homogenous barrier and contains a complex epidermal path-

way, residing mainly in the stratum corneum, and an appendageal pathway, through hair follicles and other skin shunts, as illustrated in Fig. 4.1. In addition, structure-permeation relationship dependency relates to the nature of the barrier and it is difficult to find a general relationship to describe skin permeation overall. Besides considering a structure permeability relationship for permeation through the intact epidermis, physicochemical properties that favour a follicular pathway are also considered in this section.

Skin is a complex barrier, through which there are different parallel penetration routes via the intact epidermis and the appendages (hair follicles and sweat ducts) as well as serial barriers, including the stratum corneum, the viable epidermis, the dermis, etc. (Fig. 4.1). Even the stratum corneum (SC) contains parallel and serial pathways; the intercellular and transcellular routes. The SC is considered to be the main barrier to transdermal delivery in most cases. The transdermal permeation process, therefore, involves solute partitioning into and permeation through the appendageal pathway (App), partitioning into and permeation through the SC (transcellular or intercellular routes), partitioning between the SC and viable epidermis (VE), permeation through the VE, dermis and aqueous diffusion layers, and finally uptake by blood vessels or permeation through the hypodermis to underlying tissues [modified from (Zhang et al. 2009)]. This transport is expressed quantitatively, in its simplest form, as the steady state rate of permeation or flux ( $J_s$ ) through the skin and is defined by the amount of solute ( $Q$ ) passing through an area of skin ( $A$ ) over a period of time ( $T$ ) at steady state (i.e.  $T >$  an apparent lag time for permeation to occur and can be related to the maximum flux ( $J_{\max}$ ) (that will be similar for all vehicles not affecting the skin) and fractional solubility in a given vehicle ( $f_v$ ) (Roberts 2013) (Eq. 4.2), which, in principle, is related to the individual fluxes for solutes through the individual skin layers (stratum corneum, sc; viable epidermis, ve; dermis, de) and appendageal pathways (app) (Eq. 4.3):

$$J_s^{\text{skin}} = \frac{Q}{A \cdot T} = J_{\max} f_v \quad (4.2)$$

$$J_s^{\text{skin}} = \left( \frac{1}{J_s^{\text{sc}}} + \frac{1}{J_s^{\text{ve}}} + \frac{1}{J_s^{\text{dermis}}} \right)^{-1} + J_s^{\text{app}} \quad (4.3)$$

As we will see later, dermal perfusion also affects the clearance of solutes from the dermis and the clearance of solutes across the dermis into deeper tissues, which, in turn, may affect viable epidermal concentrations. In this section, permeation of drugs through intact epidermis and the appendageal pathway will be discussed in relation to physicochemical properties of molecules.

#### 4.4 Permeation Through Intact Epidermis

Considerable efforts have been made to establish a relationship between skin permeation and the molecular structure descriptors of solutes. The dependency of skin penetration on lipid-water partition coefficients, solubility, melting point and molecular size (molecular weight or molar volume) has been widely discussed in early studies published in this area (Scheuplein and Blank 1971; Lien and Tong 1973; Michaels et al. 1975; Roberts et al. 1977; Potts and Guy 1992; Du Plessis et al. 2002). In these studies, the SC was considered as the main barrier to permeation of drugs through the skin, but they recognised that the underlying viable epidermis, aqueous diffusion layer and dermis may also contribute to the skin resistance. Two main approaches have been used in defining these relationships: one is to express relationships in terms of observed fluxes through the skin and the other in terms of the physicochemical determinants often used to understand the variability in fluxes between different solutes and different formulations. The two approaches differ in that the first has its origins in the work of Higuchi (Higuchi 1960) and often relates permeation to the maximal permeation from a given vehicle, recognising that the flux of solutes from saturated solutions vehicles that have not affected the skin permeation should all be the same (Roberts 2013). In contrast, the second appears to arise from the conventions associated with

epithelial permeability in biological systems where low solute concentrations are used. This approach defines transport in terms of a permeability coefficient; flux÷vehicle concentration (Kuswahyuning and Roberts 2014) and is limited by the variability in permeability coefficient between vehicles, in accordance with the variation in solute solubility in the different vehicles (Roberts 2013). Care should be applied when using such relationships, as most vehicles do in fact affect skin permeability, they may affect dermal blood flow, and solutes could be in solution in a supersaturated form, i.e. above the usual solubility of the solute in the vehicle and therefore be associated with higher fluxes. The use of saturated or maximum flux has the advantage of directly showing the maximum dose deliverable over a period of time (Magnusson et al. 2004; Sloan et al. 2006; Milewski and Stinchcomb 2012). Further, if neither the formulation nor the solute affects the membrane, it should be an invariant in the thermodynamic description of the penetration process, whereas the permeability coefficient depends on the formulation used (Zhang et al. 2009; Scheuplein 2013). However, a changed maximum flux after formulation application may suggest an alteration of the skin bioproperties by the components of the vehicle, either during solute partitioning or the diffusion process.

Relevant to the first approach, we showed that the main determinant for maximal (or more accurately, saturated) solute flux from aqueous vehicles is the solute size (molecular weight or molecular volume) with an  $r^2$  of 0.688 ( $n=278$ ,  $p<0.001$ ) (Magnusson et al. 2004):

$$\log J_{s,\text{sat}} = \log J_{\text{max}} = -4.52 - 0.0141\text{MW} \quad (4.4)$$

A limitation of Eq. 4.3 is that it really only reflects the effect of diffusivity on skin transport, noting the diffusivity is a function of solute size, as defined by free volume and other theories (Kasting et al. 1987). It does not reflect the contribution of solubility of solutes to the flux. The theoretical importance of solubility is evident when it is assumed that the SC is the main barrier for solute penetration and when the saturated solute flux is expressed in terms of its underlying determinants for skin penetration: diffusivity in the SC ( $D_{\text{sc}}$ ), the path length for transport across the SC ( $h_{\text{sc}}$ ) and the solubility in the SC ( $S_{\text{sc}}$ ). Hence, incorporating these into Eq. 4.1 and expanding by recognising that the SC-water partition coefficient ( $K_{\text{sc},v}$ ) is given by ( $S_{\text{sc}}/S_v$ ) yields:

$$\begin{aligned} J_{s,\text{sat}}^{\text{skin}} &= \frac{Q}{A \cdot T} = \frac{D_{\text{sc}}}{h_{\text{sc}}} S_{\text{sc}} \\ &= \frac{D_{\text{sc}}}{h_{\text{sc}}} K_{\text{sc},v} S_v = k_p^{\text{skin}} S_v \end{aligned} \quad (4.5)$$

Thus, it is evident from Eq. 4.5 that the solubility of the solute in the SC,  $S_{\text{sc}}$ , can be expressed in terms of a solubility of the solute in the vehicle and a partition coefficient  $K_{\text{sc},v}$  between the SC and vehicle (i.e.  $S_{\text{sc}} = K_{\text{sc},v} \times S_v$ ) and, in turn, the permeability coefficient is the product of this partition coefficient multiplied by  $D_{\text{sc}}/h_{\text{sc}}$  (i.e.  $k_p = K_{\text{sc},v} \times D_{\text{sc}} / h_{\text{sc}}$ ). We have previously applied  $S_{\text{sc}} = K_{\text{sc},v} \times S_v$  and the relationships between  $\log K_{\text{sc}}$  and  $\log P$  (Roberts et al. 1996), the dependence of solubility of the solutes in water on the octanol-water partition coefficient and the solute melting point above 25 °C (Yalkowsky and Valvani 1980) to yield (Roberts et al. 2002):

$$\log S_{\text{sc}} = \log K_{\text{sc}-w} + \log S_w = -0.48 \log P - 0.012(\text{MP} - 25) + 0.77 \quad (4.6)$$

Thus, the overall saturated flux is given by a combination of Eqs. 4.3 and 4.4. A difficulty in this area is the accuracy of the predictions for both SC-water partition coefficients and in water

solubility of different solutes. The most recent relationship, recognising most of the previous studies, suggests the slope for the linear relationship for a large data set of lipophilic solutes is

0.69 (Wang et al. 2010), slightly higher than the slope of 0.57 we found for our data set. Hewitt et al. (2009) recently evaluated the generalised solubility model used by Yalkowsky and colleagues (Yalkowsky and Valvani 1980) and commented: “The final conclusion of this study must be that predicting aqueous solubility is indeed still a formidable challenge! The results obtained in this study clearly indicate that no one model was able to predict solubility accurately.” Indeed, Ali et al. (2012) are also advocating the inclusion of the total polar surface area in estimation of aqueous solubility for some solutes. Magnusson et al., in recognising SC solubility as a determinant of flux, showed that inclusion of melting point (MP) and hydrogen bond acceptor ability increases the  $r^2$  for the prediction of saturated fluxes (Eq. 4.3) to 0.760.

The effect of solubility will be most evident for a group of solutes that are approximately similar in size (i.e. similar diffusivity). We and others have shown that there is a parabolic relationship between the saturated solute flux for such solutes and  $\log P$  (a measure of solute polarity) (Yano et al. 1986; Hinz et al. 1991; Magnusson et al. 2006; Zhang et al. 2009). Several other studies have shown a parabolic relationship between maximum flux and solute lipophilicity in vitro in humans (Cross et al. 2001), hairless rat (Diez et al. 1991) and hairless mouse skin (Hinz et al. 1991) and in vivo (Yano et al. 1986; Bucks and Maibach 2005). Parabolic relationships seen in our data (Zhang et al. 2009) with epidermal membranes and that of Yano (humans in vivo) and Hinz (hairless mouse skin) are illustrated in Fig. 4.2.

We also showed a parabolic relationship between the SC solubility and  $\log P$  for phenols and that the saturated flux versus SC solubility was linear (Fig. 4.3), with a  $\log P$  independent diffusivity for these similar size solutes, showing that this saturated flux –  $\log P$  relationship was defined by a variation in SC solubility with  $\log P$ .

We then extended this study by using a propylene glycol-water co-solvent vehicle (Zhang et al. 2011), concluding that propylene glycol containing vehicles enhanced the maximum flux

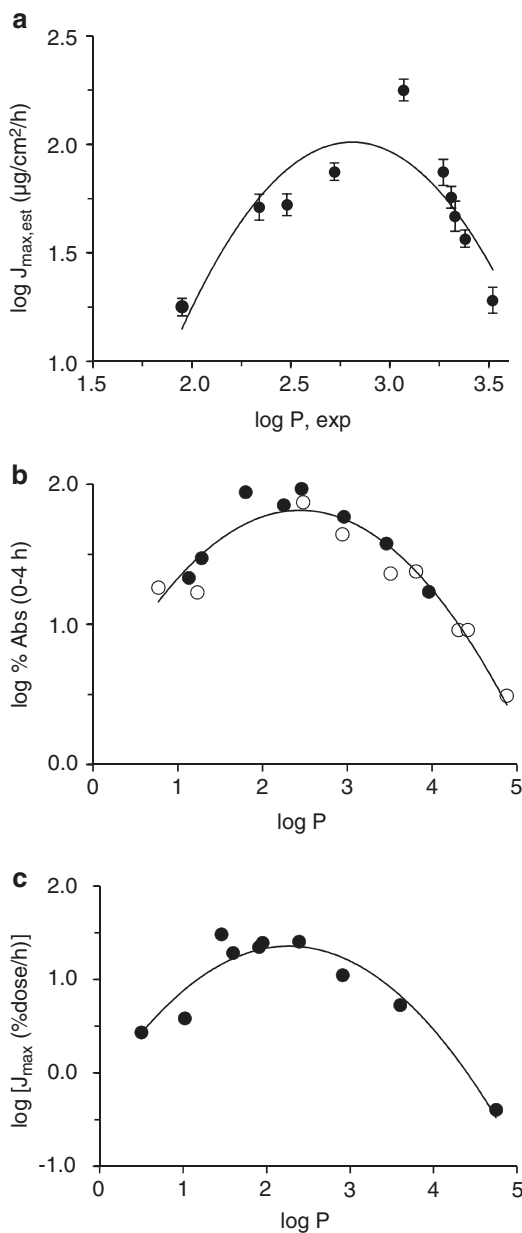


**Fig. 4.2** Convex dependence on  $\log P$  seen in (a)  $\log J_{\max}$  a series of similar-sized phenols (MW approx. 150) applied in aqueous solutions to excised human epidermal membranes. (Original data from Zhang et al. 2009). (b)  $\log (\% \text{ absorption over 4 h})$  for salicylates (closed symbols) and non-steroidal anti-inflammatory drugs (open symbols) applied to human skin in vivo. Original data from (Yano et al. 1986) and (c)  $\log J_{\max}$  for a series of phenols across hairless mouse skin in vitro (Original data from (Hinz et al. 1991)). The curves are for illustrative purposes only

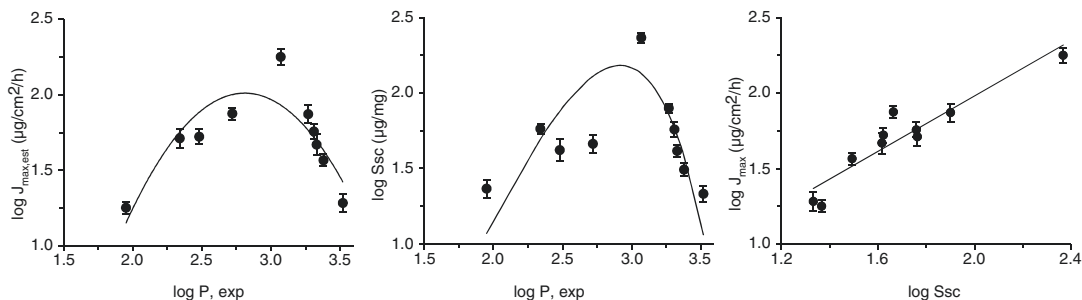


**Fig. 4.3** Relationships between maximum flux ( $J_{\max}$ , estimated from a 10% solution), stratum corneum solubility ( $S_{sc}$ ) and  $\log P$  (experimentally determined) for a series of similar-sized phenols applied in aqueous solu-

tions to excised human epidermal membranes. (a)  $J_{\max}$  vs  $\log P$ ; (b)  $\log S_{sc}$  vs  $\log P$ ; (c) linear relationship between  $\log J_{\max}$  and  $\log S_{sc}$  (Data adapted from (Zhang et al. 2009)). The curves are for illustrative purposes only

of these solutes by increasing their solubility in the intercellular lipids of the SC, but again showing that diffusivity was not dependent on the lipophilicity of the solute.

The second approach is to examine skin permeation in terms of the skin permeability coefficient ( $k_p$ ), which is defined by two main parameters: diffusion and partition coefficients (Eq. 4.5). Traditionally, these have been represented by a combination of organic – water partition coefficients (presented by  $\log P$ ) and size (represented by molecular weight MW or molecular volume MV) (Lien et al. 1971). The most comprehensive analysis of  $k_p$  in terms of solute size and lipophilicity was presented by Potts and Guy (Potts and Guy 1992), as shown in Eq 4.7:

$$\begin{aligned} \log k_p = & -6.3 + 0.71 \log P \\ & - 0.0061 \text{MW} \\ & (n = 93; r^2 = 0.67) \end{aligned} \quad (4.7)$$

Many others have since attempted to improve estimation of  $k_p$  (Lian et al. 2008; Chen et al. 2010; Moss et al. 2012). In a recent work, Milewski and Stinchcomb (Milewski and Stinchcomb 2012) have arrived at a predictive model for saturated skin fluxes by combining the Potts Guy (Eq. 4.7) with that from the Yalkowsky group (Yalkowsky and Valvani 1980) for water solubility to yield Eq. 4.8 for estimation of  $J_{s,\text{sat}}$  from  $\log P$ , MW and MP ( $n = 208, r^2 = 0.81$ ).

Whilst this model probably is currently limited to aqueous solutions, it may be applied to other vehicles if the concentration of the solute in the vehicle can be expressed as a fractional solubility in a simple or complex vehicle, Raoult's Law is approximately obeyed and the vehicle has either not affected the skin or its extent of skin permeation enhancement is known. We have pointed out that when the fractional solubilities for the vehicle  $f_v (= C_v / S_v)$  and skin  $f_s (= C_s / S_s)$  can be assumed to be equal, the skin flux is given by Eq. 4.1, i.e.  $J_s = J_{s,\text{sat}} \times f_v$  (Roberts 2013). Despite much effort in developing quantitative structure–activity relationship (QSAR) models, the predictability and quality of these models for risk assessment purposes can be further improved. A key issue is the large set of historical experimental data, in which variability is likely to have arisen from the use of different experimental approaches and human skin donors. In an attempt to cover as many formulations and conditions as possible, Samaras et al. (Samaras et al. 2012) examined the in vitro skin fluxes from the EDETOX database in their regression analyses in terms of not only the molecular descriptors of the penetrants and the vehicle, but also the range of various experimental and vehicle conditions used – including finite/infinite dosing, skin pre-hydration, occlusion and the skin thickness. They concluded that the donor concentration, solute lipophilicity, solute size and solute polar-

$$\log J_{s,\text{sat}} = 4.6 - 0.219 \log P - 0.0086 \text{MW} - 0.0102 (\text{MP} - 25) (n = 208, r^2 = 0.81) \quad (4.8)$$



ity, as well as the vehicle melting and boiling points were prominent factors influencing skin flux.

In reality, the SC is a heterogeneous membrane consisting of several layers of corneocytes with the space filled with lipids. Some hydrophilic and polar solutes penetrate through the SC faster than would be anticipated based on lipophilicity alone (Nitsche et al. 2006; Wang et al. 2007; Mitragotri et al. 2011). Consequently, the “porous pathway” model was introduced to address this challenge by describing skin permeability to hydrophilic solutes (Peck et al. 1994; Lai and Roberts 1999; Tang et al. 2001; Tezel et al. 2002; Mitragotri 2003). In this model, hydrophilic solutes are assumed to diffuse through pores in the skin, where pore size distribution, skin porosity and tortuosity are considered. The “brick-and-mortar” model has also been adapted and expressed in different forms (Wang et al. 2006, 2007; Chen et al. 2010, 2013). This mathematic model aims to include permeation through the corneocytes (i.e. trans-cellular pathway) and intercellular lipids (inter-cellular pathway), where the geometrical and compositional parameters of the SC have been included.

---

#### 4.5 Physicochemical Properties That Favour Appendageal Permeation

As an alternative to the stratum corneum inter- and intracellular permeation routes, the “bulk pathway” or “shunt pathway” by appendages such as hair follicles also acts as a permeation route through the skin (Fig. 4.1). This pathway has previously been considered as insignificant as appendageal structures only make up 0.1–1 % (forearm to forehead) of the total skin surface area (Otberg et al. 2004). However, in recent years, hair follicles and their associated pilosebaceous structures acting as a permeation pathway and/or reservoirs have been increasingly explored and received more attention, especially for nanoparticle delivery (Lademann et al. 2008; Patzelt and Lademann 2013).

The pilosebaceous unit comprises four different areas for topical application: the sebaceous gland, the bulb region, the hair matrix cells and the hair follicle infundibulum. Sebum excreted by the sebaceous gland is composed of short-chain fatty acids, resulting in a microenvironment that is rich in neutral, non-polar lipids (Meidan et al. 2005). The lower infundibulum provides decreased barrier properties and is surrounded by a dense network of blood capillaries. The infundibulum increases the possible surface area for targeted delivery and is an area of additional absorption. The immediate region surrounding the infundibulum is rich in antigen-presenting cells, whereas the lower bulge region is surrounded by stem cells (Patzelt and Lademann 2013), providing target sites for penetrated molecules (Knorr et al. 2009).

Work by a number of groups has found that the follicular route predominates for hydrophilic molecules (Essa et al. 2002; Ogiso et al. 2002; Mitragotri 2003) that cannot permeate the epidermal pathway easily. A study by Frum et al. (2007) quantified the influence of the drug lipophilicity on follicular penetration by using a range of drugs with similar molecular weights. A parabolic profile shows a maximal follicular contribution occurs at log  $P$  around 1. The two most lipophilic drugs, estradiol and corticosterone, had minimal entry into the follicular pores, whereas a 34 % contribution to total skin flux was found for hydrophilic adenosine (log  $P = -1.05$ ). For mannitol, which is also hydrophilic (log  $P = -2.47$ ) there was a 54 % follicular contribution associated with its flux through human skin, though its molecular size is slightly smaller than the above penetrants (Essa et al. 2002).

The in vivo follicular penetration of caffeine was also systemically examined using pharmacokinetic modelling (Liu et al. 2011). There was a 10 times faster absorption from hair follicles, and a 10-min delay for transport through the stratum corneum, with the follicular route contributing 25–35 % to the overall skin absorption. The in vivo absorption of caffeine was fast and high compared to the in vitro absorption, and this was considered to be mainly due to a fast resorption by in vivo blood flow, the physiological differ-

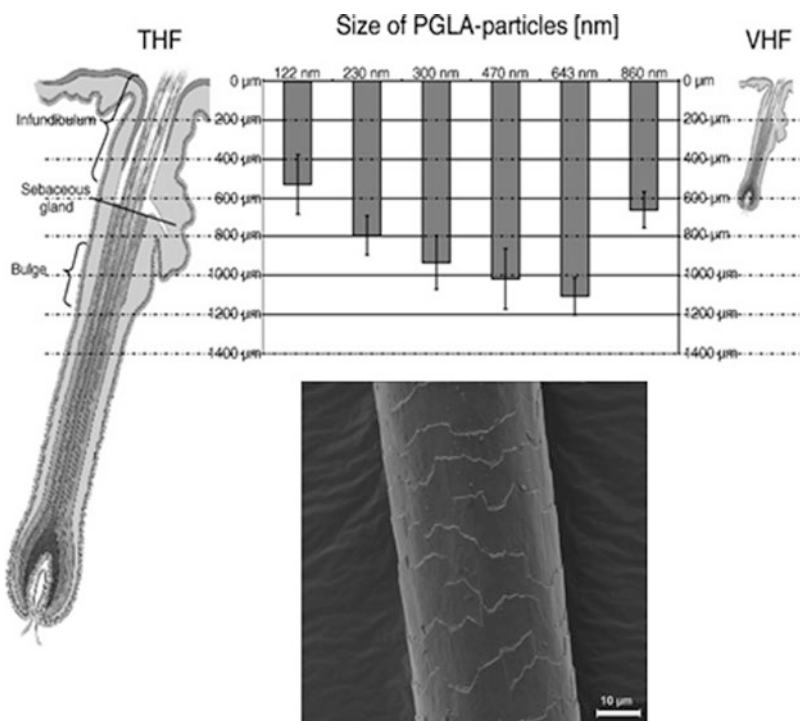


**Fig. 4.4** Above: Penetration depths in  $\mu\text{m}$  of different sizes of PLGA particles in relation to the target sites within terminal hair follicles (THF) and vellus hair follicles (VHF).

Below: The hair surface structure, showing the layers of overlapping cells (cuticula pili) (Reproduced with permission from Patzelt et al. 2011 and Lademann et al. 2011)

ence in hair follicles of the investigated skin and a contraction of hair follicles of the excised skin.

Besides polar molecules, the transfollicular pathway is also an important route for nanoparticles, which may be targeted to deep follicular regions and function as drug delivery vehicles (Lademann et al. 2007). Topically applied polymeric particles were shown to penetrate porcine skin with massage via the follicular pathway in a size-dependent manner (Patzelt et al. 2011), with 643-nm particles penetrating deepest into the follicle, to a maximum depth of approximately 1100  $\mu\text{m}$  (see Fig. 4.4).

Lademann has suggested that the optimal size of particles for deep penetration is governed by the size of the cuticula on the hair shafts (Lademann et al. 2011) (see Fig. 4.4), which may act as “geared pumps” to drive the particles into the follicles during massage (Lademann et al. 2009). The effect of massage is demonstrated in Fig. 4.5, where both particles and dye molecules remain in the superficial regions of the follicle

without massage, whereas, massage drives the particles – but not the dye – deep into the follicle (Lademann et al. 2007).

Particles, which may be solid or vesicular, with therapeutic substances bound to the surface or encapsulated, may be ideal follicular delivery agents, because of their long residence time within the follicle and their targetable penetration depth (Lademann et al. 2008). In addition, Vogt et al. found that antigen-presenting cells surrounding the infundibulum are able to internalise 40-nm particles that have permeated through the follicular epithelium (Vogt et al. 2006), thus providing a promising mechanism for vaccination via the follicular route.

Targeted follicular delivery can be achieved by manipulating the formulation (i.e. particle-/vesicle-based dosage forms and using sebum miscible ingredients) or modifying the target molecule (optimising physicochemical properties such as size, lipophilicity, solubility parameters and charge) (Trommer and Neubert 2006).

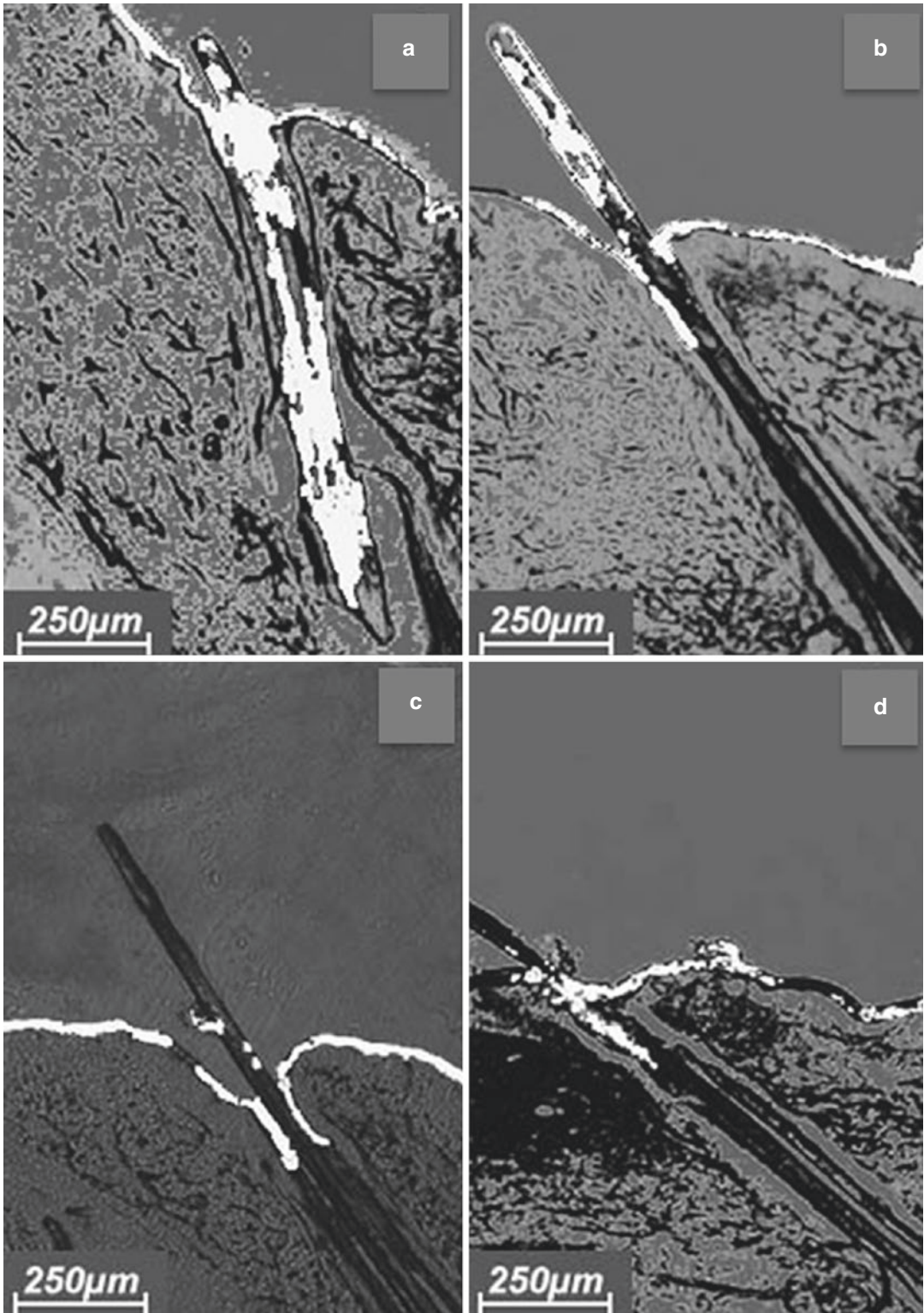


**Fig. 4.5** Superposition of transmission and fluorescent images, demonstrating the in vitro penetration of the dye-containing formulation into the hair follicles of porcine skin after application of massage. (a) Dye in particle form

and (b) dye in non-particle form – with massage. (c) Particle form and (d) non-particle form – without massage (Reproduced with permission from Lademann et al. 2007)

An example reported by Grice et al. (2010) shows that formulations that contained ethanol could enhance the early minoxidil uptake into the hair follicles. As minoxidil is six times more soluble in ethanol as it is in water, this was likely due to the partitioning of ethanol (plus minoxidil) through the lipid rich compartments. Some other methods like fractional laser and massage could also selectively enhance permeant targeting to follicles (Lademann et al. 2007; Lee et al. 2013).

The importance and required molecular and particular properties for an optimum follicular delivery are yet to be fully investigated.

---

#### **4.6 Physicochemical Properties That Favour Direct Subcutaneous and Deeper Tissue Permeation**

There are now a large number of studies showing that deep tissue penetration can occur after topical application to specific areas of the body. Various human biopsy (Rabinowitz et al. 1982; Grundmann-Kollmann et al. 2002; Anissimov and Roberts 2011) or cutaneous microdialysis (Cross et al. 1998; Benfeldt et al. 1999; Brunner et al. 2005) studies have been used to show direct and deep tissue penetration of solutes after topical application.

Rat wound deposition studies have been used to show that the main determinant for the penetration of solutes into deeper tissues after topical application is the size of the solute (Singh and Roberts 1996; Cross and Roberts 1999; Kretsos et al. 2008). The cutaneous vascular appears to be implicated in the penetration of solutes in studies conducted in rats, pigs and man (McNeill et al. 1992; Monteiro-Riviere et al. 1993; Cross et al. 1999).

Dancik et al. (2012) combined experimental percutaneous permeation studies with the available microdialysis literature on the penetration of topically compounds into subcutaneous tissue and muscle. The solutes studied were of similar size and included diclofenac, ibuprofen, fluconazole, lidocaine, nicotine, propranolol, ethanol, 5-fluorouracil, methyl salicylate, salicylic acid, salicylic compounds and trolamine salicylate.

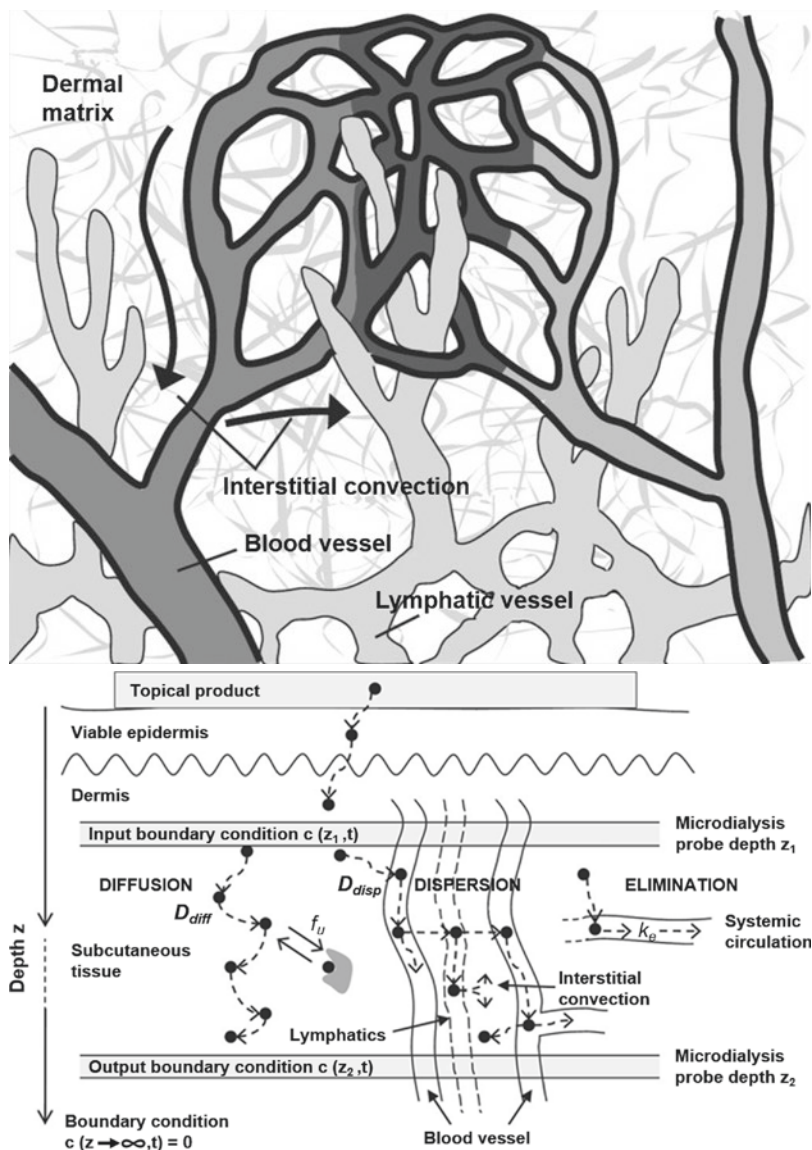
They observed that, in general, the concentration gradients for highly protein bound drugs for deeper tissue penetration tended to be shallow, whereas the poorly bound drugs showed an exponential concentration gradient. They applied a physiological pharmacokinetic analysis to this data and concluded that highly plasma protein bound drugs, in addition to normal diffusive transport, may be transported in deeper tissues via the blood and lymphatic circulation as well as via interstitial convection (Fig. 4.6) and that these transport routes may dominate in some cases. Such vascular transport can increase deep tissue concentrations beyond those resulting from extravascular diffusion alone, and decrease the drug's lag time into deep dermis, subcutaneous and muscle tissue.

---

#### **4.7 Skin Hydration and Percutaneous Absorption**

Transdermal delivery can also be controlled by the extent of skin hydration, which mainly refers to the extent of hydration in the SC. A major controller of hydration is natural moisturising factor (NMF). The original bricks and mortar description of the SC has been refined substantially and it is now described as being a continuous poly-proteinaceous structure, with the bricks being likened to NMF-containing keratin sponges. NMF functions as a plasticiser of the stratum corneum under basal conditions (Laden 1967; Jokura et al. 1995). Following the addition of water or under conditions of high humidity, the NMF-bound water assists in the swelling of the corneocytes. Swelling is at its greatest in regions where the NMF concentration is at its highest (Bouwstra et al. 2003). It has been shown that when the skin is highly hydrated, water is predominantly located either in the intercellular regions in separate domains or trapped in corneocytes (Roberts et al. 2008). In addition, swollen corneocytes and separation of lipid bilayers in the intercellular space to form cisternae and networks of spherical particulates are found in porcine skin after a 4–10-h hydration period

**Fig. 4.6** Physiological pharmacokinetic model for topical drug transport processes in deeper skin. (a) Blood vessels, lymphatic vessels and interstitial convection in dermis. (b) Schematic of physiological pharmacokinetic model used to analyse human cutaneous microdialysis data at two depths, the concentration–time profile in the superficial microdialysis probe being used as an input to predict the deeper microdialysis probe concentration–time profile (Reproduced with permission from (Dancik et al. 2012))



(Tan et al. 2010). Figure 4.7 shows high magnification cryo-scanning electron microscopy images of human SC in various hydration states, showing clearly the swollen corneocytes and water pools present at high levels of hydration (Bouwstra et al. 2003).

The hydration state of the stratum corneum is mainly influenced by environmental humidity, temperature, transepidermal water loss (TEWL) rate, keratinisation rate and the type of moisturisers (Vergnanini et al. 2010). The inverse relationship between TEWL and SC hydration is well

known, just as disturbed skin barrier function has been correlated with low SC hydration (Proksch et al. 2008).

In the presence of an intact barrier, increasing the water content of the skin can have substantial effects on the transdermal delivery of penetrants by altering skin physiology. In clinical practice, occlusion of the skin, by which the hydration of the SC can be greatly increased, is widely used to enhance the penetration of topically applied drugs (Hafeez and Maibach 2013). A number of factors could contribute to the increased permea-

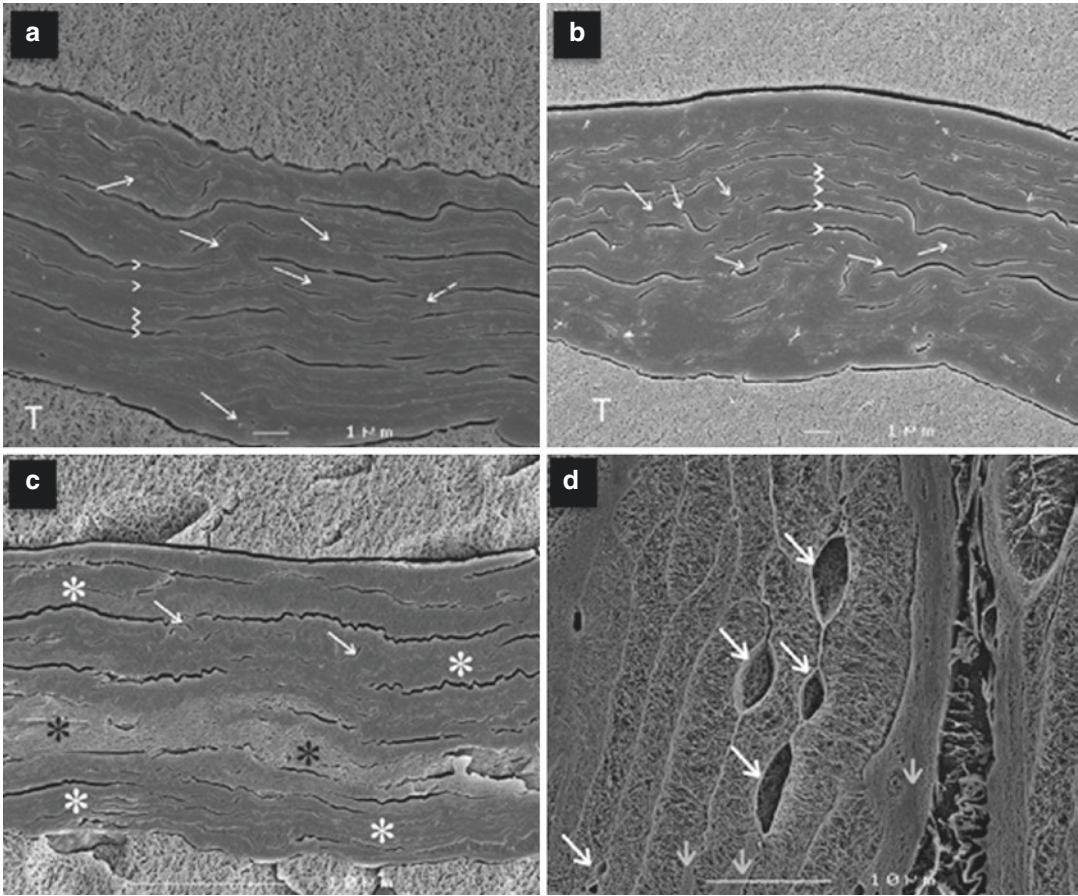


**Fig. 4.7** High magnification cryo-scanning electron microscopy images of SC hydrated to various levels. *Arrows* indicate undulations or interdigitations of cells. *Arrowheads* indicate the cell boundaries. **(a)** Dry SC characterised by low contrast images. The cells are approximately 360 nm in thickness. The spaces between the corneocytes are mostly air-filled, possibly caused by drying of the SC required for low hydration levels. *Arrows* indicate undulations or interdigitations of cells. *Arrowheads* indicate the cell boundaries. T, tissue-freezing medium. **(b)** SC hydrated to 17% wt/wt reveals a low contrast image, similar to that observed for dry skin. This indicates the absence of water pools. **(c)** SC hydrated to 70% wt/wt reveals in the central part slightly swollen cells with a higher contrast (see

*black asterisks*) indicating the presence of water. In the upper and lower part, the appearance of the SC is similar to that of dry skin (*white asterisks*). **(d)** A high magnification of a fully hydrated SC sheet. The keratin network is clearly depicted. This network is surrounded by the cornified envelope. Between the cells frequently large and very small water pools are observed (see *white arrows*). If no water pools are present a close cell to cell contact is observed. The cell ends are round and fewer undulations are observed compared to dry SC or SC hydrated to approximately 20% wt/wt. A difference in the degree of swelling between the various cells is noticed. The cells that are less swollen are indicated by short arrows (Reproduced with permission from Bouwstra et al. 2003)

bility. Firstly, it is likely to be due to an increase in the solubility of the permeant in the SC. This increases the partitioning of the solute from the vehicle into the membrane. Another possibility is that the increased hydration could lead to swelling of the structure and rearrangement of the lipids. Recent work using Raman spectroscopy demonstrated that increased amounts of unbound

water in the stratum corneum, also illustrated by cryo- electron microscopy (Fig. 4.7) could disorder the structures of lipids and proteins (Vyumvuhore et al. 2013), thereby altering the permeation rate of topically applied solutes. Changes in skin hydration may affect skin permeation by several orders of magnitude as previously described (Roberts 1991; Roberts and

Walker 1993). Evidence shows that increasing room humidity can lead to a marked increase in absorption for a range of solutes including aspirin, fusidic acid, methylethylketone, various corticosteroids, etc. (Roberts and Walker 1993).

Interestingly, current findings suggest that there are no quantitatively defined relationships between hydration-enhanced skin permeability and the lipophilicity and molecular structure of the solutes, although the early study by Wurster and Kramer (1961) suggested that hydration preferentially enhanced the skin penetration of the more polar salicylate esters.

Taylor et al. (2002) found that occlusion of the skin affected the skin penetration of linoleic acid and glycerol differently, with occlusion suppressing the delivery of linoleic acid from an ethanolic vehicle compared to the unoccluded condition, but with little influence on the percutaneous absorption of glycerol. Work by Hikima and Maibach (2006) showed a random distribution in human skin fluxes of steroids in relation to their lipophilicity or molecular weight when the skin was either hydrated or dehydrated. A similar result was found by Bucks and Maibach (2005), where a series of phenolic compounds with varying lipophilicity was examined. In the same study, the more lipophilic steroids appear to have a greater enhancement by occlusion than the more polar ones (Fig. 4.8).

It should be noted that the effects of occlusion on skin permeation are not clearly defined or uniform (Roberts et al. 2004; Pellanda et al. 2007). For example, Cevc et al. (2008) found that skin occlusion suppressed the permeation of ketoprofen delivered from ultra-deformable, hydrophilic transfersome carriers by apparently eliminating the transcutaneous water gradient that normally drives the transfersomes across the skin. In contrast, the permeability of topically applied free ketoprofen was promoted by occlusion. Samaras et al. (2012) further showed that skin occlusion had a significant non-linear effect in their statistically valid QSAR developed from an extended database. Hafeez and Maibach (2013) recently concluded that occlusion was more effective in enhancing permeation of very lipophilic compounds than in relatively hydrophilic compounds, but emphasised that no clear relationship between

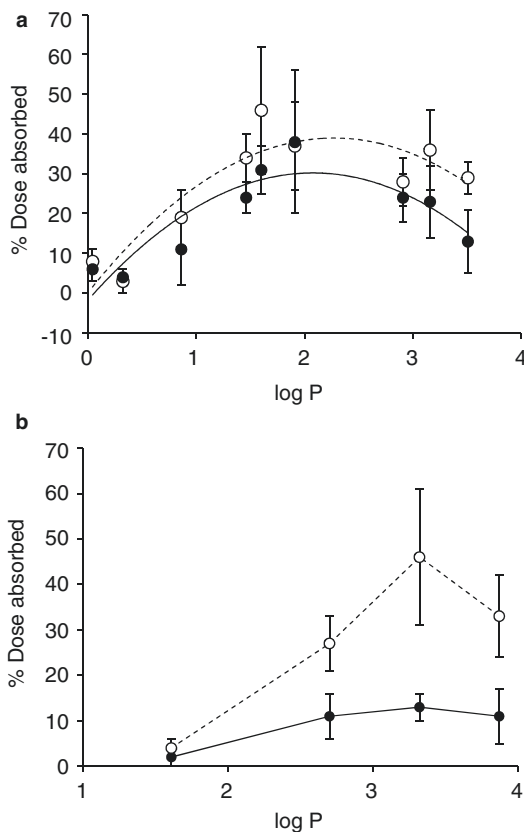


**Fig. 4.8** Occlusivity does not uniformly enhance penetration of solutes with varying octanol water partition coefficient ( $\log P$ ) across human skin in vivo: (a) Phenols, (b) steroids; open symbols occluded, closed symbols unoccluded (Data modified from (Bucks and Maibach 2005))

lipophilicity and occlusion-induced permeation enhancement could be discerned.

Occlusion is not the only means of increasing skin hydration. Chemical and physical enhancement methods can also affect skin hydration. For instance, iontophoresis may hydrate the stratum corneum due to the formation of water pools in the intercellular regions (Fatouros et al. 2006). Water-binding agents (humectants and or hydrating agents) are also classified as moisturisers that prevent water loss and have a softening and soothing effect on the skin. For example, urea, an ingredient in some hair conditioners, facial cleansers, bath oils, skin softeners and lotions, has good water-binding and exfoliating properties for skin when used in small amounts. Some studies have also shown that urea may act as a

penetration enhancer (Wohlrab 1984, 1990; Beastall et al. 1986). Glycerin based creams, very familiar to most consumers, also have humectant properties. Humectants with a small molecular size (e.g. urea and glycerin) are assumed to penetrate into the stratum corneum, mimicking the role of natural moisturising factors to retain moisture (Caussin et al. 2007). However, the mode of action is still poorly understood (Loden 2008).

#### 4.8 Age-Related Skin Barrier Performance

Epidermal development, including SC structure, is complete in utero by 34 weeks. Pre-term babies have elevated levels of both TEWL and transcutaneous heat transfer, which as expected, are largely dependent on how premature the baby is. Ultra-low birth weight infants from the ages of 23–25 weeks were shown to need at least 4 weeks to develop a fully functional SC, whereas babies of 30–32 weeks had barrier functions comparable to adults (Kalia et al. 1998; Fluhr et al. 2004).

It has been widely reported that premature infant skin is more susceptible to penetration than fully formed infant skin. A study by Anderson et al. showed that when hexachlorophene was used as a disinfectant on the skin of pre-term infants, dermal absorption occurred which resulted in myelinopathy in the premature infants (Anderson et al. 1975). Another study by Barker et al. examined the permeation of sodium salicylate through ex vivo newborn infant skin. It was found that absorption of the compound was 100–1000 times higher in infants who had a gestation period of 30 weeks or less, compared to full term infants (Barker et al. 1987).

Giusti et al. measured the TEWL, capacitance and pH of the volar forearm and buttocks of 70 infants aged 8–24 months and compared these to values in adult skin (Giusti et al. 2001). As expected, no differences in TEWL were found between the infants and adults at either site, confirming that the infant skin had a fully developed barrier function. Capacitance values, which quantify the amount of water in the SC, were

found to be higher in infants, as were the pH readings. No TEWL, capacitance or pH variations were observed in infants according to sex or age.

As the skin ages, certain structural changes occur, so that the aged SC is considerably drier than that of a young adult, it has a reduced lipid content and frequently has a less extensive micro-circulation. The epidermis becomes thinner and the keratinocytes become less adjacent to one another. The dermis also becomes relatively atrophic, acellular and avascular. Collagen, elastin and glycosaminoglycan are also altered. Exactly how the penetration barrier of the skin changes with age remains unclear; however, it should be assumed that aged skin provides a more variable environment for the diffusion of topically applied drugs, as discussed below (Byl 1995).

Waller and Maibach reviewed the literature on the effect of aging on blood flow, pH, thickness and ultrasound echogenicity (Waller and Maibach 2005). They concluded that the data which described age-related changes in skin structure and function were often conflicting and difficult to interpret. The cutaneous blood flow results suggested that there may be a trend towards decreased cutaneous perfusion in older individuals, especially in photo-aged areas. The skin pH data were more convincing, as it appears that skin pH is constant throughout adulthood to approximately 70 years of age. After 70, the pH increased, which was suggested to be due to stasis of blood, especially in the lower limbs. The change in thickness of the skin layers seemed to have been influenced more by site on the body than by age. The epidermis thickens with age on certain sites such as the volar and dorsal upper arm, but remains constant in areas such as the buttock, dorsal forearm and shoulder. Similar variations were noted for dermal thickness.

TEWL has been used as an indication of the effect of aging on barrier function. Hillebrand and Wickett noted considerable variability in TEWL with age in Chinese female women living in Beijing, with a quadratic regression showing little change between 10 and 70 years (Hillebrand and Wickett 2008). They point out that an alternative explanation for these findings is that the



women in the different age groups experienced different stresses (sun, diet, exercise) depending on where they were born, which may dominate any relationship between TEWL and skin age. In another study of adults aged 19–85 years showing no correlation of ventral forearm TEWL with age, Roskos and Guy concluded that the ability of the SC to control evaporation from the skin is not age-dependent and its ability to prevent dehydration is also maintained as a subject ages (Roskos and Guy 1989). When the SC barrier was deliberately perturbed by occlusion, the water activity gradient was lost more rapidly in the younger group (age 19–42) than the older group (age 69–85). The time it took for water to diffuse through the SC was longer for older patients. It was explained that when the tissue was occluded, less water may have been required for the SC to achieve the fully hydrated equilibrium state. As older skin has been shown to have reduced water content, it requires more water to achieve a fully hydrated state. It is possible that occlusion in the older subjects produces a hydration-induced structural alteration of the intercellular lipid organisation. The subsequent dehydration (and reorganisation of this structural modification) could manifest slower release kinetics. Similar findings of a minimal effect of age on TEWL at six different body sites in women were reported by Luebberding et al. (2013). In the same study, significant decreases in sebum production were seen with increasing age, with the lowest skin surface lipid levels seen in subjects over 70 years old.

Despite the minimal effects of age on barrier function with regard to TEWL, age-related changes in percutaneous permeation have been reported. Roskos et al. examined the penetration of a range of drugs in young (18–40) and old (>65) volunteers, to test whether permeation through aging skin varies across a range of penetrants with different physicochemical properties (Roskos et al. 1989). Testosterone (TST), estradiol (EST), hydrocortisone (HC), benzoic acid (BA), acetylsalicylic acid (ASA) and caffeine (CS) were administered topically to the ventral forearms of volunteers. The permeation of HC, BA, ASA and CS was significantly lower in older volunteers,

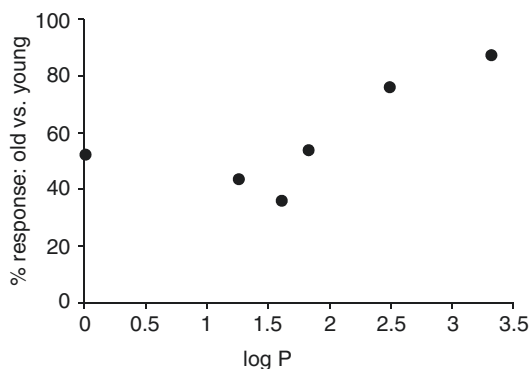


**Fig. 4.9** Percutaneous permeation data. Cumulative % dose absorbed for six drugs, expressed as the ratio of responses in old (>65 years) and young (22–40 year) subjects, versus log P of the drug. Drugs, in order of increasing log P, are caffeine, acetylsalicylic acid, hydrocortisone, benzoic acid, estradiol, testosterone. The effect of age is most pronounced for the more hydrophilic compounds (Data modified from (Roskos et al. 1989))

while the absorption of both of the most lipophilic compounds TST and EST was similar in the older and younger volunteers (see Fig. 4.9).

Rougier et al. showed a similar age-related decrease in benzoic acid permeation in older male subjects (65–80 years), compared to younger subjects (20–30 and 45–55 years), in the absence of changes in TEWL (Rougier et al. 1988), which appeared related to changes in corneocyte surface area (see Sect. 9, below). These results indicate that the more hydrophilic the compounds are, the more their permeation is affected by the age of the volunteer's skin. This work agrees with the previous findings showing that, as the skin ages, the SC surface becomes drier and sebaceous gland activity is reduced. The authors concluded that reduced lipid content in aging skin results in a poorer dissolution medium for topically applied chemicals. Accordingly, the percutaneous permeation of the more hydrophilic molecules is more affected than lipophilic molecules. As aged skin is drier, the reduced water content also favours the permeation of more lipophilic molecules.

To conclude, it seems that two main age-related changes in barrier properties of skin are expected: decreased barrier performance in pre-term babies and moderate change in skin barrier

performance in elderly; the effects of which, however, depend on the physicochemical properties of the permeant. However, there are also a number of confounding environmental and genetic factors at play and these may dominate over any underlying apparent relationship between skin permeation and aging. A combination of factors, including reduced lipid and water content of the SC, may be responsible for the permeation behaviour of certain types of molecules through aging skin.

#### 4.9 Site-Related Skin Barrier Performance

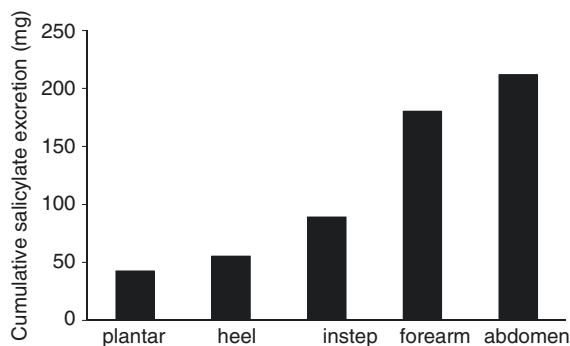
Site-related or regional variations in SC structure are well recognised and may be reflected in differences in permeability of the skin (Feldmann and Maibach 1967; Scheuplein and Blank 1971). A key determinant for differences between sites is SC thickness, which can vary from 400 to 600  $\mu\text{m}$  for the plantar and palmar callus to 10–20  $\mu\text{m}$  for the back, arms, legs, and abdomen (Rushmer et al. 1966). The differences in thickness are manifested in delayed responses to materials applied to plantar and palmar skin, compared to other sites. As seen in data for water permeation quoted by Scheuplein and Blank, the greater thickness of plantar skin leads to longer lag times, despite its having greater permeability to water than abdominal skin. The increased lag time effectively masks the increased permeability (Scheuplein and Blank 1971). Indeed, it has been suggested that plantar and palmar SC should be considered separately from the thinner horny layers at other sites (Kligman 1964; Scheuplein and Blank 1971). Results from the Roberts group showing 48-h cumulative urinary salicylate excretion following topical application of methyl salicylate on five separate body sites for 10 h (Fig. 4.10) clearly show the effect of increased SC thickness (Roberts et al. 1982).

Various studies mapping the regional variations in TEWL, hydration and other skin parameters skin (Marrakchi and Maibach 2007; Kleesz et al. 2012; Luebberding et al. 2013) and the permeability of hydrocortisone (Feldmann and

Maibach 1967), pesticides (Maibach et al. 1971) and other chemicals (Rougier et al. 1987) have been reported, with scrotal, forehead and wrist skin generally more permeable than skin on the trunk and periphery. Rougier et al. showed a good correlation between benzoic acid permeation (measured as  $^{14}\text{C}$ -benzoic acid excretion and TEWL) across seven different body sites in humans (Rougier et al. 1988). This work also showed the forehead to be the site of greatest permeability for water loss (scrotal skin was not examined).

In addition to mapping, attempts have been made to relate the regional variations in skin permeability to skin properties. Early work by Plewig and Marples showed significant regional differences in corneocyte dimensions, with the smallest cells found in the forehead (Plewig and Marples 1970). The authors suggested that these cellular variations could explain previous observations of regional differences in TEWL (Baker and Kligman 1967) and hydrocortisone (Feldmann and Maibach 1967). Recent work from Hadgraft's laboratory (Hadgraft and Lane 2009; Machado et al. 2010a) has suggested a mechanism, in which smaller corneocytes can pack more closely together, resulting in a shorter intercellular path length for permeating molecules to traverse the layers of corneocytes. Machado et al. have calculated the intercellular path length from the corneocyte surface area and the number of cell layers at six body sites, and shown an excellent correlation between the reciprocal of path length and TEWL (Machado et al. 2010a). As noted previously, the forehead had the smallest corneocyte surface area, the smallest number of cell layers and the greatest TEWL. Earlier work by Rougier et al. (1988) examined the effect of corneocyte size on benzoic acid permeation as well as TEWL in humans and concluded that regional differences in permeation could not be entirely explained by corneocyte size alone and that other factors were important, especially for corneocytes  $<600\ \mu\text{m}^2$  or  $>1000\ \mu\text{m}^2$ . A re-analysis of Rougier et al.'s data for benzoic acid permeation supports this conclusion. If  $1/\text{path}$

**Fig. 4.10** Cumulative urinary salicylate excretion showing the effect of stratum corneum thickness at five different body sites on the percutaneous absorption rate of methyl salicylate (commercial 25% formulation) applied to a 50 cm<sup>2</sup> area for 10 h (Data modified from (Roberts et al. 1982))



length is calculated and plotted against TEWL and permeation results for four body sites, the correlation for TEWL ( $R^2=0.98$ ) is very strong, while that for benzoic acid permeation is weaker ( $R^2=0.75$ ).

Noting that the forehead contains a high concentration of sebaceous glands, Maibach explained the relatively high hydrocortisone permeation at this site by suggesting that a substantial amount of permeation was probably occurring through the follicles rather than the SC (Feldmann and Maibach 1967; Rougier et al. 1987). This may be considered unlikely, since it had been accepted that hair follicles made up less than 0.1% of the surface area of the skin (Schaefer and Redelmeier 1996). However, the Lademann group has identified significant regional variations in follicle size and distribution in seven body sites (Otberg et al. 2004). The volume and surface area of the follicular infundibula per square centimetre of skin was greatest in the forehead and least in the forearm, with the overall pattern of follicular distribution being similar to that seen in variations in TEWL (Rougier et al. 1988) and chemical permeation (Feldmann and Maibach 1967; Maibach et al. 1971; Scheuplein and Blank 1971; Rougier et al. 1987, 1988). These correlations indicate that the follicular route may contribute significantly to chemical permeation and water transport and that variations in follicular size and distribution may contribute to regional variations in skin permeability. It is not clear whether the significantly greater sebum content on the forehead skin surface (Rougier et al. 1987;

Luebberding et al. 2013) impacts on the permeation of molecules with different physicochemical properties, although decreasing or artificially increasing the level of sebum on the skin surface has no effect on transepidermal water loss (Kligman 1963).

Based on their results from permeation of water and salicylic acid across abdominal and leg skin, Elias et al. have suggested that the regional variations in skin permeability arise mainly from differences in the lipid content in the epidermal layers (Elias and Brown 1978). The permeation of each solute was found to correlate inversely with the percentage lipid content in each piece of skin but did not relate to the number of cell layers or the SC thickness. Given the relatively low permeation of chemicals at these two sites compared to the forehead (Wester et al. 1984), their similarity in SC thickness (Ya-Xian et al. 1999) and the likelihood of a similar contribution by follicles (Otberg et al. 2004) Elias and Brown may have been able to reveal a dependence on SC lipids in the absence of other strong contributing differences.

Laser Doppler techniques allow the measurement of blood flow to surface tissues. Johnson et al. found regional differences in basal skin blood flow across the forearm (Johnson et al. 1984), while in kinetic studies with topical application of the vasodilator benzyl nicotinate, variations in cutaneous blood flow, temperature and redness were seen across the forehead, forearm and calf, both basally and in response to the drug (Jacobi et al. 2006). The forehead had a higher blood flow and

greater and more rapid responses to the vasodilator. These results suggest that differences in cutaneous blood flow may also account for regional differences in skin permeability *in vivo*.

Figure 4.11 attempts to summarise the state of knowledge on regional variations in skin permeation and some of the factors that may contribute to this.

In conclusion, the influence of the site of application on percutaneous permeation of topical formulations or any material which comes into contact with the skin is substantial and depends on different variables as discussed above. This implies that for optimised delivery, dermatological formulations should be designed in a way that the formulation, and not the skin, controls the rate of delivery if it is designed for different skin areas.

As well, the site of application should be specified on the product if the site dependency in absorption affects the treatment or safety.

#### 4.10 Gender-Related Skin Barrier Performance

As far as the skin structure is concerned, studies by Fluhr et al. in 33 pre-menopausal women, 21 post-menopausal women on no hormone replacement and 25 male subjects found that the skin of pre-menopausal women contained significantly smaller corneocytes compared to the other two groups (Fluhr et al. 2004). The authors hypothesised that sex hormones may have an effect on corneocyte area, since sex hormone levels are normally elevated in pre-/ post-menopausal

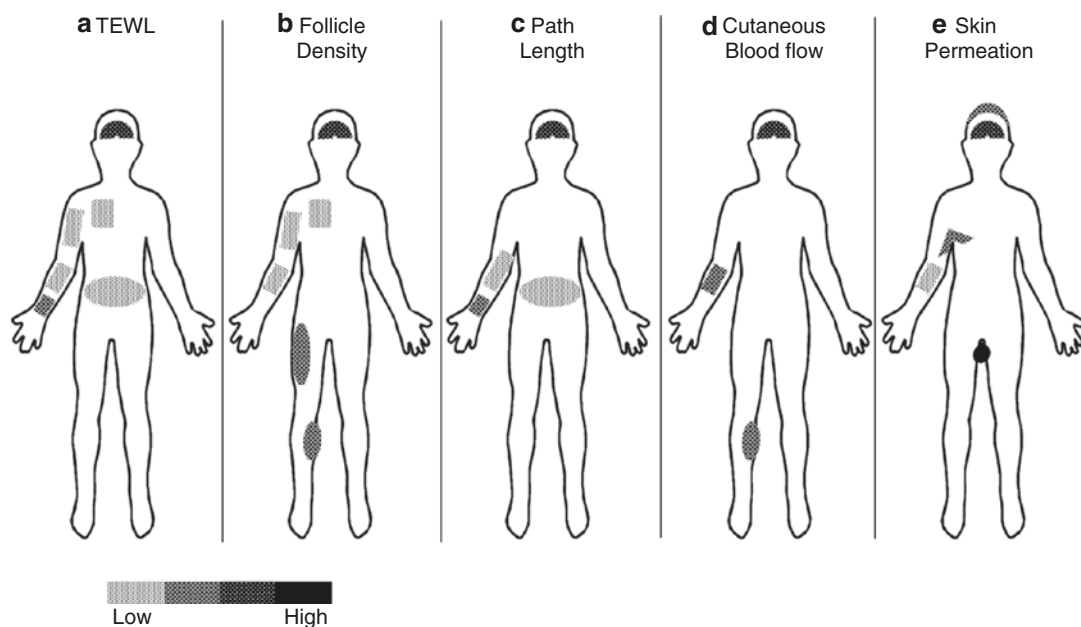


**Fig. 4.11** Regional differences in responses and properties of human skin based on rank order. (a) TEWL (Rougier et al. 2005); (b) follicle density, expressed as infundibular surface area  $\text{mm}^2$  per  $\text{cm}^2$  of skin (Otberg et al. 2004); (c) minimum intercellular path length through the stratum corneum, based on corneocyte surface area

and the number of cell layers (Machado et al. 2010a); (d) cutaneous blood flow determined by Laser Doppler flowmetry (Jacobi et al. 2006); (e) skin permeation of hydrocortisone (Feldman and Maibach 1967) and parathion (Maibach et al. 1971), both measured as total urinary excretion of the  $^{14}\text{C}$ -compound over five days

women compared to the other two groups. No differences in corneocyte size were observed by Machado et al. when male and female subjects aged 20–60 years were compared (Machado et al. 2010a).

Prather et al. carried out a study in which the differences in permeation of nicotine from a Nicoderm® transdermal delivery system (Alza Corp.) based on gender was examined (Prather et al. 1993). Following a 24-h application of the transdermal nicotine system, the levels in nicotine plasma concentration ( $C_{\max}$ ) and area under the curve (AUC) did not vary significantly between women and normal-sized men.

A recent review by Machado et al. supports the above observations, and suggests that skin barrier function does not seem to vary with gender (Machado et al. 2010b). Reed et al. also concluded that there were no gender-related differences in barrier integrity and barrier recovery and that any conflicting results may be due to changes in the skin's barrier function related to the menstrual cycle (Reed et al. 1995).

To conclude, the above-mentioned studies might reveal that among different biological factors, gender seems to have lowest effect on percutaneous absorption of drugs. Accordingly, as a rule of thumb, and until proven otherwise, all laboratories use mixtures of male and female skin samples for their investigations indiscriminately and there is no gender-specified product in the market.

---

## 4.11 Barrier Performance in Cosmetically Treated Skin

Application of products on the skin for cosmetic purposes is widespread. Some products, such as moisturising creams, insect repellents and sunscreen creams are used by everyone irrespective of age and gender, while depilatory creams, deodorants, antiperspirants, and anti-aging products are more age and gender specific. Cosmetic products contain ingredients that can alter both the structure and function of the skin and a

change in barrier performance is, therefore, anticipated. This is important because the application of therapeutic agents is sometimes accompanied by the application of cosmetics. As a result, impaired skin barrier properties that may occur in cosmetically treated skin can increase the risk of dermatotoxicity. In this section, we will examine the influence of certain actives found in cosmetic products on skin barrier function.

### 4.11.1 Insect Repellents

Insect repellent creams, lotions and sprays are widely used products, having been available to the public for more than 50 years. N,N-diethyl-m-toluamide (DEET), a hydrophobic compound, is the most common ingredient of insect repellents with more than 200 million people using products containing various concentrations of this active (10% or higher) worldwide (Debboun et al. 2006). The absorption of DEET into the circulatory system and its relative toxicity are topics that have been of interest. However, it is equally interesting to note that DEET is also considered to be a permeation enhancer, shown to improve the dermal and transdermal delivery of a variety of drugs through hairless mouse skin (Windheuser et al. 1982).

Kondo et al. (1988) reported no increase of absorption of nifedipine in the presence of DEET while Ogiso et al. (2002) observed a slight increase in indomethacin flux. However, it has been reported that mixtures of DEET and DES (diethyl sebacate, a lipophilic vehicle with enhancer properties used in medications and cosmetics such as shaving lotions) resulted in a remarkable increase in nifedipine penetration (Kondo et al. 1988). This finding might indicate that DEET is not an effective permeation enhancer when employed alone. It would be interesting to discover if the application of a cosmetic cream containing DES before or after the application of insect repellent would increase the penetration of the actives contained in the aforementioned cream.

### 4.11.2 Chemical Depilatories

A plethora of products and services is available on the market for hair removal, ranging from high-tech laser removal to the more conventional systems, such as shaving and depilatory formulations, that are the subject of the present review. The two main components of these formulations are calcium thioglycolate and potassium thioglycolate. Keratin filaments contained in hair strands are strengthened by intercellular disulphide bridges formed between two cysteine residues. Calcium and potassium thioglycolates reduce these intercellular bonds thus compromising the structural integrity of hair strands. As a result, the hair can be easily removed by scraping or rubbing (Goddard and Michaelis 1934).

The absence of the hair shaft is influential in promoting cutaneous absorption through the transfollicular route. Hair removal induces the hair follicle and greatly enhances the low-resistance character of this pathway (Han et al. 2004). Corneocytes also contain keratin filaments, which constitute a major structural protein, located within the cornified cells and in the cell envelope (Madison 2003). Therefore, depilatory agents will also be able to reduce the disulphide bridges contained in corneocytes, weakening their structure. Lee et al. found that the transdermal penetration of both hydrophilic and lipophilic compounds through rat skin pre-treated with a depilatory agent was significantly enhanced and that this enhancement persisted for 24 h after application (Lee et al. 2008). This suggests that the structural changes induced by the depilatory agent may be restored later.

The mechanism of thioglycolate-induced permeation enhancement is not well understood. It has been reported that the structural changes induced by thioglycolate-based depilatory creams enhanced drug delivery through both the transcellular and intercellular SC pathways (Lee et al. 2008). Shiozuka et al. also reported changes in SC structure after treatment by a depilatory agent (Shiozuka et al. 2010). Whereas the normal SC is characterised by tight packing of clearly defined cells, treatment with a depilatory agent produced some highly noticeable morphological changes. Firstly, struc-

tural changes in the SC were observed and the definition of cell borders was disrupted, presenting a 'homogenised' pattern (Lee et al. 2008). Secondly, the volume of intercellular spaces and gaps increased (Shiozuka et al. 2010). Consequently, the barrier function of the SC is compromised and resistance to transdermal delivery is greatly reduced. However, no studies have been conducted to date exploring the effects of chronic application of calcium or potassium thioglycolate. Therefore, one would not be able to conclude if continued use of depilatory creams induces any long-term structural or permeability changes in the skin. Some other hair removal methods also can affect skin permeation of compounds. It has been shown that shaved skin enhances the permeation of aluminium salts (Anane et al. 1997).

### 4.11.3 Peeling Agents

The anti-ageing industry, worth billions of dollars, has an overwhelming number of products and treatments promising to turn back the clock. One example is chemical peeling, which involves treating the skin with low concentrations of phenol or  $\alpha$ -hydroxy acids (AHAs), such as glycolic or salicylic acid to remove the superficial layer of the skin, the SC and to stimulate its renewal. These acids are known to cause irritation to the skin by producing one of the following reactions: keratolysis or keratocoagulation (Brown et al. 1961). Keratolysis leads to the necrosis of the SC and its separation from the viable epidermis whereas keratocoagulation involves the irreversible phenomenon of denaturation and coagulation of keratin (Rothman 1943). Consequently, the skin barrier function is significantly altered after this procedure. AHAs reduce the skin barrier integrity by reducing corneocyte cohesion and their influence extends to the newly forming layers of the SC, resulting in the formation of more supple superficial layers (Van Scott and Yu 1984). In this direction, Song et al. reported that the increase in TEWL observed in vivo after glycolic acid treatment returned to pre-treatments values after one day (Song et al. 2004).

#### 4.11.4 Other Cosmetic Products

There are many other cosmetic products that can affect barrier performance of the skin or percutaneous absorption of drugs. One group is moisturising agents that affect hydration level of skin, as described in previous sections of this chapter. Surfactant-containing products may also affect percutaneous absorption. Some surfactants (e.g. sodium lauryl sulphate) are well known for their enhancement effects on drug absorption through the skin. Other cosmetic products contain ingredients such as glycols or barrier creams that can decrease permeation of drugs, as explained later in this chapter.

To conclude, this review shows that cosmetic products are not permeability-inert compounds and, therefore, their effects on the permeation of other compounds that are possibly applied concomitantly, should be considered. Such considerations will help optimised drug delivery and minimise side effects.

---

### 4.12 Compromised Barrier Performance

The SC barrier can be compromised by a range of insults, including exposure to environmental or industrial chemicals; excess water; cosmetic ingredients such as surfactants, which may cause irritation; physical damage, including abrasion or burns; and various skin disorders. Hillebrand and Wickett point out that TEWL can also vary with the time of the day and year (Hillebrand and Wickett 2008). Generally, TEWL is higher in the day than at night and in the winter rather than in the summer months. The rate of barrier repair appears to be slower in the aged.

#### 4.12.1 Intrinsic Barrier Defects

It is likely that intrinsic defects in the skin barrier, which may be genetic in origin, contribute to conditions whereby irritant chemicals penetrate the skin more readily, driving the development of atopic dermatitis in susceptible individuals (Elias and Schmuth 2009). Thus, in Netherton syn-

drome there is a strong association between defective serine protease expression, causing an abnormally thin SC barrier and the severe atopic dermatitis characterising this condition (Hachem et al. 2006). Similarly, loss-of-function mutations in the filaggrin (FLG) gene cause a range of SC barrier defects (Hudson 2006), including abnormalities in hydration due to reduced NMF content (Kezic et al. 2008). Reduced filaggrin expression has been linked to atopic dermatitis and ichthyosis vulgaris (Elias and Schmuth 2009). In addition to the underlying, intrinsic barrier defect, environmental or other stressors may be involved or required for the inflammatory condition to become manifest. This may be exemplified by a study in children with atopic dermatitis, where even clinically uninvolved skin was shown to have defective barrier function by TEWL, pH and capacitance, compared to normal subjects (Seidenari and Giusti 1995).

#### 4.12.2 Thermally Damaged Skin and Its Manipulation

Burn injuries to the skin may result in enzyme malfunction, lipid damage, denaturation of proteins and destruction of protein architecture, impaired blood flow and subsequently ischemia and necrosis and creation of a dead eschar (Moritz and Henriques 1947; Jackson 1953; Bullock 1996). Microorganisms may also colonise the burn wound, proliferate on the eschar and progress in depth and make the structure of the barrier more complicated (Moritz and Henriques 1947; Jackson 1953; Monafo and West 1990; Bullock 1996). While topical therapy is a mainstay of burn treatment (Moghimi and Manafi 2009), a better understanding of the permeation properties of burnt tissue and its barrier performance towards the permeation of different drugs could lead to improvements in this area.

Early studies by the Flynn group in the 1980s, using excised mouse skin, showed that scalding with 60 °C water increased the permeability of skin to water, methanol, ethanol, n-butanol and n-octanol by up to three times (Behl et al. 1980). They further showed that permeability to all compounds

continued to increase with increasing temperature, with a sharp transition in barrier properties occurring between 70 and 80 °C (Behl et al. 1981). The effects at lower temperatures were attributed to the increased hydration associated with scalding, while at higher temperatures, the increase in permeability was attributed to morphological and/or chemical alterations in the SC (Behl et al. 1981).

The effects of higher temperatures have been studied recently by Park et al. using full-thickness skin, epidermis and SC samples from human and porcine cadavers heated to temperatures ranging from 100 to 315 °C. They found that skin permeability was increased by a few fold after heating to 100–150 °C, by one to two orders of magnitude after heating to 150–250 °C and by three orders of magnitude after heating above 300 °C. These permeability changes were respectively attributed to the disordering of SC lipid structure for temperatures lower than 150 °C, disruption of SC keratin network structure at 150–250 °C and finally decomposition and vaporisation of keratin to create micron-scale holes in the SC above 300 °C (Park et al. 2008).

The experiments mentioned above were performed on burnt skin separated from the body, whereas in the *in vivo* situation, barrier function is more fully reflective of the range of skin responses caused by the burn. *In vivo* experiments also allow the dynamic effects of the burn to be studied. Flynn et al. followed the progress of mice burned with an 80 °C metal surface and showed that the permeability to methanol and butanol gradually increased after the burn, reaching a maximum on the tenth day, then decreasing until termination of the studies at 14 days (Flynn et al. 1982). The Moghimi group has investigated barrier function in humans, showing increased permeability of fully hydrated full-thickness (1500 µm) third-degree burn eschar to silver sulfadiazine (Zadeh et al. 2008, 2010).

Despite the evidence of reduced barrier function in burned skin, it has been shown that some drugs cannot permeate the burn eschar in therapeutic amounts to overcome infection and drug delivery to and through burn eschar is still a challenge (Moghimi and Manafi 2009). Wang et al. also showed that while fetuin-A (40 kDa) cannot per-

meate the burn eschar, the underlying tissues are permeable to such a macromolecule (Wang et al. 2009). Consequently, there has been interest in techniques to enhance burn eschar permeability to therapeutic substances. For example, Zadeh and Moghimi showed that the permeability of human third-degree burn eschar was very sensitive to the level of hydration and that prolonged exposure to water might open the compact structure of eschar and increase drug permeation through this barrier (Zadeh et al. 2008). The Moghimi group has also achieved success in the use of chemical penetration enhancers with burn eschar. While outside the scope of this review, the work showing that water, glycerin, hexane:ethanol and ethyl acetate:ethanol (Manafi et al. 2008) as well as terpenes such as limonene, geraniol, 1,8-cineole and  $\alpha$ -pinene oxide (Moghimi et al. 2009) were able to increase permeation of silversulfadiazine significantly through human third-degree burn eschar should be noted.

---

#### 4.13 Prevention of Percutaneous Permeation: A Possibility and a Necessity

Intact skin is a very effective barrier and inhibits permeation of most compounds; therefore, skin permeation enhancement has been the subject of much research over last few decades. In spite of this, skin penetration retardation is also a very crucial issue, not only to prevent permeation of toxic chemicals, but also due to the fact that some materials (e.g. polyethylene glycol) that are employed in dermatological formulations for another purposes (e.g. as solvents) can reduce percutaneous absorption of drugs (Moghimi and Shakerinejad 1998).

Human skin is exposed to a number of irritants and toxic material in daily life, some of which have the ability to permeate the skin barrier in toxic amounts and cause local or systemic toxicities, particularly if the barrier is damaged (O'Flaherty 2000). Organophosphates, such as parathion and malathion that are used as insecticides, have caused toxicity and deaths after absorption through the skin (Aaron 2001). The nerve agent VX (an organophosphorus ester)



shows a percutaneous LD<sub>50</sub> of 10 mg for a 70 kg person (Somani and Romano 2000). Another example is hexane that can produce a peripheral neurotoxicity through the skin (O'Flaherty 2000). Different techniques have been developed over time to overcome such transdermal toxicities, as discussed below.

Protective clothing and gloves can provide some degree of protection and are considered to be essential protective items. However, care is necessary, as some gloves cannot prevent penetration of low molecular weight chemicals (Wigger-Alberti and Elsner 1998; Moghimi et al. 2010). Another class of protectants is barrier creams, which contain ingredients that are supposed to trap or transform unwanted material or prevent/delay their contact with the skin by forming a protective barrier at the skin surface (Berndt et al. 2000). Similar to other creams, barrier creams contain different materials such as surfactants (that can act as penetration enhancers) and oily phases (that can increase skin hydration), so that under some circumstances, barrier creams have the potential to increase the permeation of drugs. For example, it has been shown that the percutaneous absorption of trimethylbenzene was increased through skin treated with barrier creams (Korinth et al. 2003). Therefore, in practice, barrier creams are recommended only for low-grade irritants and should be not used as primary protection against high-risk substances. This area has been extensively reviewed (Machado et al. 2010b).

Although beyond the scope of this chapter, other approaches based on the manipulation of formulations for preventing or retarding the percutaneous absorption of chemicals will be briefly mentioned here. The Moghimi group has shown permeation retardation with a range of additives, including complexation with high molecular weight compounds that show low skin permeation, such as polyethylene glycol and  $\beta$ -cyclodextrin (Moghimi and Shakerinejad 1998), the highly hydrophilic polymer, polyacrylamide (Erfan et al. 2012) and polyamidoamine (PAMAM) dendrimers (Moghimi et al. 2010). Kaushik has postulated that the decreased percutaneous permeation seen with certain chemical

retardants may be explained by their actions to increase the organisation of SC lipids (Kaushik et al. 2008, 2010; Kaushik and Michniak-Kohn 2010). Stabilisation of lipid lamellae in the more ordered orthorhombic phase has been associated with enhanced SC barrier properties (Pilgram et al. 1999).

## Conclusion

The interaction of a penetrant with the skin barrier determines its rate of percutaneous absorption and is influenced by the physico-chemical properties of the molecule or particle and the properties of the barrier itself. There is considerable variability in the skin barrier, due to factors such as the degree of hydration, age, gender, anatomical site, abnormalities due to disease or injury and prior treatment with various skin treatments. While most research has concentrated on finding ways to increase percutaneous absorption, retardation may be necessary in some situations, for example, to prevent permeation of toxic chemicals.

**Acknowledgements** Thanks go to the National Health & Medical Research Council of Australia for financial support. The authors also thank Navin Chandrasekaran (Therapeutics Research Centre, School of Medicine, the University of Queensland) for help in drawing figures and Dr Amy Holmes, from (Therapeutics Research Centre, School of Pharmacy and Medical Sciences, University of South Australia), for assistance in editing the chapter.

## References

- Aaron CK (2001) Organophosphates and carbamates. In: Clinical toxicology. WB Saunders Company, Philadelphia, pp 819–828
- Ali J, Camilleri P, Brown MB, Hutt AJ, Kirton SB (2012) Revisiting the general solubility equation: in silico prediction of aqueous solubility incorporating the effect of topographical polar surface area. *J Chem Inf Model* 52(2):420–428
- Anane R, Bonini M, Creppy EE (1997) Transplacental passage of aluminium from pregnant mice to fetus organs after maternal transcutaneous exposure. *Hum Exp Toxicol* 16(9):501–504
- Anderson JM, Kilshaw BH, Harkness RA, Kelly RW (1975) Spongiform myelinopathy in premature infants. *Br Med J* 2(5964):175–176

- Anissimov YG, Roberts MS (2011) Modelling dermal drug distribution after topical application in human. *Pharm Res* 28(9):2119–2129
- Baker H, Kligman AM (1967) A simple in vivo method for studying the permeability of the human stratum corneum. *J Invest Dermatol* 48(3):273–274
- Barker N, Hadgraft J, Rutter N (1987) Skin permeability in the newborn. *J Invest Dermatol* 88(4):409–411
- Beastall J, Guy RH, Hadgraft J, Wilding I (1986) The influence of urea on percutaneous absorption. *Pharm Res* 3:294–297
- Behl CR, Flynn GL, Kurihara T, Smith W, Gatmaitan O, Higuchi WI, Ho NF, Pierson CL (1980) Permeability of thermally damaged skin: I. Immediate influences of 60 degrees C scalding on hairless mouse skin. *J Invest Dermatol* 75(4):340–345
- Behl CR, Flynn GL, Barrett M, Walters KA, Linn EE, Mohamed Z, Kurihara T, Ho NF, Higuchi WI, Pierson CL (1981) Permeability of thermally damaged skin II: immediate influences of branding at 60 C on hairless mouse skin permeability. *Burns* 7(6):389–399
- Benfeldt E, Serup J, Menne T (1999) Effect of barrier perturbation on cutaneous salicylic acid penetration in human skin: in vivo pharmacokinetics using microdialysis and non-invasive quantification of barrier function. *Br J Dermatol* 140(4):739–748
- Berndt U, Wigger-Alberti W, Gabard B, Elsner P (2000) Efficacy of a barrier cream and its vehicle as protective measures against occupational irritant contact dermatitis. *Contact Dermatitis* 42(2):77–80
- Bickers DR, Kappas A (1978) Human skin aryl hydrocarbon hydroxylase. Induction by coal tar. *J Clin Invest* 62(5):1061–1068
- Bouwstra JA, de Graaff A, Gooris GS, Nijssse J, Wiechers JW, van Aelst AC (2003) Water distribution and related morphology in human stratum corneum at different hydration levels. *J Invest Dermatol* 120(5):750–758
- Brown AM, Kaplan LM, Brown ME (1961) Phenol-induced histological skin changes: hazards, technique, and uses. *Br J Plast Surg* 13:158–169
- Brunner M, Dehghanyar P, Seigfried B, Martin W, Menke G, Muller M (2005) Favourable dermal penetration of diclofenac after administration to the skin using a novel spray gel formulation. *Br J Clin Pharmacol* 60(5):573–577
- Bucks DA, Maibach H (2005) Occlusion does not uniformly enhance penetration in vivo. In: Bronaugh RL, Maibach H (eds) *Percutaneous absorption*. Marcel Dekker, New York, pp 65–83
- Bullock BL (1996) *Pathophysiology: adaptations and alterations in function*. Williams and Wilkins, Lippincott
- Byl NN (1995) The use of ultrasound as an enhancer for transcutaneous drug delivery: phonophoresis. *Phys Ther* 75(6):539–553
- Caussin J, Groenink HW, de Graaff AM, Gooris GS, Wiechers JW, van Aelst AC, Bouwstra JA (2007) Lipophilic and hydrophilic moisturizers show different actions on human skin as revealed by cryo scanning electron microscopy. *Exp Dermatol* 16(11):891–898
- Cevc G, Mazgareanu S, Rother M, Vierl U (2008) Occlusion effect on transcutaneous NSAID delivery from conventional and carrier-based formulations. *Int J Pharm* 359(1–2):190–197
- Chen LJ, Lian GP, Han LJ (2010) Modeling transdermal permeation. Part I. Predicting skin permeability of both hydrophobic and hydrophilic solutes. *Am Inst Chem Eng J* 56(5):1136–1146
- Chen LJ, Han LJ, Lian GP (2013) Recent advances in predicting skin permeability of hydrophilic solutes. *Adv Drug Deliv Rev* 65(2):295–305
- Coomes MW, Norling AH, Pohl RJ, Muller D, Fouts JR (1983) Foreign compound metabolism by isolated skin cells from the hairless mouse. *J Pharmacol Exp Ther* 225(3):770–777
- Cross SE, Roberts MS (1999) Defining a model to predict the distribution of topically applied growth factors and other solutes in excisional full-thickness wounds. *J Invest Dermatol* 112(1):36–41
- Cross SE, Anderson C, Roberts MS (1998) Topical penetration of commercial salicylate esters and salts using human isolated skin and clinical microdialysis studies. *Br J Clin Pharmacol* 46(1):29–35
- Cross SE, Megwa SA, Benson HA, Roberts MS (1999) Self promotion of deep tissue penetration and distribution of methylsalicylate after topical application. *Pharm Res* 16(3):427–433
- Cross SE, Pugh WJ, Hadgraft J, Roberts MS (2001) Probing the effect of vehicles on topical delivery: understanding the basic relationship between solvent and solute penetration using silicone membranes. *Pharm Res* 18(7):999–1005
- Dancik Y, Jepps OG, Roberts MS (2008) Physiologically based pharmacokinetics and pharmacodynamics of skin. In: Roberts MS, Walters KA (eds) *Dermal absorption and toxicity assessment*, vol 177. Informa Healthcare, New York, pp 179–207
- Dancik Y, Thompson C, Krishnan G, Roberts MS (2010) Cutaneous metabolism and active transport in transdermal drug delivery. In: Monteiro-Riviere NA (ed) *Toxicology of the skin*. Informa Healthcare USA Inc., New York, pp 69–82
- Dancik Y, Anissimov YG, Jepps OG, Roberts MS (2012) Convective transport of highly plasma protein bound drugs facilitates direct penetration into deep tissues after topical application. *Br J Clin Pharmacol* 73(4):564–578
- Debboun M, Frances SP, Strickman DA (2006) *Insect repellents: principles, methods, and uses*. CRC Press, Boca Raton
- Diez I, Colom H, Moreno J, Obach R, Peraire C, Domenech J (1991) A comparative in vitro study of transdermal absorption of a series of calcium channel antagonists. *J Pharm Sci* 80(10):931–934
- Du Plessis J, Pugh WJ, Judefeind A, Hadgraft J (2002) Physico-chemical determinants of dermal drug deliv-

- ery: effects of the number and substitution pattern of polar groups. *Eur J Pharm Sci* 16(3):107–112
- Elias PM, Brown BE (1978) The mammalian cutaneous permeability barrier: defective barrier function is essential fatty acid deficiency correlates with abnormal intercellular lipid deposition. *Lab Invest* 39(6):574–583
- Elias PM, Schmuth M (2009) Abnormal skin barrier in the etiopathogenesis of atopic dermatitis. *Curr Opin Allergy Clin Immunol* 9(5):437–446
- Erfan M, Moghimi HR, Haeri A, Jafarzadeh Kashi TS, Jafarzade F (2012). Poly (CPP-SA) anhydride as a reactive barrier matrix against percutaneous absorption of toxic chemicals, US Patent 20,120,237,471
- Essa EA, Bonner MC, Barry BW (2002) Human skin sandwich for assessing shunt route penetration during passive and iontophoretic drug and liposome delivery. *J Pharm Pharmacol* 54(11):1481–1490
- Fatouros DG, Groenink HW, de Graaff AM, van Aelst AC, Koerten HK, Bouwstra JA (2006) Visualization studies of human skin in vitro/in vivo under the influence of an electrical field. *Eur J Pharm Sci* 29(2):160–170
- Feldmann RJ, Maibach HI (1967) Regional variation in percutaneous penetration of 14C cortisol in man. *J Invest Dermatol* 48(2):181–183
- Finnen MJ, Herdman ML, Shuster S (1984) Induction of drug metabolising enzymes in the skin by topical steroids. *J Steroid Biochem* 20(5):1169–1173
- Fluhr JW, Pelosi A, Lazzarini S, Dikstein S, Berardesca E (2004) Differences in corneocyte surface area in pre- and post-menopausal women. *Skin Pharmacol Physiol* 14(Suppl 1):10–16
- Flynn GL, Behl CR, Linn EE, Higuchi WI, Ho NFH, Pierson CL (1982) Permeability of thermally damaged skin v: permeability over the course of maturation of a deep partial-thickness wound. *Burns* 8(3):196–202
- Frum Y, Bonner MC, Eccleston GM, Meidan VM (2007) The influence of drug partition coefficient on follicular penetration: in vitro human skin studies. *Eur J Pharm Sci* 30(3–4):280–287
- Giusti F, Martella A, Bertoni L, Seidenari S (2001) Skin barrier, hydration, and pH of the skin of infants under 2 years of age. *Pediatr Dermatol* 18(2):93–96
- Goddard DR, Michaelis L (1934) A study on keratin. *J Biol Chem* 106(2):605–614
- Grice JE, Ciotti S, Weiner N, Lockwood P, Cross SE, Roberts MS (2010) Relative uptake of minoxidil into appendages and stratum corneum and permeation through human skin in vitro. *J Pharm Sci* 99(2):712–718
- Grundmann-Kollmann M, Podda M, Brautigam L, Hardt-Weinelt K, Ludwig RJ, Geisslinger G, Kaufmann R, Tegeder I (2002) Spatial distribution of 8-methoxypsoralen penetration into human skin after systemic or topical administration. *Br J Clin Pharmacol* 54(5):535–539
- Hachem JP, Wagberg F, Schmuth M, Crumrine D, Lissens W, Jayakumar A, Houben E, Mauro TM, Leonardsson G, Brattsand M, Egelrud T, Roseeuw D, Clayman GL, Feingold KR, Williams ML, Elias PM (2006) Serine protease activity and residual LEKTI expression determine phenotype in Netherton syndrome. *J Invest Dermatol* 126(7):1609–1621
- Hadgraft J, Lane ME (2009) Transepidermal water loss and skin site: a hypothesis. *Int J Pharm* 373(1–2):1–3
- Hafeez F, Maibach H (2013) Occlusion effect on in vivo percutaneous penetration of chemicals in man and monkey: partition coefficient effects. *Skin Pharmacol Physiol* 26(2):85–91
- Han I, Kim M, Kim J (2004) Enhanced transfollicular delivery of adriamycin with a liposome and iontophoresis. *Exp Dermatol* 13(2):86–92
- Hewitt M, Cronin MT, Enoch SJ, Madden JC, Roberts DW, Dearden JC (2009) In silico prediction of aqueous solubility: the solubility challenge. *J Chem Inf Model* 49(11):2572–2587
- Higuchi T (1960) Physical chemical analysis of percutaneous absorption process from creams and ointments. *J Soc Cosmet Chem* 11(2):85–97
- Hikima T, Maibach H (2006) Skin penetration flux and lag-time of steroids across hydrated and dehydrated human skin in vitro. *Biol Pharm Bull* 29(11):2270–2273
- Hillebrand GG, Wickert RR (2008) Epidemiology of skin barrier function: host and environmental factors. In: Walters KA, Roberts MS (eds) *Dermatologic, cosmeceutic, and cosmetic development: therapeutic and novel approaches*. Informa Healthcare, New York, pp 129–156
- Hinz RS, Lorence CR, Hodson CD, Hansch C, Hall LL, Guy RH (1991) Percutaneous penetration of para-substituted phenols in vitro. *Fundam Appl Toxicol* 17(3):575–583
- Hotchkiss SAM (1998) Dermal metabolism. In: Roberts MS, Walters KA (eds) *Dermal absorption and toxicity assessment*. Marcel Dekker, New York, pp 43–101
- Hudson TJ (2006) Skin barrier function and allergic risk. *Nat Genet* 38(4):399–400
- Imhof PR, Vuillemin T, Gerardin A, Racine A, Muller P, Follath F (1984) Studies of the bioavailability of nitroglycerin from a transdermal therapeutic system (Nitroderm TTS). *Eur J Clin Pharmacol* 27(1):7–12
- Jackson DM (1953) The diagnosis of the depth of burning. *Br J Surg* 40(164):588–596
- Jacobi U, Kaiser M, Sterry W, Lademann J (2006) Kinetics of blood flow after topical application of benzyl nicotine on different anatomic sites. *Arch Dermatol Res* 298(6):291–300
- Johnson JM, Taylor WF, Shepherd AP, Park MK (1984) Laser-Doppler measurement of skin blood flow: comparison with plethysmography. *J Appl Physiol Respir Environ Exerc Physiol* 56(3):798–803
- Jokura Y, Ishikawa S, Tokuda H, Imokawa G (1995) Molecular analysis of elastic properties of the stratum corneum by solid-state <sup>13</sup>C-Nuclear Magnetic Resonance spectroscopy. *J Invest Dermatol* 104(5):806–812
- Kalia YN, Nonato LB, Lund CH, Guy RH (1998) Development of skin barrier function in premature infants. *J Invest Dermatol* 111(2):320–326

- Kasting GB, Smith R, Cooper E (1987) Effect of lipid solubility and molecular size on percutaneous absorption. In: Shroot B, Schaefer H (eds) *Pharmacology and the skin*, vol 1. Karger, Basel, pp 138–153
- Kaushik D, Michniak-Kohn B (2010) Percutaneous penetration modifiers and formulation effects: thermal and spectral analyses. *AAPS PharmSciTech* 11(3):1068–1083
- Kaushik D, Batheja P, Kilfoyle B, Rai V, Michniak-Kohn B (2008) Percutaneous permeation modifiers: enhancement versus retardation. *Expert Opin Drug Deliv* 5(5):517–529
- Kaushik D, Costache A, Michniak-Kohn B (2010) Percutaneous penetration modifiers and formulation effects. *Int J Pharm* 386(1–2):42–51
- Kezic S, Kemperman PM, Koster ES, de Jongh CM, Thio HB, Campbell LE, Irvine AD, McLean WH, Puppels GJ, Caspers PJ (2008) Loss-of-function mutations in the filaggrin gene lead to reduced level of natural moisturizing factor in the stratum corneum. *J Invest Dermatol* 128(8):2117–2119
- Kleesz P, Darlenski R, Fluhr JW (2012) Full-body skin mapping for six biophysical parameters: baseline values at 16 anatomical sites in 125 human subjects. *Skin Pharmacol Physiol* 25(1):25–33
- Kligman AM (1963) The uses of sebum. *Br J Dermatol* 75:307–319
- Kligman AM (1964) The biology of the stratum corneum. In: Montagna W, Lobitz WC (eds) *The epidermis*. Academic, New York, pp 387–433
- Knorr F, Lademann J, Patzelt A, Sterry W, Blume-Peytavi U, Vogt A (2009) Follicular transport route – research progress and future perspectives. *Eur J Pharm Biopharm* 71(2):173–180
- Kondo S, Mizuno T, Sugimoto I (1988) Effects of penetration enhancers on percutaneous absorption of nifedipine. Comparison between Deet and Azone. *J Pharmacobiodyn* 11(2):88
- Korinth G, Geh S, Schaller KH, Drexler H (2003) In vitro evaluation of the efficacy of skin barrier creams and protective gloves on percutaneous absorption of industrial solvents. *Int Arch Occup Environ Health* 76(5):382–386
- Kretsos K, Miller MA, Zamora-Estrada G, Kasting GB (2008) Partitioning, diffusivity and clearance of skin permeants in mammalian dermis. *Int J Pharm* 346(1–2):64–79
- Kuswahyuning R, Roberts MS (2014) Concentration dependency in nicotine skin penetration flux from aqueous solutions reflects vehicle induced changes in nicotine stratum corneum retention. *Pharm Res* 31(6):1501–1511
- Lademann J, Richter H, Teichmann A, Otberg N, Blume-Peytavi U, Luengo J, Weiß B, Schaefer UF, Lehr C-M, Wepf R, Sterry W (2007) Nanoparticles – an efficient carrier for drug delivery into the hair follicles. *Eur J Pharm Biopharm* 66(2):159–164
- Lademann J, Knorr F, Richter H, Blume-Peytavi U, Vogt A, Antoniou C, Sterry W, Patzelt A (2008) Hair follicles – an efficient storage and penetration pathway for topically applied substances. Summary of recent results obtained at the Center of Experimental and Applied Cutaneous Physiology, Charité -Universitätsmedizin Berlin, Germany. *Skin Pharmacol Physiol* 21(3):150–155
- Lademann J, Patzelt A, Richter H, Antoniou C, Sterry W, Knorr F (2009) Determination of the cuticula thickness of human and porcine hairs and their potential influence on the penetration of nanoparticles into the hair follicles. *J Biomed Opt* 14(2):021014
- Lademann J, Richter H, Schanzer S, Knorr F, Meinke M, Sterry W, Patzelt A (2011) Penetration and storage of particles in human skin: perspectives and safety aspects. *Eur J Pharm Biopharm* 77(3):465–468
- Laden KSR (1967) Identification of a natural moisturising agent in skin. *J Soc Cosmet Chem* 18:351–361
- Lai PM, Roberts MS (1999) An analysis of solute structure-human epidermal transport relationships in epidermal iontophoresis using the ionic mobility: pore model. *J Control Release* 58(3):323–333
- Lau WM, Ng KW, Sakenyte K, Heard CM (2012) Distribution of esterase activity in porcine ear skin, and the effects of freezing and heat separation. *Int J Pharm* 433(1–2):10–15
- Lee JN, Jee SH, Chan CC, Lo W, Dong CY, Lin SJ (2008) The effects of depilatory agents as penetration enhancers on human stratum corneum structures. *J Invest Dermatol* 128(9):2240–2247
- Lee WR, Shen SC, Al-Suwayeh SA, Yang HH, Li YC, Fang JY (2013) Skin permeation of small-molecule drugs, macromolecules, and nanoparticles mediated by a fractional carbon dioxide laser: the role of hair follicles. *Pharm Res* 30(3):792–802
- Lian G, Chen L, Han L (2008) An evaluation of mathematical models for predicting skin permeability. *J Pharm Sci* 97(1):584–598
- Lien EJ, Tong GL (1973) Physicochemical properties and percutaneous absorption of drugs. *J Soc Cosmet Chem* 24(6):371–384
- Lien E, Koda RT, Tong GL (1971) Physicochemical properties, bioavailability of drugs – buccal and percutaneous absorptions. *Drug Intelligence Clin Pharm* 5(2):38–41
- Liu P, Higuchi WI, Song WQ, Kurihara-Bergstrom T, Good WR (1991) Quantitative evaluation of ethanol effects on diffusion and metabolism of beta-estradiol in hairless mouse skin. *Pharm Res* 8(7):865–872
- Liu X, Grice JE, Lademann J, Otberg N, Trauer S, Patzelt A, Roberts MS (2011) Hair follicles contribute significantly to penetration through human skin only at times soon after application as a solvent deposited solid in man. *Br J Clin Pharmacol* 72(5):768–774
- Lockley DJ, Howes D, Williams FM (2005) Cutaneous metabolism of glycol ethers. *Arch Toxicol* 79(3):160–168
- Loden M (1985) The in vitro hydrolysis of diisopropyl fluorophosphate during penetration through human full-thickness skin and isolated epidermis. *J Invest Dermatol* 85(4):335–339

- Loden M (2008) Skin barrier function: effects of moisturizers. In: Wiechers JW (ed) *Skin Barrier: chemistry of skin delivery systems*. Allured publishing corporation, Carol Stream, pp 105–115
- Luebberding S, Krueger N, Kerscher M (2013) Age-related changes in skin barrier function – quantitative evaluation of 150 female subjects. *Int J Cosmet Sci* 35(2):183–190
- Machado M, Salgado TM, Hadgraft J, Lane ME (2010a) The relationship between transepidermal water loss and skin permeability. *Int J Pharm* 384(1–2):73–77
- Machado M, Hadgraft J, Lane ME (2010b) Assessment of the variation of skin barrier function with anatomic site, age, gender and ethnicity. *Int J Cosmet Sci* 32(6):397–409
- Madison KC (2003) Barrier function of the skin: “la raison d’être” of the epidermis. *J Invest Dermatol* 121(2):231–241
- Magnusson BM, Anissimov YG, Cross SE, Roberts MS (2004) Molecular size as the main determinant of solute maximum flux across the skin. *J Invest Dermatol* 122(4):993–999
- Magnusson BM, Cross SE, Winckle G, Roberts MS (2006) Percutaneous absorption of steroids: determination of in vitro permeability and tissue reservoir characteristics in human skin layers. *Skin Pharmacol Physiol* 19(6):336–342
- Maibach HI, Feldman RJ, Milby TH, Serat WF (1971) Regional variation in percutaneous penetration in man. *Pesticides. Arch Environ Health* 23(3):208–211
- Manafi A, Hashemlou A, Momeni P, Moghimi HR (2008) Enhancing drugs absorption through third-degree burn wound eschar. *Burns* 34(5):698–702
- Marrakchi S, Maibach HI (2007) Biophysical parameters of skin: map of human face, regional, and age-related differences. *Contact Dermatitis* 57(1):28–34
- McNeill SC, Potts RO, Francoeur ML (1992) Local enhanced topical delivery (LETD) of drugs: does it truly exist? *Pharm Res* 9(11):1422–1427
- Meidan VM, Bonner MC, Michniak BB (2005) Transfollicular drug delivery – is it a reality? *Int J Pharm* 306(1–2):1–14
- Michaels AS, Chandrasekaran SK, Shaw JE (1975) Drug permeation through human skin – theory and in vitro experimental measurement. *Am Inst Chem Eng J* 21(5):985–996
- Milewski M, Stinchcomb AL (2012) Estimation of maximum transdermal flux of nonionized xenobiotics from basic physicochemical determinants. *Mol Pharm* 9(7):2111–2120
- Mitragotri S (2003) Modeling skin permeability to hydrophilic and hydrophobic solutes based on four permeation pathways. *J Control Release* 86(1):69–92
- Mitragotri S, Anissimov YG, Bunge AL, Frasch HF, Guy RH, Hadgraft J, Kasting GB, Lane ME, Roberts MS (2011) Mathematical models of skin permeability: an overview. *Int J Pharm* 418(1):115–129
- Moghimi HR, Manafi A (2009) The necessity for enhancing of drugs absorption through burn eschar. *Burns* 35(6):902–904
- Moghimi HR, Shakerinejad A (1998). Retardation effects of  $\beta$ -cyclodextrin and polyethylene glycol on percutaneous absorption of nitroglycerin. 6th International Conference on Perspectives in Percutaneous Penetration, Leiden
- Moghimi HR, Makhmalzadeh BS, Manafi A (2009) Enhancement effect of terpenes on silver sulphadiazine permeation through third-degree burn eschar. *Burns* 35(8):1165–1170
- Moghimi HR, Varshochian R, Kobarfard F, Erfan M (2010) Reduction of percutaneous absorption of toxic chemicals by dendrimers. *Cutan Ocul Toxicol* 29(1):34–40
- Monafo WW, West MA (1990) Current treatment recommendations for topical burn therapy. *Drugs* 40(3):364–373
- Monteiro-Riviere NA, Inman AO, Riviere JE, McNeill SC, Francoeur ML (1993) Topical penetration of piroxicam is dependent on the distribution of the local cutaneous vasculature. *Pharm Res* 10(9):1326–1331
- Moritz AR, Henriques FC Jr (1947) Studies of thermal injury: II. The relative importance of time and surface temperature in the causation of cutaneous burns. *Am J Pathol* 23(5):695
- Moss GP, Wilkinson SC, Sun Y (2012) Mathematical modelling of percutaneous absorption. *Curr Opin Colloid Interface Sci* 17(3):166–172
- Nakashima E, Noonan PK, Benet LZ (1987) Transdermal bioavailability and first-pass skin metabolism: a preliminary evaluation with nitroglycerin. *J Pharmacokinet Biopharm* 15(4):423–437
- Nitsche JM, Wang TF, Kasting GB (2006) A two-phase analysis of solute partitioning into the stratum corneum. *J Pharm Sci* 95(3):649–666
- O’Flaherty EJ (2000) Absorption, distribution, and elimination of toxic agents. In: *Principles of toxicology: environmental and industrial applications*, 2nd edn. Wiley, New York, pp 35–55
- Osigo T, Shiraki T, Okajima K, Tanino T, Iwaki M, Wada T (2002) Transfollicular drug delivery: penetration of drugs through human scalp skin and comparison of penetration between scalp and abdominal skins in vitro. *J Drug Target* 10(5):369–378
- Otberg N, Richter H, Schaefer H, Blume-Peytavi U, Sterry W, Lademann J (2004) Variations of hair follicle size and distribution in different body sites. *J Invest Dermatol* 122(1):14–19
- Park JH, Lee JW, Kim YC, Prausnitz MR (2008) The effect of heat on skin permeability. *Int J Pharm* 359(1):94–103
- Patzelt A, Lademann J (2013) Drug delivery to hair follicles. *Expert Opin Drug Deliv* 10(6):787–797
- Patzelt A, Richter H, Knorr F, Schäfer U, Lehr C-M, Dähne L, Sterry W, Lademann J (2011) Selective follicular targeting by modification of the particle sizes. *J Control Release* 150(1):45–48
- Peck KD, Ghanem AH, Higuchi WI (1994) Hindered diffusion of polar molecules through and effective pore radii estimates of intact and ethanol treated human epidermal membrane. *Pharm Res* 11(9):1306–1314

- Pellanda C, Strub C, Figueiredo V, Ruffi T, Imanidis G, Surber C (2007) Topical bioavailability of triamcinolone acetonide: effect of occlusion. *Skin Pharmacol Physiol* 20(1):50–56
- Pilgram GS, Engelsma-van PAM, Bouwstra JA, Koerten HK (1999) Electron diffraction provides new information on human stratum corneum lipid organization studied in relation to depth and temperature. *J Invest Dermatol* 113(3):403–409
- Plewig G, Marples RR (1970) Regional differences of cell sizes in the human stratum corneum. Part I. *J Invest Dermatol* 54(1):13–18
- Potts RO, Guy RH (1992) Predicting skin permeability. *Pharm Res* 9(5):663–669
- Prather RD, Tu TG, Rolf CN, Gorsline J (1993) Nicotine pharmacokinetics of Nicoderm<sup>®</sup> (nicotine transdermal system) in women and obese men compared with normal-sized men. *J Clin Pharmacol* 33(7):644–649
- Proksch E, Brandner JM, Jensen JM (2008) The skin: an indispensable barrier. *Exp Dermatol* 17(12):1063–1072
- Rabinowitz JL, Feldman ES, Weinberger A, Schumacher HR (1982) Comparative tissue absorption of oral 14C-aspirin and topical triethanolamine 14C-salicylate in human and canine knee joints. *J Clin Pharmacol* 22(1):42–48
- Reed JT, Ghadially R, Elias PM (1995) SKin type, but neither race nor gender, influence epidermal permeability barrier function. *Arch Dermatol* 131(10):1134–1138
- Roberts MS (1991) Structure-permeability considerations in percutaneous absorption. In: Scott RC, Guy RH, Hadgraft J, Bodde HE (eds) *Prediction of percutaneous penetration – methods, measurement and modelling*, vol 2. IBC Technical Services Ltd, London, pp 210–228
- Roberts MS (2013) Solute-vehicle-skin interactions in percutaneous absorption: the principles and the people. *Skin Pharmacol Physiol* 26(4–6):356–370
- Roberts MS, Walker M (1993) Water – the most natural penetration enhancer. In: Walters KA, Hadgraft J (eds) *Skin penetration enhancement*. Marcel Dekker, New York, pp 1–30
- Roberts MS, Anderson RA, Swarbrick J (1977) Permeability of human epidermis to phenolic compounds. *J Pharm Pharmacol* 29(11):677–683
- Roberts MS, Favretto WA, Meyer A, Reckmann M, Wongseelashote T (1982) Topical bioavailability of methyl salicylate. *Aust N Z J Med* 12(3):303–305
- Roberts MS, Pugh WJ, Hadgraft J (1996) Epidermal permeability: penetrant structure relationships. 2. The effect of h-bonding groups in penetrants on their diffusion through the stratum corneum. *Int J Pharm* 132(1–2):23–32
- Roberts MS, Cross SE, Pellett MA (2002) Skin transport. In: Walters KA (ed) *Dermatological and transdermal formulations*. Marcel Dekker, Inc., New York, pp 89–196
- Roberts MS, Cross SE, Anissimov YG (2004) Factors affecting the formation of a skin reservoir for topically applied solutes. *Skin Pharmacol Physiol* 17(1):3–16
- Roberts MS, Bouwstra J, Pirot F, Falson F (2008) Skin hydration-A key determinant in topical absorption. In: Walters KA, Roberts MS (eds) *Dermatologic, cosmeceutic, and cosmetic development: therapeutic and novel approaches*. Informa Healthcare, New York, pp 115–128
- Roskos KV, Guy RH (1989) Assessment of skin barrier function using transepidermal water loss: effect of age. *Pharm Res* 6(11):949–953
- Roskos KV, Maibach HI, Guy RH (1989) The effect of aging on percutaneous absorption in man. *J Pharmacokinet Biopharm* 17(6):617–630
- Rothman S (1943) The principles of percutaneous absorption. *J Lab Clin Med* 28:1305–1321
- Rougier A, Lotte C, Maibach HI (1987) In vivo percutaneous penetration of some organic compounds related to anatomic site in humans: predictive assessment by the stripping method. *J Pharm Sci* 76(6):451–454
- Rougier A, Lotte C, Corcuff P, Maibach HI (1988) Relationship between skin permeability and corneocyte size according to anatomic site, age, and sex in man. *J Soc Cosmetic Chem* 39(1):15–26
- Rougier A, Lotte C, Maibach HI (2005) In vivo relationship between percutaneous absorption and transdermal water loss. In: Bronaugh RL, Maibach HI (eds) *Percutaneous absorption*. Taylor Francis, Boca Raton, pp 95–106
- Rushmer RF, Buettner KJ, Short JM, Odland GF (1966) The skin. *Science* 154(3747):343–348
- Samaras EG, Riviere JE, Ghafourian T (2012) The effect of formulations and experimental conditions on in vitro human skin permeation-data from updated EDETOX database. *Int J Pharm* 434(1–2):280–291
- Schaefer H, Redelmeier TE (1996) Skin barrier. Principles of percutaneous absorption. S. Karger AG, Basel
- Scheuplein RJ (2013) A personal view of skin permeation (1960–2013). *Skin Pharmacol Physiol* 26(4–6):199–212
- Scheuplein RJ, Blank IH (1971) Permeability of the skin. *Physiol Rev* 51(4):702–747
- Seidenari S, Giusti G (1995) Objective assessment of the skin of children affected by atopic dermatitis: a study of pH, capacitance and TEWL in eczematous and clinically uninvolved skin. *Acta Derm Venereol* 75(6):429–433
- Shiozuka M, Wagatsuma A, Kawamoto T, Sasaki H, Shimada K, Takahashi Y, Nonomura Y, Matsuda R (2010) Transdermal delivery of a readthrough-inducing drug: a new approach of gentamicin administration for the treatment of nonsense mutation-mediated disorders. *J Biochem* 147(4):463–470
- Singh P, Roberts MS (1996) Local deep tissue penetration of compounds after dermal application: structure-tissue penetration relationships. *J Pharmacol Exp Ther* 279(2):908–917
- Sloan KB, Wasdo SC, Rautio J (2006) Design for optimized topical delivery: prodrugs and a paradigm change. *Pharm Res* 23(12):2729–2747
- Somani SM, Romano JA Jr (2000) Chemical warfare agents: toxicity at low levels. CRC Press, Boca Raton

- Song JY, Kang HA, Kim MY, Park YM, Kim HO (2004) Damage and recovery of skin barrier function after glycolic acid chemical peeling and crystal microdermabrasion. *Dermatol Surg* 30(3):390–394
- Tan G, Xu P, Lawson LB, He J, Freytag LC, Clements JD, John VT (2010) Hydration effects on skin microstructure as probed by high-resolution cryo-scanning electron microscopy and mechanistic implications to enhanced transcutaneous delivery of biomacromolecules. *J Pharm Sci* 99(2):730–740
- Tang H, Mitragotri S, Blankschtein D, Langer R (2001) Theoretical description of transdermal transport of hydrophilic permeants: application to low-frequency sonophoresis. *J Pharm Sci* 90(5):545–568
- Taylor LJ, Lee RS, Long M, Rawlings AV, Tubek J, Whitehead L, Moss GP (2002) Effect of occlusion on the percutaneous penetration of linoleic acid and glycerol. *Int J Pharm* 249(1–2):157–164
- Tezel A, Sens A, Mitragotri S (2002) A theoretical analysis of low-frequency sonophoresis: dependence of transdermal transport pathways on frequency and energy density. *Pharm Res* 19(12):1841–1846
- Trommer H, Neubert RH (2006) Overcoming the stratum corneum: the modulation of skin penetration. A review. *Skin Pharmacol Physiol* 19(2):106–121
- Van Scott EJ, Yu RJ (1984) Hyperkeratinization, corneocyte cohesion, and alpha hydroxy acids. *J Am Acad Dermatol* 11(5):867–879
- Vergnanini AL, Aoki V, Takaoka R, Madi J (2010) Comparative effects of pimecrolimus cream vehicle and three commercially available moisturizers on skin hydration and transepidermal water loss. *J Dermatolog Treat* 21(3):126–129
- Vogt A, Combadiere B, Hadam S, Stieler KM, Lademann J, Schaefer H, Autran B, Sterry W, Blume-Peytavi U (2006) 40 nm, but not 750 or 1,500 nm, nanoparticles enter epidermal CD1a+ cells after transcutaneous application on human skin. *J Invest Dermatol* 126(6):1316–1322
- Vyumvuhore R, Tfayli A, Duplan H, Delalleau A, Manfait M, Baillet-Guffroy A (2013) Effects of atmospheric relative humidity on Stratum Corneum structure at the molecular level: ex vivo Raman spectroscopy analysis. *Analyst* 138(14):4103–4111
- Waller JM, Maibach HI (2005) Age and skin structure and function, a quantitative approach (I): blood flow, pH, thickness, and ultrasound echogenicity. *Skin Res Technol* 11(4):221–235
- Wang TF, Kasting GB, Nitsche JM (2006) A multiphase microscopic diffusion model for stratum corneum permeability. I. Formulation, solution, and illustrative results for representative compounds. *J Pharm Sci* 95(3):620–648
- Wang TF, Kasting GB, Nitsche JM (2007) A multiphase microscopic diffusion model for stratum corneum permeability. II. Estimation of physicochemical parameters, and application to a large permeability database. *J Pharm Sci* 96(11):3024–3051
- Wang XQ, Hayes MT, Kempf M, Cuttle L, Mill J, Kimble RM (2009) The poor penetration of topical burn agent through burn eschar on a porcine burn model. *Burns* 35(6):901–902
- Wang L, Chen L, Lian G, Han L (2010) Determination of partition and binding properties of solutes to stratum corneum. *Int J Pharm* 398(1–2):114–122
- Wester RC, Noonan PK, Smeach S, Kosobud L (1983) Pharmacokinetics and bioavailability of intravenous and topical nitroglycerin in the rhesus monkey: estimate of percutaneous first-pass metabolism. *J Pharm Sci* 72(7):745–748
- Wester RC, Maibach HI, Bucks DA, Aufrere MB (1984) In vivo percutaneous absorption of paraquat from hand, leg, and forearm of humans. *J Toxicol Environ Health* 14(5–6):759–762
- Wigger-Alberti W, Elsner P (1998) Do barrier creams and gloves prevent or provoke contact dermatitis? *Am J Contact Dermatitis* 9(2):100–106
- Windheuser JJ, Haslam JL, Caldwell L, Shaffer RD (1982) The use of N, N-diethyl-m-toluamide to enhance dermal and transdermal delivery of drugs. *J Pharm Sci* 71(11):1211–1213
- Wohrlab W (1984) The influence of urea on the penetration kinetics of topically applied corticosteroids. *Acta Derm Venereol* 64(3):233–238
- Wohrlab W (1990) The influence of urea on the penetration kinetics of vitamin-A-acid into human skin. *Z-Hautkr* 65:803–805
- Wurster DE, Kramer SF (1961) Investigation of some factors influencing percutaneous absorption. *J Pharm Sci* 50:288–293
- Yalkowsky SH, Valvani SC (1980) Solubility and partitioning I: solubility of nonelectrolytes in water. *J Pharm Sci* 69(8):912–922
- Yano T, Nakagawa A, Tsuji M, Noda K (1986) Skin permeability of various non-steroidal anti-inflammatory drugs in man. *Life Sci* 39(12):1043–1050
- Ya-Xian Z, Suetake T, Tagami H (1999) Number of cell layers of the stratum corneum in normal skin – relationship to the anatomical location on the body, age, sex and physical parameters. *Arch Dermatol Res* 291(10):555–559
- Zadeh BS, Moghimi H, Santos P, Hadgraft J, Lane ME (2008) A comparative study of the in vitro permeation characteristic of sulphadiazine across synthetic membranes and eschar tissue. *Int Wound J* 5(5):633–638
- Zadeh BSM, Moghimi H, Santos P, Hadgraft J, Lane ME, Rahim F (2010) Formulation of microemulsion systems for improvement of nitrofurazone permeation through silicon membrane as burn wound imitating coverage. *Int J Pharm* 6:264–270
- Zhang Q, Grice JE, Li P, Jepps OG, Wang GJ, Roberts MS (2009) Skin solubility determines maximum transepidermal flux for similar size molecules. *Pharm Res* 26(8):1974–1985
- Zhang Q, Li P, Roberts MS (2011) Maximum transepidermal flux for similar size phenolic compounds is enhanced by solvent uptake into the skin. *J Control Release* 154(1):50–57

# The Influence of Emollients on Dermal and Transdermal Drug Delivery

5

V.R. Leite-Silva, Jeffrey E. Grice,  
Yousuf Mohammed, Hamid R. Moghimi,  
and Michael S. Roberts

## Contents

5.1	<b>Introduction</b> .....	77	5.3.2	How Do the Emollients Differ in their Ability to Affect and Enter the Skin (Size and Solubility Parameter Determined) and to Promote Skin Penetration of Actives? .....	86
5.2	<b>Current Emollients, Their Modes of Action, and Their Use in Practice</b> .....	79	5.3.3	What Do Other Ingredients in a Moisturizing Formulation Do to Enhance or Inhibit the Effects of Emollients on Skin Penetration?.....	87
5.2.1	Sebum .....	79	5.4	<b>Practical Aspects</b> .....	89
5.2.2	Emollient Classes and Properties .....	80	<b>Conclusion</b> .....	90	
5.2.3	Effect of Emollients on Skin Lubrication .....	80	<b>References</b> .....	91	
5.2.4	Effect of Emollients on Skin TEWL and Skin Hydration .....	82			
5.2.5	Emollient Substantivity .....	83			
5.2.6	An Overall Comparison of Emollient Properties.....	84			
5.3	<b>Effects of Emollients on Percutaneous Absorption</b> .....	84			
5.3.1	How Do the Various Emollients Differ in their Ability to Dissolve and Release Different Actives? .....	84			

V.R. Leite-Silva  
Universidade Federal de São Paulo, Instituto de Ciências Ambientais Químicas e Farmacêuticas, Diadema, SP, Brazil  
e-mail: [vania.leite@unifesp.br](mailto:vania.leite@unifesp.br)

J.E. Grice • Y. Mohammed  
Therapeutics Research Centre, School of Medicine, University of Queensland, Translational Research Institute, Woolloongabba, QLD 4102, Australia  
e-mail: [jeff.grice@uq.edu.au](mailto:jeff.grice@uq.edu.au)

H.R. Moghimi  
Therapeutics Research Centre, School of Pharmacy and Medical Sciences, University of South Australia, Adelaide, SA 5000, Australia

School of Pharmacy, Shahid Beheshti University of Medical Sciences, Tehran, Iran  
e-mail: [hrmoghimi@sbmu.ac.ir](mailto:hrmoghimi@sbmu.ac.ir)

## 5.1 Introduction

The word “emollient” is derived from the Latin *emollire*, meaning to soften (from *ex*, out and *molli*, soft). According to the *Oxford English Dictionary*, an emollient is a substance “that has the power of softening or relaxing the living animal textures,” with the first use of the name being

M.S. Roberts (✉)  
Therapeutics Research Centre, School of Pharmacy and Medical Sciences, University of South Australia, Adelaide, SA 5000, Australia

School of Medicine, University of Queensland, Translational Research Institute, Woolloongabba, QLD 4102, Australia  
e-mail: [m.roberts@uq.edu.au](mailto:m.roberts@uq.edu.au)



**Table 5.1** The nature, uses, and various definitions of emollients over time

Source	Date	Definition
<i>Oxford English Dictionary</i>	1643	Substance “that has the power of softening or relaxing the living animal textures”
Edwards (1940)	1940	“Since oils, fats and glycerin when applied to the skin tend to soften the epidermis they are termed emollients...” “An adhesive coat is produced which prevents the irritation of drying, and the access of bacterial, chemical and mechanical irritants”
Blank (1957)	1957	Any material that tends to prevent or alleviate the symptoms and signs of dry skin
Idson (1982)	1982	Emollients – substances lubricating and/or occluding the skin with water-insoluble material (Moisturizers – substances actively increasing the water content of the skin)
Wilkinson and Moore (1982)	1982	Emolliency is only associated with imparting smoothness and general sense of well-being to the skin, as determined by touch
Wehr and Krochmal (1987)	1987	Emollients – systems that smooth the roughened surface of the SC, but do not occlude the skin. No effect on TEWL after application
Loden (1992)	1992	Similar action to moisturizers
Dederen et al. (2012)	2012	Emollients – oily ingredients used for skin care formulations

recorded in 1643. In general, emollients are lipid in nature and are ingredients in a product, which when applied to the skin deposit a lipid film that can also replenish any lost skin lipids. The resultant effect is improved skin lubrication, a smoother skin surface, a soothing effect as it protects the exposed viable epidermis, and hydration of the stratum corneum (by moisturizing the skin through reduced transepidermal water loss). Overall, the skin treated with an emollient is described as being soft and supple, whereas that treated with a humectant (a substance that attracts water to the skin (Idson 1992), improving its hydration) has the sensory feel of softness due to moisturization of the stratum corneum, but without the sensorial suppleness feel associated with the “oily” film. A moisturizer usually refers to a product, and it may contain an emollient and/or a humectant and/or water to provide direct hydration of the stratum corneum. In practice, however, the term “emollients” has been interchangeable with “moisturizers” and “lubricants,” and being used as “bases,” “vehicles,” or to make “vanishing creams,” “revitalizing creams,” or “regenerating milk” (Nola et al. 2003). Regrettably, the nature and actions of an emollient, a humectant, and a moisturizer often have become blurred in the

press over the years, leading to the terms often being used interchangeably, although the sensory responses are different.

With a history of several thousands of years, the nature, uses, and various definitions of emollients have changed with time (Table 5.1). Many of the earliest emollients were derived from animal fats. Marks refers to Egyptians and ancient Greeks using “oils and pleasant smelling fatty concoctions on the skin,” the use of wool fat by the Greeks in about 700 BC, the processing of lanolin from sheep’s wool by a Greek physician in a *Materia Medica* in 60 AD, and the patenting of petrolatum (also known as petroleum jelly, white soft paraffin, and Vaseline) in 1872. As he points out, lanolin is a complex emollient in being a two-phase liquid and wax system consisting of multiple complex sterols, fatty alcohols, and fatty acids, dependent on the nature of the sheep sourced, its manufacturing, and its storage (Marks 2001). Interestingly, goose grease and even human fat have been used as emollients, and emolliency has also been referred to in the soothing of the throat (Coxe 1825). A prevailing view is that “lipids (fats, waxes, and oils) are seen as the essential components of emollients” and that the total lipid content in an emollient formulation is usually 20–40% (Marks 2001).

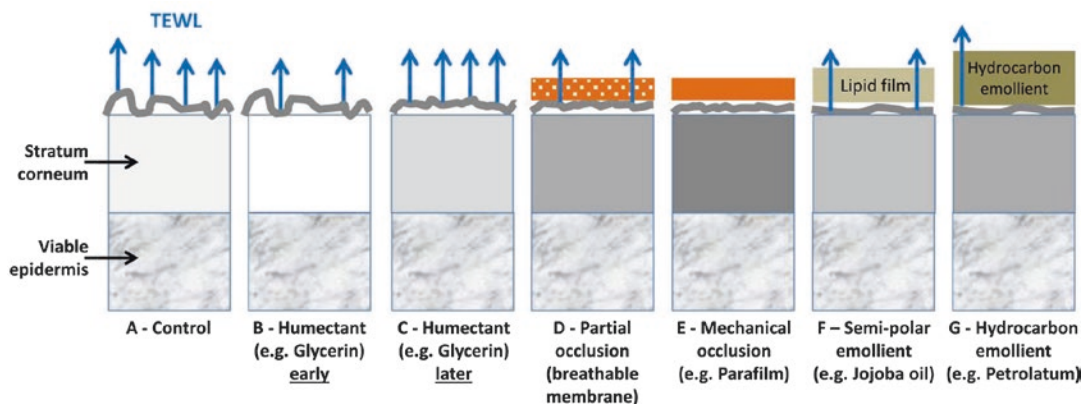


**Fig. 5.1** The effect of various products on the stratum corneum, ranked in order of increasing lubrication of the stratum corneum surface after several hours of application (except B) for: (a). Control; (b). Humectant, early times only; (c). Humectant, later times; (d). Partial mechanical occlusion with a breathable membrane; (e). Mechanical

occlusion, for example, with a plastic covering; (f). Semipolar emollient; (g). Hydrocarbon emollient. The figure also shows (i) the effect of products on stratum corneum hydration (the darker the box, the higher the skin hydration) and (ii) the transepidermal water loss (TEWL), with the number of arrows indicating the magnitude of the TEWL.

Other definitions of emollients have included the preparations themselves (Ray and Blank 1940; Harry 1941), and ointments designed for deeper skin penetration (Wild 1911). Confusion has arisen, in part, from the early emphasis on the emollient lipid film interactions with skin lipids and scales and the more mechanistic approach advocated by Blank, in 1957, which emphasized the skin hydration associated with emolliency. He defined an emollient as “any externally applied material that tends to prevent or counteract the symptoms and signs of dryness of the skin” (Blank 1957). An occlusive dressing is also often used to increase skin moisturization.

Figure 5.1 summarizes our current view of the effects of humectants, semipermeable or impermeous occlusive films, semipolar emollients, and hydrocarbon emollients on stratum corneum (SC) roughness, hydration, and transepidermal water loss (TEWL). It is evident from this figure that emollients differ in their actions on normal skin, compared with other skin treatments such as application of humectants and occlusive dressings. As shown in Fig. 5.1, emollients affect both the transepidermal water loss and the roughness of skin surface through the oily film that they create. The lipid surface film on the stratum corneum and its resulting lubrication of the surface gives a feel of suppleness. The reduction in tran-

sepidermal water loss (TEWL) promotes skin hydration. The application of a semipolar emollient like vegetable oil is likely to reduce TEWL to promote skin hydration to a lesser effect than the more occlusive hydrocarbon emollient.

We now describe the emollients used in practice, their potential effects on percutaneous absorption, and some practical examples of products containing emollients. In recognizing that the stratum corneum is the main barrier for both dermal and transdermal absorption, we have focused this chapter on the effects of emolliency on skin function and the skin penetration of the active.

## 5.2 Current Emollients, Their Modes of Action, and Their Use in Practice

### 5.2.1 Sebum

Sebum is the natural emollient of skin. It is produced from the sebaceous glands adjacent to the hair follicle and consists predominantly of squalene, wax esters, triglycerides, cholesterol esters, and possibly free cholesterol (Stewart 1992). The sebum provides a pliable film on the skin surface that lubricates the skin, inhibits percutaneous absorption of unwanted substances, and impairs

TEWL, leading to increased skin hydration (Stoughton 1959). As well as providing lubrication and hydration of the skin, the sebum can also provide immunological and antimicrobial protection through its surfactant proteins and peptides, especially when their expression in human skin is upregulated (Mo et al. 2007). In addition, the sebum can also act as a buffer, impairing adverse irritation from acidic or basic compounds.

Regular washing of the skin, however, can remove the sebum and result in greater skin roughness and reduce stratum corneum hydration. Low sebum levels have been regarded as a contributing factor in the development of dry skin (Clarys and Barel 1995). Emollients are widely used to provide the desired lubrication and skin hydration that is normally supported by the sebum. In addition, a number of common skin care ingredients, including mineral oil, white petrolatum, and isopropyl myristate, have been shown to enhance sebocyte counts, and hence, potentially, sebum production, in a hairless mouse model (Lesnik et al. 1992).

Sebum has been shown to contribute to stratum corneum hydration by a glycerol-dependent mechanism. Based on the identification of glycerol as the putative product of triglyceride hydrolysis in sebaceous glands, Fluhr et al (2003) treated asebia mice, showing profound sebaceous gland hypoplasia, with glycerol, and were able to restore normal stratum corneum hydration. Urea, another commonly used humectant, had no effect.

### 5.2.2 Emollient Classes and Properties

Members of the different classes of emollients have different physicochemical properties that result in a range of functional and sensorial effects when left as a lipid film after being applied to the skin in a cosmetic or dermatological product. Traditionally, emollients have been regarded as having a number of common properties: (i) fat solubility, (ii) the ability to soften the skin, and (iii) an oily feel. However, they can differ quite markedly in their physicochemical properties. Some emollients are partially soluble in water

(e.g., PEG-150 distearate, PEG/PPG-8/3 laurate) and are used not only for skin but also for hair (e.g., PEG-7 glyceryl cocoate, PPG-3 benzyl ether myristate). Others may feel dry to the touch (e.g., oleyl alcohol, C12–15 alkyl benzoate, phenethyl benzoate, cyclomethicone, and isononyl isononanoate). In general, the lipophilicities of the emollients in (Table 5.2) are such that those containing hydrogen bonding groups, such as ethers, esters, vegetable oils, and lanolin are more polar than those without these groups, for example, hydrocarbons. Today's emollients are used to meet many different functional needs and to support multiple "claims," and hence, a formulator has to select appropriate emollients to meet not only the consumer and regulatory needs but also to cater for whether the final product is designed for a cosmetic or a therapeutic application.

### 5.2.3 Effect of Emollients on Skin Lubrication

The choice of an emollient is often based on the tactile properties of these substances on the skin surface and is often of higher importance in cosmetology than in the formulation of topical therapeutic drugs, where sensory properties are not necessarily the main priority (Dederen et al. 2012). A plethora of imaginative terms may be used to describe these subjective properties. Words such as "tacky," "oily," "dry-velvety," or "waxy" are readily understood, whereas other more esoteric terms such as "scroopy" (the textile chemist's description of the rough, soft-draggy feel of raw silk) are less obvious (Goldemberg and De La Rosa 1971). All these terms are used in an attempt to describe the sensory responses caused by the lubricating actions of emollients on the skin. A special issue of the *Journal of Investigative Dermatology* was devoted to the effects of emollients on the mechanical properties of the skin in 1977, with articles on the viscoelastic (Christensen et al. 1977) and frictional (Highley et al. 1977) properties of human skin, as well as measurement of skin hydration (Campbell et al. 1977), among others.

To the formulator, the tactile sensory properties of the neat oils are the first consideration in

**Table 5.2** Common emollients used in topical formulations

Chemical class	INCI name	CAS number	Physical form at 25°C
Esters	Isopropyl palmitate	142-91-6	Liquid
	Isopropyl myristate	110-27-0	Liquid
	Ethylhexyl palmitate	29806-73-3	Liquid
	Octyl stearate	109-36-4	Liquid
	Cetyl palmitate	540-10-3	Solid
	Cetyl lactate	35274-05-6	Semi-solid
	Myristyl lactate	1323-03-1	Semi-solid
	C12–15 alkyl benzoate	68411-27-8	Liquid
	Ethylhexyl isononanoate	71566-49-9	Liquid
	Isononyl isononanoate	59219-71-5	Liquid
	Cetyl isononanoate	84878-33-1	Liquid
	Decyl oleate	3687-46-5	Liquid
	Diisopropyl adipate	6938-94-9	Liquid
	Diisobutyl adipate	141-04-8	Liquid
	Glyceryl stearate	123-94-4	Solid
	Propylene glycol stearate	1323-39-3	Solid
	Glycol stearate	31566-31-1	Solid
Glycol distearate	627-83-8	Solid	
Ethers	Dicaprylyl ether	629-82-3	Liquid
	PPG-15 stearyl ether	25231-21-4	Liquid
	PEG-7 glyceryl cocoate	68201-46-7	Liquid
Triglycerides	Capric/caprylic triglycerides	65381-09-01	Liquid
Fatty alcohols	Cetyl alcohol	36653-82-4	Solid
	Cetearyl alcohol	8005-44-5	Solid
	Stearyl alcohol	112-92-5	Solid
	Oleyl alcohol	143-28-2	Liquid
	Octyldodecanol	34513-50-3	Liquid
Fatty acids	Oleic acid	112-80-1	Liquid
	Linoleic acid	60-33-3	Liquid
Hydrocarbons	Liquid paraffin	8012-95-1/8042-47-5	Liquid
	Petrolatum	8009-03-8	Solid
	C9–14 isoparaffin	246538-73-8	Liquid
	Polyisobutene	9003-27-4	Liquid
	Isohexadecane	93685-80-4	Liquid
Vegetal butters	<i>Butyrospermum parkii</i> butter (Shea butter)	194043-92-0	Semi-solid
	<i>Theobroma cacao</i> seed butter (cocoa butter)	84649-99-0	Semi-solid
	<i>Mangifera indica</i> seed butter (mango butter)	90063-86-8	Semi-solid
Vegetal oils	<i>Prunus Amygdalus Dulcis</i> seed oil (sweet almond oil)	8007-69-0	Liquid
	<i>Vitis vinifera</i> seed oil (grape seed oil)	8024-22-4	Liquid
	<i>Simmondsia chinensis</i> seed oil (Jojoba oil)	90045-98-0	Liquid
	<i>Triticum vulgare</i> germ oil (wheat germ oil)	68917-73-7	Liquid
	<i>Sesamum indicum</i> oil (sesame oil)	8008-74-0	Liquid
Esterols	Lanolin	8006-54-0	Semi-solid
Silicones	Cyclopentasiloxane	541-02-6	Liquid
	Dimethicone	9006-65-9	Liquid
	Dimethiconol	31692-79-2/70131-67-8	Liquid

**Table 5.3** Spreading values for selected ester emollients

High spreading values	>850 mm <sup>2</sup> /10 min	For example, isopropyl myristate and isopropyl palmitate
Medium spreading values	501–850 mm <sup>2</sup> /10 min	For example, ethylhexyl stearate and decyl oleate
Low spreading values	0–500 mm <sup>2</sup> /10 min	For example, C12–15 alkyl benzoate

choosing an emollient for a cosmetic product (Goldemberg and De La Rosa 1971; Zeidler 1992). The key property of the emollient that this is reflecting is its ability to lubricate and reduce any friction between the skin surface and its environment (skin with skin, clothing with skin, etc.), as this reduces possible discomfort, irritation, and pain (Dederen et al. 2012). The lubrication intensity of the emollient on the skin can be partly explained by the properties of the emollient itself; the residual film thickness, by dynamic spreadability and the viscosity. However, the skin is not a rigid, inert surface, and emollients can directly or indirectly modify its mechanical properties. This must also contribute to the overall sensory response (Dederen et al. 2012). This important property of emollients is defined by their ability to disperse more or less quickly on the skin surface by forming a film. This can be assessed quantitatively using a parameter known as the spreading value. A common technique for determining the spreading values has been described by Zeidler (1985). Spreading values, in units of mm<sup>2</sup>/10 min, are determined by applying 20  $\mu$ l of an emollient to the center of an ashless, medium-to-fast filter paper at 25 °C and measuring the area covered by the applied material in 10 min. Examples of spreading values for some of the most widely used group of emollient for skin lubrication, the esters, are shown in Table 5.3. Esters are useful to formulators because of their versatility and the unique properties they can give to the final product, influenced by the chemical properties, including chain length, of their constituent fatty acids and alcohols. As can be seen, changes in the

constituent chain lengths can alter the skin-surface spreading characteristics of ester emollients. For example, isopropyl myristate and palmitate, with short-chain alcohol components and the shortest acid chain lengths (C14 and C16, respectively) in this table, have the highest spreading values. The C16 palmitate is greasier than the C14 myristate, but the spreading values are similar. Ethylhexyl stearate and decyl oleate, with longer chain components, have medium spreading values, whereas the longer chain alcohol (C12–C15), alkyl benzoates, are low spreading esters.

Many attempts have been made to achieve a measure of sensory softness of the skin. In 2013, Nakatani suggested that conventional methods for measuring the mechanical properties of the skin, such as the elongation in response to suction, elastic responses to ballistic impact, and rheological responses to torsional stress, were restricted to measuring the properties of the whole skin and were unable to look at different skin layers separately. They developed a novel piezoelectric tactile sensor system that could simultaneously measure the mechanical properties of the whole skin and its superficial layer. Such a technique has obvious advantages to the cosmetic industry, but can also be applied clinically to the quantitative evaluation of skin disorders such as atopic dermatitis (Nakatani et al. 2013).

#### 5.2.4 Effect of Emollients on Skin TEWL and Skin Hydration

The residual lipid film on the stratum corneum surface after the application of products containing emollients will limit the evaporation of water from the skin surface and therefore cause an increase in skin hydration. Accordingly, emollients have been described as indirect skin moisturizers (Dederen et al. 2012). In general, the presence of hydrogen bonds in emollients also facilitates the transport of water through the lipid films, so that for lipid films of similar thickness and viscosity, the semipolar emollients will be more permeable to water than the hydrocarbon emollients, resulting in a lower occlusive state than that induced by the hydrocarbon emollients. However, these findings can differ significantly,

depending on the nature of the emollient. Patzelt et al (2012) recently showed that vegetable oils (except Jojoba oil) led to a similar occlusion of the human skin surface *in vivo* as paraffin oil, but the semisolid, petrolatum, was the most effective occlusive. The occlusive effects of an emollient then result in a reduced transepidermal water loss (TEWL) and, in turn, an increase in the hydration of the stratum corneum relative to normal moisture conditions. By occluding the skin and providing an additional barrier to water loss, skin hydration can be increased by up to 50% (Hafeez and Maibach 2013a). This increase in hydration as an effect of occlusion has also been seen with physical occlusives like wound dressings and bandages (Voegeli et al. 2009, 2011). Increasing the thickness of the lipid film and/or increasing the viscosity of the lipid film will reduce the TEWL and increase stratum corneum hydration, so that a wax will have a low TEWL and higher SC hydration than an oil.

The presence of water in a formulation can add to the moisturizing properties of that formulation on the skin, but generally for only a short time. Indeed, the moisturizing effect of topically applied water is often lost after 10–20 min of application (Batt and Fairhurst 1986; Paepe and Rogiers 2009). Blank showed that the main effect associated with skin moisturization was an increase in its softness and pliability (Blank 1952). The moisturizing effect of water can be prolonged when an emollient is present in the moisturizing formulation. The presence of a humectant, such as glycerol, in the aqueous phase, as well as the emollient will increase the moisturization of the skin. Indeed, Batt et al. showed that the enhanced moisturizing effect of glycerol by different emollients and oils was present even 12 h after application (Batt et al. 1988).

Nonphysiological occlusive moisturizers such as petrolatum remain on the skin surface without being incorporated into the deeper skin layers. While they may provide some benefit by improving skin hydration, they are not effective in directly treating the disordered lipid states in such diseases. For example, petrolatum treatment had no effect on the abnormal lipid organization associated with barrier defects in patients with atopic dermatitis or lamellar ichthyosis (Pilgram et al.

2001). On the other hand, some moisturizers do act by penetrating the intercellular lipid regions. A novel mechanism known as “internal occlusion” (Wiechers et al. 2009) has been described, where moisturizers such as isostearyl isostearate and isopropyl isostearate cause improved skin hydration and barrier function by stabilizing the SC lipid organization in the more tightly packed orthorhombic phase (Caussin et al. 2007).

A different approach to the emollient treatment of skin diseases such as atopic dermatitis, relying on the use of emollient treatments containing ceramide-dominant physiological mixtures of the three key lipids, cholesterol, free fatty acids, and ceramides at the appropriate physiological pH, has been pioneered by Elias (Chamlin et al. 2002; Elias 2010). The mechanism leading to skin barrier enhancement is believed to involve more than a simple augmentation of intercellular lipid populations and structure. On passing through the SC, the applied lipids migrate to the nucleated cell regions, to be taken up by keratinocytes and then trafficked to lamellar bodies, where they are mixed with endogenous epidermal lipids. The augmented lipid mixture is then secreted into the SC intercellular spaces (Mao-Qiang et al. 1995; Chamlin et al. 2002) to enhance skin barrier function and normalize skin hydration. According to Elias, the effectiveness of any such treatment depends primarily on understanding the mechanism responsible for a particular skin barrier defect, in order to judge whether lipid replacement is appropriate for that condition (Chamlin et al. 2002). An alternative approach to address imbalance in the SC proteolytic cascade leading to dry skin is to use serine protease inhibitors to treat mild-to-severe barrier abnormalities (Voegeli et al. 2009; Rawlings and Voegeli 2013).

### 5.2.5 Emollient Substantivity

This is defined here as a measure of the retention of an emollient in and persistence of its effect on the skin after exposure to water, perspiration, and resistance to being rubbed off. Another definition of substantivity is: “the property of continuing therapeutic action despite removal of the vehicle, such as the action of certain shampoos” (Mosby

2009). (*MediLexicon* 2013), referring to *Stedman's Medical Dictionary* (Stedman's 2011), suggests substantivity is a "term comprising the adherent qualities of a sunscreen and its ability to be retained after the skin is exposed to water and perspiration. Persistence of effect of a topically applied drug or cosmetic, determined by the degree of physical and chemical bonding to the surface; resistance to removal or inactivation by sweating, swimming, bathing, and friction, among other factors." In general, emollient substantivity is poor for an aqueous gel but comparatively better for an O/W emulsion. Greater substantivity would be expected for a W/O emulsion and more particularly for an ointment. It has been suggested that silicone ingredients have a higher substantivity than the more common emollients, as silicone chains are entangled (Sene 2003).

### 5.2.6 An Overall Comparison of Emollient Properties

Wiechers began his pioneering work on skin care products by working with panels of human subjects. He tested a broad spectrum of materials (Wiechers 1997), quantitatively assessing moisturization by skin hydration (using a Corneometer, with glycerin as a positive control and untreated skin as a negative control), elasticity (using a Dermal Torque Meter, with water applied 30 min under occlusion as a positive control and untreated skin as a negative control), and substantivity (using a Sebumeter, with petrolatum as a positive control and untreated skin as the negative control). For each property, he then derived a relative performance index (RPI). A value of  $\geq 70\%$  for a particular property indicated a good performing ingredient, while ingredients with RPI values between 30 and 70% were regarded as medium

performers. Figure 5.2 shows Wiechers' RPI values for moisturization, elasticity, and substantivity for a range of selected emollients. It is apparent that there are many more medium–good performing moisturizing and substantivity ingredients than there are elasticity ingredients, so that a good RPI for moisturization, for example, did not necessarily predict a similar result for the other parameters. This led Wiechers to conclude that multiple mechanisms were present (Wiechers and Barlow 1999) and that multiple emollients are needed for enhanced overall emollient performance (Wiechers et al. 2002). Most recently, we combined forces to use the principles described here and in his work to predict the skin penetration of actives from complex practical formulations (Wiechers et al. 2012).

## 5.3 Effects of Emollients on Percutaneous Absorption

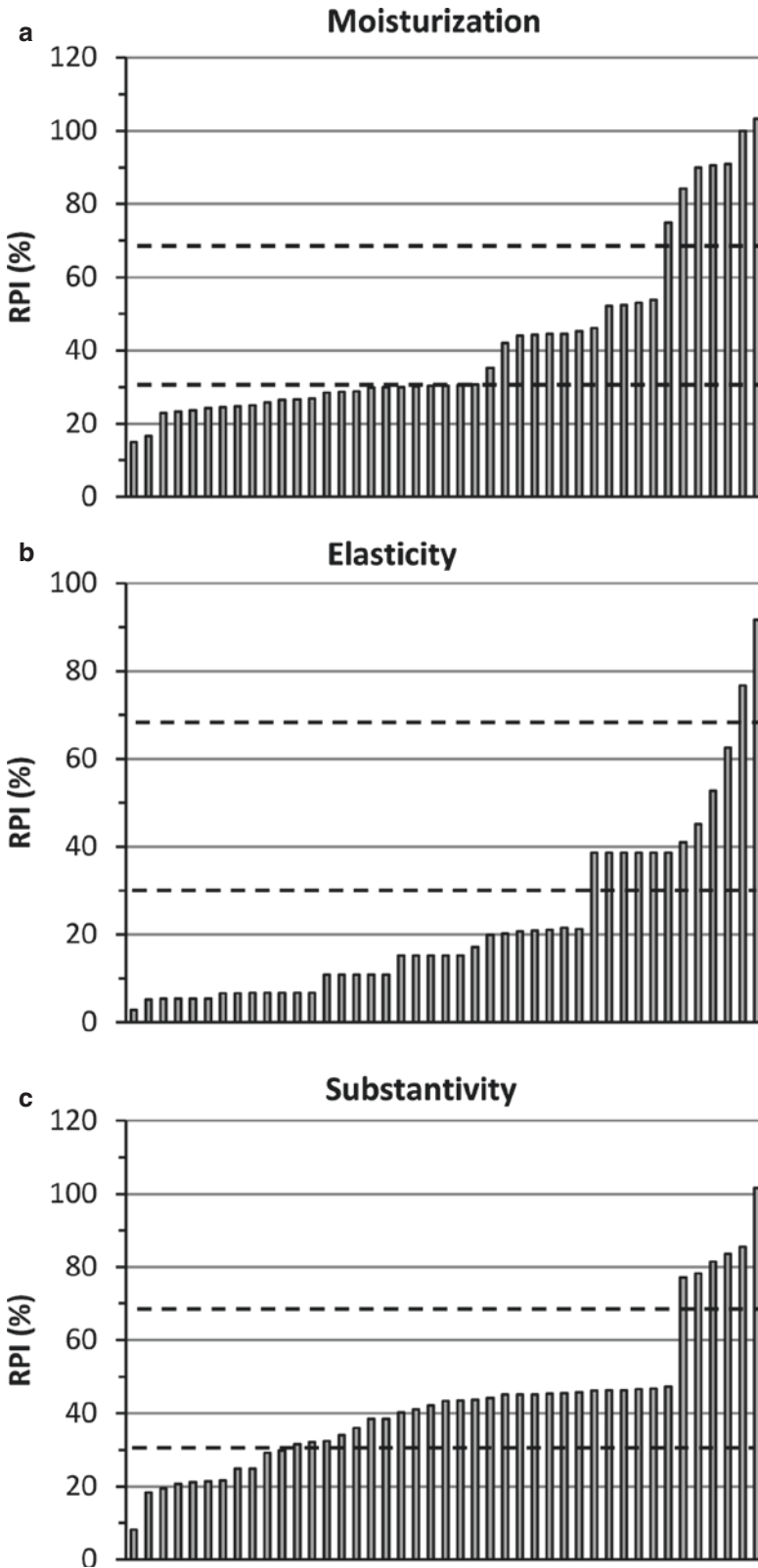
As discussed in the earlier sections, emollients can differ greatly in their properties and in their effects on the skin. These in turn can greatly affect how these emollients in formulations impact on the percutaneous absorption of actives in various formulations. We now consider each of the mechanisms by which emollients can affect percutaneous absorption in turn.

### 5.3.1 How Do the Various Emollients Differ in their Ability to Dissolve and Release Different Actives?

An overarching view of percutaneous absorption is that maximal penetration for an active in a stable formulation will occur at its maximum

**Fig. 5.2** Relative performance indices (RPI, as %) for a range of emollient ingredients shown as individual bars. (a) Moisturization (by skin hydration using a Corneometer, with glycerin as a positive control and untreated skin as a negative control); (b) Elasticity (using a Dermal Torque Meter, with water applied 30 min under occlusion as a positive control and untreated skin as a negative control) and (c)

Substantivity (using a Sebumeter, with petrolatum as a positive control and untreated skin as the negative control). For each property, ingredients were classified as: good-performing ingredients, RPI  $\geq 70\%$ ; medium-performing ingredients, RPI between 30 and 70%; low-performing ingredients, RPI  $\leq 30\%$ . The 30 and 70% cutoffs are shown as *dotted lines* (Adapted from Wiechers et al. 1997)





solubility in the formulation, that is, at saturation, providing the formulation does not affect the skin. Accordingly, the maximal flux for smaller actives is greater than that for larger ones, and those with the lowest melting point (Magnusson et al. 2004) and highest flux for a series of actives of similar size will occur at a lipophilicity similar to that of the skin lipids (a log  $P$  of about 3) (Zhang et al. 2009). There are two general principles defining the ability of an emollient to dissolve an active: “Like dissolves like” and “Oils ain’t all oils”! In other words, lipid-soluble actives generally dissolve better in emollients than polar actives, AND not all emollients have the same properties. In general, actives dissolve better in semipolar emollients (e.g., esters) than in nonpolar, for example, hydrocarbon emollients. Actives can dissolve in both liquid and waxy emollients after heating, but will be released more slowly from the waxy than the liquid emollient. However, increasing the viscosity of a formulation can sometimes result in an enhanced skin penetration as a result of the formulation excipients on evaporation, leaving behind a semi-solid barrier that may impede TEWL, promote skin hydration, and in turn skin penetration flux (Cross et al. 2001a).

These findings have the following implications for how the solubility of an active in an emollient may affect its percutaneous absorption. Firstly, the thermodynamic activity for two equal concentrations of an active in two emollients will be higher in the hydrocarbon than in the semipolar emollient in accordance with their different relative fractional solubilities, resulting in a higher flux of the active through the skin (Wiechers et al. 2012; Roberts 2013). Hence, an active formulated with a hydrocarbon emollient will usually have a faster rate of skin penetration than the one formulated in a semipolar emollient. Accordingly, the skin flux for the sunscreen oxybenzone for petrolatum was found to be greater than that for an oil-in-water (o/w) emulsion (Kurul and Hekimoglu 2001). However, there can be a downside. As the active in the hydrocarbon emollient has a limited solubility, it will also exhaust much more quickly than in the semipolar emollient, that is, the semipolar emollient will

generally deliver its active for a longer period of time. On the other hand, with a semipolar emollient, the product will be more readily washed off by water. Silicone emollients appear to offer both persistence in their retention in the skin and a high solubility, and thus substantivity, for actives dissolved in them (Sene 2003).

### **5.3.2 How Do the Emollients Differ in their Ability to Affect and Enter the Skin (Size and Solubility Parameter Determined) and to Promote Skin Penetration of Actives?**

The primary action by which an emollient promotes skin penetration is by hydration of the stratum corneum. When the skin barrier is normal, increasing the water content by occlusion can lead to enhanced penetration of some, but not all compounds (Hafeez and Maibach 2013a). Some possible mechanisms include increased solubility of the compound in the SC, increased partitioning from the vehicle into the hydrated membrane, and structural alterations due to the swelling of corneocytes and a rearrangement of the intercellular lipid domains (Bjorklund et al. 2010; Hafeez and Maibach 2013b). Occlusion is a well-recognized strategy for enhancing skin penetration (Roberts et al. 2008). The recent reviews by Hafeez and Maibach examined literature data on the effects of occlusion on the penetration of compounds of varying lipophilicities in vivo (Hafeez and Maibach 2013b) and in vitro (Hafeez and Maibach 2013a). They concluded that occlusion tends to enhance the penetration of lipophilic compounds more than hydrophilic compounds, which would be expected, given the relatively lipophilic nature of the intercellular domains into which the compound must partition. However, there appears to be a fall-off in penetration for very lipophilic compounds, which would also be expected as the hydrated conditions under occlusion increase the water content in the intercellular regions. Additionally, the penetration of highly lipophilic compounds may be further limited, as they will not readily

partition from the stratum corneum to an increasingly hydrated viable epidermis. These findings show an interesting parallel to those of Zhang, who showed a parabolic relationship between maximum flux and lipophilicity for a series of phenols penetrating human skin *in vitro*. Zhang saw the greatest penetration at an octanol–water partition coefficient of about 3, with a reduced flux at higher values, and concluded that the relationship was driven by the solubility of the compound in the stratum corneum (Zhang et al. 2009). In both of these examples, stratum corneum solubility can be seen to be largely dependent on the relative lipophilicities of the penetrating compound and the intercellular lipid domain.

As we have seen, a large part of the strategy of using emollients to moisturize and soften the skin is concerned with replacing, replenishing, and reorganizing the population of intercellular lipids. At the same time, a restored lipid domain may strengthen the skin barrier and most likely lead to a reduced permeability to applied chemicals. Results from infrared spectroscopy on human stratum corneum suggested that increased lipid organization occurred as a result of increased hydrogen bonding (Kaushik and Michniak-Kohn 2010). On the other hand, petrolatum (Ghadially et al. 1992) and nonphysiological lipophilic moisturizers (Caussin et al. 2007) were shown to become localized in separate intercellular domains, with little effect on lamellar organization or barrier function.

Conversely, the application of emollients to the skin may have the effect of reducing barrier function and enhancing the penetration of applied compounds. This may occur as a result of a direct effect on intercellular lipids, where they become disrupted or fluidized (Kaushik and Michniak-Kohn 2010). Certain silicone polymers, although functioning as effective moisturizers, were shown by electron microscopy to disrupt lipid bilayers, leading to reduced barrier function (Menon and Ghadially 1997).

In the same way as active solutes will penetrate the skin according to their size, melting point, and lipophilicity, similar considerations determine how emollients enter the skin. Thus, of

the ester emollients in Table 5.2, the liquid diisopropyl adipate (MW 230 Da) is most likely to enter the skin, whereas the solid, glycol distearate (MW 595 Da) is the least likely to enter. Zhang et al (2013) showed that the ester emollient isopropyl myristate (MW 270 Da) rapidly enters the skin and could change its properties, whereas the hydrocarbon emollient liquid paraffin appears not to enter the skin. Thus, isopropyl myristate is an emollient that enhanced the skin penetration of phenols, whereas mineral oil did not. The main effect of isopropyl myristate was to carry the phenols into skin lipids, increasing their overall solubility and maximum flux. However, isopropyl myristate also appeared to act as a reservoir, retarding the penetration for the more lipophilic phenols.

Limited information is available about the extent to which emollients can modify the skin reservoir effect. It seems likely that, in a similar way to occlusion, emollients may promote the release of actives from the horny layer (Roberts et al. 2004). However, there may be some waxy emollients which have a very slow release rate of actives. Therefore, such emollients, if retained in the horny layer, could potentially cause an enhanced reservoir effect. A more desirable effect is to have an enhanced substantivity as a consequence of the emollient's substantive properties, as shown for silicone esters (Sene 2003).

### 5.3.3 What Do Other Ingredients in a Moisturizing Formulation Do to Enhance or Inhibit the Effects of Emollients on Skin Penetration?

Formulations, especially emulsions, may contain a wide range of ingredients with many different functions, including: preservatives, coloring materials, fragrances, thickeners, surfactants, humectants, emollients, buffers to control the pH, chelating agents, and others. The balance between them is very important for the stability and final function of the formulation. For example, if a fragrance causes skin irritation, it may also change

skin penetration of actives. As they are major ingredients in many topical formulations, the effects of humectants and surfactants on the skin barrier may be significant.

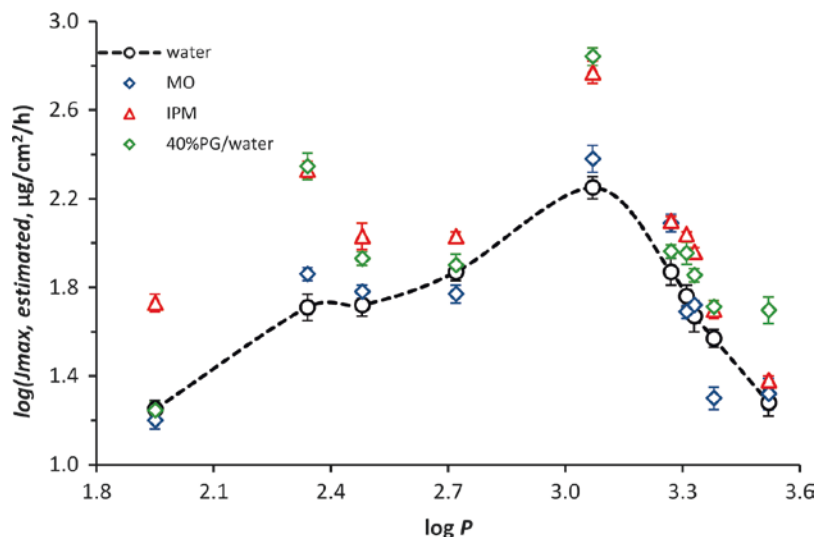
Humectants such as glycerol, propylene glycol, or sorbitol are used to accentuate moisturization, but can also accentuate emollient effects on skin lipids by inhibiting the SC lipid phase transition. Indeed, in a 1990 study done in a dry atmosphere, Froebe et al. (1990) showed that glycerol acts as a skin moisturizer by inhibiting the lipid phase transition from liquid to solid crystal, rather than by acting primarily as a humectant. More recently, *in vitro* studies using mixtures of glycerol and the powerful skin irritant and penetration enhancer, sodium dodecyl sulfate (SDS), showed that glycerol was able to attenuate the effects of SDS on the skin barrier by reducing the ability of SDS to penetrate into the SC (Ghosh and Blankschtein 2007).

Surfactants are used widely in topical formulations, usually to solubilize more lipophilic actives. As the name suggests, they interact at membrane interfaces and, in particular, are capable of modifying the structure and properties of the skin (Williams and Barry 2004). Anionic and cationic surfactants in particular may cause irritation and skin damage by strong binding and denaturing of skin surface proteins with swelling and disruption of the corneocytes, as well as

disordering of the intercellular lipid structure. Nonionic surfactants tend to cause less irritation and barrier damage, with polysorbates being accorded GRAS (generally regarded as safe) status by the US Food and Drug Administration (Predmore and Li 2011). They act to fluidize lipids and bind to keratin filaments (Nokhodchi et al. 2003). As expected, alterations in SC barrier properties by surfactants may lead to enhanced permeation of topically applied materials. Most studies have examined the effects of anionic and nonionic surfactants, with the more disruptive anionic materials such as sodium lauryl sulfate and sodium dodecyl sulfate causing the greatest enhancement (Williams and Barry 2004). Nonionic surfactants like ethers and polysorbates (e.g., Tween 80) cause more modest degrees of enhancement (Som et al. 2012). Nonionic surfactants have also been incorporated into W/O emulsions which are compatible with the lipophilic sebum environment in hair follicles, in order to target the follicular route of skin penetration by hydrophilic solutes (Wu et al. 2001).

Figure 5.3 shows maximum fluxes for a series of phenols of similar molecular weight applied to human epidermal membranes from a range of simple vehicles, plotted against  $\log P$  (Zhang et al. 2013). It is clear that the maximum fluxes for water and the occlusive emollient mineral oil

**Fig. 5.3**  $\log(J_{\max})$ , estimated versus  $\log P$ . Estimated maximum fluxes ( $n=5$ , mean  $\pm$  SD) for ten phenolic compounds of similar molecular weight from water, mineral oil (MO), isopropyl myristate (IPM), and a mixture of 40% PG/water, plotted against lipophilicity of the phenolic compound. The dotted line interpolates data from the water vehicle and is included as a reference only (Adapted from Zhang et al. 2013)



(MO) are similar across this range of log  $P$ , as expected for “inert” solvents that do not permanently alter the properties of the skin (Barry et al. 1985; Cross et al. 2001b). In contrast, the ester emollient IPM led to increased maximum fluxes, particularly for the more polar phenols, which was due to penetration of IPM into deeper layers of the stratum corneum (Zhang et al. 2013), where it has been suggested that it integrates into the stratum corneum lipid matrix and disrupts the organization of the lipid lamellae (Brinkmann and Muller-Goymann 2005). Figure 5.3 also illustrates similar increases in maximum flux seen with mixtures of the humectant propylene glycol and water, most likely due to increased solubility of the phenols in stratum corneum lipids following propylene glycol absorption (Zhang et al. 2011). Such a mechanism was also used to explain the enhanced penetration of minoxidil into human skin from vehicles containing propylene glycol (Grice et al. 2010).

## 5.4 Practical Aspects

Table 5.4 shows five formulations containing different emollients and their likely effect on the skin properties and on the skin penetration of an active. The first impression that a consumer has in using a product is the sensorial feel. Formulation 1 feels light and soft, because it lacks oils but is capable of lowering TEWL sufficiently to increase hydration and potentially promote skin penetration of an active. The second formulation contains ester emollients to give a smooth and soft feel. The smoothness derives from the lubrication of the skin surface by the ester emollient’s lipid film. As this film has a greater effect on TEWL and skin hydration than formulation 1, it may promote skin penetration more. On the other hand, the lipid active is probably more soluble in formulation 2, and this may inhibit skin penetration of the active. Formulation 3 contains mineral oil as an emollient, and it will feel oily and very soft, as this is

**Table 5.4** Examples of some formulations containing different emollients and their effects on the skin and the likely skin penetration of an active

Raw materials	1 (control)	2 (ester)	3 (mineral oil)	4 (animal fat)	5 (IPM)
Cetareth-20	2.0%	2.0%	2.0%	2.0%	2.0%
Cetearyl alcohol	3.0%	3.0%	3.0%	3.0%	3.0%
Triethanolamine	pH5.5–6.5	pH5.5–6.5	pH5.5–6.5	pH5.5–6.5	pH5.5–6.5
Carbomer	0.15%	0.15%	0.15%	0.15%	0.15%
Caprylic/capric triglyceride (CCT)	–	5%	–	–	–
Lanolin	–	–	–	5%	–
Mineral oil	–	–	5%	–	–
Isopropyl myristate	–	–	–	–	5%
Glycerin	4.0%	4.0%	4.0%	4.0%	4.0%
Phenoxyethanol and parabens (methyl, ethyl, and propyl)	0.8%	0.8%	0.8%	0.8%	0.8%
Water	Qsp 100%	Qsp 100%	Qsp 100%	Qsp 100%	Qsp 100%
<i>Effects on skin</i>					
Sensorial feel	Light and soft	Smooth and soft	Oily and soft	Greasy and heavy	Smooth and soft
Reduction in TEWL	↓	↓	↓↓↓	↓↓	↓↓
Skin hydration	↑	↑↑	↑↑↑	↑↑	↑↑
Change in solubility of nonpolar active	–	↑	↑	↑↑	↑↑
Potential effect on skin penetration	↑	↑↑↑	↑↑↑	↑↑↑	↑↑↑

the most occlusive formulation of all described formulations and therefore will provide the greatest inhibition of TEWL and the greatest skin hydration. An active is also likely to have poorer solubility in formulation 3. Accordingly, this formulation is likely to provide better skin penetration of the active. Formulation 4 feels greasy, because it contains animal fat such as lanolin, and heavy because of the lanolin waxes. This formulation is expected to be occlusive and to promote the solubility of the active. However, lanolin also contains cholesterol, cholesterol derivatives, and free fatty acids, which may act as skin penetration enhancers. The overall effect is likely to be an enhancement of skin penetration. Formulation 5 is very similar to formulation 2. However, it contains the ester emollient, isopropyl myristate, a well-known skin penetration enhancer. Accordingly, formulation 5 should provide greater skin penetration of the active than formulation 2.

There are other practical considerations in the use of emollients. They can provide a number of functions, including the relief of potential discomfort and irritation caused by solvents, promotion of penetration, particle coating, stabilization of suspensions, brightness control for makeup, among others (Dederen et al. 2012). Another practical consideration is emollient stability. Ester emollient stability may be affected at low or high pH, due to the possibility of hydrolysis or saponification, respectively. While formulations are generally prepared at neutral or slightly acidic pH, care must be taken to ensure that these conditions will be maintained in a product over time. There are some raw materials that can promote stability of emollient esters at extreme pH. Additionally, it should be recognized that if the finished products are to come into contact with the mouth (e.g., in lipstick), emollients and other ingredients must not have an unpleasant taste. In summary, each product has unique physicochemical properties that can promote different interactions and reactions with the skin surface.

Another consideration is the potential irritancy of the formulations. As a general principle, in order to minimize skin irritancy, the sensitizing lanolin alcohols should be used in formulations in concentrations less than 3% (Marks

2001). Other ingredients, such as the humectant, propylene glycol (>15%), and ingredients used to stabilize emollients in products, such as surfactants (e.g., oleic acid), can also cause irritation (Marks 2001).

## Conclusion

This chapter has attempted to clarify the definition of an emollient, show the range of emollients available in the market, and explore how these emollients are likely to affect skin penetration. The chapter concludes with an examination of some emollient-containing products and their effects on the skin and on the likely skin penetration of an active.

The key property of an emollient is that it softens the skin through occlusion and resultant moisturization as well as by forming a lipid film which smooths the skin by lubrication. Moisturization of the skin is well known to be the main means by which skin penetration enhancement can be achieved (Roberts et al. 2008). However, emollients can also affect the solubility of an active and penetration enhancers, and thus their effects on the skin penetration of an active may be uncertain. The final section discusses some potential outcomes for different formulations containing emollients.

It also needs to be recognized that all cosmetic and pharmaceutical products contain different ingredients, each of which can impinge on the sensorial feel and skin penetration properties of a product. One concern is the potential skin irritation caused by these ingredients. Of the emollients, lanolin and isopropyl myristate are the most likely to be associated with skin irritation. The most inert emollient is probably mineral oil and, as it is very hydrophobic, it may also promote skin penetration by inducing a high thermodynamic activity of the active as a consequence of the active's low solubility in the mineral oil.

Treatments designed to improve dry skin or treat skin diseases, such as lipid replenishment, may also enhance the skin barrier function and reduce its permeability to topical chemicals. On the other hand, emollients may

enhance the barrier's permeability by mechanisms such as increased hydration following occlusion, disruption of the intercellular lipid organization, or increasing the solubility of a chemical or active ingredient in the stratum corneum. Formulation strategies designed to enhance skin penetration can be devised by the judicious choice of emollient ingredients; however, it is important to stress that each skin characteristic varies widely between individuals. In addition, factors such as safety, cost, sensory properties, sustainability, and marketing will all be considered by a formulator in choosing a suitable emollient.

**Acknowledgments** This chapter is dedicated to Johann Wiechers who was to write this chapter and brought us all together. It was his fervent wish that we looked at the impact of practical formulations on skin penetration. We thank the NHMRC of Australia for its support of our work. We are also grateful to Ricardo Azzini, Fabricio Sousa, and Joaosinho Di Domenico for their valuable guidance on the construction of Table 5.2 and their general comments.

## References

- Barry BW, Harrison SM, Dugard PH (1985) Vapour and liquid diffusion of model penetrants through human skin; correlation with thermodynamic activity. *J Pharm Pharmacol* 37(4):226–236
- Batt MD, Fairhurst E (1986) Hydration of the stratum corneum. *Int J Cosmet Sci* 8(6):253–264
- Batt MD, Davis WB, Fairhurst E, Gerrard WA, Ridge BD (1988) Changes in the physical-properties of the stratum-corneum following treatment with glycerol. *J Soc Cosmetic Chem* 39(6):367–381
- Bjorklund S, Engblom J, Thuresson K, Sparr E (2010) A water gradient can be used to regulate drug transport across skin. *J Control Release* 143(2):191–200
- Blank IH (1952) Factors which influence the water content of the stratum corneum. *J Invest Dermatol* 18(6):433–440
- Blank IH (1957) Action of emollient creams and their additives. *JAMA* 164(4):412–415
- Brinkmann I, Muller-Goymann CC (2005) An attempt to clarify the influence of glycerol, propylene glycol, isopropyl myristate and a combination of propylene glycol and isopropyl myristate on human stratum corneum. *Pharmazie* 60(3):215–220
- Campbell SD, Kraning KK, Schibli EG, Momii ST (1977) Hydration characteristics and electrical resistivity of stratum corneum using a noninvasive four-point microelectrode method. *J Invest Dermatol* 69(3):290–295
- Caussin J, Gooris GS, Groenink HW, Wiechers JW, Bouwstra JA (2007) Interaction of lipophilic moisturizers on stratum corneum lipid domains in vitro and in vivo. *Skin Pharmacol Physiol* 20(4):175–186
- Chamlin SL, Kao J, Frieden IJ, Sheu MY, Fowler AJ, Fluhr JW, Williams ML, Elias PM (2002) Ceramide-dominant barrier repair lipids alleviate childhood atopic dermatitis: changes in barrier function provide a sensitive indicator of disease activity. *J Am Acad Dermatol* 47(2):198–208
- Christensen MS, Hargens CW 3rd, Nacht S, Gans EH (1977) Viscoelastic properties of intact human skin: instrumentation, hydration effects, and the contribution of the stratum corneum. *J Invest Dermatol* 69(3):282–286
- Clarys P, Barel A (1995) Quantitative evaluation of skin surface lipids. *Clin Dermatol* 13(4):307–321
- Coxe JR (1825) *The American dispensatory*. Carey & Lea, Philadelphia
- Cross SE, Jiang R, Benson HA, Roberts MS (2001a) Can increasing the viscosity of formulations be used to reduce the human skin penetration of the sunscreen oxybenzone? *J Invest Dermatol* 117(1):147–150
- Cross SE, Pugh WJ, Hadgraft J, Roberts MS (2001b) Probing the effect of vehicles on topical delivery: understanding the basic relationship between solvent and solute penetration using silicone membranes. *Pharm Res* 18(7):999–1005
- Dederen JC, Chavan B, Rawlings AV (2012) Emollients are more than sensory ingredients: the case of isostearyl isostearate. *Int J Cosmet Sci* 34(6):502–510
- Edwards LD (1940) The role of fats and fat materials in pharmaceutical and cosmetic preparations. *Oil Soap* 17(4):82–84
- Elias PM (2010) Therapeutic implications of a barrier-based pathogenesis of atopic dermatitis. *Ann Dermatol* 22(3):245–254
- Fluhr JW, Mao-Qiang M, Brown BE, Wertz PW, Crumrine D, Sundberg JP, Feingold KR, Elias PM (2003) Glycerol regulates stratum corneum hydration in sebaceous gland deficient (asebia) mice. *J Invest Dermatol* 120(5):728–737
- Froebe CL, Simion A, Ohlmeyer H, Rhein LD, Mattai J, Cagan RH, Friberg SE (1990) Prevention of stratum corneum lipid phase transitions in vitro by glycerol – an alternative mechanism for skin moisturization. *J Soc Cosmet Chem* 41:51–65
- Ghadially R, Halkier-Sorensen L, Elias PM (1992) Effects of petrolatum on stratum corneum structure and function. *J Am Acad Dermatol* 26(3 Pt 2):387–396
- Ghosh S, Blankshtein D (2007) The role of sodium dodecyl sulfate (SDS) micelles in inducing skin barrier perturbation in the presence of glycerol. *J Cosmet Sci* 58(2):109–133
- Goldemberg RL, De La Rosa CP (1971) Correlation of skin feel of emollients to their chemical structure. *J Soc Cosmet Chem* 22(10):635–654

- Grice JE, Ciotti S, Weiner N, Lockwood P, Cross SE, Roberts MS (2010) Relative uptake of minoxidil into appendages and stratum corneum and permeation through human skin in vitro. *J Pharm Sci* 99(2):712–718
- Hafeez F, Maibach H (2013a) Do partition coefficients (lipophilicity/hydrophilicity) predict effects of occlusion on percutaneous penetration in vitro: a retrospective review. *Cutan Ocul Toxicol* 32(4):299–303
- Hafeez F, Maibach H (2013b) Occlusion effect on in vivo percutaneous penetration of chemicals in man and monkey: partition coefficient effects. *Skin Pharmacol Physiol* 26(2):85–91
- Harry RG (1941) Skin penetration. *Br J Dermatol Syphilis* 53(3):65–82
- Highley DR, Coomey M, Denbeste M, Wolfram LJ (1977) Frictional-properties of skin. *J Invest Dermatol* 69(3):303–305
- Idson B (1982) Moisturizers, emollients, and bath oils. In: Frost P, Horwitz SN (eds) *Principles of cosmetics for the dermatologist*. The C.V. Mosby Company, St Louis
- Idson B (1992) Dry skin: moisturizing and emolliency. *Cosmet Toiletr* 107:69
- Kaushik D, Michniak-Kohn B (2010) Percutaneous penetration modifiers and formulation effects: thermal and spectral analyses. *AAPS PharmSciTech* 11(3):1068–1083
- Kurul E, Hekimoglu S (2001) Skin permeation of two different benzophenone derivatives from various vehicles. *Int J Cosmet Sci* 23(4):211–218
- Lesnik RH, Kligman LH, Kligman AM (1992) Agents that cause enlargement of sebaceous glands in hairless mice. I. Topical substances. *Arch Dermatol Res* 284(2):100–105
- Loden M (1992) The increase in skin hydration after application of emollients with different amounts of lipids. *Acta Derm Venereol* 72(5):327–330
- Magnusson BM, Anissimov YG, Cross SE, Roberts MS (2004) Molecular size as the main determinant of solute maximum flux across the skin. *J Invest Dermatol* 122(4):993–999
- Mao-Qiang M, Brown BE, Wu-Pong S, Feingold KR, Elias PM (1995) Exogenous nonphysiologic vs physiologic lipids. Divergent mechanisms for correction of permeability barrier dysfunction. *Arch Dermatol* 131(7):809–816
- Marks R (2001) Constituents of emollients. In: Marks R (ed) *Sophisticated emollients*. Georg Thieme Verlag, Stuttgart, pp 40–48
- MediLexicon. Medical Dictionary, Medical Terminology. Retrieved 25 Nov 2013. 2013. From <http://www.mediLexicon.com/medicaldictionary.php>.
- Menon G, Ghadially R (1997) Morphology of lipid alterations in the epidermis: a review. *Microsc Res Tech* 37(3):180–192
- Mo YK, Kankavi O, Masci PP, Mellick GD, Whitehouse MW, Boyle GM, Parsons PG, Roberts MS, Cross SE (2007) Surfactant protein expression in human skin: evidence and implications. *J Invest Dermatol* 127(2):381–386
- Mosby, Inc. (2009) *Mosby's medical dictionary*. Elsevier – Health Sciences Division, St Louis
- Nakatani M, Fukuda T, Arakawa N, Kawasoe T, Omata S (2013) Softness sensor system for simultaneously measuring the mechanical properties of superficial skin layer and whole skin. *Skin Res Technol* 19(1):e332–e338
- Nokhodchi A, Shokri J, Dashbolaghi A, Hassan-Zadeh D, Ghafourian T, Barzegar-Jalali M (2003) The enhancement effect of surfactants on the penetration of lorazepam through rat skin. *Int J Pharm* 250(2):359–369
- Nola I, Kostovic K, Kotrulja L, Lugovic L (2003) The use of emollients as sophisticated therapy in dermatology. *Acta Dermatovenerol Croatica ADC* 11(2):80–87
- Paepe K, Rogiers V (2009) Glycerol as humectant in cosmetic formulations. In: Rawlings AV, Leyden JJ (eds) *Skin moisturization*. Informa Healthcare, New York, pp 279–294
- Patzelt A, Lademann J, Richter H, Darvin ME, Schanzer S, Thiede G, Sterry W, Vergou T, Hauser M (2012) In vivo investigations on the penetration of various oils and their influence on the skin barrier. *Skin Res Technol* 18(3):364–369
- Pilgram GS, Vissers DC, van der Meulen H, Pavel S, Lavrijsen SP, Bouwstra JA, Koerten HK (2001) Aberrant lipid organization in stratum corneum of patients with atopic dermatitis and lamellar ichthyosis. *J Invest Dermatol* 117(3):710–717
- Predmore A, Li J (2011) Enhanced removal of a human norovirus surrogate from fresh vegetables and fruits by a combination of surfactants and sanitizers. *Appl Environ Microbiol* 77(14):4829–4838
- Rawlings AV, Voegeli R (2013) Stratum corneum proteases and dry skin conditions. *Cell Tissue Res* 351(2):217–235
- Ray LF, Blank IH (1940) Effect of ointment bases on the skin I. Results of patch tests with commonly used ointment bases. *Arch Derm Syphilol* 42(2):285–289
- Roberts MS (2013) Solute-vehicle-skin interactions in percutaneous absorption: the principles and the people. *Skin Pharmacol Physiol* 26(4–6):356–370
- Roberts MS, Cross SE, Anissimov YG (2004) Factors affecting the formation of a skin reservoir for topically applied solutes. *Skin Pharmacol Physiol* 17(1):3–16
- Roberts MS, Bouwstra JA, Pirot F, Falson F (2008) Skin hydration—a key determinant in topical absorption. In: Walters KA, Roberts MS (eds) *Dermatologic, cosmetic, and cosmetic development*. Informa Healthcare USA, Inc, New York, pp 115–128
- Sene C (2003) Silicone excipients for aesthetically superior and substantive topical pharmaceutical formulations. *Pharma Chem* 2(5):17–20
- Som I, Bhatia K, Yasir M (2012) Status of surfactants as penetration enhancers in transdermal drug delivery. *J Pharmacy Bioallied Sci* 4(1):2–9
- Stedman's TL (2011) *Stedman's medical dictionary for the health professions and nursing*. Lippincott Williams & Wilkins, Philadelphia
- Stewart ME (1992) Sebaceous gland lipids. *Semin Dermatol* 11(2):100–105

- Stoughton RB (1959). Relation of the anatomy of normal and abnormal skin to its protective function. In: Rothman S (ed) *The human integument. Normal and abnormal*. American Association for the Advancement of Science, Washington, DC
- Voegeli R, Rawlings AV, Breternitz M, Doppler S, Schreier T, Fluhr JW (2009) Increased stratum corneum serine protease activity in acute eczematous atopic skin. *Br J Dermatol* 161(1):70–77
- Voegeli R, Doppler S, Joller P, Breternitz M, Fluhr JW, Rawlings AV (2011) Increased mass levels of certain serine proteases in the stratum corneum in acute eczematous atopic skin. *Int J Cosmet Sci* 33(6):560–565
- Wehr RF, Krochmal L (1987) Considerations in selecting a moisturizer. *Cutis* 39(6):512–515
- Wiechers J (1997) Relative performance testing: introducing a tool to facilitate cosmetic ingredient selection. *Cosmet Toiletr* 112(9):79–84
- Wiechers JM, Barlow T (1999) Skin moisturisation and elasticity originate from at least two different mechanisms. *Int J Cosmet Sci* 21(6):425–435
- Wiechers JW, Verboom C, Wortel VAL, Starmans WA (2002) Multifunctionality: from “One in More” to “More in One”. *Cosmet Toiletr* 117(4):73–78
- Wiechers JW, Dederen JC, Rawlings AV (2009) Moisturization mechanisms: internal occlusion by orthorhombic lipid phase stabilizers—a novel mechanism of action of skin moisturization. In: Rawlings AV, Leyden JJ (eds) *Skin moisturization*. Informa Healthcare USA, Inc, New York, pp 309–321
- Wiechers JW, Watkinson AC, Cross SE, Roberts MS (2012) Predicting skin penetration of actives from complex cosmetic formulations: an evaluation of inter formulation and inter active effects during formulation optimization for transdermal delivery. *Int J Cosmet Sci* 34(6):525–535
- Wild RB (1911) On the official ointments, with special reference to the substances used as bases. *Br Med J* 1911:161–162
- Wilkinson JB, Moore RJ (1982). *Skin creams*. In: Wilkinson JB (ed) *Harry’s cosmeticology*. Chemical Publishing, New York, p 62
- Williams AC, Barry BW (2004) Penetration enhancers. *Adv Drug Deliv Rev* 56(5):603–618
- Wu H, Ramachandran C, Weiner ND, Roessler BJ (2001) Topical transport of hydrophilic compounds using water-in-oil nanoemulsions. *Int J Pharm* 220(1–2): 63–75
- Zeidler U (1985) On the spreading of lipids on the skin. *Fette Seifen Anstrichmittel* 87(10):403–408
- Zeidler U (1992) Über die taktilen Eigenschaften kosmetischer Öle. *SÖFW* 118:1001–1007
- Zhang Q, Grice JE, Li P, Jepps OG, Wang GJ, Roberts MS (2009) Skin solubility determines maximum transepidermal flux for similar size molecules. *Pharm Res* 26(8):1974–1985
- Zhang Q, Li P, Roberts MS (2011) Maximum transepidermal flux for similar size phenolic compounds is enhanced by solvent uptake into the skin. *J Control Release* 154(1):50–57
- Zhang Q, Li P, Liu D, Roberts MS (2013) Effect of vehicles on the maximum transepidermal flux of similar size phenolic compounds. *Pharm Res* 30(1):32–40



# The Effects of Vehicle Mixtures on Transdermal Absorption: Thermodynamics, Mechanisms, Assessment, and Prediction

Jason T. Chittenden and Jim E. Riviere

## Contents

6.1	<b>Introduction</b> .....	95
6.2	<b>Thermodynamics of Mixtures</b> .....	96
6.2.1	Solubility .....	97
6.2.2	Partition Coefficient .....	98
6.2.3	Diffusion .....	99
6.3	<b>Potential Mechanisms of Interaction</b> .....	99
6.3.1	Skin Surface .....	99
6.3.2	Stratum Corneum .....	101
6.3.3	Epidermis and Dermis .....	102
6.4	<b>Experimental Assessment of Interactions</b> ..	103
6.4.1	Diffusion Cells .....	103
6.4.2	Isolated Perfused Porcine Skin Flap .....	103
6.4.3	Model Membrane Systems .....	104
6.5	<b>Predicting Absorption from Complex Vehicle Mixtures</b> .....	104
	<b>Conclusion</b> .....	113
	<b>References</b> .....	113

J.T. Chittenden (✉)  
Biomathematics, North Carolina State University,  
Raleigh, NC, USA

Pharsight Corporation,  
5520 Dillard Drive, suite 260, Cary, NC 27518, USA  
e-mail: [jason.chittenden@certara.com](mailto:jason.chittenden@certara.com)

J.E. Riviere, DVM, PhD, DSc(hon), ATS  
Coles 207, Department of Anatomy and Physiology,  
Institute of Computational Comparative Medicine,  
College of Veterinary Medicine, Kansas State  
University, Manhattan, KS 66506-5802, USA  
e-mail: [jriviere@ksu.edu](mailto:jriviere@ksu.edu)

## 6.1 Introduction

In industrial settings, dermal exposure to toxic substances usually occurs with the substance carried in a liquid mixture. The mixture may contain solvents used in extraction processes, reaction by-products, wetting agents, surfactants, etc. For pharmaceutical applications, a dosing vehicle is used to stabilize the formulation and modulate absorption. In either case, the composition of the vehicle affects the thermodynamic and transport properties of the penetrant. The ability to predict the effect of vehicle composition on the relevant properties of the penetrant and model exposure to the penetrant would be valuable for evaluating the risk in toxic exposure or maximizing the therapeutic value in pharmaceutical applications.

The impact of different vehicles and enhancers on percutaneous absorption has been studied extensively (Carpentieri-Rodrigues et al. 2007; Cross et al. 2001; Dias et al. 2007; Dupuis et al. 1986; Hotchkiss et al. 1992; Jepson and McDougal 1999; de la Maza et al. 1998; Van der Merwe and Riviere 2005a; Mills 2007; Mills et al. 2005, 2006; Sherertz et al. 1987; Traynor et al. 2007; Tsuruta 1996; Walker and Smith 1996; Williams and Barry 2004). A large number of studies have demonstrated synergistic effects of combinations of solvents and/or penetration enhancers (Carpentieri-Rodrigues et al. 2007; Karande and Mitragotri 2009). Several studies have shown permeability enhancement in binary

or ternary mixtures (Baynes and Riviere 2004; Baynes et al. 2001; El Maghraby et al. 2009; Van der Merwe and Riviere 2005b; Monti et al. 1995; Rosado et al. 2003). Enhancement of diazepam permeability in rat skin from a 50:50 mixture of propylene glycol and water was found to vary with the concentration of added surfactants (Shokri et al. 2001). One study explored over 4000 binary vehicles to develop rules for predicting synergistic permeability enhancements (Karande et al. 2006). An extensive study of up to quaternary combinations of ten enhancers on skin permeability found synergistic enhancement, with the best results on average for ternary combinations (Arora et al. 2010). Despite such a large body of work, a comprehensive understanding of the effect of complex vehicle mixtures is still elusive.

A review (Moss et al. 2002) of quantitative structure to permeability relationships (QSPRs) for percutaneous permeation prior to 2002 showed only one example where a vehicle effect was accounted for, and it only provided an indicator variable to adapt between two vehicles. Most of the prior work on skin absorption is done with few compounds, aqueous or single vehicles, and in nonstandardized conditions. Building models to predict vehicle mixture effects requires an extensive dataset with dosing applied in various vehicle compositions. Single penetrant or enhancer studies, even if combined, are not suitable to study synergistic effects. Studies should be specifically designed for the purpose. Thus, it is only recently that predictive models that include vehicle effects, and especially mixture effects, have been developed.

The goal of this chapter is to exhibit some of the most recent works in the modeling and prediction of skin permeability from complex vehicle mixtures. The chemical thermodynamics that underlie many of the interactions are briefly reviewed to highlight the mixture effects that can affect some key properties driving permeability. The structure of the skin is discussed in the context of potential mechanisms for interaction with vehicle constituents. An overview of some of the

experimental apparatuses gives insight into the strengths and limitations of available data. Finally, a thorough review of the available literature on predicting mixture effects on permeability shows the promise and failings of work to date.

## 6.2 Thermodynamics of Mixtures

The key properties – solubility, partition coefficient, and diffusivity – that drive transdermal absorption can be related back to a single property of a penetrant, the chemical potential, which is a function of the composition of the multicomponent system also including solvents and enhancers. The chemical potential measures the differential change in Gibbs energy of a system with respect to one of its constituents. In practical terms, the chemical potential is the definitive property which is equated in various equilibria (e.g., reaction, phase, adsorption). For component  $i$  in a solution, one can write the chemical potential  $\mu_i$  as

$$\mu_i = \left( \frac{\partial G}{\partial N_i} \right)_{T,P,N_{j \neq i}} = RT \ln \gamma_i x_i + \mu_i^\circ,$$

where  $R$  is the ideal gas constant,  $T$  and  $P$  are temperature and pressure,  $x_i$  is the mole fraction of component  $i$ ,  $N_j$  are the numbers of molecules of each component  $j$ ,  $\mu_i^\circ$  is the chemical potential of pure component  $i$  at a reference state ( $T^\circ, P^\circ$ ), and  $\gamma_i$  is the activity coefficient. Rearranging the equation leads to an expression of the change in the partial Gibbs energy of mixing ( $\Delta G_i$ ) as a function of concentration:

$$\begin{aligned} \Delta G_i &= \mu_i - \mu_i^\circ = RT \ln x_i + RT \ln \gamma_i \\ &= \Delta G_i^{ID} + \Delta G_i^{EX}, \end{aligned}$$

where  $\Delta G_i^{ID}$  and  $\Delta G_i^{EX}$  are the ideal and excess Gibbs mixing energies for component  $i$ . The activity coefficient of component  $i$  can then be taken as:

$$\frac{\Delta G_i^{EX}}{RT} = \ln \gamma_i$$

Chemical potential is the driving force behind solubility, phase equilibrium, and diffusion. The activity coefficient captures the departure from ideality for real mixtures and provides a mechanism to link that departure to the mixture composition. Activity coefficient models, which incorporate parameters that describe the interactions between mixture components, provide a way to include mixture composition effects in chemical property predictions.

### 6.2.1 Solubility

Predicting the solubility of a compound in various vehicles is important both in manufacturing processes and in the formulation of drug products. The solubility of a compound in a solvent is the equilibrium expressed as:

$$x_i^L \gamma_i^L f_i^{\circ,L} = x_i^S \gamma_i^S f_i^{\circ,S}$$

If the solid is pure, then this reduced to

$$x_i^L = \frac{f_i^{\circ,S}}{\gamma_i^L f_i^{\circ,L}}$$

$$\ln x_i^L = \frac{\Delta H_{m,i}}{RT} \left( 1 - \frac{T}{T_m} \right) - \ln \gamma_i^L$$

where  $\Delta H_{m,i}$  is the enthalpy of fusion,  $T_m$  is the melting point,  $x_i^L$  is the solubility,  $\gamma_i^L$  is the liquid activity at saturation, and  $f_i^{\circ,L}$  and  $f_i^{\circ,S}$  are the fugacity of the pure liquid and solid phases. So, prediction of solubility can be based on accessible physical properties, and a model for liquid phase activity, of the solute.

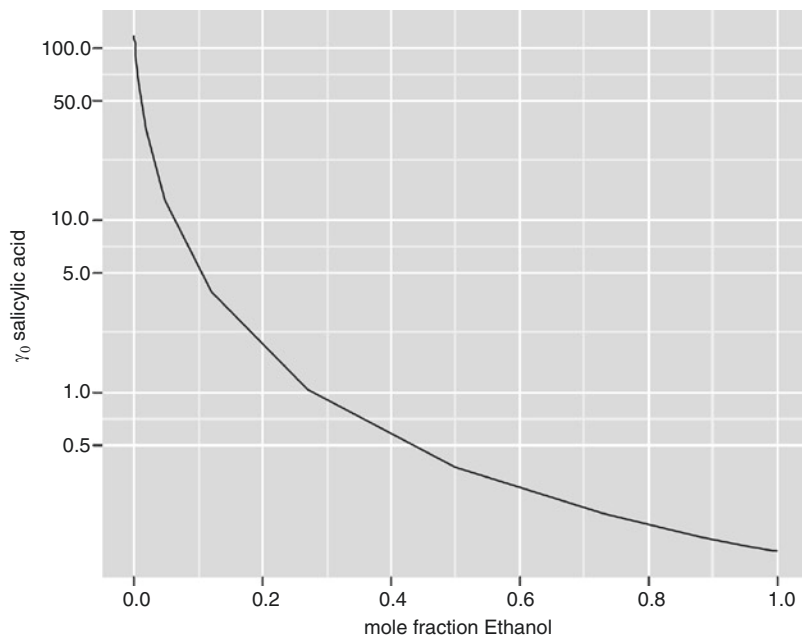
Many activity coefficient models have been developed and applied to solubility in drug-like compounds. These range from simple models to complex computational chemistry-based simulations. Many are incremental improvements on already existing models such as the Non-Random Two-Liquid (NRTL) and UNiversal QUasiChemical (UNIQUAC).

Mirmehrabi proposed a simple activity coefficient model, similar to the Margules model but extended to mixtures, and used it to predict vapor-liquid equilibria in 41 systems and solubility of stearic acid in a solvent mixture with better results than UNIFAQ (UNIQUAC Functional Activity Coefficients) (Mirmehrabi et al. 2006a). The same proposed model was tested with three drugs in pure and mixed solvents showing that while it performed well for binary systems, UNIQUAC and NRTL outperformed in mixture systems (Mirmehrabi et al. 2006b). A simple one-parameter Wilson model has been used to predict the solubility of four drugs in water plus cosolvents of either ethanol, methanol, or 1,4-dioxane (Matsuda et al. 2010). Computations of the infinite dilution activity coefficient of salicylic acid in water and ethanol, performed with the one-parameter Wilson model of Matsuda et al. (2010), highlight the large change in activity due to variation of the mixture composition from pure water to pure ethanol (Fig. 6.1).

The basic NRTL model was successfully applied to correlate simvastatin solubility in 15 solvents, with the goal of predicting solubility in mixtures (Nti-Gyabaah et al. 2009). The polymer NRTL model of Chen (1993) was extended by Chen and Song (2004) by introducing the concept of a segment activity coefficient (SAC) to create the NRTL-SAC model. The NRTL-SAC model decomposes molecules into recognized segments and adjusts the activity prediction based on the segments' hydrophilicity, hydrophobicity, and polarity. The NRTL-SAC model has been used to model 14 drug compounds' solubility in up to 14 solvents (Chen and Song 2004). Application of the NRTL-SAC model to vehicle mixtures showed good agreement with experimental data (Chen and Crafts 2006), even in associating systems such as ethanol/water, and captured the solubility peak at minimum activity.

An adapted version of the UNIFAC model, A-UNIFAC, was developed by Mengarelli to extend its capabilities to associating systems

**Fig. 6.1** Activity coefficient of salicylic acid in water and ethanol mixture, by one parameter (Wilson model with parameters from Matsuda et al. 2010)



(Mengarelli et al. 1999). The A-UNIFAC model was extended and compared with NRTL-SAC in predicting solubility for seven drug-like compounds in up to 28 pure solvents and was found to be adequate, though the NRTL-SAC model gave generally better results (Mota et al. 2012). A comparison of UNIFAC, Conductor-like Screening Model for Realistic Solvents (COSMO-RS), NRTL-SAC, and a pharma-modified UNIFAC was made, using up to 17 drugs in 15 pure solvents and a few mixtures, in which NRTL-SAC and the modified UNIFAC fared best (Diedrichs and Gmehling 2010). Tung compared a SAC version of COSMO and NRTL-SAC for four drugs in 13 solvents and found that while NRTL-SAC predicted better overall, including in solvent mixtures, COSMO-SAC had the advantage of being an ab initio method (Tung et al. 2008).

Gross and Sadowski developed the perturbed chain statistical associating fluid theory (PC-SAFT) (Gross and Sadowski 2001) as an equation of state for modeling vapor-liquid and liquid-liquid systems. It was extended to associating systems such as ethanol/water (Gross and Sadowski 2002), and has been applied to the prediction of solubility of six drugs in up to 17 pure solvents and several mixtures (Spyriouni et al. 2011).

## 6.2.2 Partition Coefficient

The partition coefficient is the ratio of concentrations of a solute in two different liquid phases. At a minimum, this represents a ternary system in equilibrium. The equilibrium between two liquid phases  $\alpha$  and  $\beta$  at a constant temperature ( $T$ ) and pressure ( $P$ ) is governed by:

$$\begin{aligned}\mu_i^\alpha &= \mu_i^\beta \\ RT \ln \gamma_i^\alpha x_i^\alpha + \mu_i^\circ &= RT \ln \gamma_i^\beta x_i^\beta + \mu_i^\circ \\ x_i^\alpha \gamma_i^\alpha &= x_i^\beta \gamma_i^\beta \\ P = \frac{C^\alpha}{C^\beta} &= \frac{x_i^\alpha v^\alpha}{x_i^\beta v^\beta} = \frac{\gamma_i^\beta v^\alpha}{\gamma_i^\alpha v^\beta}\end{aligned}$$

where  $C^\alpha$  and  $C^\beta$  are the concentration of solute in the two phases,  $P$  is the partition coefficient, and  $v_\alpha$  and  $v_\beta$  are the molar densities of the two phases. The equilibrium concentrations are determined by the activity coefficients (or vice versa to compute activity from observed data). The NRTL and UNIQUAC? models have been used to correlate partition coefficient data for atenolol and propranolol in a water/n-octanol system, with both showing the ability to predict  $P$  as a function of temperature (Mohsen-Nia et al. 2012). The SPARC performs automated reasoning in

chemistry (SPARC) system has been used to predict solubility ( $N=707$ ,  $RMS=0.487$ ), activity coefficient ( $N=2647$ ,  $RMS=.272$ ), and distribution coefficient ( $N=698$ ,  $RMS=0.44$ ) (Hilal et al. 2004), where  $N$  is the number of compounds in the dataset and  $RMS$  is the root mean square error in the prediction in log units. Ingram used COSMO-RS in the prediction of partition and distribution coefficients of 19 ionizable drugs over a range of pH and with various counterions (Ingram et al. 2011).

### 6.2.3 Diffusion

Chemical potential plays a role in diffusion as well. The generalized Maxwell-Stefan equation relates the diffusional flux of components of a mixture to the driving force for diffusion (Taylor and Kooijman 1991):

$$d_i = \sum_{j=1}^n \left( \frac{x_i J_j - x_j J_i}{c_i D_{ij}} \right)$$

$$d_i = \frac{x_i}{RT} \nabla \mu_i = \sum_{j=1}^{n-1} \left( \delta_{ij} + x_i \frac{\partial \ln \gamma_i}{\partial x_j} \right) \nabla x_j$$

$$= \sum_{j=1}^{n-1} \Gamma_{ij} \nabla x_j$$

In a binary system (or perhaps one with only one diffusing solute), the equation simplifies to:

$$J_1 = -c_1 D_{12} \Gamma \nabla x_1 = -c_1 D \nabla x_1$$

$$D = D_{12} \Gamma = D_{12} \left( 1 + x_1 \frac{\partial \ln \gamma_1}{\partial x_1} \right)$$

The diffusion coefficient usually estimated from experimental data is the Fickian diffusion coefficient  $D$ , which is the product of the Maxwell diffusion coefficient  $D_{12}$  and the thermodynamic factor  $\Gamma$ . Note that the mixture molar density  $c_i$  is taken to be constant here. The thermodynamic factor can be computed from any activity coefficient model.

The activity-adjusted diffusion coefficient  $D_{12}$  has been computed from observed Fickian diffusion coefficients  $D$  for several binary systems (Vignes 1966). The results showed that  $D$  could

vary by an order of magnitude with the concentration of the solute and that the Maxwellian diffusivity  $D_{12}$  as a function of concentration of solute was log-linear, being described by:

$D_{12} = (D_{12}^\circ)^{x_1} (D_{12}^\circ)^{x_2}$ , where  $D_{12}^\circ$  and  $D_{12}^\circ$  are the infinite dilution diffusivities. The implication is that with an activity coefficient model for a solvent/solvent system, and a prediction of dilute diffusivity, that diffusivity can be predicted over the entire range of concentrations.

## 6.3 Potential Mechanisms of Interaction

Thermodynamics provides a mechanism for understanding how components in a mixture can interact to modulate key properties related to transdermal penetration. How these properties interact, however, at different levels of the penetration process is the key driver of the rate and extent of absorption. As the penetrant moves from the dosing vehicle (if there is one), into solution at the skin surface, then into the stratum corneum and dermis, it encounters different environments at each level. The vehicle can then have synergistic effects by acting in multiple levels. In addition, mechanisms that change the composition of the solvent and/or absorption environment can have dynamic effects on the chemical properties related to penetration and absorption.

### 6.3.1 Skin Surface

Several mechanisms at the skin's surface affect the dissolution, diffusion, and penetration of drug from the dosing vehicle into the stratum corneum. Transport of the penetrant from the dosing vehicle to the surface of the skin may be limited by the solubility of the penetrant in the dosing vehicle or the rate of diffusion across a boundary layer. If the penetrant is dosed as a suspension, then dissolution may also become a rate-limiting factor. In the case of a neutral solute (penetrant) in a pure solvent, the

thermodynamics of the system are relatively simple, even if not ideal (in the sense of “ideal” thermodynamic behavior). For binary or higher mixtures of solvents, however, the combined effects on the solute properties such as solubility and diffusion coefficient are not necessarily simple combinations of the properties in the pure solvent systems, and as such may exhibit synergistic effects.

Consider a boundary layer of the dosing vehicle sandwiched between the skin surface and some bulk fluid or dosing apparatus (e.g., a drug eluting patch). The flux of penetrant through the boundary layer at steady state is determined by Fick’s law as:  $J = -D \frac{\partial C}{\partial z}$ , where  $J$  is flux of penetrant,  $C$  is concentration of penetrant,  $D$  is the diffusion coefficient,  $z$  is the distance through the boundary layer. Assuming a constant gradient  $J = -D(C_h - C_0)/h$ , where  $C_h$  is the bulk concentration at the top of the layer and  $C_0$  is the penetrant concentration at the skin surface (note, not in SC membrane itself). If the bulk concentration of penetrant is near saturation, then the mixture effects that increase solubility can increase flux as long as diffusion to the skin surface is the rate-limiting step.

One way to increase solubility is to add surfactants, which can aid in the solvation of hydrophobic molecules. Solvation imposes increased order around the solute molecule, however, and reduces rate of diffusion, as the solute and surrounding surfactant molecules have an increased tendency to move as a unit. In essence, the effective radius of the solute increases. This implies a trade-off between increased solubility increasing flux and reduced diffusivity reducing flux. When surfactant concentrations are above the critical micelle concentration (CMC), phase separation into micelles will occur, further complicating the system. Micelles diffuse much more slowly than the single solute molecule, but due to their size, can deliver multiple solute molecules instantaneously when they disassemble at the stratum corneum interface. Nonetheless, with the introduction of micelles, penetration is generally reduced (Wiechers 1989).

If volatile solvents are used, evaporation can cause an increase in solute concentration as the effective volume of solvent decreases (Stinchcomb et al. 1999). This disappearance of solvent volume can also reduce the depth of the boundary layer, which also increases flux. When a solvent mixture is used, the evaporation of one of the solvents results in a change in the solvent composition over time (except in the case of an azeotrope), which can drastically change the physical properties of solubility, diffusivity, and partition coefficient. As the solute concentrates due to solvent evaporation, it may begin to precipitate. If the solvent evaporates completely before the solute is fully absorbed into the stratum corneum, rapid initial flux will give way to slower flux and crystallization of penetrant on the skin surface, with the end result of incomplete absorption (Oliveira et al. 2012b). If, however, the solvent evaporates more slowly than the absorption rate, the effect will be to increase the overall absorption rate. One other possibility is that the solvent does not evaporate completely, which is more likely in a solvent mixture where one of the components is not volatile.

In the case of incomplete evaporation, the impact on absorption is more complex. Up to the point of precipitation, the absorption rate may be increased, presuming no other effects on solubility or diffusion coefficient. Supersaturation of lipophilic solutes in the donor well has been shown to increase their penetration by increasing thermodynamic activity while not affecting the stratum corneum barrier function (Moser et al. 2001). When the evaporation stops,  $C_h$  will be at (or possibly above) the saturation concentration  $C_{sat}$  and should remain at the saturation concentration, until all the precipitated drug redissolves. If redissolution is slow, the net effect may be an initial increase in flux followed by lowering of flux to the dissolution rate, which may be overall slower than if the system were occluded and evaporation could not occur. These same effects may occur if, instead of evaporation, loss of solvent is through its penetration into the skin.

### 6.3.2 Stratum Corneum

The transit and accumulation of a penetrant through the stratum corneum is governed primarily by partitioning and diffusion. The interaction of these phenomena and the potential for mixture components to influence one or both of them amplifies the impact of the mixture. The “brick and mortar” model of the stratum corneum (Michaels et al. 1975) suggests that the main pathway for diffusion is the intracellular lipid lamellae, which provide a hydrophobic barrier to water loss from the underlying tissue. The mechanisms by which vehicle constituents could affect the stratum corneum barrier function are extraction of lipids from the lamellae; alteration of the partition coefficient between the vehicle and stratum corneum lipids; disruption of the lipid bilayers; displacement of water domains; or loosening of the keratin structure in corneocytes (Daniels and Knie 2007).

The stratum corneum is composed of flattened corneocytes stacked in layers with an intracellular matrix of lipid lamellae, corneocyte envelopes, corneocyte lipid envelopes, enzymes, and structural proteins (Elias 2012). The barrier function of the skin is primarily due to the stratum corneum (Baroni et al. 2012; Bouwstra 1997), with the lipid lamellae contributing the majority of that function (Squier et al. 1991). The effectiveness of the barrier to water transit is modulated by the total lipid content of the stratum corneum (Grubauer et al. 1989; Squier et al. 1991). The only continuous pathway through the stratum corneum is via the lipid multilayer, and any molecules diffusing through the stratum corneum must traverse the lipid multilayer or move within it (Bouwstra 1997). In addition, the overlapping arrangement of the corneocytes in the “brick and mortar” model of the stratum corneum creates a tortuous path that effectively increases the length of the lipid pathway by about an order of magnitude (factor of 12.7 in human skin samples) (Michaels et al. 1975; Talreja et al. 2001).

The lipid lamellae are arranged in a multilayer, which is generally oriented parallel to the stratum corneum surface (Bouwstra 1997). A lipid monolayer is chemically bonded to the

keratinized cell membranes of the corneocytes (Swartzendruber et al. 1987; Wertz et al. 1989) with various ceramides, free fatty acids, and cholesterol (Bouwstra 1997) comprising the lamellae between them. The lipids are organized primarily in crystalline phases, though some liquid phase may be present, and the presence of free fatty acids results in a denser packing structure (Bouwstra et al. 2003). The presence of the denser, orthorhombic packing structure, as opposed to the hexagonal or liquid-crystal phases, correlates with the effectiveness of the stratum corneum barrier (Damien and Boncheva 2009). It has been determined that the presence of endogenous proteins does not affect the lipid organization (Bouwstra et al. 2003).

As previously stated, the diffusional barrier is the intercellular lamellae of lipids. These are primarily neutral lipids and sphingolipids (largely ceramides) (Lampe et al. 1983) with some polar lipid and cholesterol sulfate. These lipids are formed into bilayers that span the gap between corneocytes in several layers, with the lipid head groups oriented at the corneocyte membranes. The lamellar layers consist of a crystalline regime on both sides where the lipid head groups of adjacent layers meet, and a more disordered fluid phase between them with embedded head groups of the shorter chain lipids and cholesterol filling in. The lamellae are stacked multiple times over to fill in the intercellular pathway. The tight packing of the head groups in the crystalline regime and the orderliness of the fluid regime provide a strong barrier to diffusion of large and hydrophilic compounds. The lateral diffusion of lipophilic solutes in the stratum corneum lipids is dependent on the weight and size of the molecule (Johnson et al. 1996).

Disruptions to the packing structure in the crystalline regime or introduction of moieties that displace the small chain lipids and cholesterol in the fluid phase can weaken the diffusional barrier by disrupting the ordered structure of the layer and increasing fluidity. Some vehicle components may completely disrupt the lipid layers, resulting in their extraction. Many permeation-enhancing compounds, such as alcohols and alkanes, can extract lipids from the intercellular

lipid domains of the stratum corneum (Walker and Smith 1996). At high concentrations, ethanol has been shown to extract lipids, while at lower concentrations it disrupts the lipid head groups resulting in disruption of the crystal structure and increased permeability (Krill et al. 1992; Suhonen et al. 1999). Fatty acids (Aungst 1989), various ceramides (Vávrová et al. 2003), a variety of other compounds including ethers and alcohols (Ibrahim and Li 2010), and numerous terpenes (Williams and Barry 1991) have been shown to increase permeation by fluidization of the lipid lamellae. Acidic pH may also contribute to fluidization (Kitagawa et al. 1995).

Modulation of the partition coefficient can occur by modification of the mixture properties on the skin surface or through changes induced in the stratum corneum lipid structure. The partition coefficient between the stratum corneum lipids and the vehicle at the skin surface is

$$P_{sc} = \frac{C_{sc}}{C_0} = \frac{v_{sc}x_{sc}\gamma_{sc}}{v_0x_0\gamma_0},$$

which is a function of the mixture composition through the activity coefficients. So, vehicle components that raise  $\gamma_{sc}$  or lower  $\gamma_0$  of the penetrant increase the partitioning into the stratum corneum. A study of the effect of vehicle mixtures of SLS, water, ethanol, and propylene glycol demonstrated that partitioning into the stratum corneum was determined by the relative solubility of the solute in the vehicle and stratum corneum lipids (Van der Merwe and Riviere 2005b). Experiments in model membranes and skin support a model of vehicle interactions where high solvent uptake promotes drug partitioning by enabling the solute to exist within the solvent fraction/solvent-rich areas inside the membrane or skin by increasing solubility in the membrane (Oliveira et al. 2012a). Conversely, lowering the solubility in the vehicle has been found to also contribute to greater partitioning into the stratum corneum (Hilton et al. 1994).

Another potential interaction in the stratum corneum is binding of the drug to proteins in the keratinocytes (Frasch et al. 2011), which may cause a depot effect of the drug. That is, penetrant may move rapidly into the stratum corneum but accumulate there rather than enter the epidermis. For example, partition coefficient in delipidized stratum

corneum increased for some compounds, possibly due to increased exposure to a protein domain that is normally shielded by the lipid domain (Surber et al. 1990). Depending upon the desorption rate, this could result in an extended time of absorption or even reduced absorption, if desorption is so slow that the penetrant is eliminated by desquamation. For penetrants with local action or toxicity, modulation of this accumulation may be crucial.

Hydration of the stratum corneum results in the inclusion of bulk water that may pool in corneocytes or within the intercellular lipid matrix (Pieper et al. 2003). Inclusion of water in the stratum corneum, as a function of relative humidity (RH), was found to sharply increase the diffusivity of water in the membrane at values over 80% RH (Wiechers 1989). These results may indicate the formation of a hydrophilic pathway, when the stratum corneum is in a highly hydrated state.

### 6.3.3 Epidermis and Dermis

As the penetrant moves through the epidermis, it must cross cell membranes and diffuse through cells (Monteiro-Riviere 2010). Alternatively, it is possible that small polar molecules could follow an aqueous paracellular pathway through tight junctions to the basal lamina (Brandner 2009; O'Neill and Garrod 2011). By the time the penetrant arrives in the epidermis, it is likely to be separated from the hydrophilic penetration enhancers and other vehicle components. Remaining components can interact in a few interesting ways to enhance absorption rate. Increasing the partitioning into the cell membranes or the fluidity of the membranes will increase diffusion of the penetrant. Metabolizing enzymes in the epidermis may reduce overall bioavailability of the penetrant (Stinchcomb 2003; Storm et al. 1990), though a co-penetrant that inhibits or downregulates expression of the enzymes will diminish that effect.

In the dermis, the vasculature acts as the final barrier between the skin and the systemic availability of the penetrant. Systemic uptake is a function of the perfusion rate and the partitioning between the tissue and plasma. Penetration enhancers that increase blood flow would create a stronger sink condition for diffusion, increasing



permeation rate (Riviere and Williams 1992; Wiechers 1989). Co-penetrants that affect protein binding of the penetrant in the extracellular spaces of the dermis or blood plasma will affect the equilibration into the blood and the eventual venous uptake of the penetrant. Finally, like many tissues in the body, the skin expresses several drug transporter systems. The P-glycoprotein (P-gp) transporter system is one of the most important in presenting barriers to drug uptake by tissues. In the dermis, P-gp is concentrated at the vasculature and presents a barrier to drug uptake from the systemic circulation. For penetrants, P-gp may provide a boost to penetration rate that co-penetrants could inhibit (Skazik et al. 2011).

---

## 6.4 Experimental Assessment of Interactions

The interaction of vehicle constituents to modify the transport properties of a penetrant can be assessed in several ways. *In vivo* experiments offer the most direct assessment of effects via endpoints such as  $C_{\max}$  (maximum plasma concentration) and  $T_{\max}$  (time of  $C_{\max}$ ), which indicate rate of exposure, and AUC (area under the concentration profile) which indicates extent of exposure. But, *in vivo* experiments can be expensive, time consuming, unethical (in the case of toxicants), and may not provide much information on the mechanism of the interaction. *In vitro* and *ex vivo* experiments provide a way to isolate mechanisms of interaction as well as increase the throughput of experiments. In trying to identify molecular properties of vehicle constituents that contribute to changes in penetrant transport properties, collection of data over several penetrants and vehicle mixture combinations is required and only feasible in a high-throughput system.

### 6.4.1 Diffusion Cells

Diffusion cells, whether static or flow-through, presents a conceptually simple system for determining skin permeation rate. A donor well above the fixated membrane sample is dosed with a penetrant and vehicle mixture. The pene-

trant (and perhaps some of the vehicle constituents) partition into and diffuse through the membrane to the receptor well. In the Franz-type static cells, the receptor well is a closed system which is periodically sampled, while in the flow-through cell, fresh perfusate is continually introduced and collected (Bronaugh and Stewart 1985; Franz 1975). In both cases, it is common to include a binding agent such as albumin in the perfusate to create a sink condition on the receptor side. If the boundary layer in the donor and receptor wells is kept small, by stirring or turbulence, or if diffusion is rapid, then the rate-limiting barrier to permeation will be diffusion through the membrane.

The use of different membranes such as silastic and porcine skin allows the combination of the obtained data to factor out the contributions from the membrane and account for effects in the donor and receptor wells, such as solubility, evaporation, binding, and if the penetrant partitioning/binding to silicone membrane is negligible or otherwise accounted for – diffusivity.

### 6.4.2 Isolated Perfused Porcine Skin Flap

A deficiency with *in vitro* systems is the inability to assess effects due to perfusion or metabolism which only manifest in viable, integrated tissues. The isolated perfused porcine skin flap (IPPSF) addresses these deficiencies by providing an *ex vivo* system for percutaneous penetration studies. The IPPSF is surgically prepared *in situ* on weanling swine and excised after closure of the incisions. The flap is cannulated and perfused with a modified Krebs-Ringer solution containing glucose, antimicrobial agents, and serum albumin to maintain viability. The perfusate effluent can be collected or sampled for analysis to determine the absorptive flux of penetrants placed on the surface of the flap. The integral, viable nature of the IPPSF allows the investigation of effects on permeation and partitioning due to changes in perfusion, metabolism, inflammation, and cytokine signaling (Riviere et al. 1986; Riviere and Monteiro-Riviere 1991).

### 6.4.3 Model Membrane Systems

Model membrane systems have been developed and used to understand diffusion and partitioning of compounds as well as the effects of vehicles on membrane structure. These systems lack the complex structure and interactions encountered with *in vitro* and *in vivo* stratum corneum, such as corneocyte envelop boundaries and metabolic interactions. They do, however, allow for a finer focus on the structural changes induced by vehicle components and potential correlations to transport properties. Lipids extracted from the stratum corneum (SC) can be studied as liposomes or lamellar sheets (Kitagawa et al. 1995; Suhonen et al. 2008; Wertz et al. 1986). Incorporation of phospholipids into SC lipid liposomes increases fluidity of the membranes and partitioning of estradiol, progesterone, and propranolol into the liposomes (Kirjavainen et al. 1999). A study of the interaction of sodium dodecyl sulfate with SC lipid-like liposomes found that increasing cholesterol sulfate content in the membrane increased the resistance of the membrane to solubilization (López et al. 2000). Partitioning of absorption enhancers into SC lipid liposomes has been correlated to increased permeability through fluidization of the membrane (Ibrahim and Li 2010).

Fixation of model membranes to an ancillary structure is an effective approach for enabling high-throughput experiments. The Parallel Artificial Membrane Permeability Assay (PAMPA) has been used for years to assess intestinal permeability (Avdeef 2012). PAMPA consists of membrane constituents fixed on a filter material on a 96-well microtiter plate and placed in a 96-well receptor plate containing buffer. Half of the wells are used with the membrane and half are used as controls (Kansy et al. 1998). Permeant solutions are introduced on the donor side, and flux is measured after a suitable incubation time. Recent developments have led to a modified PAMPA system that shows promise for predicting transdermal permeability (Sinkó et al. 2012). The use of a PAMPA system to predict the effects

of vehicles on dermal absorption has been recently reported (Karadzovska and Riviere 2013).

Another high-throughput technique for permeability assay is the membrane-coated fiber (MCF) array, wherein model membranes are immobilized on fibers. The fibers are exposed to the donor solution for a fixed incubation time, after which the entire fiber can be processed by GC/MS. Samples taken well before equilibrium can be used to assess permeability, while at equilibrium they will assess partitioning. Silicone-MCF partition coefficient correlated well ( $R^2 = 0.927$ ) with the octanol/water partition coefficient (Xia et al. 2003). The MCF technique is bolstered by a descriptive mathematical model that can be used to regress data and obtain partition coefficient estimates when equilibration time is inconveniently long (Xia et al. 2004). The composite approach (MCF with regression) was used to estimate partitioning and absorption of jet fuel components in polydimethylsiloxane (PDMS-MCF) and polyacrylate (PA-MCF) membranes, showing excellent correlations between partitioning and observed  $\log K_{o:w}$  (Xia et al. 2005). Extending the idea of using multiple MCFs in an array has led to a unique assay for transdermal permeation using PDMS-MCF, PA-MCF, and Wax-MCF (CarboWaxcoated) partition coefficients jointly to predict porcine skin diffusion cell  $\log K_p$  with high fidelity ( $R^2 = 0.93$ ) in 32 compounds (Xia et al. 2007). The multiple MCF approach has also been applied to the study of vehicle mixture interactions (Baynes et al. 2008; Riviere et al. 2007, 2010). The major limitation of this method is the need for study compounds to be amenable to assay by gas chromatography.

---

### 6.5 Predicting Absorption from Complex Vehicle Mixtures

A quantitative structure to permeability relationship (QSPR) is a mathematical equation that relates a property of permeability, such as diffu-

sion or partition coefficients, to chemical descriptors of the permeant (and possibly vehicle) such as molecular weight,  $K_{o:vw}$ , dipolarity, etc. An early relationship that could be considered a QSPR related partition coefficient in skin to solubility parameters, which in turn is a method for computing activity coefficients (Barton 1975; Sloan et al. 1986). Sloan reasoned that for small molecules of a similar size, diffusivity would be approximately constant, and therefore the permeability rate constant  $k_p$  would depend only on partition coefficient. Using a relationship for the activity coefficient of the solute  $i$  in solution  $n$ :

$$\ln \gamma_i^{v(n)} = \left( \delta_i - \delta_{v(n)} \right)^2 V_i \phi_{v(n)}^2 / RT$$

where  $V$  is the molar volume,  $\delta_i$  and  $\delta_{v(n)}$  are the solubility parameters of the solute  $i$  and vehicle  $n$ ,  $\phi_{v(n)}$  is the volume fraction of solvent  $n$  (which approaches unity for dilute solutions),  $R$  is the gas constant, and  $T$  is temperature. Substituting into the definition of partition coefficient:

$$\ln P_i^{v(2,1)sat} = \ln \frac{X_i^{v(2)sat}}{X_i^{v(1)sat}} = \ln \frac{\gamma_i^{v(1)sat}}{\gamma_i^{v(2)sat}}$$

for vehicle  $n$  and skin  $s$ , gives:

$$\log P_i^{s,v(n)sat} = \left( \left( \delta_i - \delta_{v(n)} \right)^2 - \left( \delta_i - \delta_s \right)^2 \right) \frac{V_i}{2.3RT}$$

The correlation of the predicted partition coefficients to skin permeability coefficient worked well for theophylline in various vehicles, including dimethylformamide, propylene glycol, ethylene glycol, and formamide. However, it failed to predict much higher fluxes from isopropyl myristate and octanol vehicles, which have similar solubility parameters to skin. This might have been due to an interaction between the skin and vehicle that changed the diffusivity or chemical nature of the skin, resulting in a permanent change of barrier function – lipid extraction, for instance. So, this approach does not provide a mechanism for predicting changes in barrier function due to vehicle application. An addi-

tional problem with this approach is that it relies on saturation conditions in the donor well; so, it may be of limited use in practical application.

Another approach to the incorporation of activity coefficients is through linear free energy relations (LFER) (Karadzovska et al. 2013a). These are models that relate a property of interest, which has its basis in Gibbs free energy, to a linear function of chemical descriptors. LFERs have been used to relate various molecular properties to overall permeability coefficients. The use of LFER equations for predicting  $K_p$  has arisen from their use in predicting various other physicochemical properties such as log partition coefficient (Abraham and Martins 2004). Extrapolation across experimental systems should not be expected.

Potts and Guy found that a simple model (6.1) that accounts for lipid partitioning and molecular size is sufficient to describe stratum corneum permeability, and they discount competing ideas that aqueous pathways play a significant role in the absorption kinetics in SC (Potts and Guy 1992).

$$\log(k_p) = \log\left(\frac{D^0}{\delta}\right) + f \log(K_{oct}) - \beta' MW$$

$D^0$  - hypothetical diffusivity of MW = 0 compound

$\delta$  - diffusion path length

$K_{oct}$  - octanol : water partition coefficient

$MW$  - Molecular weight

(6.1)

In (6.1), molecular weight is a surrogate for molecular size (volume) and  $K_{oct}$  is a surrogate for SC lipid partitioning. This first widely accepted QSAR for predicting skin permeability coefficient showed a strong correlation ( $R^2 = 0.67$ ) for the 93 compounds in the Flynn dataset (Flynn 1990).

Abraham and Martins performed a metastudy involving experiments on human skin for 119 compounds. They note that ionization of the compounds does not necessarily have a deleterious effect on absorption, especially in the case of

hydrogen-basic molecules. They fit a model of the form:

$$sp = c + eE + sS + aA + bB + vV$$

$$sp - \log(k_p) \text{ or } \log(k_{sc})$$

$E$  – excess molar volume

$S$  – dipolarity / polarizability

$A$  –  $\sum$ hydrogen bond acidity

$B$  –  $\sum$ hydrogen bond basicity

$V$  – McGowan characteristic volume

The final fitted model for  $k_p$  shows it is decreasing for all terms except characteristic volume:

$$\log(k_p) = -5.426(\pm 0.101) - 0.106(\pm 0.129)$$

$$E - .473(\pm 0.095)S$$

$$-0.473(\pm 0.148)A - 3.000(\pm 0.152)$$

$$B + 2.296(\pm 0.137)V$$

$$N = 119, R^2 = 0.832, SD = 0.461, F = 112$$

The positive term for volume seems nonintuitive, but is due to negative correlation between molecular volume and hydrophilicity (Geinoz et al. 2002).

Hostynek and Magee proposed a model involving molar refractivity (MR), number of hydrogen bond acceptors (HBA), and number of hydrogen bond donors (HBD). This model also accounts for effects of lipophilicity and molecular size (Hostynek and Magee 1997). One additional feature of their model is a factor for dosing vehicle (VEH):

$$\log(k_p) = i + aVEH + bMR + cHBA + dHBD$$

Accounting for the vehicle effects on the permeability constant is an important aspect in transdermal absorption modeling. Because most exposure to, or dosing of, compounds will occur in the presence of solubilizers and/or permeability enhancers, the accurate prediction of the uptake of the compound must necessarily include some factor to account for the presence of the dosing vehicle. Yet, in most of the literature up to the turn of the 21st century, these important aspects were integrated into the experimental

system rather than separated out as features of interest (Moss et al. 2002). Hostynek and Magee (1997) provide a simple model for accounting for the vehicle effect, but the approach lacks general applicability, because it uses an indicator variable that ignores the relative concentrations of the vehicle and compound. In addition, the relationship is not extensible to new vehicle effects.

Rosado et al. (2003) examined the effect of pretreating skin samples with various vehicles before applying permeants in a diffusion cell. Flux and retention enhancement ratios were calculated for four compounds over 13 vehicles. While most of the studied vehicles enhanced partitioning into SC, a few modulated diffusion coefficients of the permeants.

To separate and model the effect of complex vehicle mixtures on the permeability of a particular compound, Qiao et al. (1996) proposed a mechanistically defined chemical mixture (MDCM) experimental design. The MDCM is defined as containing a penetrant, solvent(s), and selectively a surfactant, a reducing agent, and/or a vasodilator. The effects of 16 MDCMs on parathion absorption in IPPSF were evaluated in a full 2x4 factorial design, with the MDCMs composed of a solvent (acetone or, full name, dimethyl sulfoxide (DMSO)), surfactant (sodium lauryl sulfate (SLS)), metabolism modifier (stannous chloride), a vasoactive compound (methyl nicotinic acid (MNA)), and 20% water. Assessment of absorption and residue levels indicated not only effects due to single vehicles, but also interaction effects. A similar approach was also used to study benzidine absorption in IPPSF (Baynes et al. 1996).

Williams et al. (1996) used the MDCM data of Qiao et al. (1996) to predict and compare transdermal flux and skin residues using a multicompartment dermatopharmacokinetic model for parathion that compared quite well to the observed flux in IPPSF. In this model, each of the components of the MDCM is modeled, and their concentrations in the various compartments are allowed to affect the rate parameters in mechanistically chosen, nearby compartments, according to a modified Hill equation. That is, for instance, DMSO in the SC increases the

permeability of parathion, but does not affect its transfer to the depot compartment. Parameter values for vehicle transit were directly gathered from previous studies, while those for parathion were adjusted from a previous study. While this model is certainly mechanistic and thorough, it requires many parameters for each penetrant, and many more for the interactions, making estimation and validations of such a large model impractical for prospective applications.

Extending the experimental approach of the MDCMs, Riviere and Brooks have found significant improvements in LFER fits, using the Abraham and Martins models to describe permeability in porcine skin flow-through (PSFT) cells by accounting for mixture effects with a mixture factor (MF) (Riviere and Brooks 2005). The MF approach adds a new term to the LFER that is a mass fraction weighted mixture property of the penetrant-vehicle mixture. The basic form of the mixture factor (MF) is as follows:

$$MF = \sum_{chemical=i} m_i p_i$$

$m_i$  – mass fraction of chemical  $i$

$p_i$  – property of chemical  $i$

These experiments examined 20 chemical properties to assess the influence of their MF on permeability, including descriptors of molecular size, volume, boiling point, hydrogen bonding properties, polarizability, refractivity, melting point (MP), and more. Twelve chemically diverse penetrants and 24 vehicle mixtures (comprised of water, ethanol, propylene glycol, sodium lauryl sulfate, and methyl nicotinate) were studied in PSFT in a full factorial design resulting in 288

treatments with four to five replicates per treatment. A validation dataset with five compounds (also included triazine) in various chemical mixtures added 56 additional treatments. Finite doses were applied which resulted in dynamic flux profiles; so, permeability constant ( $k_p$ ) was assessed from the regressed slope of the cumulative flux profiles.

Among the 16 LFER relationships reviewed by Geinoz et al. (2004), the training set of 288 treatments was fit well by Abraham's model, which was used as a baseline fit for investigating potential mixture factors. Potential MFs were identified by trends in residual values against MF values. Three MFs identified as having potential to reduce the residual variance (based on  $R^2$  of the trend) were refractive index, polarizability, and  $\log(1/HC)$ . Inclusion of these MFs in the LFER improved the correlation as shown in Table 6.1. Predictions on the validation set data showed that the MF approach extended well to the new treatment combinations as well.

It is worth noting that the descriptors used in the MFs have a link back to chemical thermodynamics that make their effectiveness less than surprising. Consider that Abraham's LFER accounts for diffusivity and partitioning components of  $k_p$  and that the primary role of the MF is to account for a change in partitioning due to the vehicle. The partition coefficient is a function of the activity coefficients of the solute in the vehicle and skin, but the LFER is optimized for an aqueous vehicle. Correcting a partition coefficient for the vehicle composition, then, would require multiplying by the ratio of activity coefficients in vehicle and water. Henry's law con-

**Table 6.1** Coefficient of determination ( $R^2$ ), of predicted vs. observed  $\log k_p$  and regression residuals vs. mixture factor (MF) value

Mixture factor	Original dataset (288 treatments)		Validation dataset (56 treatments)	
	Predicted vs. observed $\log k_p$	Residuals vs. MF	Predicted vs. observed $\log k_p$	Residuals vs. MF
None	0.58	0	0.62	0
Refractive index	0.80	0.53	0.78	0.41
Polarizability	0.76	0.43	0.69	0.17
$\log(1/HC)$	0.77	0.45	0.75	0.34

Table modified from Riviere and Brooks (2005)

$HC$  Henry's law constant,  $\log Kp$  log of permeability coefficient,  $MF$  mixture factor

stant is the activity coefficient of an infinitely dilute solute; so, it has direct bearing on the computation. Polarizability relates to the attractive forces between molecules in solution, which have direct bearing on activity. Refractive index itself is influenced by polarizability with a positive correlation. The MFs, however, are an imperfect measure of the required activity coefficient ratio due to the incomplete information provided by these descriptors and the potentially inadequate linear mass fraction mixing rule used. Nonetheless, the success with this approach highlights the promise and necessity of incorporating the vehicle mixture properties when predicting skin permeability.

A further study used the same data from PSFT cells (Riviere and Brooks 2005) and additional data for ten penetrants in five vehicle mixtures in IPPSF to investigate the effect of adding mixture factors to the LFERs of Potts and Guy, Hostyneck and Magee, and Abraham and Martins (Riviere and Brooks 2007). The mixture factor approach was able to improve the  $k_p$  prediction in each of the LFERs tested in PSFT. The results from the Abraham and Martins based model are shown in Fig. 6.2. Note the vertical banding in (a) due to the penetrant predictions being unadjusted for mixture effects, as well as the large variation in observed  $\log k_p$  values. In many cases, the variance within a penetrant, due to the formulation effects, is larger than the variance between penetrants. Inclusion of topical polar surface area (TPSA) as a MF allows the predictions to vary within a penetrant, removing the banding effect, and reducing the prediction error. Application of MFs to predict area under the flux curve (AUC) in IPPSF also improved the prediction over the unmodified LFER models.

Influential MFs in PSFT were number of hydrogen bond acceptors, refractive index, and TPSA. TPSA provided the best fit among all of the investigated LFERs. For IPPSF, octanol:water partition coefficient and inverse water solubility were important MFs for the Potts and Guy LFER, while log water solubility and ovality (a measure of deviation from spherical shape) were important in the other two LFERs investigated. The results showed that the MF approach works in two

different experimental systems to extrapolate single-compound LFER models across different dosing vehicles, although the specific chemical property that best describes the vehicle effect has yet to be identified. An additional study in PSFTs using a different set of compounds (caffeine, cortisone, diclofenac, mannitol, salicylic acid, and testosterone) was recently reported where the optimal MF was 1/MP for these drugs (Karadzovska et al. 2013b). This study also allowed the incorporation of datasets from different in vitro models (infinite versus finite dosing, saturation level, vehicle) to be accomplished by incorporating indicator variables and a MF of 1/MP.

A QSAR model developed with the already published data (Riviere and Brooks 2005) again highlighted the importance of vehicle effects by finding a significant correlation of  $k_p$  with the difference between melting and boiling point of the vehicle (Ghafourian et al. 2010a). Stepwise regression with descriptors for the penetrants including connectivity indices, quantum molecular properties, and group counts, along with vehicle mixture properties comprising melting point, boiling point, solubility, vapor pressure, and Henry's law constant, resulted in a best fit model which included octanol/water partition coefficient, ninth order molecular connectivity index, and difference in boiling and melting point of the solvent system.

$$\log k_p = -0.909 - 0.610 \log K_{o:w} + 2.62 \chi_{p,9} - 0.00917 (BP_s - MP_s) \quad (6.2)$$

In the resulting model, Eq. (6.2),  $K_{o:w}$  is the octanol-water partition coefficient,  $\chi_{p,9}$  is the ninth order molecular connectivity index, and  $BP_s$  and  $MP_s$  are the boiling and melting points of the solvent. The negative effect of partition coefficient was surprising, and it was hypothesized that this was due to the overall lipophilic nature of the dataset. This motivated the author to compare the chemical space of the dataset with the datasets of Flynn (1990) and Wilschut et al. (1995). The comparison was conducted using principal component analysis, where linear combinations of the descriptors are used to describe the variability of the response variable.

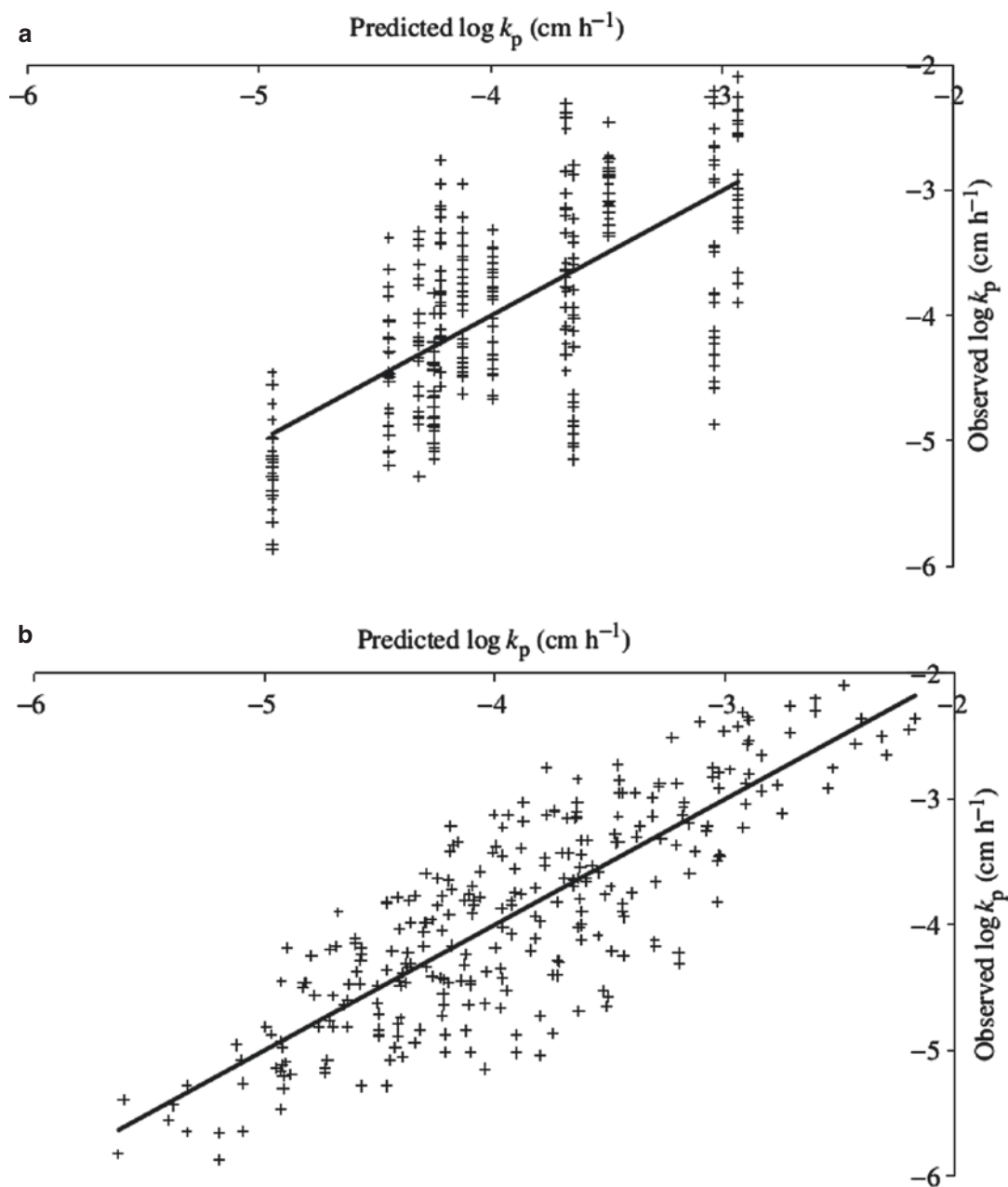


**Fig. 6.2** Predicted vs. observed of penetrant absorption in PSFT cells, with the Abraham and Martins LFER (Abraham and Martins 2004). (a) With no MF. (b) MF is

topical polar surface area (Figure from (Riviere and Brooks 2007), used with permission)

Plotting the first two principal components against each other (Fig. 6.3) is enlightening as it demonstrates that the chemical space of the dataset is quite constrained when compared to the chemical space of the Flynn and Wilschut datasets.

With the data for the four additional chemicals expanding the dataset to 384 treatments and increasing the diversity of the chemical space, a QSAR study was again performed using stepwise selection across a wide array of chemical

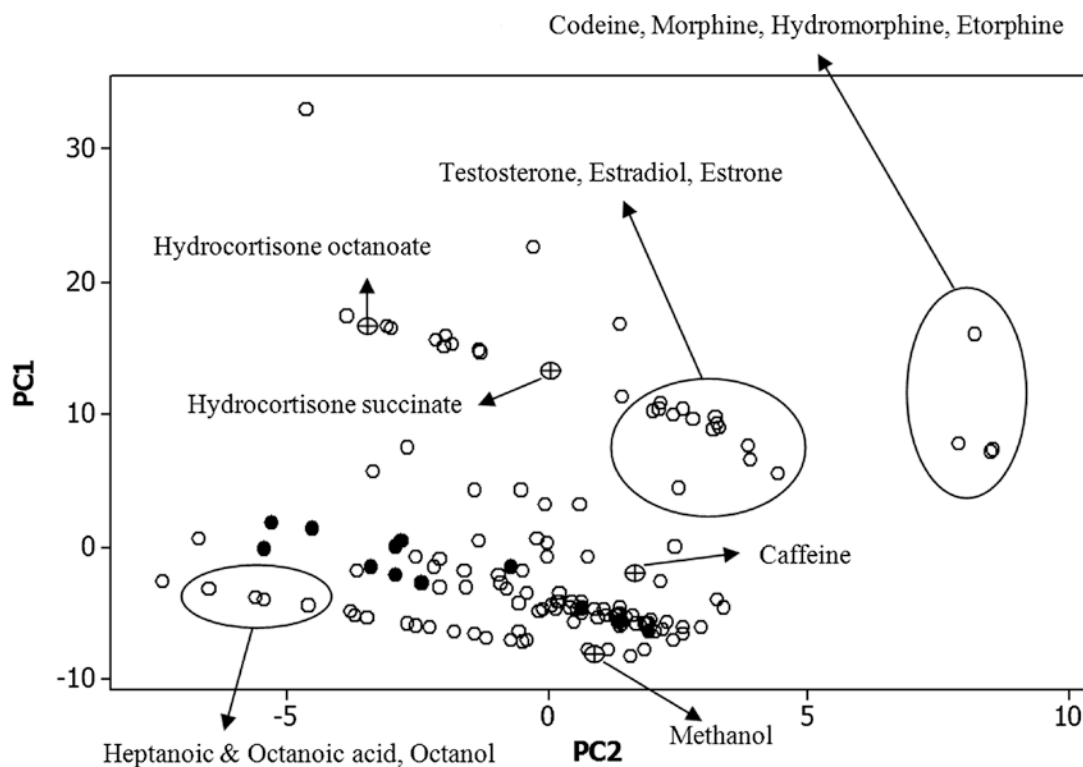


**Fig. 6.3** The chemical diversity of the combined datasets (Riviere – solid circles, Flynn (1990) and Wilschut et al. (1995) – empty circles) using all of the chemical descriptors

in PCA analysis (Figure modified from (Ghafourian et al. 2010a), reprinted with permission. \*PC1 and PC2 are the first and second principal components of the chemical space)

descriptors and physicochemical properties of the penetrant and solvent mixture (Ghafourian et al. 2010b). Solvent mixture properties were computed by mass weighted average, similar to the MF approach. The model size was constrained to no more than four descriptors to avoid spurious correlations. The model (6.3) with the best fit ( $R^2 = 0.701$ ) included descriptors for: the difference in melting point between the vehicle and penetrant ( $\Delta mp = mp_v - mp_p$ ); Wiener's topological index of the penetrant ( $W_p$ ); boiling point of the vehicle ( $BP_v$ ); and lipole of the penetrant ( $L_p$ ).

$$\log k_p = -0.956 - 0.00322\Delta mp - 0.000320W_p - 0.0121BP_v - 0.114L_p \quad (6.3)$$

The implications of this model are that penetrants with lower melting points will have higher absorption rates. In addition, vehicles with

higher boiling points will result in lower absorption. The Wiener topological index, which is a measure of molecular size, accounts for reduction in permeability with increasing molecular volume. The negative contribution of lipole may reflect the fact that this descriptor combines lipophilicity, which is usually seen to increase permeability, with molecular size, which should decrease permeability. Testosterone, the largest molecule by  $W_p$ , showed the greatest variation in permeability due to vehicle composition and was an outlier in some of the treatments, which indicates that the QSAR is not able to account fully for vehicle effects in some of the mixtures.

A study that combined data from PSFT (16 penetrants in 384 treatments) and IPPSF experiments (20 penetrants in 119 treatments) resulted in a total set of 27 penetrants in vehicles composed of mixtures of water, methylnicotinic acid,



sodium lauryl sulfate, propylene glycol, and ethanol (Riviere and Brooks 2011). A dataset with seven compounds in mixtures of 14 vehicle components (89 treatments) in IPPSF was used for validation. QSPR models based on the LFERs of Potts and Guy, and Abraham and Martins, were estimated separately for the two experimental systems. A stepwise selection process was applied to the mixture factor components added to the LFER models, resulting in the final QSPRs (6.4) and (6.5).

$$\log \Psi = i + mMF + a \sum \alpha_2^H + b \sum \beta_2^H + s\pi_2^H + eR_2 + vV_x \quad (6.4)$$

$$\log \Psi = i + mMF + a \log K_{o:w} + bMW \quad (6.5)$$

In Eqs. (6.4) and (6.5),  $\Psi$  is a placeholder for either  $k_p$  (in the case of PSFT) or AUC (in the case of IPPSF); MF is a placeholder for a specific mixture factor;  $\sum \alpha_2^H$  is hydrogen bond donor acidity;  $\sum \beta_2^H$  is hydrogen bond acceptor basicity;  $\pi_2^H$  is dipolarity/polarizability;  $R_2$  is excess molar refractivity;  $V_x$  is McGowan volume;  $K_{o:w}$  is octanol:water partition coefficient; MW is molecular weight; and  $m$ ,  $a$ ,  $b$ ,  $s$ ,  $e$ ,  $v$ , and  $i$  are estimated parameters. In both the PSFT and IPPSF datasets, the MFs that contributed most to improving the model, as evaluated by correlation coefficients and cross-validation metrics, were the number of hydrogen bond acceptors (HBA) and the inverse of melting point (1/MP). However, different MFs were needed in each model system to achieve the best fit. The QSPR based on the model of Abraham and Martins could be simplified by removing a parameter, but it was a different parameter in each of the model systems: hydrogen bond donor basicity in PSFT and polarizability in IPPSF. The addition of a MF to a LFER model has little impact on the estimated parameters (Table 6.2) for the chemical descriptors, which indicates the independence of the MF from the descriptors.

The results would indicate that different barrier functions are being evaluated between the two systems, but they could also indicate a fundamental difference between predicting rate and extent of

absorption. The IPPSF includes dermis, vasculature, active enzymes, and is a live tissue – all of which can contribute to not only differences in barrier function, but also to tissue partitioning and depot effects. In addition, the MF approach appears to confound effects in the solvent with effects in the barrier, such that for the same vehicle mixture different MFs are required. It is suggested that using the estimation from PSFT to fix some portion of the model for IPPSF may help to isolate effects that are particular to the ex vivo IPPSF system.

A QSPR for the absorption of cosmetic and dermatological formulations in human skin was developed from a model for predicting cumulative absorption (Bunge et al. 1995; Bunge and Cleek 1995; Cleek and Bunge 1993), adjusting it to account for ionization of the penetrant in the vehicle as well as distribution to aqueous and organic phases of an emulsion (Grégoire et al. 2009). The adjustment for ionization affects the prediction of partitioning into skin and is accomplished by replacing the  $\log P_{o:w}$  term in the Potts and Guy LFER with the log distribution coefficient of the penetrant in the octanol-water system at the pH of the vehicle ( $\log D_{pH}$ ). The effective area of diffusion was corrected for the aqueous fraction, which is assumed to be the phase contributing the majority of the flux. The model assumes steady-state diffusion, ignores the effect of penetration enhancers, approximates all vehicles as emulsions, and considers only absorption from the aqueous phase of the vehicle.

The dataset comprised cumulative amount of absorbed measurements from human skin in 101 individual studies, with a total of 36 compounds in various vehicles and experimental settings. The estimated parameter of the model is a coefficient to control the distribution of the penetrant between the phases of the emulsion. The resulting QSPR predicted 91 % of the data within 0.2 to 5-fold ( $R^2 = 0.7115$ ). This model is unique in the literature in incorporating biphasic vehicle and ionization interactions, but more research needs to be done to extend it to ionic or metabolized compounds, monophasic vehicles, and to account for penetration-enhancing excipients.

**Table 6.2** Compilation of QSPR results from Riviere and Brooks (2011), showing best fits with and without mixture factor (MF)

$R^2$	System	Equation	MF	$m$	$i$	$a$	$b$	$s$	$e$	$v$
0.53	PSFT	(6.4)	–	–	2.55	1.45	0.01	0.27	–0.55	–1.39
0.73	PSFT	(6.4)	HBA	–1.21	4.27	1.44	–	0.28	–0.55	–1.38
0.60	IPPSF	(6.4)	–	–	1.61	–2.00	–0.39	0.04	0.38	–1.54
0.69	IPPSF	(6.4)	1/MP	35.63	1.81	–2.00	–0.35	–	0.47	–1.61
0.33	PSFT	(6.5)	–	–	1.13	–0.10	–0.0058			
0.55	PSFT	(6.5)	HBA	–1.23	2.89	–0.10	–0.0058			

HBA hydrogen bond acceptors, MP melting point, PSFT porcine skin flow-through cell, IPPSF isolated perfused porcine skin flap,  $m$ ,  $i$ ,  $a$ ,  $b$ ,  $s$ ,  $e$ ,  $v$ , which are parameters in Eqs. 6.4 or 6.5, as indicated by the equation column (NB Parameters carry different meanings in the two equations)

The effects of vehicle properties and experimental conditions have recently been studied in a large database of 536 flux data points from excised human skin (Samaras et al. 2012). The QSARs that were developed account for different dosing conditions, vehicles, membrane thickness, and sample pretreatment. Vehicle properties were computed by weighted averaging. For melting and boiling points, solute effects of boiling point elevation and freezing point depression were factored in. Models were estimated by stepwise regression as well as regression tree. Regression tree models split the problem space according to covariate regions (leaves) and fit simpler models (often just the mean of the data) in each leaf. The RT models were used to investigate the effects of experimental conditions, but only one condition at a time. That is, no model included all of the experimental condition effects, possibly because the response space would become too fractured, resulting in subsets too small to estimate parameters for even simple models.

Neither stepwise regression nor regression tree models selected variables for skin thickness, infinite vs. finite dosing, prehydration of the membrane, or occlusion. The failure to automatically select for what were found to be otherwise statistically significant effects may be due to the large number of descriptors (375) used in the automated procedure. The most significant variable selected in both models was donor concentration, with other descriptors for molecular size, hydrophilicity, lipophilicity, and polarizability. The regression equation also selected the difference between vehicle boiling

and melting point ( $BP - MP(\text{mix})$ ), showing the strong contribution of vehicle effect on permeability. Each of the factors for experimental condition was then added to the regression equation, whereby skin thickness and exposure type were found to be statistically significant variables. With the RT models, inclusion of  $BP - MP(\text{mix})$  had the lowest mean absolute error (MAE) on the full dataset. These results clearly indicate the importance of accounting for the vehicle mixture.

It has also been demonstrated that results from one model system can extend to predictions in another model system. The MCF array has been used to predict absorption in IPPSF in a study that tested the effect of two surfactants (SLS and linear alkylbenzene sulfate (LAS)) on penetration of six compounds (Riviere et al. 2010). Penetrant partition coefficient from each vehicle into MCFs coated with PA, PDMS, and CW was determined by mass balance. The partition coefficients were then used in a QSPR (6.6) to predict  $\log AUC$  ( $R^2 = 0.718$ ).

$$\log AUC = I + a(\log K_{PDMS}) + b(\log K_{PA}) + c(\log K_{CW}) \quad (6.6)$$

The rank ordering of absorption, penetration, and peak flux across the three mixtures in IPPSF was consistent: water > SLS > LAS, except for simazine, where SLS > water > LAS. Remarkably, rank ordering of  $\log K_{MCF}$  followed the same pattern (water > SLS > LAS) except for simazine in all of the MCFs, and propazine in just the CW MCF, where the ordering was water > LAS > SLS. Seeing

the effect in both experimental systems should rule out an effect due to skin irritation by LAS. The uniformly higher absorption from water is due to the lipophilic nature of the chemicals studied. The results are promising in that a simple in vitro system may be used to predict some results of a more complex biological system, though more research must be done on an expanded chemical space that should include highly water-soluble, hydrophilic compounds.

### Conclusion

Real-life exposures to chemicals are rarely in neat solutions under simple conditions. Complex interactions between penetrants, vehicle components, and skin can lead to synergistic modulation of skin penetration that is not generally predictable from knowledge of the effects of the single components. Thermodynamics gives some structure to understanding the effects of composition on the key properties of solubility, partitioning, and diffusion that affect skin permeation, but cannot readily account for some interactions with the tissue such as lipid extraction and metabolism. Recent studies that incorporate effects due to mixture composition in QSPR models have shown promise in explaining the variation in permeability observed among complex vehicle mixtures. Results in this area are far from complete, and additional research is required to refine the models of mixture effects, expand the inference space of predictions, extend models between different experimental systems, and extrapolate results to in vivo exposure scenarios.

### References

- Abraham MH, Martins F (2004) Human skin permeation and partition: general linear free-energy relationship analyses. *J Pharm Sci* 93:1508–1523
- Arora A, Kisak E, Karande P et al (2010) Multicomponent chemical enhancer formulations for transdermal drug delivery: more is not always better. *J Controll Release* 144:175–180
- Aungst BJ (1989) Structure/effect studies of fatty acid isomers as skin penetration enhancers and skin irritants. *Pharm Res* 6:244–247
- Avdeef A (2012) Absorption and drug development: solubility, permeability, and charge state, John Wiley & Sons, Inc., Hoboken, New Jersey, 2nd edn. p 742
- Baroni A, Buommino E, De Gregorio V et al (2012) Structure and function of the epidermis related to barrier properties. *Clin Dermatol* 30:257–262
- Barton AFM (1975) Solubility parameters. *Chem Rev* 75:731–753
- Baynes R, Riviere J (2004) Mixture additives inhibit the dermal permeation of the fatty acid, ricinoleic acid. *Toxicol Lett* 147:15–26
- Baynes RE, Brooks JD, Budsaba K et al (2001) Mixture effects of JP-8 additives on the dermal disposition of jet fuel components. *Toxicol Appl Pharmacol* 175: 269–281
- Baynes RE, Brownie C, Freeman H, Riviere JE (1996) In vitro percutaneous absorption of benzidine in complex mechanistically defined chemical mixtures. *Toxicol Appl Pharmacol* 141:497–506
- Baynes RE, Xia XR, Imran M, Riviere JE (2008) Quantification of chemical mixture interactions modulating dermal absorption using a multiple membrane fiber array. *Chem Res Toxicol* 21:591–599
- Bouwstra JA (1997) The skin barrier, a well-organized membrane. *Colloids Surf* 123–124:403–413
- Bouwstra JA, Honeywell-Nguyen PL, Gooris GS, Ponc M (2003) Structure of the skin barrier and its modulation by vesicular formulations. *Prog Lipid Res* 42:1–36
- Brandner JM (2009) Tight junctions and tight junction proteins in mammalian epidermis. *Eur J Pharm Biopharm* 72:289–294
- Bronaugh RL, Stewart RF (1985) Methods for in vitro percutaneous absorption studies iv: the flow-through diffusion cell. *J Pharm Sci* 74:64–67
- Bunge A, Cleek R, Vecchia B (1995) A new method for estimating dermal absorption from chemical exposure. 3. Compared with steady-state methods for prediction and data analysis. *Pharm Res* 12:972–982
- Bunge AL, Cleek RL (1995) A new method for estimating dermal absorption from chemical exposure: 2. Effect of molecular weight and octanol-water partitioning. *Pharm Res* 12:88–95
- Carpentieri-Rodrigues LN, Zanluchi JM, Grebogi IH (2007) Percutaneous absorption enhancers: mechanisms and potential. *Braz Arch Bio Tech* 50:949–961
- Chen C-C (1993) A segment-based local composition model for the gibbs energy of polymer solutions. *Fluid Phase Equilib* 83:301–312
- Chen C-C, Crafts PA (2006) Correlation and prediction of drug molecule solubility in mixed solvent systems with the nonrandom two-liquid segment activity coefficient (NRTL-SAC) model. *Ind Eng Chem Res* 45:4816–4824
- Chen C-C, Song Y (2004) Solubility modeling with a nonrandom two-liquid segment activity coefficient model. *Ind Eng Chem Res* 43:8354–8362
- Cleek RL, Bunge AL (1993) A new method for estimating dermal absorption from chemical exposure. 1. General approach. *Pharm Res* 10:497–506

- Cross S, Pugh WJ, Hadgraft J, Roberts M (2001) Probing the effect of vehicles on topical delivery: understanding the basic relationship between solvent and solute penetration using silicone membranes. *Pharm Res* 18:999–1005
- Damien F, Boncheva M (2009) The extent of orthorhombic lipid phases in the stratum corneum determines the barrier efficiency of human skin in vivo. *J Invest Dermatol* 130:611–614
- Daniels R, Knie U (2007) Galenics of dermal products: vehicles, properties and drug release. *J Dtsch Dermatol Ges* 5:367–383
- Dias M, Hadgraft J, Lane ME (2007) Influence of membrane–solvent–solute interactions on solute permeation in skin. *Int J Pharm* 340:65–70
- Diedrichs A, Gmehling J (2010) Solubility calculation of active pharmaceutical ingredients in alkanes, alcohols, water and their mixtures using various activity coefficient models. *Ind Eng Chem Res* 50:1757–1769
- Dupuis D, Rougier A, Roguet R, Lotte C (1986) The measurement of the stratum corneum reservoir: a simple method to predict the influence of vehicles on in vivo percutaneous absorption. *Br J Dermatol* 115:233–238
- El Maghraby GM, Alanazi FK, Alsarra IA (2009) Transdermal delivery of tadalafil. I. Effect of vehicles on skin permeation. *Drug Dev Ind Pharm* 35:329–336
- Elias PM (2012) Structure and function of the stratum corneum extracellular matrix. *J Invest Dermatol* 132:2131–2133
- Flynn G (1990) Physicochemical determinants of skin absorption. In: Gerrity T, Henry C (eds) *Principles of route-to-route extrapolation for risk assessment*. Elsevier, New York, pp 93–127
- Franz TJ (1975) Percutaneous absorption. On the relevance of in vitro data. *J Invest Dermatol* 64:190–195
- Frasch HF, Barbero AM, Hettick JM, Nitsche JM (2011) Tissue binding affects the kinetics of theophylline diffusion through the stratum corneum barrier layer of skin. *J Pharm Sci* 100:2989–2995
- Geinoz S, Guy R, Testa B, Carrupt P-A (2004) Quantitative structure-permeation relationships (QSPeRs) to predict skin permeation: a critical evaluation. *Pharm Res* 21:83–92
- Geinoz S, Rey S, Boss G et al (2002) Quantitative structure-permeation relationships for solute transport across silicone membranes. *Pharm Res* 19:1622–1629
- Ghafourian T, Samaras EG, Brooks JD, Riviere JE (2010a) Modelling the effect of mixture components on permeation through skin. *Int J Pharm* 398:28–32
- Ghafourian T, Samaras EG, Brooks JD, Riviere JE (2010b) Validated models for predicting skin penetration from different vehicles. *Eur J Pharm Sci* 41:612–616
- Grégoire S, Ribaud C, Benech F et al (2009) Prediction of chemical absorption into and through the skin from cosmetic and dermatological formulations. *Br J Dermatol* 160:80–91
- Gross J, Sadowski G (2001) Perturbed-chain SAFT: an equation of state based on a perturbation theory for chain molecules. *Ind Eng Chem Res* 40:1244–1260
- Gross J, Sadowski G (2002) Application of the perturbed-chain SAFT equation of state to associating systems. *Ind Eng Chem Res* 41:5510–5515
- Grubauer G, Feingold K, Harris R, Elias P (1989) Lipid content and lipid type as determinants of the epidermal permeability barrier. *J Lipid Res* 30:89–96
- Hilal SH, Karickhoff SW, Carreira LA (2004) Prediction of the solubility, activity coefficient and liquid/liquid partition coefficient of organic compounds. *QSAR Comb Sci* 23:709–720
- Hilton J, Woollen BH, Scott RC et al (1994) Vehicle effects on in vitro percutaneous absorption through rat and human skin. *Pharm Res* 11:1396–1400
- Hostynek J, Magee P (1997) Modelling in vivo human skin absorption. *Q Struct Act Relat* 16:473–479
- Hotchkiss SAM, Miller JM, Caldwell J (1992) Percutaneous absorption of benzyl acetate through rat skin in vitro. 2. Effect of vehicle and occlusion. *Food Chem Toxicol* 30:145–153
- Ibrahim SA, Li SK (2010) Chemical enhancer solubility in human stratum corneum lipids and enhancer mechanism of action on stratum corneum lipid domain. *Int J Pharm* 383:89–98
- Ingram T, Richter U, Mehling T, Smirnova I (2011) Modelling of pH dependent n-octanol/water partition coefficients of ionizable pharmaceuticals. *Fluid Phase Equilib* 305:197–203
- Jepson G, McDougal J (1999) Predicting vehicle effects on the dermal absorption of halogenated methanes using physiologically based modeling. *Toxicol Sci* 48:180–188
- Johnson ME, Berk DA, Blankschtein D et al (1996) Lateral diffusion of small compounds in human stratum corneum and model lipid bilayer systems. *Biophys J* 71:2656–2668
- Kansy M, Senner F, Gubernator K (1998) Physicochemical high throughput screening: parallel artificial membrane permeation assay in the description of passive absorption processes. *J Med Chem* 41:1007–1010
- Karadzovska D, Brooks JD, Monteiro-Riviere NA, Riviere JE (2013a) Predicting skin permeability from complex vehicles. *Adv Drug Delivery Rev* 65:265–277
- Karadzovska D, Brooks JD, Riviere JE (2013b) Modeling the effect of experimental variables on the in vitro permeation of six model compounds across porcine skin. *Int J Pharm* 443:58–67
- Karadzovska D, Riviere JE (2013) Assessing vehicle effects on skin absorption using artificial membrane systems. *Eur J Pharm Sci* 50(5):569–576
- Karande P, Jain A, Mitragotri S (2006) Insights into synergistic interactions in binary mixtures of chemical permeation enhancers for transdermal drug delivery. *J Controll Release* 115:85–93
- Karande P, Mitragotri S (2009) Enhancement of transdermal drug delivery via synergistic action of chemicals. *Biochim Biophys Acta Biomem* 1788:2362–2373
- Kirjavainen M, Mönkkönen J, Saukkosaari M et al (1999) Phospholipids affect stratum corneum lipid bilayer fluidity and drug partitioning into the bilayers. *J Controll Release* 58:207–214

- Kitagawa S, Yokochi N, Murooka N (1995) Ph-dependence of phase transition of the lipid bilayer of liposomes of stratum corneum lipids. *Int J Pharm* 126:49–56
- Krill SL, Knutson K, Higuchi WI (1992) Ethanol effects on the stratum corneum lipid phase behavior. *Biochim Biophys Acta Biomem* 1112:273–280
- Lampe MA, Burlingame AL, Whitney J et al (1983) Human stratum corneum lipids: characterization and regional variations. *J Lipid Res* 24:120–130
- López O, Cócera M, de la Maza A et al (2000) Different stratum corneum lipid liposomes as models to evaluate the effect of the sodium dodecyl sulfate. *Biochim Biophys Acta Biomem* 1508:196–209
- Matsuda H, Kaburagi K, Kurihara K et al (2010) Prediction of solubilities of pharmaceutical compounds in water+co-solvent systems using an activity coefficient model. *Fluid Phase Equilib* 290:153–157
- de la Maza A, Lopez O, Coderch L, Parra JL (1998) Interactions of oxyethylenated nonylphenols with liposomes mimicking the stratum corneum lipid composition. *Colloids Surf A* 145:83–91
- Mengarelli AC, Brignole EA, Bottini SB (1999) Activity coefficients of associating mixtures by group contribution. *Fluid Phase Equilib* 163:195–207
- Michaels AS, Chandrasekaran SK, Shaw JE (1975) Drug permeation through human skin: theory and invitro experimental measurement. *AICHE J* 21:985–996
- Mills PC (2007) Vehicle effects on the in vitro penetration of testosterone through equine skin. *Vet Res Comm* 31:227–233
- Mills PC, Magnusson BM, Cross SE (2006) The effects of vehicle and region of application on in vitro penetration of testosterone through canine skin. *Vet J* 171:276–280
- Mills PC, Magnusson BM, Cross SE (2005) Effects of vehicle and region of application on absorption of hydrocortisone through canine skin. *Am J Vet Res* 66:43–47
- Mirmehrabi M, Rohani S, Perry L (2006a) Thermodynamic modeling of activity coefficient and prediction of solubility: part 1. *Predict Models J Pharm Sci* 95:790–797
- Mirmehrabi M, Rohani S, Perry L (2006b) Thermodynamic modeling of activity coefficient and prediction of solubility: part 2. *Semipredictive or semiempirical models. J Pharm Sci* 95:798–809
- Mohsen-Nia M, Ebrahimabadi AH, Niknahad B (2012) Partition coefficient n-octanol/water of propranolol and atenolol at different temperatures: experimental and theoretical studies. *J Chem Thermodyn* 54:393–397
- Monteiro-Riviere NA (2010) Structure and function of skin. In: Monteiro-Riviere NA (ed) *Toxicology of the skin: target organ series*. Informa Healthcare, USA, Inc, New York, pp 1–18
- Monti D, Saettone MF, Giannaccini B, Galli-Angeli D (1995) Enhancement of transdermal penetration of dapiprazole through hairless mouse skin. *J Control Release* 33:71–77
- Moser K, Kriwet K, Froehlich C et al (2001) Supersaturation: enhancement of skin penetration and permeation of a lipophilic drug. *Pharm Res* 18:1006–1011
- Moss GP, Dearden JC, Patel H, Cronin MTD (2002) Quantitative structure-permeability relationships (QSPRs) for percutaneous absorption. *Toxicol Vitro* 16:299–317
- Mota FL, Queimada AJ, Andreatta AE et al (2012) Calculation of drug-like molecules solubility using predictive activity coefficient models. *Fluid Phase Equilib* 322–323:48–55
- Nti-Gyabaah J, Chan V, Chiew YC (2009) Solubility and limiting activity coefficient of simvastatin in different organic solvents. *Fluid Phase Equilib* 280:35–41
- O'Neill CA, Garrod D (2011) Tight junction proteins and the epidermis. *Exp Dermatol* 20:88–91
- Oliveira G, Hadgraft J, Lane ME (2012a) The role of vehicle interactions on permeation of an active through model membranes and human skin. *Int J Cosmet Sci* 34:536–545
- Oliveira G, Hadgraft J, Lane ME (2012b) The influence of volatile solvents on transport across model membranes and human skin. *Int J Pharm* 435:38–49
- Pieper J, Charalambopoulou G, Steriotis T et al (2003) Water diffusion in fully hydrated porcine stratum corneum. *Chem Phys* 292:465–476
- Potts RO, Guy RH (1992) Predicting skin permeability. *Pharm Res* 9:663–669
- Qiao GL, Brooks JD, Baynes RE et al (1996) The use of mechanistically defined chemical mixtures (MDCM) to assess component effects on the percutaneous absorption and cutaneous disposition of topically exposed chemicals: I. Studies with parathion mixtures in isolated perfused porcine skin. *Toxicol Appl Pharmacol* 141:473–486
- Riviere J, Bowman K, Monteiro-Riviere N et al (1986) The isolated perfused porcine skin flap (IPPSF). I. A novel in vitro model for percutaneous absorption and cutaneous toxicology studies. *Fundam Appl Toxicol* 7:444–453
- Riviere J, Brooks J (2005) Predicting skin permeability from complex chemical mixtures. *Toxicol Appl Pharmacol* 208:99–110
- Riviere J, Brooks J (2007) Prediction of dermal absorption from complex chemical mixtures: incorporation of vehicle effects and interactions into a QSPR framework. *SAR QSAR Environ Res* 18:31–44
- Riviere J, Monteiro-Riviere N (1991) The isolated perfused porcine skin flap as an in vitro model for percutaneous absorption and cutaneous toxicology. *Crit Rev Toxicol* 21:329–344
- Riviere JE, Baynes RE, Xia X-R (2007) Membrane-coated fiber array approach for predicting skin permeability of chemical mixtures from different vehicles. *Toxicol Sci* 99:153–161
- Riviere JE, Brooks JD (2011) Predicting skin permeability from complex chemical mixtures: dependency of quantitative structure permeation relationships on biology of skin model used. *Toxicol Sci* 119:224–232
- Riviere JE, Brooks JD, Yeatts JL, Koivisto EL (2010) Surfactant effects on skin absorption of model organic

- chemicals: implications for dermal risk assessment studies. *J Toxicol Environ Health Part A* 73: 725–737
- Riviere JE, Williams PL (1992) Pharmacokinetic implications of changing blood flow in skin. *J Pharm Sci* 81:601–602
- Rosado C, Cross SE, Pugh WJ et al (2003) Effect of vehicle pretreatment on the flux, retention, and diffusion of topically applied penetrants in vitro. *Pharm Res* 20:1502–1507
- Samaras EG, Riviere JE, Ghafourian T (2012) The effect of formulations and experimental conditions on in vitro human skin permeation—data from updated edetox database. *Int J Pharm* 434:280–291
- Sherertz EF, Sloan KB, McTiernan RG (1987) Effect of skin pretreatment with vehicle alone or drug in vehicle on flux of a subsequently applied drug: results of hairless mouse skin and diffusion cell studies. *J Invest Dermatol* 89:249–252
- Shokri J, Nakhodchi A, Dashbolaghi A et al (2001) The effect of surfactants on the skin penetration of diazepam. *Int J Pharm* 228:99–107
- Sinkó B, Garrigues TM, Balogh GT et al (2012) Skin-PAMPA: a new method for fast prediction of skin penetration. *Eur J Pharm Sci* 45:698–707
- Skazik C, Wenzel J, Marquardt Y et al (2011) P-glycoprotein (ABCB1) expression in human skin is mainly restricted to dermal components. *Exp Dermatol* 20:450–452
- Sloan KB, Koch SAM, Siver KG, Flowers FP (1986) Use of solubility parameters of drug and vehicle to predict flux through skin. *J Invest Dermatol* 87:244–252
- Spyriouni T, Krokidis X, Economou IG (2011) Thermodynamics of pharmaceuticals: prediction of solubility in pure and mixed solvents with PC-SAFT. *Fluid Phase Equilib* 302:331–337
- Squier CA, Cox P, Wertz PW (1991) Lipid content and water permeability of skin and oral mucosa. *J Invest Dermatol* 96:123–126
- Stinchcomb A, Pirot F, Touraille G et al (1999) Chemical uptake into human stratum corneum in vivo from volatile and non-volatile solvents. *Pharm Res* 16:1288–1293
- Stinchcomb AL (2003) Xenobiotic bioconversion in human epidermis models. *Pharm Res* 20:1113–1118
- Storm EJ, Collier WS, Steward FR, Bronaugh RL (1990) Metabolism of xenobiotics during percutaneous penetration: role of absorption rate and cutaneous enzyme activity. *Toxicol Sci* 15:132–141
- Suhonen M, Li SK, Higuchi WI, Herron JN (2008) A liposome permeability model for stratum corneum lipid bilayers based on commercial lipids. *J Pharm Sci* 97:4278–4293
- Suhonen TM, Bouwstra JA, Urtti A (1999) Chemical enhancement of percutaneous absorption in relation to stratum corneum structural alterations. *J Controll Release* 59:149–161
- Surber C, Wilhelm K-P, Hori M et al (1990) Optimization of topical therapy: partitioning of drugs into stratum corneum. *Pharm Res* 7:1320–1324
- Swartzendruber DC, Wertz PW, Madison KC, Downing DT (1987) Evidence that the corneocyte has a chemically bound lipid envelope. *J Invest Dermatol* 88:709–713
- Talreja P, Kasting G, Kleene N et al (2001) Visualization of the lipid barrier and measurement of lipid path-length in human stratum corneum. *AAPS J* 3:48–56
- Taylor R, Kooijman HA (1991) Composition derivatives of activity coefficient models (for the estimation of thermodynamic factors in diffusion). *Chem Eng Commun* 102:87–106
- Traynor MJ, Wilkinson SC, Williams FM (2007) The influence of water mixtures on the dermal absorption of glycol ethers. *Toxicol Appl Pharmacol* 218:128–134
- Tsuruta H (1996) Skin absorption of solvent mixtures—effect of vehicles on skin absorption of toluene. *Ind Health* 34:369–378
- Tung H-H, Tabora J, Variankaval N et al (2008) Prediction of pharmaceutical solubility via NRTL-SAC and COSMO-SAC. *J Pharm Sci* 97:1813–1820
- Van der Merwe D, Riviere JE (2005a) Comparative studies on the effects of water, ethanol and water/ethanol mixtures on chemical partitioning into porcine stratum corneum and silastic membrane. *Toxicol Vitro* 19:69–77
- Van der Merwe D, Riviere JE (2005b) Effect of vehicles and sodium lauryl sulphate on xenobiotic permeability and stratum corneum partitioning in porcine skin. *Toxicology* 206:325–335
- Vávrová K, Hrabálek A, Doležal P et al (2003) Synthetic ceramide analogues as skin permeation enhancers: structure–activity relationships. *Bioorg Med Chem* 11:5381–5390
- Vignes A (1966) Diffusion in binary solutions. Variation of diffusion coefficient with composition. *Ind Eng Chem Fund* 5:189–199
- Walker RB, Smith EW (1996) The role of percutaneous penetration enhancers. *Adv Drug Delivery Rev* 18:295–301
- Wertz PW, Abraham W, Landmann L, Downing DT (1986) Preparation of liposomes from stratum corneum lipids. *J Invest Dermatol* 87:582–584
- Wertz PW, Madison KC, Downing DT (1989) Covalently bound lipids of human stratum corneum. *J Invest Dermatol* 92:109–111
- Wiechers JW (1989) The barrier function of the skin in relation to percutaneous absorption of drugs. *Pharm World Sci* 11:185–198
- Williams AC, Barry BW (2004) Penetration enhancers. *Adv Drug Delivery Rev* 56:603–618
- Williams AC, Barry BW (1991) Terpenes and the lipid-protein-partitioning theory of skin penetration enhancement. *Pharm Res* 8:17–24
- Williams PL, Thompson D, Qiao G et al (1996) The use of mechanistically defined chemical mixtures (MDCM) to assess mixture component effects on the percutaneous absorption and cutaneous disposition of topically exposed chemicals: II. Development of a general dermatopharmacokinetic model for use in risk assessment. *Toxicol Appl Pharmacol* 141:487–496

- Wilschut A, ten Berge WF, Robinson PJ, McKone TE (1995) Estimating skin permeation. The validation of five mathematical skin permeation models. *Chemosphere* 30:1275–1296
- Xia X-R, Baynes R, Monteiro-Riviere N et al (2003) A novel in-vitro technique for studying percutaneous permeation with a membrane-coated fiber and gas chromatography/mass spectrometry: part I. Performances of the technique and determination of the permeation rates and partition coefficients of chemical mixtures. *Pharm Res* 20:275–282
- Xia XR, Baynes RE, Monteiro-Riviere NA, Riviere JE (2004) A compartment model for the membrane-coated fiber technique used for determining the absorption parameters of chemicals into lipophilic membranes. *Pharm Res* 21:1345–1352
- Xia XR, Baynes RE, Monteiro-Riviere NA, Riviere JE (2005) Membrane uptake kinetics of jet fuel aromatic hydrocarbons from aqueous solutions studied by a membrane-coated fiber technique. *Toxicol Mech Methods* 15:307–316
- Xia X-R, Baynes RE, Monteiro-Riviere NA, Riviere JE (2007) An experimentally based approach for predicting skin permeability of chemicals and drugs using a membrane-coated fiber array. *Toxicol Appl Pharmacol* 221:320–328

S. Kevin Li and William I. Higuchi

## Contents

7.1	<b>Introduction</b> .....	119
7.2	<b>Methods</b> .....	120
7.2.1	Animal Model.....	120
7.2.2	Transport Experiments.....	121
7.2.3	Partition Experiments.....	124
7.3	<b>Results and Discussion</b> .....	126
7.3.1	Isoenhancement Concentrations and Enhancer Effects.....	126
7.3.2	Effects of Alkyl Chain Length.....	126
7.3.3	Effects of Polar Head Functional Groups.....	127
7.3.4	Effects of Hydrocarbon Chain Carbon–Carbon Double Bond.....	128
7.3.5	Effects of Branched Alkyl Chain.....	129
7.3.6	Equilibrium Partition Enhancement of ES into SC Intercellular Lipids.....	130
7.3.7	Transport Rate-Limiting Domain and Equilibrium Partitioning Domain.....	131
7.3.8	Effects of Permeation Enhancement on Permeants of Different Molecular Sizes.....	131
7.3.9	Permeation Enhancers in a Nonaqueous System in Transdermal Drug Delivery.....	133
	<b>Conclusion</b> .....	134
	<b>References</b> .....	135

## 7.1 Introduction

Most of the chemical permeation enhancer studies in the past decades have been aimed at gaining better insights into the relationship between the nature of the enhancers and their effectiveness in permeation enhancement. In typical in vitro studies of chemical permeation enhancers, the enhancer in question is usually applied with a drug in solution or suspension to one side of the membrane, and the effectiveness of the enhancer compared to a control is determined by the rate of transport of the drug. Under this approach, the different relationships among the enhancer molecular structures and their effects as permeation enhancers have been studied (e.g., reviewed in Lee et al. 1991; Smith and Maibach 1995; Hadgraft 2001).

Our laboratory has been studying the mechanism of action of permeation enhancers for more than a decade. A different experimental approach has been employed in these studies (Kim

---

S.K. Li (✉)  
Division of Pharmaceutical Sciences,  
College of Pharmacy, University of Cincinnati,  
3225 Eden Ave, Rm 160, Cincinnati,  
OH 45267-0004, USA  
e-mail: [kevin.li@uc.edu](mailto:kevin.li@uc.edu)

W.I. Higuchi  
Pharmaceutics and Pharmaceutical Chemistry,  
College of Pharmacy, University of Utah,  
30 S 2000 E, Skaggs Hall, Salt Lake City,  
UT 84112, USA



et al. 1992; Yoneto et al. 1995; Warner et al. 2003; He et al. 2004). First, if mechanistic insight is to be collected directly, a symmetric and equilibrium configuration (with respect to the enhancer) should be used. In the symmetric configuration, the enhancer is present at equal concentrations in both the donor and receiver chambers of a side-by-side diffusion cell and in equilibrium with the membrane. Under these conditions, the complications arising from enhancer concentration (or activity) gradients across the membrane (Liu et al. 1991, 1992; Chantasart and Li 2010) can be avoided. These enhancer gradients would otherwise lead to a situation in which the local permeation enhancement varies with the position within the membrane and make mechanistic data analysis difficult. With the symmetric configuration, the permeability coefficients obtained for the permeants can be used directly to determine the effectiveness of an enhancer in enhancing transdermal transport (enhancer potency). Second, good enhancers are usually lipophilic and relatively water-insoluble. Because they are water-insoluble, well absorbed, and need to be solubilized for effective presentation, they cannot be systematically investigated conveniently for structure–enhancement activity. Establishing equilibrium between the enhancer and the membrane is therefore necessary in obtaining mechanistic insights into the action of permeation enhancers and for establishing a structure–enhancement relationship. Third, model analyses to separate the effects of permeation enhancement on transport across the lipoidal and pore transport pathways using model permeants of different polarity have been used. The effects of the enhancers upon the intercellular lipoidal and pore pathway transport have been delineated in order to understand the mechanism of action of the enhancers. Last, in the assessment of skin permeation enhancement, changes in the chemical potential (activity) of the permeant in the enhancer solution with respect to that in the buffer solution (the control) are corrected for, so the effects of permeant activity alteration upon transport in the presence of the enhancers are taken into account. Taking the above issues into consideration, we have developed a research strategy to gain mechanistic insights into the effects of enhancers upon

transport across skin, to determine the intrinsic potencies of the enhancers, and to establish a quantitative structure–enhancement relationship between the enhancers and permeation enhancement. This chapter is a review of our studies employing this strategy and the experimental approaches.

---

## 7.2 Methods

### 7.2.1 Animal Model

Experiments were conducted with freshly separated hairless mouse skin (HMS) obtained from the abdomen region and freed from adhering fat and other visceral debris. HMS was selected as the model for human skin for the following reasons. HMS has relatively constant lipid content (Yoneto et al. 1998), and a large body of HMS data is available in the literature allowing the direct comparisons of our results with those in previous studies. HMS stratum corneum (SC) lipid composition (Grubauer et al. 1989) is also similar to that of human skin (Lampe et al. 1983). In certain cases, such as for experiments requiring long-term skin stability in aqueous solution, HMS is not a good model of human skin (Lambert et al. 1989). However, in the investigation of chemical permeation enhancers for the lipoidal pathway and where relatively short experimental times are involved, HMS can be an adequate quantitative model for human skin (Kim et al. 1992; Li et al. 1997). For example, Chantasart et al. (2007) compared the effects of permeation enhancers on the permeability coefficients of the lipoidal pathways of HMS and human epidermal membrane (HEM) under the symmetric and equilibrium configuration. The quantitative structure–enhancement relationships of the enhancers in HMS and HEM were also compared. The results suggest that for the assessment of skin permeation across the lipoidal pathway and for the mechanistic studies of the effects of skin permeation enhancers upon this pathway, HMS can be a reliable model for human skin. There is no direct evidence of significant discrepancies between the mechanisms of action of permeation enhancers in HMS and human skin.

## 7.2.2 Transport Experiments

### 7.2.2.1 Permeability Coefficient Determination

The permeability experiments were carried out as previously described with a two-chamber side-by-side diffusion cell in phosphate buffered saline (PBS) at 37 °C (Yoneto et al. 1995; Warner et al. 2003). Each compartment has a 2-mL volume and an effective diffusional area of 0.67 cm<sup>2</sup>. The skin membrane was sandwiched between the two half cells and an enhancer solution in PBS was pipetted into both chambers. A list of the enhancers investigated is shown in Fig. 7.1. To attain equilibrium of the enhancer with the HMS, the enhancer solution in both diffusion cell chambers was replaced until the SC was essentially in equilibrium with the enhancer solution (enhancer/PBS). With highly hydrophobic enhancers (e.g., 1-dodecyl-2-pyrrolidone), due to the extensive depletion of the enhancers in the aqueous phase that made it difficult to achieving an equilibrium of the enhancers between the aqueous phase and the SC at the target concentrations, an aqueous reservoir system (enhancer solubilizing system of micelles or cyclodextrin) that neither significantly interacts with the SC nor acts as a permeation enhancer was used (Warner 2003; Shaker et al. 2003; Warner et al. 2008). The concentrations of the enhancers in the diffusion cell chambers were frequently checked by HPLC or GC. The loss or depletion of all the enhancers was less than 5% in most cases and less than 15% in the extreme case at the end of the transport experiments.

Corticosterone (CS) was the main model permeant. Estradiol (ES) and hydrocortisone (HC) were the two other steroidal permeants tested in the studies. Other permeants used will be discussed in the section on “Effects of Permeation Enhancement on Permeants of Different Molecular Sizes.” The steroidal permeant at radiotracer levels and at concentrations far below its solubility was added to the donor chamber following enhancer equilibration. Samples were withdrawn from the donor and receiver chambers at predetermined time intervals and analyzed. Permeability experiments with model ionic polar

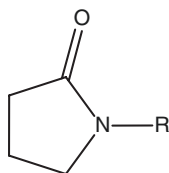
permeant tetraethylammonium ion (TEA) were conducted in essentially the same manner. The total permeability coefficients ( $P_T$ ) were determined from data obtained under steady-state conditions (experiment time points around three to five times longer than the lag times). The permeability coefficient of the dermis–epidermis combination ( $P_{D/E}$ ) was obtained in the same manner, but the skin was stripped 30 times with 3 M Scotch tape prior to excision and assembly into the diffusion cell.

Another method to evaluate the potency of permeation enhancers, particularly highly lipophilic enhancers, is the direct equilibration of the skin with liquid enhancers and the subsequent skin transport experiments with PBS as the donor and receiver solution in a side-by-side diffusion cell in the absence of cosolvents or solubilizing agents (Ibrahim and Li 2009a, b). With highly lipophilic enhancers, the depletion of the enhancers from the skin to the aqueous solution in the diffusion cell chambers is expected to be minimal, and essentially constant enhancer concentration can be maintained in the SC over the duration of the permeability experiments. This method was recently used to study the structure–enhancement relationship of highly lipophilic chemical enhancers and evaluate enhancer effectiveness under the condition when the SC was saturated with the enhancer at thermodynamic activity equivalent to its pure state (i.e., at the solubility of the enhancer in the SC lipids). A disadvantage of this approach is the inability to control the enhancer concentration in the diffusion cell chamber (i.e., always at saturation in the aqueous solution) and hence in the skin. In other words, this approach cannot be used to evaluate the effects of enhancer concentration upon skin permeation enhancement. Permeation enhancer studies using this approach (Ibrahim and Li 2009a, b; Chantasart and Li 2012) will not be discussed in this chapter but have been discussed in a recent book chapter (Li and Higuchi 2015).

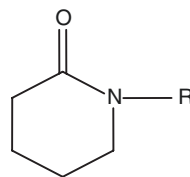
#### 7.2.2.2 Reversibility Study

Diffusion cells were assembled with full thickness HMS as described for a typical permeation experiment under the symmetric and equilibrium

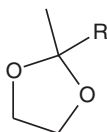
**Fig. 7.1** Chemical structures of the enhancers.  $R, R'$  = alkyl chain



1-alkyl-2-pyrrolidones (AP)



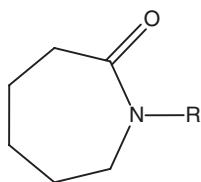
1-alkyl-2-piperidinones (API)



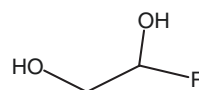
2-(1-alkyl)-2-methyl-1,3-dioxolanes (MD)



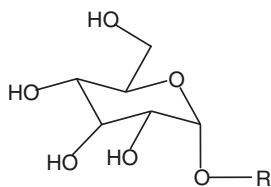
1-alkanols (AL)



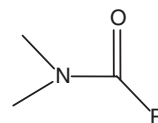
1-alkyl-2-azacycloheptanones (AZ)



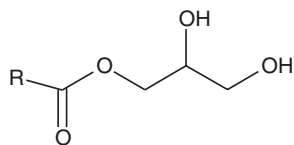
1,2-alkanediols (AD)



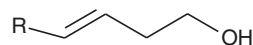
*n*-alkyl- $\beta$ -D-glucopyranosides (AG)



N,N-dimethyl alkanamides (AM)



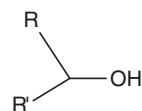
1,2-dihydroxypropyl alkanoates (MG)



trans-3-alken-1-ols (TAL)



cis-3-alken-1-ols (CAL)



Branched alkanols (bAL)

configuration, and equilibrium between the membrane and the enhancer solution was allowed to take place. However, in this protocol, both chambers of the diffusion cell were then rinsed with PBS to remove the enhancer equilibrated in the membrane. Following the PBS rinsing regime, transport studies were carried out with PBS in both chambers. The permeability coefficients obtained with PBS after pretreatment with enhancers were then compared with those obtained with pretreatment with PBS only. Except for the highly lipophilic enhancers, all enhancers were tested for reversibility at enhancer concentrations up to enhancement factor ( $E$ ) at  $E=10$  (Warner et al. 2001, 2003; He et al. 2003, 2004; Chantasart et al. 2004), and their effects upon permeation across SC were shown to be essentially reversible (permeability coefficients in PBS after enhancer pretreatment were within a factor of 2 of those in PBS without enhancer pretreatment).

### 7.2.2.3 Model Description and Analysis of Experimental Data

The permeability coefficient ( $P$ ) of a probe permeant was calculated according to Eq. (7.1) (Warner et al. 2001):

$$P = \frac{1}{AC_D} \frac{dQ}{dt} \quad (7.1)$$

where  $A$  is the diffusional area of the diffusion cell,  $C_D$  is the concentration in the donor chamber, and  $dQ/dt$  is the slope of the linear region of the cumulative amount of permeant in receiver chamber ( $Q$ ) vs. time plot.

Total permeability coefficient expression for full-thickness skin is written as follows:

$$P_T = \frac{1}{\frac{1}{P_{SC}} + \frac{1}{P_{D/E}}} \quad (7.2)$$

where  $P_{SC}$  is the permeability coefficient for the stratum corneum (SC) and  $P_{D/E}$  is the permeability coefficient for the epidermis-dermis combination (D/E) and can be obtained from experiments of tape-stripped skin.  $P_{SC}$  can be further divided

into parallel lipoidal and pore pathway components in SC via the following equation:

$$P_{SC} = P_L + P_P \quad (7.3)$$

where  $P_L$  and  $P_P$  are the permeability coefficients for the lipoidal pathway and the pore pathway (TEA is used as the probe permeant for estimating the magnitude of  $P_P$ ), respectively, in the SC. The intercellular lipid domain in SC is generally accepted as the lipoidal transport pathway across SC. Substituting Eq. (7.3) into Eq. (7.2) yields:

$$P_T = \frac{1}{\frac{1}{P_L + P_P} + \frac{1}{P_{D/E}}} \quad (7.4)$$

Based on the results from previous studies, the use of CS as the probe permeant allows Eq. (7.4) to be approximated by:

$$P_T \approx P_L \quad (7.5)$$

For other steroidal permeants,  $P_L$  can be calculated by Eq. (7.4) with  $P_{D/E}$  and  $P_P$  values obtained from transport experiments with stripped skin and TEA, respectively. The equation for the lipoidal pathway transport enhancement factor ( $E$ ) is:

$$E = \frac{P_{L,X} S_X}{P_{L,O} S_O} \quad (7.6)$$

where  $P_{L,X}$  and  $P_{L,O}$  are the permeability coefficients for the lipoidal pathway when the solvent is enhancer/PBS and PBS, respectively, and  $S_X$  and  $S_O$  are the permeant solubilities in enhancer/PBS and in PBS, respectively. The solubility ratio corrects for any activity coefficient differences between the activity coefficient in PBS and that in the enhancer solution. Use of the solubility ratio assumes that Henry's law is obeyed for the permeant in both PBS and enhancer solutions (Kim et al. 1992).

### 7.2.2.4 Permeant Solubility Determination

The solubilities of the steroidal permeants in PBS and the enhancer solutions were determined by adding excess crystals of the permeant into the

enhancer solution in Pyrex culture tubes. The drug suspension was shaken for 72 h at 37 °C. The culture tubes were then centrifuged for 15 min at 3500 rpm, and the clear supernatants were analyzed for permeant concentrations with HPLC.

### 7.2.2.5 Determination of Partition Coefficient in Bulk Organic Solvent/PBS Systems

Organic solvent/PBS partition coefficients were obtained at the aqueous enhancer concentrations corresponding to  $E=10$  and at one tenth of the  $E=10$  concentration, the latter to test whether Henry's law is obeyed in the two liquid phases. The two-phase systems were maintained at 37 °C for 72 h. Both the organic and aqueous phases were centrifuged, and aliquots were carefully withdrawn from both phases and appropriately diluted for subsequent analysis using HPLC or GC.

## 7.2.3 Partition Experiments

### 7.2.3.1 n-Heptane Treatment and SC preparation

Before SC preparation, HMS was rinsed with heptane for  $3 \times 10$  s to remove the SC surface lipids. This rinsing protocol (the number of rinses and the rinse time) was shown to remove approximately 20% of the SC lipids but did not disrupt the SC barrier (He et al. 2003). Similar treatments with nonpolar organic solvent were also shown to remove skin surface lipids (e.g., Abrams et al. 1993; Nicolaides 1974). SC was then prepared according to the method described by Kligman and Christophers (1963) and Yoneto et al. (1998). Briefly, the skin was placed, dermis side down, on a filter paper (quantitative filter paper No. 1, Whatman®) mounted on a Petri dish. The Petri dish was filled with 0.2% trypsin in PBS solution up to the surface of SC. The Petri dish was covered and maintained at 37 °C for 16 h. When the skin membrane was placed in distilled water after the trypsin treatment, the dermis and viable epidermal layers would separate and fall away from the SC. The SC was then rinsed with distilled water several times and swabbed with Kimwipe® tissue paper to remove excess water. Then, the SC was placed on aluminum foil

and dried at room temperature. After drying, the SC was kept in a freezer for later use.

### 7.2.3.2 HMS SC Delipidization

Heptane-treated HMS SC samples were prepared as described in the previous section. The delipidized HMS SC was prepared according to the method described previously (Yoneto et al. 1998). Briefly, dried *n*-heptane-treated SC samples (about 1–2 mg) were weighed and transferred into 5 mL  $\text{CHCl}_3/\text{MeOH}$  (2:1) mixture and equilibrated for 48 h at room temperature. The residue of SC was then rinsed several times with fresh  $\text{CHCl}_3/\text{MeOH}$  (2:1) mixture and dried under room temperature for 24 h. The dried residue was carefully weighed and used for the partition experiments.

### 7.2.3.3 Partition Experiments with Heptane-Treated and Delipidized HMS SC

Partition experiments were carried out to determine the uptake amounts of the chemical permeation enhancer and of probe permeant ES into *n*-heptane-treated or delipidized HMS SC. Two different partition experimental setups were used in our laboratory. The old setup used a Franz diffusion cell (Yoneto et al. 1998) and would not be discussed here. The following is a brief description of the other method (Chantasart et al. 2004). Heptane-treated SC (about 1–2 mg) or delipidized SC sample was carefully weighed and equilibrated in about 20 mL of enhancer solution ( $E=10$  concentration) containing trace amounts of radiolabeled ES ( $^3\text{H-ES}$ ) in a screw-capped glass vial. The vial was sealed with parafilm to prevent enhancer solution evaporation and put in a water bath with shaking at  $37 \pm 0.1$  °C for 12 h. The 12-h incubation period was chosen because preliminary studies showed that equilibrium of enhancer and  $^3\text{H-ES}$  with the SC sample took place in less than 12 h and that a longer incubation period might result in too fragile a membrane sample for the partitioning experiments. After 12 h, the SC sample was taken out from the solution by tweezers and blotted by Kimwipe® tissue paper. The enhancer and ES concentrations of the solution in the screw-capped glass vial were checked. The wet SC sample was carefully weighed in a

snap-capped glass bottle. Then, 5 mL of 100% ethanol was added into the bottle to extract the enhancer and ES from the sample for 48 h at room temperature with occasional gentle agitation. The extracted solution was then transferred to a screw-capped Pyrex test tube. The test tube was centrifuged at 3500 rpm for 15 min. The supernatant was analyzed for the enhancer by GC or HPLC and for ES by a scintillation counter.

The uptake amount of enhancer in the heptane-treated SC or delipidized SC was calculated as follows:

$$A_{\text{corrected},i} = \frac{A_{\text{extracted},i}}{W_{\text{dry}}} - (W_{\text{wet}} - W_{\text{dry}}) \frac{C_i}{W_{\text{dry}}} \quad (7.7)$$

where  $A_{\text{extracted},i}$  is the amount enhancer extracted from heptane-treated or delipidized HMS SC,  $W_{\text{dry}}$  is the dried heptane-treated or delipidized SC weight, and the subscript  $i$  represents the enhancer. A correction for the enhancer in the aqueous compartment(s) of the SC was calculated according to the wet weight of SC ( $W_{\text{wet}}$ ) and the concentration of the enhancer in aqueous bulk phase ( $C_i$ ). The partition coefficient of ES ( $K_{\text{ES}}$ ) for partitioning from the aqueous phase into  $n$ -heptane-treated SC or delipidized SC was calculated as follows:

$$K_{\text{ES}} = \frac{[A'_{\text{extracted}} - (W_{\text{wet}} - W_{\text{dry}})C'_i] / W_{\text{dry}}}{C'_i} \frac{S'_x}{S'_o} \quad (7.8)$$

where  $A'_{\text{extracted}}$  is the amount of extracted  $^3\text{H}$ -ES,  $C'_i$  is the concentration of  $^3\text{H}$ -ES in aqueous bulk phase, and  $S'_x$  and  $S'_o$  are the solubilities of ES in enhancer solution and in PBS, respectively. The solubility ratio corrects for any activity coefficient differences between the activity coefficient of ES in PBS and that in the enhancer solution.

#### 7.2.3.4 Permeant Partitioning into the Transport Rate-Limiting Domain and Equilibrium Permeant Partitioning into the Stratum Corneum Intercellular Lipids

An important question raised in the above transport and equilibrium partition studies was: is the

equilibrium partition enhancement data of ES a direct correlate of the partition enhancement of ES in SC permeation? To address this question, the partition enhancement in SC permeation was determined in skin transport experiments using a nonsteady state transport analysis (He et al. 2005). However, a direct comparison of the partition enhancement data obtained in transport experiments and those data obtained in equilibrium partitioning experiments of ES was not practical due to the D/E layer being a significant barrier for ES permeation across HMS. Furthermore, significant ES metabolism was observed in ES transdermal permeation. Because of these difficulties, nonsteady state ES transport analysis was complicated, and it was decided to employ CS as the surrogate permeant for ES in the following study. The strategy here was to examine the relationship between the transport partitioning enhancement of CS and the equilibrium partitioning enhancement of ES, with the assumption that ES and CS should likely behave similarly. This assumption was considered to be reasonable because previous studies had shown similar permeability coefficient enhancement effects of chemical enhancers with ES and CS for permeation across the lipoidal pathway of HMS SC (Yoneto et al. 1995).

The skin transport model (He et al. 2005) is a two-layer numerical transport simulation with a least squares-fitting software Scientist (MicroMath, Salt Lake City, UT). This model assumes that both SC and D/E are homogenous and divides the SC and D/E into a sufficient number of layers characterized by partition, diffusion, and dimension parameters. The permeant concentration in the donor chamber was assumed constant, which was true in all transport experiments carried out in the study. The receiver chamber concentration was kept at sink conditions. The transport data of full-thickness HMS were analyzed using the model to obtain the partition coefficient ( $K_{\text{SC}}$ ) and diffusion coefficient ( $D_{\text{SC}}$ ) of SC. The reduced parameters  $K_{\text{SC}}'$  and  $D_{\text{SC}}'$  of SC were then calculated:

$$D_{\text{SC}}' = D_{\text{SC}} / L^2 \quad (7.9)$$

$$K_{\text{SC}}' = K_{\text{SC}}L \quad (7.10)$$

where  $L$  is the effective path length across SC. These reduced parameters  $K_{SC}'$  and  $D_{SC}'$  were defined (Okamoto et al. 1988) to avoid the difficulty and uncertainty in assigning the  $L$  value and to minimize the number of parameters for least square fitting in model analyses of the experimental transport data. The enhancement of  $K_{SC}'$  and  $D_{SC}'$  ( $E_{K, SC}$  and  $E_{D, SC}$ , respectively) was calculated by dividing the  $K_{SC}'$  and  $D_{SC}'$  parameters obtained with the enhancers at  $E=10$  by those with PBS control.

## 7.3 Results and Discussion

### 7.3.1 Isoenhancement Concentrations and Enhancer Effects

Figure 7.2 shows a representative plot of enhancement factor vs. aqueous enhancer concentration for ES, CS, and HC permeation across the SC lipoidal pathway with 1-butyl-2-pyrrolidone, 1-hexyl-2-pyrrolidone, and 1-octyl-2-pyrrolidone as permeation enhancers (Yoneto et al. 1995). Similar enhancement factor vs. aqueous enhancer concentration plots were observed for the enhanc-

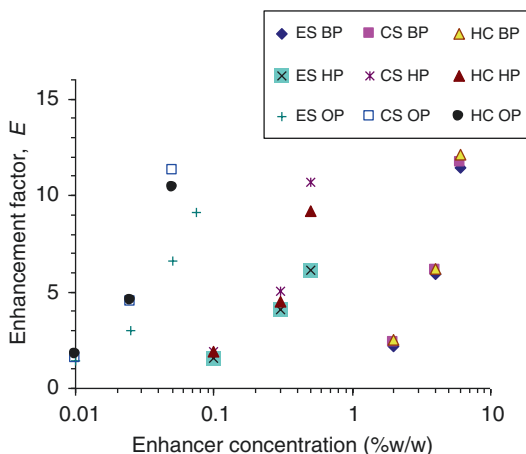


**Fig. 7.2** Transport enhancement factors of estradiol (ES), corticosterone (CS), and hydrocortisone (HC) across the SC lipoidal pathway in the presence of 1-butyl-2-pyrrolidone (BP), 1-hexyl-2-pyrrolidone (HP), and 1-octyl-2-pyrrolidone (OP). The transport enhancement factors were calculated using Eq. (7.6)

ers studied. The enhancement factor profiles at increasing aqueous enhancer concentrations are essentially the same for the steroidal permeants of different lipophilicity, suggesting the same mechanism of permeation enhancement for these steroidal permeants.

### 7.3.2 Effects of Alkyl Chain Length

The isoenhancement concentrations at  $E=10$  for more than 20 different enhancers are presented in Fig. 7.3 (Warner et al. 2003); isoenhancement concentration is defined as the aqueous concentrations of enhancers to induce the same enhancement factor and in this case  $E=10$ . These isoenhancement concentrations were interpolated from the  $E$  vs. aqueous enhancer concentration plots similar to those in Fig. 7.2. Figure 7.3 shows the relationship between the  $E=10$  enhancer concentration and the carbon number of the enhancer  $n$ -alkyl group (at constant permeant thermodynamic activity). The major conclusion deduced from the data in Fig. 7.3 is a slope of around  $-0.55$  found for each enhancer series (enhancers have the same polar head functional group but different alkyl chain length) in the figure. The value of  $-0.55$  translates into an around

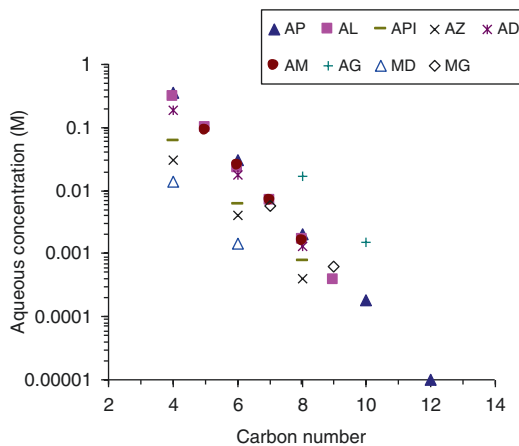


**Fig. 7.3** Relationships between the aqueous  $E=10$  isoenhancement concentrations of the enhancers and the carbon number of the enhancer alkyl chain. Each data point represents the average value without showing the standard deviation because the error bar generally lies within the symbol in the plot. Enhancer abbreviations are provided in Fig. 7.1

3.5-fold increase in potency per methylene group for the enhancers. In other words, the aqueous concentration required to induce  $E=10$  increases 3.5-fold when the alkyl chain length of the enhancer decreases by one methylene group. The constant slope of  $-0.55$  for the different enhancer series suggests a hydrophobic effect involving the transfer of the methylene group from the aqueous phase to a relatively nonpolar organic phase (e.g., Tanford 1980).

The results of the equilibrium partition experiments with the enhancers conducted to determine the amount of enhancers in the SC intercellular lipids under the isoenhancement  $E=10$  conditions (He et al. 2003, 2004) are shown in Fig. 7.4. Note that the scale of the y-axis in Fig. 7.4 is the same as that in Fig. 7.3. The data in Fig. 7.4 suggest that there was little effect of the enhancer alkyl chain length upon the enhancer potency based on the concentrations of the enhancers in the intercellular lipid lamellae (relative to that based on the  $E=10$  aqueous enhancer concentrations in Fig. 7.3), thus suggesting that the intrinsic potency of the enhancers at their site of action, generally believed to be the SC intercellular lipids, is relatively independent of their alkyl group chain length and lipophilicity.

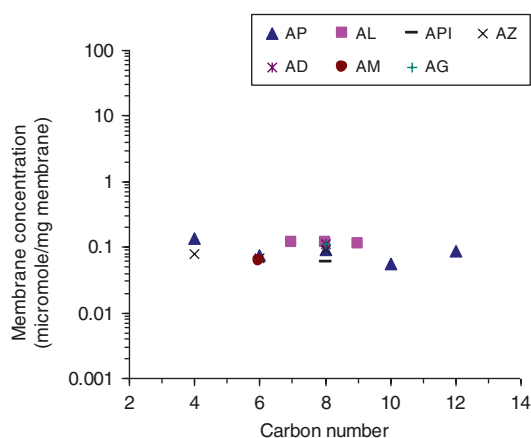


**Fig. 7.4** Relationship between the enhancer concentrations in the intercellular lipid domain of the SC membrane at the  $E=10$  isoenhancement conditions and the carbon number of the enhancer alkyl chain. Each data point represents the average value. Enhancer abbreviations are provided in Fig. 7.1

### 7.3.3 Effects of Polar Head Functional Groups

The data in Fig. 7.3 also show that some enhancer polar functional groups are more effective (more potent) than the others in inducing permeation enhancement. For example, the  $E=10$  isoenhancement concentrations of 1-alkyl-2-azacycloheptanones are consistently around tenfold lower than those of 1-alkyl-2-pyrrolidones at the same  $n$ -alkyl chain length, suggesting that the azacycloheptanone group makes the 1-alkyl-2-azacycloheptanones more effective permeation enhancers as compared with the pyrrolidone group of the 1-alkyl-2-pyrrolidones based on their concentrations in the aqueous phase in the donor and receiver chambers. However, the relative constant concentration of enhancer uptake into the SC lipid domain at  $E=10$  in Fig. 7.4 reveals that there is little effect of the enhancer polar head functional group upon the enhancer potency based on the concentrations of the enhancers at their site of action. This is an interesting finding because studies using conventional experimental methods in the literature have demonstrated the influence of the polar head functional group of an enhancer upon its effectiveness in transdermal permeation enhancement (e.g., Smith and Maibach 1995). In particular, it has been suggested that the azacycloheptanone functional group is more potent than other polar head functional groups in general due to specific interactions between the functional group and the ceramide lipid matrix (e.g., Brain and Walters 1993; Hadgraft et al. 1996). The data in Fig. 7.4, however, imply that the polar head and alkyl groups of the enhancers act only to transfer the enhancers from the aqueous phase to the hydrocarbon phase of the SC lipid lamellae and make available the enhancers for their action in the SC transport rate-limiting domain.

Figure 7.5 is a replot of the data shown in Fig. 7.3 to demonstrate a structure-enhancement relationship for the enhancers (Warner et al. 2003). The correlation between the  $E=10$  isoenhancement concentrations and the octanol/PBS partition coefficients of the enhancers with a slope of around  $-1$  suggests that the potencies of



the enhancers for the steroidal permeants are related to the enhancer lipophilicities. Together with the data analysis in Figs. 7.3 and 7.4, it is reasonable to hypothesize that (a) permeation enhancement is related to the ability of the permeation enhancer to partition into the transport rate-limiting domain in SC, (b) the polar head group assists the translocation of the enhancer to the site of action through a free energy of transfer from the bulk aqueous phase to the transport rate-limiting domain, and (c) the transport rate-limiting domain has a microenvironment with polarity similar to the polarity of bulk octanol. These hypotheses and the results of Fig. 7.5 have been discussed in detail in a recent book chapter (Li and Higuchi 2015).

### 7.3.4 Effects of Hydrocarbon Chain Carbon–Carbon Double Bond

The effects of substituting a single carbon–carbon bond on the *n*-alkyl chain of an enhancer with a carbon–carbon double bond have been investigated, and the  $E=10$  isoenhancement concentrations of the *cis*- and *trans*-3-alken-1-ols (closed symbols) are plotted against the carbon numbers of the enhancer hydrocarbon chains in Fig. 7.6 (He et al. 2004). The data for the

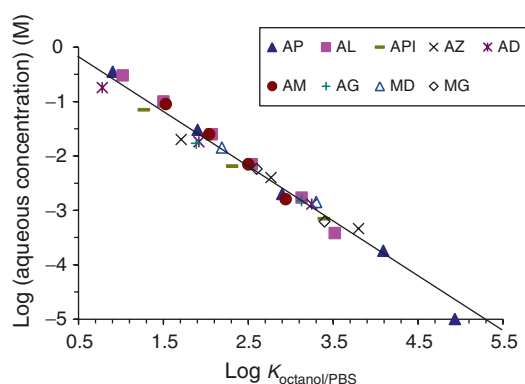


**Fig. 7.5** Correlation between the aqueous  $E=10$  isoenhancement concentration of the enhancer and its octanol/PBS partition coefficient ( $K_{\text{octanol/PBS}}$ ). The slope of the line is  $-1$ . Each data point represents the average value without showing the standard deviation because the error bar generally lies within the symbol in the plot. Enhancer abbreviations are provided in Fig. 7.1

*n*-alkanols reported in Fig. 7.3 are also included in Fig. 7.6 for comparison. In Fig. 7.6, it is seen that the  $E=10$  isoenhancement concentrations of the *cis*- and *trans*-3-alken-1-ols are two to three times higher than those of the corresponding *n*-alkanols (open squares). Based on the criterion that the  $E=10$  isoenhancement (aqueous) concentration is a measure of the enhancer potency, the results in Fig. 7.6 would suggest the *cis*- and *trans*-3-alken-1-ols are less potent than the *n*-alkanols by a factor of 2 to 3. However, when the  $E=10$  isoenhancement concentrations of the *cis*- and *trans*-3-alken-1-ols and of the *n*-alkyl enhancers are plotted against their octanol/PBS partition coefficients ( $K_{\text{octanol/PBS}}$ ) in Fig. 7.7, the *cis*- and *trans*-3-alken-1-ol data fall closely on the correlation line in the figure (same correlation line as that in Fig. 7.5) when the lipophilicity of the enhancers is taken into consideration. The correlation between the  $E=10$  isoenhancement concentration and octanol/PBS partition coefficient here is consistent with the demonstrated structure–enhancement relationship for the *n*-alkyl enhancers in Fig. 7.5.

In the equilibrium partition experiments of the *cis*- and *trans*-3-alken-1-ols, the concentrations of the enhancers in the SC intercellular lipid

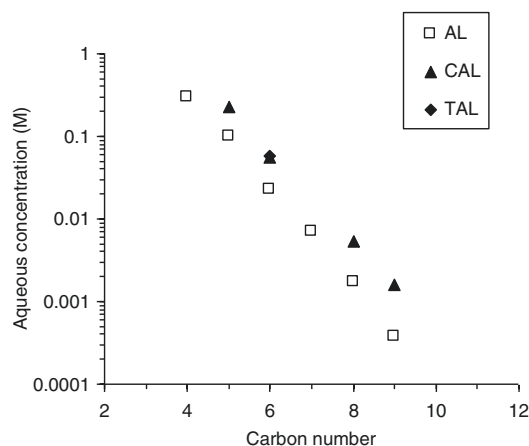


**Fig. 7.6** Relationships between the aqueous  $E=10$  isoenhancement concentrations of the enhancers and the carbon number of the enhancer alkyl chain. Each data point represents the average value without showing the standard deviation because the error bar generally lies within the symbol in the plot. Enhancer abbreviations are provided in Fig. 7.1

domain under the isoenhancement  $E=10$  conditions are essentially constant (Fig. 7.8). The substitution of a single carbon–carbon bond with a carbon–carbon double bond on the alkyl chain here has little effect upon the enhancer potency based on the concentrations of the enhancers in the SC intercellular lipid domain. This is somewhat surprising because enhancers with unsaturated hydrocarbon chains are expected to be more

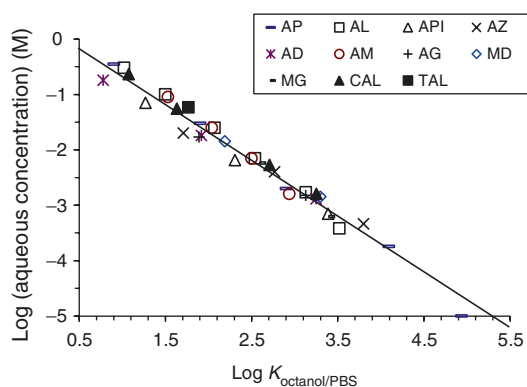


**Fig. 7.7** Correlation between the aqueous  $E=10$  isoenhancement concentration of the enhancer and its octanol/PBS partition coefficient ( $K_{\text{octanol/PBS}}$ ). Each data point represents the average value without showing the standard deviation because the error bar generally lies within the symbol in the plot. The slope of the line is  $-1$ . Enhancer abbreviations are provided in Fig. 7.1

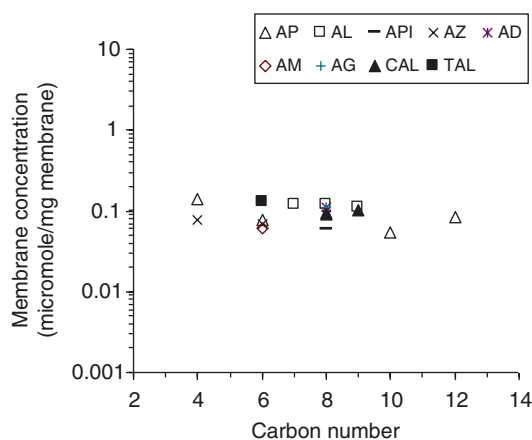


**Fig. 7.8** Relationship between the enhancer concentrations in the intercellular lipid domain of the SC membrane at the  $E=10$  isoenhancement conditions and the carbon number of the enhancer alkyl chain. Each data point represents the average value. Enhancer abbreviations are provided in Fig. 7.1

potent than enhancers with saturated hydrocarbon chains based on molecular modeling of skin permeation and previous experimental results (Golden et al. 1987; Aungst 1989; Brain and Walters 1993; Tenjarla et al. 1999).

### 7.3.5 Effects of Branched Alkyl Chain

Branched chain alkanols (2-alkanols, 3-alkanols, 4-alkanols, and 5-nonanol) were also investigated as another group of skin permeation enhancers to provide insights into the mechanism of action of both  $n$ -alkyl and branched chain enhancers (Chantasart et al. 2004). The 2-alkanols, 3-alkanols, and 4-alkanols are 2-hexanol, 2-heptanol, 2-octanol, 2-nonanol; 3-hexanol, 3-heptanol, 3-octanol, 3-nonanol; and 4-heptanol, 4-octanol, and 4-nonanol, respectively. In Fig. 7.9, the isoenhancement concentrations at  $E=10$  of the branched alkanols (closed symbols) are plotted against their  $K_{\text{octanol/PBS}}$  values. Again, the data of the  $n$ -alkyl enhancers (including the  $n$ -alkanols) are included in Fig. 7.9, and the straight line shown in the figure is a best fit line based on the data for more than 20  $n$ -alkyl enhancers in Fig. 7.5. Different from the random deviations for the  $n$ -alkyl enhancers (crosses), the

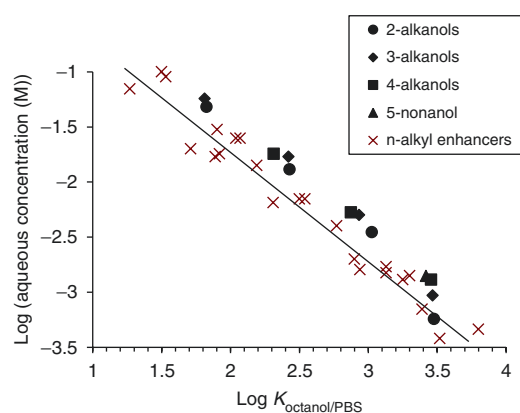


**Fig. 7.9** Correlation between the aqueous  $E=10$  isoenhancement concentration of the enhancer and its octanol/PBS partition coefficient ( $K_{\text{octanol/PBS}}$ ). Each data point represents the average value without showing the standard deviation because the error bar generally lies within the symbol in the plot. The slope of the line is  $-1$

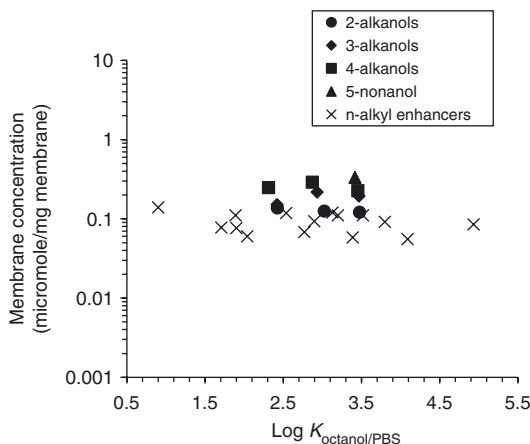


**Fig. 7.10** Relationship between the enhancer concentrations in the intercellular lipid domain of the SC membrane at the  $E=10$  isoenhancement conditions and the octanol/PBS partition coefficient ( $K_{\text{octanol/PBS}}$ ) of the enhancers. Each data point represents the average value

branched chain alkanols (closed symbols) show modest but consistent positive deviations (in the direction of lower potency) from the quantitative structure–enhancement correlation (the straight line). These deviations support the view, based on the assumption that  $K_{\text{octanol/PBS}}$  is a valid predictor of enhancer potency, that the branched chain alkanols are slightly less potent than the  $n$ -alkyl enhancers. The lower potencies based on the  $E=10$  aqueous concentrations of the branched chain alkanols could be attributed to decreasing intrinsic potency and increasing effective hydrophilicity of the enhancers when the hydroxyl group moves from the terminal end towards the center of the enhancer alkyl chain. Nevertheless, the results of the branched chain alkanols continue to support the hypothesis previously established for the  $n$ -alkyl enhancers that the potency of an enhancer based on its aqueous concentration increases with enhancer lipophilicity.

Figure 7.10 presents the concentrations of the branched chain alkanols and  $n$ -alkyl enhancers in the SC intercellular lipids under the isoenhancement conditions of  $E=10$ . Whereas the intrinsic potencies of the  $n$ -alkyl enhancers are essentially the same and independent of their alkyl chain length, branching of the alkyl chain decreases the intrinsic potencies of the enhancers; the

concentrations of the branched alkanols in the SC intercellular lipid domain (closed symbols) required to induce the  $E=10$  conditions are generally higher than those of the  $n$ -alkyl enhancers (crosses in the figure). This result is consistent with the relatively lower intrinsic potency of the branched chain alkanols suggested with the data in Fig. 7.9.

Despite the observed deviation of the branched chain alkanols from the  $n$ -alkyl chain enhancers, it should be noted that the correlation between the logarithm of the enhancer partition coefficient from the aqueous phase to the SC intercellular lipid phase ( $\log K_{\text{SC lipid/PBS}}$ ) and  $\log K_{\text{octanol/PBS}}$  continues to hold for the branched chain alkanols. The microenvironment of the enhancer site of action remains essentially the same and independent of alkyl-chain branching; the  $n$ -alkanols, branched chain alkanols, and all other studied enhancers fall on the same regression line (Fig. 5.9 in a recent book chapter; Li and Higuchi 2015).

### 7.3.6 Equilibrium Partition Enhancement of ES into SC Intercellular Lipids

In addition to the equilibrium partition experiments of the enhancers, experiments were also conducted with a model steroidal compound ES (He et al. 2003, 2004; Chantasart et al. 2004). The goal here was to determine the enhancement of the partitioning of a lipophilic permeant into the SC intercellular lipids under the isoenhancement  $E=10$  conditions. Figure 7.11 shows the plots of the partition coefficients of ES from the aqueous phase into the SC intercellular lipid domain ( $K_{\text{ES}}$ ) under the  $E=10$  conditions of more than 20 different enhancers vs. the  $K_{\text{octanol/PBS}}$  values of the enhancers. The  $K_{\text{ES}}$  values were determined with Eq. (7.8). The dotted line represents the  $K_{\text{ES}}$  value in PBS control. As can be seen in the figure, approximately the same enhancement of  $K_{\text{ES}}$  (four- to sevenfold) was induced under the isoenhancement conditions of  $E=10$  for all the enhancers studied. The relatively constant four- to sevenfold enhancement in permeant partitioning suggests that (a) the same target site in the SC

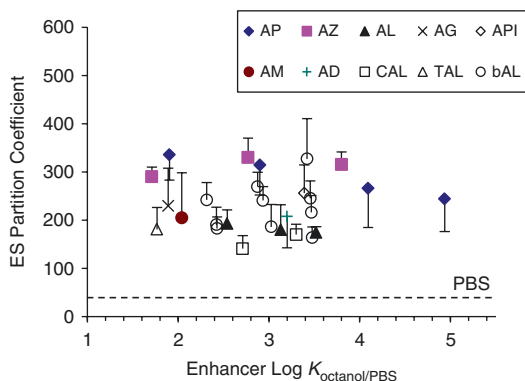


**Fig. 7.11** Relationship between the partition coefficients of ES ( $K_{ES}$ ) for partitioning from the aqueous phase into the SC intercellular lipid domain and the enhancer octanol/PBS partition coefficients ( $K_{octanol/PBS}$ ). The dotted line represents the  $K_{ES}$  value in PBS control. Each data point represents the average and its standard deviation ( $n > 3$ ). The standard deviations of  $\text{Log } K_{octanol/PBS}$  are not shown because the error bars generally lie within the symbols in the plot. Enhancer abbreviations are provided in Fig. 7.1

lipid lamellae is fluidized by the studied enhancers, (b) the uptake domain probed in these partitioning studies is at the same time the transport rate-limiting domain and the enhancer site of action, and (c) the tenfold permeation enhancement corresponds to around a 4- to 7-fold and 1.5- to 2.5-fold enhancement in permeant partitioning and diffusion, respectively, in the transport rate-limiting domain.

### 7.3.7 Transport Rate-Limiting Domain and Equilibrium Partitioning Domain

It would be inappropriate to conclude that the uptake domain probed in the equilibrium partitioning experiments is at the same time the transport rate-limiting domain and the enhancer site of action with only the  $K_{ES}$  data above. Comparison of the partition enhancement in permeant transport across the SC rate-limiting domain and the partition enhancement in the equilibrium partitioning experiments is required. Consistent enhancer effects upon transport and equilibrium partitioning would suggest that the SC intercellular lipid domain probed in the partitioning experiments is

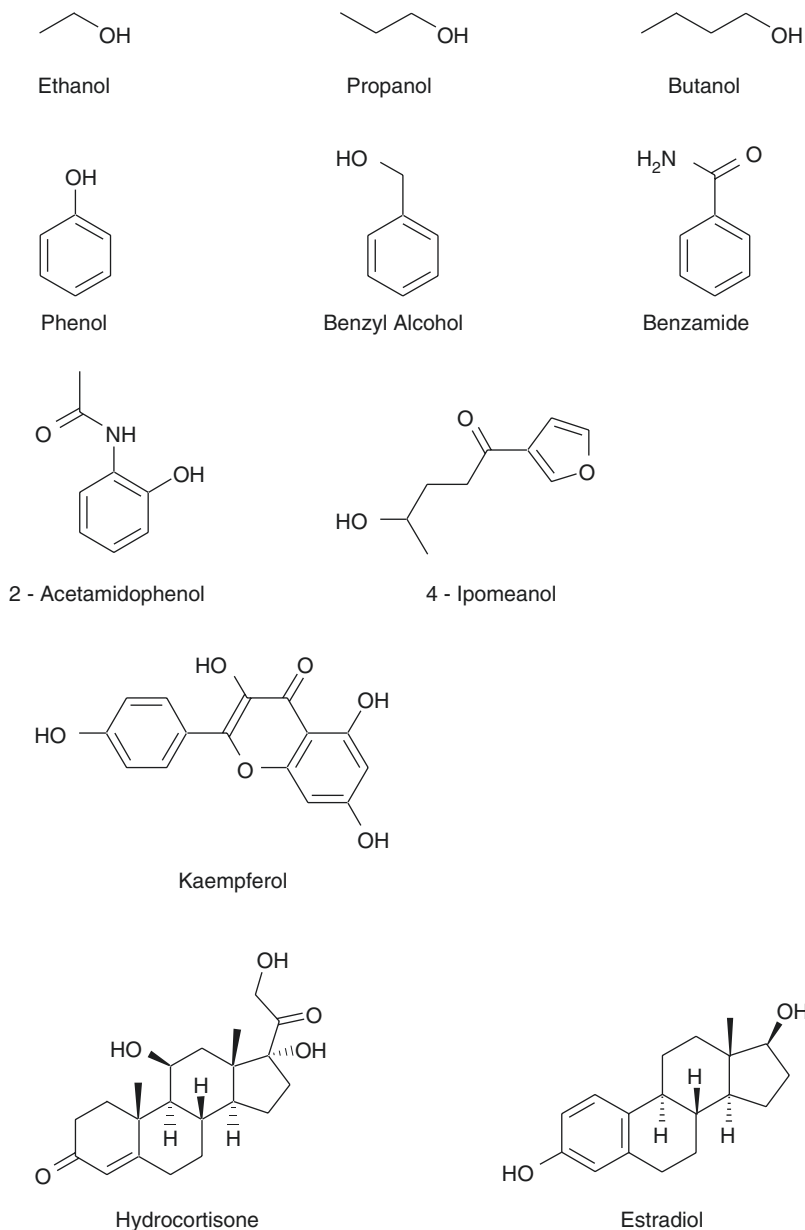
the same as the transport rate-limiting domain for permeation across SC.

As described in the Experimental section, the cumulative amount of CS transported across HMS vs. time profiles in CS transport experiments were analyzed with a transport model to obtain the least squares-fitting  $K_{SC}'$  and  $D_{SC}'$  of CS in PBS, 1-octyl-2-pyrrolidone (OP), and 1-hexyl-2-azacycloheptanone (HAZ) (He et al. 2005). The least squares fittings of the CS transport data were satisfactory, and the results show that the enhancement of permeant partitioning into the transport rate-limiting domain of HMS is significantly higher than the enhancement of permeant diffusion coefficient in the domain. When the total flux enhancement ( $E$ ) was 12 for OP,  $E_{K,SC}$  was  $6.0 \pm 1.9$  and  $E_{D,SC}$  was  $1.8 \pm 0.9$  (mean  $\pm$  SD,  $n \geq 3$ ). For HAZ with  $E$  of 11,  $E_{K,SC}$  was  $7.9 \pm 2.8$  and  $E_{D,SC}$  was  $1.3 \pm 0.6$  (mean  $\pm$  SD,  $n \geq 3$ ). This suggests that the transport enhancement of CS was mainly driven by partition enhancement in the rate-limiting domain of SC. The consistency between the partitioning enhancement of transport found with the SC rate-limiting domain ( $E_{K,SC}$  around 6–8) and the equilibrium partitioning enhancement of ES with the SC intercellular lipids (in the range of 4–7) is quite significant. This finding provides quantitative evidence that the rate-limiting domain for the transport of the model permeants through the SC lipoidal pathway and the intercellular lipid domain probed in the equilibrium partitioning experiments have similar properties regarding the partitioning enhancement effects of chemical permeation enhancers upon the lipophilic model permeants and therefore that these domains are likely to be the same. This result also supports the conclusions on quantitative structure enhancement relationship of enhancers presented in a recent book chapter (Li and Higuchi 2015).

### 7.3.8 Effects of Permeation Enhancement on Permeants of Different Molecular Sizes

Most of the work so far presented in this chapter was based on the data of a single model steroidal permeant CS. Two other steroidal permeants HC

**Fig. 7.12** Chemical structures of the probe permeants



and ES were also employed to examine the generality of the transport enhancement results, and essentially the same permeation enhancement was observed with all three steroidal permeants (e.g., Fig. 7.2). However, the physicochemical properties of a permeant can influence the transport of the permeant across SC. For example, it is general knowledge that there may be a steep-permeant molecular size dependence in permeation across lipid bilayers (e.g., Stein 1986;

Xiang and Anderson 1994), and when enhancers fluidize the SC lipids, the increase in the bilayer free volume can have different consequences on transport enhancement of permeants with different molecular sizes (Mitragotri 2001).

To examine the effects of permeant molecular size upon transport enhancement, transport experiments were conducted using permeants of different molecular sizes and lipophilicities (Fig. 7.12) under the  $E=10$  enhancer conditions

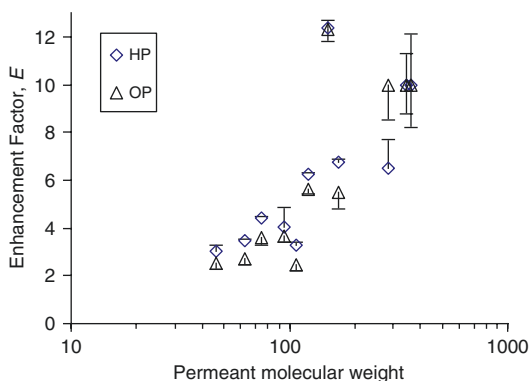


**Fig. 7.13** Relationship between the transport enhancement factors and the molecular weight of the permeants under the  $E=10$  condition for the steroidal permeants with 1-hexyl-2-pyrrolidone (HP) or 1-octyl-2-pyrrolidone (OP) as the enhancers. Each data point represents the average and its standard deviation ( $n>3$ )

for CS (Warner 2003). 1-Hexyl-2-pyrrolidone (HP) and OP were the model permeation enhancers in this study. Figure 7.13 presents the results of the enhancement factors of transport across the SC lipoidal pathway vs. the molecular weight of the permeants under the isoenhancement conditions:  $E=10$  for steroidal permeants. The enhancement factors are calculated using Eqs. (7.4 and 7.6) and with the assumption that the presence of the enhancers did not affect the thermodynamic activities of the permeants in the aqueous solution. As discussed earlier, the enhancement factors for ES, CS, and HC are essentially the same in Fig. 7.13. However, there is a strong permeant molecular weight dependence upon permeation enhancement. This strong molecular weight dependence is consistent with an enhancer-induced increase in the free volume of the SC intercellular lipids, which favors the transport enhancement of permeants of large molecular sizes. The effect of permeant lipophilicity upon permeation enhancement was minimal, and no significant dependency between permeation enhancement and permeant lipophilicity was observed among the studied permeants (provided that the SC lipoidal pathway is the dominant transport pathway for permeation). Given the results in Fig. 7.13, caution needs to be exercised in generalizing the results presented in

this chapter to permeants of different physico-chemical properties. Further investigation on this subject is required.

### 7.3.9 Permeation Enhancers in a Nonaqueous System in Transdermal Drug Delivery

Although the studies presented in this chapter did not include nonaqueous vehicles or conventional cosolvents, the conclusions derived from these experiments are expected not to be limited only to the aqueous system. First, unless the vehicle is able to partition into the SC intercellular lipid “phase” and itself behaves as an enhancer, a nonaqueous system should not affect the intrinsic potency of the enhancer. In this scenario, the nonaqueous vehicle or cosolvent may only alter the thermodynamic activity of the enhancer in the dosage form such as a transdermal patch and alter the partitioning tendency of the enhancer from the patch vehicle into the SC. The concentration of the enhancer at its site of action may therefore be lowered or raised, but this effect can be predicted from thermodynamics. Further discussion can be found in a recent book chapter (Li and Higuchi 2015).

Another important issue is the symmetric situation with the enhancers in equilibrium with skin in our study of permeation enhancers. In transdermal drug delivery, enhancer permeation occurs across the SC from the transdermal patch to the blood sink, this resulting in an asymmetric enhancer situation with an enhancer concentration gradient in the SC. This enhancer concentration gradient is related to the permeability coefficients  $P_{SC}$  and  $P_{D/E}$  of the enhancer. For illustrative purposes, Fig. 7.14 qualitatively shows the SC concentration gradients of two enhancers with different lipophilicities and permeability coefficients across the SC. As can be seen in the figure, the absorption of the more lipophilic enhancer (Enhancer A) is largely dermis-controlled and therefore exhibits a relatively constant concentration across the SC compared with that of the other enhancer (Enhancer B). For Enhancer B, due to its relatively low

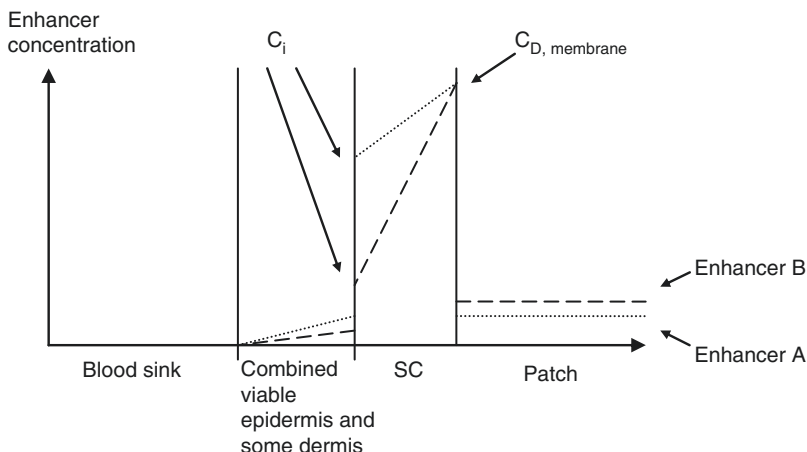


**Fig. 7.14** Enhancer concentration profiles in SC in transdermal drug delivery (see Eq. 7.2): dotted line, Enhancer A; dashed line, Enhancer B.  $P_{D/E}$  for Enhancers A and B are the same,  $\log K_{\text{octanol/PBS}}$  for Enhancer A > Enhancer B, and  $P_{SC}$  for Enhancer A > Enhancer B. This analysis assumes SC is homogenous and does not

account for (a) enhancer-induced variation in local enhancement (permeation and partition enhancement) at different locations within the SC and (b) enhancer-induced enhancement for the enhancer. Such enhancement will affect the enhancer concentration in SC and lead to nonlinear profiles

permeability across the SC, a much more significant concentration drop across the SC is observed. Thus, a large portion of the SC is not affected by Enhancer B and this region of the SC becomes the rate-limiting barrier for drug transport. The relatively constant concentration of Enhancer A in the SC would suggest that lipophilic enhancers are likely to be more effective in providing uniform transport enhancement over the entire SC and a high overall flux enhancement of drug transport across SC. However, simply applying the most lipophilic enhancer does not guarantee success. The solubility of the enhancer and depletion of the enhancer in the transdermal patch are other factors that need to be considered.

The appropriateness of extrapolating the permeation experiment findings under the symmetric and equilibrium enhancer configuration to the asymmetric situation in practice has been examined in a recent study (Chantasart and Li 2010). In this study, the effects of enhancers upon the permeation of CS across HEM under the symmetric and asymmetric configurations were compared. The data show a correlation between transdermal permeation enhancement under the symmetric and asymmetric configurations. This suggests that the mechanisms of the enhancers

for skin permeation under the symmetric and asymmetric configurations are likely to be the same and supports the utility of the findings in the symmetric transport studies for skin permeation under the asymmetric configurations in practice.

### Conclusion

New insights into the factors influencing the effectiveness of chemical permeation enhancers for the lipoidal pathway of the SC have been obtained. The present study supports the view that (a) the potency of an *n*-alkyl enhancer (based on its aqueous concentration) is related to the enhancer lipophilicity, this being the case because of the lipophilic nature of the enhancer site of action, which is well mimicked by liquid *n*-octanol; (b) the intrinsic potency of the enhancer (as represented by its concentration at the target site of action) is relatively independent of its lipophilicity; (c) the substitution of a carbon-carbon single bond on the hydrocarbon chain of the enhancer with a carbon-carbon double bond does not significantly affect its intrinsic potency; and (d) with modest effects, branching of the *n*-alkyl chain of the enhancer generally

reduces the intrinsic potency of the enhancer. To date, we have not encountered any enhancer candidates that are inconsistent with this view in our research. However, skin penetration retarders have been reported (e.g., Hadgraft et al. 1996). This suggests that further studies are needed for greater generalization of the present findings. Nevertheless, the present study has demonstrated useful concepts and effective methodologies for mechanistic studies of chemical permeation enhancers.

**Acknowledgments** The authors thank Drs. Kevin S. Warner, Ning He, Doungdaw Chantasart, and Sarah A. Ibrahim for their contributions in the project and the financial support by NIH Grants GM 043181 and GM 063559.

## References

- Abrams K, Harvell JD, Shriner D, Wertz P, Maibach H, Maibach HI, Rehfeld SJ (1993) Effect of organic solvents on *in vitro* human skin water barrier function. *J Invest Dermatol* 101:609–613
- Aungst BJ (1989) Structure/effect studies of fatty acid isomers as skin penetration enhancers and skin irritants. *Pharm Res* 6:244–247
- Brain KR, Walters KA (1993) Molecular modeling of skin permeation enhancement by chemical agents. In: Walters KA, Hadgraft J (eds) *Pharmaceutical skin penetration enhancement*. Marcel Dekker, New York, pp 389–416
- Chantasart D, Li SK (2010) Relationship between the enhancement effects of chemical permeation enhancers on the lipoidal transport pathway across human skin under the symmetric and asymmetric conditions *in vitro*. *Pharm Res* 27:1825–1836
- Chantasart D, Li SK (2012) Structure enhancement relationship of chemical penetration enhancers in drug transport across the stratum corneum. *Pharmaceutics* 4:71–92
- Chantasart D, Li SK, He N, Warner KS, Prakongpan S, Higuchi WI (2004) Mechanistic studies of branched-chain alkanols as skin permeation enhancers. *J Pharm Sci* 93:762–779
- Chantasart D, Sa-Nguandeeekul P, Prakongpan S, Li SK, Higuchi WI (2007) Comparison of the effects of chemical permeation enhancers on the lipoidal pathways of human epidermal membrane and hairless mouse skin and the mechanism of enhancer action. *J Pharm Sci* 96:2310–2326
- Golden GM, McKie JE, Potts RO (1987) Role of stratum corneum lipid fluidity in transdermal drug flux. *J Pharm Sci* 76:25–28
- Grubauer G, Feingold KR, Harris RM, Elias PM (1989) Lipid content and lipid type as determinants of the epidermal permeability barrier. *J Lipid Res* 30:89–96
- Hadgraft J (2001) Modulation of the barrier function of the skin. *Skin Pharmacol Appl Skin Physiol* 14(Suppl 1): 72–81
- Hadgraft J, Peck J, Williams DG, Pugh J, Allan G (1996) Mechanisms of action of skin penetration enhancers/retarders: azone and analogues. *Int J Pharm* 141:17–25
- He N, Li SK, Suhonen TM, Warner KS, Higuchi WI (2003) Mechanistic study of alkyl azacycloheptanones as skin permeation enhancers by permeation and partition experiments with hairless mouse skin. *J Pharm Sci* 92:297–310
- He N, Warner KS, Chantasart D, Shaker DS, Higuchi WI, Li SK (2004) Mechanistic study of chemical skin permeation enhancers with different polar and lipophilic functional groups. *J Pharm Sci* 93:1415–1430
- He N, Warner KS, Higuchi WI, Li SK (2005) Model analysis of flux enhancement across hairless mouse skin induced by chemical permeation enhancers. *Int J Pharm* 297:9–21
- Ibrahim SA, Li SK (2009a) Effects of chemical enhancers on human epidermal membrane: structure-enhancement relationship based on maximum enhancement ( $E_{max}$ ). *J Pharm Sci* 98:926–944
- Ibrahim SA, Li SK (2009b) Effects of solvent deposited enhancers on transdermal permeation and their relationship with  $E_{max}$ . *J Control Release* 136:117–124
- Kim YH, Ghanem AH, Higuchi WI (1992) Model studies of epidermal permeability. *Semin Dermatol* 11: 145–156
- Kligman AM, Christophers E (1963) Preparation of isolated sheets of human stratum corneum. *Arch Dermatol* 88:702–705
- Lambert WJ, Higuchi WI, Knutson K, Krill SL (1989) Effects of long-term hydration leading to the development of polar channels in hairless mouse stratum corneum. *J Pharm Sci* 78:925–928
- Lampe MA, Williams ML, Elias PM (1983) Human epidermal lipids: characterization and modulations during differentiation. *J Lipid Res* 24:131–140
- Lee VHL, Yamamoto A, Kompella UB (1991) Mucosal penetration enhancers for facilitation of peptide and protein drug absorption. *Crit Rev Ther Drug Carrier Syst* 8:91–192
- Li SK, Higuchi WI (2015) Quantitative structure-enhancement relationship and the microenvironment of the enhancer site of action. In: Dragicevic N, Maibach HI (eds) *Percutaneous penetration enhancers, chemical methods in penetration enhancement: modification of the stratum corneum*. Springer, New York, Ch. 5
- Li SK, Ghanem A-H, Yoneto K, Higuchi WI (1997) Effects of 1-alkyl-2-pyrrolidones on the lipoidal pathway of human epidermal membrane: a comparison with hairless mouse skin. *Pharm Res* 14:S-303
- Liu P, Higuchi WI, Song WQ, Kurihara-Bergstrom T, Good WR (1991) Quantitative evaluation of ethanol effects on diffusion and metabolism of beta-estradiol in hairless mouse skin. *Pharm Res* 8:865–872



- Liu P, Higuchi WI, Ghanem A-H, Kurihara-Bergstrom T, Good WR (1992) Assessing the influence of ethanol in simultaneous diffusion and metabolism of estradiol in hairless mouse skin for the 'asymmetric' situation *in vitro*. *Int J Pharm* 78:123–136
- Mitragotri S (2001) Effect of bilayer disruption on transdermal transport of low-molecular weight hydrophobic solutes. *Pharm Res* 18:1018–1023
- Nicolaides N (1974) Skin lipids: their biochemical uniqueness. *Science* 186:19–26
- Okamoto H, Hashida M, Sezaki H (1988) Structure-activity relationship of 1-alkyl or 1-alkenylazacycloalkanone derivatives as percutaneous penetration enhancers. *J Pharm Sci* 77:418–424
- Shaker DS, Ghanem AH, Li SK, Warner KS, Hashem FM, Higuchi WI (2003) Mechanistic studies of the effect of hydroxypropyl-beta-cyclodextrin on *in vitro* transdermal permeation of corticosterone through hairless mouse skin. *Int J Pharm* 253:1–11
- Smith EW, Maibach HI (1995) Percutaneous penetration enhancers. CRC Press, Inc., Boca Raton
- Stein W (1986) Transport and diffusion across cell membranes. Academic, New York
- Tanford C (1980) The hydrophobic effect: formation of micelles and biological membranes, 2nd edn. Wiley, New York
- Tenjarla SN, Kasina R, Puranajoti P, Omar MS, Harris WT (1999) Synthesis and evaluation of N-acetylproline esters – novel skin penetration enhancers. *Int J Pharm* 192:147–158
- Warner KS (2003) Mechanistic aspects of chemical skin permeation enhancers. PhD Thesis, University of Utah
- Warner KS, Li SK, Higuchi WI (2001) Influences of alkyl group chain length and polar head group on chemical skin permeation enhancement. *J Pharm Sci* 90:1143–1153
- Warner KS, Li SK, He N, Suhonen TM, Chantasart D, Bolikal D, Higuchi WI (2003) Structure-activity relationship for chemical skin permeation enhancers: probing the chemical microenvironment of the site of action. *J Pharm Sci* 92:1305–1322
- Warner KS, Shaker DS, Molokhia S, Xu Q, Hao J, Higuchi WI, Li SK (2008) Silicone elastomer uptake method for determination of free 1-alkyl-2-pyrrolidone concentration in micelle and hydroxypropyl- $\beta$ -cyclodextrin systems used in skin transport studies. *J Pharm Sci* 97:368–380
- Xiang TX, Anderson BD (1994) The relationship between permeant size and permeability in lipid bilayer membranes. *J Membr Biol* 140:111–122
- Yoneto K, Ghanem AH, Higuchi WI, Peck KD, Li SK (1995) Mechanistic studies of the 1-alkyl-2-pyrrolidones as skin permeation enhancers. *J Pharm Sci* 84:312–317
- Yoneto K, Li SK, Higuchi WI, Shimabayashi S (1998) Influence of the permeation enhancers 1-alkyl-2-pyrrolidones on permeant partitioning into the stratum corneum. *J Pharm Sci* 87:209–214

# High Throughput Screening of Transdermal Penetration Enhancers: Opportunities, Methods, and Applications

8

Amit Jain, Pankaj Karande, and Samir Mitragotri

## Contents

8.1	<b>Introduction</b> .....	137
8.2	<b>Overview of INSIGHT Screening</b> .....	140
8.2.1	Skin Impedance–Skin Permeability Correlation.....	141
8.3	<b>Validation of INSIGHT with FDC</b> .....	144
8.4	<b>Applications of INSIGHT Screening</b> .....	145
8.4.1	Discovery of Rare Formulations .....	145
8.4.2	Generation of Database for Quantitative Understanding .....	146
	<b>References</b> .....	147

## 8.1 Introduction

The idea of delivering drugs through the skin is as old as human civilization, but the excitement has increased in recent times after the introduction of the first transdermal patch in the 1970s. Though transdermal route of drug administration offers several advantages such as reduced first-pass drug metabolism, no gastrointestinal degradation, long-term delivery (>24 h), and control over delivery and termination, only few drug molecules have been formulated into transdermal patches (Barry 2001). The cause of this imbalance between the benefits of this route and the number of products in the market lies in the skin itself. Skin's topmost layer, stratum corneum (SC), forms a barrier against permeation of xenobiotics into the body and water evaporation out of the body. This barrier must be altered to maximize the advantages of transdermal route of drug administration. This has engaged pharmaceutical scientists, dermatologists, and engineers alike in research over the last couple of decades (Mitragotri 2004). High research activity in this field has led to the introduction of a variety of techniques including formulation-based approaches (Williams and Barry 2004), iontophoresis (Kalia et al. 2004), electroporation (Prausnitz 1999; Weaver et al. 1999), acoustical methods (Mitragotri and Kost 2004), microneedles (Prausnitz 2004), jet injection (Hingson and Figge 1952), and thermal poration (Sintov et al. 2003).

---

A. Jain (✉) • S. Mitragotri  
Corium International Inc., Menlo Park, CA, USA  
e-mail: [ajain13@gmail.com](mailto:ajain13@gmail.com)

P. Karande  
Howard Isermann Department of Chemical  
and Biological Engineering, Rensselaer Polytechnic  
Institute, Troy, NY, USA

Center for Biotechnology and Interdisciplinary  
Sciences, Rensselaer Polytechnic Institute,  
Troy, NY, USA

All of the above techniques have their own benefits and specific applications. Formulation-based approaches have a number of unique advantages such as design simplicity and flexibility, and ease of application over a large area (Prausnitz et al. 2004). The last 20 years have seen extensive research in the field of chemical enhancers, which form the core component of formulation-based strategies for transdermal drug delivery. More than 200 chemicals have been shown to enhance skin permeability to various drugs. These include molecules from a diverse group of chemicals including fatty acids (Golden et al. 1987; Aungst et al. 1990; Jain and Panchagnula 2003), fatty esters (Chukwumerije et al. 1989), nonionic surfactants (Lopez et al. 2000), anionic surfactants (Nokhodchi et al. 2003), and terpenes (Williams and Barry 1991; Jain et al. 2002). However, identification of potent yet safe permeation enhancers has proved challenging. To date, only few chemicals are to be found in currently marketed transdermal products. These include oleic acid, sorbitan monooleate, and methyl laurate among others.

Even though individual chemical penetration enhancers (CPEs) have found limited applications, combinations of CPEs represent a huge opportunity that has been sparsely tapped. Several reports have indicated that combinations of CPEs offer better enhancements of transdermal drug transport compared to their individual constituents (Mitragotri 2000; Thomas and Panchagnula 2003). However, such combinations do not necessarily yield safer enhancers. It should be feasible, in principle, to use CPEs as building blocks to construct new microstructures and novel formulations that offer enhancement without irritation. However, the challenge now shifts to screening the potency of enhancer combinations. Random mixtures of CPEs are likely to exhibit additive properties, that is, their potency and irritancy are likely to be averages of corresponding properties of their individual constituents. Occurrence of truly synergistic combinations is likely to be rare. In the absence of capabilities to predict the occurrence of such rare mixtures,

one has to rely on a brute force screening approach. Starting with a pool of >200 individual CPEs, millions of binary and billions of higher order formulations can be designed. Screening of these mixtures is a mammoth task.

Screening of chemical enhancers can be performed *in vitro* as well as *in vivo*. *In vivo* experiments are likely to yield better results; however, several issues including variability, cost, and practicality limit their applications for screening a large database of enhancers. Accordingly, *in vitro* screening based on excised tissue (human or animal) presents a more practical alternative (Priborsky and Muhlbachova 1990). A number of models exist to predict *in vivo* pharmacokinetics based on *in vitro* data (Naito and Tsai 1981; Guy et al. 1982; Ogiso et al. 1989; Takayama and Nagai 1991; Wu et al. 2000). The use of *in vitro* models for screening is also supported by the fact that SC, the principle site of enhancer action, shows similar behavior *in vivo* and *in vitro* except for the extent of metabolic activity (Chang et al. 1998). Majority of *in vitro* studies on transdermal drug transport have been performed using Franz diffusion cells (FDCs). The throughput of this traditional setup of diffusion chamber is very low, not more than 10–15 experiments at a time. These permeation studies are time consuming and are resource expensive as analytical methods such as high-pressure liquid chromatography (HPLC) or radiolabeled drugs for liquid scintillation counting are expensive. Automated in-line flow through diffusion cells has been developed in the last few years to increase the throughput of skin permeation experiments (Bosman et al. 1996; Cordoba-Diaz et al. 2000). Although these methods have facilitated the experiments, the throughput of these methods has not been significantly improved. Furthermore, these methods are also cost prohibitive. Accordingly, standard FDCs still dominate the screening of CPEs.

The urgent need to increase experimental throughput has led to the development of high throughput screening methods. Though in early stages, these methods have already shown promise in discovering novel formulations for transdermal drug delivery. A high throughput assay to

be used for screening of transdermal formulations should meet the following requirements:

(i) *Ability to screen a large number of formulations*

Increasing the throughput by at least 2–3 orders of magnitude would result in significant reduction in the effort and time spent in the very first stage of formulation development (Karande and Mitragotri 2002).

(ii) *Use of a surrogate end point that is quick, easy and independent of the physicochemical properties of the model permeant*

Permeation experiments using radiolabeled (Rosado et al. 2003), fluorescent (Ogiso et al. 1996), HPLC-detectable (Wu et al. 2000), or RIA/ELISA-detectable (Xing et al. 1998; Magnusson and Runn 1999) markers necessitate the need of extensive sample handling and sample analysis. This accentuates the cost of sample analysis and overall time spent in characterizing the efficacy of formulations. Furthermore, current state-of-the-art fluidics systems put a fundamental limit on the number of samples handled in a given time. Permeation of a model solute across the skin in the presence of an enhancer is dependent not only on the inherent capacity of the enhancer to permeabilize skin but also on the physicochemical interactions of the enhancer with the model solute (Lee and Kim 1987; Takács-Novak and Szász 1999; Auner et al. 2003a, b). An end point, to characterize the effect of an enhancer on skin permeability, should be able to decouple these two effects to assure the generality of the results.

(iii) *Low incubation times to further increase the throughput and hence time efficiency*

FDC experiments typically use incubation times of 48–96 h thereby reducing the throughput of permeation experiments. Low incubation times favor high turnover frequencies for assay utilization.

(iv) *Minimal use of test chemicals and efficient utilization of model membrane such as animal skin*

FDCs typically require application of 1–2 ml of enhancer formulations over about 3–4 cm<sup>2</sup> of skin per experiment. This makes it cost prohibitive to include candidates that are expensive in the test libraries as well as to screen a large number of formulations.

(v) *Adaptability to automation to reduce human interference*

Typical FDC setup requires manual sampling with little opportunities for process automation (Cordoba-Diaz et al. 2000).

In addition to these requirements of the assay tool, the high throughput screening methodology should also satisfy, if possible, the following experimental constraints:

(vi) *Use of a common model membrane to represent human skin*

It is common to find in transdermal literature the use of a variety of different models to represent human skin such as rat skin (Schmook et al. 2001), pig skin (Sekkat et al. 2002), snake skin (Itoh et al. 1990), excised human skin, etc. While human skin is difficult to procure on a large scale, animal models show deviations in permeability characteristics from human skin (Panchagnula et al. 1997; Schmook et al. 2001; Auner et al. 2003a, b). Also, results on one model cannot be directly translated to a different model.

(vii) *Use of consistent thermodynamic conditions for enhancer formulations*

Permeation enhancement efficacy of a CPE is a function of its chemical potential (Francoeur et al. 1990; Shokri et al. 2001), temperature (Ongpipattanukul et al. 1991; Narishetty and Panchagnula 2004), and cosolvent (Yamane et al. 1995; Larrucea et al. 2001) among other thermodynamic parameters. These thermodynamic conditions need to be standardized for all the enhancers that are being tested to create direct comparison of their efficacies in increasing skin permeation.

This chapter focuses on a specific high throughput screening method called INSIGHT, *In vitro* Skin Impedance Guided High

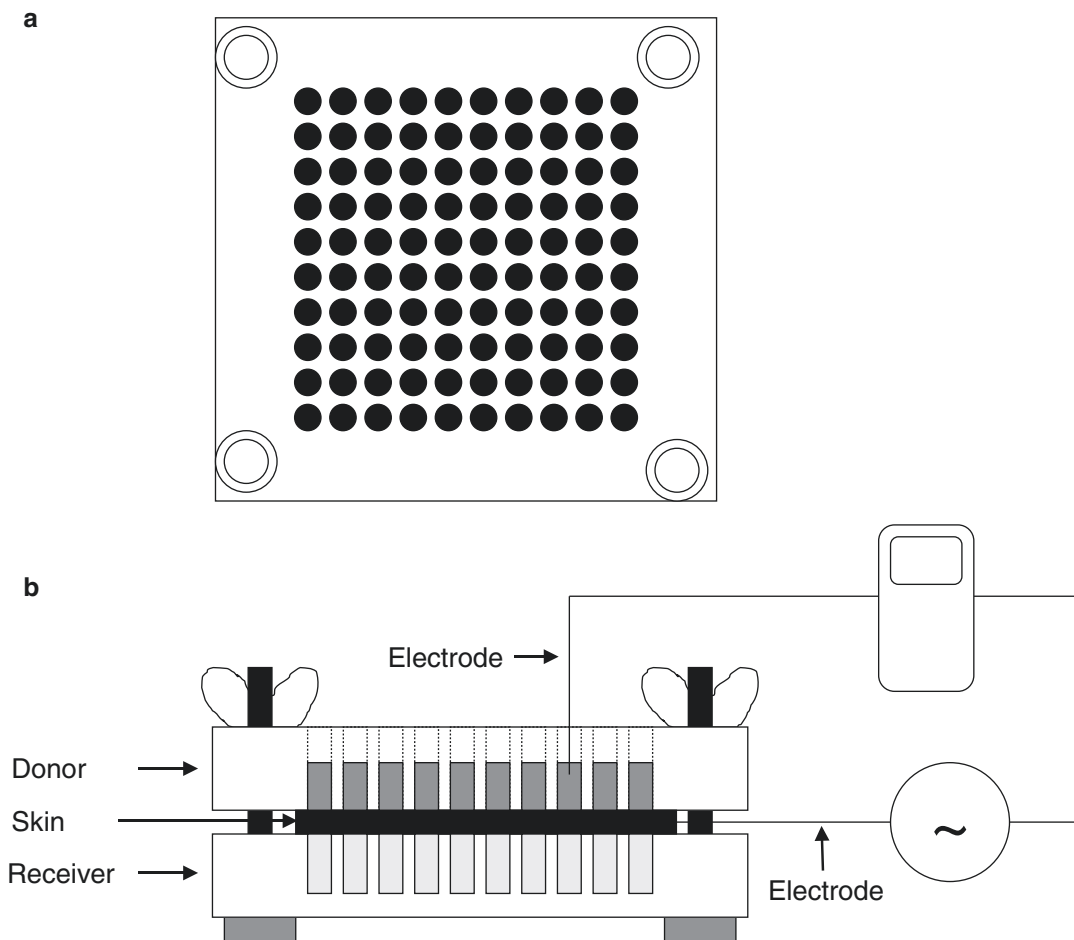


**Fig. 8.1** Schematic of the INSIGHT screening apparatus. The INSIGHT screen is made up of a donor array (*top*) and a symmetric receiver array (*bottom*). A single screen can screen 100 formulations at one time. The skin is sandwiched between the donor (Teflon) and receiver (Polycarbonate)

and the formulations contact the stratum corneum from the donor array. Conductivity measurements are made with one electrode inserted in the dermis and a second electrode moved sequentially in the donor wells. (a) and (b) is top and side view of the INSIGHT apparatus, respectively

Throughput screening that was recently introduced (Karande et al. 2004). This method is described in detail with respect to its fundamentals, validation, and outcomes.

## 8.2 Overview of INSIGHT Screening

INSIGHT screening offers >100-fold improvement in screening rates of transdermal formulations (Karande et al. 2004). This improvement in

efficiency comes from two factors. First, the INSIGHT, in its current version, can perform up to 50 tests per square inch of skin compared to about >2 cm<sup>2</sup> of skin per test in the case of Franz diffusion cells (Fig. 8.1). About 100 formulations can be screened per INSIGHT array. Second, INSIGHT screening uses skin impedance as a surrogate marker for skin permeability.

Skin impedance has been previously used: (i) to assess the skin integrity for in vitro dermal testing (Lawrence 1997; Fasano et al. 2002; Davies et al. 2004), (ii) to evaluate the irritation potential

of chemicals in a test known as skin integrity function test (SIFT) (Heylings et al. 2001), and (iii) to monitor skin barrier recovery *in vivo* following the application of current during iontophoresis (Turner et al. 1997; Curdy et al. 2002). Since it is evident from the literature that skin impedance can be used to confirm skin integrity, it is logical to hypothesize that alteration in skin barrier due to chemical enhancers can be used as an *in vitro* surrogate marker for permeability. Scattered literature data support this hypothesis. A study by Yamamoto and Yamamoto (1976a, b) showed that total skin impedance reduces gradually with tape stripping and after 15 stripping skin impedance approaches the impedance value of deep tissues (Yamamoto and Yamamoto 1976a, b). However, quantitative relationships between skin impedance and permeability in the presence of chemical enhancers and their validity for a wide range of markers have not been previously documented.

### 8.2.1 Skin Impedance–Skin Permeability Correlation

Stratum corneum is a composite of proteins and lipids in which protein-rich corneocytes are surrounded by lipid bilayers (Madison et al. 1987). Approximately 70–100 bilayers are stacked between two corneocytes (Elias et al. 1977; Elias 1983). Because of its architecture the SC is relatively nonconductive and possesses high electrical impedance (Lackermeier et al. 1999). Skin impedance (AC) can be measured either by applying a constant current and measuring the potential across the skin or by measuring transepidermal current following the application of a constant AC potential. Data reported in this chapter are based on measurement of transepidermal current following the application of a constant potential (100 mV rms). Frequency of the applied potential is also an important parameter. Due to the capacitive components of the skin, the measured electrical impedance of the skin decreases with increasing frequency (Yamamoto and Yamamoto 1976a, b). While the use of higher frequencies facilitates measurements due to decreased impedance, the correlation between

electrical impedance and solute permeability is stronger at lower frequencies. Thus, an optimal frequency must be chosen. All experiments reported in chapter were performed at a frequency of 100 Hz.

INSIGHT screening is founded on the relationship between skin's electrical impedance (reciprocal of skin conductance) and solute permeability. There is a dearth of literature on skin impedance (conductivity) and permeability relationship, and moreover in most of the studies this relationship was used to elucidate the mechanism of transport of hydrophilic molecules across the skin under the influence of temperature (Peck et al. 1995), hydration (Tang et al. 2002), electric current (Sims et al. 1991; Li et al. 1998), or ultrasonic waves (Tang et al. 2001; Tezel et al. 2003). Therefore existing data cannot be used to generalize the relationship between skin impedance and permeability. Accordingly, a large dataset was first generated to assess the correlation between skin impedance and permeability to small (mannitol) and macromolecule (inulin) hydrophilic solutes in the presence of different chemical enhancer formulations. A set of 22 enhancer formulations, chosen from the candidate pool was used to validate the relationship between skin conductivity and skin permeability. The candidate pool comprised of 15 single enhancer formulations and seven binary enhancer formulations. In order to establish the correlation between skin impedance and permeability for wide range of chemical enhancers, formulations were made from different classes of chemicals including cationic surfactants (CTAB, cetyl trimethyl ammonium bromide; BDAC, benzyl dodecyl ammonium chloride), anionic surfactants (NLS, N-laurylsarcosine sodium; SLA, sodium laureth sulfate; SLS, sodium lauryl sulfate), zwitterionic surfactants (HPS, N-hexadecyl-N,N-dimethyl-3-ammonio-1-propanesulfonate), nonionic surfactants (PEGE, polyethylene dodecyl glycol ether; S20, sorbitan monolaurate; T20, polyoxyethylene sorbitan monolaurate), fatty acids and their sodium salts (LA, lauric acid; OL, oleic acid; SOS, sodium octyl sulfate; SO, sodium oleate), fatty acid esters (TET, tetra-caine HCl; IPM, isopropyl myristate), and others

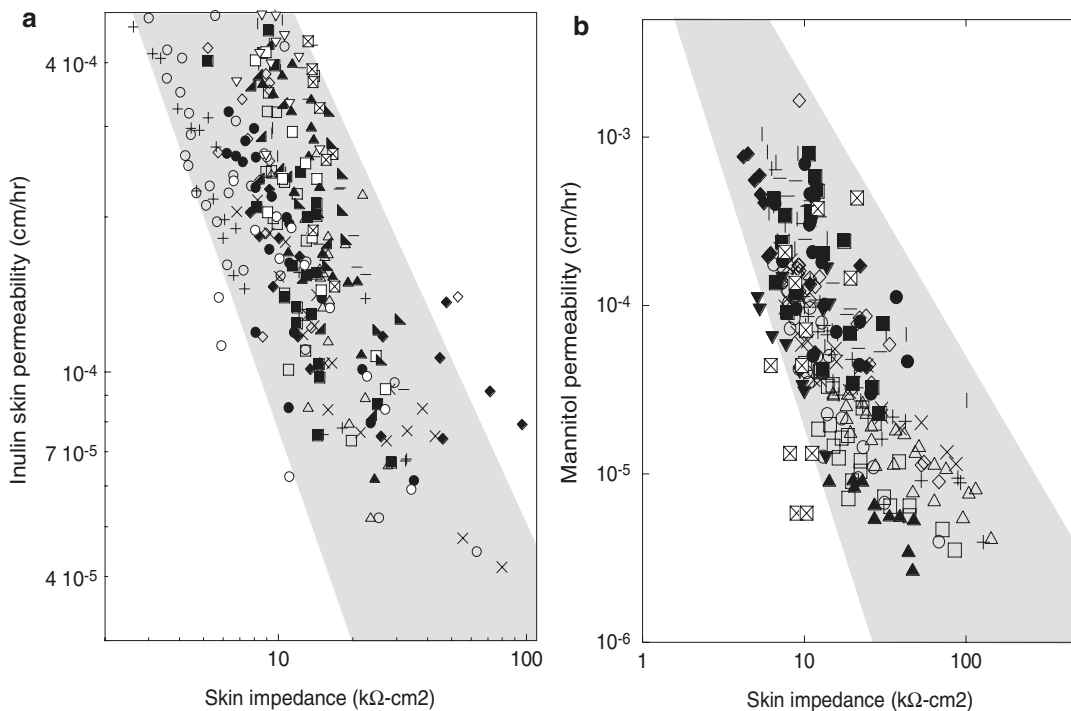


**Fig. 8.2** Skin impedance–permeability correlation for (a) inulin and (b) mannitol. Test formulations used in this study (in parenthesis total concentration of chemical enhancer w/v, weight fraction used): (a) ●-MEN (1.5%w/v); ■-SO (1.5%w/v); ▲-PEGE (1.5%w/v); △-OL (1.5%w/v); ■-S20 (1.0%w/v); ○-DMP (1.5%w/v); ▽-OL: MEN (1.5%w/v, 0.4:0.6); ◇-IPM (1.5%w/v); ×-TET (2.0%w/v); + -LA (1.5%w/v); ◆-NLS (1.0%w/v); ○-SOS (2.0%w/v); ⊠-NLS:S20 (1.0%w/v, 0.6:0.4); ⊡-TET:SLS (1.0%w/v, 0.6:0.4);

▲-TET:HPS (2.0%w/v, 0.1:0.9); ▲-MEN:T20 (2.0%w/v, 0.5:0.5); \* -DMP:TET (2.0%w/v, 0.4:0.6); γ-CTAB (1.0%w/v). (b) γ-OL (1.5%w/v); ▲-DMP (2.0%w/v); ▼-DMP:TET (2.0%w/v, 0.4:0.6); △-PEGE (1.5%w/v); ⊠-TET (2.0%w/v); ×-LA (1.5%w/v); + -S20 (1.0%w/v); ■-HPS (1.5%w/v); ○-NLS (1.0%w/v); □-BDAC (1.5%w/v); ◇-MEN (1.5%w/v); ◆-DMP:HPS (1.5%w/v, 0.6:0.4); ⊠-NLS:S20 (1.0%w/v, 0.6:0.4); ●-DMP (1.5%w/v)

(DMP, N-dodecyl 2-pyrrolidone; MEN, menthol). Skin impedance and permeability to two model solutes, mannitol and inulin, were measured. Inulin (MW 5 kDa) was selected as a model solute as it satisfactorily represents a macromolecular hydrophilic drug. Mannitol (MW 182.2 Da,  $\log K_{o/w} -3.1$ ) was used as a representative of small hydrophilic drugs.

A strong correlation was observed between skin impedance and permeability of mannitol and inulin for different enhancer formulations (Figs. 8.2, 8.3, and 8.4). The measurements reported in Fig. 8.2a, b were performed in FDCs. There is a reasonable scatter in these data, which is inherent to biological systems such as skin that exhibits high variability. Also, measurements

reported in Fig. 8.2a, b represent an aggregate of experiments performed over several different animals and anatomical regions. The correlation between skin permeability and impedance was improved when data for individual enhancers were plotted separately; example for inulin (with DMP enhancer  $r^2=0.85$ ) and mannitol (with OL enhancer  $r^2=0.86$ ) is given in (Fig. 8.3a, b). The correlation between skin permeability and impedance can be clearly seen in Fig. 8.4a, b where data in Fig. 8.2a, b are replotted after averaging over  $\sim 5$  kΩ-cm<sup>2</sup> intervals (inulin  $r^2=0.86$  and for mannitol  $r^2=0.90$ ). Permeability data of mannitol and inulin with a variety of chemical enhancer formulations showed that skin impedance is inversely related to permeability of hydrophilic

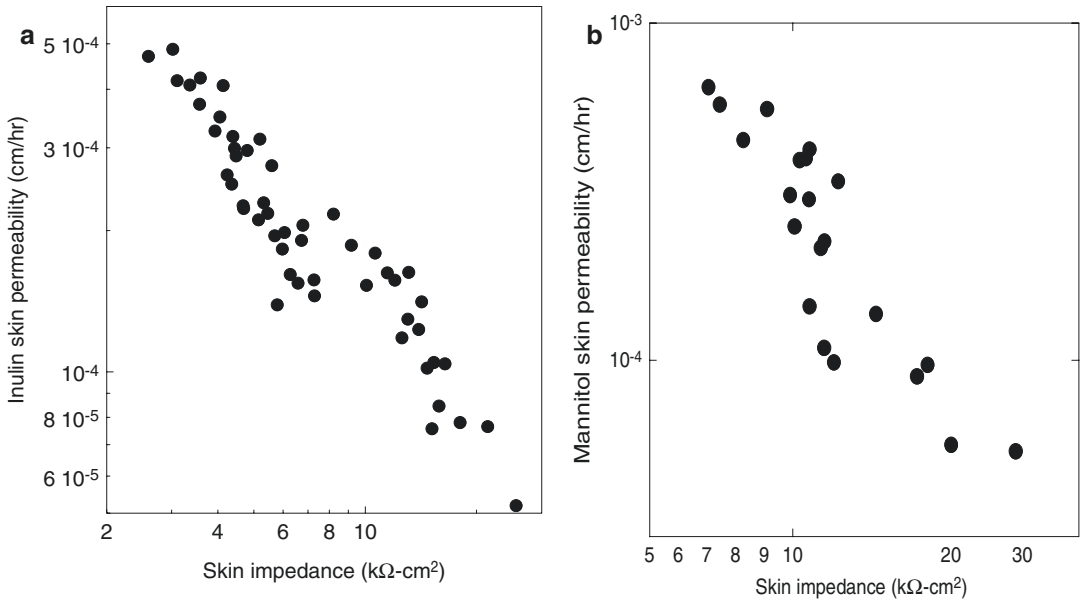


**Fig. 8.3** Skin impedance-permeability correlation for single enhancer. (a) Plot of skin permeability to inulin vs. skin impedance in the presence of DMP (1.5%w/v in 1:1 EtOH:PBS); (b) Plot of skin permeability to mannitol vs. skin impedance in the presence of NLS (1.5%w/v in 1:1 EtOH:PBS). A much tighter correlation can be observed compared to Fig. 8.2

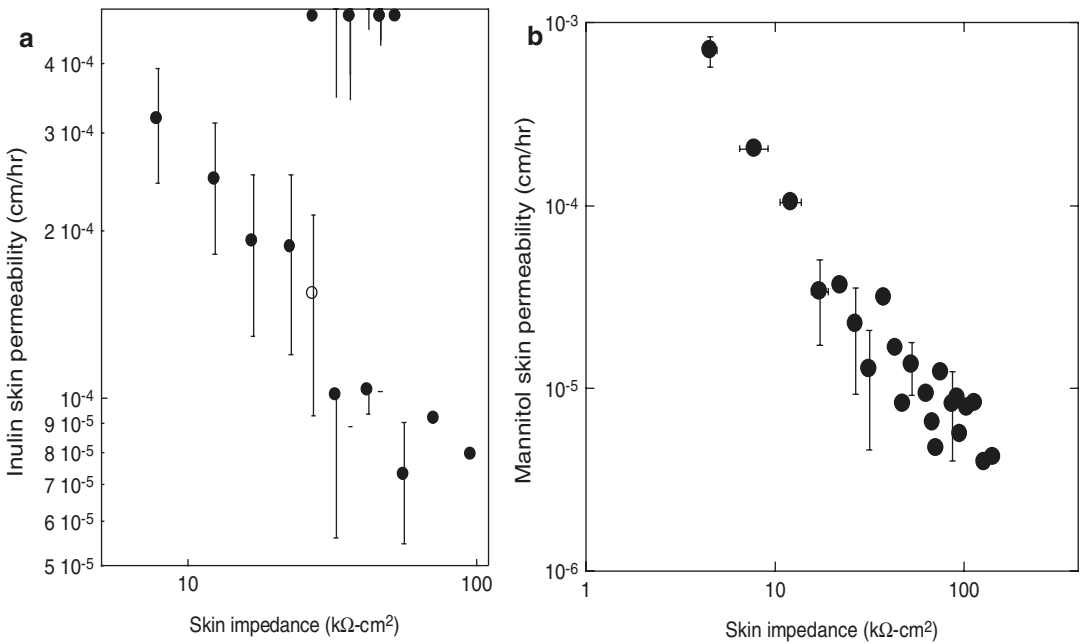


**Fig. 8.4** Skin impedance – permeability correlation for different enhancers are grouped in the bins of  $5 \text{ k}\Omega\text{-cm}^2$  along the x-axis representing skin impedance. The correlation is much tighter as compared to the one in Fig. 8.2



solutes, which is in agreement with existing data in literature. Correlation coefficient (inulin  $r^2=0.86$  and mannitol  $r^2=0.90$ ) of average data for all enhancer formulations indicates that a remarkable correlation exists between skin permeability and impedance for single and binary enhancers formulations irrespective of the nature of the formulation. These results indicate that skin impedance can be used as a parameter to measure the extent of barrier alteration by chemicals irrespective of their mode of action (which, in most cases, is not precisely known). Specifically, good correlations were observed between permeability and skin impedance for enhancers, which act by lipid extraction (NLS, MEN, BDAC) or by lipid bilayer fluidization (OL, LA, IPM). Note, however, that the nature of these correlations is an integral function of the physicochemical properties of the drug or permeant. Educated discretion must therefore be exercised when selecting a delivery formulation for a particular model permeant or drug of interest.

### 8.3 Validation of INSIGHT with FDC

Conductivity enhancement ratio (ER), that is, the ratio of skin impedances at time zero and 24 h following the application of enhancer formulation, measurements in INSIGHT were plotted against conductivity enhancement and permeability enhancements in FDCs (Fig. 8.5a). Inulin was used as a model permeant in these studies. Results shown in Fig. 8.5a reflect that the predictions obtained from INSIGHT on the potency of enhancer formulations are essentially the same as those obtained from FDCs. However, INSIGHT allows collection of information at a much greater speed ( $\sim 1000$  per day) and less skin utilization (about  $0.07 \text{ cm}^2$  per experiment as compared to  $2 \text{ cm}^2$  in a 16 mm diameter FDC,  $>25$ -fold reduction in skin utilization).

Further improvements in INSIGHT screening speed can be obtained by reducing the formulation incubation period. Capabilities of INSIGHT in assessing formulation potency after a 4-h

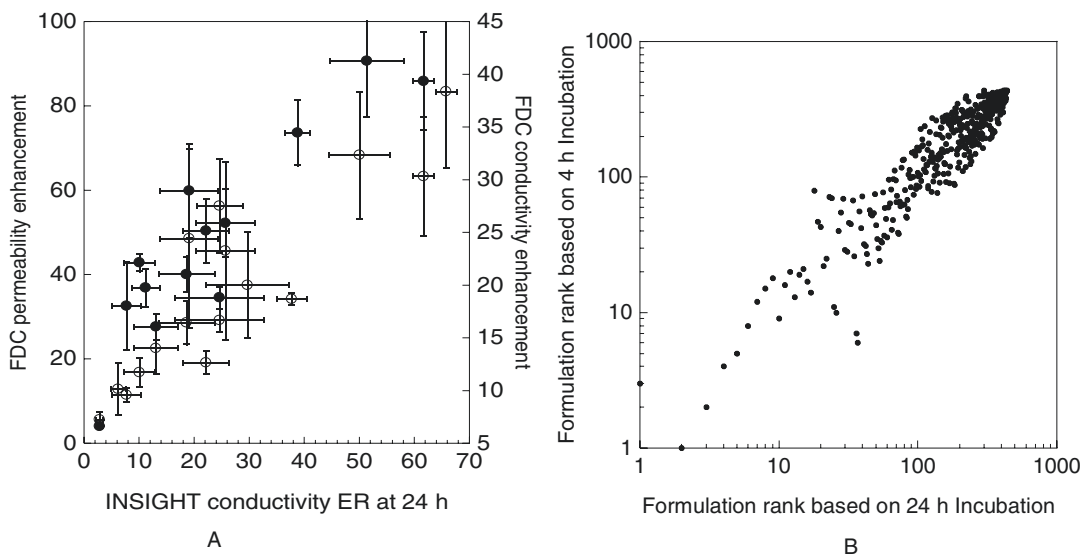


**Fig. 8.5** Validation of INSIGHT predictions with FDC. Plot of conductivity enhancement ratios in INSIGHT at 24 h vs. conductivity and permeability enhancement ratios in FDC at 96 h for 19 enhancer formulations. A strong linear correlation indicates the validity of observations in INSIGHT when compared with those from traditional tools like FDC. The closed circles indi-

cate conductivity enhancement numbers, and the filled circles indicate permeability enhancement numbers in FDC. (a) Plot of 24 h predictions in INSIGHT vs. 4 h predictions in INSIGHT on the potency of enhancer formulations. A strong correlation indicates that predictions on potency of formulations can be obtained at significantly lower incubation periods of 4 h

incubation are demonstrated in Fig. 8.5b where potency rankings of 438 single and binary formulations randomly prepared from the enhancer library based on 4-h screening are compared to those based on 24-h screening. Rank 1 corresponds to most potent formulation in the library and rank 438 to the weakest formulation. The predictions of the potency made in 4 h were consistent with those made after a contact time of 24 h, thus indicating that the efficiency of INSIGHT screening can be further improved.

## 8.4 Applications of INSIGHT Screening

### 8.4.1 Discovery of Rare Formulations

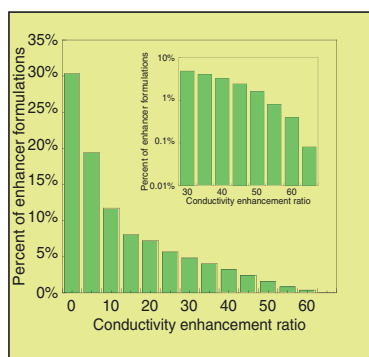
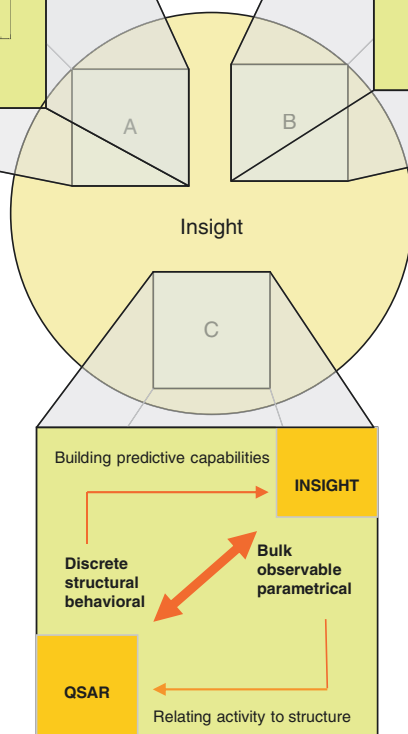
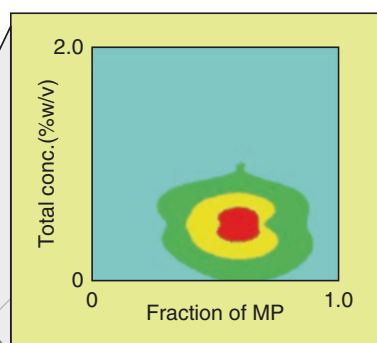
INSIGHT screening can be used to screen huge libraries of chemicals within a short span of time and without the fear of failure that exists with traditional tools. Many current single enhancers are also potent irritants to the skin at concentrations necessary to induce meaningful penetration enhancement. Attempts have been made to synthesize novel chemical enhancers such as laurocapram (Azone); however, achieving sufficient potency without irritancy has proved challenging, especially for macromolecules. A number of studies have shown that formulations made up of combination of chemical enhancers are more potent than its individual components (Karande et al. 2004; Tezel et al. 2002; Mitragotri 2000). The addition of components increases the number of formulations exponentially. However, the use of INSIGHT screening allows one to tackle this challenge in a more cost-effective way compared to FDCs. In addition, synergies between CPEs not only lead to new transdermal formulations but also potentially offer insight into mechanisms by which CPEs enhance skin permeability. Prediction of synergies from the first principles is challenging. INSIGHT screening offers an effective tool for identifying synergies (positive or negative) between the CPEs.

To identify synergistic combinations of penetration enhancers (SCOPE) formulations, a library of chemical enhancers was first generated

from 32 chemicals chosen from a list of >250 chemical enhancers belonging to various categories. Random pairing of CPEs from various categories led to 496 binary chemical enhancers pairs. For each pair, 44 distinct chemical compositions were created with the concentration of each chemical enhancer ranging from 0–2% w/v, yielding a library of 25,000 candidate SCOPE formulations. About 20% of this library (5,040 formulations) was screened using INSIGHT, the largest ever-cohesive screening study reported in the transdermal literature. Each formulation was tested at least four times in over 20,000 experiments (Karande et al. 2004). Using the traditional tools for formulation screening, it would have taken over 7 years to do these many experiments. With INSIGHT screening, the same task was accomplished in about 2 months with screening rate of 500–1,000 experiments per day.

Binary formulations exhibited a wide range of enhancements. The percent of randomly generated enhancer combinations that exhibit ER above a certain threshold decreases rapidly with increasing threshold (Fig. 8.6a). The inset shows a section of the main figure corresponding to high ER values. Less than 0.1% of formulations exhibited more than 60-fold enhancement of skin conductivity. Discovery of such rare formulations by brute force experimentation is contingent on the throughput of the experimental tool. INSIGHT screening opens up the possibility of discovering such rare formulations.

One of the formulations discovered by INSIGHT, SLA:PP (sodium laureth sulfate:phenyl piperazine) was shown to increase the permeability of macromolecules such as inulin across porcine skin by 80–100 fold compared to passive skin permeability of inulin (Karande et al. 2004). SLA:PP also increased the skin permeability of molecules such as methotrexate, low molecular weight heparin, luteinizing hormone releasing hormone (LHRH), and oligonucleotides by 50–100 fold. Animal experiments in hairless rats also confirmed delivery of a synthetic analogue of LHRH, leuprolide acetate in vivo. The amount of leuprolide acetate delivered using a SCOPE formulation (SLA:PP) is significantly higher than that delivered from a control solution and lies in the therapeutic window.

**a. Discovery of rare formulations****b. Exploration of synergy****c. Database for QSAR**

**Fig.8.6** Applications of INSIGHT screening. (a) Discovery of rare enhancer formulations that is significantly potent in increasing skin permeability. Such formulations are difficult to discover using the traditional tools like FDC due to their low experimental throughput. The success rate of discovering these potent formulations is very small (~0.1%) requiring a tool with high experimental throughput. (b) INSIGHT

screening is used to quantify the extent of interactions between the components of CPE mixtures in terms of Synergy. Regions of high synergy almost always overlap with the regions of high potency. (c) INSIGHT screening can be used to generate large volumes of data on the interaction of CPEs with skin. The information is used to relate chemistry of the enhancer to its potency using QSAR

### 8.4.2 Generation of Database for Quantitative Understanding

Looking beyond searching for potent combinations of enhancers, the sheer volume of information generated via INSIGHT screening on the behavior of a wide variety of penetration enhanc-

ers will provide, for the first time, a platform to build further investigations of the fundamental aspects of enhancer-skin interactions. Quantitative descriptions of structure-activity relations (QSARs) for CPEs, which have had limited success in the past (Moss et al. 2002; Walker et al. 2003), may lead to better outcomes in light of the availability of large volumes of data collected in a

consistent manner. As exemplified in Fig. 8.6, this information should help in generating hypotheses relating the chemistry of CPEs to their potencies. For working hypotheses, this knowledge can then help refine our selection rules for designing next generation transdermal formulations. Repeating the experiment-hypothesis loop over a vast but limited number of candidate penetration enhancers will provide the missing pieces in solving a vast multivariate problem. Also, this knowledge should significantly reduce the cost and effort of designing therapeutics for use on skin in the future.

## References

- Auner BG, Valenta C et al (2003a) Influence of lipophilic counter-ions in combination with phloretin and 6-ketocholestanol on the skin permeation of 5-aminolevulinic acid. *Int J Pharm* 255(1–2):109–116
- Auner BG, Valenta C et al (2003b) Influence of phloretin and 6-ketocholestanol on the skin permeation of sodium-fluorescein. *J Control Release* 89(2):321–328
- Aungst BJ, Blake JA et al (1990) Contributions of drug solubilization, partitioning, barrier disruption, and solvent permeation to the enhancement of skin permeation of various compounds with fatty acids and amines. *Pharm Res* 7(7):712–718
- Barry BW (2001) Novel mechanisms and devices to enable successful transdermal drug delivery. *Eur J Pharm Sci* 14(2):101–114
- Bosman IJ, Lawant AL et al (1996) Novel diffusion cell for in vitro transdermal permeation, compatible with automated dynamic sampling. *J Pharm Biomed Anal* 14(8–10):1015–1023
- Chang P, Rosenquist MD et al (1998) A study of functional viability and metabolic degeneration of human skin stored at 4 degrees C. *J Burn Care Rehabil* 19(1 Pt 1): 25–28
- Chukwumerije O, Nash RA et al (1989) Studies on the efficacy of methyl esters of n-alkyl fatty acids as penetration enhancers. *J Invest Dermatol* 93(3): 349–352
- Cordoba-Diaz M, Nova M et al (2000) Validation protocol of an automated in-line flow-through diffusion equipment for in vitro permeation studies. *J Control Release* 69(3):357–367
- Curdy C, Kalia YN et al (2002) Post-iontophoresis recovery of human skin impedance in vivo. *Eur J Pharm Biopharm* 53(1):15–21
- Davies DJ, Ward RJ et al (2004) Multi-species assessment of electrical resistance as a skin integrity marker for in vitro percutaneous absorption studies. *Toxicol In Vitro* 18(3):351–358
- Elias PM (1983) Epidermal lipids, barrier function, and desquamation. *J Invest Dermatol* 80(Suppl):44s–49s
- Elias PM, McNutt NS et al (1977) Membrane alterations during cornification of mammalian squamous epithelia: a freeze-fracture, tracer, and thin-section study. *Anat Rec* 189(4):577–594
- Fasano WJ, Manning LA et al (2002) Rapid integrity assessment of rat and human epidermal membranes for in vitro dermal regulatory testing: correlation of electrical resistance with tritiated water permeability. *Toxicol In Vitro* 16(6):731–740
- Francoeur ML, Golden GM et al (1990) Oleic acid: its effects on stratum corneum in relation to (trans)dermal drug delivery. *Pharm Res* 7(6):621–627
- Golden GM, McKie JE et al (1987) Role of stratum corneum lipid fluidity in transdermal drug flux. *J Pharm Sci* 76(1):25–28
- Guy RH, Hadgraft J et al (1982) A pharmacokinetic model for percutaneous absorption. *Int J Pharm* 11: 119–129
- Heylings JR, Clowes HM et al (2001) Comparison of tissue sources for the skin integrity function test (SIFT). *Toxicol In Vitro* 15(4–5):597–600
- Hingson RA, Figge FH (1952) A survey of the development of jet injection in parenteral therapy. *Curr Res Anesth Analg* 31(6):361–366
- Itoh T, Xia J et al (1990) Use of shed snake skin as a model membrane for in vitro percutaneous penetration studies: comparison with human skin. *Pharm Res* 7(10): 1042–1047
- Jain AK, Panchagnula R (2003) Transdermal drug delivery of tricyclic antidepressants: effect of fatty acids. *Methods Find Exp Clin Pharmacol* 25(6):413–421
- Jain AK, Thomas NS et al (2002) Transdermal drug delivery of imipramine hydrochloride. I. Effect of terpenes. *J Control Release* 79(1–3):93–101
- Kalia YN, Naik A et al (2004) Iontophoretic drug delivery. *Adv Drug Deliv Rev* 56(5):619–658
- Karande P, Mitragotri S (2002) High throughput screening of transdermal formulations. *Pharm Res* 19(5): 655–660
- Karande P, Jain A et al (2004) Discovery of transdermal penetration enhancers by high-throughput screening. *Nat Biotechnol* 22(2):192–197
- Lackermeier AH, McAdams ET et al (1999) In vivo ac impedance spectroscopy of human skin. Theory and problems in monitoring of passive percutaneous drug delivery. *Ann N Y Acad Sci* 873:197–213
- Larrucea E, Arellano A et al (2001) Combined effect of oleic acid and propylene glycol on the percutaneous penetration of tenoxicam and its retention in the skin. *Eur J Pharm Biopharm* 52(2):113–119
- Lawrence JN (1997) Electrical resistance and tritiated water permeability as indicators of barrier integrity of in vitro human skin. *Toxicol In Vitro* 11:241–249
- Lee SJ, Kim SW (1987) Hydrophobization of ionic drugs for transport through membranes. *J Control Release* 6:3–13
- Li SK, Ghanem AH et al (1998) Characterization of the transport pathways induced during low to moderate voltage iontophoresis in human epidermal membrane. *J Pharm Sci* 87(1):40–48

- Lopez A, Llinares F et al (2000) Comparative enhancer effects of Span20 with Tween20 and Azone on the in vitro percutaneous penetration of compounds with different lipophilicities. *Int J Pharm* 202(1–2):133–140
- Madison KC, Swartzendruber DC et al (1987) Presence of intact intercellular lipid lamellae in the upper layers of the stratum corneum. *J Invest Dermatol* 88:714–718
- Magnusson BM, Runn P (1999) Effect of penetration enhancers on the permeation of the thyrotropin releasing hormone analogue pGlu-3-methyl-His-Pro amide through human epidermis. *Int J Pharm* 178(2):149–159
- Mitragotri S (2000) Synergistic effect of enhancers for transdermal drug delivery. *Pharm Res* 17(11):1354–1359
- Mitragotri S (2004) Breaking the skin barrier. *Adv Drug Deliv Rev* 56(5):555–556
- Mitragotri S, Kost J (2004) Low-frequency sonophoresis: a review. *Adv Drug Deliv Rev* 56(5):589–601
- Moss GP, Dearden JC et al (2002) Quantitative structure-permeability relationships (QSPRs) for percutaneous absorption. *Toxicol In Vitro* 16(3):299–317
- Naito SI, Tsai YH (1981) Percutaneous absorption of indomethacin from ointment bases in rabbits. *Int J Pharm* 8:263–276
- Narishetty ST, Panchagnula R (2004) Transdermal delivery of zidovudine: effect of terpenes and their mechanism of action. *J Control Release* 95(3):367–379
- Nokhodchi A, Shokri J et al (2003) The enhancement effect of surfactants on the penetration of lorazepam through rat skin. *Int J Pharm* 250(2):359–369
- Ogiso T, Ito Y et al (1989) A pharmacokinetic model for the percutaneous absorption of indomethacin and the prediction of drug disposition kinetics. *J Pharm Sci* 78:319–323
- Ogiso T, Niinaka N et al (1996) Mechanism for enhancement effect of lipid disperse system on percutaneous absorption. *J Pharm Sci* 85(1):57–64
- Ongpipattanakul B, Burnette RR et al (1991) Evidence that oleic acid exists in a separate phase within stratum corneum lipids. *Pharm Res* 8(3):350–354
- Panchagnula R, Stemmer K et al (1997) Animal models for transdermal drug delivery. *Methods Find Exp Clin Pharmacol* 19(5):335–341
- Peck KD, Ghanem AH et al (1995) The effect of temperature upon the permeation of polar and ionic solutes through human epidermal membrane. *J Pharm Sci* 84(8):975–982
- Prausnitz MR (1999) A practical assessment of transdermal drug delivery by skin electroporation. *Adv Drug Deliv Rev* 35(1):61–76
- Prausnitz MR (2004) Microneedles for transdermal drug delivery. *Adv Drug Deliv Rev* 56(5):581–587
- Prausnitz MR, Mitragotri S et al (2004) Current status and future potential of transdermal drug delivery. *Nat Rev Drug Discov* 3(2):115–124
- Priborsky J, Muhlbachova E (1990) Evaluation of in-vitro percutaneous absorption across human skin and in animal models. *J Pharm Pharmacol* 42(7):468–472
- Rosado C, Cross SE et al (2003) Effect of vehicle pretreatment on the flux, retention, and diffusion of topically applied penetrants in vitro. *Pharm Res* 20(9):1502–1507
- Schmook FP, Meingassner JG et al (2001) Comparison of human skin or epidermis models with human and animal skin in in-vitro percutaneous absorption. *Int J Pharm* 215(1–2):51–56
- Sekkat N, Kalia YN et al (2002) Biophysical study of porcine ear skin in vitro and its comparison to human skin in vivo. *J Pharm Sci* 91(11):2376–2381
- Shokri J, Nokhodchi A et al (2001) The effect of surfactants on the skin penetration of diazepam. *Int J Pharm* 228(1–2):99–107
- Sims SM, Higuchi WI et al (1991) Skin alteration and convective solvent flow effects during iontophoresis: I. Neutral solute transport across human skin. *Int J Pharm* 69(2):109–121
- Sintov AC, Krymberk I et al (2003) Radiofrequency-driven skin microchanneling as a new way for electrically assisted transdermal delivery of hydrophilic drugs. *J Control Release* 89(2):311–320
- Takács-Novak K, Szász G (1999) Ion-pair partition of quaternary ammonium drugs: the influence of counter ions of different lipophilicity, size, and flexibility. *Pharm Res* 16:1633–1638
- Takayama K, Nagai T (1991) Simultaneous optimization for several characteristics concerning percutaneous absorption and skin damage of ketoprofen hydrogels containing Dlinomene. *Int J Pharm* 74:115–126
- Tang H, Mitragotri S et al (2001) Theoretical description of transdermal transport of hydrophilic permeants: application to low-frequency sonophoresis. *J Pharm Sci* 90(5):545–568
- Tang H, Blankschtein D et al (2002) Prediction of steady-state skin permeabilities of polar and nonpolar permeants across excised pig skin based on measurements of transient diffusion: characterization of hydration effects on the skin porous pathway. *J Pharm Sci* 91(8):1891–1907
- Tezel A, Sens A et al (2002) Synergistic effect of low-frequency ultrasound and surfactants on skin permeability. *J Pharm Sci* 91(1):91–100
- Tezel A, Sens A et al (2003) Description of transdermal transport of hydrophilic solutes during low-frequency sonophoresis based on a modified porous pathway model. *J Pharm Sci* 92(2):381–393
- Thomas NS, Panchagnula R (2003) Combination strategies to enhance transdermal permeation of zidovudine (AZT). *Pharmazie* 58(12):895–898
- Turner NG, Kalia YN et al (1997) The effect of current on skin barrier function in vivo: recovery kinetics post-iontophoresis. *Pharm Res* 14(9):1252–1257
- Walker JD, Rodford R et al (2003) Quantitative structure-activity relationships for predicting percutaneous absorption rates. *Environ Toxicol Chem* 22(8):1870–1884
- Weaver JC, Vaughan TE et al (1999) Theory of electrical creation of aqueous pathways across skin transport barriers. *Adv Drug Deliv Rev* 35(1):21–39
- Williams AC, Barry BW (1991) Terpenes and the lipid-protein-partitioning theory of skin penetration enhancement. *Pharm Res* 8(1):17–24

- Williams AC, Barry BW (2004) Penetration enhancers. *Adv Drug Deliv Rev* 56(5):603–618
- Wu PC, Huang YB et al (2000) Evaluation of pharmacokinetics and pharmacodynamics of captopril from transdermal hydrophilic gels in normotensive rabbits and spontaneously hypertensive rats. *Int J Pharm* 209(1–2):87–94
- Xing QF, Lin S et al (1998) Transdermal testosterone delivery in castrated Yucatan minipigs: pharmacokinetics and metabolism. *J Control Release* 52(1–2):89–98
- Yamamoto T, Yamamoto Y (1976a) Dielectric constant and resistivity of epidermal stratum corneum. *Med Biol Eng* 14(5):494–500
- Yamamoto T, Yamamoto Y (1976b) Electrical properties of the epidermal stratum corneum. *Med Biol Eng* 14(2):151–158
- Yamane MA, Williams AC et al (1995) Terpene penetration enhancers in propylene glycol/water co-solvent systems: effectiveness and mechanism of action. *J Pharm Pharmacol* 47(12A):978–989

---

## Part II

# Methods for Measuring the Percutaneous Drug Penetration

---

# Models, Methods, and Measurements in Transdermal Drug Delivery

# 9

Donald M. Cropek and Pankaj Karande

## Contents

9.1	<b>Introduction</b> .....	153
9.1.1	Transdermal Drug Delivery .....	154
9.1.2	Scope of Review .....	155
9.2	<b>Structure of Skin</b> .....	155
9.2.1	Ultra-structure of Stratum Corneum .....	156
9.2.2	Lipids of Stratum Corneum .....	157
9.2.3	Proteins of Stratum Corneum .....	157
9.3	<b>Routes of Permeation</b> .....	158
9.3.1	Skin Appendages .....	158
9.3.2	Intracellular Route .....	159
9.3.3	Intercellular Route .....	159
9.4	<b>In Vitro Skin Models</b> .....	160
9.4.1	Excised Human skin .....	160
9.4.2	Excised Animal Skin .....	161
9.4.3	Living Skin Equivalents .....	162
9.4.4	Polymers .....	163
9.4.5	Lipids .....	164
9.5	<b>Evaluation of Skin Permeability in Vitro</b> .....	164
9.5.1	Diffusion Measurements .....	165
9.5.2	Tape Stripping .....	167
9.5.3	Impedance Spectroscopy .....	167
9.5.4	Infrared Spectroscopy .....	168
9.5.5	Trans Epidermal Water Loss .....	169
9.6	<b>Evaluation of Skin Permeability in Vivo</b> .....	170
9.6.1	Diffusion Measurements .....	170
9.6.2	Pharmacological Response .....	170
9.6.3	Other Approaches .....	170
	<b>Conclusion</b> .....	172
	<b>References</b> .....	172

---

## 9.1 Introduction

Commonly employed delivery systems include injections, pills, and to some extent topical and mucosal formulations. Oral delivery is by far the easiest and most convenient way of delivering drugs especially when repeated or routine administration is required (Chen and Langer 1998). This advantage, however, is offset for protein and peptide-based drugs sensitive to enzymatic degradation in the gastrointestinal tract. Drugs based on proteins and peptides now form a significant fraction of the therapeutic spectrum, primarily due to accelerated advances in understanding protein chemistry and drug interactions. Thus, while the bygone drug delivery systems have been domi-

---

D.M. Cropek (✉)

Environmental Chemistry Laboratory, Construction Engineering Research Laboratory, U.S. Army Corps of Engineers, Engineering Research and Development Center, 2902 Newmark Dr, Champaign, IL 61822, USA  
e-mail: [Donald.M.Cropek@usace.army.mil](mailto:Donald.M.Cropek@usace.army.mil)

P. Karande (✉)

Howard Isermann Department of Chemical and Biological Engineering, Center for Biotechnology and Interdisciplinary Sciences, Rensselaer Polytechnic Institute, Rm. 3217, 110 8th St., Troy, NY 12180, USA  
e-mail: [karanp@rpi.edu](mailto:karanp@rpi.edu)



nated by the oral route, the next millennia of health care will demand more accommodating delivery systems for sensitive drug classes.

Injections comprise the next most commonly used method for administering therapeutics into humans. The World Health Organization (WHO) estimates that 12 billion injections are given annually (Kermode 2004). Despite the common use, needle-based drug administration has several limitations. Needle phobia is a significant issue in adults and children alike (Nir et al. 2003) and makes drug administration stressful (Breau et al. 2001). Accidental needle sticks also add to the limitations of needle use in developed and developing countries alike (Kane et al. 1999; Miller and Pisani 1999). Further, hepatic metabolism results in rapid clearance of active drug from the blood plasma making repeated administration inevitable. This only aggravates the problem of needle pain especially for patients requiring multiple administrations on a daily basis.

It is thus sufficiently obvious that as we move toward the next era of health care, compliant, noninvasive, and sustained delivery will become the key features desirable of any drug delivery system. Several advances to this effect have been made in the last two to three decades and novel drug delivery systems have been brought to the forefront (Drachman 1989; Vanbrunt 1989; Langer 1990). A large contribution to these novel systems appeared as modifications to the active drug or formulation excipients to modulate drug pharmacokinetics, safety, efficacy, and metabolism. A more radical approach has been to explore newer interfaces on the body for introducing therapeutics. One such approach, transdermal drug delivery, makes use of human skin as a port of entry for systemic delivery of drug molecules (Guy 1996; Prausnitz 1997; Barry 2001a, b; Pillai et al. 2001; Prausnitz et al. 2004; Thomas and Finnin 2004).

### 9.1.1 Transdermal Drug Delivery

Transdermal drug delivery (TDD) offers an advantageous mode of drug administration by eliminating first-pass hepatic metabolism and

providing sustained drug release for a prolonged period of time. It is painless compared to needles and therefore offers superior patient compatibility. However, skin is the first line of defense of an organism and the last barrier separating the organism from its hostile environment of viruses, pathogens, and toxics. Evolved to impede the flux of exogenous molecules into the body, the skin naturally offers a very low permeability to the movement of foreign molecules across it. A unique hierarchical structure of lipid-rich matrix with embedded keratinocytes in the upper strata (15  $\mu\text{m}$ ) of skin, stratum corneum (SC), is responsible for this barrier (Bouwstra 1997). In addition to its role as a barrier, both physical and biological, skin performs a complimentary role, which is that of a transport regulator. Skin routinely regulates the flux of water molecules into and out of the body. It also permits the influx of a variety of small molecules that are fairly lipophilic (partition coefficient,  $\log P > 1.5$ ) and have molecular weight (MW) less than 500 Da (Bos and Meinardi 2000). As a result there has been a natural bias of transdermal delivery systems to cash in on therapeutics that meet these requirements. Drug molecules currently administered via the transdermal route fall within a narrow range of MW and lipophilicity. They are typically characterized by high  $\log P$  ( $> 1.5$ ) and low MW ( $< 500$  Da), thereby taking advantage of the natural selectivity of skin membrane. A large fraction of drug molecules lie outside these bounds. These are mostly peptide- and protein-based drugs that will become the key therapeutics in the future. The biggest challenge in transdermal drug delivery today is to open the skin safely and reversibly to these high molecular weight hydrophilic drugs.

Several technological advances have been made in the past couple of decades to overcome this challenge. These advances can be broadly divided into two categories: (1) physical approaches including but not limited to iontophoresis (Panchagnula et al. 2000; Delgado-Charro and Guy 2001), sonophoresis (Mitragotri and Kost 2004; Ogura et al. 2008), microneedles (McAllister et al. 2000; Prausnitz 2004; Sivamani et al. 2007), and electroporation (Pliquett 1999; Denet et al. 2004) that use some form of physical

energy to modulate the SC ultrastructure, and (2) chemical approaches that employ chemical formulations to modulate skin transport barrier (Sinha and Kaur 2000; Williams and Barry 2004). Each of these methods has its individual benefits and limitations.

### 9.1.2 Scope of Review

The early 1990s of the last century brought the first transdermal patch to the market. The market for patch-based therapeutics has since grown to \$4 billion per annum worldwide, a small but significant proportion of the total revenues from pharmaceuticals (Barry 2001a, b). After more than a quarter of a century since the introduction of the first patch, the number of marketed transdermal patches has not exceeded beyond a couple of dozen. Another four dozen are in the developmental phases. Although somewhat satisfactory on the face value, these numbers are misleading since a huge fraction is made up of generic replicas of similar drugs. Only 11 independent drugs make up these 80 odd products, almost all exclusively below 500 Da and characteristically lipophilic in nature. Most efforts to push the envelope on molecular weight have shown limited success. Only one physical method (i.e., iontophoresis) has successfully entered the market share of transdermal delivery technologies but it is being used to deliver a low molecular weight drug, lidocaine (235 Da). On the other hand, laurocapram (Azone<sup>®</sup>), the most widely studied chemical permeation enhancer with high expectations, has failed to gain clinical acceptance in transdermal delivery due to its skin irritation (Okamoto et al. 1988; Lashmar et al. 1989; Wong et al. 1989). The landscape of transdermal delivery opportunities seems grim and one cannot help but ask, “Is transdermal drug delivery research still important today?” (Barry 2001a, b). The concept of transdermal drug delivery is rooted in strong scientific acumen even though the practical realization of it has been less fascinating than expected. A sound engineering approach coupled with fundamental understanding of a complex biological tissue is required.

Equally important is adoption of the right platform of models, methods, and measurement techniques to evaluate new and traditional transdermal delivery strategies in light of the knowledge gained in the last five decades in this field of research. The number of original publications with “transdermal delivery” in the title has well approached 1000 with the numbers rising rapidly. These numbers form one metric to indicate that new scientists continue to be attracted to this field. This review aims to provide a synopsis of the “nuts and bolts” in transdermal drug delivery research to a new scientist. A short introduction on skin structure and constituents is followed by a description of different model systems and methods employed in this area.

---

## 9.2 Structure of Skin

Elucidation of skin structure, especially in relation to its barrier function, has drawn countless researchers since the early 1950s (Blank 1952; Breathnach et al. 1973; Elias and Friend 1975). The human skin is a sandwich of two layers: a thin layer of epidermis stacked upon a much thicker substrate, the dermis. The dermis is highly vascularized and permeable, consisting predominantly of a fibrous collagen meshwork that is sparsely populated with cells. It houses sweat glands, sebaceous glands, hair follicles, and a network of capillaries supported by the connective tissue. The dermis provides most of the bulk and toughness of the skin. The epidermis is devoid of blood vessels, receiving all of its nutrients and disposing of its waste products by diffusional exchange with the dermis. It is maintained by continuous cell division in the germinative basal layer. Differentiating daughter cells, the keratinocytes move outward toward the surface of skin. During this process, there is a change in the morphology and composition of keratinocytes. Ultimately, the keratinocytes undergo terminal differentiation, forming dead, flattened corneocytes; 20–30 layers of corneocytes embedded in a matrix of lipid, extruded from the cells immediately before cornification, form the SC. Corneocytes continually exfoliate from the

SC to maintain a constant thickness of this layer at ~20–30  $\mu\text{m}$  (Elias and Friend 1975; Odland 1983; Matoltsy 1986; Downing 1992). In the last 60 years of close scrutiny of the skin structure, the SC has received by far the most attention. And not surprisingly, since this superficial layer is where the barrier property of skin resides. The seminal work of Scheuplein et al. conclusively summarized the locus and origin of the molecular impermeability of skin and established it to be a passive rather than biologically active property (Scheuplein 1965, 1966, 1967, 1972, 1978; Blank and Scheuplein 1973). Through their studies of the permeability of excised human skin in vitro to a large number of permeants, they were able to show conclusively that the principal barrier to permeation is provided by the SC. Separating the epidermis from the underlying dermis by heat stripping followed by enzymatic removal of the live epidermal layer, Scheuplein et al. measured the permeability of the residual SC and dermis independently. These measurements indicated that the SC is at least three, and frequently as much as five, orders of magnitude less permeable to most substances than the dermis. Moreover, the permeability of the entire epidermis was found to be indistinguishable from that of the SC alone. This prompted Scheuplein to model the skin as a three-layer laminate of SC, epidermis, and dermis, with permeation occurring by Fickian diffusion of the penetrating species through the three layers in series. Since the dominant resistance to permeation of most compounds is offered by the SC, the gradient in penetrant concentration across the entire skin is, for all practical purposes, localized within the SC.

### 9.2.1 Ultra-structure of Stratum Corneum

Several models have been proposed for the structure of the SC. These include the classic “brick and mortar” model of Michaels, the “domain mosaic” model of Forslind, the “single gel phase” model of Norlen, “molecular lipid lamellae” models of Swartzendruber and Fenske, and “membrane folding” model of Norlen (Michaels et al. 1975; Swartzendruber et al. 1989; Fenske et al. 1994;

Forslind 1994; Kitson et al. 1994; Engström et al. 1995; Menon and Elias 1997; Bouwstra et al. 1998; Menon et al. 1998; Norlen 2001; Norlén 2001). A comprehensive all encompassing model seems to be elusive as newer observations continually require modulating the physical picture of this membrane (Wertz et al. 1987; Norlén et al. 1998). While newer models are being proposed to accommodate minor nuances, the coarse macroscopic–microscopic structure is well agreed upon. The most simplistic model in this respect is still the “brick and mortar” model of Michaels et al.; the term itself coined by Elias (Elias and Friend 1975; Michaels et al. 1975). This model treats the skin barrier as a simplified two-compartment system with discontinuous protein pockets embedded in a continuous, homogeneous lipid matrix. Proteins held within corneocyte lipid envelopes thus form the bricks held by the mortar of a continuous lipid phase in the “brick and mortar” model. The bricks occupy, by far, the larger volume of this assembly. Early solvent extraction experiments indicated that lipids, especially polar lipids, play a critical role in the barrier (Matoltsy et al. 1968; Sweeney and Downing 1970). The freeze fracture studies of the SC established conclusively that lipids form multiple broad bilayers filling the corneocyte intercellular spaces (Breathnach et al. 1973). These bilayers, shown to exist throughout the SC, provide the barrier to water permeability as determined by Elias and Squier through freeze-fracture, thin-section, and tracer studies (Squier 1973; Elias et al. 1977; Madison et al. 1987; Wertz et al. 1987).

A general observation of mammalian cells indicates that their membranes do not provide a formidable barrier to water or water-soluble molecules. These membranes are typically composed of phosphoglycerides, sphingomyelin, and cholesterol where the lipid fatty acyl chains extend to 16 through 20 carbons with a varied degree of unsaturation (Fettiplace and Haydon 1980). Occasionally, methyl branching is also observed on the interior of the fatty acyl chains. This methyl branching coupled with unsaturation in the interior of the chains inhibits formation of a highly ordered membrane. The membrane is disordered or fluid with high permeability to small hydrophilic solutes and water. Interesting to note

is the lack of any phospholipids or the usual fatty acyl chain structures in the SC (Yardley and Summerly 1981; Yardley 1983; Wertz 1986). Instead, the SC bilayers are made of cholesterol, fatty acids, and ceramides (Wertz et al. 1987; Hedberg et al. 1988). The molecular structure and composition of these constituents play an important role in defining the barrier properties of the bilayers and in turn of the SC membrane.

Subsequent sections provide a brief description of the corneocyte proteins and the lipids of the SC.

## 9.2.2 Lipids of Stratum Corneum

### 9.2.2.1 Ceramides

Ceramides (1–6) constitute ~42 % of the material in the bilayers followed by cholesterol (~40 % along with cholesteryl sulfate and cholesteryl esters) and fatty acids (~13 %) (Wertz and Downing 1983a, b; Abraham et al. 1985; Long et al. 1985; Wertz et al. 1985). The ceramides include both sphingosines (ceramides 1, 2, 4, and 5) and phytosphingosines (ceramides 3 and 6). Also, the amide-linked fatty acids include nonhydroxy acids (ceramides 2 and 3),  $\alpha$ -hydroxy acids (ceramides 4, 5, and 6), and  $\omega$ -hydroxy acids (ceramide 1). In addition, ester-linked fatty acids (ceramide 1) are also present in the epidermal ceramides. The ceramides are straight and saturated with the exception of ceramide 1. Also the unsaturation is placed exclusively at the polar end of these ceramide chains thus providing little room for formation of kinks. This architecture is well poised to provide a highly ordered structure to the membrane formed from these ceramides. In addition, there is a considerable chain length variation in the ceramides, i.e., from 15 to 48. This provides room for interdigitation of the hydrocarbon chains, an interaction highly favorable during bilayer formation. Also, the lipids are characteristically amphiphilic in nature capable of extensive hydrogen bonding, once again a primo in formation of self-assembled lamellae.

### 9.2.2.2 Cholesterol

Free cholesterol is the second most abundant lipid in the SC, amounting to 25 % of extractable

lipid. In addition, 15 % of the SC lipids are made of cholesteryl sulfate and cholesteryl esters. Cholesterol plays a key role in providing barrier property of the SC. This was shown conclusively by Feingold et al. in 1990 based on their observation that barrier recovery was severely inhibited in skin treated with an enzyme that inhibits cutaneous cholesterol synthesis (Feingold et al. 1990). Later Takahashi et al. showed that cholesterol at high concentrations (>30 % molar basis) promotes lamellar structures, regarded generally to provide superior barrier properties (Takahashi et al. 1996). Cholesterol also increases the chain mobility of lipids in the gel state making them more pliable and thus, potentially, more resistant to mechanical stresses (de Kruffyff et al. 1974). In addition, cholesterol broadens phase transition regions or in some cases may entirely abolish subtransitions between gel phases thereby stabilizing them (McMullen and McElhaney 1995; Takahashi et al. 1996).

### 9.2.2.3 Fatty Acids

Fatty acids make up ~13 % of the SC lipids. The origin of these fatty acids is not completely understood, although it is believed that some of them are a result of hydrolysis of ceramides. The composition of the mixture of fatty acids is unusual in consisting predominantly of very long chain (20–28 carbons) saturated acids, with only 6 % of monounsaturated and 1 % of diunsaturated acids (Wertz et al. 1987; Downing 1992). Presence of fatty acids along with cholesterol and ceramides is essential to the barrier property of the SC. In addition to providing structural integrity to the SC, free fatty acids are also responsible for providing a low pH or acidic surface (Blank 1939; Draize 1942; Beare et al. 1958; Baden and Pathak 1967; Qiang et al. 1993). This may be critical to the antimicrobial activity of the SC thereby making it a physical as well as physiological barrier (Fluhr et al. 2001).

## 9.2.3 Proteins of Stratum Corneum

Protein pockets, the bricks in the “brick and mortar” model, form the second important component of the SC. These pockets are included in flat,

hexagonal, and physiologically dead corneocytes. The SC proteins are typically composed of keratin. Keratins are a family of  $\alpha$ -helical polypeptides ranging from 40 to 70 kDa in size (Green et al. 1982; Wertz and Downing 1989). They are relatively poor in cysteine, rich in serine and glycine, and contain N-acetylserine at the amino terminus (Steinert and Cantieri 1983). Keratins accumulate throughout epidermal differentiation and represent the major component of the SC as well as of epidermal appendages such as hair and nails (Baden et al. 1973). Earlier in epidermal differentiation, low molecular weight keratins predominate, whereas higher molecular weight polypeptides are found in the SC (Skerrow and Hunter 1978). Individual keratin molecules aggregate to form superhelices, the detailed structures of which are still under investigation (Steinert and Cantieri 1983). They are stabilized by disulfide bridges that can be solubilized only by reducing agents. The keratin in the SC is probably responsible for maintaining the hexagonal shapes of the corneocytes and may contribute to the toughness and flexibility of the SC (Wertz and Downing 1989).

The corneocyte envelope enclosing the keratin filaments is made of two layers. The inner portion of the envelope consists of cross linked proteins, predominantly involucrin and at least six other soluble and membrane-associated proteins (Rice and Green 1977; Watt and Green 1981; Simon and Green 1984). The outer portion is made of ester-linked  $\omega$ -hydroxyacyl-sphingosines. These hydroxyceramide molecules contain mainly 30–34 carbon  $\omega$ -hydroxyacyl chains and represent 2% of the dry weight of the SC (Wertz and Downing 1989). At least 50% of the hydroxyceramides are linked to the protein envelope through the  $\omega$ -hydroxy terminus. This helps the sphingosine moieties to interdigitate with the lipid lamellae (Wertz and Downing 1987). This may explain why unlike other membranous structures the lipid envelope persists even after extensive extraction with methanol–chloroform mixture (Swartzendruber et al. 1987; Wertz and Downing 1987). The lipid envelope hydroxyceramides anchor the corneocytes to the intercellular lipids. As a result, even

when all the intercellular lipids are extracted the covalently bound hydroxyceramides can interdigitate in a zip-like manner to close the intercellular space and thus maintain the integrity of the SC.

---

## 9.3 Routes of Permeation

There are three major routes of permeation for passive diffusion of a molecule across the SC. These include: (a) diffusion through appendages such as sweat ducts, sebaceous glands, and hair follicles; (b) diffusion through the corneocytes of the SC; and (c) diffusion through the lipids of the SC. Diffusion across the corneocytes and lipids of the intact SC comprises the predominant route through which most molecules penetrate. The appendageal area available for diffusion is significantly lower,  $\sim 0.1\%$ , but has received considerable attention as an important permeation pathway for ions or large polar molecules that have slow permeation across the SC (Barry 2001a, b).

### 9.3.1 Skin Appendages

The involvement of skin appendages in transcutaneous permeation has received considerable attention over six decades. Early studies by many investigators implicated skin appendages as important avenues for penetration of topically applied chemicals (Mackee et al. 1945; Shelley and Melton 1949; Fredriksson 1961; Tregear 1961; Vankooten and Mali 1966; Wahlberg 1968; Rutherford and Black 1969; Wallace and Barnett 1978). Using full-thickness mouse skin maintained as short-term organ cultures in an *in vitro* experimental system, Kao et al. demonstrated that permeation of topically applied benzo[*a*]pyrene was higher in haired mice skin compared to hairless mice skin (Kao et al. 1988). Histochemical techniques, autoradiographic techniques, and fluorescence microscopy have been used to visualize and quantitate appendageal absorption. These studies revealed that topically applied agents concentrated and persisted in

the hair follicles and sebaceous glands (Grasso and Lansdown 1972; Foreman et al. 1979; Holland et al. 1984).

Of all the appendageal routes, the hair follicle has received the most attention as a prominent route of permeation. It also serves as an important cutaneous reservoir for topically applied molecules (Lademann et al. 2006). Hueber et al. and Tenjarla et al. showed that the penetration of corticosteroids is considerably lower in hairless skin compared to haired skin (Hueber et al. 1994; Tenjarla et al. 1999). Hydrocortisone permeability increased in tissue engineered skin on insertion of hair follicles (Michel et al. 1999). Permeation enhancers that specifically target hair follicles have been investigated with great success. Of these, liposomes have been shown to deliver DNA (Li et al. 1993), plasmids (Domashenko et al. 2000), monoclonal antibodies (Balsari et al. 1994), calcein (Lieb et al. 1992), and melanin (Li and Hoffman 1997) to hair follicles. Lee et al. reported that the auxiliary SC associated with the sweat glands has a reduced barrier function (Lee et al. 2001). Following up with elegant immunostaining studies, Wilke et al. proposed that the active permeation barriers in sweat ducts in the epidermis and dermis are functionally and morphologically distinct (Wilke et al. 2005, 2006). The innermost layer of the intra-epidermal duct is completely keratinized (Zelickson 1961; Hashimot et al. 1965). In contrast, the dermal ducts lack the presence of cornified corneocytes but contain luminal tight junctions, which seem to be absent from the epidermal duct lining (Hashimot 1971a, b). Similar to the dermal ducts, the secretory coils of the sweat glands themselves lack cornified layers but are rich in tight junctions as evidenced by the colocalization of occludin and claudin-4 (Hashimot 1971a, b). In light of these observations, Wilke et al. propose that dermal sweat ducts and the sweat glands could serve as potential permeation routes (Wilke et al. 2006). Only a few experimental studies have actually been dedicated to evaluating the contribution of sweat glands and ducts to transcutaneous permeation (Vankootte and Mali 1966).

### 9.3.2 Intracellular Route

Certain permeation enhancers can open up the dense keratin structure in corneocytes creating porous pathways for diffusion across them. For example, decylmethyl sulfoxide interacts with keratin and is hypothesized to enhance permeability by opening up aqueous channels within the corneocyte (Cooper 1982). Dimethyl sulfoxide can induce reversible changes in protein structures of isolated corneocytes (Mendelsohn et al. 2006). Hexamethyl sulfoxide and dimethyl sulfoxide convert  $\alpha$ -helical keratins in the corneocyte to  $\beta$ -sheets (Oertel 1977). Lee et al. have demonstrated the capability of thioglycolates in depilatory creams in disrupting intracellular keratin matrix and the protein envelope using multiphoton microscopy (Lee et al. 2008). He et al. have shown that N-trimethyl chitosan is capable of increasing transcutaneous permeation by affecting secondary structure of keratins within the corneocytes (He et al. 2008). Azone<sup>®</sup> can act on the keratin fibers of the corneocytes converting their rigid  $\alpha$ -helical conformation to a flexible  $\beta$ -sheet confirmation (Xueqin et al. 2005). Lauric acid enhances the permeability of verapamil by interacting with skin proteins (Shah et al. 1992). Dithiothreitol enhances flux of sucrose and mannitol across the SC exclusively through interactions with corneocyte keratin matrix (Goates and Knutson 1993). Oleic acid and isopropyl myristate increase the permeability of the corneocytes for polar substances after pretreatment of the skin (Eder and Müller-Goymann 1995).

### 9.3.3 Intercellular Route

Several chemicals can alter or disrupt the organization of lipid molecules in the SC bilayers thereby facilitating the diffusion of molecules across the SC. Barry postulated different ways in which permeation enhancers can modify SC lipids (Barry 1988, 1991, 2004). Enhancers can act on polar head groups of lipids and modify the hydrogen bonding and ionic forces between them resulting in a disruption of the packing geometry. Fluidity caused at the polar plane due to the

disruption of packing geometry accelerates the diffusion of solute molecules across the lipid bilayers. An alternate consequence of disrupting packing geometry of lipid head groups is the creation of aqueous pockets that facilitate diffusion of hydrophilic molecules. In addition to fluidizing bilayers, enhancers that disrupt lipid head group interactions can cause extraction of lipid molecules, phase separation, or micelle formation (Barry 2004). Enhancers can also insert themselves between the hydrocarbon chains of the lipid bilayers and thereby disrupt the packing of lipid molecules. Consequent fluidization of the lipid bilayers facilitates the diffusion of permeants. Disruption in packing of lipid chains can in turn alter the packing of polar head groups of the lipid molecules, thereby accelerating, to a small extent, the diffusion of permeants.

Karande et al. studied permeation enhancers from eight different categories: anionic surfactants, cationic surfactants, zwitterionic surfactants, fatty acids, fatty alcohols, fatty amines, fatty esters, and azone-like molecules, and showed that chemicals in all these categories could be classified, more simply, as lipid extractors or lipid fluidizers (Karande et al. 2005). Lipid extractors increased SC permeability by extracting lipids from bilayers or the corneocyte envelope. Loss of lipids from the SC was monitored as a decrease in the signal intensity of methylene groups of lipid chains in Fourier transform infrared (FT-IR) spectroscopy. Lipid fluidizers increased SC permeability by partitioning themselves in the bilayers and disrupting the bilayers packing structure. Fluidization was monitored as an increase in the signal intensity of methylene groups (from hydrocarbon tails of the enhancer) and disappearance of peaks related to the ordered packing of lipids in FT-IR spectroscopy. Extent of extraction or fluidization correlated very well with the extent of skin permeabilization.

---

## 9.4 In Vitro Skin Models

### 9.4.1 Excised Human skin

Human skin is the obvious choice in experiments for determining the permeability of model

compounds or therapeutics (Rao and Misra 1994; McCullough et al. 2006; Suppasrivasuseth et al. 2006; Elewski 2007; Kim et al. 2008). Freshly excised skin from autopsies, cadaver skin, or discarded skin from breast reduction procedures are excellent sources of human skin (Bronaugh et al. 1986; Wester and Maibach 1989; Friend 1992). The primary barrier to transport of molecules across the skin is the SC. In comparison the epidermis and dermis offer minimal resistance to passive diffusion of solutes. The SC is composed of lipids and terminally differentiated, fully keratinized corneocytes. It is, therefore, intuitively expected for ex vivo skin to maintain the barrier integrity of the SC for an extended period of time after harvesting when stored under appropriate conditions. Some investigators have indeed verified that skin can be frozen for up to 12 months without significant deterioration of barrier properties (Franz 1975; Harrison et al. 1984). Barry et al. found that human cadaver skin stored at  $-18^{\circ}\text{C}$  for 466 days did not show any significant change in permeability toward tritiated water (Harrison et al. 1984). Interestingly, Barry et al. also found that the skin obtained from an iceman 5000 years old and buried in glacial ice was very well preserved. Several reports have documented the comparison between in vivo and ex vivo SC and have shown that it retains its barrier properties for several days after harvesting (Berenson and Burch 1951; Galey et al. 1976). Wester et al. monitored glucose metabolism in skin as a measure of its viability and showed that the metabolic activity was highest during the first 18 h after the skin was harvested. The metabolic activity showed a decrease by day 2 but stayed steady until day 8 (Wester et al. 1998a).

In spite of the several advantages of using human skin in permeation experiments there are several problems associated with its use such as safety concerns, difficulty in procurement, limited supply, and regulatory considerations. Also the permeability measurements obtained on human skin samples vary greatly between individuals as well as between samples from different anatomical sites on the same individual (Wester and Maibach 1992; Norlen et al. 1999; Robert Peter Chilcott 2000). Chilcott et al. have shown that there is a statistically significant

variation in the skin barrier property with relation to gender, chirality, time of the day when measurement was obtained, and to some extent the dietary habits of the individual (Robert Peter Chilcott 2000). Akomeah measured the permeability of caffeine, methyl paraben, and butyl paraben on skin samples from several donors and found interdonor variabilities between 33 % and 44 % (Akomeah et al. 2007). In general, the inter-subject skin sample variability in skin permeation was higher than that observed within the same subject. Similar observations have been reported by other investigators (Southwell et al. 1984; Langguth et al. 1986; Rochefort et al. 1986). Further, these permeability measurements show a non-Gaussian distribution (Williams et al. 1992; Cornwell and Barry 1995).

#### 9.4.2 Excised Animal Skin

In view of the difficulties associated with human skin, animal skin is routinely used as a model for human skin in *in vitro* experiments (Haigh and Smith 1994). Mouse (Bonina et al. 1993; Roy et al. 1994; Panchagnula et al. 1997; Bhandari et al. 2008; Cho et al. 2008), rat (Panchagnula et al. 1997; Hai et al. 2008; Zhao et al. 2008), guinea pig (Panchagnula et al. 1997; Tipre and Vavia 2003; Pabla and Zia 2007), rabbit (Panchagnula et al. 1997; Ogiso et al. 2001; Artusi et al. 2004; Sebastiani et al. 2005; Elgorashi et al. 2008), porcine (Panchagnula et al. 1997; Karande et al. 2004; Ben-Shabat et al. 2007), monkey (Wester and Maibach 1987; Roy and Degroot 1994; Panchagnula et al. 1997), dog (Sato et al. 1991; Panchagnula et al. 1997; Rohatagi et al. 1997), hamster (Coutelegros et al. 1992; Panchagnula et al. 1997; Bach and Lippold 1998), fish (Watanabe et al. 1989; Masson et al. 2002), snake (Megrab et al. 1995; Suh and Jun 1996; Panchagnula et al. 1997), cow (Panchagnula et al. 1997; Netzlaff et al. 2006b), frog (Dewhurst and Williams 1993; Smith 1993), sheep (Panchagnula et al. 1997), and marmoset (Scott et al. 1991) are some of the animal skin models studied to represent human skin. Animal skin offers advantages over human skin in that the age and sex of the animal can be controlled as well as

large quantities of skin can be obtained for experimental purpose (Friend 1992).

One needs to be cautious, however, in extrapolating animal skin data to human skin. Several differences exist and have been documented. Skin from experimental animals is different from human skin in thickness, composition, and constitution of the SC, and distribution and density of appendages such as sweat glands and hair follicles (Schalla and Schaefer 1982; Bronaugh et al. 1983). Panchagnula et al. have documented follicular density, SC thickness, epidermis thickness, and full skin thickness for 16 animal models including human skin (Panchagnula et al. 1997). These parameters vary significantly between the different species studied. For two model compounds used in this study, water and 7-hydroxycoumarin, lag time and permeability varied significantly across the skin models. While both compounds have similar permeabilities across human skin, their permeabilities across other skin models vary drastically. The lipid content of the skin is a major determinant in its barrier potential and differs between species or between sites on the same animal (Elias et al. 1980, 1981). Hairless mouse skin which is commonly used as a model for human skin is comparatively fragile. While permeability of human skin exposed to water increases only twofold in 10 days, hydration can completely disintegrate hairless mouse skin (Bond and Barry 1988a, b, c). A 2-min treatment with acetone has negligible effect on human skin but can increase hairless mouse skin permeability by 15-fold (Bond and Barry 1988a, b, c, d). Hairless mouse skin model overestimates the effect of permeation enhancers on skin permeability by sevenfold (Bond and Barry 1988a, b, c). In contrast, another common model, shed snake skin, underestimates the effect of permeation enhancers on skin permeability when compared to human skin (Rigg and Barry 1990). In general, it has been observed that animal skin permeability is higher than human skin permeability (Panchagnula et al. 1997).

Of all animal skin models studied, porcine skin, and particularly porcine ear skin, is closest to human skin in terms of its biochemical composition and histological features (Gray and Yardley 1975; Dick and Scott 1992; Wester et al. 1998b;



Sekkat et al. 2002; Muhammad et al. 2004; Jacobi et al. 2007). Porcine skin resembles human skin most in terms of the SC thickness (Holbrook and Odland 1974; Wester and Maibach 1989; Jacobi et al. 2007), epidermis thickness (Wester and Maibach 1989; Sandby-Moller et al. 2003; Jacobi et al. 2007), follicular structure and density (Jacobi et al. 2007), lipid composition (Gray and Yardley 1975), and the underlying vasculature (Simon and Maibach 2000). As a result, the porcine skin has gained wide acceptance as a representative model for human skin.

### 9.4.3 Living Skin Equivalents

Skin samples obtained from different species show varying permeability responses in presence of the same permeation enhancer on account of the differences in their constituents, composition, and microstructure. In addition to an interspecies variation, there is also a variation observed in skin permeability with age and anatomical location within the same species (Bronaugh et al. 1982; Dupuis et al. 1986; Hughes et al. 1994; Duncan et al. 2002). Cell culture or tissue culture-based models of human skin can potentially overcome this problem by offering a more consistent skin representation (Roguet et al. 1998; Faller and Bracher 2002; Lotte et al. 2002). In general, *in vitro* cell culture models of living tissues offer several advantages such as high reproducibility, rapid assessment of permeability and metabolism of drugs, stricter control over experimental conditions, well-defined end points, and potential time and cost savings when compared to animal use. The biggest advantage of cell culture models, however, is their amenability to high-throughput studies for drug discovery or formulation optimization studies (Audus et al. 1990).

Reconstruction of skin *in vitro* typically starts with obtaining keratinocytes from full thickness or split thickness skin by enzymatic digestion using trypsin (Larsen et al. 1988), dispase (Green et al. 1979), or thermolysin (Walzer et al. 1989). Basal keratinocytes are isolated and grown at an air-liquid interface on a substrate that is equivalent of the dermis. Dermal equivalents that have

been used successfully include permeable synthetic membranes such as nylon mesh (Slivka et al. 1993; Crooke et al. 1996) and polycarbonate membranes (MonteiroRiviere et al. 1997; Poumay et al. 2004; Kandarova et al. 2006), collagen (Fransson et al. 1998; Flamand et al. 2006), collagen lattices (Bell et al. 1981), glycated collagen (Pageon and Asselineau 2005), collagen-glycosaminoglycan matrices (Boyce et al. 1988), chitosan-cross-linked collagen-glycosaminoglycan matrices (Shahabeddin et al. 1990), fibrin (Holland et al. 2008), dead de-epidermized dermis (Regnier et al. 1998; Rehder et al. 2004), synthetic scaffolds (Shakespeare 2001; Mansbridge 2002), biodegradable scaffolds (El Ghalbzouri et al. 2004), or combinations thereof (Slivka et al. 1993; Lee et al. 2000; Barker et al. 2004; Sobral et al. 2007). Keratinocytes receive nutrients from the lower surface of the culture while being pushed upward in a process of progressive differentiation. In 14–21 days, the topmost layer achieves terminal differentiation and manifests characteristics remarkably similar to those of normal SC, i.e., completely cornified cells surrounded by a lipid intercellular matrix (Nabila Sekkat 2001). Today, several cell culture-based skin models are commercially available for ready use in skin permeation or skin toxicity studies. These include TestSkin<sup>®</sup> and TestSkin<sup>®</sup> II by Organogenesis, Canton, MA (Davis 1990; Moody et al. 1995; Elyan et al. 1996; Rodriguez et al. 2004; Shibayama et al. 2008), EpiDerm<sup>™</sup> and EpiDermFT<sup>™</sup> (Hayden et al. 2004, 2005; Kandarova et al. 2007; Borgia et al. 2008; Schafer-Korting et al. 2008) by MatTek Corp., Ashland, MA, EpiSkin<sup>®</sup> and SkinEthic RHE<sup>®</sup> (Botham 2004; Schafer-Korting et al. 2006, 2008; Luu-The et al. 2007; Netzlaff et al. 2007) by SkinEthic Labs., Nice, France, Vitrolife-Skin (Uchino et al. 2002; Morikawa et al. 2007) by Gunze, Kyoto, Japan. Netzlaff et al. have reviewed the EpiDerm<sup>™</sup>, EpiSkin<sup>®</sup>, and SkinEthic<sup>®</sup> models based on their morphology, lipid composition, biochemical markers, and their applicability in tests for evaluating phototoxicity, corrosivity, irritancy, and transport properties (Netzaff et al. 2005). The architecture, homeostasis, and lipid composition of these models come close to human

skin (Ponec and Kempenaar 1995; Ponec et al. 2000, 2002). Faller et al. compared the models in their ability to secrete extracellular enzymes glutamic oxaloacetic transaminase (GOT) and lactate dehydrogenase (LDH), and interleukin-1 $\alpha$  on treatment with sodium lauryl sulfate (SLS). EpiDerm<sup>TM</sup> was the most resistant to SLS and most reproducible (Faller and Bracher 2002).

In general, the reconstructed skin models have higher permeabilities compared to excised human skin (Gysler et al. 1999). Schmook et al. compared the permeabilities of four topical dermatological compounds of varying polarity—salicylic acid, hydrocortisone, clotrimazole and terbinafine, across rat, human and pig skin as well as two models of human skin—Graftskin<sup>TM</sup> LSE<sup>TM</sup> and Skinethic<sup>TM</sup> HRE (Schmook et al. 2001). In these studies pig skin performed similar to human skin with comparable flux of solute across both tissues. Graftskin<sup>TM</sup> LSE<sup>TM</sup> provided an adequate barrier to salicylic acid, but clotrimazole flux across it was 1000-fold higher and its skin concentration 50-fold higher when compared with human skin. Skinethic<sup>TM</sup> HRE was approximately sevenfold more permeable compared to human skin for salicylic acid and 900-fold more permeable to clotrimazole. In a similar study Marty et al. reported that trinitroglycerol and estradiol were about 20-fold more permeable across Skinethic<sup>TM</sup> HRE compared to split-thickness human skin (Marty et al. 1997). In cutaneous bioavailability studies on topical formulations, vehicle effects were observed to be vastly different in EpiDerm<sup>TM</sup> and EpiSkin<sup>®</sup> models compared to ex vivo human skin (Dreher et al. 2002). Although the reconstructed human skin models underperform significantly in reproducing the barrier properties of ex vivo human skin they can still be used to rank order the permeabilities of solutes based on their permeabilities. Such a rank order has been shown to match the order obtained on ex vivo human skin for several different molecules. Lotte et al. have shown that the skin absorption and permeability of lauric acid, mannitol, and caffeine follow the same rank order as they would on ex vivo human skin (Lotte et al. 2002). Dreher et al. found that the EpiSkin<sup>®</sup> and EpiDerm<sup>TM</sup> models showed the same rank

order permeability as human skin for caffeine and  $\alpha$ -tocopherol acetate from a water in oil (w/o)-emulsion, an oil in water (o/w)-emulsion, a liposomal dispersion and a hydrogel (Dreher et al. 2002). In addition, a multilab study verified that the permeability ranking across EpiSkin<sup>®</sup>, EpiDerm<sup>TM</sup>, and Skin Ethic<sup>TM</sup> RHE models was comparable to the permeation through human epidermis for caffeine and testosterone (Schafer-Korting et al. 2008).

The biggest shortcoming of commercially available skin models is their relatively weak barrier function. Impaired desquamation (Vicanova et al. 1996a, b), impaired transfer of desmosomes (Vicanova et al. 1996a, b), and presence of unkeratinized microscopic foci (Mak et al. 1991) are cited as reasons for this poor performance. Another significant impediment to the use of reconstructed human skin models is their high cost. This has limited the use of such models mostly to industry and out of reach of most academic labs and small enterprises. Furthermore, all commercially available models use proprietary chemically defined media and sources for cells that can put additional constraints on the flexibility of using such models. All three leading models, EpiDerm<sup>TM</sup>, EpiSkin<sup>®</sup>, and SkinEthic<sup>TM</sup> RHE are based on the epidermis raised on a minimal dermal equivalent such as collagen gel scaffold encapsulating fibroblasts. In contrast, Nakamura et al. report that full-thickness models based on organ cultures of skin explants match the in vivo situation more closely (Nakamura et al. 1990).

#### 9.4.4 Polymers

Model membrane systems can provide tremendous insight into mechanistic details of solute diffusion and thermodynamics of solute–membrane and solvent–membrane interactions (Corrigan et al. 1980; Flynn 1985; Beastall et al. 1986; Haigh and Smith 1994). Diffusion of a solute molecule across a membrane is governed by physical factors such as molecule size and shape, pore size, pore distribution, path length and tortuosity, and chemical factors such as hydrogen bonding, hydrophobic interactions, and electrostatic interactions. The

contribution from each of these factors can potentially be decoupled by a systematic study with model membranes. Synthetic membranes and polymers such as silicone (Hou and Flynn 1997; Cross et al. 2001), cellulose acetate (Barry and Eleini 1976; Barry and Brace 1977; Farinha et al. 2003), poly(dimethylsiloxane) (Cronin et al. 1998; Du Plessis et al. 2002; Farinha et al. 2003; Frum et al. 2007), polyvinylidene difluoride (Olivella et al. 2006), polyvinyl chloride, polyether sulfone (Farinha et al. 2003), ethyl vinyl acetate (Farinha et al. 2003), multimembrane laminates (Scheuplein and Bronaugh 1983; Houk and Guy 1988), and a mixture of isopropyl myristate and silicone oil (Ottaviani et al. 2006) have been used to this end. In spirit of the “fluid—mosaic model” of the skin, organic solvents such as 1-octanol, alkanes, ether, chloroform, esters, and paraffins have also been used to model diffusion through skin (Houk and Guy 1988). Relatively less studied synthetic membrane systems are porous materials. In diffusion studies across model biomembranes, filter supports have typically gained prominence as support membranes. A few studies, however, have used filter supports or filter supports filled with organic liquid to study diffusion of topical agents (Tanaka et al. 1978; Demeere and Tomlinson 1984; Turakka et al. 1984; Viegas et al. 1986). Schramm-Baxter et al. have used polyacrylamide gels to model human skin and study the energetics of liquid jet penetration into skin (Schramm-Baxter et al. 2004). Dyer et al. have tested zeolites as model systems (Dyer et al. 1979). Although such models are simplistic and lack all the functional and structural complexity of skin, they provide several other advantages such as uniformity of structure, sample-to-sample reproducibility, and ease of procurement.

#### 9.4.5 Lipids

In vitro models based on lipids, model lipids, or mixtures of natural or model lipids have been evaluated for studying percutaneous absorption in humans. An artificial lipid membrane composed of isopropyl myristate (IPM) supported in a rotating diffusion cell has been used to simulate the epidermal barrier. Reasonable correlation was

obtained between diffusion of a wide range of compounds across the IPM membrane and excised skin. Transport resistance across the model membrane, however, was 1000-fold lower as compared to excised skin (Hadgraft and Ridout 1987). A three-component mixture of dipalmitoyl phosphatidylcholine, linoleic acid, and tetradecane showed an order of magnitude improvement in transport resistance when compared to IPM membrane (Hadgraft and Ridout 1988). Matsuzaki et al. developed a model skin membrane by fixing liposomes composed of SC lipids: ceramides, palmitic acid, cholesterol, and cholesterol-3-sulfate onto a supporting filter, Biodyne B (Matsuzaki et al. 1993; Miyajima et al. 1994). Drug permeability through this system correlated very well ( $r=0.88$ ) with that through guinea pig skin although permeability through the model system was an order of magnitude higher. Moghimi et al. constructed a model lipid matrix from cholesterol, water, and free fatty acids of the SC and their sodium salts (Moghimi et al. 1996). This model matrix was shown to be a good representation of the SC barrier based on the permeability of a model hydrophobic drug, 5-fluorouracil. Using a similar approach, de Jager et al. created a SC substitute (SCS) by applying a mixture of synthetic SC lipids, free fatty acids, and cholesterol on a porous substrate. The composition, organization, and orientation of lipids in the SCS bore high resemblance to that of the intercellular barrier lipids in SC (de Jager et al. 2006a, b). Other groups have reported studies on membranes reconstituted from porcine SC lipids or porcine brain ceramides on porous substrates. These models have been shown to reproduce the permeability of water and some other permeants across intact SC (Abraham and Downing 1989; Friberg and Kayali 1989; Friberg et al. 1990; Kittayanond et al. 1992; Lieckfeldt et al. 1993; Kuempel et al. 1998).

---

## 9.5 Evaluation of Skin Permeability In Vitro

The ability to measure skin permeability is of utmost importance for percutaneous absorption and transdermal delivery applications. Several methods have been proposed to quantify skin permeability.

### 9.5.1 Diffusion Measurements

Diffusion cells are by far the oldest and most commonly used apparatus in measuring permeation of solutes across the skin. A typical diffusion cell assembly contains a donor chamber coupled to a receiver chamber by means of a spring clamp or screw. The membrane, in this case skin, whose permeability is to be assessed, is sandwiched between the donor and receiver chambers such that the SC is exposed to the donor and the epidermis/dermis to the receiver. A solute whose permeability across skin is to be measured is placed in the donor chamber by formulating it in a suitable solvent. Appearance of the solute in the receiver chamber is periodically monitored using appropriate analytical methods. The rate of appearance of the solute in the receiver chamber is then expressed as a permeability profile in the form amount vs. time.

#### 9.5.1.1 Theory

A number of relationships have been used to describe the permeation of drugs across skin. While the basis for these relationships can be complex, the amount of solute ( $M_t$ ) crossing the skin in time  $t$  can be related to skin permeability ( $P$ ) by a reasonably straightforward relation.

For an infinite dose of solute in the donor,

$$M_t = C_0 KL \left[ \frac{Dt}{L^2} - \frac{1}{6} - \frac{2}{\pi^2} \sum_{n=1}^{\infty} \exp\left(\frac{-Dn^2\pi^2 t}{L^2}\right) \right] \quad (9.1)$$

where  $C_0$  is the concentration of the solute in the donor chamber,  $K$  is the partition coefficient, or log  $P$  of the solute into skin (SC),  $D$  is the effective diffusion coefficient across the skin,  $L$  is the path length of diffusion.

At steady state ( $t \rightarrow \infty$ ), Eq. (9.1) above can be rewritten in a simpler form as

$$M_t = \frac{C_0 KD}{L} \left[ t - \frac{L^2}{6D} \right] \quad (9.2)$$

This represents the permeability profile of a solute diffusing across skin. The slope of this profile provides flux of the solute across skin,

$$\frac{dM_t}{dt} = \frac{C_0 KD}{L} \quad (9.3)$$

The permeability profile is linear in time but

$$t_L = \frac{L^2}{6D}$$

exhibits a lag time,

The terms  $K$ ,  $D$  and  $L$  are grouped together and defined as a single term,  $P = \frac{KD}{L}$ , the skin permeability. Solute permeability can then be estimated from flux of the solute across the skin and its concentration in the donor chamber.

$$P = \frac{\frac{dM_t}{dt}}{C_0} \quad (9.4)$$

Several simplifying assumptions have been made in deriving this relationship (Foreman and Kelly 1976; Osborne 1986). Nevertheless, Eq. (9.4) above provides a straightforward way of determining skin permeability to different solutes by measuring their flux.

#### 9.5.1.2 Model Solutes

The solute, whose permeability is to be assessed across the skin, needs to be detected in the receiver chamber by means of appropriate analytical methods. These may include spectrometry, chromatography, biochemical methods such as ELISA, western blots, etc. The solute itself may be labeled using a fluoropore or radioisotope for direct detection. Care needs to be taken that labeling of the solute does not alter its physicochemical properties, which may affect skin permeability resulting in misleading conclusions.

#### 9.5.1.3 Diffusion Cells

A wide variety of diffusion cell systems have been developed for measuring solute permeation through membranes (Frantz 1990; Bronaugh and Collier 1991; Gummer and Maibach 1991; Friend 1992). The most common configurations are vertical cells, where the donor chamber is atop the receiver chamber separated by the membrane in between, and horizontal diffusion cells where the donor and receiver chamber are arranged side-by-side. Mixing

of the chambers to create homogeneous compartments is critical in horizontal diffusion cells. In case of vertical diffusion cells, mixing is not critical. However, a homogeneous well-mixed receiver chamber better mimics *in vivo* conditions and prevents the formation of a static boundary layer of high-solute concentration in the receiver chamber. Formation of unmixed zones is especially critical when assessing the permeability of a hydrophobic solute in an aqueous receiver compartment (Tsuruta 1977; Bronaugh and Stewart 1984, 1986). Efficient mixing can be obtained using small magnetic stir bars. Flow-through diffusion cells in which the receptor fluid is continuously refreshed to mimic *in vivo* sink conditions (i.e., metabolism and diffusion into the subdermal vasculature) have also been used successfully (Ainsworth 1960). Temperature control of the diffusion cell can be attained using water jackets or simply submerging the entire cell assembly into a water bath. For studying permeation of highly hydrophobic compounds, solubilizing solvents can be added to the aqueous receiver chamber. These include Triton X-100 (Bronaugh and Stewart 1984), bovine serum albumin (Brown and Ulsamer 1975), Poloxamer 188 (Hoelgaard and Mollgaard 1982), PEG 400 (Valia et al. 1984), and ethanol (Scott et al. 1986). Caution needs to be exercised when using solubilizing agents that they do not alter inherent membrane properties. Hydration effect on membrane integrity needs to be considered when assessing solute permeability over extended periods of time. Some studies have reported that long-term hydration in rodent skin, and in particular hairless mouse skin, can lead to changes in permeation rates (Whitton and Everall 1973; Bond and Barry 1988a, b, c, d; Hinz et al. 1989). Finally, the area of diffusion of the donor chamber has been shown to have some effects on the permeation rates (Karande and Mitragotri 2003). Water penetration into the skin introduces a lateral strain at the edges of the donor chamber due to swelling. This scales as the strain edge available per unit area and results in higher observed permeation rates in smaller donor chambers.

#### (a) Horizontal diffusion cells

Several designs have been suggested and used successfully for this type of diffusion cell. These include the T-shape configuration

(Washitake et al. 1980), L-shape configuration (Dyer et al. 1979; Tojo et al. 1985a), glass conical flasks configuration (Wurster et al. 1979), vertical membrane, equi-compartment diffusion cell with high area to volume ratio (Flynn and Smith 1971), glass diffusion cells with steel mesh (Southwell and Barry 1983), Valia-Chien cells (Tojo et al. 1985a, b), and flow through system with central inlet and peripheral effluent ports (Astley and Levine 1976). In recent years, several modified versions of these early designs have been used (Morell et al. 1996; Aramaki et al. 2003; Bakand et al. 2006; Soni et al. 2006; Tas et al. 2007).

#### (b) Vertical cells

Vertical diffusion cells are closer to *in vivo* situation in obtaining permeability data across the skin (Friend 1992). The Coldman cell represents the earliest of all vertical diffusion cells (Coldman et al. 1969). A glass cell with a side arm for sampling and stir bar for mixing forms the receiver chamber. Skin is sandwiched between the donor and receiver using a clamp. Whitton et al. studied a similar cell with the sampling arm located at the bottom of the receiver (Whitton and Everall 1973). The Franz diffusion cell remains the most widely studied vertical diffusion cell today (Franz 1978). The original design had poor mixing properties which have been addressed in subsequent modifications (Nacht et al. 1981; Loftsson 1982; Kao et al. 1983; Dugard et al. 1984; Hawkins and Reifenrath 1986; Gummer et al. 1987; Tiemessen et al. 1989). In the past two decades several modifications of the Coldman cell have been used successfully. These include the release cells (Morell et al. 1996), enhancer cells (Bosman et al. 1996), Kelder cells in combination with the Automatic Sample Preparation with Extraction Columns system (Bosman et al. 1996), Oak Ridge National Laboratory Skin Permeability Chamber (Holland et al. 1984), and Ussing type chambers (Li et al. 2006; Ito et al. 2007).

#### (c) Skin Flaps

In addition to the conventional diffusion systems discussed above, novel *in vitro* systems that measure effect of perfusion rates on

solute permeation have also been designed. Isolated Perfused Porcine Skin Flap (IPPSF) is a model system of porcine skin flap perfused by the caudal superficial epigastric artery and its associated veins and mounted on a diffusion cell (Williams et al. 1990; Riviere et al. 1991). Bovine udder is used in a similar fashion for permeation studies (Kietzmann et al. 1993).

## 9.5.2 Tape Stripping

Tape stripping is a technique that has been found useful in dermatopathological and dermatopharmacological research for selectively or at times exhaustively removing the SC (Surber et al. 1999). Typically, an adhesive tape is applied to the skin and removed abruptly. This application can be repeated between 10 and 100 times (Sheth et al. 1987; Ohman and Vahlquist 1994). The observation that skin may serve as a reservoir for chemicals was first reported in 1955 (Malkinson and Ferguson 1955). Drugs like corticosteroids were shown to localize within the SC (Vickers 1963; Carr and Wieland 1966). These observations led to the use of the tape stripping technique in investigating the barrier and reservoir function of the skin (Rougier et al. 1983; Tojo and Lee 1989). This technique is now being increasingly used in measuring drug concentration and its concentration profile in the SC (Pershing et al. 1990; Pellett et al. 1997; Shah et al. 1998).

### 9.5.2.1 Theory

Solute diffusion in the SC can be described by Fick's law (Crank 1975) as follows

$$\frac{\partial C_s}{\partial t} = D \frac{\partial^2 C_s}{\partial x^2} \quad (9.5)$$

where  $D$  is the average solute diffusion coefficient in the SC,  $C_s$  is the solute concentration in the SC, and  $x$  is the distance from the SC surface. Eq. (9.1) can be solved with the following boundary conditions:

$$\begin{aligned} C_s(x=0) &= KC_0 \\ C_s(x=L) &= 0 \end{aligned}$$

where  $x=0$  corresponds to the SC surface and  $x=L$  corresponds to the end of the SC,  $K$  is the average solute partition coefficient in the SC, and  $C_0$  is the donor concentration of the solute. The resulting equation for solute concentration in the SC,  $C_s$  is given as follows (Crank 1975):

$$\frac{C_s(t)}{C_\infty} = 1 - \frac{8}{\pi^2} \sum_{n=0}^{\infty} \frac{1}{(2n+1)^2} \exp\left\{-\frac{D(2n+1)^2 \pi^2 t}{L^2}\right\} \quad (9.6)$$

where  $C_\infty$  is the solute concentration in SC at steady state ( $C_\infty = \frac{KC_0}{2}$ ). For short times, i.e.,

low values of  $\frac{Dt}{L^2}$ , Eq. (9.6) can be simplified as

$$\frac{C_s(t)}{C_0} \approx \frac{4DKt}{L^2} \quad (9.7)$$

Using the definition of permeability  $P$ , the above Eq. (9.7) further simplifies to

$$C_s(t) = \frac{4Pt}{L} C_0 \quad (9.8)$$

Equation (9.8) shows that the solute concentration in the SC measured at short times is proportional to its steady-state permeability. Accordingly, solute concentration can be measured via tape stripping in the SC to infer its steady-state permeability. An analytical technique such as high-performance liquid chromatography (HPLC) or an immunoassay or radioimmunoassay is required in conjunction to accurately determine solute concentration. Several studies have successfully applied this method to determine the skin permeability of a wide range of solutes (Stinchcomb et al. 1999; Alberti et al. 2001a, b, c; Moser et al. 2001).

## 9.5.3 Impedance Spectroscopy

Methods based on measuring solute diffusion across skin may not always provide the sensitivity required to measure small perturbations in skin permeability or follow permeability changes over short intervals of time. Electrical

measurements across the SC provide improved sensitivity (Dugard and Scheuple 1973). Electrical properties of SC parallel those of permeability and play a dominant role in the control of current flow (Lawler et al. 1960; Tregear 1966). A review of factors governing the passage of electricity across skin has been presented by Tregear (Tregear 1966).

### 9.5.3.1 Theory

Flow of ions across skin under an electric field is analogous to diffusion of solutes under a chemical gradient. Current across skin can thus be related to permeability of skin. Skin and its appendages can be represented by an equivalent circuit containing a resistance  $R$  shunted by capacitance  $C$  (Lackermeier et al. 1999). The impedance,  $Z$ , of this equivalent skin model can be represented as

$$Z = \left[ R^2 + \frac{1}{(2\pi fC)^2} \right]^{\frac{1}{2}} \quad (9.9)$$

where  $f$  is the frequency of the applied alternating current (AC) signal. A formal porous pathway theory based on Nernst–Planck flux equations and the Nernst–Einstein relations for ideal solutions has been developed that relates skin impedance to skin permeability (Lakshminarayanaiah 1965; Srinivasan and Higuchi 1990; Li et al. 1998, 1999; Tezel et al. 2003).

A simplified correlation between skin resistivity,  $R$ , and skin permeability,  $P$ , is provided by Tang et al. (2001) as

$$\log P = \log C - \log R \quad (9.10)$$

where  $C$  is dependent on the properties of the solute and the solvent in which it is dissolved.

The impedance of intact skin is in the range of several hundred kilo ohms (k $\Omega$ ). As the skin is permeabilized, impedance drops finally attaining a value of  $\sim 1$  k $\Omega$ , which corresponds to removal of the entire barrier (Naik et al. 2001). Skin impedance measurements have been used to study the effect of sonophoresis (Mitragotri et al. 1996; Tezel et al. 2001; Paliwal et al. 2006), iontophoresis (Burnette and Bagnieski 1988;

Kalia et al. 1996; Kumar and Lin 2008), and chemical enhancers on skin permeability (Karande et al. 2004; Karande et al. 2006a, b).

In comparison to diffusion measurements of solute permeability in diffusion cells, electrical impedance measurements are relatively simpler, faster, and more sensitive. Impedance-based permeability assessment provides direct readout of barrier integrity and does not require subsequent analysis, which may be tedious, time consuming, and expensive. Also, since these measurements can be performed rapidly and by use of automated systems the throughput of impedance-based assays is significantly larger compared to diffusion cells. Karande et al. have described the design of an impedance based high-throughput assay to determine the effect of chemical permeation enhancers on skin permeability (Karande et al. 2004, 2006a, b). This system, *in vitro* impedance Guided High Throughput (INSIGHT) screen, is capable of assessing thousands of formulations per day for their ability to modulate skin permeability. The authors discovered synergistic formulations of permeation enhancers using this screen, which were capable of delivering a biologically active hormone across the skin at therapeutically relevant doses. One downside of using impedance to assess skin permeability is that impedance serves only as a surrogate measure of actual skin permeability. The actual flux of a solute needs to be assessed by conventional diffusion methods.

## 9.5.4 Infrared Spectroscopy

Transport of solute molecules in the skin can be studied using spectroscopic techniques. Fourier transform infrared (FTIR) spectroscopy has been used extensively in determining skin structure, properties, hydration, and effect of permeation enhancers (Potts and Francoeur 1993; Moore and Rerek 1998; Karande et al. 2005; Mendelsohn et al. 2006).

### 9.5.4.1 Theory

FTIR spectroscopy is used to track solute molecules in the epidermis by recording their

molecular vibrations. The integrated absorbance of these vibrations is directly proportional to the amount of solute present in the skin. Depth-dependant profiling of the solute in the skin can be achieved by attenuated total reflectance (ATR)-FTIR spectroscopy. ATR-FTIR spectroscopy generally provides infor-

mation in the superficial 1–2  $\mu\text{m}$  layer of the skin. Repeated tape stripping can be used to scan successive layers of the skin for solute penetration. Transport properties for the solute can then be obtained from an unsteady state solution for Eq. (9.5) given as (Piro et al. 1997)

$$C(x) = C_0 \left( 1 - \frac{x}{L} \right) - \sum_{n=1}^{\infty} \frac{2}{n\pi} C_0 \sin \left( \frac{n\pi x}{L} \right) \exp \left( \frac{-Dn^2\pi^2 t}{L^2} \right) \quad (9.11)$$

where  $C(x)$  is the concentration of solute at a depth  $x$  from skin surface and  $C_0$  is the concentration of the solute at the skin surface.  $L$  is the total thickness of skin and  $D$  is the effective diffusivity of the solute in skin. The rate per unit area at which the solute diffuses out of the skin can be obtained by differentiation of Eq. (9.11) as

$$-D \left( \frac{\partial C}{\partial x} \right)_{x=0}$$

with time yields the total amount of solute diffusing across skin in a given time. This information can be used to obtain the permeability profile of the solute and hence its permeability across the skin. Several assumptions have been made in deriving this correlation that is discussed in Piro et al. (1997). One downside of using ATR-FTIR spectroscopy is that the solute to be monitored needs to be IR active and have a signature distinct from those of the SC components. This limitation can, in theory, be overcome using spectral correction techniques (Naik et al. 2001).

Several other methods have been used to study permeation and absorption of material into and across skin. Xiao et al. have used Raman microscopy and imaging to track penetration of phospholipids in skin (Xiao et al. 2005a, b). Williams et al. provide a critical comparison of different Raman spectroscopy techniques and their application in vivo (Williams et al. 1993). Sonavane et al. have used a combination of UV-vis spectroscopy, X-ray spectroscopy, and inductive coupled mass spectroscopy to track permeation of gold nanoparticles in the rat skin (Sonavane et al. 2008). Other groups have used photoacoustic spectroscopy for studying permeation of Carbopol 940 and transdermal gels (Christ et al.

2001; Rocha et al. 2007; Rossi et al. 2008). Remittance spectroscopy and photothermal deflection are a few of the other methods that have been suggested in this area (Gotter et al. 2008).

### 9.5.5 Trans Epidermal Water Loss

Mammalian skin has evolved to regulate the transport of material into and out of the body. One of the primary functions of skin is to regulate the loss of water from the body. It follows, then, that the quantitative measure of water loss from the skin is indicative of its barrier integrity. A device, such as an evaporimeter, that can adequately and accurately measure the water vapor flux at the skin surface, and hence the rate of trans-epidermal water loss (TEWL), can be used to assess barrier integrity of the skin. A quantitative correlation between TEWL and skin permeability has been reported (Rougier et al. 1989) and is found to be consistently reproducible in vivo and in vitro (Pinnagoda et al. 1989, 1990). Several studies have reported the use of TEWL to assess the effect of permeation enhancers on skin permeability (Loden 1992; Kanikkannan and Singh 2002; Luzardo-Alvarez et al. 2003; Tokudome and Sugibayashi 2004). A comprehensive review of their findings is provided by Levin and Maibach (Levin and Maibach 2005). This review also sheds light on possible reasons why two particular studies did not observe quantitative correlation between percutaneous absorption and TEWL (Tsai et al. 2001; Chilcott et al. 2002). Recent literature continues to provide opposing views on the use of TEWL as a



measure of skin barrier integrity (Fluhr et al. 2006; Netzlaff et al. 2006a). Nevertheless, several commercial devices based on this principle are readily available today for laboratory work.

---

## 9.6 Evaluation of Skin Permeability In Vivo

In vivo methods for quantification of solute permeation across the skin serve as a gold standard in transdermal drug delivery. Such methods can potentially eliminate variables associated with using excised human or animal skin, surrogate endpoints as well as faithfully reproduce metabolic, pharmacokinetic, and pharmacodynamic behavior of the drug molecule. Wherever possible, and practically feasible, in vivo measurements are considered reliable and superior to measurements made on model systems in vitro.

### 9.6.1 Diffusion Measurements

Diffusion cells have been designed that can be filled with drug solution and strapped on to an animal in vivo or the arm of a human volunteer (Wurster and Kramer 1961; Quisno and Doyle 1983; Leopold and Lippold 1992). Such a system allows one to study the passive permeation of a solute across the skin in vivo in much the same way as diffusion cells with excised skin or model membranes. Different endpoints can then be used to quantify permeation rates across the skin.

#### 9.6.1.1 Systemic Bioavailability

A solute whose percutaneous absorption is to be measured is applied topically to the skin and its concentration measured in blood plasma or urine over a period of time. These amounts generally tend to be very low and hence a sensitive detection technique such as radiolabeling with  $^3\text{H}$  or  $^{14}\text{C}$  is necessary (Wester et al. 1983; Gschwind et al. 2008). Caution needs to be exercised when using such techniques if the drug is susceptible to metabolism. Metabolism can lead to by-products that have significantly different pharmacokinetics

and pharmacodynamics than the parent compound and can give misleading results.

#### 9.6.1.2 Surface Loss

Alternate approach to determine in vivo percutaneous absorption is to measure the loss of solute from the surface as it penetrates the skin. This can be achieved when all residual material, contained in a reservoir, can be recovered. Difference between concentration or amount at time zero and at time of recovery provides an estimate of amount absorbed. Generally, the method used to detect the residual amount needs to be sensitive enough, especially in supersaturated systems, as the reservoir can be infinitely large when compared to the amount absorbed. Also, this method assumes that the skin does not act as a reservoir, which in itself can be a poor assumption.

### 9.6.2 Pharmacological Response

A good method to assess percutaneous absorption is to measure the biological or pharmacological response to the drug. Vasoconstriction can be used as an endpoint to measure transdermal delivery of topically applied corticosteroids (Barry 1983) and vasodilation as an endpoint for topically applied nicotines (Le and Lippold 1995). Laser Doppler flowmetry (LDF) has been used to study absorption of prostaglandin  $\text{E}_1$  ( $\text{PGE}_1$ ) (Foldvari et al. 1998), methylnicotinate (Wilkin et al. 1985; Poelman et al. 1989), and minoxidil (Wester et al. 1984) in vivo by measuring changes in cutaneous microcirculation. Reduction in blood glucose levels has been used as an endpoint to determine the efficacy of transdermal delivery of insulin (Mitragotri et al. 1995; Chen et al. 2006). The downside of this method is that it works only for drugs that have a detectable biological endpoint and can tend to be more qualitative than quantitative.

### 9.6.3 Other Approaches

Several of the methods discussed above for in vitro skin barrier assessment can be adopted

for *in vivo* measurements with little or no modification at all. Tape stripping and TEWL measurements in particular are attractive for *in vivo* measurements as they are relatively straightforward and minimally invasive or noninvasive. The amount of solute that penetrates the SC can be quantified *in vivo*, in humans, by tape stripping with an appropriate adhesive tape (Tsai et al. 1991). In case of animal studies, *in vivo*, it is possible to quantify penetration in deeper skin layers by sacrificing the animal and harvesting its skin. The concentration profiles can then be used to determine solute permeability as suggested in Eq. (9.8). Umemura et al. have used tape stripping *in vivo* in healthy human subjects to determine the pharmacokinetics of topically applied maxacalcitol from an ointment and lotion (Umemura et al. 2008). Puglia et al. have used tape stripping to quantify skin penetration of lipid nanoparticles (Puglia et al. 2008). A review of tape-stripping methods in determining percutaneous absorption *in vivo* is provided by Herkenne et al. (Herkenne et al. 2008). Several reports have documented the use of TEWL to assess the barrier integrity after treatment with physical or chemical enhancers of skin permeability (Atrux-Tallau et al. 2008; Kolli and Banga 2008). Maibach et al. have documented the effect of successive tape strippings on TEWL *in vivo* in human subjects as well as compared two different configurations for devices measuring TEWL (Zhai et al. 2007). Xhaufaire-Uhoda et al. have used TEWL measurements to study barrier repair after the application of miconazole nitrate and tape stripping (Xhaufaire-Uhoda et al. 2006). Among the various spectroscopic techniques, ATR-FTIR spectroscopy has been used extensively in tracking solute permeation in the skin (Ayala-Bravo et al. 2003; Tsai et al. 2003; Curdy et al. 2004; Escobar-Chavez et al. 2005; Remane et al. 2006). A comprehensive review of ATR-FTIR spectroscopy and its use in *in vivo* studies appears in Naik et al. (Naik et al. 2001). Raman spectroscopy, similar in principle to FTIR spectroscopy, has also been used in studying transdermal solute penetration *in vivo*. A big advantage of Raman spectroscopy is that it does not require tape stripping of the skin for depth profiling and

is thus a truly noninvasive technique. Stamatias et al. have used *in vivo* confocal Raman microspectroscopy to study the uptake of vegetable oils and paraffin oil in infants (Stamatias et al. 2008). Pudney et al. have demonstrated the use of Raman spectroscopy to obtain depth profiles of trans-retinol in the epidermis for 10 h after application in an *in vivo* setting (Pudney et al. 2007). Caspers et al. have used confocal Raman spectroscopy to detect dimethyl sulfoxide in the SC (Caspers et al. 2002). For both techniques, ATR-FTIR and Raman spectroscopy, the molecule of interest should have an active IR signature of sufficient intensity that is distinct from the signatures of skin components. An additional drawback of using Raman spectroscopy is that it can only provide relative concentrations as against absolute amounts of the diffusing solute in different layers of the skin. Impedance spectroscopy is a highly sensitive and relatively straightforward technique that can be used *in vivo* to assess skin barrier integrity. Curdy et al. have used impedance spectroscopy to follow barrier recovery after the application of iontophoresis (Curdy et al. 2002). Dujardin et al. describe the use of impedance measurements to assess effects of electroporation on barrier function *in vivo* in rats (Dujardin et al. 2002). Kalia et al. have looked at the effect of surfactant treatment and iontophoresis on skin impedance *in vivo* (Kalia and Guy 1997).

In addition, several other techniques have been utilized to quantify *in vivo* transdermal delivery (Herkenne et al. 2008). These include creation of suction blisters and punch biopsies. Although relatively straightforward, these are painful and invasive procedures that are less popular in studying percutaneous absorption of solutes, especially in human subjects. Recently, microdialysis has been suggested as a novel technique to measure the diffusion of solutes across the skin (Kreilgaard 2002; Mathy et al. 2005). A thin probe perfused with a physiological solution is implanted under the dermis where, on equilibration, it can exchange material with the extracellular tissue components by passive diffusion. The perfusate from the probe can then be analyzed for the solute diffusing across the skin. A

time-based concentration profile of the solute diffusing across the skin into the probe can be used to determine the pharmacokinetics of the solute. A practical challenge associated with this method is the careful and reproducible insertion of the probe in the deeper layers of the skin. Also, extremely sensitive detection methods are required to analyze the small amounts of material obtained from the perfusate.

### Conclusion

The field of transdermal drug delivery research has come of age and is rich with opportunities and promises. A combination of improved representative systems that meet regulatory considerations and capture relevant biophysical properties of the skin, reliable and accurate quantification methods, as well as innovative skin permeabilization strategies will expedite the appearance of transdermal delivery systems in this new century.

### References

- Abraham W, Downing DT (1989) Permeability studies on model membranes prepared from stratum-corneum lipids. *J Invest Dermatol* 92(3):393
- Abraham W, Wertz PW et al (1985) Linoleate-rich acylglucosylceramides of pig epidermis: structure determination by proton magnetic resonance. *J Lipid Res* 26:761–766
- Ainsworth M (1960) Methods for measuring percutaneous absorption. *J Soc Cosmet Chem* 11:69–78
- Akomeah FK, Martin GP et al (2007) Variability in human skin permeability in vitro: comparing penetrants with different physicochemical properties. *J Pharm Sci* 96(4):824–834
- Alberti I, Kalia YN et al (2001a) Effect of ethanol and isopropyl myristate on the availability of topical terbinafine in human stratum corneum, in vivo. *Int J Pharm* 219(1–2):11–19
- Alberti I, Kalia YN et al (2001b) In vivo assessment of enhanced topical delivery of terbinafine to human stratum corneum. *J Control Release* 71(3):319–327
- Alberti I, Kalia YN et al (2001c) Assessment and prediction of the cutaneous bioavailability of topical terbinafine, in vivo, in man. *Pharm Res* 18(10):1472–1475
- Aramaki Y, Arima H et al (2003) Intradermal delivery of anti-sense oligonucleotides by the pulse depolarization iontophoretic system. *Biol Pharm Bull* 26(10):1461–1466
- Artusi M, Nicoli S et al (2004) Effect of chemical enhancers and iontophoresis on thiocholchicoside permeation across rabbit and human skin in vitro. *J Pharm Sci* 93(10):2431–2438
- Astley JP, Levine M (1976) Effect of dimethyl-sulfoxide on permeability of human skin in vitro. *J Pharm Sci* 65(2):210–215
- Atrux-Tallau N, Huynh NTT et al (2008) Effects of physical and chemical treatments upon biophysical properties and micro-relief of human skin. *Arch Dermatol Res* 300(5):243–251
- Audus KL, Bartel RL et al (1990) The use of cultured epithelial and endothelial-cells for drug transport and metabolism studies. *Pharm Res* 7(5):435–451
- Ayala-Bravo HA, Quintanar-Guerrero D et al (2003) Effects of sucrose oleate and sucrose laureate on in vivo human stratum corneum permeability. *Pharm Res* 20(8):1267–1273
- Bach M, Lippold BC (1998) Percutaneous penetration enhancement and its quantification. *Eur J Pharm Biopharm* 46(1):1–13
- Baden HP, Pathak MA (1967) The metabolism and function of urocanic acid in skin. *J Invest Dermatol* 48:11–17
- Baden HP, Goldsmith EL et al (1973) A comparative study of the physicochemical properties of human keratinized tissues. *Biochim Biophys Acta* 322:269–278
- Bakand S, Winder C et al (2006) An experimental in vitro model for dynamic direct exposure of human cells to airborne contaminants. *Toxicol Lett* 165(1):1–10
- Balsari AL, Morelli D et al (1994) Protection against doxorubicin-induced alopecia in rats by liposome-entrapped monoclonal-antibodies. *FASEB J* 8(2):226–230
- Barker CL, McHale MT et al (2004) The development and characterization of an in vitro model of psoriasis. *J Invest Dermatol* 123(5):892–901
- Barry BW (1983) *Dermatological formulations Percutaneous absorption*. Marcel Dekker, New York
- Bary BW (1988) Action of skin penetration enhancers – the lipid protein partitioning theory. *Int J Cosmet Sci* 10(6):281–293
- Barry BW (1991) Lipid-protein-partitioning theory of skin penetration enhancement. *J Control Release* 15(3):237–248
- Barry BW (2001a) Is transdermal drug delivery research still important today? *Drug Discov Today* 6(19):967–971
- Barry BW (2001b) Novel mechanisms and devices to enable successful transdermal drug delivery. *Eur J Pharm Sci* 14(2):101–114
- Barry BW (2004) Breaching the skin's barrier to drugs. *Nat Biotechnol* 22(2):165–167
- Barry BW, Brace AR (1977) Permeation of estrone, estradiol, estriol and dexamethasone across cellulose-acetate membrane. *J Pharm Pharmacol* 29(7):397–400
- Barry BW, Eleini DID (1976) Influence of nonionic surfactants on permeation of hydrocortisone, dexamethasone, testosterone and progesterone across cellulose-acetate membrane. *J Pharm Pharmacol* 28(3):219–227

- Beare JM, Cheeseman EA et al (1958) The pH of the skin surface of children with seborrheic dermatitis compared with unaffected children. *Br J Dermatol* 70:233
- Beastall J, Guy RH et al (1986) The influence of urea on percutaneous-absorption. *Pharm Res* 3(5):294–297
- Bell E, Ehrlich HP et al (1981) Living tissue formed in vitro and accepted as skin-equivalent tissue of full thickness. *Science* 211(4486):1052–1054
- Ben-Shabat S, Baruch N et al (2007) Conjugates of unsaturated fatty acids with propylene glycol as potentially less-irritant skin penetration enhancers. *Drug Dev Ind Pharm* 33(11):1169–1175
- Berenson GS, Burch GE (1951) Studies of diffusion of water through dead human skin – the effect of different environmental states and of chemical alterations of the epidermis. *Am J Trop Med* 31(6):842–853
- Bhandari KH, Lee DX et al (2008) Evaluation of skin permeation and accumulation profiles of a highly lipophilic fatty ester. *Arch Pharm Res* 31(2):242–249
- Blank IH (1939) Measurement of pH of the skin surface. *J Invest Dermatol* 2:67
- Blank IH (1952) Factors which influence the water content of stratum corneum. *J Invest Dermatol* 18:433–440
- Blank IH, Scheuplein RJ (1973) Mechanism of percutaneous absorption. IV. Penetration of nonelectrolytes (alcohols) from aqueous solutions and from pure liquids. *J Invest Dermatol* 60(5):286–296
- Bond JR, Barry BW (1988a) Damaging effect of acetone on the permeability barrier of hairless mouse skin compared with that of human-skin. *Int J Pharm* 41(1–2):91–93
- Bond JR, Barry BW (1988b) Hairless mouse skin is limited as a model for assessing the effects of penetration enhancers in human-skin. *J Invest Dermatol* 90(6):810–813
- Bond JR, Barry BW (1988c) Limitations of hairless mouse skin as a model for in vitro permeation studies through human-skin – hydration damage. *J Invest Dermatol* 90(4):486–489
- Bonina FP, Montenegro L et al (1993) In-vitro percutaneous-absorption evaluation of phenobarbital through hairless mouse, adult and premature human skin. *Int J Pharm* 98(1–3):93–99
- Borgia SL, Schupp P et al (2008) In vitro skin absorption and drug release – a comparison of six commercial prednicarbate preparations for topical use. *Eur J Pharm Biopharm* 68(2):380–389
- Bos JD, Meinardi MHM (2000) The 500 dalton rule for the skin penetration of chemical compounds and drugs. *Exp Dermatol* 9(3):165–169
- Bosman IJ, Lawant AL et al (1996) Novel diffusion cell for in vitro transdermal permeation, compatible with automated dynamic sampling. *J Pharm Biomed Anal* 14(8–10):1015–1023
- Botham PA (2004) The validation of in vitro methods for skin irritation. *Toxicol Lett* 149(1–3):387–390
- Bouwstra JA (1997) The skin, a well organized membrane. *Colloids Surf A* 123–124:403–413
- Bouwstra JA, Gooris GS et al (1998) Role of ceramide 1 in the molecular organisation of the stratum corneum lipids. *J Lipid Res* 39:186–196
- Boyce ST, Christianson DJ et al (1988) Structure of a collagen-gag dermal skin substitute optimized for cultured human epidermal-keratinocytes. *J Biomed Mater Res* 22(10):939–957
- Breathnach AS, Goodman T et al (1973) Freeze fracture replication of cells of stratum corneum of human epidermis. *J Anat* 114:65–81
- Breau LM, McGrath PJ et al (2001) Facial expression of children receiving immunizations: a principal components analysis of the child facial coding system. *Clin J Pain* 17(2):178–186
- Bronaugh RL, Collier S (1991) Preparation of human and animal skin. In: Bronaugh RL, Maibach HI (eds) *In vitro percutaneous absorption: principles, fundamentals, and applications*. CRC Press, Boca Raton, pp 1–6
- Bronaugh RL, Stewart RF (1984) Methods for in vitro percutaneous-absorption studies. 3. Hydrophobic compounds. *J Pharm Sci* 73(9):1255–1258
- Bronaugh RL, Stewart RF (1986) Methods for in vitro percutaneous-absorption studies. 6. Preparation of the barrier layer. *J Pharm Sci* 75(5):487–491
- Bronaugh RL, Stewart RF et al (1982) Methods for in vitro percutaneous absorption studies II. Animal models for human skin. *Toxicol Appl Pharmacol* 62(3):481–488
- Bronaugh RL, Stewart RF et al (1983) Differences in permeability of rat skin related to sex and body site. *J Soc Cosmet Chem* 34(3):127–135
- Bronaugh RL, Stewart RF et al (1986) Methods for in vitro percutaneous-absorption studies. 7. Use of excised human-skin. *J Pharm Sci* 75(11):1094–1097
- Brown DWC, Ulsamer AG (1975) Percutaneous penetration of hexachlorophene as related to receptor solutions. *Food Cosmet Toxicol* 13(1):81–86
- Burnette RR, Bagniefski TM (1988) Influence of constant current iontophoresis on the impedance and passive na+ permeability of excised nude-mouse skin. *J Pharm Sci* 77(6):492–497
- Carr RD, Wieland RG (1966) Corticosteroid reservoir in stratum corneum. *Arch Dermatol* 94(1):81–84
- Caspers PJ, Williams AC et al (2002) Monitoring the penetration enhancer dimethyl sulfoxide in human stratum corneum in vivo by confocal Raman spectroscopy. *Pharm Res* 19(10):1577–1580
- Chen H, Langer R (1998) Oral particulate delivery: status and future trends. *Adv Drug Deliv Rev* 34(2–3):339–350
- Chen YP, Shen YY et al (2006) Transdermal protein delivery by a coadministered peptide identified via phage display. *Nat Biotechnol* 24(4):455–460
- Chilcott RP, Dalton CH et al (2002) Transepidermal water loss does not correlate with skin barrier function in vitro. *J Invest Dermatol* 118(5):871–875
- Cho CW, Choi JS et al (2008) Development of the ambroxol gels for enhanced transdermal delivery. *Drug Dev Ind Pharm* 34(3):330–335

- Christ A, Szurkowski J et al (2001) Drug penetration into a membrane investigated by photoacoustic and FTIR-ATR spectroscopy. *Anal Sci* 17:S371–S373
- Coldman MF, Poulsen BJ et al (1969) Enhancement of percutaneous absorption by use of volatile – nonvolatile systems as vehicles. *J Pharm Sci* 58(9):1098–1102
- Cooper ER (1982) Effect of decylmethyl sulfoxide on skin penetration. In: Mittal KL, Fendler EJ (eds) *Solution behaviour of surfactants: theoretical and applied aspects*. Plenum Press, New York, pp 1505–1516
- Cornwell PA, Barry BW (1995) Effects of penetration enhancer treatment on the statistical distribution of human skin permeabilities. *Int J Pharm* 117(1):101–112
- Corrigan OI, Farvar MA et al (1980) Drug membrane-transport enhancement using high-energy drug polyvinylpyrrolidone (PVP) co-precipitates. *Int J Pharm* 5(3):229–238
- Coutelegros A, Maitani Y et al (1992) Combined effects of ph. cosolvent and penetration enhancers on the in vitro buccal absorption of propranolol through excised hamster-cheek pouch. *Int J Pharm* 84(2):117–128
- Crank J (1975) *The Mathematics of diffusion*. Oxford University Press, Inc., New York
- Cronin MTD, Dearden JC et al (1998) An investigation of the mechanism of flux across polydimethylsiloxane membranes by use of quantitative structure-permeability relationships. *J Pharm Pharmacol* 50(2):143–152
- Crooke RM, Crooke ST et al (1996) Effect of antisense oligonucleotides on cytokine release from human keratinocytes in an in vitro model of skin. *Toxicol Appl Pharmacol* 140(1):85–93
- Cross SE, Pugh WJ et al (2001) Probing the effect of vehicles on topical delivery: understanding the basic relationship between solvent and solute penetration using silicone membranes. *Pharm Res* 18(7):999–1005
- Curdy C, Kalia YN et al (2002) Post-iontophoresis recovery of human skin impedance in vivo. *Eur J Pharm Biopharm* 53(1):15–21
- Curdy C, Naik A et al (2004) Non-invasive assessment of the effect of formulation excipients on stratum corneum barrier function in vivo. *Int J Pharm* 271(1–2):251–256
- Davis DA (1990) TestSkin racks up in vitro converts. *Drug Cosmet Indust* 146(5):40
- de Jager M, Groenink W et al (2006a) A novel in vitro percutaneous penetration model: evaluation of barrier properties with P-aminobenzoic acid and two of its derivatives. *Pharm Res* 23(5):951–960
- de Jager M, Groenink W et al (2006b) Preparation and characterization of a stratum corneum substitute for in vitro percutaneous penetration studies. *Biochim Biophys Acta Biomembranes* 1758(5):636–644
- de Kruyff B, van Dijck PWM et al (1974) Non random distribution of cholesterol in phosphatidylcholine bilayers. *Biochim Biophys Acta* 356:1–7
- Delgado-Charro MB, Guy RH (2001) Transdermal iontophoresis for controlled drug delivery and non-invasive monitoring. *STP Pharma Sci* 11(6):403–414
- Demeere ALJ, Tomlinson E (1984) Physicochemical description of the absorption rate of a solute between water and 2,2,4-trimethylpentane. *Int J Pharm* 22(2–3):177–196
- Denet AR, Vanbever R et al (2004) Skin electroporation for transdermal and topical delivery. *Adv Drug Deliv Rev* 56(5):659–674
- Dewhurst DG, Williams A (1993) Frog-skin – a computer-simulation of experiments performed on frog-skin in vitro to investigate the epithelial transport of ions. *ATLA Altern Lab Anim* 21(3):350–358
- Dick IP, Scott RC (1992) Pig ear skin as an in vitro model for human skin permeability. *J Pharm Pharmacol* 44(8):640–645
- Domashenko A, Gupta S et al (2000) Efficient delivery of transgenes on human hair follicle progenitor cells using topical lipoplex. *Nat Biotechnol* 18(4):420–423
- Downing DT (1992) Lipid and protein structures in the permeability barrier of mammalian epidermis. *J Lipid Res* 33:301–313
- Drachman D (1989) Novel drug delivery systems-opportunities and caveats. *Neurobiol Aging* 10(5):632–633
- Draize JH (1942) The determination of pH of the skin of man and common laboratory animals. *J Invest Dermatol* 5:77
- Dreher F, Fouchard F et al (2002) Comparison of cutaneous bioavailability of cosmetic preparations containing caffeine or alpha-tocopherol applied on human skin models or human skin ex vivo at finite doses. *Skin Pharmacol Appl Skin Physiol* 15:40–58
- Du Plessis J, Pugh WJ et al (2002) The effect of the nature of H-bonding groups on diffusion through PDMS membranes saturated with octanol and toluene. *Eur J Pharm Sci* 15(1):63–69
- Dugard PH, Scheuple RJ (1973) Effects of ionic surfactants on permeability of human epidermis – electro-metric study. *J Invest Dermatol* 60(5):263–269
- Dugard PH, Walker M et al (1984) Absorption of some glycol ethers through human-skin in vitro. *Environ Health Perspect* 57:193–197
- Dujardin N, Staes E et al (2002) In vivo assessment of skin electroporation using square wave pulses. *J Control Release* 79(1–3):219–227
- Duncan EJ, Brown A, Lundy P, Sawyer TW, Hamilton M, Hill I, Conley JD (2002) Site-specific percutaneous absorption of methyl salicylate and VX in domestic swine. *J Appl Toxicol* 22(3):141–148
- Dupuis D, Rougier A et al (1986) In vivo relationship between percutaneous absorption and transepidermal water loss according to anatomic site in man. *J Soc Cosmet Chem* 37(5):351–357
- Dyer A, Hayes GG et al (1979) Diffusion through skin and model systems. *Int J Cosmet Sci* 1(2):91–100
- Eder I, Müller-Goymann CC (1995) In vivo amino acid extraction from human stratum corneum as indicator for penetration enhancing properties of oleic acid and isopropylmyristate. *Pharm Pharmacol Lett* 1:14–17
- El Ghalbzouri A, Lamme EN et al (2004) The use of PEGT/PBT as a dermal scaffold for skin tissue engineering. *Biomaterials* 25(15):2987–2996

- Elewski BE (2007) Percutaneous absorption kinetics of topical metronidazole formulations in vitro in the human cadaver skin model. *Adv Ther* 24(2):239–246
- Elgorashi AS, Heard CM et al (2008) Transdermal delivery enhancement of haloperidol from gel formulations by 1,8-cineole. *J Pharm Pharmacol* 60(6):689–692
- Elias PM, Friend DS (1975) The permeability barrier in mammalian epidermis. *J Cell Biol* 65:180–191
- Elias PM, McNutt NS et al (1977) Membrane alterations during cornification of mammalian squamous epithelia: a freeze-fracture, tracer and thin-section study. *Anat Rec* 189:577–594
- Elias PM, Brown BE et al (1980) The permeability barrier in essential fatty-acid deficiency – evidence for a direct role for linoleic-acid in barrier function. *J Invest Dermatol* 74(4):230–233
- Elias PM, Cooper ER et al (1981) Percutaneous transport in relation to stratum-corneum structure and lipid-composition. *J Invest Dermatol* 76(4):297–301
- Elyan BM, Sidhom MB et al (1996) Evaluation of the effect of different fatty acids on the percutaneous absorption of metaproterenol sulfate. *J Pharm Sci* 85(1):101–105
- Engström, S, Forslind B et al (1995) Lipid polymorphism – a key to the understanding of skin penetration. In: Brain KR, James VJ, Walters KA (eds) *Proceedings of prediction of percutaneous penetration*, vol 4b. STS Publishing Ltd., Cardiff, pp 163–166
- Escobar-Chavez JJ, Quintanar-Guerrero D et al (2005) In vivo skin permeation of sodium naproxen formulated in pluronic F-127 gels: effect of Azone (R) and Transcutol (R). *Drug Dev Ind Pharm* 31(4–5):447–454
- Faller C, Bracher M (2002) Reconstructed skin kits: reproducibility of cutaneous irritancy testing. *Skin Pharmacol Appl Skin Physiol* 15:74–91
- Farinha A, Toscano C et al (2003) Permeation of naproxen from saturated solutions and commercial formulations through synthetic membranes. *Drug Dev Ind Pharm* 29(4):489–494
- Feingold K, Qiang M et al (1990) Cholesterol synthesis is required for cutaneous barrier function in mice. *J Clin Invest* 86:1738–1745
- Fenske DB, Thewalt JL et al (1994) Models of stratum corneum intercellular membranes: 2H NMR of macroscopically oriented multilayers. *Biophys J* 67:1562–1573
- Fettiplace R, Haydon DA (1980) Water permeability of lipid membranes. *Phys Rev* 60:510–550
- Flamand N, Marrot L et al (2006) Development of genotoxicity test procedures with Episkin®, a reconstructed human skin model: towards new tools for in vitro risk assessment of dermally applied compounds? *Mut Res (Genetic Toxicology and Environmental Mutagenesis)* 606(1–2):39–51
- Fluhr J, Kao J et al (2001) Generation of free fatty acids from phospholipids regulates stratum corneum acidification and integrity. *J Invest Dermatol* 117:44–51
- Fluhr JW, Feingold KR et al (2006) Transepidermal water loss reflects permeability barrier status: validation in human and rodent in vivo and ex vivo models. *Exp Dermatol* 15(7):483–492
- Flynn GL (1985) Mechanism of percutaneous absorption from physicochemical evidence. In: Bronaugh RL, Maibach H (eds) *Percutaneous absorption: mechanisms-methodology-drug delivery*. Marcel Dekker, New York, pp 17–42
- Flynn GL, Smith EW (1971) Membrane diffusion I: design and testing of a new multifaceted diffusion cell. *J Pharma Sci* 60(11):1713–1717
- Foldvari M, Oguejiofor CJ et al (1998) Transcutaneous delivery of prostaglandin E1: in vitro and laser doppler flowmetry study. *J Pharm Sci* 87(6):721–725
- Foreman MI, Kelly I (1976) The diffusion of nandrolone through hydrated human cadaver skin. *Br J Dermatol* 95(3):265–270
- Foreman MI, Picton W et al (1979) Effect of topical crude coal-tar treatment on unstimulated hairless hamster skin. *Br J Dermatol* 100(6):707–715
- Forslind B (1994) A domain mosaic model of the skin barrier. *Acta Derm Venereol* 74:1–6
- Fransson J, Heffler LC et al (1998) Culture of human epidermal Langerhans cells in a skin equivalent. *Br J Dermatol* 139(4):598–604
- Frantz SW (1990) Instrumentation and methodology for in vitro diffusion cells. In: Kemppainen BW, Reifenrath WG (eds) *Methods for skin absorption*. CRC Press, Boca Raton, pp 35–59
- Franz TJ (1975) Percutaneous absorption – relevance of in vitro data. *J Invest Dermatol* 64(3):190–195
- Franz TJ (1978) The finite dose technique as a valid in vitro model for the study of percutaneous absorption in man. *Curr Probl Dermatol* 7:58–68
- Fredriksson T (1961) Studies on percutaneous absorption of parathion and paraoxon. 2. Distribution of 32p-labelled parathion within skin. *Acta Derm Venereol* 41(5):344
- Friberg SE, Kayali I (1989) Water evaporation rates from a model of stratum-corneum lipids. *J Pharm Sci* 78(8):639–643
- Friberg SE, Kayali I et al (1990) Water permeation of reaggregated stratum-corneum with model lipids. *J Invest Dermatol* 94(3):377–380
- Friend DR (1992) In vitro skin permeation techniques. *J Control Release* 18(3):235–248
- Frum Y, Eccleston GM et al (2007) Evidence that drug flux across synthetic membranes is described by normally distributed permeability coefficients. *Eur J Pharm Biopharm* 67(2):434–439
- Galey WR, Lonsdale HK et al (1976) In vitro permeability of skin and buccal mucosa to selected drugs and tritiated-water. *J Invest Dermatol* 67(6):713–717
- Goates CY, Knutson K (1993) Enhanced permeation and stratum-corneum structural alterations in the presence of dithiothreitol. *Biochim Biophys Acta* 1153(2):289–298
- Gotter B, Faubel W et al (2008) Optical methods for measurements of skin penetration. *Skin Pharmacol Physiol* 21(3):156–165

- Grasso P, Lansdown AB (1972) Methods of measuring, and factors affecting, percutaneous absorption. *J Soc Cosmet Chem* 23(8):481
- Gray GM, Yardley HJ (1975) Lipid compositions of cells isolated from pig, human, and rat epidermis. *J Lipid Res* 16(6):434–440
- Green H, Kehinde O et al (1979) Growth of cultured human epidermal-cells into multiple epithelia suitable for grafting. *Proc Natl Acad Sci U S A* 76(11):5665–5668
- Green H, Fuchs E et al (1982) Differentiated structural components of the keratinocyte. *Cold Spring Harbor Symp Quant Biol* 1:293–301
- Gschwind H-P, Waldmeier F et al (2008) Pimecrolimus: skin disposition after topical administration in minipigs in vivo and in human skin in vitro. *Eur J Pharm Sci* 33(1):9–19
- Gummer CL, Maibach HI (1991) Diffusion cell design. In: Bronaugh RL, Maibach HI (eds) *In vitro percutaneous absorption: principles, fundamentals, and applications*. CRC Press, Boca Raton, pp 7–16
- Gummer CL, Hinz RS et al (1987) The skin penetration cell – a design update. *Int J Pharm* 40(1–2):101–104
- Guy RH (1996) Current status and future prospects of transdermal drug delivery. *Pharm Res* 13(12):1765–1769
- Gysler A, Kleuser B et al (1999) Skin penetration and metabolism of topical glucocorticoids in reconstructed epidermis and in excised human skin. *Pharm Res* 16(9):1386–1391
- Hadgraft J, Ridout G (1987) Development of model membranes for percutaneous absorption measurements. I. Isopropyl myristate. *Int J Pharm* 39(1–2):149–156
- Hadgraft J, Ridout G (1988) Development of model membranes for percutaneous absorption measurements. II. Dipalmitoyl phosphatidylcholine, linoleic acid and tetradecane. *Int J Pharm* 42(1–3):97–104
- Hai NT, Kim J et al (2008) Formulation and biopharmaceutical evaluation of transdermal patch containing benzotropine. *Int J Pharm* 357(1–2):55–60
- Haigh JM, Smith EW (1994) The selection and use of natural and synthetic membranes for in-vitro diffusion experiments. *Eur J Pharm Sci* 2(5–6):311–330
- Harrison SM, Barry BW et al (1984) Effects of freezing on human-skin permeability. *J Pharm Pharmacol* 36(4):261–262
- Hashimoto K (1971a) Demonstration of intercellular spaces of human eccrine sweat gland by lanthanum. I. Secretory coil. *J Ultrastruct Res* 36(1–2):249
- Hashimoto K (1971b) Demonstration of intercellular spaces of human eccrine sweat gland by lanthanum. 2. Duct. *J Ultrastruct Res* 37(5–6):504
- Hashimoto K, Gross BG et al (1965) Ultrastructure of skin of human embryos. i. Intraepidermal eccrine sweat duct. *J Invest Dermatol* 45(3):139
- Hawkins GS, Reifenrath WG (1986) Influence of skin source, penetration cell fluid, and partition-coefficient on in vitro skin penetration. *J Pharm Sci* 75(4):378–381
- Hayden PJ, Burnham B et al (2004) Wound healing response or a full thickness in vitro human skin equivalent (EpiDerm-FT 200) after solar UV-irradiation. *J Invest Dermatol* 122(3):A141
- Hayden PJ, Petrali JP et al (2005) Development of a full thickness in vitro human skin equivalent (EpiDerm-FT) for sulfur mustard research. *J Invest Dermatol* 124(4):A29
- He W, Guo XX et al (2008) Transdermal permeation enhancement of N-trimethyl chitosan for testosterone. *Int J Pharm* 356(1–2):82–87
- Hedberg CL, Wertz PW et al (1988) The time course of biosynthesis of epidermal lipids. *J Invest Dermatol* 91(2):169–174
- Herkenne C, Alberti I et al (2008) In vivo methods for the assessment of topical drug bioavailability. *Pharm Res* 25(1):87–103
- Hinz RS, Hodson CD et al (1989) In vitro percutaneous penetration – evaluation of the utility of hairless mouse skin. *J Invest Dermatol* 93(1):87–91
- Hoelgaard A, Mollgaard B (1982) Permeation of linoleic acid through skin in vitro. *J Pharm Pharmacol* 34(9):610–611
- Holbrook KA, Odland GF (1974) Regional differences in thickness (cell layers) of human stratum-corneum – ultrastructural analysis. *J Invest Dermatol* 62(4):415–422
- Holland JM, Kao JY et al (1984) A multisample apparatus for kinetic evaluation of skin penetration in vitro – the influence of viability and metabolic status of the skin. *Toxicol Appl Pharmacol* 72(2):272–280
- Holland DB, Bojar RA et al (2008) Microbial colonization of an in vitro model of a tissue engineered human skin equivalent – a novel approach. *FEMS Microbiol Lett* 279(1):110–115
- Hou SYE, Flynn GL (1997) Influences of 1-dodecylazacycloheptan-2-one on permeation of membranes by weak electrolytes. 1. Theoretical analysis of weak electrolyte diffusion through membranes and studies involving silicone rubber membranes. *J Pharm Sci* 86(1):85–91
- Houk J, Guy RH (1988) Membrane models for skin penetration studies. *Chem Rev* 88(3):455–471
- Hueber F, Besnard M et al (1994) Percutaneous-absorption of estradiol and progesterone in normal and appendage-free skin of the hairless rat – lack of importance of nutritional blood-flow. *Skin Pharmacol* 7(5):245–256
- Hughes MF, Fisher HL et al (1994) Effect of age on the in-vitro percutaneous-absorption of phenols in mice. *Toxicol In Vitro* 8(2):221–227
- Ito K, Kato Y et al (2007) Involvement of organic anion transport system in transdermal absorption of flurbiprofen. *J Control Release* 124(1–2):60–68
- Jacobi U, Kaiser M et al (2007) Porcine ear skin: an in vitro model for human skin. *Skin Res Technol* 13(1):19–24

- Kalia YN, Guy RH (1997) Interaction between penetration enhancers and iontophoresis: effect on human skin impedance in vivo. *J Control Release* 44(1):33–42
- Kalia YN, Nonato LB et al (1996) The effect of iontophoresis on skin barrier integrity: non-invasive evaluation by impedance spectroscopy and transepidermal water loss. *Pharm Res* 13(6):957–960
- Kandarova H, Liebsch M et al (2006) Assessment of the human epidermis model SkinEthic RHE for in vitro skin corrosion testing of chemicals according to new OECD TG 431. *Toxicol In Vitro* 20(5):547–559
- Kandarova H, Richter H et al (2007) Stratum corneum architecture of reconstructed human skin models monitored by fluorescent confocal laser scanning microscopy. *Laser Phys Lett* 4(4):308–311
- Kane A, Lloyd J et al (1999) Transmission of hepatitis B, hepatitis C and human immunodeficiency viruses through unsafe injections in the developing world: model-based regional estimates. *Bull World Health Organ* 77(10):801–807
- Kanikkannan N, Singh M (2002) Skin permeation enhancement effect and skin irritation of saturated fatty alcohols. *Int J Pharm* 248(1–2):219–228
- Kao J, Hall J et al (1983) Quantitation of cutaneous toxicity – an in vitro approach using skin organ-culture. *Toxicol Appl Pharmacol* 68(2):206–217
- Kao J, Hall J et al (1988) In vitro percutaneous-absorption in mouse skin – influence of skin appendages. *Toxicol Appl Pharmacol* 94(1):93–103
- Karande P, Mitragotri S (2003) Dependence of skin permeability on contact area. *Pharm Res* 20(2):257–263
- Karande P, Jain A et al (2004) Discovery of transdermal penetration enhancers by high-throughput screening. *Nat Biotechnol* 22(2):192–197
- Karande P, Jain A et al (2005) Design principles of chemical penetration enhancers for transdermal drug delivery. *Proc Natl Acad Sci U S A* 102(13):4688–4693
- Karande P, Jain A et al (2006a) Relationships between skin's electrical impedance and permeability in the presence of chemical enhancers. *J Control Release* 110(2):307–313
- Karande P, Jain A et al (2006b) Synergistic combinations of penetration enhancers and their discovery by high-throughput screening. In: Katdare A, Chaubal M (eds) *Excipient development for pharmaceutical, biotechnology, and drug delivery systems*. Informa Healthcare, New York/London
- Kermode M (2004) Unsafe injections in low-income country health settings: need for injection safety promotion to prevent the spread of blood-borne viruses. *Health Promot Int* 19(1):95–103
- Kietzmann M, Loscher W et al (1993) The isolated-perfused bovine udder as an in-vitro model of percutaneous drug absorption skin viability and percutaneous-absorption of dexamethasone, benzoyl peroxide, and etofenamate. *J Pharmacol Toxicol Methods* 30(2):75–84
- Kim YC, Park JH et al (2008) Synergistic enhancement of skin permeability by N-lauroylsarcosine and ethanol. *Int J Pharm* 352(1–2):129–138
- Kitson N, Thewalt J et al (1994) A model membrane approach to the epidermal permeability barrier. *Biochemistry* 33(21):6707–6715
- Kittayanond D, Dowton SM et al (1992) Development of a model of the lipid constituent phase of the stratum corneum. 2. Preparation of artificial membranes from synthetic lipids and assessment of permeability properties using in vitro diffusion experiments. *J Soc Cosmet Chem* 43(5):237–249
- Kolli CS, Banga AK (2008) Characterization of solid maltose microneedles and their use for transdermal delivery. *Pharm Res* 25(1):104–113
- Kreilgaard M (2002) Assessment of cutaneous drug delivery using microdialysis. *Adv Drug Deliv Rev* 54(Suppl 1):S99–S121
- Kuempel D, Swartzendruber DC et al (1998) In vitro reconstruction of stratum corneum lipid lamellae. *Biochim Biophys Acta Biomembranes* 1372(1):135–140
- Kumar MG, Lin SS (2008) Transdermal iontophoresis: impact on skin integrity as evaluated by various methods. *Crit Rev Ther Drug Carrier Syst* 25(4):381–401
- Lackermeier AH, McAdams ET et al (1999) In vivo AC impedance spectroscopy of human skin: theory and problems in monitoring of passive percutaneous drug delivery. *Ann N Y Acad Sci* 873(Electrical Bioimpedance Methods: Applications to Medicine and Biotechnology):197–213
- Lademann J, Richter H et al (2006) Hair follicles – a long-term reservoir for drug delivery. *Skin Pharmacol Physiol* 19(4):232–236
- Lakshminarayanaiah N (1965) Transport phenomena in artificial membranes. *Chem Rev* 65(5):491
- Langer R (1990) Novel drug delivery systems. *Chem Br* 26(3):232
- Langguth P, Spahn H et al (1986) Variations of in vitro nitroglycerine permeation through human-epidermis. *Pharm Res* 3(1):61–63
- Larsen CG, Larsen FG et al (1988) Preparation of human epidermal tissue for functional immune studies. *Acta Derm Venereol* 68(6):474–479
- Lashmar UT, Hadgraft J et al (1989) Topical application of penetration enhancers to the skin of nude-mice – a histopathological study. *J Pharm Pharmacol* 41(2):118–121
- Lawler JC, Davis MJ et al (1960) Electrical characteristics of the skin – the impedance of the surface sheath and deep tissues. *J Invest Dermatol* 34(5):301–308
- Le VH, Lippold BC (1995) Influence of physicochemical properties of homologous esters of nicotinic-acid on skin permeability and maximum flux. *Int J Pharm* 124(2):285–292
- Lee D-Y, Ahn H-T et al (2000) A new skin equivalent model: dermal substrate that combines de-epidermized dermis with fibroblast-populated collagen matrix. *J Dermatol Sci* 23(2):132–137



- Lee RS, Watkinson A et al (2001) Barrier function of the axillary stratum corneum. *J Invest Dermatol* 117(3):810–810
- Lee J-N, Jee S-H et al (2008) The effects of depilatory agents as penetration enhancers on human stratum corneum structures. *J Invest Dermatol* 128:2240–2247
- Leopold CS, Lippold BC (1992) A new application chamber for skin penetration studies in vivo with liquid preparations. *Pharm Res* 9(9):1215–1218
- Levin J, Maibach H (2005) The correlation between transepidermal water loss and percutaneous absorption: an overview. *J Control Release* 103(2):291–299
- Li LN, Hoffman RM (1997) Topical liposome delivery of molecules to hair follicles in mice. *J Dermatol Sci* 14(2):101–108
- Li LN, Lishko V et al (1993) Liposome targeting of high-molecular-weight DNA to the hair-follicles of histocultured skin – a model for gene-therapy of the hair-growth processes. *In Vitro Cell Dev Biol Anim* 29A(4):258–260
- Li SK, Suh W et al (1998) Lag time data for characterizing the pore pathway of intact and chemically pretreated human epidermal membrane. *Int J Pharm* 170(1):93–108
- Li SK, Ghanem AH et al (1999) Pore induction in human epidermal membrane during low to moderate voltage iontophoresis: a study using AC iontophoresis. *J Pharm Sci* 88(4):419–427
- Li Q, Tsuji H et al (2006) Characterization of the transdermal transport of flurbiprofen and indomethacin. *J Control Release* 110(3):542–556
- Lieb LM, Ramachandran C et al (1992) Topical delivery enhancement with multilamellar liposomes into pilo-sebaceous units. I. In vitro evaluation using fluorescent techniques with the hamster ear model. *J Invest Dermatol* 99(1):108–113
- Lieckfeldt R, Villalain J et al (1993) Diffusivity and structural polymorphism in some model stratum-corneum lipid systems. *Biochim Biophys Acta* 1150(2):182–188
- Loden M (1992) The increase in skin hydration after application of emollients with different amounts of lipids. *Acta Derm Venereol* 72(5):327–330
- Loftsson T (1982) Experimental and theoretical model for studying simultaneous transport and metabolism of drugs in excised skin. *Arch Pharm Chem Sci Ed* 10:17
- Long SA, Wertz PW et al (1985) Human stratum corneum polar lipids and desquamation. *Arch Dermatol Res* 277:284–287
- Lotte C, Patouillet C et al (2002) Permeation and skin absorption: reproducibility of various industrial reconstructed human skin models. *Skin Pharmacol Appl Skin Physiol* 15:18–30
- Luu-The V, Ferraris C et al (2007) Steroid metabolism and profile of steroidogenic gene expression in Episkin (TM): high similarity with human epidermis. *J Steroid Biochem Mol Biol* 107(1–2):30–36
- Luzardo-Alvarez A, Delgado-Charro MB et al (2003) In vivo iontophoretic administration of ropinirole hydrochloride. *J Pharm Sci* 92(12):2441–2448
- Mackee GM, Sulzberger MB et al (1945) Histologic studies on percutaneous penetration with special reference to the effect of vehicles. *J Invest Dermatol* 6(1):43–61
- Madison KC, Swartzendruber DC et al (1987) Presence of intercellular lipid lamellae in the upper layers of stratum corneum. *J Invest Dermatol* 88:714–718
- Mak VHW, Cumpstone MB et al (1991) Barrier function of human keratinocyte cultures grown at the air-liquid interface. *J Invest Dermatol* 96(3):323–327
- Malkinson FD, Ferguson EH (1955) Percutaneous absorption of hydrocortisone-4-c-14 in 2 human subjects. *J Invest Dermatol* 25(5):281–283
- Mansbridge J (2002) Tissue-engineered skin substitutes. *Expert Opin Biol Ther* 2(1):25–34
- Marty P, Faure C et al (1997) Assessment of human skins obtained by in vitro culture as membrane models for cutaneous permeation tests. In: Brain KR, James VJ, Walters KA (eds) *Perspectives in percutaneous penetration*. STS Publishing, Cardiff, p 64
- Masson M, Sigfusson SD et al (2002) Fish skin as a model membrane to study transmembrane drug delivery with cyclodextrins. *J Incl Phenom Macrocycl Chem* 44(1–4):177–182
- Mathy FX, Ntivunwa D et al (2005) Fluconazole distribution in rat dermis following intravenous and topical application: a microdialysis study. *J Pharm Sci* 94(4):770–780
- Matoltsy AG (1986) The skin of mammals: structure and function of the mammalian epidermis. In: BereiterHahn J, Matoltsy AG, Richards KS (eds) *Biology of the integument. 2. Vertebrates*. Berlin, Springer, pp 255–277
- Matoltsy AG, Downes AM et al (1968) Studies of the epidermal water barrier. Part II. Investigation of the chemical nature of the water barrier. *J Invest Dermatol* 50:19–26
- Matsuzaki K, Imaoka T et al (1993) Development of a model membrane system using stratum-corneum lipids for estimation of drug skin permeability. *Chem Pharm Bull* 41(3):575–579
- McAllister DV, Allen MG et al (2000) Microfabricated microneedles for gene and drug delivery. *Annu Rev Biomed Eng* 2:289–313
- McCullough J, Ramirez J et al (2006) In vitro percutaneous absorption of a novel topical benzoyl peroxide formulation in human cadaver skin layers. *J Am Acad Dermatol* 54(3):AB29
- McMullen TPW, McElhaney RN (1995) New aspects of the interactions of cholesterol with dipalmitoyl phosphatidylcholine bilayers as revealed by high-sensitivity differential scanning calorimetry. *Biochim Biophys Acta* 1234:90–98
- Megrab NA, Williams AC et al (1995) Estradiol permeation across human skin, silastic and snake skin membranes – the effects of ethanol-water cosolvent systems. *Int J Pharm* 116(1):101–112
- Mendelsohn R, Flach CR et al (2006) Determination of molecular conformation and permeation in skin via IR spectroscopy, microscopy, and imaging. *Biochim Biophys Acta Biomembranes* 1758(7):923–933

- Menon GK, Elias PM (1997) Morphologic basis for a pore-pathway in mammalian stratum corneum. *Skin Pharmacol* 10:235–246
- Menon GK, Lee SH et al (1998) Ultrastructural effects of some solvents and vehicles on the stratum corneum and other skin components: evidence for an “extended mosaic partitioning” model of the skin barrier. In: Roberts MS, Walters KA (eds) *Dermal absorption and toxicity assessment*. Marcel Dekker, New York, pp 727–751
- Michaels AS, Chandrasekaran SK et al (1975) Drug permeation through human skin. Theory and in vitro experimental measurements. *AICHE J* 21(5):985–996
- Michel M, L’Heureux N et al (1999) Characterization of a new tissue-engineered human skin equivalent with hair. *In Vitro Cell Dev Biol Anim* 35(6):318–326
- Miller MA, Pisani E (1999) The cost of unsafe injections. *Bull World Health Organ* 77(10):808–811
- Mitragotri S, Kost J (2004) Low-frequency sonophoresis – a review. *Adv Drug Deliv Rev* 56(5):589–601
- Mitragotri S, Blankschtein D et al (1995) Ultrasound-mediated transdermal protein delivery. *Science* 269(5225):850–853
- Mitragotri S, Blankschtein D et al (1996) Transdermal drug delivery using low-frequency sonophoresis. *Pharm Res* 13(3):411–420
- Miyajima K, Tanikawa S et al (1994) Effects of absorption enhancers and lipid-composition on drug permeability through the model membrane using stratum-corneum lipids. *Chem Pharm Bull* 42(6):1345–1347
- Moghimi HR, Williams AC et al (1996) A lamellar matrix model for stratum corneum intercellular lipids. 1. Characterisation and comparison with stratum corneum intercellular structure. *Int J Pharm* 131(2):103–115
- MonteiroRiviere NA, Inman AO et al (1997) Comparison of an in vitro skin model to normal human skin for dermatological research. *Microsc Res Tech* 37(3):172–179
- Moody RP, Nadeau B et al (1995) In-vivo and in-vitro dermal absorption of benzo[a]pyrene in rat, guinea-pig, human and tissue-cultured skin. *J Dermatol Sci* 9(1):48–58
- Moore DJ, Rerek ME (1998) Biophysics of skin barrier lipid organization. *J Invest Dermatol* 110(4):674
- Morell JLP, Claramonte MDC et al (1996) Validation of a release diffusion cell for topical dosage forms. *Int J Pharm* 137(1):49–55
- Morikawa N, Kitagawa T et al (2007) Assessment of the in vitro skin irritation of chemicals using the Vitrolife-Skin™ human skin model. *AATEX* 14:417–423
- Moser K, Kriwet K et al (2001) Permeation enhancement of a highly lipophilic drug using supersaturated systems. *J Pharm Sci* 90(5):607–616
- Muhammad F, Brooks JD et al (2004) Comparative mixture effects of JP-8(100) additives on the dermal absorption and disposition of jet fuel hydrocarbons in different membrane model systems. *Toxicol Lett* 150(3):351–365
- Nabila Sekkat RHG (2001) Biological models to study skin permeation. In: Testa B, van de Waterbeemd H, Folkers G, Guy R (eds) *Pharmacokinetic optimization in drug research*. Verlag Helvetica Chimica Acta, Postfach, CH-8042 Zürich, Switzerland pp 155–172
- Nacht S, Yeung D et al (1981) Benzoyl peroxide – percutaneous penetration and metabolic disposition. *J Am Acad Dermatol* 4(1):31–37
- Naik A, Kalia YN et al (2001) Characterization of molecular transport across human stratum corneum in vivo. *J Toxicol Cutan Ocular Toxicol* 20(2–3):279–301
- Nakamura M, Rikimaru T et al (1990) Full-thickness human skin explants for testing the toxicity of topically applied chemicals. *J Invest Dermatol* 95(3):325–332
- Netzlaff F, Lehr CM et al (2005) The human epidermis models EpiSkin (R), SkinEthic (R) and EpiDerm (R): an evaluation of morphology and their suitability for testing phototoxicity, irritancy, corrosivity, and substance transport. *Eur J Pharm Biopharm* 60(2):167–178
- Netzlaff F, Kostka KH et al (2006a) TEWL measurements as a routine method for evaluating the integrity of epidermis sheets in static Franz type diffusion cells in vitro. Limitations shown by transport data testing. *Eur J Pharm Biopharm* 63(1):44–50
- Netzlaff F, Schaefer UF et al (2006b) Comparison of bovine udder skin with human and porcine skin in percutaneous permeation experiments. *ATLA Altern Lab Anim* 34(5):499–513
- Netzlaff F, Kaca M et al (2007) Permeability of the reconstructed human epidermis model EpiSkin (R) in comparison to various human skin preparations. *Eur J Pharm Biopharm* 66(1):127–134
- Nir Y, Paz A et al (2003) Fear of injections in young adults: prevalence and associations. *Am J Trop Med Hyg* 68(3):341–344
- Norlen L (2001) Skin barrier formation: the membrane folding model. *J Invest Dermatol* 117(4):823–829
- Norlén L (2001) Skin barrier structure and function: the single phase model. *J Invest Dermatol* 117:830–836
- Norlén L, Nicander I et al (1998) A new HPLC-based method for the quantitative analysis of inner stratum corneum lipids with special reference to the free fatty acid fraction. *Arch Dermatol Res* 290:508–516
- Norlen L, Nicander I et al (1999) Inter- and intra-individual differences in human stratum corneum lipid content related to physical parameters of skin barrier function in vivo. *J Invest Dermatol* 112(1):72–77
- Odlund GF (1983) Structure of the skin. In: Goldsmith EL (ed) *Biochemistry and physiology of the skin*. Oxford University Press, New York, pp 3–63
- Oertel RP (1977) Protein conformational-changes induced in human stratum-corneum by organic sulfoxides – IR spectroscopic investigation. *Biopolymers* 16(10):2329–2345
- Osigo T, Hata T et al (2001) Transdermal absorption of bupranolol in rabbit skin in vitro and in vivo. *Biol Pharm Bull* 24(5):588–591

- Ogura M, Pahwal S et al (2008) Low-frequency sonophoresis: current status and future prospects. *Adv Drug Deliv Rev* 60(10):1218–1223
- Ohman H, Vahlquist A (1994) In-vivo studies concerning a pH gradient in human stratum-corneum and upper epidermis. *Acta Derm Venereol* 74(5):375–379
- Okamoto H, Hashida M et al (1988) Structure activity relationship of 1-alkylazacycloalkanone or 1-alkenylazacycloalkanone derivatives as percutaneous penetration enhancers. *J Pharm Sci* 77(5):418–424
- Olivella MS, Debattista NB et al (2006) Salicylic acid permeation: a comparative study with different vehicles and membranes. *Biocell* 30(2):321–324
- Osborne DW (1986) Computational method for predicting skin permeation of chemicals. *Pharmaceutical Manufacturing* 41–48
- Ottaviani G, Martel S et al (2006) Parallel artificial membrane permeability assay: a new membrane for the fast prediction of passive human skin permeability. *J Med Chem* 49(13):3948–3954
- Pabla D, Zia H (2007) A comparative permeation/release study of different testosterone gel formulations. *Drug Deliv* 15(6):389–396
- Pageon H, Asselineau D (2005) An in vitro approach to the chronological aging of skin by glycation of the collagen – the biological effect of glycation on the reconstructed skin model. In: Maillard reaction: chemistry at the interface of nutrition, aging, and disease, vol 1043. New York, New York Academy Sciences, pp 529–532
- Paliwal S, Menon GK et al (2006) Low-frequency sonophoresis: ultrastructural basis for stratum corneum permeability assessed using quantum dots. *J Invest Dermatol* 126(5):1095–1101
- Panchagnula R, Stemmer K et al (1997) Animal models for transdermal drug delivery. *Methods Find Exp Clin Pharmacol* 19(5):335–341
- Panchagnula R, Pillai O et al (2000) Transdermal iontophoresis revisited. *Curr Opin Chem Biol* 4(4):468–473
- Pellett MA, Roberts MS et al (1997) Supersaturated solutions evaluated with an in vitro stratum corneum tape stripping technique. *Int J Pharm* 151(1):91–98
- Pershing LK, Lambert LD et al (1990) Mechanism of ethanol-enhanced estradiol permeation across human skin in vivo. *Pharm Res* 7(2):170–175
- Pillai O, Nair V et al (2001) Noninvasive transdermal delivery of peptides and proteins. *Drugs Future* 26(8):779–791
- Pinnagoda J, Tupker RA et al (1989) The intra-individual and inter-individual variability and reliability of trans-epidermal water-loss measurements. *Contact Dermatitis* 21(4):255–259
- Pinnagoda J, Tupker RA et al (1990) Guidelines for transepidermal water loss (TEWL) measurement – a report from the standardization group of the European Society of contact dermatitis. *Contact Dermatitis* 22(3):164–178
- Pirot F, Kalia YN et al (1997) Characterization of the permeability barrier of human skin in vivo. *Proc Natl Acad Sci U S A* 94(4):1562–1567
- Pliquett U (1999) Mechanistic studies of molecular transdermal transport due to skin electroporation. *Adv Drug Deliv Rev* 35(1):41–60
- Poelman MC, Piot B et al (1989) Assessment of topical non-steroidal anti-inflammatory drugs. *J Pharm Pharmacol* 41(10):720–722
- Ponec M, Kempenaar J (1995) Use of human skin recombinants as an in-vitro model for testing the irritation potential of cutaneous irritants. *Skin Pharmacol* 8(1–2):49–59
- Ponec M, Boelsma E et al (2000) Lipid and ultrastructural characterization of reconstructed skin models. *Int J Pharm* 203(1–2):211–225
- Ponec M, Boelsma E et al (2002) Characterization of reconstructed skin models. *Skin Pharmacol Appl Skin Physiol* 15:4–17
- Potts RO, Francoeur ML (1993) Infrared spectroscopy of stratum corneum lipids. In: Walters KA, Hadgraft J (eds) *Pharmaceutical skin penetration enhancement*. Marcel Dekker, New York
- Poumay Y, Dupont F et al (2004) A simple reconstructed human epidermis: preparation of the culture model and utilization in in vitro studies. *Arch Dermatol Res* 296(5):203–211
- Prausnitz MR (1997) Transdermal delivery of macromolecules: recent advances by modification of skin's barrier properties. In: Zahra Shahrokh (ed.) *Therapeutic protein and peptide formulation and delivery*, vol 675, American Chemical Society symposium series pp 124–153
- Prausnitz MR (2004) Microneedles for transdermal drug delivery. *Adv Drug Deliv Rev* 56(5):581–587
- Prausnitz MR, Mitragotri S et al (2004) Current status and future potential of transdermal drug delivery. *Nat Rev Drug Discov* 3(2):115–124
- Pudney PDA, Melot M et al (2007) An in vivo confocal Raman study of the delivery of trans-retinol to the skin. *Appl Spectrosc* 61(8):804–811
- Puglia C, Blasi P et al (2008) Lipid nanoparticles for prolonged topical delivery: an in vitro and in vivo investigation. *Int J Pharm* 357(1–2):295–304
- Qiang M, Engström S et al (1993) Fatty acids are required for epidermal permeability barrier function. *J Clin Invest* 92:791–798
- Quisno RA, Doyle RL (1983) A new occlusive patch test system with a plastic chamber. *J Soc Cosmet Chem* 34(1):13–19
- Rao VU, Misra AN (1994) Effect of penetration enhancers on transdermal absorption of insulin across human cadaver skin. *Drug Dev Ind Pharm* 20(16):2585–2591
- Regnier M, Patwardhan A et al (1998) Reconstructed human epidermis composed of keratinocytes, melanocytes and Langerhans cells. *Med Biol Eng Comput* 36(6):821–824
- Rehder J, Souto LR et al (2004) Model of human epidermis reconstructed in vitro with keratinocytes and melanocytes on dead de-epidermized human dermis. *Sao Paulo Med J* 122:22–25
- Remane Y, Leopold CS et al (2006) Percutaneous penetration of methyl nicotinate from ointments using the laser

- Doppler technique: bioequivalence and enhancer effects. *J Pharmacokinet Pharmacodyn* 33(6):719–735
- Rice RH, Green H (1977) The cornified envelope of terminally differentiated human epidermal keratinocytes consists of cross linked proteins. *Cell* 11:417–422
- Rigg PC, Barry BW (1990) Shed snake skin and hairless mouse skin as model membranes for human skin during permeation studies. *J Invest Dermatol* 94(2):235–240
- Riviere JE, Sage B et al (1991) Effects of vasoactive drugs on transdermal lidocaine iontophoresis. *J Pharm Sci* 80(7):615–620
- Robert Peter Chilcott RF (2000) Biophysical measurements of human forearm skin in vivo: effects of site, gender, chirality and time. *Skin Res Technol* 6(2):64–69
- Rocha JCB, Pedrochi F et al (2007) Ex vivo evaluation of the percutaneous penetration of proanthocyanidin extracts from *Guazuma ulmifolia* using photoacoustic spectroscopy. *Anal Chim Acta* 587(1):132–136
- Rocheffort A, Druot P et al (1986) A new technique for the evaluation of cosmetics effect on mechanical-properties of stratum-corneum and epidermis in vitro. *Int J Cosmet Sci* 8(1):27–36
- Rodriguez H, O'Connell C et al (2004) Measurement of DNA biomarkers for the safety of tissue-engineered medical products, using artificial skin as a model. *Tissue Eng* 10(9–10):1332–1345
- Roguet R, Cohen C et al (1998) An interlaboratory study of the reproducibility and relevance of Episkin, reconstructed human epidermis, in the assessment of cosmetics irritancy. *Toxicol In Vitro* 12(3):295–304
- Rohatagi S, Barrett JS et al (1997) Selegiline percutaneous absorption in various species and metabolism by human skin. *Pharm Res* 14(1):50–55
- Rossi RCP, de Paiva RF et al (2008) Photoacoustic study of percutaneous absorption of Carbopol and transdermic gels for topic use in skin. *Eur Phys J (Special Topics)* 153:479–482
- Rougier A, Dupuis D et al (1983) In vivo correlation between stratum-corneum reservoir function and percutaneous-absorption. *J Invest Dermatol* 81(3):275–278
- Rougier A, Lotte C et al (1989) In vivo relationship between percutaneous absorption and transepidermal water loss. In: Bronaugh RL, Maibach HI (eds) *Percutaneous absorption*. Marcel Dekker, New York, pp 175–190
- Roy SD, Degroot JS (1994) Percutaneous-absorption of nafarelin acetate, an LHRH analog, through human cadaver skin and monkey skin. *Int J Pharm* 110(2):137–145
- Roy SD, Hou SYE et al (1994) Transdermal delivery of narcotic analgesics – comparative metabolism and permeability of human cadaver skin and hairless mouse skin. *J Pharm Sci* 83(12):1723–1728
- Rutherford T, Black JG (1969) Use of autoradiography to study localization of germicides in skin. *Br J Dermatol* S81:75
- Sandby-Moller J, Poulsen T et al (2003) Epidermal thickness at different body sites: relationship to age, gender, pigmentation, blood content, skin type and smoking habits. *Acta Derm Venereol* 83(6):410–413
- Sato K, Sugibayashi K et al (1991) Species-differences in percutaneous-absorption of nicorandil. *J Pharm Sci* 80(2):104–107
- Schafer-Korting M, Bock U et al (2006) Reconstructed human epidermis for skin absorption testing: results of the German prevalidation study. *ATLA Altern Lab Anim* 34(3):283–294
- Schafer-Korting M, Bock U et al (2008) The use of reconstructed human epidermis for skin absorption testing: results of the validation study. *ATLA Altern Lab Anim* 36(2):161–187
- Schalla W, Schaefer H (1982) Mechanisms of penetration of drugs into the skin. In: Brandau R, Lippold BH (eds) *Dermal and transdermal absorption*. Wissenschaftlichen Verlag, Stuttgart, pp 41–70
- Scheuplein RJ (1965) Mechanism of percutaneous absorption. I. Routes of penetration and the influence of solubility. *J Invest Dermatol* 45:334–346
- Scheuplein RJ (1966) Analysis of permeability data for the case of parallel diffusion pathways. *Biophys J* 6(1):1–17
- Scheuplein RJ (1967) Mechanism of percutaneous absorption. II. Transient diffusion and the relative importance of various routes of skin penetration. *J Invest Dermatol* 48(1):79–88
- Scheuplein RJ (1972) Properties of the skin as a membrane. *Adv Biol Skin* 12:125–152
- Scheuplein RJ (1978) Permeability of the skin: a review of major concepts. *Curr Prob Dermatol* 7:172–186
- Scheuplein RJ, Bronaugh RL (1983) Percutaneous absorption. In: Goldsmith LA, ed. *Biochemistry and Physiology of the Skin*, Vol. 2. New York: Oxford University Press 1255–1295
- Schmook FP, Meingassner JG et al (2001) Comparison of human skin or epidermis models with human and animal skin in in-vitro percutaneous absorption. *Int J Pharm* 215(1–2):51–56
- Schramm-Baxter J, Katrencik J et al (2004) Jet injection into polyacrylamide gels: investigation of jet injection mechanics. *J Biomech* 37(8):1181–1188
- Scott RE, Leahy DE et al (1986) In vitro percutaneous model for quantitative structure-absorption studies. *J Pharm Pharmacol* 38(Suppl):66
- Scott RC, Corrigan MA et al (1991) The influence of skin structure on permeability: an intersite and interspecies comparison with hydrophilic penetrants. *J Invest Dermatol* 96(6):921–925
- Sebastiani P, Nicoli S et al (2005) Effect of lactic acid and iontophoresis on drug permeation across rabbit ear skin. *Int J Pharm* 292(1–2):119–126
- Sekkat N, Kalia YN et al (2002) Biophysical study of porcine ear skin in vitro and its comparison to human skin in vivo. *J Pharm Sci* 91(11):2376–2381
- Shah HS, Tojo K et al (1992) Enhancement of in vitro skin permeation of verapamil. *Drug Dev Ind Pharm* 18(13):1461–1476
- Shah VP, Flynn GL et al (1998) Bioequivalence of topical dermatological dosage forms – methods of evaluation of bioequivalence. *Pharm Res* 15(2):167–171

- Shahabeddin L, Berthod F et al (1990) Characterization of skin reconstructed on a chitosan-cross-linked collagen-glycosaminoglycan matrix. *Skin Pharmacol* 3:107–114
- Shakespeare P (2001) Burn wound healing and skin substitutes. *Burns* 27(5):517–522
- Shelley WB, Melton FM (1949) Factors accelerating the penetration of histamine through normal intact human skin. *J Invest Dermatol* 13(2):61–71
- Sheth NV, McKeough MB et al (1987) Measurement of the stratum-corneum drug reservoir to predict the therapeutic efficacy of topical iododeoxyuridine for herpes-simplex virus-infection. *J Invest Dermatol* 89(6):598–602
- Shibayama H, Hisama M et al (2008) Permeation and metabolism of a novel ascorbic acid derivative, disodium isostearyl 2-O-L-ascorbyl phosphate, in human living skin equivalent models. *Skin Pharmacol Physiol* 21(4):235–243
- Simon M, Green H (1984) Participation of membrane associated proteins in the formation of the cross linked envelope of the keratinocyte. *Cell* 36:827–834
- Simon GA, Maibach HI (2000) The pig as an experimental animal model of percutaneous permeation in man: qualitative and quantitative observations – an overview. *Skin Pharmacol Appl Skin Physiol* 13(5):229–234
- Sinha VR, Kaur MP (2000) Permeation enhancers for transdermal drug delivery. *Drug Dev Ind Pharm* 26(11):1131–1140
- Sivamani RK, Liepmann D et al (2007) Microneedles and transdermal applications. *Expert Opin Drug Deliv* 4(1):19–25
- Skerrow D, Hunter I (1978) Protein modification during the keratinization of normal and psoriatic epidermis. *Biochim Biophys Acta* 537:474–484
- Slivka SR, Landeen LK et al (1993) Characterization, barrier function, and drug-metabolism of an in vitro skin model. *J Invest Dermatol* 100(1):40–46
- Smith ICH (1993) Frog skin. *ATLA Altern Lab Anim* 21(3):392
- Sobral CS, Gragnani A et al (2007) Inhibition of proliferation of *Pseudomonas aeruginosa* by KGF in an experimental burn model using human cultured keratinocytes. *Burns* 33(5):613–620
- Sonavane G, Tomoda K et al (2008) In vitro permeation of gold nanoparticles through rat skin and rat intestine: effect of particle size. *Colloids Surf B Biointerfaces* 65(1):1–10
- Soni J, Baird AW et al (2006) Rat, ovine and bovine Peyer's patches mounted in horizontal diffusion chambers display sampling function. *J Control Release* 115(1):68–77
- Southwell D, Barry BW (1983) Penetration enhancers for human-skin – mode of action of 2-pyrrolidone and dimethylformamide on partition and diffusion of model compounds water, normal-alcohols, and caffeine. *J Invest Dermatol* 80(6):507–514
- Southwell D, Barry BW et al (1984) Variations in permeability of human-skin within and between specimens. *Int J Pharm* 18(3):299–309
- Squier CA (1973) The permeability of keratinized and nonkeratinized oral epithelium to horseradish peroxidase. *J Ultrastr Res* 43:160–177
- Srinivasan V, Higuchi WI (1990) A model for iontophoresis incorporating the effect of convective solvent flow. *Int J Pharm* 60(2):133–138
- Stamatas GN, de Sterke J et al (2008) Lipid uptake and skin occlusion following topical application of oils on adult and infant skin. *J Dermatol Sci* 50(2):135–142
- Steinert PM, Cantieri JS (1983) Epidermal keratins. In: Goldsmith AL (ed) *Biochemistry and physiology of the skin*, vol I. Oxford University Press, New York, pp 135–169
- Stinchcomb AL, Pirot F et al (1999) Chemical uptake into human stratum corneum in vivo from volatile and non-volatile solvents. *Pharm Res* 16(8):1288–1293
- Suh H, Jun HW (1996) Effectiveness and mode of action of isopropyl myristate as a permeation enhancer for naproxen through shed snake skin. *J Pharm Pharmacol* 48(8):812–816
- Suppasrivasuth J, Bellantone RA et al (2006) Permeability and retention studies of (–)Epicatechin gel formulations in human cadaver skin. *Drug Dev Ind Pharm* 32(9):1007–1017
- Surber C, Schwarb FP et al (1999) Tape-stripping technique. In: Bronough H, Maibach H (eds) *Drugs and the pharmaceutical sciences*. Marcel Dekker, New York, pp 395–409
- Swartzendruber DC, Wertz PW et al (1987) Evidence that the corneocyte has a chemically bound lipid envelope. *J Invest Dermatol* 88:709–713
- Swartzendruber DC, Wertz PW et al (1989) Molecular models of the intercellular lipid lamellae in mammalian stratum corneum. *J Invest Dermatol* 92:251–257
- Sweeney TM, Downing DT (1970) The role of lipids in the epidermal barrier to diffusion. *J Invest Dermatol* 55:135–140
- Takahashi H, Sinoda K et al (1996) Effects of cholesterol on the lamellar and the inverted hexagonal phases of dielaidoylphosphatidylethanolamine. *Biochim Biophys Acta* 1289:209–216
- Tanaka M, Fukuda H et al (1978) Permeation of drug through a model membrane consisting of millipore filter with oil. *Chem Pharm Bull* 26(1):9–13
- Tang H, Mitragotri S et al (2001) Theoretical description of transdermal transport of hydrophilic permeants: application to low-frequency sonophoresis. *J Pharm Sci* 90(5):545–568
- Tas C, Ozkan Y et al (2007) In vitro and ex vivo permeation studies of etodolac from hydrophilic gels and effect of Terpenes as enhancers. *Drug Deliv* 14(7):453–459
- Tenjarla SN, Kasina R et al (1999) Synthesis and evaluation of N-acetylprolinate esters – novel skin penetration enhancers. *Int J Pharm* 192(2):147–158
- Tezel A, Sens A et al (2001) Frequency dependence of sonophoresis. *Pharm Res* 18(12):1694–1700
- Tezel A, Sens A et al (2003) Description of transdermal transport of hydrophilic solutes during low-frequency sonophoresis based on a modified porous pathway model. *J Pharm Sci* 92(2):381–393

- Thomas BJ, Finnin BC (2004) The transdermal revolution. *Drug Discov Today* 9(16):697–703
- Tiemessen H, Bodde HE et al (1989) A human stratum-corneum silicone membrane sandwich to simulate drug transport under occlusion. *Int J Pharm* 53(2):119–127
- Tipre DN, Vavia PR (2003) Acrylate-based transdermal therapeutic system of nitrendipine. *Drug Dev Ind Pharm* 29(1):71–78
- Tojo K, Lee ARC (1989) A method for predicting steady-state rate of skin penetration in vivo. *J Invest Dermatol* 92(1):105–108
- Tojo K, Masi JA et al (1985a) Hydrodynamic characteristics of an in vitro drug permeation cell. *Ind Eng Chem Fund* 24(3):368–373
- Tojo K, Sun Y et al (1985b) Characterization of a membrane permeation system for controlled drug delivery studies. *AIChE J* 31(5):741–746
- Tokudome Y, Sugibayashi K (2004) Mechanism of the synergic effects of calcium chloride and electroporation on the in vitro enhanced skin permeation of drugs. *J Control Release* 95(2):267–274
- Tregear RT (1961) Relative penetrability of hair follicles and epidermis. *J Physiol (London)* 156(2):307
- Tregear RT (1966) Physical function of skin. Academic, New York
- Tsai JC, Weiner ND et al (1991) Properties of adhesive tapes used for stratum-corneum stripping. *Int J Pharm* 72(3):227–231
- Tsai JC, Sheu HM et al (2001) Effect of barrier disruption by acetone treatment on the permeability of compounds with various lipophilicities: implications for the permeability of compromised skin. *J Pharm Sci* 90(9):1242–1254
- Tsai JC, Lin CY et al (2003) Noninvasive characterization of regional variation in drug transport into human stratum corneum in vivo. *Pharm Res* 20(4):632–638
- Tsuruta H (1977) Percutaneous absorption of organic solvents. 2. A method for measuring the penetration rate of chlorinated solvents through excised rat skin. *Ind Health* 15:131–139
- Turakka L, Piepponen T et al (1984) Release of hydrocortisone and hydrocortisone acetate from topical vehicles in vitro. *Labo-Pharma Probl Tech* 344:540–544
- Uchino T, Tokunaga H et al (2002) Effect of squalene monohydroperoxide on cytotoxicity and cytokine release in a three-dimensional human skin model and human epidermal keratinocytes. *Biol Pharm Bull* 25(5):605–610
- Umemura K, Ikeda Y et al (2008) Cutaneous pharmacokinetics of topically applied maxacalcitol ointment and lotion. *Int J Clin Pharmacol Ther* 46(6):289–294
- Valia KH, Chien YW et al (1984) Long-term skin permeation kinetics of estradiol. 1. Effect of drug solubilizer olyethylene-glycol 400. *Drug Dev Ind Pharm* 10(7):951–981
- Vanbrunt J (1989) Novel drug delivery systems. *Biotechnology* 7(2):127–130
- Vankooten WJ, Mali JWH (1966) Significance of sweatducts in permeation experiments on isolated cadaverous human skin. *Dermatologica* 132(2):141
- Vankooten WJ, Mali JWH (1966) Significance of sweatducts in permeation experiments on isolated cadaverous human skin. *Dermatologica* 132(2):141
- Vicanova J, Mommaas AM et al (1996a) Impaired desquamation in the in vitro reconstructed human epidermis. *Cell Tissue Res* 286(1):115–122
- Vicanova J, Mommaas AM et al (1996b) Transformation of desmosomes is impaired in the in vitro reconstructed human epidermis. *J Invest Dermatol* 107(4):44
- Vickers CFH (1963) Existence of reservoir in stratum corneum – experimental proof. *Arch Dermatol* 88(1):20
- Viegas TX, Kibbe AH et al (1986) An in vitro method of evaluating tolinaftate release from topical powder. *Pharm Res* 3(2):88–92
- Wahlberg JE (1968) Transepidermal or transfollicular absorption – in vivo and in vitro studies in hairy and non-hairy guinea pig skin with sodium (22 Na) and mercuric (203 Hg) chlorides. *Acta Derm Venereol* 48(4):336
- Wallace SM, Barnett G (1978) Pharmacokinetic analysis of percutaneous absorption – evidence of parallel penetration pathways for methotrexate. *J Pharmacokin Biopharm* 6(4):315–325
- Walzer C, Benathan M et al (1989) Thermolysin treatment – a new method for dermo-epidermal separation. *J Invest Dermatol* 92(1):78–81
- Washitake M, Takashima Y et al (1980) Studies on drug release from ointment. 1. Drug permeation through eggshell membranes. *Chem Pharm Bull* 28(10):2855–2861
- Watanabe Y, Hongo S et al (1989) Evaluation of excised loach skin for studies on transdermal permeation of drugs in vitro. *Yakugaku Zasshi (Journal of the Pharmaceutical Society of Japan)* 109(9):656–661
- Watt F, Green H (1981) Involucrin synthesis is correlated with cell size in human cultures. *J Cell Biol* 90:738–742
- Wertz PW (1986) Lipids of keratinizing tissues. In: BereiterHahn J, Matoltsy AG, Richards KS (eds) *Biology of the integument*. Springer, Berlin, pp 815–823
- Wertz PW, Downing DT (1983a) Acylglucosylceramides of pig epidermis: structure determination. *J Lipid Res* 24:753–758
- Wertz PW, Downing DT (1983b) Ceramides of pig epidermis: structure determination. *J Lipid Res* 24:759–765
- Wertz PW, Downing DT (1987) Covalently bound  $\omega$ -hydroxyacylceramide in the stratum corneum. *Biochim Biophys Acta* 917:108–111
- Wertz PW, Downing DT (1989) Stratum corneum: biological and biochemical considerations. In: Hadgraft J, Guy RH (eds) *Transdermal drug delivery: developmental issues and research initiatives*. Marcel Dekker, New York and Basel, pp 1–22
- Wertz PW, Miethke MC et al (1985) The composition of the ceramides from human stratum corneum and from comedones. *J Invest Dermatol* 84:410–412
- Wertz PW, Swartzendruber DC et al (1987) The composition and morphology of epidermal cyst lipids. *J Invest Dermatol* 89:419–425
- Wester RC, Maibach HI (1987) Animal models for transdermal drug delivery. In: Kydonieus AF, Berner B

- (eds) *Transdermal delivery of drugs*, vol 1. CRC Press, Boca Raton, pp 61–70
- Wester RC, Maibach HI (1989) In vivo methods for percutaneous absorption measurements. In: Brounaugh RL, Maibach HI (eds) *Percutaneous absorption: mechanisms-methodology-drug delivery*. Marcel Dekker, New York, pp 215–237
- Wester RC, Maibach HI (1992) Percutaneous-absorption of drugs. *Clin Pharmacokinetics* 23(4):253–266
- Wester RC, Noonan PK et al (1983) Pharmacokinetics and bioavailability of intravenous and topical nitroglycerin in the rhesus-monkey – estimate of percutaneous 1st-pass metabolism. *J Pharm Sci* 72(7):745–748
- Wester RC, Maibach HI et al (1984) Minoxidil stimulates cutaneous blood-flow in human balding scalps – pharmacodynamics measured by laser doppler velocimetry and photopulse plethysmography. *J Invest Dermatol* 82(5):515–517
- Wester RC, Christoffel J et al (1998a) Human cadaver skin viability for in vitro percutaneous absorption: storage and detrimental effects of heat-separation and freezing. *Pharm Res* 15(1):82–84
- Wester RC, Melendres J et al (1998b) Percutaneous absorption of salicylic acid, theophylline, 2,4-dimethylamine, diethyl hexyl phthalic acid, and p-aminobenzoic acid in the isolated perfused porcine skin flap compared to man in vivo. *Toxicol Appl Pharmacol* 151(1):159–165
- Whitton JT, Everall JD (1973) Thickness of epidermis. *Br J Dermatol* 89(5):467–476
- Wilke K, Wepf R et al (2005) Initial investigations towards a better understanding of the barrier properties of the sweat gland apparatus. *J Invest Dermatol* 125(6):A29
- Wilke K, Wepf R et al (2006) Are sweat glands an alternate penetration pathway? Understanding the morphological complexity of the axillary sweat gland apparatus. *Skin Pharmacol Physiol* 19(1):38–49
- Wilkin JK, Fortner G et al (1985) Prostaglandins and nicotine-provoked increase in cutaneous blood-flow. *Clin Pharmacol Therap* 38(3):273–277
- Williams AC, Barry BW (2004) Penetration enhancers. *Adv Drug Deliv Rev* 56(5):603–618
- Williams PL, Carver MP et al (1990) A physiologically relevant pharmacokinetic model of xenobiotic percutaneous-absorption utilizing the isolated perfused porcine skin flap. *J Pharm Sci* 79(4):305–311
- Williams AC, Cornwell PA et al (1992) On the non-Gaussian distribution of human skin permeabilities. *Int J Pharm* 86(1):69–77
- Williams AC, Barry BW et al (1993) A critical comparison of some Raman-spectroscopic techniques for studies of human stratum-corneum. *Pharm Res* 10(11):1642–1647
- Wong O, Huntington J et al (1989) New alkyl N, N-dialkyl-substituted amino acetates as transdermal penetration enhancers. *Pharm Res* 6(4):286–295
- Wurster DE, Kramer SF (1961) Investigation of some factors influencing percutaneous absorption. *J Pharm Sci* 50(4):288
- Wurster DE, Ostrenga JA et al (1979) Sarin transport across excised human-skin. 1. Permeability and adsorption characteristics. *J Pharm Sci* 68(11):1406–1409
- Xhaufflaire-Uhoda E, Vroome V et al (2006) Dynamics of skin barrier repair following topical applications of miconazole nitrate. *Skin Pharmacol Physiol* 19(5):290–294
- Xiao CH, Moore DJ et al (2005a) Permeation of dimyristoylphosphatidylcholine into skin – structural and spatial information from IR and Raman microscopic imaging. *Vib Spectrosc* 38(1–2):151–158
- Xiao CH, Moore DJ et al (2005b) Feasibility of tracking phospholipid permeation into skin using infrared and Raman microscopic imaging. *J Invest Dermatol* 124(3):622–632
- Xueqin Z, Jing X et al (2005) Interaction of 1-dodecylazacycloheptan-2-one with mouse stratum corneum. *J Biomater Sci Polym Ed* 16(5):563–574
- Yardley HJ (1983) Epidermal lipids. In: Goldsmith AL (ed) *Biochemistry and physiology of skin*. Oxford University Press, New York, pp 363–381
- Yardley HJ, Summerly R (1981) Lipid composition and metabolism in normal and diseased epidermis. *Pharmacol Ther* 13:357–383
- Zelickson A (1961) Electron microscopic study of epidermal sweat duct. *Arch Dermatol* 83(1):106
- Zhai HB, Dika E et al (2007) Tape-stripping method in man: comparison of evaporimetric methods. *Skin Res Technol* 13(2):207–210
- Zhao LG, Fang L et al (2008) Transdermal delivery of penetrants with differing lipophilicities using O-acylmenthol derivatives as penetration enhancers. *Eur J Pharm Biopharm* 69(1):199–213

# Human Native and Reconstructed Skin Preparations for In Vitro Penetration and Permeation Studies

# 10

Ulrich F. Schaefer, D. Selzer, S. Hansen,  
and Claus-Michael Lehr

## Contents

10.1	<b>Introduction</b> .....	186	10.3.7	Duration of Exposure and Sampling Period .....	195
10.1.1	Needs for In Vitro Skin Absorption Studies .....	186	10.3.8	Quantification Methods .....	196
10.1.2	Rate Determining Processes Involved in Skin Absorption.....	186	10.3.9	Influence of Thickness of Skin Preparation .....	196
10.2	<b>In Vitro Barriers for Skin Absorption Studies</b> .....	187	10.3.10	Number of Experiments/Replicates.....	196
10.2.1	Excised Human Skin .....	187	10.3.11	Segmentation of Skin in Different Skin Layers .....	196
10.2.2	Animal Skin.....	190	10.4	<b>Results Obtained from Permeation Studies</b> .....	197
10.2.3	Bioengineered Skin .....	190	10.4.1	Infinite Dosing Studies .....	198
10.2.4	Artificial Skin Surrogates .....	191	10.4.2	Finite Dosing Studies .....	198
10.3	<b>In Vitro Experimental Setups for Skin Absorption Studies</b> .....	192	10.5	<b>Results Obtained from Penetration Studies</b> .....	198
10.3.1	Finite Versus Infinite Dosing .....	192	<b>Conclusion</b> .....		199
10.3.2	Open Versus Occluded Dosing .....	193	<b>References</b> .....		199
10.3.3	Diffusion Cells .....	193			
10.3.4	Barrier Integrity Check .....	194			
10.3.5	Temperature .....	195			
10.3.6	Selection of Receptor Fluid .....	195			

U.F. Schaefer (✉) • D. Selzer  
Biopharmaceutics and Pharmaceutical Technology,  
Saarland University, Campus A 4.1, D-66123  
Saarbruecken, Germany  
e-mail: [ufs@mx.uni-saarland.de](mailto:ufs@mx.uni-saarland.de)

S. Hansen • C.-M. Lehr (✉)  
Biopharmaceutics and Pharmaceutical Technology,  
Saarland University, Campus A 4.1, D-66123  
Saarbruecken, Germany

Department of Drug Delivery, Helmholtz-Institute  
for Pharmaceutical Research Saarland (HIPS),  
Helmholtz Center for Infection Research (HZI),  
Campus E 8.1, D-66123 Saarbruecken, Germany  
e-mail: [Claus-Michael.Lehr@helmholtz-hzi.de](mailto:Claus-Michael.Lehr@helmholtz-hzi.de)

## Abbreviations

C <sub>ss</sub>	Saturation concentration of solute in the vehicle
C <sub>v</sub>	Concentration in the vehicle
EC	European Commission
ECETOC	European Centre for Ecotoxicology and Toxicology of Chemicals
EDETOX	Evaluations and predictions of dermal absorption of toxic chemicals
EEC	European Economic Community
EFSA	European Food Safety Authority
HaCaT	Human adult low calcium high temperature keratinocytes



HPLC	High-performance liquid chromatography
$J_{\text{peak}}$	Peak flux
$J_{\text{ss}}$	Steady state flux
$J_{\text{ss(max)}}$	Maximum flux
LC	Liquid chromatography
$K^P$	Apparent permeability coefficient
MS	Mass spectrometry
NAFTA	North American Free Trade Agreement
REACH	Registration, Evaluation, Authorisation and Restriction of Chemicals
SC	Stratum corneum
SCCNFP	Scientific Committee on Cosmetic Products and Non-Food Products
SCCS	Scientific Committee on Consumer Safety
TEWL	Transepidermal water loss
$t_{\text{lag}}$	Lag-time
USEPA	US Environmental Protection Agency
WHO	World Health Organisation

## 10.1 Introduction

### 10.1.1 Needs for In Vitro Skin Absorption Studies

As an easy accessible organ our skin is used since a long time for the application of cosmetics and furthermore also for the application of drugs. Primarily, however, the skin is actually a protective organ hindering the invasion of foreign substances from the environment to our body and to maintain homeostasis. Therefore, different reasons exist to monitor the fate of compounds in contact with the skin, for example, to assure that no absorption occurs (cosmetics or hazardous substances) or vice versa to demonstrate that skin absorption does takes place, indeed (drug delivery). While the motivation and scope for skin absorption studies might be different, the same experimental setups can be used to gather the desired information. In contrast to clinical studies or animal experiments, in vitro skin absorption studies allow the screening of different formulations, without any ethical restrictions, which is a particular problem for cosmetics where animal experiments have been banned (EEC 1976; Rossignol 2005). Besides these advantages, the

major drawback of in vitro skin absorption studies is the absence of peripheral blood flow which cannot be simulated completely. Furthermore, concerning risk assessment the acceptance of in vitro skin absorption data by the authorities are different. In the European Union, dermal absorption data for many pesticides has been estimated by in vitro experiments (EC 2003a, b; EFSA 2012). In contrast, NAFTA countries (the USA, Canada, and Mexico (NAFTA 2009)) do not accept in vitro skin absorption data alone for risk assessment. However, most of the skin absorption data published in the field of cosmetic and pharmaceutical sciences is based on in vitro skin absorption studies.

### 10.1.2 Rate Determining Processes Involved in Skin Absorption

In general, skin invasion is predominantly governed by the stratum corneum, which is accepted as the main barrier of the skin. Passive diffusion according to Fick's law is considered the rate determining kinetic process for skin absorption. Modulation of this diffusion process therefore allows controlling skin invasion.

#### 10.1.2.1 Pathways Through the Healthy Skin

While for healthy skin the barrier function is typically located in the stratum corneum (SC), the bottleneck for invasion of very lipophilic substances shifts down to the conjunction of SC and viable epidermis due to their reduced solubility in the aqueous epidermis layers (Moghimi et al. 1999). This different behavior has to be regarded when in vitro skin absorption studies are carried out.

Based on the anatomical structure of the skin, two basically different pathways for substance invasion are to be considered:

1. Diffusion across the intact SC, the outermost layer of the skin.
2. Invasion via skin appendages such as hair follicles or glands.

Normally the route through the intact SC accounts for the main pathway of skin absorp-

tion, especially if small and dissolved molecules are concerned. However, for nanoparticles or submicron-sized drug delivery systems, for example, liposomes and nanoparticles, the appendageal pathway may be predominant (Lademann et al. 2006, 2007; Patzelt et al. 2011). An additional mechanical rubbing, e.g., a massage, will improve the appendageal delivery. Moreover, for healthy skin it is reported that nanoparticles >10 nm are unlikely to overcome the SC barrier (Prow et al. 2011).

Governed by the anatomical structure of the intact SC the following absorption pathways are feasible: the intercellular route and the transcellular route. The intercellular route is associated with the lipid bilayer structures in between the corneocytes and is considered to be the predominating invasion route, particularly if steady state conditions are assumed. Due to the liquid crystalline structures of the lipid matrix surrounding the corneocytes, the intercellular route provides hydrophilic as well as lipophilic domains offering the possibility that both lipophilic and hydrophilic entities diffuse via this pathway. Although the intercellular route is very tortuous and therefore much longer, the diffusion is relatively fast in this region due to the enhanced diffusion coefficient in comparison to the corneocytes. Furthermore, this pathway can easily be modulated by penetration enhancers. The transcellular route is normally regarded negligible because diffusion in the solid corneocytes is low and the necessity to partition several times between the lipidic bilayers and the more hydrophilic corneocytes. Both phenomena result in a reduced absorption with the exception if penetration enhancers are used which increase the permeability of the corneocytes, e.g., by application of urea due to keratolytic actions (Williams and Barry 2012).

As a result of the various possibilities for substance invasion through and into the SC in vitro skin absorption experiments must take into account these different pathways.

### 10.1.2.2 Pathways Through the Diseased Skin

In diseased skin the barrier function is reduced because of structural changes in the SC. For

example, the lipid bilayer structure is partly lost or the number of SC layers may be reduced. Therefore, from studies with healthy skin only limited conclusions can be drawn for diseased skin. However, there are nowadays also in vitro models available to mimic the situation of diseased skin (see Sect. 10.2.1.5).

---

## 10.2 In Vitro Barriers for Skin Absorption Studies

### 10.2.1 Excised Human Skin

Excised human skin from surgery is the best available in vitro model for skin absorption studies, it is therefore considered as the gold standard. When using skin from surgery, care has to be taken during transport and preparation. In any case, transport and preparation conditions have to be standardized and must be considered when interpreting the results. The following fundamental points have to be noted. As several cycles of freezing and thawing influence the absorption behavior of the skin, freeze-thaw cycles should be avoided at all cost. Thus, transport at reduced temperature, e.g., on ice packs with no direct contact to the skin, is appropriate. During transport and skin preparation, care must be taken to prevent the skin surface from contamination by lipids originating from the subcutaneous fatty tissue which will change the permeability characteristics of the SC (Wertz 1996). It has been shown that the storage period in a freezer (−20 to −26 °C) should be limited to 6 months (Swarbrick et al. 1982; Harrison et al. 1984; Hawkins and Reifenrath 1984; Bronaugh et al. 1986; Schaefer and Loth 1996) as otherwise the barrier function may be affected. Furthermore, evaporation should be prevented during storage by using tightly sealed bags.

#### 10.2.1.1 Full Thickness Skin

Full thickness skin consisting of SC, viable epidermis, and dermis (Fig. 10.1a) is usable for permeation studies (diffusion through the skin, see also Sect. 10.4) as well as penetration studies

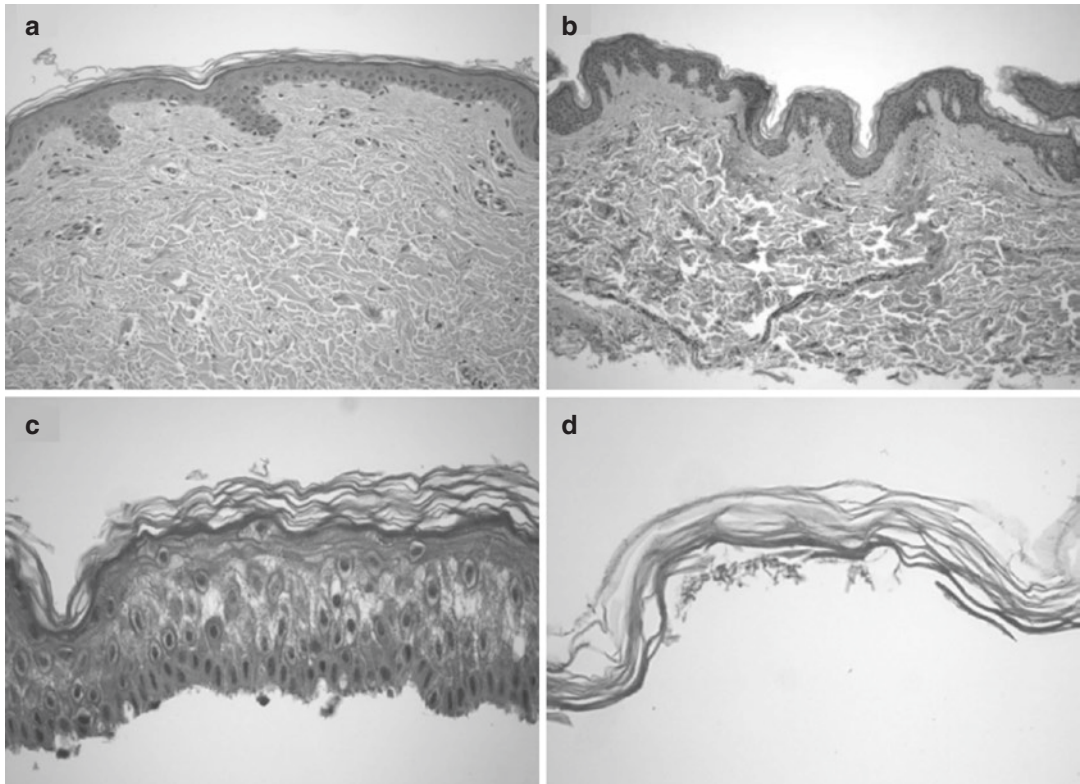


**Fig. 10.1** Different human skin membranes for absorption studies: (a) full thickness skin, (b) dermatomed skin, (c) heat separated epidermis, and (d) enzyme split stratum corneum (According to Schaefer et al. 2008)

(see Sect. 10.5), the latter addressing the substance distribution in the different skin layers. For skin permeation studies, the following aspects are noticeable: Hydrophilic substances often cause very long lag-times and may thus require extremely long observation periods. This holds true also for lipophilic substances because of reduced partitioning at the interface between stratum corneum and viable epidermis. However, long observation periods enhance the problem of microbial contamination and change of skin integrity (due to epidermal separation) and should therefore be avoided. To overcome these problems, further segmentation of the skin will be needed.

#### 10.2.1.2 Dermatomed or Split Skin

Dermatomed skin can be prepared by means of a dermatome which performs surface parallel sections, composed of the epidermis and including

the stratum corneum as well as parts of the dermis (Fig. 10.1b). Normally, a slice thickness of 200–400/500  $\mu\text{m}$  is recommended for human skin (OECD 2004b; USEPA 2004). In doing so, the hair follicles will be cut, but the resulting holes will rapidly close during incubation with the acceptor medium due to swelling of the tissue, especially if aqueous donor and receptor fluids are used. During dermatomization care must be taken to avoid mechanical damage of the SC, the main barrier of the skin. To overcome this problem, protection of the skin surface by a plastic foil is indicated (Brain et al. 1998). Typically, dermatomed skin is used for permeation studies, especially if the influence of the hydrophilic layers of the epidermis and dermis should be considered on skin absorption (influence of partition step between SC and viable epidermis/dermis). Moreover, dermatomed skin might be of particular interest to study the fate of

very lipophilic drugs (e.g., pesticides) due to the limited solubility in rather the hydrophilic viable epidermis and dermis.

### 10.2.1.3 Epidermis Sheets

For the separation of epidermis (consisting of SC and viable epidermis, see Fig. 10.1c) and dermis mechanical, thermal, and chemical techniques are available. With all techniques splitting occurs at the basal layer of the epidermis. Mechanical division can be achieved by applying a vacuum to the skin surface (suction technique (Kiistala 1968)). However, only relatively small areas can be treated in such a way. Thermal treatment is most common. This technique was established by Kligman and Christophers (Kligman and Christophers 1963). A specimen of full thickness skin is immersed in water of about 60 °C for a time period of 30–120 s. Afterwards the epidermis sheet can easily be removed from the dermis by means of a forceps or a spatula. Care has to be taken not to mechanically damage the epidermis by this procedure. Before use, the epidermis should be floated on a physiological buffer solution to unfold it completely. It was shown that this treatment does not result in changes of the barrier function. Several methods of chemical separation are reported (Kligman and Christophers 1963; Lee and Parlicharla 1986; Scott et al. 1986). However, due to the use of strong alkaline or acidic solutions, the buffer capacity of the skin will be changed and this may also influence the penetration of ionizable substances. Epidermis sheets provide a reduced resistance to permeation in comparison to dermatomed skin due to the absence of the dermis layer. They are typically used for permeation studies like dermatomed skin.

### 10.2.1.4 Stratum Corneum Sheets

Stratum corneum sheets (Fig. 10.1d) can easily be isolated by incubating full thickness skin or heat separated epidermis in an aqueous buffer solution of pH 7.4 containing trypsin for 24 h at 37 °C (Kligman and Christophers 1963). The SC may be separated from the underlying tissue by gentle shaking. To remove residual amounts of trypsin, the sheets can be rinsed in isotonic aqueous buffer solution pH 7.4. Due to its fragility the

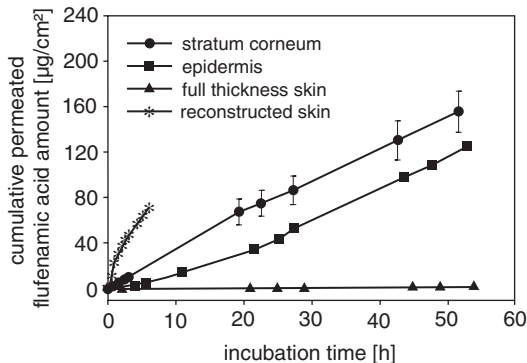


**Fig. 10.2** Permeation experiments with the FD-C. Permeation of flufenamic acid ( $\text{mg}/\text{cm}^2 \pm \text{S.E.}$ ;  $n=3-5$ ) through different skin layers in dependence on the incubation time ( $h$ ) (Figure taken from Wagner et al. (2001))

separated SC should be taken up by a supporting membrane, for example, cellulose membrane (Reichling et al. 2006). In addition, the SC can be lifted by a Teflon foil and afterwards be allowed to dry for storage. After reconstitution with isotonic aqueous buffer pH 7.4, the SC can be used for in vitro experiments.

The influence of the type of skin preparation used in permeation experiments is depicted exemplarily in Fig. 10.2. It is clearly shown that with full thickness skin the permeation is reduced compared to heat separated epidermis and SC, which do not differ in permeability but provide differences in the lag-time. SC sheets are primarily used for mechanistic studies and partition coefficient determination.

### 10.2.1.5 Skin with Impaired Barrier Function

In diseased, injured, or premature skin, the barrier function of the skin is reduced. Skin with an impaired barrier is sometimes also desired for in vitro skin absorption experiments. By stripping with adhesive tape (Wagner et al. 2000) or glue, the outermost cornified cell layers of the SC can be gradually removed, allowing to generate different levels of a decrease in barrier function, corresponding to differently increased permeabilities. In order to compare the results of such experiments, the degree of damage has to be known. In principal this can be done by different

methods, e.g., by determining the amount of SC removed (Hahn et al. 2010) or measuring the transepidermal water loss (TEWL) (Kalia et al. 1996; Russell et al. 2008). Complete removal of stratum corneum and epidermis can best be achieved preferably by rigorous dermatomization rather than by heat separation or trypsinization. The latter two methods may compromise the protein structure of the epidermal/dermal tissue due to precipitation or digestion of proteins.

### 10.2.2 Animal Skin

As human skin has only limited availability, alternatives are necessary. Besides, due to widespread demands in skin absorption studies based on regulatory aspects (e.g., REACH program of the EU (EC 1907/2006, 2006) the pressure to establish alternative models was enforced. In addition, some researchers have ethical and cultural restraints to use human skin (Hikima et al. 2012). Skin from mouse, hairless rat, hamster (cheek pouch), snake (shed skin), pig (ear, flank, abdomen, or back), and cow udder has been suggested as alternatives (Haigh and Smith 1994). However, depending on the animal species used, differences in SC thickness, number of corneocyte layers, hair density, water content, lipid profile and morphology, and different permeabilities in comparison to human skin have been found. Typically the permeability of animal skin was enhanced in comparison to human skin (Bronaugh et al. 1982; Netzlaff et al. 2006b). In general, porcine skin is reported to match human skin best. In addition, porcine skin, especially the ear, is easily available from slaughter houses. However, it has to be kept in mind that porcine skin must not be scalded. Moreover, there are references pointing also to the alternative of cow udder skin (Kietzmann et al. 1993; Netzlaff et al. 2006b; Pittermann and Kietzmann 2006). By the 7th Amendment to the Cosmetic Directive for cosmetic products (EC (2003c) Directive 2003/15/EC; Rossignol MR 2005) a ban of tests on animals and of the marketing of products/ingredients tested on animals came into action in September 2009. Since then only alternative

methods such as animal skin from sources of food supply (pig ear, cow udder) or bioengineered skin surrogates can be used.

### 10.2.3 Bioengineered Skin

For some time bioengineered skin has been introduced in the field of skin research due to the limited supply of human skin, some ethical or cultural restraints to use human skin, and the “3R”-initiative concerning animal welfare (“Refinement, Replacement, Reduction”) (Russell and Russell 1957). Firstly, skin corrosion (Kandárová et al. 2006a, b), sensitization, (Bernard et al. 2000; Spielmann et al. 2000), metabolic phenomena (Gysler et al. 1999), and phototoxicity (Liebsch et al. 1999) were addressed and afterwards skin permeability was evaluated (Dreher et al. 2002). Meanwhile various commercial reconstructed epidermis models are available (Netzlaff et al. 2005) and also accepted for skin corrosion (OECD 2004c, 2006) and irritation testing (OECD 2010). Moreover, many attempts have been made to compare in detail bioengineered skin to human skin and animal skin (Schreiber et al. 2005; Netzlaff et al. 2005, 2007). In two large studies sponsored by the German BMBF (Federal Ministry of Education and Research), the usefulness of the commercially available reconstructed epidermis models Episkin™ (L’Oreal, France), Epiderm® (MatTek corporation, USA), SkinEthic® (SkinEthic Laboratories, France) were tested with nine substances in aqueous solution covering a wide range of lipophilicities and molecular weights (Schäfer-Korting et al. 2006, 2008). As a result, it could be clearly shown that all reconstructed epidermis models were more permeable than human heat separated epidermis and dermatomed porcine skin; however, the rank order of permeability agreed reasonably among these models. Besides, it could be shown that reconstructed epidermis provides less variability in comparison to human and animal skin which is consistent with results from the EDETOX (Evaluations and Predictions of Dermal Absorption of Toxic Chemicals) project (van de Sandt et al. 2004). A review about morphology, biochemical characterization, and application of the bioengineered mod-

els Episkin™, Epiderm®, and SkinEthic® is reported by Netzlaff et al. (2005). Besides, a list of materials tested with Epiderm® is provided by MatTek, USA ([www.mattek.com/pages/products/epider/materials-tested](http://www.mattek.com/pages/products/epider/materials-tested)).

Additional reports are available for other, sometimes self-made, bioengineered skin models. Suhonen et al. reported permeability experiments for 18 compounds in buffered aqueous solutions with a cell culture model based on keratinocytes from rat skin (Suhonen et al. 2003). A close relationship to isolated human cadaver skin was found; however, again the permeability in the cell culture model was enhanced. The group of Mueller-Goymann developed an artificial skin construct based on collagen and HaCaT (human adult low calcium high temperature keratinocytes) cells cultivated at the air-liquid interface (Savic et al. 2009). Investigating the permeation of caffeine and diclofenac from various formulations containing natural surfactant/fatty alcohols mixed emulsifiers they reported that the vehicle skin interaction was mirrored in the artificial skin construct.

A full-thickness commercial skin model, the Phenion® model (Henkel AG & Co.KGaA, Germany) was tested by Ackermann et al. (2010) for percutaneous absorption testing of the OECD (Organisation of economic Co-operation and Development) reference compounds caffeine and testosterone. They concluded that the results closely paralleled human skin (Ackermann et al. 2010). One of the major problems with bioengineered skin is that the sheets must be transferred to standard diffusion cells after the cell layer has been punched out from the cultivating support. To overcome this drawback, Grégoire et al. improved the experimental setup for screening skin absorption with the reconstructed epidermis model Episkin® (Grégoire et al. 2008). By modifying the culture conditions, it was possible to omit bypass diffusion in the inserts. In contrast to studies in static diffusion cells the cell layer no longer has to be punched out. In summary, although there are references suggesting the helpfulness of bioengineered skin in skin absorption studies, the basic problem is the lack of building up a barrier at the same level as natural

human skin (see Fig. 10.2). However, the actual value of such reconstructed skin might be in the development of disease models to simulate specific situations (Semlin et al. 2011).

#### 10.2.4 Artificial Skin Surrogates

Artificial skin surrogates have a long lasting history. Starting from simple membranes of dialysis tubing and polymeric membranes for example of regenerated cellulose, cellulose derivatives, polycarbonate, polyolefines, silicon, etc. more and more complex systems became available (Haigh and Smith 1994). It was recognized early that these very simple membranes do not resemble the skin characteristics and therefore their recommended use was to determine the release of active compounds only (FDA 1997). However, by loading of porous filter materials with lipids, these surrogates better resemble the skin properties especially if native SC lipids are used. Jaeckle et al. used systematic variation of lipid composition to establish suitable membranes which provide properties similar to heat-separated epidermis (Jaeckle et al. 2003). Recently, the Bouwstra group published different methods to establish SC model membranes (De Jager et al. 2004, 2005). For benzoic acid, they could nicely demonstrate that the flux is comparable to human SC (Groen et al. 2008). Based on the PAMPA technique (parallel artificial membrane permeability Assay) that has been successfully applied to predict gastrointestinal and blood–brain barrier absorption (Avdeef 2005) Ottavianai et al. reported on the use of a PAMPA-membrane loaded with an optimized mixture of silicone (70 %) and isopropyl myristate (30 %) to address skin permeation (Ottaviani et al. 2006). They could show for 31 substances of a diverse data set a good correlation to  $k_p$ -values of human skin. Recently, two commercial models based on synthetic lipid mixtures, Strat M® (Joshi et al. 2012) and Skin-PAMPA (Sinkó et al. 2012), have become available.

The Skin-PAMPA assay mimics the lipid phase of the SC using an optimized lipid mixture composed of ceramides, free fatty acids, and chole-

terol. It can be considered as a refined approach of the method of Ottavani et al. mentioned above. The method was validated comparing the permeation ( $k_p$ ) of various solutes through three different kinds of skin preparations (isolated SC, isolated epidermis, and full thickness skin). Moreover, it could be shown that the assay is capable to predict the permeation in human skin with a reasonable correlation between Skin-PAMPA permeability and Franz cell permeability (Sinkó et al. 2012). When it comes to mimic different skin preparation, the best correlation was found for full thickness skin. Since Skin-PAMPA is a rather new approach, it should be investigated further to prove its reliability and applicability to various scenarios.

The Strat M<sup>®</sup> approach uses a synthetic membrane sandwich composed of polyether sulfone treated with synthetic lipid materials to mimic the human skin. The method was tested using various substances in different formulations in comparison to human cadaver skin in a Franz cell setup. For aspirine, nicotine, and hydrocortisone, the usefulness of the model could be demonstrated showing comparable fluxes in comparison to human skin. Furthermore, comparable vehicle effects, such as penetration enhancement, could be observed for different caffeine formulations. The authors of the study state that the model was investigated against a diverse data set but unfortunately did not state exactly which compounds were tested and what kind of human skin preparation was used in the study (Joshi et al. 2012). Besides, a definition of the lipid mixture composition is missing. Since this is also a novel approach its reliability and versatility should be shown in greater detail in further studies.

---

## 10.3 In Vitro Experimental Setups for Skin Absorption Studies

### 10.3.1 Finite Versus Infinite Dosing

For skin absorption studies one differentiates usually between two different modes of application, finite and infinite dosing. Both terms are defined in the OECD Guideline 428 (OECD 2004b) and more specifically in OECD Guidance

28 (OECD 2004a). In general, finite dosing mimics the “in use” conditions where normally a limited dose of the formulation is applied to the skin. In contrast by infinite dosing a disproportionately high amount of formulation is applied. Typically a maximum of 1–5 mg/cm<sup>2</sup> for powders, up to 10 µl/cm<sup>2</sup> for solutions, and up to 10 mg/cm<sup>2</sup> for semisolid preparations are considered finite doses. One problem with finite dosing is to spread the formulation evenly across the skin surface. Hahn et al. could demonstrate that this effect may influence the results of in vitro skin absorption studies depending on the applied drug (Hahn et al. 2012). Also, the finite dose kinetics of drug concentration over time are usually quite complex due to multifactorial overlapping processes such as the depletion of active in the donor phase (which should usually lead to a decrease in the rate of absorption), changes in the donor composition which affect the skin permeability, and elimination of the active due to metabolism and systemic clearance to name but the most relevant. The complexity of the problem shall be illustrated by the following example. If the formulation is applied without an occlusive dressing, the donor concentration may increase due to evaporation of components of the vehicle and consequently increase the rate of absorption. This may even lead to over-saturation or recrystallization of formulation components or the active on the skin which further complicates matters. Normally true finite dosing is assumed if the donor concentration depletes to at least 10 % of the initial concentration of the applied formulation after about 20–24 h (WHO 2006).

By infinite dosing, the amount of formulation should be large enough to assure that practically no donor depletion occurs. From that it follows that a maximum rate of absorption is gained and maintained over the whole experimental period. Typically the steady state flux is determined and based on that the apparent permeability coefficient is calculated. In between of finite and infinite dosing all transient cases are possible. For more details on the effects of finite, semifinite, and infinite dosing on skin invasion see Chapter 1 “Basic mathematics in skin permeation of drugs” in this volume.

As stated before finite dosing is normally related to “in use” conditions. However, the conditions during bathing or wearing closely fitting clothes are more realistic depicted by infinite dosing (WHO 2006).

### 10.3.2 Open Versus Occluded Dosing

Occlusion during in vitro skin absorption experiments will influence the results in different ways. Normally these effects are limited to the finite dose case, because for infinite dosing practically no changes of the donor compartment will take place. In the open system, due to evaporation of vehicle compounds, the concentration of active increases and may even achieve supersaturation. This changes the conditions completely depending on the magnitude of evaporation. Surber and Smith have reported this phenomenon as metamorphosis of the formulation (Surber and Smith 2005). On the other hand, if the active is volatile the concentration will decrease during experimental time. In this case, it is essential to determine the rate of evaporation during the experiment by collecting the volatile substance, for example, by using an adsorption trap (adsorptive powder) mounted on top of the diffusion cell (Rauma et al. 2013). This is essential if mass balance is addressed (Kasting and Miller 2006).

### 10.3.3 Diffusion Cells

In the past, many different protocols have been used to address skin invasion (ECETOC 1993; EC 2003a, b; SCCNFP 2003; SCCNFP/0690/03 2003; EC 2004; WHO 2006; SCCS/1358/10 2010; EFSA 2012). This results in problems of comparability of results. Meanwhile in 2004 the OECD Guideline 428 and OECD Guidance 28 became effective and provide general rules for conducting in vitro tests for dermal absorption (OECD 2004a, b). In principal special protocols are allowed; however, deviations from the recommended procedures should be restricted and have to be rationally motivated on a case-to-case basis.

In principal two different types of test chambers are available. These are either upright/vertical (Fig. 10.3a) or side-by-side/horizontal cells (Fig. 10.3b) with receptor volumes from 0.5 to 15 ml and application areas of about 0.2–2 cm<sup>2</sup> (Brain et al. 1998). As by manufacturing processes dimensions may vary in certain limits calculation of data has to be related to individual cells. Vertical cells are preferable for testing semisolid formulations which can be spread on the incubation area analogously to the in vivo situation. In addition, it is easy to realize both occlusive effects by capping the donor chamber and in-use condition (nonoccluded) by leaving the donor chamber open. Usually, in vertical cells the receptor phase is mixed by stirring with a magnetic bar. Side-by-side cells consist of two chambers separated by a membrane. Both sides are stirred leading to highly controlled diffusion conditions, including continuous concentration equilibrium in both chambers and well-defined unstirred layers. Therefore, side-by-side diffusion cells are preferable for kinetic studies, especially if solutions are tested. For testing semisolid preparations, the design of side-by-side diffusion cells has to be changed by replacing the donor side by a static system without stirring (Feldmann and Maibach 1969; Bronaugh and Stewart 1984, 1985). For vertical as well as side-by-side diffusion cells, the static and the flow-through mode are available. Using the static mode the receptor phase is not replaced continuously except for the volume exchange during sampling. This leads to a constant increase of substance in the receptor fluid, and depending on the saturation concentration of compound diffusion may be affected. In general it is agreed upon that until reaching a maximum of 10 % saturation concentration in the acceptor, diffusion will not be influenced (known as sink conditions). Therefore, care must be taken not to exceed this limit. One possibility to overcome this problem is to exchange the receptor medium completely at each sampling point. However, it has to be considered that problems with compound quantification, due to quantification limits, and air bubbles may occur.

Because of the easy handling the most widely used static diffusion cell is the Franz diffusion



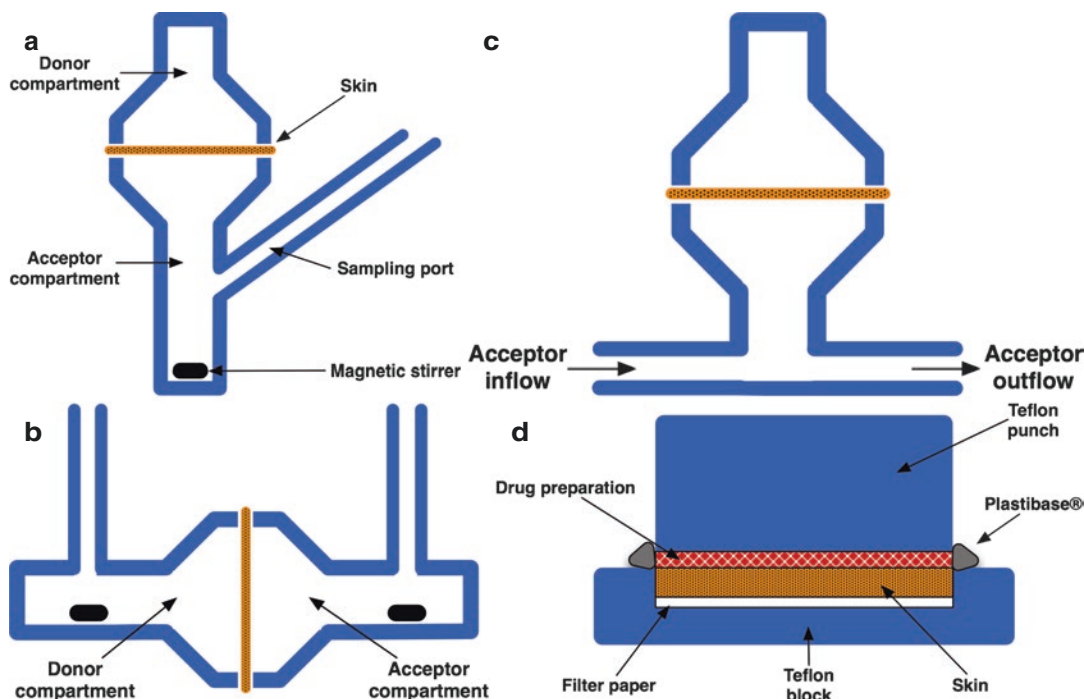


**Fig. 10.3** Sketch of a static vertical Franz diffusion-cell (a), static side-by-side diffusion cell (b), after static side-by-side diffusion cell, flow-through cell (c), and Saarbruecken penetration model (d)

cell which was introduced in 1975 (Franz 1975). As an alternative a flow-through version can be used (Fig. 10.3c). In this mode the receptor volume is continuously replaced by means of a pump, which more or less mimics the vivo conditions of drainage by the systemic circulation and facilitates maintaining sink conditions. A typical flow-through cell, based on a side-by-side diffusion cell, has been designed by Bronaugh and Stewart (1985). It has to be kept in mind that flow rate, chamber volume, and detection limit are related variables. The flow rate has to be adjusted in a way that during the entire experimental time sink conditions apply in the receptor chamber, the amount can be detected, and proper mixing exists. In addition adsorption of analytes to the tubing used to pump the receptor medium may influence the results. A real benefit of flow-through systems especially for higher numbers of tests such as in an industrial setting is that continuous replacement of the receptor fluid can easily be automated (Moody 1997, 2000). Automation of sampling is available for vertical

diffusion cells too, for example, described by Solich et al. (2001, 2003). In general several comparative studies have shown the equivalence of static and flow-through cells (Bronaugh and Maibach 1985; Bronaugh and Stewart 1985). Due to the easy handling and realization of in-use application conditions, static Franz diffusion cells are generally preferred. However, for studies where metabolic effects are involved flow-through systems like the Bronaugh cell are superior because the continuous solvent replacement better mimics the in vivo situation (Bronaugh 2004a, b).

### 10.3.4 Barrier Integrity Check

Barrier integrity has to be checked prior or after in vitro skin invasion experiments. Common physical methods are measurement TEWL or transcutaneous resistance or alternatively the measurement of the permeation of a marker substance, mostly tritiated water. TEWL measurements are well

established for in vivo studies. For in vitro experiments, it is strongly recommended to use a closed chamber measurement setup (e.g., Aquaflex AF200, Biox, London, UK; VapoMeter, Delfin Technologies, Kuopio, Finland). In contrast, Netzlaff et al. reported that devices using the open chamber principle (e.g., the Tewameter<sup>®</sup> TM 300, Courage-Khazaka Electronic, Koeln, Germany) are not sensitive enough to detect small defects of the skin which nonetheless influence skin permeation (Netzlaff et al. 2006a). However, it has to be kept in mind that TEWL threshold values that might indicate a violation of barrier integrity depend on the TEWL instrument used as well as the skin preparation and therefore no general limits can be provided (Elkeeb et al. 2010). Using tritiated water as a marker is also a well-established method although the exclusion criteria for damaged skin are nowadays under discussion. Too many samples may be rejected using a permeability coefficient of water of  $2.5 \times 10^{-3}$  cm/h as the upper limit to reject cells with damaged barrier (Wilkinson et al. 2004). Another problem is the use of tritiated water before doing the experiment. During the removal of the remaining tritiated water barrier damage may occur. Therefore, the use of tritiated water must be evaluated critically.

### 10.3.5 Temperature

Diffusion processes are temperature dependent and therefore in vitro permeation experiments should be carried out at the physiological temperature of the skin surface, i.e.,  $32 \pm 1$  °C (OECD 2004a, b). This should be maintained during the entire experimental duration. If diffusion cells with a water jacket are used in line configuration may cause a temperature gradient between the first cell and the last cell. To overcome this problem parallel connection of the cells is recommended. Other possibilities are to insert the cells in a water bath (in this case care must be taken that no water enters the cells) or a metal bloc or alternatively to store the cells in an oven with constant temperature (Schäfer-Korting et al. 2006).

### 10.3.6 Selection of Receptor Fluid

The selection of the right receptor fluid is essential for the results. The following points have to be considered: the receptor fluid should enable sufficient solubility of the active compound under investigation (see also Sect. 10.3.3 for explanation of sink conditions), allow unhindered partitioning of the active from the skin to the receptor fluid, and not disturb the barrier integrity of the skin. For water soluble compounds, normal saline or isotonic buffer systems of pH 7.4 are appropriate. To prevent microbial influences on skin integrity preservatives, preferentially sodium azide (0.05 % wt/V), should be added. To maintain viability of fresh skin cell culture medium is feasible. For lipophilic substances additives to enhance the solubility are needed (OECD 2004a). For example, for essential oils ethanol water mixtures of different concentrations may be used (Reichling et al. 2006). Furthermore, the addition of surfactants (Challapalli and Stinchcomb 2002; OECD 2004a), bovine serum albumin (Dal Pozzo et al. 1991), or cyclodextrines (Sclafani et al. 1995) are reported. In all these cases, the influence of the additives on permeability must be clarified, e.g., by testing different concentrations of a solubilizer. Besides, it has to be considered that the analytical procedure may be affected by the additives.

### 10.3.7 Duration of Exposure and Sampling Period

Exposure times of the skin with the formulation should always reflect in-use conditions and consequently will vary, e.g., for rinse-off products exposure time will only be a few minutes. However, the sampling time should cover at least a period of 24 h (OECD 2004b). For kinetic studies, e.g., determination of permeability coefficients under infinite conditions or lag time (i.e., the time to reach steady state of diffusion) an extension to 48 h may be needed. Even longer sampling times normally result in impairment of the skin barrier and freshness and the results are questionable. Moreover, where static cells are

concerned a sufficiently large number of sampling points should be planned so that a representative number of data points are available especially during steady state (rule of thumb: preferentially at least five sampling points which are evenly spread out during steady state) to describe the permeation kinetics properly. Especially concentration changes between sampling points should be large enough to be detected by the analytical procedure.

### 10.3.8 Quantification Methods

For risk assessment frequently radioactive labeled compounds are used (Poet and McDougal 2002). In this context, it has to be demonstrated that the intact molecule is measured by scintillation counting. In addition one cannot fully exclude that labeling may result in a change of permeability properties. Meanwhile new highly sensitive and selective quantification methods are available, e.g., high-performance liquid chromatography (HPLC), Liquid chromatography-mass spectrometry (LC-MS-MS), etc. With these methods simultaneous quantification of the mother compound as well as metabolites or degradation products is possible. Therefore, it is recommended to use such methods preferentially.

### 10.3.9 Influence of Thickness of Skin Preparation

It is well known that the thickness of the skin preparation may influence the results of in vitro skin absorption experiments in various manners depending on compound, formulation, and dosing (finite/infinite) (Wagner et al. 2002; Veccia and Bunge 2003; EDETOX 2004; Wilkinson et al. 2004, 2006; Henning et al. 2008, 2009). Due to the complexity of the skin invasion process and lack of data, relations to physico-chemical characteristics are difficult to establish. However, in general if using full thickness skin steady state conditions may often not be achieved

within feasible experimental time periods (<48 h, in well-founded exceptional cases up to 72 h). Therefore, it is generally recommended to use split-thickness human skin for permeation studies, if possible (Van De Sandt et al. 2000; SCCS/1358/10 2010). If full thickness skin is needed, rational has to be provided for that. Moreover, the use of epidermal membranes must be justified. Due to their fragility, heat separated epidermis may cause problems with tape stripping which is needed for establishing a mass balance to address the content inside the SC in finite dose experiments especially if skin absorption of pesticides etc. is addressed. In this case, the amount in the SC is often considered as not absorbed depending on substance properties and application (EFSA 2012).

### 10.3.10 Number of Experiments/Replicates

As basic criteria concerning the number of samples to assess in vitro absorption of cosmetic ingredients eight samples from four different donors are recommended by (SCCS/1358/10 2010). In addition a minimum of 0.64 cm<sup>2</sup> skin area should be covered by the formulation (SCCS/1358/10 2010). Furthermore, the total recovery should be in the range of 85–115% (SCCS/1358/10 2010). However, for risk assessments of chemicals the recovery limits are 90–110% but may be extended in special justified cases (OECD 2004b).

### 10.3.11 Segmentation of Skin in Different Skin Layers

To localize the active compound in different skin layers, e.g., to determine depot effects, a segmentation of the skin is needed. Incubation of the skin can be done either in diffusion cells or in a special apparatus, the so-called Saarbruecken penetration model (SB-M, Fig. 10.3d) (Wagner et al. 2000). In contrast to diffusion cells, the SB-M

does not have a liquid receptor phase and therefore the original hydration state of the skin is preserved. Normally full thickness skin is used for this model, and experiments are done for a series of incubation times to obtain drug-concentration skin depth profiles. For more details, please refer to (Wagner et al. 2000; Melero et al. 2011).

Skin dissection can be done first by tape stripping to remove the stratum corneum layer-by-layer using adhesive tapes and afterwards by segmentation of epidermis and dermis into surface parallel slices by means of a cryomicrotome. Skin segmentation in in vitro absorption experiments is only meaningful if skin of a certain thickness, e.g., dermatomed or full thickness skin, is used.

#### 10.3.11.1 Removal of the Stratum Corneum by Tape Stripping

Many protocols exist for tape stripping in vitro as well as in vivo (Shah et al. 1998; Surber et al. 1999; Voegeli et al. 2007; Lademann et al. 2009; Melero et al. 2011). Normally tape stripping is not possible for epidermis sheets due to their fragility. Furthermore, for longer incubation times or strong interaction of excipients with the SC tape stripping may be altered.

To obtain valid results, the following points have to be considered:

The surface of the skin must be properly cleaned, for example, by cotton swabs or by a washing procedure. The washing step removes the remaining formulation from the skin surface and thus assures that the tape strips may stick to the skin surface. Especially, organic solvents should be avoided due to the effect of substance extraction at least from the outermost stratum corneum layers.

For homogeneous tape stripping, the problem of wrinkles has to be eliminated and a constant pressure has to be applied. That can be done, for example, by mounting the skin disk under stretching on cork disks in a special apparatus (Wagner et al. 2000) and charging each strip with a constant weight for a predetermined time period or using a special roller (Lademann et al. 2009). Furthermore, to be able to calculate the

corresponding skin depths the removed amount of stratum corneum has to be determined. This can be done, e.g., by weighing (Russell and Guy 2012) or by a more advanced method such as infrared densitometry (Hahn et al. 2010; Franzen et al. 2012) protein extraction and quantification (Dreher et al. 2005) or other optical methods (Weigmann et al. 2003). For human skin and pig skin, it could also be demonstrated that infrared densitometry offers the possibility to determine the point of total removal of the stratum corneum (Hahn et al. 2010; Franzen et al. 2012). For more detailed instructions see (Melero et al. 2011).

#### 10.3.11.2 Segmentation of the Deeper Skin Layers Consisting of Viable Epidermis and Dermis (Cryosectioning)

The best way for segmentation of the deeper skin layers is surface parallel cryosectioning. After removal of the SC the skin specimen is mounted on a metal bloc, the surface is adjusted horizontally, and rapidly frozen, for example, by expanding carbon dioxide. Subsequently, the sample is transferred into a cryomicrotome and the skin is segmented into horizontal slices. The corresponding skin depth can easily be related to the weight of the slice. For details see reference (Melero et al. 2011).

---

## 10.4 Results Obtained from Permeation Studies

Permeation studies are normally conducted to determine the transdermal/systemic availability of a compound. Therefore, the main experimental parameter which is addressed is the amount permeated per  $\text{cm}^2$  into the receptor compartment over time. Two different dosing regimens are available. The infinite dosing regimen serves to determine kinetic constants such as the steady state flux or the apparent permeability coefficient and lag time, whereas finite dosing evaluates the amount absorbed after a certain time. Additionally by applying the technique of mass balance the

fate of a compound can be evaluated (i.e., the percentage that stays on the skin surface, enters the SC or other parts of the skin, etc.).

#### 10.4.1 Infinite Dosing Studies

Permeation studies using infinite dosing address the steady state flux of a compound from a formulation through a given membrane, e.g., SC, epidermis, dermatomed skin, or full thickness skin, according to Fick's law of diffusion. The steady state flux value  $J_{ss}$  is calculated from the linear part of a diagram of the amount of compound permeated into the receptor phase per area versus time. At the beginning of the experiment, the membrane will first be filled up with permeant until saturation (steady state) is reached. The extrapolation of the linear steady state intersects with the time-axis at the lag time  $t_{lag}$  which can be used to calculate the apparent diffusion coefficient. Moreover, based on the steady state flux ( $J_{ss}$ ) the apparent permeability coefficient  $K_p = J_{ss}/C_v$ , with  $C_v$  = concentration in the vehicle can be calculated. Permeability coefficients may be used for the comparison of different formulations. Furthermore, the maximum flux ( $J_{ss(max)}$ ) of the solute, which denotes the maximal possible dermal delivery from a given vehicle, can be estimated by  $K_{p(max)} = J_{ss(max)}/C_{ss}$ , with  $C_{ss}$  = saturation concentration of the solute in the vehicle (Roberts et al. 2002; Magnusson et al. 2004). For more details see Chap. 1 "Basic Mathematics in Skin Permeation of Drugs" in this volume (Selzer et al. 2013).

#### 10.4.2 Finite Dosing Studies

Based on the permeated amount of compound into the receptor phase per  $cm^2$  versus time dependency the amount permeated can be calculated for selected time points. These values can serve for comparison of different formulations. Moreover, the highest flux value (Also: peak flux,  $J_{peak}$ ) during the experimental time period can be determined. For finite dosing studies after the end of the

experiment a mass balance is inevitable. Total recovery should be in the range of 85–115% according to guidelines or references (SCCNFP/0690/03 2003; SCCS/1358/10 2010). However, for risk assessments of chemicals the recovery limits are set to 90–110% but may be extended in special justified cases (OECD 2004b).

---

### 10.5 Results Obtained from Penetration Studies

The scope of penetration studies is to determine the distribution of a compound within the different skin layers. Therefore, skin segmentation is needed (see Sect. 10.3.11). Within each skin segment the amount of drug must be determined selectively and completely. For doing that an extraction procedure has to be established and validated which allows the determination of very low concentrations with a high accuracy and recovery. This may lead to complications if quantification techniques like HPLC, LC-MS, etc. are used. Furthermore, due to quantification limits consecutive segments may need to be pooled (Wagner et al. 2000; Hansen et al. 2008). However, this reduces the precision of the results. Besides, for the construction of concentration skin depth profiles the exact segment position in the skin has to be known (Hahn et al. 2010). Examples for SC profiles of infinite dosing and finite dosing are shown in Fig. 10.4.

Due to potential contamination by not completely removed formulation often the two first strips are discarded. Based on such profiles diffusion parameters according to Fick's law can be calculated. For more details, please refer to reference (Selzer et al. 2013). Apart from that additional information can be gained. Wagner et al. demonstrated by applying a model based on a Michaels Menten kinetic that the time to reach 50% of saturation within the SC can be related to the permeability coefficients for heat-separated epidermis sheets (Wagner et al. 2002). Moreover, calculation of total amounts in different skin layers, e.g., SC and deeper skin layer, may allow the identification of skin depots.

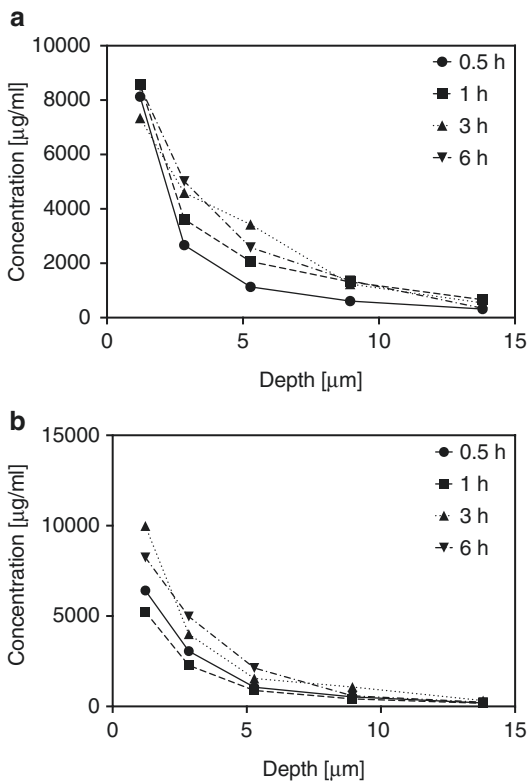


**Fig. 10.4** Stratum corneum concentration-depth profiles of 0.9% flufenamic acid in wool wax alcohol ointment for the infinite (a) and finite dose case (b) in dependency of incubation time. Standard deviations are not shown for clarity (Data taken H. Wagner, PhD thesis, Charakterisierung des Arzneistofftransportes in Humanhaut unter in-vitro und in-vivo Bedingungen sowie unter Berücksichtigung des Einflusses zweier in-vitro Testsysteme” (2001), Saarland University, Saarbruecken, Germany)

## Conclusion

In vitro approaches to study skin absorption are useful tools in dermal product development as well as in risk assessment. Within the last years enormous efforts have been done to standardize experimental setups (SCCNFP/0690/03 2003; OECD 2004a, b; WHO 2006). However, due to the diversity of the requirements deviations from the standard protocols are often needed. This chapter provides a basic overview of the main topics of in vitro skin absorption techniques. Especially, different skin layers and artificial membranes for permeation studies are addressed. In general, the major

problem for advanced data interpretation is the lack of systematic experimental studies and standardized procedures.

## References

- Ackermann K, Lombardi Borgia S, Korting HC, Mewes KR, Schäfer-Korting M (2010) The phenion® full-thickness skin model for percutaneous absorption testing. *Skin Pharmacol Physiol* 23:105–112
- Avdeef A (2005) The rise of PAMPA. *Expert Opin Drug Metab Toxicol* 1:325–342
- Bernard FX, Barrault C, Deguercy A, De Wever B, Rosdy M (2000) Development of a highly sensitive in vitro phototoxicity assay using the SkinEthic™ reconstructed human epidermis. *Cell Biol Toxicol* 16:391–400
- Brain KR, Walters KA, Watkinson AC (1998) Investigation of skin permeation in vitro. In: Roberts M, Walters KA (eds) *Dermal absorption and toxicity assessment*, vol 91. Marcel Dekker, New York, pp. 161–187
- Bronaugh RL (2004a) Methods for in vitro percutaneous absorption. In: Zhai H, Maibach H (eds) *Dermatotoxicology*, 6th ed. CRC Press, New York, pp 520–526
- Bronaugh RL (2004b) Methods for in vitro skin metabolism studies. In: Zhai H, Maibach H (eds) *Dermatotoxicology*, 6th ed. CRC Press, New York, pp 622–630
- Bronaugh RL, Maibach HI (1985) Percutaneous absorption of nitroaromatic compounds: in vivo and in vitro studies in the human and monkey. *J Invest Dermatol* 84:180–183
- Bronaugh RL, Stewart RF (1984) Methods for in vitro percutaneous absorption studies III: hydrophobic compounds. *J Pharm Sci* 73:1255–1258
- Bronaugh RL, Stewart RF (1985) Methods for in vitro percutaneous absorption studies. IV: the flow-through diffusion cell. *J Pharm Sci* 74:64–67
- Bronaugh RL, Stewart RF, Congdon ER (1982) Methods for in vitro percutaneous absorption studies II. Animal models for human skin. *Toxicol Appl Pharmacol* 62:481–488
- Bronaugh RL, Stewart RF, Simon M (1986) Methods for in vitro percutaneous absorption studies VII: use of excised human skin. *J Pharm Sci* 75:1094–1097
- Challapalli PVN, Stinchcomb AL (2002) In vitro experiment optimization for measuring tetrahydrocannabinol skin permeation. *Int J Pharm* 241:329–339
- Dal Pozzo A, Liggeri E, Delucca C, Calabrese G (1991) Prediction of skin permeation of highly lipophilic compounds: in vitro model with a modified receptor phase. *Int J Pharm* 70:219–223
- De Jager MW, Gooris GS, Dolbnya IP, Bras W, Ponc M, Bouwstra JA (2004) Novel lipid mixtures based on synthetic ceramides reproduce the unique stratum corneum lipid organization. *J Lipid Res* 45:923–932
- De Jager MW, Gooris GS, Ponc M, Bouwstra JA (2005) Lipid mixtures prepared with well-defined synthetic

- ceramides closely mimic the unique stratum corneum lipid phase behavior. *J Lipid Res* 46:2649–2656
- DI G, Gooris GS, Ponec M, Bouwstra JA (2008) Two new methods for preparing a unique stratum corneum substitute. *Biochim Biophys Acta Biomembranes* 1778:2421–2429
- Dreher F, Patouillet C, Fouchard F, Zanini M, Messager A, Roguet R et al (2002) Improvement of the experimental setup to assess cutaneous bioavailability on human skin models: dynamic protocol. *Skin Pharmacol Appl Skin Physiol* 15:31–39
- Dreher F, Modjtahedi BS, Modjtahedi SP, Maibach HI (2005) Quantification of stratum corneum removal by adhesive tape stripping by total protein assay in 96-well microplates. *Skin Res Technol* 11:97–101
- EC (2003a) European Commission, Health & Consumer protection directorate, directorate E, Food safety: plant health, animal health and welfare, international questions, Flufenacet 7469/VI/98, Brussels, Belgium, <https://www.fluoridealert.org/wp-content/pesticides/flufenacet.eu.july.2003.pdf>
- EC (2003b) European Commission, Health & Consumer protection directorate, directorate E, Food safety: plant health, animal health and welfare, international questions. Propineb SANCO/7574/VI/97-final, Brussels, Belgium, [http://ec.europa.eu/food/fs/sfp/ph\\_ps/pro/eva/existing/list1-34\\_en.pdf](http://ec.europa.eu/food/fs/sfp/ph_ps/pro/eva/existing/list1-34_en.pdf)
- EC (2003c) Directive 2003/15/EC of the European Parliament and of the Council of 27 February 2003, <http://eur-lex.europa.eu/legal-content/EN/TXT/?uri=CELEX%3A32003L0015>
- EC (2004) Guidance on dermal absorption, Sanco/22s2/2000rev.7, European Commission, Brussels, Belgium, [http://ec.europa.eu/food/plant/docs/pesticides\\_ppp\\_app-proc\\_guide\\_tox\\_dermal-absorp-2004.pdf](http://ec.europa.eu/food/plant/docs/pesticides_ppp_app-proc_guide_tox_dermal-absorp-2004.pdf)
- EC 1907/2006 (2006) Registration, Evaluation, Authorisation and Restriction of Chemicals (REACH), European Commission, Brussels, Belgium, [http://eur-lex.europa.eu/legal-content/EN/TXT/?uri=uriserv:OJ.L\\_.2006.396.01.0001.01.ENG](http://eur-lex.europa.eu/legal-content/EN/TXT/?uri=uriserv:OJ.L_.2006.396.01.0001.01.ENG)
- ECETOX (1993) ECETOX (European Centre for Ecotoxicology and Toxicology of Chemicals), Percutaneous absorption. Monograph 020, ECETOX, Brussels, Belgium, <http://www.ecetoc.org/publications/monographs/>
- EDETOX (2004) Evaluations and predictions of dermal absorption of toxic chemicals, Final report for dissemination, Faith M. Williams, [https://ec.europa.eu/research/quality-of-life/ka4/pdf/report\\_edetox\\_en.pdf](https://ec.europa.eu/research/quality-of-life/ka4/pdf/report_edetox_en.pdf)
- EEC (1976) Council directive on the approximation of laws of the Member States relating to cosmetic products (76/768/EEC), European Commission, Brussels, Belgium
- EFSA (2012) Panel on Plant Protection Products and their Residues, Guidance on Dermal Absorption, *EFSA Journal* 10(4):2665. DOI: 10.2903/j.efsa.2012.2665 <https://www.efsa.europa.eu/en/efsajournal/pub/2665>
- Elkeeb R, Hui X, Chan H, Tian L, Maibach HI (2010) Correlation of transepidermal water loss with skin barrier properties in vitro: comparison of three evaporimeters. *Skin Res Technol* 16:9–15
- FDA (1997) U.S. Food and Drug Administration, Silver Spring, MD 20993, USA Guidance SUPAC-SS: Nonsterile Semisolid Dosage Forms; Scaling-Up and Post-Approval Changes: Chemistry, Manufacturing and Controls; In Vitro Release Testing and In Vivo Bioequivalence Documentation. Food and Drug Administration, Silver Spring, MD 20993, USA, <http://www.fda.gov/ucm/groups/fdagov-public/@fdagov-drugs-gen/documents/document/ucm070930.pdf>
- Feldmann RJ, Maibach HI (1969) Percutaneous penetration of steroids in man. *J Invest Dermatol* 52:89–94
- Franz TJ (1975) Percutaneous absorption. On the relevance of in vitro data. *J Invest Dermatol* 64:190–195
- Franzen L, Windbergs M, Hansen S (2012) Assessment of near-infrared densitometry for in situ determination of the total stratum corneum thickness on pig skin: influence of storage time. *Skin Pharmacol Physiol* 25:249–256
- Grégoire S, Patouillet C, Noé C, Fossa I, Benech Kieffer F, Ribaud C (2008) Improvement of the experimental setup for skin absorption screening studies with reconstructed skin EPISKIN®. *Skin Pharmacol Physiol* 21:89–97
- Gysler A, Kleuser B, Sippl W, Lange K, Korting HC, Hölting HD et al (1999) Skin penetration and metabolism of topical glucocorticoids in reconstructed epidermis and in excised human skin. *Pharm Res* 16:1386–1391
- Hahn T, Hansen S, Neumann D, Kostka KH, Lehr CM, Muys L et al (2010) Infrared densitometry: a fast and non-destructive method for exact stratum corneum depth calculation for in vitro tape-stripping. *Skin Pharmacol Physiol* 23:183–192
- Hahn T, Selzer D, Neumann D, Kostka KH, Lehr CM, Schaefer UF (2012) Influence of the application area on finite dose permeation in relation to drug type applied. *Exp Dermatol* 21:233–235
- Haigh JM, Smith EW (1994) The selection and use of natural and synthetic membranes for in vitro diffusion experiments. *Eur J Pharma Sci* 2:311–330
- Hansen S, Henning A, Naegel A, Heisig M, Wittum G, Neumann D et al (2008) In-silico model of skin penetration based on experimentally determined input parameters. Part I: experimental determination of partition and diffusion coefficients. *Eur J Pharm Biopharm* 68:352–367
- Harrison SM, Barry BW, Dugard PH (1984) Effects of freezing on human skin permeability. *J Pharm Pharmacol* 36:261–262
- Hawkins GS Jr, Reifenrath WG (1984) Development of an in vitro model for determining the fate of chemicals applied to skin. *Fundam Appl Toxicol* 4:S133–S144
- Henning A, Neumann D, Kostka KH, Lehr CM, Schaefer UF (2008) Influence of human skin specimens consisting of different skin layers on the result of in vitro

- permeation experiments. *Skin Pharmacol Physiol* 21:81–88
- Henning A, Schaefer UF, Neumann D (2009) Potential pitfalls in skin permeation experiments: influence of experimental factors and subsequent data evaluation. *Eur J Pharm Biopharm* 72:324–331
- Hikima T, Kaneda N, Matsuo K, Tojo K (2012) Prediction of percutaneous absorption in human using three-dimensional human cultured epidermis LabCyte EPI-MODEL. *Biol Pharm Bull* 35:362–368
- Jaeckle E, Schaefer UF, Loth H (2003) Comparison of effects of different ointment bases on the penetration of ketoprofen through heat-separated human epidermis and artificial lipid barriers. *J Pharm Sci* 92:1396–1406
- Joshi V, Brewster D, Colonero P (2012) In vitro diffusion studies in transdermal research: a synthetic membrane model in place of human skin. *Drug Dev Deliv*. Issue: March 2012, <http://www.drug-dev.com/Main/Back-Issues/In-Vitro-Diffusion-Studies-in-Transdermal-Research-509.aspx>
- Kalia YN, Pirot F, Guy RH (1996) Homogeneous transport in a heterogeneous membrane: water diffusion across human stratum corneum in vivo. *Biophys J* 71:2692–2700
- Kandárová H, Liebsch M, Schmidt E, Genschow E, Traue D, Spielmann H et al (2006a) Assessment of the skin irritation potential of chemicals by using the SkinEthic reconstructed human epidermal model and the common skin irritation protocol evaluated in the ECVAM skin irritation validation study. *ATLA Altern Lab Anim* 34:393–406
- Kandárová H, Liebsch M, Spielmann H, Genschow E, Schmidt E, Traue D et al (2006b) Assessment of the human epidermis model SkinEthic RHE for in vitro skin corrosion testing of chemicals according to new OECD TG 431. *Toxicol In Vitro* 20:547–559
- Kasting GB, Miller MA (2006) Kinetics of finite dose absorption through skin 2: volatile compounds. *J Pharm Sci* 95:268–280
- Kietzmann M, Loscher W, Arens D, Maass P, Lubach D (1993) The isolated perfused bovine udder as an in vitro model of percutaneous drug absorption of dexamethasone, benzoyl peroxide, and etofenamate. *J Pharmacol Toxicol Meth* 30:75–84
- Kiistala U (1968) Suction blister device for separation of viable epidermis from dermis. *J Invest Dermatol* 50:129–137
- Kligman AM, Christophers E (1963) Preparation of isolated sheets of human stratum corneum. *Arch Dermatol* 88:702–705
- Lademann J, Richter H, Schaefer UF, Blume-Peytavi U, Teichmann A, Otberg N et al (2006) Hair follicles – a long-term reservoir for drug delivery. *Skin Pharmacol Physiol* 19:232–236
- Lademann J, Richter H, Teichmann A, Otberg N, Blume-Peytavi U, Luengo J et al (2007) Nanoparticles – an efficient carrier for drug delivery into the hair follicles. *Eur J Pharm Biopharm* 66:159–164
- Lademann J, Jacobi U, Surber C, Weigmann HJ, Fluhr JW (2009) The tape stripping procedure – evaluation of some critical parameters. *Eur J Pharm Biopharm* 72:317–323
- Lee G, Parlicharla P (1986) An examination of excised skin tissues used for in vitro membrane permeation studies. *Pharm Res* 3:356–359
- Liebsch M, Traue D, Barrabas C, Spielmann H, Gerberick GF, Prevalidation of the EpiDerm™ phototoxicity test; Alternatives to Animal Testing II. In: Clark D G, Lisansky SG, and Macmillan R. (ed.) COLIPA, Brussels, Belgium, pp.160–167.
- Magnusson BM, Anissimov YG, Cross SE, Roberts MS (2004) Molecular size as the main determinant of solute maximum flux across the skin. *J Invest Dermatol* 122:993–999
- Suhonen TM, Pasonen-Seppänen S, Kirjavainen M, Tammi M, Tammi R, Urtti A (2003) Epidermal cell culture model derived from rat keratinocytes with permeability characteristics comparable to human cadaver skin. *Eur J Pharm Sci* 20:107–113
- Melero A, Hahn TM, Schaefer UF, Schneider M (2011) In vitro human skin segmentation and drug concentration-skin depth profiles. *Methods Mol Biol* 763:33–50
- Moghimi HR, Barry BW, Williams AC (1999) Stratum corneum and barrier performance: a model lamellar structural approach. In: Bronaugh RL, Maibach H (eds) *Drugs – cosmetics – mechanisms – methodology*. Marcel Dekker, New York, Basel, Hong Kong, pp 515–553
- Moody RP (1997) Automated in Vitro Dermal Absorption (AIVDA): a new in vitro method for investigating transdermal flux. *ATLA Altern Lab Anim* 25:347–357
- Moody RP (2000) Automated In Vitro Dermal Absorption (AIVDA): predicting skin permeation of atrazine with finite and infinite (swimming/bathing) exposure models. *Toxicol In Vitro* 14:467–474
- NAFTA (2009) Detailed Review and Harmonisation of Dermal Absorption Practices – Position Paper on Use of in vitro Dermal Absorption Data in Risk Assessment. NAFTA Absorption Group, Washington, DC 20508, USA
- Netzlaff F, Lehr CM, Wertz PW, Schaefer UF (2005) The human epidermis models EpiSkin®, SkinEthic® and EpiDerm®, an evaluation of morphology and their suitability for testing phototoxicity, irritancy, corrosivity, and substance transport. *Eur J Pharm Biopharm* 60:167–178
- Netzlaff F, Kostka KH, Lehr CM, Schaefer UF (2006a) TEWL measurements as a routine method for evaluating the integrity of epidermis sheets in static Franz type diffusion cells in vitro. Limitations shown by transport data testing. *Eur J Pharm Biopharm* 63:44–50
- Netzlaff F, Schaefer UF, Lehr CM, Meiers P, Stahl J, Kietzmann M et al (2006b) Comparison of bovine udder skin with human and porcine skin in percutaneous permeation experiments. *ATLA Altern Lab Anim* 34:499–513
- Netzlaff F, Kaca M, Bock U, Haltner-Ukomadu E, Meiers P, Lehr C-M et al (2007) Permeability of the recon-



- structed human epidermis model Episkin® in comparison to various human skin preparations. *Eur J Pharm Biopharm* 66:127–134
- OECD (2004a) Guidance Document for the Conduct of Skin Absorption Studies, OECD series on testing and assessment Nr. 28, OECD Publishing, Paris. DOI: <http://dx.doi.org/10.1787/9789264078796-en>
- OECD (2004b) Test No. 428: Skin Absorption: In Vitro Method, OECD Publishing, Paris. DOI: <http://dx.doi.org/10.1787/9789264071087-en>
- OECD (2004c) Test No. 431: In Vitro Skin Corrosion: Human Skin Model Test, OECD Publishing, Paris. DOI: <http://dx.doi.org/10.1787/9789264071148-en>
- OECD (2006) Test No. 435: In Vitro Membrane Barrier Test Method for Skin Corrosion, OECD Publishing, Paris. DOI: <http://dx.doi.org/10.1787/9789264067318-en>
- OECD (2010) Test No. 439: In Vitro Skin Irritation: Reconstructed Human Epidermis Test Method, OECD Publishing, Paris. DOI: <http://dx.doi.org/10.1787/9789264090958-en>
- Ottaviani G, Martel S, Carrupt P-A (2006) Parallel artificial membrane permeability assay: a new membrane for the fast prediction of passive human skin permeability. *J Med Chem* 49:3948–3954
- Patzelt A, Richter H, Knorr F, Schaefer U, Lehr C-M, Dähne L et al (2011) Selective follicular targeting by modification of the particle sizes. *J Control Release* 150:45–48
- Pittermann WF, Kietzmann M (2006) Bovine Udder Skin (BUS): testing of skin compatibility and skin protection. *Bovine Udder Skin (BUS): Prüfung von Hautverträglichkeit und Hautschutz* 23:65–71
- Poet TS, McDougal JN (2002) Skin absorption and human risk assessment. *Chem Biol Interact* 140:19–34
- Prow TW, Grice JE, Lin LL, Faye R, Butler M, Becker W et al (2011) Nanoparticles and microparticles for skin drug delivery. *Adv Drug Deliv Rev* 63:470–491
- Rauma M, Boman A, Johanson G (2013) Predicting the absorption of chemical vapours. *Adv Drug Deliv Rev* 65:306–314
- Reichling J, Landvatter U, Wagner H, Kostka KH, Schaefer UF (2006) In vitro studies on release and human skin permeation of Australian tea tree oil (TTO) from topical formulations. *Eur J Pharm Biopharm* 64:222–228
- Roberts M, Cross S, Pellett M (2002) Skin transport. In: Walters K (ed) *Dermatological and transdermal formulations*, vol 119. Marcel Dekker, New York, pp 89–195
- Rossignol MR (2005) The 7th Amendment to the Cosmetics Directive. *Atla-Altern Lab Anim* 33:19–22
- Russell LM, Guy RH (2012) Novel imaging method to quantify stratum corneum in dermatopharmacokinetic studies. *Pharma Res* 29:2389–2397
- Russell C, Russell WMS (1957) An approach to human ethology. *Behav Sci* 2:169–200
- Russell LM, Wiedersberg S, Begoña Delgado-Charro M (2008) The determination of stratum corneum thickness. An alternative approach. *Eur J Pharm Biopharm* 69:861–870
- Savic S, Weber C, Tamburic S, Savic M, Müller-Goymann C (2009) Topical vehicles based on natural surfactant/fatty alcohols mixed emulsifier: the influence of two polyols on the colloidal structure and in vitro/in vivo skin performance. *J Pharm Sci* 98:2073–2090
- SCCNFP/0167/99, (2003), Final: Basic Criteria for the in vitro assessment of percutaneous absorption of cosmetic ingredients, adopted by the SCCNFP during the 8th plenary meeting of 23 June 1999. European Commission Health & Consumers, Directorate C: Public Health and Risk Assessment, Unit C7 - Risk Assessment Office: B232 B-1049, Brussels, Belgium
- SCCNFP/0690/03 (2003) Final: Notes of Guidance for Testing of Cosmetic Ingredients for Their Safety Evaluation, adopted by the SCCNFP during the 25th plenary meeting of 20 October 2003. European Commission Health & Consumers, Directorate C: Public Health and Risk Assessment, Unit C7 - Risk Assessment Office: B232 B-1049, Brussels, Belgium
- SCCS/1358/10 (2010) Basic criteria for the in vitro assessment of dermal absorption of cosmetic ingredients, doi: 10.2772/25843, European Commission, Health & Consumers Directorate C: Public Health and Risk Assessment, Unit C7 - Risk Assessment, Office: B232 B-1049 Brussels, Belgium, doi: 10.2772/25843
- Schaefer H, Loth H (1996) An ex vivo model for the study of drug penetration into human skin. *Pharm Res* 13:366
- Schaefer U, Hansen S, Schneider M, Luengo J, Lehr C-M (2008) Models for skin absorption and skin toxicity testing. *Drug absorption studies: in situ, in vitro and in silico models*. Springer, New York
- Schäfer-Korting M, Bock U, Gamer A, Haberland A, Haltner-Ukomadu E, Kaca M et al (2006) Reconstructed human epidermis for skin absorption testing: results of the German prevalidation study. *ATLA Altern Lab Anim* 34:283–294
- Schäfer-Korting M, Bock U, Diembeck W, Düsing HJ, Gamer A, Haltner-Ukomadu E et al (2008) The use of reconstructed human epidermis for skin absorption testing: results of the validation study. *ATLA Altern Lab Anim* 36:161–187
- Schreiber S, Mahmoud A, Vuia A, Rübhelke MK, Schmidt E, Schaller M et al (2005) Reconstructed epidermis versus human and animal skin in skin absorption studies. *Toxicol In Vitro* 19:813–822
- Scalfani J, Liu P, Hansen E, Cettina MG, Nightingale J (1995) A protocol for the assessment of receiver solution additive-induced skin permeability changes. An example with  $\gamma$ -cyclodextrin. *Int J Pharm* 124:213–217
- Scott RC, Walker M, Dugard PH (1986) In vitro percutaneous absorption experiments: a technique for the production of intact epidermal membranes from rat skin. *J Soc Cosm Chem Jap* 37:35–41
- Selzer D, Schaefer UF, Lehr C-M, Hansen S (2013) Basic mathematics in skin absorption. In: Dragicevic-Curic

- N, Maibach HI (eds) *Chemical methods in penetration enhancement*. Springer, Heidelberg
- Semlin L, Schäfer-Korting M, Borelli C, Korting HC (2011) In vitro models for human skin disease. *Drug Discov Today* 16:132–139
- Shah VP, Flynn GL, Yacobi A, Maibach HI, Bon C, Fleischer NM et al (1998) Bioequivalence of topical dermatological dosage forms – methods of evaluation of bioequivalence. *Pharm Res* 15:167–171
- Sinkó B, Garrigues TM, Balogh GT, Nagy ZK, Tsinman O, Avdeef A et al (2012) Skin-PAMPA: a new method for fast prediction of skin penetration. *Eur J Pharm Sci* 45:698–707
- Solich P, Ogrocka E, Schaefer U (2001) Application of automated flow injection analysis to drug liberations studies with the Franz diffusion cell. *Die Pharmazie* 56:787–789
- Solich P, Sklenarova H, Huclova J, Stafinsky D, Schaefer UF (2003) Fully automated drug liberation apparatus for semisolid preparations based on sequential injection analysis. *Anal Chim Acta* 499:9–16
- Spielmann H, Müller L, Averbek D, Balls M, Brendler-Schwaab S, Castell JV et al (2000) The second ECVAM workshop on phototoxicity testing: the report and recommendations of ECVAM workshop 42 1,2. *ATLA Altern Lab Anim* 28:777–814
- Surber C, Smith EW (2005) The mystical effects of dermatological vehicles. *Dermatology* 210:157–168
- Surber C, Schwarb FP, Smith EW (1999) Tape-stripping technique. In: Bronaugh RL, Maibach H (eds) *Percutaneous absorption: drugs-cosmetics-mechanisms-methodology*, vol 97, 3rd ed. Marcel Dekker, New York, pp 395–409
- Swarbrick J, Lee G, Brom J (1982) Drug permeation through human skin: I. Effect of storage conditions of skin. *J Invest Dermatol* 78:63–66
- USEPA (2004) In vitro dermal absorption rate testing of certain chemicals of interest to the Occupational Safety and Health Administration; Final rule. *Fed Regist*; 69(80):22402–41. <https://www.gpo.gov/fdsys/pkg/FR-2004-04-26/pdf/04-9409.pdf>
- Van De Sandt JJM, Meuling WJA, Elliott GR, Cnubben NHP, Hakkert BC (2000) Comparative in vitro-in vivo percutaneous absorption of the pesticide propoxur. *Toxicol Sci* 58:15–22
- van de Sandt JJM, van Burgsteden JA, Cage S, Carmichael PL, Dick I, Kenyon S et al (2004) In vitro predictions of skin absorption of caffeine, testosterone, and benzoic acid: a multi-centre comparison study. *Regul Toxicol Pharmacol* 39:271–281
- Veccia BE, Bunge AL (2003) Skin absorption databases and predictive equations. In: Guy R, Hadgraft J (eds) *Transdermal drug delivery*, vol 123, 2nd ed. Marcel Dekker, New York, pp 57–141
- Voegeli R, Heiland J, Doppler S, Rawlings AV, Schreier T (2007) Efficient and simple quantification of stratum corneum proteins on tape strippings by infrared densitometry. *Skin Res Technol* 13:242–251
- Wagner H, Kostka KH, Lehr CM, Schaefer UF (2000) Drug distribution in human skin using two different in vitro test systems: comparison with in vivo data. *Pharm Res* 17:1475–1481
- Wagner H, Kostka KH, Lehr CM, Schaefer UF (2001) Interrelation of permeation and penetration parameters obtained from in vitro experiments with human skin and skin equivalents. *J Control Release* 75:283–295
- Wagner H, Kostka KH, Lehr CM, Schaefer UF (2002) Correlation between stratum corneum/water-partition coefficient and amounts of flufenamic acid penetrated into the stratum corneum. *J Pharm Sci* 91:1915–1921
- Weigmann HJ, Lindemann U, Antoniou C, Tsirikas GN, Stratigos AI, Katsambas A et al (2003) UV/VIS absorbance allows rapid, accurate, and reproducible mass determination of corneocytes removed by tape stripping. *Skin Pharmacol Appl Skin Physiol* 16:217–227
- Wertz PW (1996) The nature of the epidermal barrier: biochemical aspects. *Adv Drug Deliv Rev* 18:283–294
- WHO (2006) *Dermal Absorption*. Environmental Health Criteria (EHC) 235, ISBN 978 92-4-157235, World Health Organization, Geneva
- Wilkinson SC, Mass WJM, Nielsen JB, Greaves LC, van de Sandt JJM, Williams FM (2004) Influence of skin thickness on percutaneous penetration in vitro. In: Brain KR, Walters KA (eds) *Perspectives in percutaneous penetration*, vol 9a. STS Publishing, Cardiff
- Wilkinson SC, Maas WJM, Nielsen JB, Greaves LC, van de Sandt JJM, Williams FM (2006) Interactions of skin thickness and physicochemical properties of test compounds in percutaneous penetration studies. In *Arch Occup Environ Health* 79:405–413
- Williams AC, Barry BW (2012) Penetration enhancers. *Adv Drug Deliv Rev* 64(Suppl):128–137

# Stripping Procedures for Penetration Measurements of Topically Applied Substances

# 11

Jürgen Lademann, Sabine Schanzer,  
Heike Richter, Martina C. Meinke, Hans-  
Jürgen Weigmann, and Alexa Patzelt

## Contents

11.1 Introduction .....	205
11.2 Tape Stripping .....	206
11.3 Differential Stripping .....	212
11.4 Summary .....	213
References .....	213

## 11.1 Introduction

The skin is not only the largest organ of the human body, but also it is a barrier toward the environment. This barrier consists of corneocytes, i.e., dead cells, which are surrounded by lipid layers. Providing mechanical protection, the cutaneous barrier protects us also from desiccating and from the penetration of hazardous substances and microorganisms. In general, there are three different pathways allowing substances to pass through the cutaneous barrier as schematically represented in Fig. 11.1 (Blume-Peytavi et al. 2010). The first pathway, being the intercellular penetration pathway, has been propagated to be the most relevant one for decades (Essa et al. 2002; Ochalek et al. 2012). Approximately 10 years ago also the follicular penetration pathway

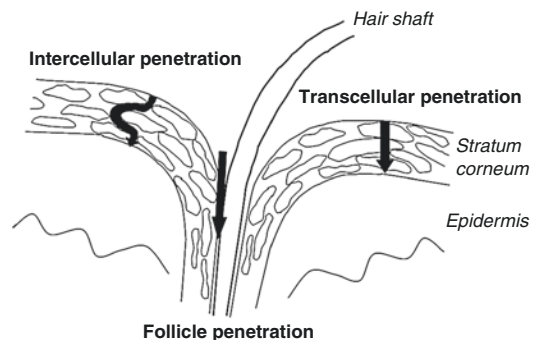


**Fig. 11.1** Schematic representation of the penetration pathways of topically applied substances

J. Lademann (✉) • S. Schanzer • H. Richter  
M.C. Meinke • H.-J. Weigmann • A. Patzelt  
Charité – Universitätsmedizin Berlin,  
Department of Dermatology, Venereology and Allergy,  
Center of Experimental and Applied Cutaneous  
Physiology, Berlin, Germany  
e-mail: [juegen.lademann@charite.de](mailto:juegen.lademann@charite.de)

was found to be a second essential pathway (Patzelt et al. 2011; Schroeter et al. 2010). The third pathway is the transcellular penetration pathway, where the substances pass through both the corneocytes and the lipid layers; this pathway seems to be of minor importance, yet.

While the intercellular penetration process has been recognized for decades, the existence of follicular penetration could be demonstrated not before a few years ago. Follicular penetration experiments require measurements at high spatial resolution (Jung et al. 2006). Only in recent years, suitable techniques for such measurements could be provided. These systems are based mainly on optical methods specifically developed or optimized for that purpose (Tfayli et al. 2012; Lademann et al. 2012; Mura et al. 2012; Forster et al. 2011; Haag et al. 2011). A further challenge is that while intercellular penetration can be usually investigated *in vitro* or *ex vivo*, follicular penetration must be analyzed *in vivo* or *ex vitro* on porcine ear model skin (Patzelt et al. 2008). This is due to the fact that skin contracts immediately after excision during surgical intervention. Although the interfollicular fibers can be expanded by stretching the excised skin to its original size for the measurements, the very dense network of fibers surrounding the hair follicles remains contracted, which is an almost irreversible process (Patzelt et al. 2008). The effect of contraction of the hair follicles in excised human skin was initially demonstrated by Patzelt et al. (2008), who could moreover show that the follicular penetration of a fluorescent dye-containing formulation was reduced by 90% in the case of *ex vitro* investigations on excised skin in comparison to *in vivo* investigations, whereby methods and skin models were identical.

As a consequence, the follicular orifices are not accessible for the penetration process in *ex vivo* models, which has to be considered when certain methods are employed such as the diffusion cell experiment. Diffusion cell experiments (Okuda et al. 2011; Baert et al. 2010) are widely used for penetration investigations on split or full-thickness skin. However, the hair follicles reach deeply into the subcutaneous tissue, which is mostly removed before the skin probes are clamped onto the diffusion cell meaning that the

hair follicles are somewhere cut in their middle. This would imply, if the hair follicles were accessible and not plugged by the contraction process, that the topically applied substances would pass directly through the hair follicle stump into the receptor medium. Since, however, the hair follicles are plugged due to contraction, intercellular penetration can be investigated more or less properly by this method whereas follicular penetration is not measurable. Thus, follicular penetration must be investigated either *in vivo* or *ex vivo* on porcine ear model skin, which strongly resembles human skin in terms of composition and structure. The advantage of the porcine ear skin model is that the skin remains tightly attached to the cartilage even after truncation of the ear and does not contract. However, it has to be taken into consideration that the porcine hair follicles extend deeper into the skin and are larger in diameter than human hair follicles (Lademann et al. 2010; Hutton et al. 1978).

The present chapter will summarize the easy and wide application possibilities of the different stripping methods, which can be applied for investigating intercellular and follicular penetration pathways.

---

## 11.2 Tape Stripping

One of the oldest methods used in penetration studies is the tape stripping method. Briefly, tape stripping comprises the successive removal of adhesive films pressed onto the skin after the topical application and penetration of the substance under investigation. With each adhesive tape, a certain amount of corneocytes is removed including the topically applied substances contained within this layer. The tape stripping method is illustrated in Fig. 11.2 in detail. After application with a syringe Fig. 11.2a and homogeneous distribution by means of a saturated rubber glove finger Fig. 11.2b, the applied formulation is then allowed to penetrate for a determined time. Thereafter, the individual adhesive strips are pressed one by one onto the skin by a roller Fig. 11.2c or stamp leading to a smoothing of the skin surface and are then removed quickly Fig. 11.2d. The smoothing of the skin surface

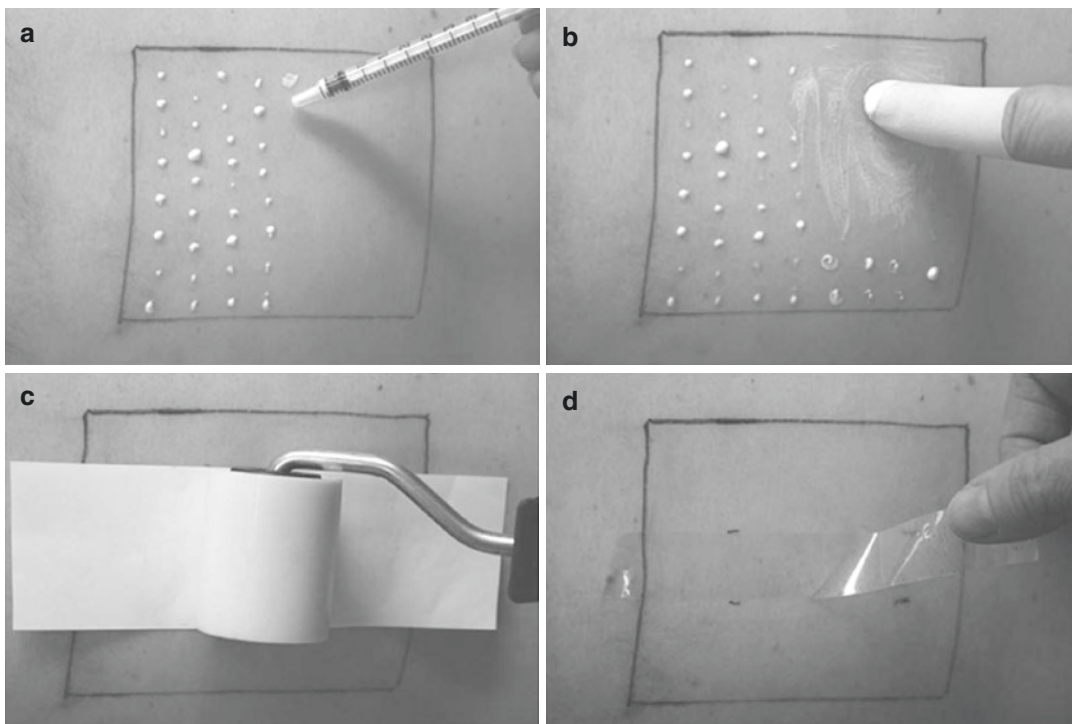


**Fig. 11.2** Images presenting the tape stripping method. (a) Application of the formulation with a syringe. (b) Distribution of the formulation using a saturated rubber glove finger. (c) Adhesive tapes are pressed onto the skin by using a roller. (d) Adhesive tapes are rapidly removed from the skin

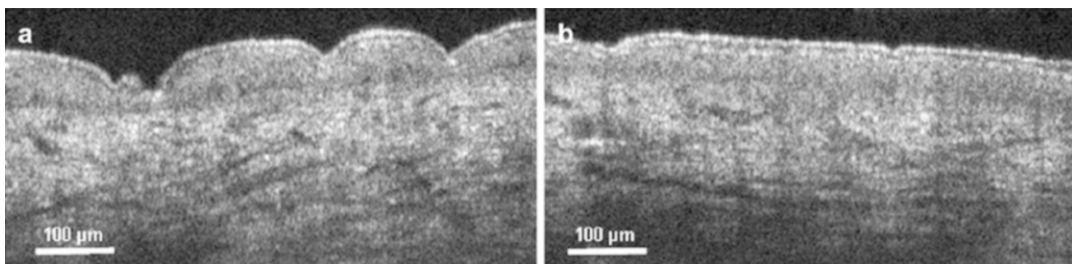


**Fig. 11.3** Influence of the roller smoothing the skin surface. (a) Skin furrows before rolling. (b) Smoothed skin surface after rolling (Lademann et al. 2005)

represents an important step in the tape stripping protocol as by pressing the adhesive film onto the skin, the influence of furrows and wrinkles can be avoided or at least minimized (Lademann et al. 2005). In Fig. 11.2c, a roller is used for smoothing (Mohammed et al. 2012; Bettoni et al. 2012; Lademann et al. 2006, 2009) the skin surface. The principle of smoothing the skin surface by a roller is represented in Fig. 11.3 using optical coherence tomography (OCT). After rolling the skin, the previously structured skin surface

(Fig. 11.3a) has been converted into a flat surface (Fig. 11.3b). During the rolling process, the adhesive film is permitted to contact the surface of the respective skin area completely. The adhesive films pressed onto the skin are subsequently removed and analyzed for the amount of stratum corneum and the amount of the topically applied substance. In Fig. 11.4, the image of a typical tape strip after removal from the human skin is shown. The corneocyte cover is clearly recognizable on the adhesive film.

Thus, tape stripping is a well-established method to investigate the penetration of topically applied substances into the complete stratum corneum; however, it is not suited to remove cells from the viable epidermis located beneath the stratum corneum. In Fig. 11.5, a biopsied human skin sample prior to (Fig. 11.5a) and after tape stripping (Fig. 11.5b) is shown, demonstrating that this procedure is capable of removing the stratum corneum completely. Prior to tape stripping, the wrinkles and furrows in the skin surface structure are clearly recognizable, yet, whereas a flat skin surface is visible after tape stripping. This is due to the tape stripping procedure causing a light swelling of the skin surface.

When the tape stripping method was introduced, the number of the individual tapes had

initially been considered as a measure for the stratum corneum depth at which the tape strip was removed. Applying the tape stripping method with growing expertise and experience, it became evident that the tape number is not a reproducible value characterizing the depth of the stratum corneum at which the tape strip is removed. This is attributable to the fact that different formulations influence the amount of stratum corneum adhering to the tape strip differently. Whereas greasy formulations may reduce the adhesive strength of a tape strip, meaning that less stratum corneum is removed per tape strip, an ethanolic formulation may increase the amount of stratum corneum removed. In addition, also the pressure used for pressing the adhesive film onto the skin and the type of adhesive film decisively influences the amount of stratum corneum removed by each tape strip. The literature reports of a variety of methods to quantify the amount of stratum corneum on the respective tape strips which further allow the determination of the depth at which the tape strips were removed. This can be performed, for instance, by weighing the tape strips prior to and after their application to the skin (Weigmann et al. 2005). A decisive shortcoming of this method is, however, that the weight of the first tape strips is not only determined by the corneocytes, but also by the topically applied substances penetrated into the uppermost layers of the corneocytes. Moreover, in deeper layers of the stratum corneum interstitial fluid may escape, which could also increase the weight. As an alternative

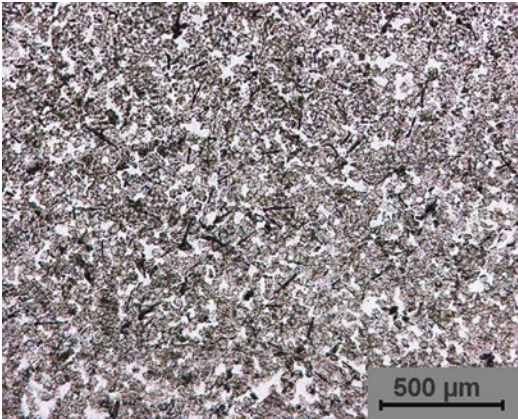


**Fig. 11.4** Microscopic image of a tape strip removed from the skin

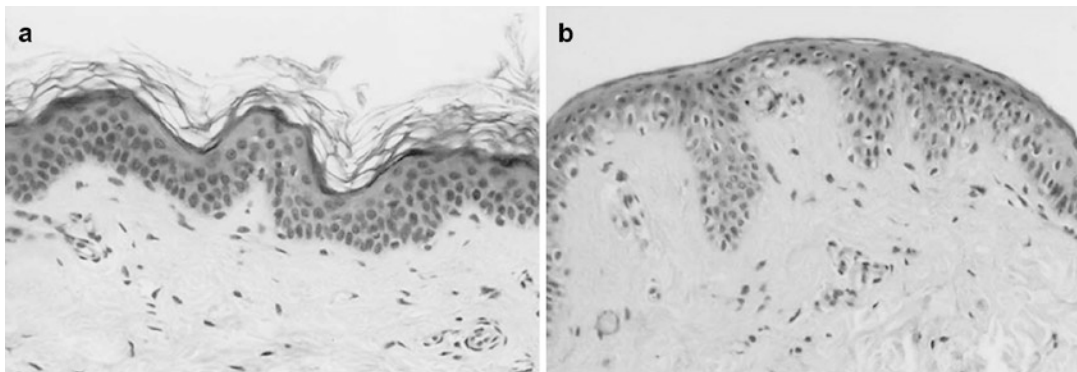


**Fig. 11.5** Histological sections from biopsies removed prior to (a) and after (b) tape stripping, demonstrating that the stratum corneum can be removed completely (Lademann et al. 2005)

method, Lindemann et al. (2003) proposed to use the pseudoabsorption at 430 nm as a measure for the amount of stratum corneum on the tape strips. The pseudoabsorption characterizes the attenuation of the light penetrating through the tape strip. It is determined by the absorption, reflectance, and scattering of the corneocytes. These signals are known to depend on the wavelength, and the shorter the wavelength, the stronger the signal, indicating that the scattering effect is more pronounced in shorter wavelength. However, wavelengths below 400 nm are unsuitable for these investigations as a variety of formulations, including sunscreens, have absorption bands in this spectral range. A third method for the determination of the amount of stratum corneum on the tape strips, which is meanwhile commercially available, was suggested by Voegeli et al. (2007, 2009). This method uses the infrared absorption of the corneocytes for determining the amount of stratum corneum. The measuring device is based on an infrared densitometer permitting indirect measurements of the stratum corneum protein content on the removed tape strip by means of absorption. This measuring method is a nondestructive technique so that the tape strips can subsequently be used for other analyses. It provides a clear advantage as it is not influenced by the absorption of applied formulations in the ultraviolet (UV) spectral range, and it is not influenced by nanoparticles. A further method suggested by Dreher et al. is based on staining the corneocytes after removal so that the amount of stratum corneum on the tape strips can be determined by absorbance measurements using a UV/VIS spectrometer (Dreher et al. 2005).

Taking into consideration the above-mentioned facts, it became established as a standard that instead of the number of tape strips, the amount of stratum corneum is now used for the calculation of penetration profiles of drugs into the stratum corneum. A comparison of the traditional and the extended method is schematically shown in Fig. 11.6, highlighting the advantages of the extended method. The traditional tape stripping procedure only considers the amount of substance in relation to the tape strip number, whereas the information about the amount of

stratum corneum is neglected in contrast to the extended method where this essential part of information is likewise considered. In this way, it can be clearly seen that although the amount of corneocytes may vary between the individual tape strips, on average it is declining with the increasing tape strip number. Therefore, based on the investigations of the amount of removed stratum corneum, the tape strips were used to calculate the profile of the horny layer. Here, the space between two horizontal lines corresponds to the amount of stratum corneum removed with the specific tape strip. In the deeper layers of the stratum corneum the distances between the horizontal lines are getting smaller. The top line of the horny layer profile shown in this figure represents the surface of the stratum corneum, while the bottom horizontal line represents the boundary to the living cells.

The amount of topically applied substance removed with a single tape strip can be determined by classical analytical methods like high-performance liquid chromatography (HPLC) and mass spectroscopy. If the information on the amount of topically applied substance detected on the respective tape strips is added to the horny layer profile, a penetration profile is obtained. This is illustrated in Fig. 11.7 showing part of a histological section. The adjacent penetration profile of a UV filter exhibits the distribution of this substance in the stratum corneum.

As already mentioned above, the tape stripping procedure is unsuitable for the investigation of transdermal penetration as tape strips only remove the stratum corneum. However, it could be shown that tape stripping can moreover be used for analyzing the dermatopharmacokinetics of topically applied substances intended for penetration through the cutaneous barrier, such as steroids (Pelchrzim et al. 2004). In a previous study, two different formulations of 0.05 % clobetasol propionate were topically applied and the penetration profile was determined 2 h after topical application. It was observed that clobetasol propionate in the Temovate® emollient (Glaxo Wellcome Inc.; Research Triangle Park, NC, USA) was predominantly located on the skin surface (Fig. 11.8b). Contrary to that, clobetasol propionate in the

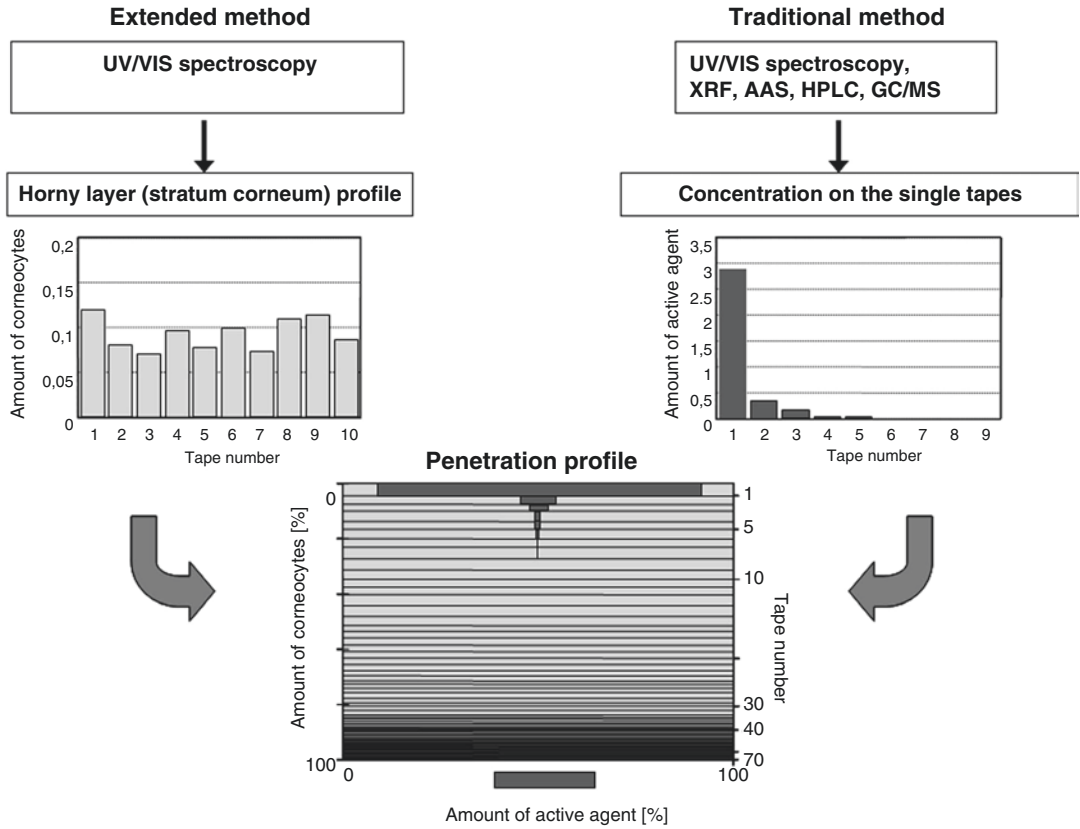


**Fig. 11.6** Principle of the calculation of the penetration profile. The amount of corneocytes on each tape strip is determined by UV/VIS spectroscopy. The concentration of the applied substance on each tape strip is determined by traditional methods such as UV/VIS spectroscopy,

X-ray fluorescence (XRF), atomic absorption spectroscopy (AAS), high-performance liquid chromatography (HPLC), or gas chromatography in combination with mass spectroscopy (GC/MS). The combination of both results allows the calculation of a penetration profile

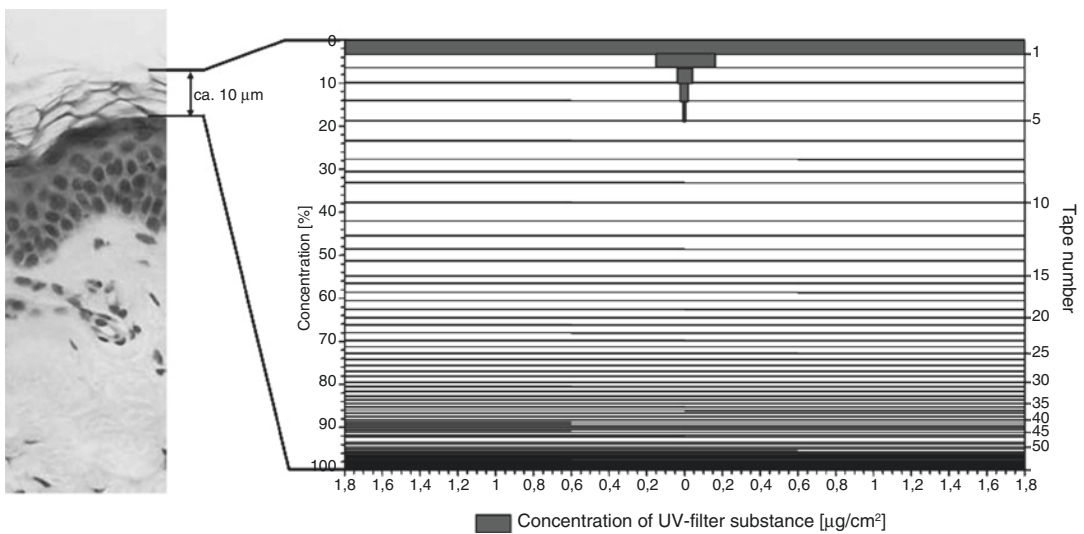


**Fig. 11.7** Distribution of a UV filter substance (sunscreen) in the stratum corneum determined by tape stripping



Temovate® cream penetrated significantly deeper into the stratum corneum (Fig. 11.8a). The amount of cream detected on the skin surface was essentially reduced compared to the emollient, indicating that the cream is penetrating better through the skin barrier. As clobetasol does not vaporize after topical application, the various steroid concentrations in the stratum corneum permit conclusions about the efficiency of drug penetration through the cutaneous barrier (Pelchrzim et al. 2004; Weigmann et al. 2001). Additionally, differences in the reservoir formation depending on the formulation applied could be correlated to a biological response in the form of a blanching effect (Fig. 11.9), which has already been described by

other authors (Gorne et al. 2007). Six hours after application of the two formulations, only weak blanching effects were visible for the Temovate® emollient, whereas intensive blanching occurred after application of the Temovate® cream indicating its higher local concentration.

Thus, tape stripping is not only a suitable and simple method for the detection of topically applied substances in the stratum corneum, but it provides also information about the dermatopharmacokinetics of these substances when they are passing through the cutaneous barriers. The tape stripping procedure can be applied both in vivo and ex vivo on human skin and on porcine

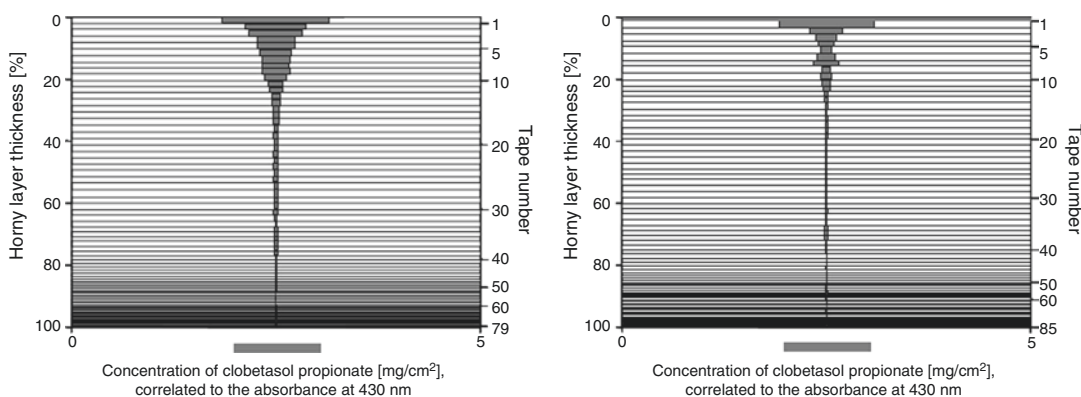


**Fig. 11.8** Penetration profiles of two commercially available clobetasol propionate preparations into the stratum corneum. (a) Temovate cream® and (b) Temovate®

emollient both were purchased from Glaxo Wellcome, Inc. (Weigmann et al. 2001)

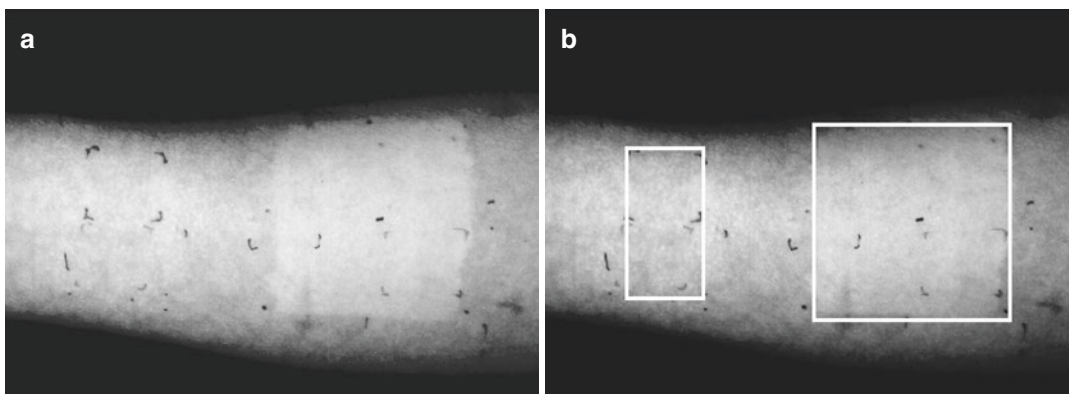


**Fig. 11.9** The blanching effect as a biological response of the skin to the steroid application corresponds to the penetration profiles. The formulation, which shows the best penetration (Temovate® cream), produced the highest

vasoconstriction (blanching effect) (a), while this effect is considerably lower in the case of the Temovate® emollient (b). Temovate® cream and Temovate® emollient were both purchased from Glaxo Wellcome Inc

ear skin. It is suited to investigating intercellular, but not follicular penetration.

### 11.3 Differential Stripping

The method of differential stripping was developed to distinguish between the amounts of topically applied substances that penetrated into the stratum corneum and into the hair follicles, respectively (Teichmann et al. 2005). The hair follicles represent an important target structure as they are surrounded by a dense network of blood capillaries and dendritic cells necessary for drug delivery and immune responses (Meinke et al. 2010; Teichmann et al. 2005). Additionally, they are host of the stem cells in the bulge region (Nagao et al. 2012; Blume-Peytavi and Vogt 2011), which are likely to become an important factor in regenerative medicine.

The differential stripping procedure combines the above-described classical tape stripping procedure with cyanoacrylate surface biopsies (Teichmann et al. 2005). This procedure is schematically represented in Fig. 11.10. After topical application of a substance, it is spreading in the stratum corneum and in the hair follicle. Subsequently, the stratum corneum is removed by tape stripping as described above. Thereafter, the amounts of penetrated substance adhering to the individual tape strips are quantified. Once the stratum corneum has been completely removed by tape stripping, the topically applied substance is only contained in the hair follicles, yet. These hair follicle contents are then removed by cyano-

acrylate surface biopsy. For this purpose, cyanoacrylate (super glue) is placed on the stripped skin areas and is then covered with a glass slide. After polymerization, the glass slide is removed quickly and contains follicular casts and contents that can be likewise analyzed quantitatively for the substance applied by conventional methods.

During the development of differential stripping, the method has been also evaluated by histological sections (Teichmann et al. 2005). It could be demonstrated histologically that after tape stripping, the stratum corneum can be removed completely, whereas the hair follicles remained intact. Only after cyanoacrylate skin surface biopsy, the follicular content was removed completely.

Unfortunately, this procedure lends itself only for *in vivo* investigations on human skin. As already explained, excised human skin immediately contracts; the follicular orifices being contracted and not open for penetration. Porcine ear skin also proved unsuitable for such investigations, as the hair follicles extend considerably deeper into porcine skin than into human skin, so that the cyanoacrylate glue either cannot penetrate into the hair follicles completely or gets stuck there during removal. In this context, Knorr et al. (2009) developed a method which resembles the differential stripping procedure but can be also utilized *ex vivo* on porcine ear skin. Using this method, the stratum corneum is likewise removed by tape stripping after topical drug application. Subsequently, a biopsy is removed, which is subsequently extracted in ethanol and then analyzed for the amount of penetrated sub-

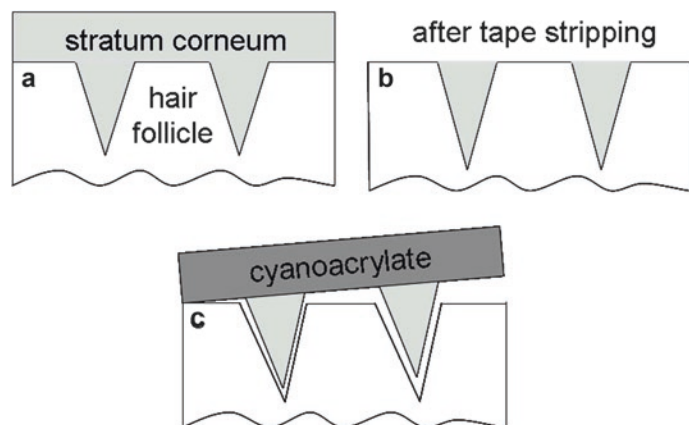


**Fig. 11.10** Schematic representation of the differential stripping method combining tape stripping with cyanoacrylate skin surface biopsy. (a) after its application the substances is penetrating into the stratum corneum and hair follicles. (b) the stratum corneum is completely removed by tape stripping and the substance is now contained only in the hair follicles. (c) the hair follicle contents are removed by cyanoacrylate skin surface biopsy

stances by fluorescence microscopy. This method is based on the fact that once the stratum corneum has been removed, the substances are exclusively located in the hair follicles; thus, the extraction of the biopsies only reveals the amount penetrated into the hair follicles. The amount of topically applied substances, which may have penetrated through the cutaneous barrier using the intercellular or follicular pathways, is almost less than 1%. Therefore, it can be neglected compared to the amount of substances penetrated into the hair follicles (Feldmann and Maibach 1969).

## 11.4 Summary

In summary it can be stated that stripping methods are simple and low-cost procedures for analyzing the penetration of topically applied substances into the stratum corneum and into the hair follicles. Using these procedures correctly, the following is to be taken into consideration: both tape stripping and differential stripping are noninvasive methods. For tape stripping the skin surface must be stretched during application of the adhesive film so that the influence of furrows and wrinkles can be neglected. This can be easily performed by pressing the adhesive film onto the skin surface with a roller. In addition, the depth from which the corresponding tape strip is removed should not be related to the tape strip number, but to the amount of stratum corneum removed. In this way, the penetration profile becomes reproducible, independent of the investigator and the type of adhesive film applied.

Also for differential stripping it is essential that the skin surface is stretched by pressing the adhesive film onto the skin surface by using a roller. Only in this case the stratum corneum can be removed completely also from the furrows and wrinkles. Otherwise, parts of the stratum corneum remain on the skin surface and will consequently be removed by the cyanoacrylate biopsy. This falsifies the measuring results in terms of follicular penetration. Notwithstanding their many advantages, the stripping methods have also limitations insofar as a removed skin area can be analyzed only once. Consequently, this skin area is not available for kinetic measure-

ments as would be the case if optical spectroscopic measurements were applied.

## References

- Baert B, Boonen J, Burvenich C, Roche N, Stillaert F, Blondeel P et al (2010) A new discriminative criterion for the development of Franz diffusion tests for transdermal pharmaceuticals. *J Pharm Pharm Sci* 13(2): 218–230
- Bettoni CC, Felippi CC, de Andrade C, Raffin RP, Jager A, Guterres SS et al (2012) Isotretinoin-loaded nanocapsules: stability and cutaneous penetration by tape stripping in human and pig skin. *J Biomed Nanotechnol* 8(2):258–271
- Blume-Peytavi U, Massoudy L, Patzelt A, Lademann J, Dietz E, Rasulev U et al (2010) Follicular and percutaneous penetration pathways of topically applied minoxidil foam. *Eur J Pharm Biopharm* 76(3):450–453. S0939-6411(10)00159-1 [pii]. doi:10.1016/j.ejpb.2010.06.010
- Blume-Peytavi U, Vogt A (2011) Human hair follicle: reservoir function and selective targeting. *Br J Dermatol* 165(Suppl 2):13–17. doi:10.1111/j.1365-2133.2011.10572.x
- Dreher F, Modjtahedi BS, Modjtahedi SP, Maibach HI (2005) Quantification of stratum corneum removal by adhesive tape stripping by total protein assay in 96-well microplates. *Skin Res Technol* 11(2):97–101. SRT103 [pii]. doi:10.1111/j.1600-0846.2005.00103.x
- Essa EA, Bonner MC, Barry BW (2002) Human skin sandwich for assessing shunt route penetration during passive and iontophoretic drug and liposome delivery. *J Pharm Pharmacol* 54(11):1481–1490
- Feldmann RJ, Maibach HI (1969) Percutaneous penetration of steroids in man. *J Invest Dermatol* 52(1):6
- Forster M, Bolzinger MA, Montagnac G, Briancon S (2011) Confocal Raman microspectroscopy of the skin. *Eur J Dermatol* 21(6):851–863. ejd.2011.1494 [pii]. doi:10.1684/ejd.2011.1494
- Gorne RC, Greif C, Metzner U, Wigger-Alberti W, Elsner P (2007) Assessment of topical corticosteroid activity using the vasoconstriction assay in healthy volunteers. *Skin Pharmacol Physiol* 20(3):133–140
- Haag SF, Fleige E, Chen M, Fahr A, Teutloff C, Bittl R et al (2011) Skin penetration enhancement of core-multishell nanotransporters and invasomes measured by electron paramagnetic resonance spectroscopy. *Int J Pharm* 416(1):223–228. S0378-5173(11)00597-7 [pii]. doi:10.1016/j.ijpharm.2011.06.044
- Hutton RD, Kerbs S, Yee K (1978) Scanning electron microscopy of experimental *Trichophyton mentagrophytes* infections in guinea pig skin. *Infect Immun* 21(1):247–253
- Jung S, Otberg N, Thiede G, Richter H, Sterry W, Panzner S et al (2006) Innovative liposomes as a transfollicular drug delivery system: Penetration into porcine hair fol-

- icles. *J Invest Dermatol* 126(8):1728–1732. doi:[10.1038/sj.jid.5700323](https://doi.org/10.1038/sj.jid.5700323).
- Knorr F, Lademann J, Patzelt A, Sterry W, Blume-Peytavi U, Vogt A (2009) Follicular transport route--research progress and future perspectives. *Eur J Pharm Biopharm* 71(2):173–180
- Lademann J, Ilgevicus A, Zurbau O, Liess HD, Schanzer S, Weigmann HJ et al (2006) Penetration studies of topically applied substances: optical determination of the amount of stratum corneum removed by tape stripping. *J Biomed Opt* 11(5):054026. doi:[10.1117/1.2359466](https://doi.org/10.1117/1.2359466)
- Lademann J, Jacobi U, Surber C, Weigmann HJ, Fluhr JW (2009) The tape stripping procedure--evaluation of some critical parameters. *Eur J Pharm Biopharm* 72(2):317–323
- Lademann J, Meinke MC, Schanzer S, Richter H, Darwin ME, Haag SF et al (2012) In vivo methods for the analysis of the penetration of topically applied substances in and through the skin barrier. *Int J Cosmet Sci* 34(6):551–559. doi:[10.1111/j.1468-2494.2012.00750.x](https://doi.org/10.1111/j.1468-2494.2012.00750.x)
- Lademann J, Richter H, Meinke M, Sterry W, Patzelt A (2010) Which skin model is the most appropriate for the investigation of topically applied substances into the hair follicles? *Skin Pharmacol Physiol* 23(1):47–52
- Lademann J, Weigmann HJ, Schanzer S, Richter H, Audring H, Antoniou C et al (2005) Optical investigations to avoid the disturbing influences of furrows and wrinkles quantifying penetration of drugs and cosmetics into the skin by tape stripping. *J Biomed Opt* 10(5):054015. doi:[10.1117/1.2055507](https://doi.org/10.1117/1.2055507)
- Lindemann U, Weigmann HJ, Schaefer H, Sterry W, Lademann J (2003) Evaluation of the pseudo-absorption method to quantify human stratum corneum removed by tape stripping using protein absorption. *Skin Pharmacol Appl Skin Physiol* 16(4):228–236
- Meinke MC, Patzelt A, Richter H, Schanzer S, Sterry W, Filbry A et al (2010) Prevention of follicular penetration: barrier-enhancing formulations against the penetration of pollen allergens into hair follicles. *Skin Pharmacol Physiol* 24(3):144–150. 000323018 [pii]. doi:[10.1159/000323018](https://doi.org/10.1159/000323018)
- Mohammed D, Yang Q, Guy RH, Matts PJ, Hadgraft J, Lane ME (2012) Comparison of gravimetric and spectroscopic approaches to quantify stratum corneum removed by tape-stripping. *Eur J Pharm Biopharm* 82(1):171–174. doi:[10.1016/j.ejpb.2012.05.018](https://doi.org/10.1016/j.ejpb.2012.05.018). S0939-6411(12)00185-3 [pii]
- Mura S, Manconi M, Fadda AM, Sala MC, Perricci J, Pini E et al (2012) Penetration enhancer-containing vesicles (PEVs) as carriers for cutaneous delivery of minoxidil: in vitro evaluation of drug permeation by infrared spectroscopy. *Pharm Dev Technol*. doi:[10.3109/10837450.2012.685661](https://doi.org/10.3109/10837450.2012.685661)
- Nagao K, Kobayashi T, Moro K, Ohyama M, Adachi T, Kitashima DY et al (2012) Stress-induced production of chemokines by hair follicles regulates the trafficking of dendritic cells in skin. *Nat Immunol* 13(8):744–752. doi:[10.1038/ni.2353](https://doi.org/10.1038/ni.2353). ni.2353 [pii]
- Ochalek M, Heissler S, Wohlrab J, Neubert RH (2012) Characterization of lipid model membranes designed for studying impact of ceramide species on drug diffusion and penetration. *Eur J Pharm Biopharm* 81(1):113–120. S0939-6411(12)00041-0 [pii]. doi:[10.1016/j.ejpb.2012.02.002](https://doi.org/10.1016/j.ejpb.2012.02.002)
- Okuda M, Donahue DA, Kaufman LE, Avalos J, Simion FA, Story DC et al (2011) Negligible penetration of incidental amounts of alpha-hydroxy acid from rinse-off personal care products in human skin using an in vitro static diffusion cell model. *Toxicol In Vitro* 25(8):2041–2047. S0887-2333(11)00218-9 [pii]. doi:[10.1016/j.tiv.2011.08.005](https://doi.org/10.1016/j.tiv.2011.08.005)
- Patzelt A, Richter H, Buettemeyer R, Huber HJ, Blume-Peytavi U, Sterry W et al (2008) Differential stripping demonstrates a significant reduction of the hair follicle reservoir in vitro compared to in vivo. *Eur J Pharm Biopharm* 70(1):234–238
- Patzelt A, Richter H, Knorr F, Schaefer U, Lehr CM, Dahne L et al (2011) Selective follicular targeting by modification of the particle sizes. *J Control Release* 150(1):45–48. S0168-3659(10)00919-3 [pii]. doi:[10.1016/j.jconrel.2010.11.015](https://doi.org/10.1016/j.jconrel.2010.11.015).
- Pelchrzrim R, Weigmann HJ, Schaefer H, Hagemeister T, Linscheid M, Shah VP et al (2004) Determination of the formation of the stratum corneum reservoir for two different corticosteroid formulations using tape stripping combined with UV/VIS spectroscopy. *J Dtsch Dermatol Ges* 2(11):914–919
- Schroeter A, Engelbrecht T, Neubert RH, Goebel AS (2010) New nanosized technologies for dermal and transdermal drug delivery. A review. *J Biomed Nanotechnol* 6(5):511–528
- Teichmann A, Jacobi U, Ossadnik M, Richter H, Koch S, Sterry W et al (2005) Differential stripping: determination of the amount of topically applied substances penetrated into the hair follicles. *J Invest Dermatol* 125(2):264–269
- Tfayli A, Guillard E, Manfait M, Baillet-Guffroy A (2012) Molecular interactions of penetration enhancers within ceramides organization: a Raman spectroscopy approach. *Analyst* 137(21):5002–5010. doi:[10.1039/c2an35220f](https://doi.org/10.1039/c2an35220f)
- Voegeli R, Heiland J, Doppler S, Rawlings AV, Schreier T (2007) Efficient and simple quantification of stratum corneum proteins on tape strippings by infrared densitometry. *Skin Res Technol* 13(3):242–251. SRT214 [pii]. doi:[10.1111/j.1600-0846.2007.00214.x](https://doi.org/10.1111/j.1600-0846.2007.00214.x)
- Voegeli R, Rawlings AV, Breternitz M, Doppler S, Schreier T, Fluhr JW (2009) Increased stratum corneum serine protease activity in acute eczematous atopic skin. *Br J Dermatol* 161(1):70–77. BJD9142 [pii]. doi:[10.1111/j.1365-2133.2009.09142.x](https://doi.org/10.1111/j.1365-2133.2009.09142.x)
- Weigmann HJ, Jacobi U, Antoniou C, Tsirikas GN, Wendel V, Rapp C et al (2005) Determination of penetration profiles of topically applied substances by means of tape stripping and optical spectroscopy: UV filter substance in sunscreens. *J Biomed Opt* 10(1):14009
- Weigmann HJ, Lademann J, Schanzer S, Lindemann U, von Pelchrzrim R, Schaefer H et al (2001) Correlation of the local distribution of topically applied substances inside the stratum corneum determined by tape-stripping to differences in bioavailability. *Skin Pharmacol Appl Skin Physiol* 14(Suppl 1):98–102. doi:[10.1016/j.ejpb.2012.02.002](https://doi.org/10.1016/j.ejpb.2012.02.002)

# Application of EPR-spin Probes to Evaluate Penetration Efficiency, Storage Capacity of Nanotransporters, and Drug Release

Stefan F. Haag, Jürgen Lademann,  
and Martina C. Meinke

## Contents

12.1	<b>Introduction</b> .....	215
12.2	<b>Nanocarriers</b> .....	216
12.2.1	Invasomes .....	216
12.2.2	Core Multishell Nanotransporters .....	217
12.2.3	Nanostructured Lipid Carriers .....	217
12.3	<b>Electron Paramagnetic Resonance Spectroscopy</b> .....	218
12.4	<b>Stable Nitroxide Spin Probes—Aminoxyl Radicals</b> .....	220
12.5	<b>Applications</b> .....	220
12.5.1	Partitioning of a Drug Within a Carrier .....	220
12.5.2	Skin Penetration Enhancement .....	222
12.5.3	Stabilization of Nitroxides— Determination of Sustained Release of TEMPO .....	223
12.5.4	Further Applications .....	226
	<b>Conclusion</b> .....	226
	<b>References</b> .....	227

## 12.1 Introduction

Drug delivery to the skin requires intensive research into the synthesis of new carrier systems, which promote an effective and selective delivery of pharmaceuticals to the site of interest. For a variety of active compounds, incorporation into a carrier system is important as (a) the compound could be poorly soluble in water or traditional formulations and (b) to increase skin penetration of the compound while avoiding absorption into systemic circulation, which minimizes adverse effects, or to achieve a sustained release of the compound from the carrier to the skin. Therefore, it is important to create new carrier systems by means of a technique that corresponds to the therapeutic needs (Martini and Ciani 2009). To achieve these goals, the physicochemical properties of the drug-loaded carrier systems must be fully understood.

Besides optical methods, electron paramagnetic resonance (EPR) or electron spin resonance spectroscopy is a unique method that provides information about the localization of a drug within a carrier system, and it offers dynamic and structural information concerning a carrier system and lends itself excellently for the observation of drug release processes. In order to observe these processes, paramagnetic material has to be added to the systems. Spin probes, mainly

S.F. Haag • J. Lademann • M.C. Meinke (✉)  
Department of Dermatology, Venereology and Allergy, Charité – Universitätsmedizin Berlin, Center of Experimental and Applied Cutaneous Physiology, 10117 Berlin, Germany  
e-mail: [martina.meinke@charite.de](mailto:martina.meinke@charite.de)

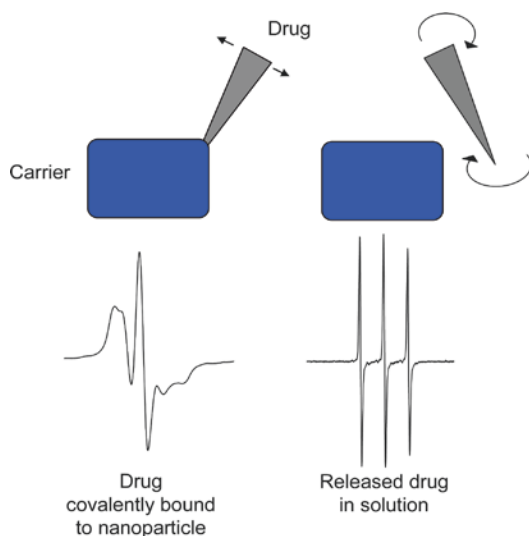


**Fig. 12.1** Example of EPR spectra of a covalently bound drug/spin probe and of one released in solution

nitroxides, can be used as model agents, or drugs can be spin labeled and incorporated into the carrier systems.

Besides microviscosity and micropolarity, the EPR spectra of nitroxides can provide even more information about the microenvironment of the carrier system, for example, with pH-sensitive nitroxides the microacidity can be measured (Bobko et al. 2010), local oxygen concentration can be determined (Khan et al. 2011; Velan et al. 2000), high local concentrations of nitroxides in carrier compartments can be quantified (Martini et al. 1985), or covalently bonded nitroxides can be differentiated from released nitroxides, which is one of the main features of EPR spectroscopy in the drug release research (Fig. 12.1).

## 12.2 Nanocarriers

As well as penetration enhancers like ethanol and dimethylsulfoxide, various nano- and micrometer scaled carrier systems are used in pharmaceuticals and cosmetics for enhanced skin penetration. Liposomes were the first nanosized drug carriers for the topical route of administration of triamcinolone, being the first drug liposomally encapsulated and applied to the skin of rabbits

(Mezei and Gulasekharan 1980). Furthermore, microemulsions and nanoemulsions are used as drug carriers as well as lipid based nanoparticles. Polymer-based macromolecules, for example, dendrimers appear to be also promising nanocarriers.

In the following paragraphs, a selection of nanocarriers for dermal application is described in more detail.

### 12.2.1 Invasomes

Invasomes are highly fluidic, ultra-deformable, elastic liposomal vesicles, which consist of phosphatidylcholine, ethanol, and terpenes (Dragicevic-Curic et al. 2008). Due to their fluidic membrane, liquid-state vesicles exhibit superior drug penetration enhancement ability compared to conventional, rigid gel-state liposomes (El Maghraby et al. 2001). Liposomes are of spherical shape, whereas invasomes are often of deformed spherical shape due to their highly fluidic and deformable membrane. Visualization of invasomes revealed that they appear unilamellar and bilamellar, which is independent of the loaded agent (Chen et al. 2011).

Moreover, it could be shown that the combination of ethanol and terpenes can enhance skin penetration of drugs, e.g., the highly lipophilic drug midazolam (Ota et al. 2003), as well as the water-soluble diclofenac sodium (Obata et al. 1990, 1991). Therefore, invasomes promote the penetration of drugs with unfavorable partition coefficient ( $\log P$  value) and molecular weight (MW), e.g., the lipophilic drug temoporfin (MW = 681 g/mol,  $\log P = 9.3$ ) (Dragicevic-Curic et al. 2008, 2009; Chen et al. 2011) and the hydrophilic model agent carboxyfluorescein (MW = 378 g/mol,  $\log P = -1.5$ ) (Chen et al. 2011). Two mechanisms are described in the literature, which explain how the interaction of elastic vesicles with the skin appears to enhance penetration. The first mechanism proposes that vesicles or vesicle constituents disorganize and disrupt intercellular lipids, affecting the ultrastructure of the stratum corneum by the creation or modification of pathways for possible drug

penetration, thus leading to increased skin permeability. However, treatment with rigid vesicles did not affect stratum corneum ultrastructure or permeability (van den Bergh et al. 1999). The second mechanism postulates that ultraflexible vesicles can penetrate the skin unfragmented on areas with low penetration resistance, e.g., between neighboring corneocyte clusters with no lateral overlapping of the corneocytes (Schätzlein and Cevc 1998; Cevc et al. 2002). Moreover, it was found that ultraflexible vesicles penetrate intact into deeper stratum corneum layers; however, only small amounts were found in the deepest stratum corneum layers. These findings could not be observed after the application of rigid gel-state vesicles (Honeywell-Nguyen et al. 2002).

### 12.2.2 Core Multishell Nanotransporters

Core multishell (CMS) nanotransporters are chemical chameleons, which, similar to liposomes, can encapsulate both hydrophilic and lipophilic guest molecules. Additionally, they can be dissolved in a variety of solvents, ranging from water to toluene. The unimolecular architecture of CMS nanotransporters contains a hydrophilic core, followed by a hydrophobic middle layer, and a hydrophilic outer shell. This architecture mimics the structure of liposomes, which are lipid vesicles that comprise of an aqueous inner phase, enclosed by a phospholipid membrane and surrounded by an exterior aqueous phase. As described above, the liposome architecture was found to have a penetration enhancing effect. It has been suggested that liposomes adhere to the skin surface and destabilize, fuse, or mix with the lipid matrix, resulting in a loosening of the lipid structure, which lowers the barrier strength of the skin and enhances skin penetration of loaded drugs or agents (Elsayed et al. 2007; Kirjavainen et al. 1996). Due to their liposome-like architecture, CMS nanotransporters might exhibit a similar penetration enhancing efficiency and additionally, as polymer-based nanotransporters, an improved stability.

The terminal shell provides a good solubility of the particle in water as well as in organic solvents and a high degree of biocompatibility. Furthermore, as well as the core, it serves as a matrix for encapsulation of hydrophilic agents. The nonpolar inner shell allows incorporation of hydrophobic guest molecules (Radowski et al. 2007).

CMS nanotransporters comprise of small unimers, 5 nm in size, but if the critical aggregation concentration of 0.1 g/l is reached, larger aggregates are formed with a diameter of approximately 30–50 nm.  $\beta$ -Carotene loaded CMS nanotransporters form aggregates up to 144 nm in size (Radowski et al. 2007).

CMS nanotransporters were shown to enhance skin penetration of the lipophilic dye Nile red (Küchler et al. 2009b) and the hydrophilic dye rhodamine B (Küchler et al. 2009a) and thus appear to be of outstanding versatility. Furthermore, CMS nanotransporters are used for tumor targeting (Quadir et al. 2008), cellular copper uptake by yeast cells (Treiber et al. 2009), or as stabilizers for catalytic platinum nanoparticles (Keilitz et al. 2010).

### 12.2.3 Nanostructured Lipid Carriers

Nanostructured lipid carriers (NLCs) consist of a solid lipid matrix formed by, e.g., glycerol tristearate (Dynasan® 118; Cognis, Monheim, Germany) and are loaded with liquid lipids of, e.g., caprylic/capric triglycerides (medium chain triglycerides, Miglyol® 812, Caelo, Hilden, Germany). NLCs are dispersed in water and stabilized by an emulsifying agent. However, the structure of NLCs is described differently in the literature. One theory describes NLCs as spherical nanoparticles with droplets of liquid lipid within the solid lipid matrix (Müller et al. 2002), whereas another group describes them as lipid platelets with oil spots located on the surface of the solid lipid matrix (Jores et al. 2004). Preparation of NLCs is performed by high-pressure homogenization (HPH), applying two to three cycles at 500 bar. HPH can be performed at high temperatures, e.g., 80 °C but also cold HPH

is known (Müller et al. 2000). HPH at room temperature is particularly interesting for the loading of temperature-sensitive agents to NLCs. The disadvantage of cold HPH is the increase in particle size. Mean particle size exhibits a wide range from 50 to 1000 nm. The lipid content of a formulation/nanodispersion can be from 5 to 40 % (Schäfer-Korting et al. 2007). NLCs were used for the controlled release of the highly lipophilic drug clotrimazole (Souto et al. 2004). Moreover, topical application of NLCs results in the formation of an occlusive film on the skin which improves skin hydration (Müller et al. 2002). Nevertheless, NLCs failed to enhance the uptake of Nile red (Lombardi Borgia et al. 2005) and cyproterone acetate (Stecova et al. 2007) when compared to the uptake from solid lipid nanoparticles.

### 12.3 Electron Paramagnetic Resonance Spectroscopy

EPR is a powerful tool for the detection of free radicals and other paramagnetic molecules (molecules with one or more free, unpaired electrons in the outer orbital shell). The concept of EPR spectroscopy is similar to nuclear magnetic resonance (NMR) spectroscopy. Both are based on the interaction of electromagnetic radiation with magnetic moments. In EPR spectroscopy the magnetic moment originates from free unpaired electrons of a molecule, whereas in NMR spectroscopy the magnetic moment arises from the proton spin of hydrogen nuclei.

Therefore, EPR spectroscopy is concerned with resonant absorption of microwave energy by an unpaired free electron within an applied magnetic field. The energy of a free electron in a magnetic field splits into two distinct energy levels, which is called the Zeeman effect (Fig. 12.2). If the energy of the microwave radiation corresponds to the energy difference of the two distinct energy levels of an electron in a magnetic field, resonance conditions are fulfilled and spin conversion occurs. This results in a change of microwave energy, which is detected in EPR spectroscopy.

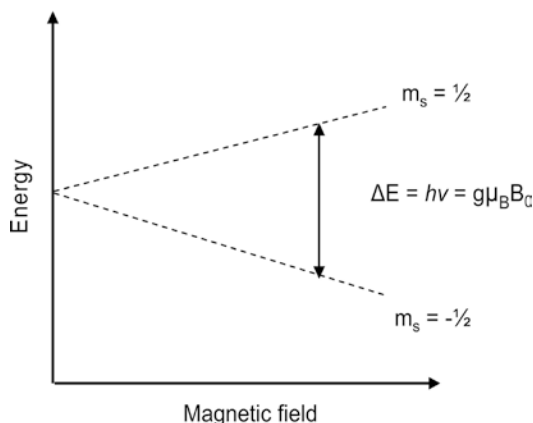


**Fig. 12.2** Zeeman effect. The magnetic field splits the energy of a free electron into two distinct energy levels. Resonance conditions are fulfilled if the microwave energy fits the energy difference between the two energy levels

The fundamental equation of EPR spectroscopy is given in formula Eq. 12.1:

$$h\nu = g\mu_B B_0 \quad (12.1)$$

with  $h$  as the Planck constant,  $\nu$  the microwave frequency,  $g$  the Landé  $g$ -factor,  $\mu_B$  the Bohr magneton, and  $B_0$  the magnetic field strength.

EPR spectrometers are classified by the microwave frequency, which ranges from 0.3 GHz (Alecci et al. 1994) to 360 GHz (Fuchs et al. 2002). L-band EPR spectrometers operate at a frequency of 1.3 GHz, X-band at 9.4 GHz, Q-band at 34 GHz, and W-band at 94 GHz, and the frequency determines the measuring sensitivity of an EPR spectrometer. Sensitivity is directly related to the square of operating frequency (Fuchs et al. 2001).

Moreover, the dependency of microwave frequency with microwave penetration into biological tissue is of high importance: At L-band frequency, microwave penetration amounts to 20 mm and is reduced exponentially at X-band frequency to below 1 mm (Fuchs et al. 2001). This can be explained by the high water content of biological samples, which causes high nonresonant, dielectric absorption of microwaves. Nonresonant absorption is a function of frequency and increases with increasing frequency.



Besides detection and quantification of nitroxides or other paramagnetic molecules, EPR spectroscopy can provide information on the physicochemical properties of the molecule as well as information about its immediate surrounding, i.e., polarity and viscosity. This information can be derived from the line shape of the EPR spectrum. EPR spectra of nitroxides in solution comprise of three resonant lines (Fig. 12.3), which are due to the magnetic moment of the neighboring nitrogen nucleus. Interactions of free, unpaired electrons with the magnetic moment of the nitrogen nucleus are described as  $^{14}\text{N}$  hyperfine coupling, which splits the EPR spectrum in three lines. The  $^{14}\text{N}$  hyperfine coupling constant ( $a_{\text{iso}}$ ) is strongly influenced by hydrogen bonds between solvent molecules and the oxygen of the nitroxide and therefore, gives information about the polarity of the immediate surrounding of the paramagnetic molecule. It was found that  $a_{\text{iso}}$  increases proportionally with the concentration of hydrogen donor groups of the solvent (Gagua et al. 1978).

The  $g$ -factor indicates the position of the resonant lines within the magnetic field. Moreover, it also reflects the polarity of its immediate surrounding when measuring at high

frequencies as shown in Fig. 12.4 for Q- and W-band measurements. The  $g$ -factor increases with increasing lipophilicity of the microenvironment. A further indicator of the polarity is the hyperfine coupling constant,  $a_{\text{iso}}$ , which reflects the polarity independent of the applied frequency. Low values of  $a_{\text{iso}}$  represent a lipophilic environment, whereas high values a hydrophilic one, e.g., the nitroxide 2,2,6,6-tetramethyl-1-piperidinyloxy (TEMPO; Sigma Aldrich, Steinheim, Germany) has an  $a_{\text{iso}}$  of 1.74 mT in water and 1.59 mT in a mix of phosphatidylcholine and lysophosphatidylcholine (Haag et al. 2011c).

An indicator of the microviscosity is the rotational correlation time in seconds, which is

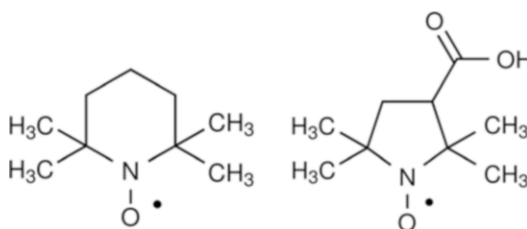


**Fig. 12.4** Chemical structure of selected nitroxide spin probes: TEMPO (left) and PCA (right)

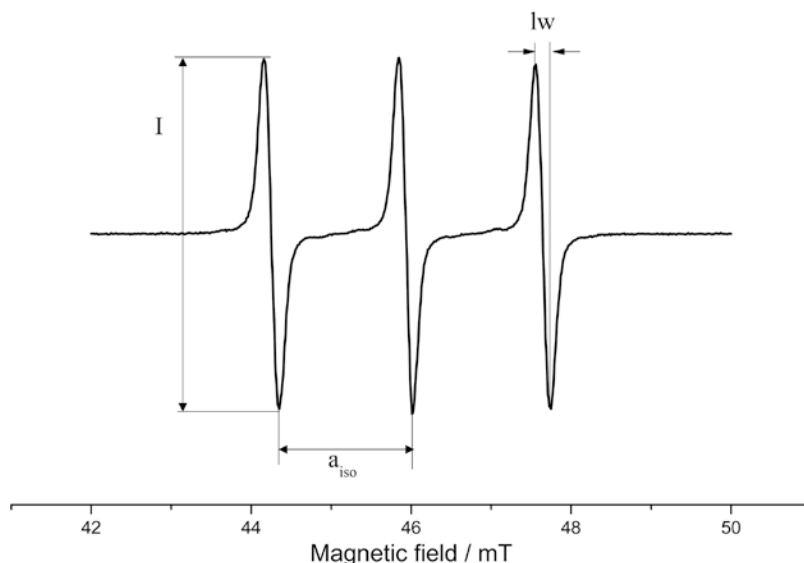


**Fig. 12.3** EPR spectrum of the nitroxide PCA that illustrates typical EPR parameters: I: signal amplitude,  $a_{\text{iso}}$ : hyperfine coupling constant, lw: peak to peak line width

defined as the time it takes for the spin probe to rotate once around its own axis. This is one of the main features of EPR spectroscopy when studying drug release processes, e.g., a spin probe or spin labeled drug that is incorporated in a carrier system can be differentiated from a released one, especially if it is covalently bound to a nanoparticle (see spectra in Fig. 12.1).

Additionally, in the case of highly concentrated paramagnetic substances within carrier systems a broadening of the signals appears due to spin–spin coupling. In the case of release, the broadening disappears.

The four described EPR parameters can be derived from the EPR spectrum by using simulation software, e.g., the EasySpin toolbox (Stoll and Schweiger 2006).

## 12.4 Stable Nitroxide Spin Probes—Aminoxyl Radicals

Nitroxides are versatile spin probes for various applications in biology, medicine, and pharmaceuticals. Nitroxides are paramagnetic species, possessing a free, unpaired electron in the outer shell of the molecule and are therefore detectable by EPR spectroscopy. While all have a free electron at the nitrogen in common, the chemical structures and thus physicochemical properties can differ significantly. Most commonly applied nitroxides are six-ring systems (piperidines) and five-ring systems (pyrrolidines). The stability of the free radical arises from the delocalized electron from the NO bond and steric hindrance by the four methyl groups.

Two representative spin probes are 3-carboxy-2,2,5,5-tetramethyl-1-pyrrolidinyloxy (PCA; Sigma Aldrich, Steinheim, Germany), ( $\log P = -1.7$ ; MW = 186 g/mol) and TEMPO ( $\log P = 2.3$ ; MW = 156 g/mol) (Fig. 12.4). The stability of the nitroxide is mainly determined by its ring structure, PCA with its five-ring system is significantly more stable than TEMPO with its six-ring system (Fuchs et al. 1993). Both spin probes can be applied in vivo (Fuchs et al. 1997).

## 12.5 Applications

### 12.5.1 Partitioning of a Drug Within a Carrier

EPR spectroscopy allows distinguishing between environments differing in polarity (Kempe et al. 2010). Smirnov et al. (1995) could show TEMPO partitioning between the aqueous and lipid domains of liposomes. Previously, Haag et al. (2011a) studied ultraflexible liposomes (invasomes) and nanostructured lipid carriers, which had also been prepared with TEMPO. Partitioning of TEMPO between lipid and aqueous phases could be observed and quantified. Changes in partitioning after application to the skin resulted in a sustained release of TEMPO to the skin. In Fig. 12.5, EPR spectra of TEMPO-loaded invasomes (solid, black line) recorded at different microwave frequencies are shown. Sensitivity is directly related to the square of operating frequency, which means the higher the frequency, the higher the measuring sensitivity of the spectrometer. Due to the low magnetic field strength at L-band frequency (1.3 GHz), spectra from phases originating from different polar environments appear as a single three-line spectrum, because the spectra from the different environments overlap. By increasing the frequency to X- and Q-band, spectra from the different phases are separated more efficiently. Measurements at W-band frequency (94 GHz) can completely separate the spectra from environments differing in polarity due to the high magnetic field strength, which results in two spectra. In this case one from the phosphatidylcholine/lysophosphatidylcholine phase and one from the aqueous phase of the invasomes. Since we can separate the spectra at W-band, the magnetic parameters can be fully derived from the spectra in each phase (i.e.,  $g$ -value indicates the position of the spectra within the magnetic field),  $^{14}\text{N}$  hyperfine coupling ( $a_{\text{iso}}$ , distance between low field and central line, high values indicate a hydrophilic environment and vice versa), and the rotational correlation time (the time it takes for a spin probe to turn once around its own axis). This is a prerequisite

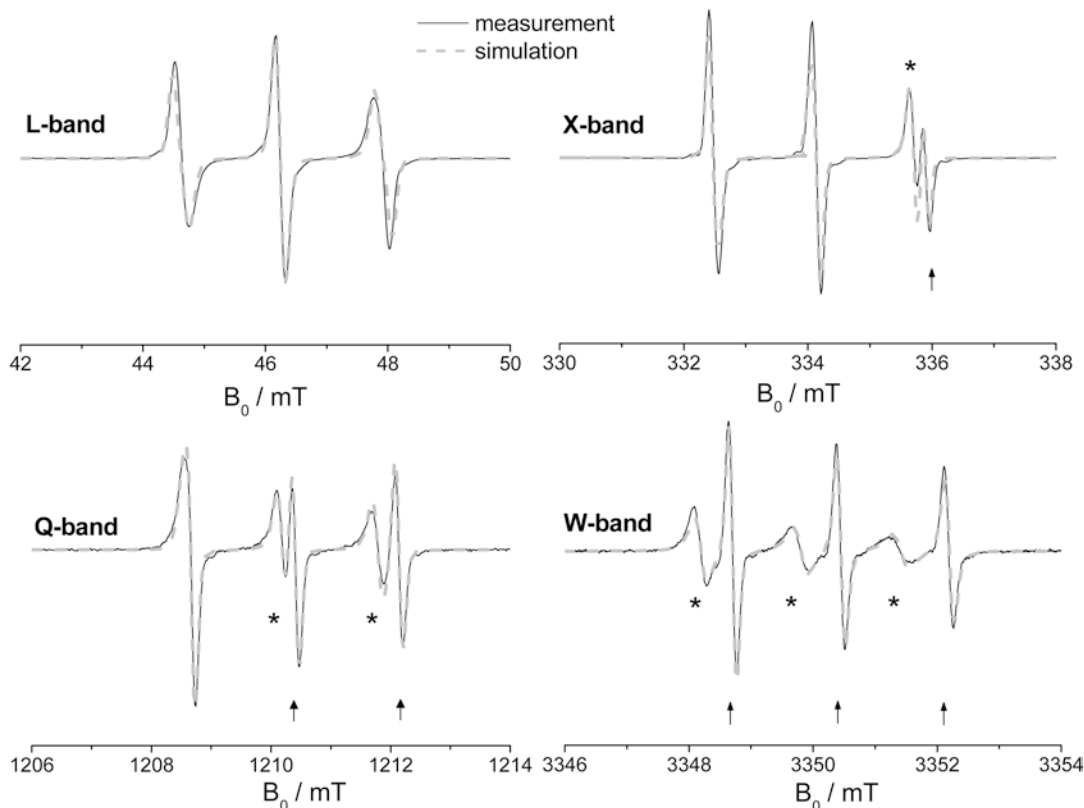


**Fig. 12.5** Multifrequency measurement of the spin probe TEMPO within an invasome dispersion. The asterisk indicates signals of TEMPO from the lipophilic membrane and the arrows from the aqueous phase

for spectral simulation of spectra recorded at lower frequencies. By entering these parameters into computer software, e.g., EasySpin the spectra can be simulated at each frequency as shown in Fig. 12.5 (gray, dashed line).

The L-band low frequency measurement shows a broadened low and high-field line. The spectrum at X-band frequency shows a partitioned high-field line. When measuring at Q-band frequency, two lines of the lipophilic TEMPO EPR spectrum already appear and are shifted down-field due to higher  $g$ -values. The measurement at W-band clearly resolves three lines from each of the two phases. As demonstrated in Fig. 12.5, the resolution increases with increasing frequency. At W-band frequency the distribution between phases of different polarity can be determined, and most importantly quantified. This is especially important for the development of

lipid-based carrier systems for a specific purpose, e.g., in the surfactant shell of the nanoparticle for burst release or in the core of a liquid lipid emulsion for sustained release. At W-band frequency, the distribution can be easily determined and quantified..

The use of different spectrometers operating at diverse microwave frequencies allows comprehensive studies of pharmaceutical formulations. At high frequency W-band (94 GHz) the localization of a spin probe or a spin-labeled drug within a carrier matrix becomes feasible allowing the observation of drug-carrier interactions. This can be the localization in a certain polar environment in a two-phase system like invasomes, or the localization of a spin probe in the core of a lipid nanoparticle or within the surfactant shell. Especially interesting for the investigation of topical dermatics is the low frequency L-band

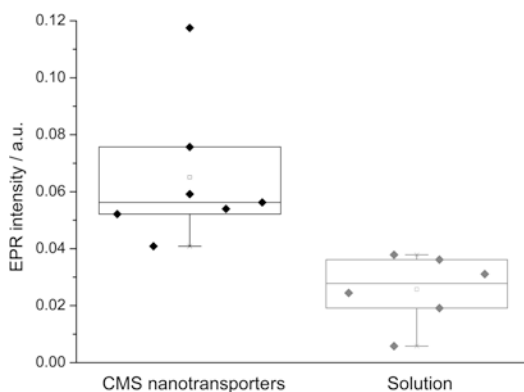
(1.3 GHz) EPR spectroscopy, because measurements of formulations containing spin probes applied to the skin *ex vivo* and *in vivo* are feasible. This allows the determination of penetration efficiency after skin application of spin probe loaded carriers. Moreover, it can be determined whether a carrier system releases its payload slowly in a depot manner.

Measurements to investigate the stability of delivery systems were further performed by Yucel et al. (2012), who investigated the distribution of the hydrophobic nitroxide 4-phenyl-2,2,5,5-tetramethyl-3-imidazoline-1-oxyl (PTMIO). PTMIO was homogenized with eicosane and a sodium caseinate solution. After cooling, solid lipid nanoparticles were formed, because eicosane is crystalline at 21.5 °C. Moreover, a further emulsion-based delivery system with tetradecane as the lipid phase was produced the same way. The only difference is that tetradecane forms liquid droplets at 21.5 °C. For both delivery systems, two different sizes were produced, fine droplets with a diameter of 0.2 µm and coarse droplets with 1.3 µm in diameter. The distribution of the probe can be obtained from analysis of the spectra, and the chemical stability by measurements of reduction kinetics (e.g., vitamin C, which turns PTMIO EPR silent) as demonstrated in Fig. 12.9 where the degradation of TEMPO by the antioxidant system of the skin is shown. Analysis of the resulting EPR spectra revealed populations of the spin probe in two discrete environments (i.e., aqueous and lipid). PTMIO is largely hydrophobic with 77 and 70% present in the coarse and the fine liquid lipid droplets of tetradecane, respectively. In the solid droplets (i.e., eicosane droplets) the probe was completely excluded from the droplets into the aqueous environment. Yucel et al. (2012) presumed that during the crystallization process the probe moves out of the solid lipid to the aqueous environment where it is more affected by the presence of the aqueous portions of the interfacial protein (sodium caseinate solution). Braem et al. (2007) showed that the EPR active cholestane is only located in the surfactant shell of solid lipid nanoparticles but not in the solid lipid core.

## 12.5.2 Skin Penetration Enhancement

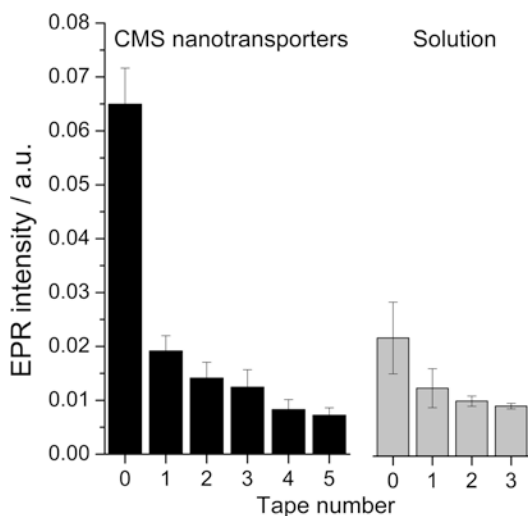
The amount of drug and/or carrier in the skin after its topical application can be quantified by EPR spectroscopy. Figure 12.6 shows the signal intensities of the nitroxide PCA in the skin following the application of two test formulations containing PCA for 30 min to porcine skin and removal of the surplus formulation from the skin surface. Investigated were CMS nanotransporters containing PCA and the free spin probe dissolved in the same solvent as the CMS nanotransporters (Haag et al. 2011b). Compared to the solution PCA penetration was 2.5-fold enhanced when applied within CMS nanotransporters. Statistical analysis revealed significant ( $p < 0.05$ ) penetration enhancement compared to PCA solution.

Figure 12.7 represents the results from the tape stripping experiments, which are in accordance with the penetration efficiency depicted in Fig. 12.6. Following the application of CMS nanotransporters PCA penetration was particularly high in unstripped skin and declined exponentially as being derived from the decline of signal intensity of the skin with subsequently taken tape strips. In fact, after one strip the intensity declines to only 25% and an EPR signal can no longer be detected after tape 6, indicating that



**Fig. 12.6** Boxplot of the EPR intensity of PCA-treated skin after a 30-min penetration time and removal of remaining liquid from the skin surface

the spin probe within the carrier and/or the spin probe itself only penetrate the upper stratum corneum. Applying PCA solution, the spin label penetrates the stratum corneum only poorly. The signal is low from start on, and after tape 4 it is below the detection limit.

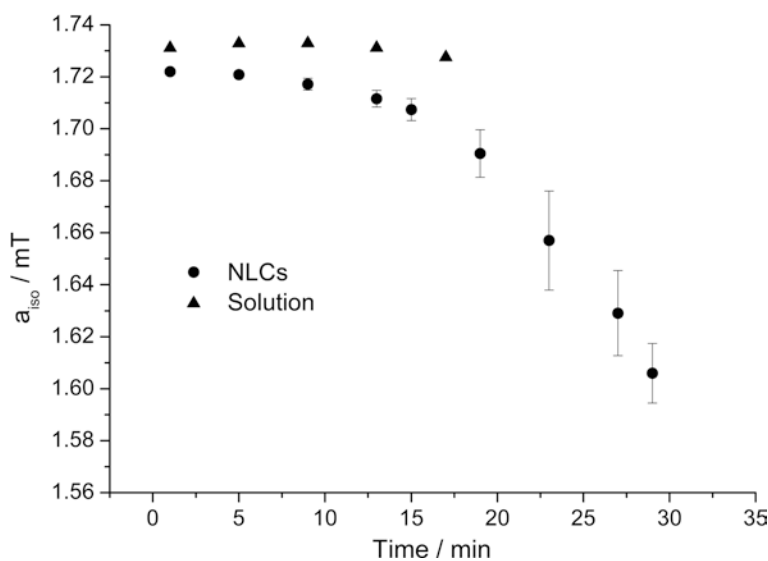


**Fig. 12.7** Spin label intensity of tape stripped porcine skin 30 min after application of PCA formulations. Tape number 0 corresponds to the intensity after penetration and removal of remaining liquids, number 1–5 correspond to the PCA-related signal intensity of the skin after each tape strip is taken

### 12.5.3 Stabilization of Nitroxides—Determination of Sustained Release of TEMPO

The next application of nitroxide stabilization is related to the possible sustained release of TEMPO incorporated into NLCs, i.e., the possibility that the formulation/carrier could act as a depot system. In this context NLCs were investigated (Haag et al. 2011a). Repetitive EPR spectra were recorded after the application of the TEMPO containing NLC formulations onto porcine ear skin. The change of  $a_{\text{iso}}$ , as a measure of the polarity of the immediate surrounding of the spin probe, over time was determined and is represented in Fig. 12.8. High values of  $a_{\text{iso}}$  represent a hydrophilic and low values indicate a lipophilic microenvironment. The  $a_{\text{iso}}$  of free TEMPO remains almost stable over time, indicating that TEMPO that interacts with the skin is immediately reduced to the EPR-silent hydroxylamine by skin antioxidants. For TEMPO in NLCs a slow decline is shown for approximately 15 min followed by a strong decline. This means that the polarity of the environment of the spin probe within the NLCs after skin application changes with time, from high values corresponding to a hydrophilic environment to low values,

**Fig. 12.8** Change of TEMPO micropolarity after the application of NLCs to porcine skin ex vivo



corresponding to a lipophilic environment. That indicates that TEMPO has a higher surviving probability in lipophilic environments, for example, in the liquid lipid droplets of the NLCs.

In Fig. 12.9 the EPR intensity decline of TEMPO measured at L-band is shown for solution and NLCs. As soon as TEMPO penetrates the skin it reacts with antioxidants and is reduced to the EPR-silent hydroxylamine, which results in intensity decline of TEMPO. EPR intensity rapidly decreases when applied in solution and is below the detection limit after 17 min, indicating that TEMPO penetrates the skin well and is quickly reduced. NLCs delayed TEMPO interaction with the skin resulting in prolonged signal detection by 12 min, when compared to solution. Thus, NLCs increase the measurement time *ex vivo* 1.7-fold, indicating that NLCs prevent TEMPO from reacting with the skin antioxidants and act therefore as slow release depot systems for TEMPO penetration into the skin. Statistical analysis revealed significance between solution and NLCs ( $p \leq 0.05$ ).

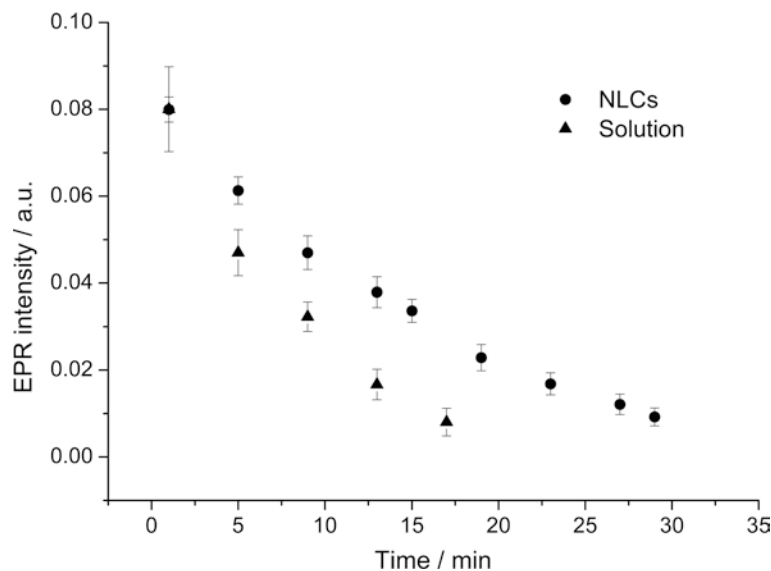
The decrease in EPR spectra intensity (Fig. 12.9) of TEMPO and the change in  $a_{\text{iso}}$  (Fig. 12.8) give information about the interaction of the NLCs with the skin. TEMPO penetrating the skin reacts with reducing agents, which turn the spin probe EPR silent that unprotected

TEMPO is reduced much faster than protected TEMPO. The slower reduction rate of TEMPO containing NLCs compared to solution indicates a fast reduction of unprotected TEMPO from the aqueous compartments of the suspension and first a stabilization of TEMPO in the liquid lipid compartments. After a longer penetration time, the liquid lipid compartments get to interact with the skin and TEMPO turns EPR silent. This indicates a delayed reduction of lipid-associated TEMPO and, therefore, slow release of TEMPO from the NLCs.

For TEMPO in NLCs a change of  $a_{\text{iso}}$  toward a more lipophilic microenvironment could be observed over time. The exponential  $a_{\text{iso}}$  decline can be explained by the distribution profile of TEMPO within the nanocarrier dispersion. NLCs had 35% of TEMPO associated with the liquid lipid droplets and 65% with the aqueous phase, as illustrated in Fig. 12.10. This becomes obvious when plotting intensity versus  $a_{\text{iso}}$  as shown in Fig. 12.10.

After the application of TEMPO-loaded nanocarriers to the skin and upon interaction of unprotected TEMPO of the aqueous phase with the skin, it is reduced quickly to the corresponding EPR-silent hydroxylamine, which results in a rapid change of signal intensity with primarily a slow decline of  $a_{\text{iso}}$ . With decreasing amounts of

**Fig. 12.9** Change of TEMPO intensity after the application of NLCs to porcine skin *ex vivo*



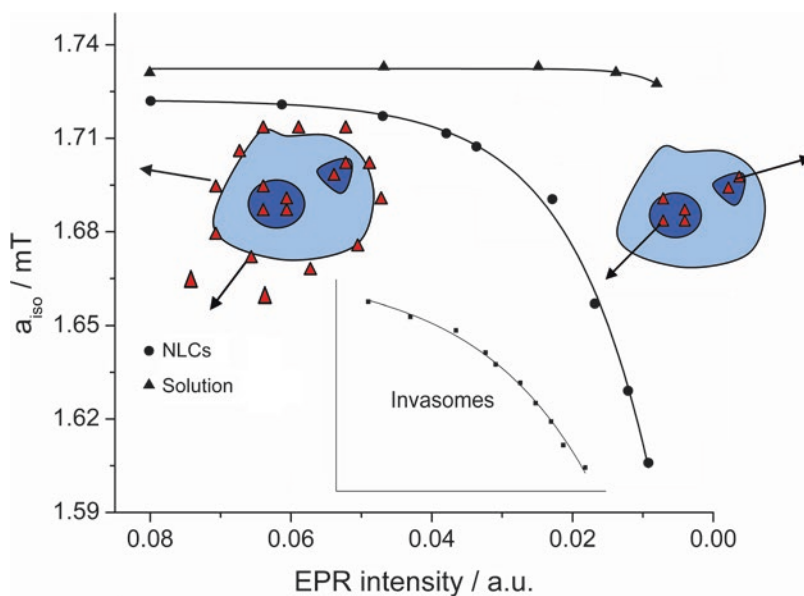


**Fig. 12.10** Plot of EPR intensity versus  $a_{\text{iso}}$  of the NLCs and solution during penetration into porcine ear skin ex vivo, TEMPO, NLC. The insert is the plot for invasomes of intensity versus  $a_{\text{iso}}$

TEMPO in the hydrophilic compartments  $a_{\text{iso}}$  is strongly influenced by lipid protected TEMPO. The reaction of TEMPO from both phases leads to a somewhat linear decrease of  $a_{\text{iso}}$  with intensity. Fig. 12.10 clearly indicates that the decline of  $a_{\text{iso}}$  with intensity depends on the distribution of TEMPO within the carrier. Since NLCs had 35% of TEMPO associated with the lipid phase, the decline is less steep in the beginning. As soon as more TEMPO is associated with lipid compartments, as shown by Haag et al. (2011c) for invasomes, which had 56% TEMPO in the lipid phase, the decline of  $a_{\text{iso}}$  with intensity turns less steep (see insert in Fig. 12.10) (Haag et al. 2011a; Haag et al. 2011c). The different intensity decline between solution and the nano-carriers was also observed in vivo (Haag et al. 2011a). This shows that EPR spectroscopy also allows the determination of sustained release on the skin of human volunteers.

In order to distinguish between different phases in a system, dissimilar spin probes that possess different EPR spectra can be used. Kempe et al. (2010) have shown with an oil and water chitosan-based gelling emulsion the distribution and release of a spin probe that served as model for

a low molecular weight drug. In order to investigate the release mechanisms, they incorporated the lipophilic spin probe HD-PMI (2-heptadecyl-2,3,4,5,5-pentamethyl-imidazoline-1-oxyl) and the hydrophilic spin probe  $^{15}\text{N}$ -PCM (3-carbamoyl-2,2,5,5-tetramethyl-3-pyrrolidin-1-oxyl- $^{15}\text{N}$ ) into the gelling emulsion. The spin probes could be distinguished from each other due to the  $^{15}\text{N}$ -PCM, which possesses a nitrogen isotope that exhibits two resonant lines only, in contrast to HD-PMI that has a typical three-line spectrum. Analysis of the micropolarity revealed that the hydrophilic  $^{15}\text{N}$ -PCM is located in the outer aqueous phase and the lipophilic HD-PMI is located in the oil droplets of the gelling emulsion. Although the gelling emulsion was rather viscous, the spin probes were not hindered in motion in their microenvironment. This could be derived from the sharp spectral lines of the spectrum. Subsequently, the release of  $^{15}\text{N}$ -PCM from the aqueous phase was analyzed and it was found that after 3 h the spin probe was completely released in vivo, whereas in vitro the release was completed after 6 h. This could be observed, because the intensity of the spectral lines of the two-line spectrum of  $^{15}\text{N}$ -PCM decreased over

time. The three-line spectrum of HD-PMI did not change in intensity, which indicates that the spin probe is protected by the oil droplets of the gelling emulsion. The use of different spin probes that possess different spectra allows distinguishing between environments differing in polarity and/or viscosity. Moreover, the localization of a spin probe within a carrier system is possible. The possibility of determination of the aforementioned parameters makes EPR spectroscopy a powerful tool in drug release research.

### 12.5.4 Further Applications

Besides the determination of spin probe distribution between environments differing in polarity, precise positioning of a spin probe in or on a nanoparticle is possible using EPR spectroscopy. Braem et al. (2007) loaded the EPR-active cholestane (which is close in its chemical structure to steroidal drugs) to solid lipid nanoparticles (SLN). SLNs consist of a lipid that is solid at skin temperature and are manufactured similarly to NLCs. Braem et al. (2007) established that cholestane could not be incorporated in the lipid matrix of the SLN, but they found two distinct compartments of attachment to the surface of the SLN, at the rim and the flat surface of the SLN. This was made possible because EPR spectroscopy allows the measurement of movement of an EPR-active compound. Cholestane attached to the flat surface of the SLN was more restricted in movement than cholestane at the rim. Moreover, due to its free electron, cholestane can be easily reduced by antioxidants. A reduction assay with vitamin C revealed that the velocity of cholestane reduction is faster for SLNs than for NLCs, which is due to incorporated cholestane in the liquid lipid droplets of the NLCs that protect cholestane from reduction. Therefore, they could conclude, based on the restricted movement and the fast reduction of cholestane by vitamin C that the spin probe is not incorporated in the solid lipid matrix.

In contrast to integrative EPR spectroscopy the EPR imaging technique allows, for example, the determination of nitroxide spin probe

localization in a human body. Burks et al. (2011) investigated the clearance and distribution of nitroxides encapsulated in different liposomes. The encapsulation in sterically stabilized liposomes allowed the transport to different organs like spleen, kidney, liver, and a breast tumor in a mouse model to be followed. By characterizing the pharmacological properties of nitroxides in liposomes, it could be demonstrated that only modest improvements are required to enable high-contrast EPR images of a mouse breast tumor (Hc7 tumors) *in vivo*. This shows that by the use of liposomes sufficient amounts of spin probe can be delivered to the site of interest.

### Conclusion

The different applications demonstrate that EPR spectroscopy is well suited for drug delivery studies.

1. It can be used to determine the localization within a carrier or formulation.
2. Stability studies of the formulation, carriers, or transporter can be performed.
3. Drug delivery into the skin or body can be investigated with regard to efficiency, localization, and distribution. Comparative studies of different carriers or formulations can be performed with regard to measuring the penetration efficiency.
4. Drug release by carriers can be followed giving additional mechanistic information about the uptake into the surrounding skin structures.

An advantage of EPR spectroscopy is that it is completely nondestructive, therefore the results are measurements of actual structure and properties and kinetic information is easily available.

A further application is the labeling of drugs and/or carriers with spin probes because nitroxides are of low molecular weight, hence not altering the physicochemical properties of the drug or carrier to the extent as in the case of fluorescence dye, which have a high molecular weight by nature. With the use of isotopic or different spin probes the drug and carrier



label can be distinguished. Drug release can also be triggered by external or internal triggers such as pH, temperature, etc., allowing the observation of release by EPR spectroscopy.

**Acknowledgment** This work was funded by the Freie Universität (FU) Berlin, Focus Area Functional Nanoscale Materials. Furthermore, we thank Ming Chen and Alfred Fahr (Department of Pharmacy, Friedrich-Schiller-Universität Jena) for providing the invasomes, Emanuel Fleige and Rainer Haag (Department of Chemistry, FU-Berlin) for providing the CMS-nanotransporters, and Daniel Peters and Cornelia Keck (Department of Pharmacy, FU-Berlin) for providing the nanostructured lipid carriers. We also thank Robert Bittl and Christian Teutloff (Department of Physics, FU-Berlin) for Q- and W-band measurements as well as their valuable support regarding spectra analysis, and Monika Schäfer-Korting (Department of Pharmacy, FU-Berlin) for fruitful discussions.

## References

- Alceci M, Ferrari M, Quaresima V, Sotgiu A, Ursini CL (1994) Simultaneous 280 MHz EPR imaging of rat organs during nitroxide free radical clearance. *Biophys J* 67(3):1274–1279
- Bobko AA, Kirilyuk IA, Gritsan NP, Polovyanenko DN, Grigor'ev IA, Khramtsov VV et al (2010) EPR and quantum chemical studies of the pH-sensitive imidazoline and imidazolidine nitroxides with bulky substituents. *Appl Magn Reson* 39(4):437–451
- Braem C, Blaschke T, Panek-Minkin G, Herrmann W, Schlupp P, Paepenmuller T et al (2007) Interaction of drug molecules with carrier systems as studied by par-electric spectroscopy and electron spin resonance. *J Control Release* 119(1):128–135
- Burks SR, Legenzov EA, Rosen GM, Kao JP (2011) Clearance and biodistribution of liposomally encapsulated nitroxides: a model for targeted delivery of electron paramagnetic resonance imaging probes to tumors. *Drug Metab Dispos Biol Fate Chem* 39(10):1961–1966
- Cevc G, Schätzlein A, Richardsen H (2002) Ultradeformable lipid vesicles can penetrate the skin and other semi-permeable barriers unfragmented. Evidence from double label CLSM experiments and direct size measurements. *Biochim Biophys Acta* 1564(1):21–30
- Chen M, Liu X, Fahr A (2011) Skin penetration and deposition of carboxyfluorescein and temoporfin from different lipid vesicular systems: in vitro study with finite and infinite dosage application. *Int J Pharm* 408(1–2):223–234
- Dragicevic-Curic N, Scheglmann D, Albrecht V, Fahr A (2008) Temoporfin-loaded invasomes: development, characterization and in vitro skin penetration studies. *J Control Release* 127(1):59–69
- Dragicevic-Curic N, Scheglmann D, Albrecht V, Fahr A (2009) Development of different temoporfin-loaded invasomes-novel nanocarriers of temoporfin: characterization, stability and in vitro skin penetration studies. *Colloids Surf B Biointerfaces* 70(2):198–206
- El Maghraby GM, Williams AC, Barry BW (2001) Skin delivery of 5-fluorouracil from ultradeformable and standard liposomes in-vitro. *J Pharm Pharmacol* 53(8):1069–1077
- Elsayed MM, Abdallah OY, Naggar VF, Khalafallah NM (2007) Lipid vesicles for skin delivery of drugs: reviewing three decades of research. *Int J Pharm* 332(1–2):1–16
- Fuchs J, Freisleben HJ, Podda M, Zimmer G, Milbradt R, Packer L (1993) Nitroxide radical biostability in skin. *Free Radic Biol Med* 15(4):415–423
- Fuchs J, Groth N, Herrling T, Zimmer G (1997) Electron paramagnetic resonance studies on nitroxide radical 2,2,5,5-tetramethyl-4-piperidin-1-oxyl (TEMPO) redox reactions in human skin. *Free Radic Biol Med* 22(6):967–976
- Fuchs J, Herrling T, Groth N (2001) Detection of free radicals in skin: a review of the literature and new developments. *Curr Probl Dermatol* 29:1–17
- Fuchs MR, Schleicher E, Schnegg A, Kay CWM, Törring JT, Bittl R et al (2002) g-tensor of the neutral flavin radical cofactor of DNA photolyase revealed by 360-GHz electron paramagnetic resonance spectroscopy. *J Phys Chem B* 106(34):8885–8890
- Gagua AV, Malenkov GG, Timofeev VP (1978) Hydrogen-bond contribution to isotropic hyperfine splitting constant of a nitroxide free radical. *Chem Phys Lett* 56(3):470–473
- Haag SF, Chen M, Peters D, Keck CM, Taskoparan B, Fahr A et al (2011a) Nanostructured lipid carriers as nitroxide depot system measured by electron paramagnetic resonance spectroscopy. *Int J Pharm* 421:364–369
- Haag SF, Fleige E, Chen M, Fahr A, Teutloff C, Bittl R et al (2011b) Skin penetration enhancement of core-multishell nanotransporters and invasomes measured by electron paramagnetic resonance spectroscopy. *Int J Pharm* 416(1):223–228
- Haag SF, Taskoparan B, Bittl R, Teutloff C, Wenzel R, Fahr A et al (2011c) Stabilization of reactive nitroxides using invasomes to allow prolonged electron paramagnetic resonance measurements. *Skin Pharmacol Physiol* 24(6):312–321
- Honeywell-Nguyen PL, de Graaff AM, Groenink HW, Bouwstra JA (2002) The in vivo and in vitro interactions of elastic and rigid vesicles with human skin. *Biochim Biophys Acta* 1573(2):130–140
- Jores K, Mehnert W, Drechsler M, Bunjes H, Johann C, Mäder K (2004) Investigations on the structure of solid lipid nanoparticles (SLN) and oil-loaded solid lipid nanoparticles by photon correlation spectroscopy, field-flow fractionation and transmission electron microscopy. *J Control Release* 95(2):217–227

- Keilitz J, Schwarze M, Nowag S, Schomäcker R, Haag R (2010) Homogeneous stabilization of Pt nanoparticles in dendritic core-multishell architectures: application in catalytic hydrogenation reactions and recycling. *ChemCatChem* 2(7):863–870
- Kempe S, Metz H, Mader K (2010) Application of electron paramagnetic resonance (EPR) spectroscopy and imaging in drug delivery research – chances and challenges. *Eur J Pharm Biopharm* 74(1):55–66
- Khan N, Blinco JP, Bottle SE, Hosokawa K, Swartz HM, Micallef AS (2011) The evaluation of new and isotopically labeled isoindoline nitroxides and an azaphenylene nitroxide for EPR oximetry. *J Magn Reson* 211(2):170–177
- Kirjavainen M, Urtti A, Jääskeläinen I, Suhonen TM, Paronen P, Valjakka-Koskela R et al (1996) Interaction of liposomes with human skin in vitro – the influence of lipid composition and structure. *Biochim Biophys Acta* 1304(3):179–189
- Küchler S, Abdel-Mottaleb M, Lamprecht A, Radowski MR, Haag R, Schäfer-Korting M (2009a) Influence of nanocarrier type and size on skin delivery of hydrophilic agents. *Int J Pharm* 377(1–2):169–172
- Küchler S, Radowski MR, Blaschke T, Dathe M, Plendl J, Haag R et al (2009b) Nanoparticles for skin penetration enhancement – a comparison of a dendritic core-multishell-nanotransporter and solid lipid nanoparticles. *Eur J Pharm Biopharm* 71(2):243–250
- Lombardi Borgia S, Regehy M, Sivaramakrishnan R, Mehnert W, Korting HC, Danker K et al (2005) Lipid nanoparticles for skin penetration enhancement – correlation to drug localization within the particle matrix as determined by fluorescence and paretic spectroscopy. *J Control Release* 110(1):151–163
- Martini G, Ciani L (2009) Electron spin resonance spectroscopy in drug delivery. *Phys Chem Chem Phys* 11(2):211–254
- Martini G, Bindi M, Ottaviani MF, Romanelli M (1985) Dipolar and spin exchange effects in the electron-spin-resonance spectra of nitroxide radicals in solution. 2. Water solutions adsorbed on porous silica-gels. *J Colloid Interface Sci* 108(1):140–148
- Mezei M, Gulasekharan V (1980) Liposomes – a selective drug delivery system for the topical route of administration. Lotion dosage form. *Life Sci* 26(18):1473–1477
- Müller RH, Jenning V, Mäder K, Lippacher A, Inventors (2000) Lipid particles on the basis of mixtures of liquid and solid lipids and methods for producing same. Germany
- Müller RH, Radtke M, Wissing SA (2002) Solid lipid nanoparticles (SLN) and nanostructured lipid carriers (NLC) in cosmetic and dermatological preparations. *Adv Drug Deliv Rev* 54(Suppl 1):S131–S155
- Obata Y, Takayama K, Okabe H, Nagai T (1990) Effect of cyclic monoterpenes on percutaneous absorption in the case of a water-soluble drug (diclofenac sodium). *Drug Des Deliv* 6(4):319–328
- Obata Y, Takayama K, Machida Y, Nagai T (1991) Combined effect of cyclic monoterpenes and ethanol on percutaneous absorption of diclofenac sodium. *Drug Des Discov* 8(2):137–144
- Ota Y, Hamada A, Nakano M, Saito H (2003) Evaluation of percutaneous absorption of midazolam by terpenes. *Drug Metab Pharmacokinet* 18(4):261–266
- Quadir MA, Radowski MR, Kratz F, Licha K, Hauff P, Haag R (2008) Dendritic multishell architectures for drug and dye transport. *J Control Release* 132(3):289–294
- Radowski MR, Shukla A, von Berlepsch H, Böttcher C, Pickaert G, Rehage H et al (2007) Supramolecular aggregates of dendritic multishell architectures as universal nanocarriers. *Angew Chem Int Ed Engl* 46(8):1265–1269
- Schäfer-Korting M, Mehnert W, Korting HC (2007) Lipid nanoparticles for improved topical application of drugs for skin diseases. *Adv Drug Deliv Rev* 59(6):427–443
- Schätzlein A, Cevc G (1998) Non-uniform cellular packing of the stratum corneum and permeability barrier function of intact skin: a high-resolution confocal laser scanning microscopy study using highly deformable vesicles (Transfersomes). *Br J Dermatol* 138(4):583–592
- Smirnov AI, Smirnova TI, Morse PD 2nd (1995) Very high frequency electron paramagnetic resonance of 2,2,6,6-tetramethyl-1-piperidinyloxy in 1,2-dipalmitoyl-sn-glycero-3-phosphatidylcholine liposomes: partitioning and molecular dynamics. *Biophys J* 68(6):2350–2360
- Souto EB, Wissing SA, Barbosa CM, Müller RH (2004) Development of a controlled release formulation based on SLN and NLC for topical clotrimazole delivery. *Int J Pharm* 278(1):71–77
- Stecova J, Mehnert W, Blaschke T, Kleuser B, Sivaramakrishnan R, Zouboulis CC et al (2007) Cyproterone acetate loading to lipid nanoparticles for topical acne treatment: particle characterisation and skin uptake. *Pharm Res* 24(5):991–1000
- Stoll S, Schweiger A (2006) EasySpin, a comprehensive software package for spectral simulation and analysis in EPR. *J Magn Reson* 178(1):42–55
- Treiber C, Quadir MA, Voigt P, Radowski M, Xu S, Munter LM et al (2009) Cellular copper import by nanocarrier systems, intracellular availability, and effects on amyloid beta peptide secretion. *Biochemistry (Mosc)* 48(20):4273–4284
- van den Bergh BA, Bouwstra JA, Junginger HE, Wertz PW (1999) Elasticity of vesicles affects hairless mouse skin structure and permeability. *J Control Release* 62(3):367–379
- Velan SS, Spencer RG, Zweier JL, Kuppusamy P (2000) Electron paramagnetic resonance oxygen mapping (EPROM): direct visualization of oxygen concentration in tissue. *Magn Reson Med* 43(6):804–809
- Yucel U, Elias RJ, Coupland JN (2012) Solute distribution and stability in emulsion-based delivery systems: an EPR study. *J Colloid Interface Sci* 377(1):105–113

# Confocal Raman Spectroscopy as a Tool to Investigate the Action of Penetration Enhancers Inside the Skin

# 13

Stéphanie Briançon, Marie-Alexandrine Bolzinger,  
and Yves Chevalier

## Contents

13.1	<b>Introduction</b> .....	229
13.2	<b>Confocal Raman Microscopy for Cutaneous Absorption Experiments</b> .....	230
13.3	<b>Confocal Raman Microscopy for Studying the Mechanism of Action of Penetration Enhancers</b> .....	234
13.3.1	Water as Penetration Enhancer .....	234
13.3.2	DMSO as a Penetration Enhancer .....	236
13.3.3	Iminosulfuranes as Penetration Enhancers .....	238
13.4	<b>Penetration Enhancement of Drugs Followed by Confocal Raman Microscopy</b> .....	238
13.4.1	Penetration Enhancement of Trans- retinol Followed by Confocal Raman Microscopy .....	238
13.4.2	Penetration Enhancement of Various Drugs Followed by Confocal Raman Microscopy .....	242
	<b>Conclusion</b> .....	243
	<b>References</b> .....	244

## 13.1 Introduction

Penetration enhancers have been recognized since a long time to improve the delivery of poorly penetrating drugs inside the deep skin layers, and finally into the systemic circulation (Walker and Smith 1996; Williams and Barry 2004). Many drugs are either too hydrophilic or too hydrophobic to cross the primary skin barrier of *stratum corneum* (SC) and reach the viable skin layers or the systemic circulation in case of transdermal drug delivery. The outermost skin layer, the SC consists of corneocytes embedded in a lipid matrix. The intercellular lipids are mainly cholesterol, ceramides, and free fatty acids organized into multilamellar stacks of bilayers. The state of intercellular lipids strongly influences the skin permeability of drugs that diffuse through the intercellular pathway. Hence, the lipid organization in SC is of primary importance for the control of drug delivery to skin. Various skin penetration enhancers have been used since a long time to decrease the barrier resistance to drug diffusion. They include dimethylsulfoxide (DMSO), *N,N*-diethyl-*m*-toluamide, *N*-methyl-2-pyrrolidone, laurocapram (Azone® or 1-dodecylazacycloheptan-2-one), oleic acid, terpenes, and various surfactants (Montes and Day 1967; Chandrasekharan et al. 1977; Windheuser et al. 1982; Stoughton and McClure 1983; Francoeur et al. 1990; Williams and Barry 2004; Benson 2005; Aqil et al. 2007; Kaushik

S. Briançon (✉) • M.-A. Bolzinger • Y. Chevalier  
University of Lyon, Laboratoire d'Automatique et de  
Génie des Procédés (LAGEP), CNRS UMR 5007,  
Université Claude Bernard Lyon 1,  
43 bd 11 Novembre, 69622 Villeurbanne, France  
e-mail: [stephanie.briancon@univ-lyon1.fr](mailto:stephanie.briancon@univ-lyon1.fr);  
[marie.bolzinger@univ-lyon1.fr](mailto:marie.bolzinger@univ-lyon1.fr);  
[yves.chevalier@univ-lyon1.fr](mailto:yves.chevalier@univ-lyon1.fr)

et al. 2008). The exact mechanisms by which enhancers promote or delay drug diffusion through the skin are not fully understood, and even the different penetration paths of transdermal permeation are still under debate. One presumed mechanism is related to the disordering or fluidizing the SC structure upon mixing the penetration enhancers with the intercellular lipids (Benson 2005). However, the molecular organization of the SC lipids is still not firmly established. Three main structures have been disclosed: (i) the orthorhombic phase, a dense organization with crystalline hydrocarbon chains that are not equally distributed in the lattice, resulting in two different distances between lattice planes (0.37 nm and 0.41 nm); (ii) the hexagonal phase with equally spaced crystallized hydrocarbon chains; and (iii) finally the fluid lamellar phase where the lipids are in a fluid (molten) state. The current view of the lipid organization in the SC at 32 °C is the orthorhombic structure coexisting with the hexagonal packing (Pilgram et al. 1999; Norlén 2001; Babita et al. 2006; Bouwstra and Ponc 2006; Bouwstra et al. 2007). An open question with respect to lateral packing of lipids (Norlén 2001) is whether the lipid matrix is made of a single gel “phase” or several coexisting fluid and solid (crystalline and/or gel phases). Another question which has recently been addressed is whether the barrier efficiency of SC is related to the extent of the orthorhombic and lamellar structures (Boncheva et al. 2008; Damien and Boncheva 2010; Groen et al. 2011).

New insights into the mechanisms of action of penetration enhancers have been gained by implementation of noninvasive physicochemical techniques into skin absorption experiments. Among them, confocal Raman microspectroscopy (CRM) is becoming a major technique because of its nondestructive character, and the possibility of monitoring the penetration of the drug and/or penetration enhancer provided that characteristic Raman bands can be associated with the compounds (Förster et al. 2011a). The spectroscopic method allows obtaining at the

same time structural information on the conformation changes of the molecules in the skin induced by the absorption of a drug, a penetration enhancer, or any physical parameter like temperature. The Raman spectrometer is associated with a confocal microscope, providing three-dimensional spectroscopic information with the spatial resolution of an optical microscope.

In this chapter, we report on absorption measurements of drugs and penetration enhancers inside skin using this vibrational spectroscopic technique, and then on the structural modifications induced by such compounds as measured by CRM. After a brief description of the technique, the second part gives detailed examples of applications to dermatological research.

---

### 13.2 Confocal Raman Microscopy for Cutaneous Absorption Experiments

CRM is based on the combined use of spectroscopic analysis and structural observation by optical microscopy. The characteristic features of this technique are the chemical analysis by spectroscopy and the three-dimensional mapping of the sample by microscopy. CRM brings about new possibilities and definite benefits over the classical methods for assessing skin absorption.

The several classical methods for assessing skin penetration of drugs (or any other kind of molecule) from a formulation containing them rely on *in vitro* measurements of passive diffusion of drugs through excised skin (Bronaugh and Maibach 1999) in Franz cells. The diffusion of drugs through excised skin from a donor compartment containing the formulation to a receptor compartment containing a receiver fluid is measured. The permeation profile is a plot of the cumulated amount of drug that reached the receptor fluid as function of duration of exposure to the formulation. The distribution of drug molecules inside the skin layers is more difficult to measure. In a classical Franz cell experiment, the cell is

dismantled at the end of the experiment, the skin layers are separated, and an analysis of the drug is performed. This method is open to several drawbacks since all manipulations (separation of skin layers, solvent-based extraction of drug) may cause strong bias of the drug concentration. Such a method gives the distribution of drug in the vertical direction ( $z$ -direction). Information pertaining to the spatial distribution in the horizontal direction ( $x,y$  plane) and the possible modification of the skin structure induced by absorption of compounds are missing. The usual method to obtain depth-dependent profiles of the drug content is the so-called tape-stripping method; it is restricted to analysis in the SC. Chemical or spectroscopic analysis along histological sections of skin provide the distribution along the depth and one lateral direction. All these methods (tape-stripping, histological sectioning) are destructive and involve hard manipulations of the skin samples that cause several artifacts (Touitou et al. 1998). Moreover, time-resolved experiments (i.e., study of dynamic processes) are not possible and information on the possible perturbations of the structure of endogenous skin components is lacking, except if it is measured by attenuated total reflectance-infrared (ATR-IR) spectroscopy before tape-stripping (Francoeur et al. 1990; Naik et al. 1995; Zhang et al. 2007a).

CRM overcomes the limitations reported above because it is not destructive. Time-resolved 3D pictures of the distribution inside skin are collected. CRM measures vibration frequencies of chemical bonds and parts of molecules. It allows distinguishing chemical species through their characteristic vibrations and provides fingerprints for the identification of substances without requiring any labeling or dyeing.

Measurement of drug penetration *in vivo* is a much more difficult task. Adaptation of the classical *in vitro* techniques to *in vivo* measurements faces major limitations (Herkenne et al. 2008). The CRM could be adapted for allowing *in vivo* measurements with good accuracy.

Raman spectroscopy is closely related to infrared (IR) spectroscopy since in both techniques the frequencies of molecular vibrations are measured. However Raman spectroscopy is sensitive to polarizable chemical bonds, whatever their polarity, while IR absorption takes place for polar bonds for which the molecular vibration changes the dipole moment. Therefore, the spectroscopic selection rules are different for both techniques. Symmetric molecules have Raman spectra, but not many IR bands. Most molecules present in the skin have both absorption bands in Raman and IR spectroscopy, but the intensities of their bands are different.

IR spectroscopy is a classical absorption technique where the absorbance or the attenuated reflectance of the sample is measured. IR and Raman spectroscopy both measure the vibrational energy of molecules, but the interaction between the incident radiation and the compound differs. IR requires a change in the dipole moment of the molecule, whereas Raman relies on a change in the polarizability of the molecule. Raman spectroscopy measures inelastic light scattering by the sample. This makes an important difference between Raman and IR spectroscopy (Caspers et al. 2001). When using Raman spectroscopy, the sample is irradiated with an intense beam of monochromatic light from a laser; a very small part of the light ( $\sim 1$  photon out of  $10^8$ ) undergoes inelastic scattering from molecular vibrations, resulting in Stokes and anti-Stokes scattered light at frequencies different from the incident radiation. The frequency shifts correspond to the frequencies of the molecular vibrations; they are expressed as wave numbers ( $\text{cm}^{-1}$ ) as in IR spectroscopy.

The identification of peaks in the resulting spectra can be complex. There are many lists of Raman frequencies and assignments in the literature (Barry et al. 1992; Anigbogu et al. 1995; Förster et al. 2011a; Tfayli et al. 2012a). The Raman frequency assignments of the major vibrational modes for the SC of mammalian skin are given in Table 13.1.

**Table 13.1** Raman assignments of the major vibrational modes for *stratum corneum*

Raman frequency (cm <sup>-1</sup> )	Assignment
526	$\nu(\text{S-S})$
600	$\rho(\text{C-H})$
623	$\nu(\text{C}=\text{S})$
644	$\nu(\text{C}=\text{S})$ ; amide IV
746	$\rho(\text{CH}_2)$ in phase
827	$\delta(\text{CCH})$ aliphatic
850	$\delta(\text{CCH})$ aromatic
883	$\rho(\text{CH}_2)$ ; $\nu(\text{C-C})$ ; $\nu(\text{C-N})$
931	$\rho(\text{CH}_3)$ terminal; $\nu(\text{C-C})$ of proteins $\alpha$ -helix
956	$\rho(\text{CH}_3)$ ; $\delta(\text{CCH})$ alkenic
1002	$\nu(\text{C-C})$ aromatic ring
1031	$\nu(\text{C-C})$ skeletal <i>cis</i> conformation
1062	$\nu(\text{C-C})$ skeletal <i>trans</i> conformation
1082	$\nu(\text{C-C})$ skeletal random conformation
1126	$\nu(\text{C-C})$ skeletal <i>trans</i> conformation
1155	$\nu(\text{C-C})$ ; $\delta(\text{COH})$
1172	$\nu(\text{C-C})$
1244	$\delta(\text{CH}_2)$ wagging; $\nu(\text{C-N})$ amide III disordered
1274	$\nu(\text{C-N})$ ; $\delta(\text{NH})$ amide III of proteins $\alpha$ -helix
1296	$\delta(\text{CH}_2)$
1336	Not assigned
1385	$\delta(\text{CH}_3)$ symmetric
1421	$\delta(\text{CH}_3)$
1438	$\delta(\text{CH}_2)$ scissoring
1552	$\delta(\text{NH})$ ; $\nu(\text{C-N})$ amide II
1585	$\nu(\text{C}=\text{C})$ alkenic
1602	not assigned
1652	$\nu(\text{C}=\text{O})$ amide I of proteins $\alpha$ -helix
1743	$\nu(\text{C}=\text{O})$ amide I of lipids
1768	$\nu(\text{COO})$
2723	$\nu(\text{C-H})$ aliphatic
2852	$\nu(\text{C-H in CH}_2)$ symmetric
2883	$\nu(\text{C-H in CH}_2)$ asymmetric
2931	$\nu(\text{C-H in CH}_3)$ symmetric
2958	$\nu(\text{C-H in CH}_3)$ asymmetric
3060	$\nu(\text{C-H})$ alkenic
3280	$\nu(\text{O-H})$ of H <sub>2</sub> O

From Förster et al. (2011a), with permission  
 $\delta$  deformation,  $\nu$  stretch,  $\rho$  rock

The strong absorbance of water limits the application of IR spectroscopy to tissues containing water. Only thin samples can be analyzed in transmission mode, and small penetration depths are available in attenuated reflection mode. On the contrary, Raman absorbance of water is weak, and the frequency of the light can be chosen independently of the frequency range of the spectroscopic analysis. This is a definite advantage of a method relying on a scattering phenomenon. Therefore, the wavelength of the incident laser light for Raman analysis is selected such that the sample is transparent and there is no fluorescence that would disturb the analysis. In the modern equipment, several laser wavelengths are available (from green light to infrared) as excitation light to match the various sample properties. The depth of penetration in the sample can reach several 10  $\mu\text{m}$ . Since visible light is used, a confocal optical microscope is associated for collecting 3D maps of Raman spectra with the spatial resolution of optical microscopy (0.2–0.5  $\mu\text{m}$  in  $x,y$  plane; 0.5–1  $\mu\text{m}$  in  $z$ -axis).

A definite advantage of CRM is its ability to provide spatially resolved concentration and molecular structure information about skin components (protein conformation, lipid organization) while keeping the sample intact. Analyses are possible in skin up to 100  $\mu\text{m}$  depth. Measurements can be made in vitro on excised skin samples as well as in vivo.

The intensities of Raman bands are proportional to the concentration of species, so that quantitative analyses can be done (Tfayli et al. 2012a). A close selection of appropriate conditions is achieved to study the skin, especially the excitation wavelength of the laser source (Tfayli et al. 2012b). Various excitation wavelengths in the visible or near-IR (from 532 nm to 1064 nm) are available as commercial sources; they are safe regarding in vivo measurements. Wavelengths of 532, 633, and 785 nm were widely used to record Raman spectra inside the skin. This parameter affects the scattered Raman intensity, possible fluorescence background, and signal attenuation along skin depth (Tfayli

et al. 2012b). The actual  $z$ -depth in the sample is different than the optical path length because of the different refractive indices of the skin layers. A correction factor of 20% is often applied to calculate the actual depth. The correction actually depends on the  $z$ -value; it is larger at deep locus of analysis (Xiao et al. 2004; Tfayli et al. 2008).

The conformational disorder of SC lipids was extensively studied using IR spectroscopy. Utilization of classical Raman spectroscopy may suffer a lack of sensitivity in the spectral regions of interest for lipid analysis. Different Raman spectral manifestations of conformational order of lipids can be drawn from experiments performed on thin films of lipids, such as in recent works in vitro on ceramide films prepared from seven classes and subclasses of ceramides (Tfayli et al. 2010, 2012c). For example, information on intra-chain conformational order is obtained from the bands of C-C skeletal optical mode and the band of the twisting mode of CH<sub>2</sub> groups, whereas the CH<sub>2</sub> scissoring and stretching modes reflect the lateral packing of the lipid molecules, and the amide I band is used to evaluate the strength of H-bonds (Tfayli et al. 2012c). In vivo determination of lipids' ordering by Raman spectroscopy is much more difficult (Tfayli et al. 2012d).

There are several variants of classical Raman spectroscopy besides the spontaneous Raman scattering technique where the spectrum acquisition is a direct measurement of the scattered light. Surface-enhanced Raman scattering (SERS) shows enhanced intensity for molecules located in the vicinity of metal particles. The sensitivity improvement requires the deposition of metal nanoparticles at the surface of the sample. SERS allows a specific analysis of the species present at the sample surface. Resonance Raman spectroscopy provides a selective spectrum of a molecule with high sensitivity when the frequency of the laser light (of the Raman spectrometer) is tuned to a UV-VIS absorption band of the molecule. Coherent Raman spectroscopy (Min et al. 2011) relies on nonlinear effects of two-photon absorption. A resonance occurs when the fre-

quency difference between the two lights matches the frequency of the molecular vibration. A signal-to-noise ratio enhancement by several orders of magnitude is achieved when the resonance condition is met. However, such resonance methods are not spectroscopic methods because a single Raman frequency is measured at once. Coherent anti-Stokes Raman scattering (CARS) (Evans and Xie 2008) and stimulated Raman scattering (SRS) (Downes and Elfick 2010; Slipchenko et al. 2010) are the two major techniques. Several improvements of these techniques were recently introduced in order to increase the sensitivity and decrease the nonresonant background by epidection (Li et al. 2005); high speed confocal microscopy data can be collected (Saar et al. 2010). Equipment for two-color microscopy has been designed (Lu et al. 2012). SRS appears more sensitive and accurate than CARS (Nandakumar et al. 2009; Freudiger et al. 2008). Such techniques allow time-resolved confocal microscopy measurements with high sensitivity at the selected vibration frequencies of the penetrant molecules. Determination of band shifts that are characteristic of interactions of penetrant molecules and skin components requires several measurements at different specific frequency and merging of all in a full spectrum. A recent SRS technique making use of modulation of excitation Raman frequencies and signal demodulation by Fourier transform allows acquisition of several Raman bands at the same time, and possibly parts of Raman spectra (Fu et al. 2012). SRS has been used for investigating the skin absorption of *trans*-retinol, DMSO, and propylene glycol (Freudiger et al. 2008; Saar et al. 2010, 2011).

The determination of the thickness of *stratum corneum* by CRM analysis of the water absorption band is shown as an illustration of the power of CRM. Figure 13.1 shows a typical series of Raman spectra measured at 6 depths inside an excised pig skin sample. The Raman spectra were collected at different depths from 0  $\mu\text{m}$  to 20  $\mu\text{m}$ , as indicated in the picture of the

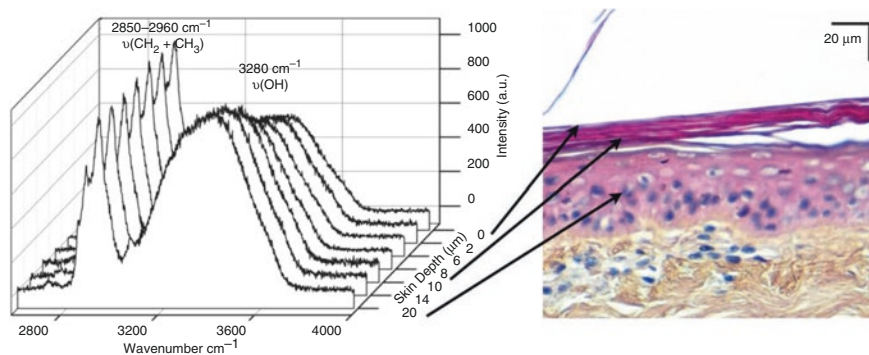


**Fig. 13.1** In depth Raman profiles of untreated pig skin between 2800 and 4000  $\text{cm}^{-1}$ . At the right side, the histological image of the skin is illustrated with the arrows

indicating skin depths (magnification  $\times 40$ ) (From Förster et al. (2011a), with permission)

histological section of skin (right side of Fig. 13.1). The intensity of the stretching band of O-H bond of water,  $\nu(\text{OH})$  at 3280  $\text{cm}^{-1}$ , increases upon going deeper from the skin surface (left side of Fig. 13.1). A sharp increase of the Raman band occurs when passing from the SC to the viable epidermis because the viable epidermis contains much more water ( $\sim 70\%$ ) than SC (an average value is 13%). The thickness of the SC can be easily measured by CRM in this way. However, quantitative analysis is not a straightforward reading of the spectra. Conversion of the Raman intensity into water concentration requires a calibration which has often been made using the  $\text{CH}_3$  band at 2935  $\text{cm}^{-1}$  as a reference (Caspers et al. 2000).

### 13.3 Confocal Raman Microscopy for Studying the Mechanism of Action of Penetration Enhancers

The role of penetration enhancers to increase or modify the permeability of drugs through the skin has been thoroughly studied (William and Barry 2004; Benson 2005). However, fewer studies have been reported on the use of CRM for studying the mechanism by which penetration enhancers improve the penetration of different compounds. It is commonly accepted that penetration enhancers are able to alter the barrier properties of the SC by disrupting temporarily its

structure. Several mechanisms have been proposed to explain their effect: lipid fluidization, lipid extraction, interaction with keratin, and pore formation (Benson 2005).

#### 13.3.1 Water as Penetration Enhancer

Many chemicals show skin penetration enhancing properties. Well-known examples are Azone<sup>®</sup>, dimethylsulfoxide, alcohols, fatty acids such as oleic acid, surfactants, solvents, and terpenes. However, the first major penetration enhancer is water. The permeability of skin for hydrophilic molecules increases dramatically as skin is hydrated. Hydration by occlusion or exposition to high humidity level results in an increase of the SC water content from 13% (standard value) to near 400% of the dry tissue weight (Williams and Barry 2004). In the SC, the water can be bound to structural elements (natural moisturizing factor (NMF), functional groups) or free. The free water acts as a solvent for hydrophilic molecules in the SC, thus increasing the solubility of drugs in the tissue. Drug partition between the formulation and the SC is then modified, and the increase of solubility leads to higher transdermal fluxes of hydrophilic substances in hydrated skin. It is not clearly established whether water can enhance the skin penetration of lipophilic drugs. It has been proposed that swelling of the polar head



group regions of the lipid bilayers by water could disrupt the lipid domains and cause higher permeability for lipophilic permeants such as steroids. However, several researchers have shown that water does not cause modification of the lipid bilayer packing (Bouwstra et al. 1991; Gay et al. 1994; Bouwstra et al. 1996; Bouwstra et al. 2003). van Hal et al. (1996) incubated human skin explants with a saline phosphate buffered solution for 24 h under occlusive or nonocclusive conditions. They proved that water penetrated in the corneocytes inducing their swelling, but also between the cells in the intercellular lipids region, mainly located in separated water pools. The images revealed these water pools and some vesicle-like structures occasionally found. However, the majority of the lipid bilayers exhibited a smooth fracture plane and no change in appearance. The amount of water in these smooth regions was low, and swelling of lamellae or lateral swelling of lipids was not observed.

Transepidermal water loss (TEWL) and electrical impedance (corneometry) measurements are two standard methods used *in vivo* to get information about the skin barrier integrity and the skin hydration level. Both methods are noninvasive and they can be considered as indirect measurements of the skin water content. CRM enables to monitor the water content in the tissue at various depths, enabling the water concentration profiles through the skin depth to be drawn (Caspers et al. 2000). The water content in the tissue can be determined from the ratio of Raman intensities of the OH stretch vibration of water at  $3390\text{ cm}^{-1}$  and the  $\text{CH}_3$  stretch of protein at  $2935\text{ cm}^{-1}$ . To improve the signal-to-noise ratio, intensities were integrated from two bands ( $I_{\text{OH}}$ :  $3350\text{--}3550\text{ cm}^{-1}$  and  $I_{\text{CH}}$ :  $2910\text{--}2965\text{ cm}^{-1}$ ). Caspers et al. (2000, 2001) proposed a quantification method to determine absolute water content by calibration of the ratio of the abovementioned areas using spectra of concentrated aqueous solutions of proteins. The profiles of water content can also be used to estimate the SC thickness, as it is well known that the water content increases sharply at the separation surface between SC and viable epidermis from about

13% in the SC to 60–70% in the viable epidermis. Several analysis methods used to determine the water depth profiles were proposed to determine the boundary between SC and viable epidermis (Caspers et al. 2000, 2003; van der Pol et al. 2007; Crowther et al. 2008; Egawa and Kajikawa 2009; Darlenski et al. 2009; Hancewicz et al. 2012). The values of water content in SC reported by various authors are rather scattered, which is mainly due to the intrinsic variability of different types of skin samples (Hancewicz et al. 2012), variation with respect to body site (Egawa et al. 2007), whether the skin is dry or freshly hydrated (Egawa and Kajikawa 2009; Hancewicz et al. 2012), and also may come from different CRM data treatments. Raman microspectroscopy data correlated with values obtained from other methods such as Karl Fisher analysis (Wu and Polefka 2008) or optical coherence microscopy for evaluating SC thickness (Crowther et al. 2008). Based on the same methodology, NMF content and depth profiles of NMF can also be determined. CRM is a useful tool for the measurements of skin hydration levels, moisturizing product efficacy, and the influence of skin hydration on drug penetration enhancement. Egawa and Kajikawa (2009) addressed by using CRM the effect of skin hydration by measuring water profile after applying water or steam on the forearm of volunteers. The incubation time of the skin with water and the water temperature were varied to study the influence of these parameters on water profile changes. Water content in the SC increased with increasing the duration of water application from 1 to 10 min. Heating the applied water from 22 to 32 °C also resulted in an increase of the penetration depth, penetrated amount, and holding time of water. Furthermore, application water-steam increased the water content in the upper part of the SC. However, this study revealed an increase of the water content by comparing the water profile before and after water application, but it was not possible to differentiate the endogenous water from that penetrated in the skin. Direct measurement of water penetration in the skin by CRM requires replacing water of natural isotopic abundance by deuterated water  $\text{D}_2\text{O}$ , which shows a Raman peak corresponding to the

O-D stretching vibration at  $2500\text{ cm}^{-1}$ , different from endogenous water and clearly distinguishable in the spectra (Förster et al. 2011b). By applying emulsions and surfactant solutions made with deuterated water, Förster et al. showed that water penetrated from the formulations into the SC with a profile similar to that of endogenous water. However, no significant differences were observed between  $\text{D}_2\text{O}$  ingress from all formulations, and no correlations could be found between water penetration and the penetration of *trans*-retinol present in the formulations.

Penetration of deuterated water in the SC after application of pure  $\text{D}_2\text{O}$  on skin sample under occlusive conditions was recently confirmed by Ashtikara (2013).

### 13.3.2 DMSO as a Penetration Enhancer

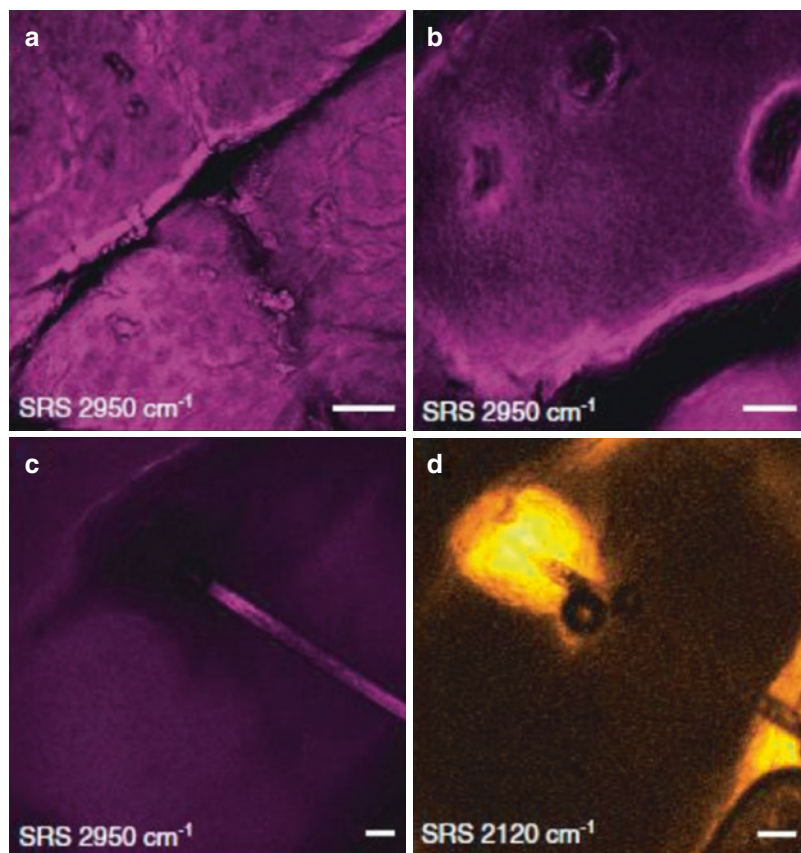
Several studies aimed at explaining the penetration enhancement mechanism of dimethylsulfoxide (DMSO), one of the most common penetration enhancers. DMSO enhances the penetration of both hydrophilic and lipophilic drugs; its action in the skin is complex and remains largely an open question. Upon interaction with keratin, DMSO changes the keratin conformation, from  $\alpha$ -helical to a  $\beta$ -sheet structure. DMSO can also interact with the polar head-groups of intercellular lipids, resulting in a perturbation of their packing. Finally, DMSO can alter the drug partition between the formulation and the skin layers due to its good solvent properties for a large number of molecules (Williams and Barry 2004).

Most studies on the behavior of SC lipids in skin have been carried out using IR spectroscopy. The poor signal-to-noise ratio in Raman spectroscopy has often limited its use for precise mechanistic investigation inside skin. Experiments using thin films of SC lipids allow devising what could be expected from measurements of skin. Tfayli et al. (2012c) studied the modification of the lipids' conformational order, lateral packing, and polar interactions induced by three penetration enhancers. The Raman investigation was carried

out on thin films of ceramides, the main lipid class of SC lipids, differing by their hydrocarbon chain length, polar head group, and the presence of a lateral group (ester or hydroxyl groups). The DMSO penetration enhancer affected mainly the polar interaction between lipid chains and the lateral packing of lipids, and its effect was dependent on the structure of the ceramides. For example, adding DMSO on ceramides IIIb resulted in the increase of the band at  $1633\text{ cm}^{-1}$  indicating weak H-bonds at the expense of the Amide I band at  $1614\text{ cm}^{-1}$  characteristic of strong H-bonds. DMSO also induced a slight change of the peak height ratio of the bands at  $2850\text{ cm}^{-1}$  ( $\nu\text{CH}_2$  sym) and  $2880\text{ cm}^{-1}$  ( $\nu\text{CH}_2$  asym) that reflected a looser lateral packing of all ceramides studied, indicating a decrease of compactness which could be associated with a higher permeability.

Finally, DMSO had a weak influence on the lipid chain conformations. Caspers et al. (2002) recorded the distribution of DMSO in the SC by CRM after application of an 80/20 mixture of DMSO and a 5% aqueous solution of propylene glycol. The mixture presented some characteristic bands, a doublet at  $671$  and  $702\text{ cm}^{-1}$  assigned to the  $\nu(\text{CSC})$  modes and a broad band at  $1030$ – $1048\text{ cm}^{-1}$  assigned to  $\nu(\text{S}=\text{O})$  stretching. After application to the skin of volunteers, there was a shift of these bands, indicating the interaction of DMSO with water and possibly other components of SC. The SC depth profile was calculated as a function of time from the ratio of DMSO/proteins bands ( $\nu(\text{CSC})677\text{ cm}^{-1}/\delta(\text{CH}_2)1450\text{ cm}^{-1}$ ). They showed that most of the applied DMSO permeated through SC within 20 min and reached the viable epidermis where a small fraction was detected. Data collected for a longer time showed evidence of a progressive penetration of DMSO through the SC. DMSO could still be detected inside skin 72 h after application. Other conclusions about DMSO–lipids or DMSO–protein interactions could not be drawn during this study. However, in a study by Zhang et al. (2007b), reversible alteration of keratin secondary structure was shown using CRM when DMSO was applied in keratinocytes culture. They reported an

**Fig. 13.2** SRS skin imaging of the forearm of a volunteer; (a–c): the frequency was tuned to the  $\text{CH}_3$  stretching vibration of proteins at  $2950\text{ cm}^{-1}$ : (a): *stratum corneum*; (b) viable epidermis; (c) hair shaft; (d) SRS skin imaging after applying deuterated  $\text{DMSO-}d_6$  (the frequency was tuned to the specific vibration of  $\text{DMSO-}d_6$   $2120\text{ cm}^{-1}$ ) in the same region as shown in (c)



appearance of  $\beta$ -sheet structures in the cellular keratin after treatment with DMSO; this change was reversible, and the original  $\alpha$ -helix structure was recovered upon rehydration. This result was explained by strong complex formation between DMSO and water, which displaced the bound water that stabilizes the secondary structure of keratin.

Saar et al. (2010) used stimulated Raman scattering (SRS) microscopy for in vivo skin optical imaging in mice, first focusing on 3 vibration bands to image skin structure: lipids ( $\text{CH}_2$  stretching,  $2845\text{ cm}^{-1}$ ), water (OH stretching,  $3250\text{ cm}^{-1}$ ), and proteins ( $\text{CH}_3$  stretching,  $2950\text{ cm}^{-1}$ ). This allowed imaging the water, lipid, and protein distribution of the SC and the viable epidermis (Fig 13.2a, b image of the protein distribution in the SC and viable epidermis). The corneocytes and the intercellular spaces clearly appeared, as well as the sebaceous glands

in the epidermis, which appeared both in lipids and water images, that is, when the incident laser frequency was tuned to the lipids ( $\text{CH}_2$  stretching) or water (OH stretching) vibrations. The sebaceous gland appeared clear when the frequency was tuned to that of lipids vibration and dark when it was tuned to the water vibration. It was possible to image the ear of living mice by SRS frequency-tuned to the protein vibration ( $\text{CH}_3$  stretching) (Fig. 13.2c). SRS was also used by the authors to explore the skin penetration of drugs and excipients (Saar et al. 2010, 2011). They explored DMSO penetration on human skin by SRS imaging using a specific vibration of deuterated  $\text{DMSO-}d_6$  at  $2120\text{ cm}^{-1}$  (2010). As shown in Fig. 13.2d, DMSO was found in the area surrounding the hair follicles, confirming the initial rapid penetration of DMSO into hair follicles. However, DMSO was not found to penetrate the hair itself.

### 13.3.3 Iminosulfuranes as Penetration Enhancers

A novel group of chemical penetration enhancers, iminosulfuranes, was studied by Song et al. (2005) on mouse and human skins. The objective was to design new penetration enhancers having high efficacy and less toxicity and irritation potency. The iminosulfurane enhancers were easily detected in the skin by their specific Raman peak at  $670\text{ cm}^{-1}$ ; its intensity was normalized to that of the amide I vibration band ( $1743\text{ cm}^{-1}$ ). The results showed penetration of the enhancer into the SC to a depth of approximately  $20\text{ }\mu\text{m}$ , the maximum content being found  $5\text{--}10\text{ }\mu\text{m}$  below the skin surface. This new enhancer did not penetrate into the viable epidermis, which meant that it might bind to the protein and/or the lipids in the SC. Furthermore, its penetration enhancing activity was proved both for a lipophilic drug (hydrocortisone) and a hydrophilic one (caffeine). The penetration enhancement of caffeine was lower than that of hydrocortisone (Song et al. 2005).

---

### 13.4 Penetration Enhancement of Drugs Followed by Confocal Raman Microscopy

CRM was used in vivo and in vitro to investigate the penetration enhancement mechanism of several compounds. Both the skin penetration of the drug and the penetration enhancer has been measured, and the CRM spectra of the SC lipids were analyzed in order to get information about lipid ordering. The penetration of several drugs of various chemical structures and physicochemical properties was studied, as far as they possess a specific Raman signature allowing their identification in the skin. Examples of *trans*-retinol, metronidazole, ibuprofen, ketoprofen, and  $\beta$ -carotene are presented below.

#### 13.4.1 Penetration Enhancement of *Trans*-retinol Followed by Confocal Raman Microscopy

*Trans*-retinol was selected as a model hydrophobic drug, because it is widely used as a reference compound for skin absorption experiments. *Trans*-retinol is also a common active substance (vitamin A) for cosmetic products (Failloux et al. 2004; Pudney et al. 2007; Mlot et al. 2009). Various kinds of penetration enhancers were investigated: surfactants, oleic acid, glycol, and ethanol. Raman spectroscopy is an appropriate technique as *trans*-retinol possesses a characteristic peak due to the  $\text{C}=\text{C}$  bond, found at  $1594\text{ cm}^{-1}$  (Mlot et al. 2009) or  $1585\text{ cm}^{-1}$  (Frster et al. 2011a), well-separated from other peaks of major skin components (Fig. 13.3).

Furthermore, *trans*-retinol does not penetrate into the deep layers of skin; hence, it can be easily detected by CRM. Frster et al. (2011b) studied the penetration behavior of *trans*-retinol from two kinds of formulations (o/w emulsion and surfactant solution) by using CRM along a diffusion experiment carried out in classical Franz cells. They used two hydrophilic surfactants, poly(ethylene glycol)-20 monolaurate (PEG20C12) and poly(ethylene glycol)-20 monooleate (PEG20C18:1), and one lipophilic, poly(ethylene glycol)-6 monooleate (PEG6C18:1), and dodecane as oil phase to prepare three solutions of retinol and three o/w emulsions loaded with retinol. Retinol penetration was higher when applying surfactant solutions than the corresponding o/w emulsions. The retinol penetration enhancement was the largest when using the PEG6 monooleate surfactant. Indeed the unsaturated alkyl chain and the small polar head are two surfactant parameters known to cause an increased penetration of drugs (Cappel and Kreuter 1991). CRM also allowed to study the organization of SC lipids by measuring the intensity ratio  $I_{2880}/I_{2850}$  of the Raman bands  $\nu_{\text{asym}}(\text{CH}_2)$  and  $\nu_{\text{sym}}(\text{CH}_2)$

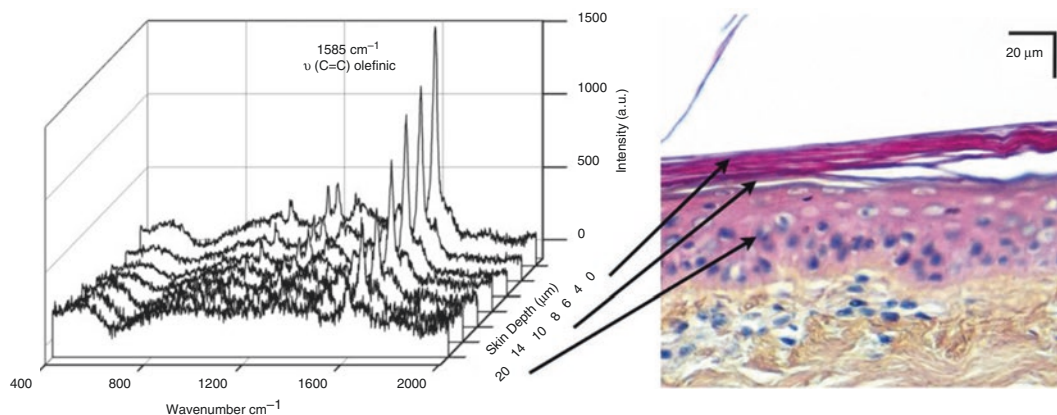


**Fig. 13.3** Raman spectra of pig skin after application of a surfactant solution containing 0.5% *trans*-retinol for 24 h. The Raman profile was measured at the surface (0  $\mu\text{m}$ ), and at 2, 6, 8, 10, 14, and 20  $\mu\text{m}$  skin depth.

Arrows indicate skin depths in the image of histological section (magnification of  $\times 40$ ) (From Förster et al. (2011a), with permission)

reflecting the lateral packing of the lipids. A low  $I_{2880}/I_{2850}$  ratio corresponds to a disorganized lipid bilayer, that is, a fluid medium. Fluidization of lipids was observed when applying surfactant solution, especially PEG6 monooleate in dodecane, pure dodecane also, resulting in a significant decrease of the  $I_{2880}/I_{2850}$  ratio. The strong decrease of the  $I_{2880}/I_{2850}$  ratio by PEG6 monooleate was correlated with the highest penetration of *trans*-retinol into the deeper skin layers (epidermis and dermis). This ratio was not correlated with the total quantity of *trans*-retinol penetrated into the skin (including the SC). CRM analyses of *trans*-retinol absorption were in agreement with skin penetration experiments performed in Franz diffusion cells.

The first *in vivo* study was reported by Mélot et al. (2009) who monitored the effect of two penetration enhancers on the delivery of *trans*-retinol through human skin. Three formulations based on 0.3% *trans*-retinol in caprylic/capric triglyceride (Myritol<sup>®</sup> 318, a nonpenetrating oil) were tested: the first one (used as control) contained no enhancer, the second one contained a lipid fluidizer, oleic acid, the third contained a lipid extractor octoxynol-9

(Triton<sup>®</sup>X100), both enhancers were introduced at 1%. Comparison was done with a very efficient delivery formulation of *trans*-retinol in propylene glycol/ethanol (30/70). Raman spectra provided depth concentration profiles of *trans*-retinol and Myritol<sup>®</sup> on the volar forearm of two male volunteers with the different formulations. Retinol solutions were spread gently on the skin surface, and measurements began 10 min after application. Raman spectra were collected from the skin surface to 30–40  $\mu\text{m}$  below with a step of 2  $\mu\text{m}$  at different locations on both treated and untreated skin area. Measurements were performed each hour up to 6 h after treatment. An improved delivery of *trans*-retinol was obtained when adding penetration enhancers in the formulation; oleic acid was found to be more efficient than Triton<sup>®</sup>X100. In the absence of a penetration enhancer, the Raman signal of *trans*-retinol was mainly confined in the first 5  $\mu\text{m}$  depth. *Trans*-retinol penetrated the skin deeper in the presence of both penetration enhancers. Oleic acid allowed the penetration to the same depth as the propylene glycol/ethanol formulation; however, the amount of *trans*-retinol penetrated into the skin was tenfold higher from the propylene glycol/ethanol system. Oleic acid

caused a phase separation in SC lipids because it is not miscible with the SC lipids. The phase separation was proved by spectroscopic studies (Ongpipattanakul et al. 1991; Naik et al. 1995) and by two-photon fluorescence microscopy showing quite large patches containing oleic acid within the SC (Yu et al. 2003). Such liquid-like inclusions are supplementary penetration pathways through the SC lipids that may be the origin of enhanced penetration of *trans*-retinol. Triton®X100 is a surfactant which can be incorporated in the lipid membrane, leading to a lipid solubilization (or extraction). When the surfactant concentration exceeds the CMC, lipid-surfactant mixed micelles form, so that lipids are extracted off the skin. The selective extraction of lipids causes a modification of the composition of the lipids remaining in the skin and an alteration of their organization in the SC results. However, this mechanism is less efficient to promote the penetration of *trans*-retinol than the phase separation caused by the penetration of oleic acid. Mélot et al. (2009) also showed that penetration enhancers are able to promote the penetration of oil (Myritol® 318) which was detected at 10  $\mu\text{m}$  depth, whereas it all remained at the skin surface when no penetration enhancers were used.

These results were recently complemented by an *in vivo* spatially resolved NMR also named magnetic resonance imaging (MRI) measurement of the penetration of skin moisturizers and the effect of penetration enhancers (Ciampi et al. 2011). The NMR relaxation parameters  $T_1$ ,  $T_2$  and the self-diffusivity  $D$  were measured at 3 h, 5 h15, and 6 h40 after application of same formulations of *trans*-retinol in Myritol® 318 containing 1% oleic acid or Triton®X100. After exposure to penetration enhancers solutions, both  $T_2$  and  $D$  decreased compared to untreated skin and to skin treated with neat Myritol® 318 showing the skin penetration of Myritol® 318 induced by oleic acid and Triton®X100. After a period of 5 h with Triton®X100 and 7 h with oleic acid,  $T_2$  and  $D$  recover their initial (preapplication) values. A moisturization of the skin by an internal occlusive mechanism was proposed as the origin of such changes in the skin properties. This was

attributed to the penetration of Myritol® 318 which interacted with the SC lipids and formed an internal barrier to water loss by an occlusion mechanism. This hypothesis was confirmed by electrical impedance measurements showing an increased water uptake in the outer SC. The effect of oleic acid in the skin lasted for a longer time than that of Triton®X100 (7 h vs. 5 h). The effect of oleic acid was explained by the interaction with the SC lipids and the formation of oleic acid-rich domains by phase separation, enhancing the Myritol® 318 penetration for a longer time compared to that induced by the surfactant that extracts the SC lipids temporarily.

Boncheva et al. (2008) used IR spectroscopy to evaluate the intercellular lipid conformation in the SC and the effect of the penetration of the penetration enhancer oleic acid and propylene glycol. The lateral packing of lipids is related to the density of the lipids within the lipid lamellae, and therefore to their barrier properties preventing skin penetration. Lipids in human SC are organized as an orthorhombic lateral packing, which is a very dense structure. The coexistence of the orthorhombic structure with a liquid phase is still under debate (Bolzinger et al. 2012). Boncheva et al. (2008) developed a method to evaluate the chain conformation and the lateral chain packing from IR spectra collected in the attenuated reflectance mode (ATR). The position and the bandwidth of the  $\text{CH}_2$  symmetric stretching band ( $2850\text{ cm}^{-1}$ ) and of the splitting of the  $\text{CH}_2$  rocking ( $\sim 720\text{ cm}^{-1}$ ) and scissoring modes ( $\sim 1468\text{ cm}^{-1}$ ) into two separate bands are indeed sensitive to the lateral packing of the hydrocarbon chains. After incubation of the skin with oleic acid, a shift of the  $\text{CH}_2$  symmetric stretching peak was observed together with the appearance of a shoulder at  $2858\text{ cm}^{-1}$  (Fig. 13.4e), indicating a minor conformational disordering of a fraction of the SC lipid chains and the formation of a new, disordered phase. Moreover, the scissoring mode of the treated samples contained the two components characteristic for orthorhombic phase centered around  $1473$  and  $1464\text{ cm}^{-1}$ , together with the component characteristic for hexagonal or liquid phase centered at  $1468\text{ cm}^{-1}$ . The treatment with oleic acid led to

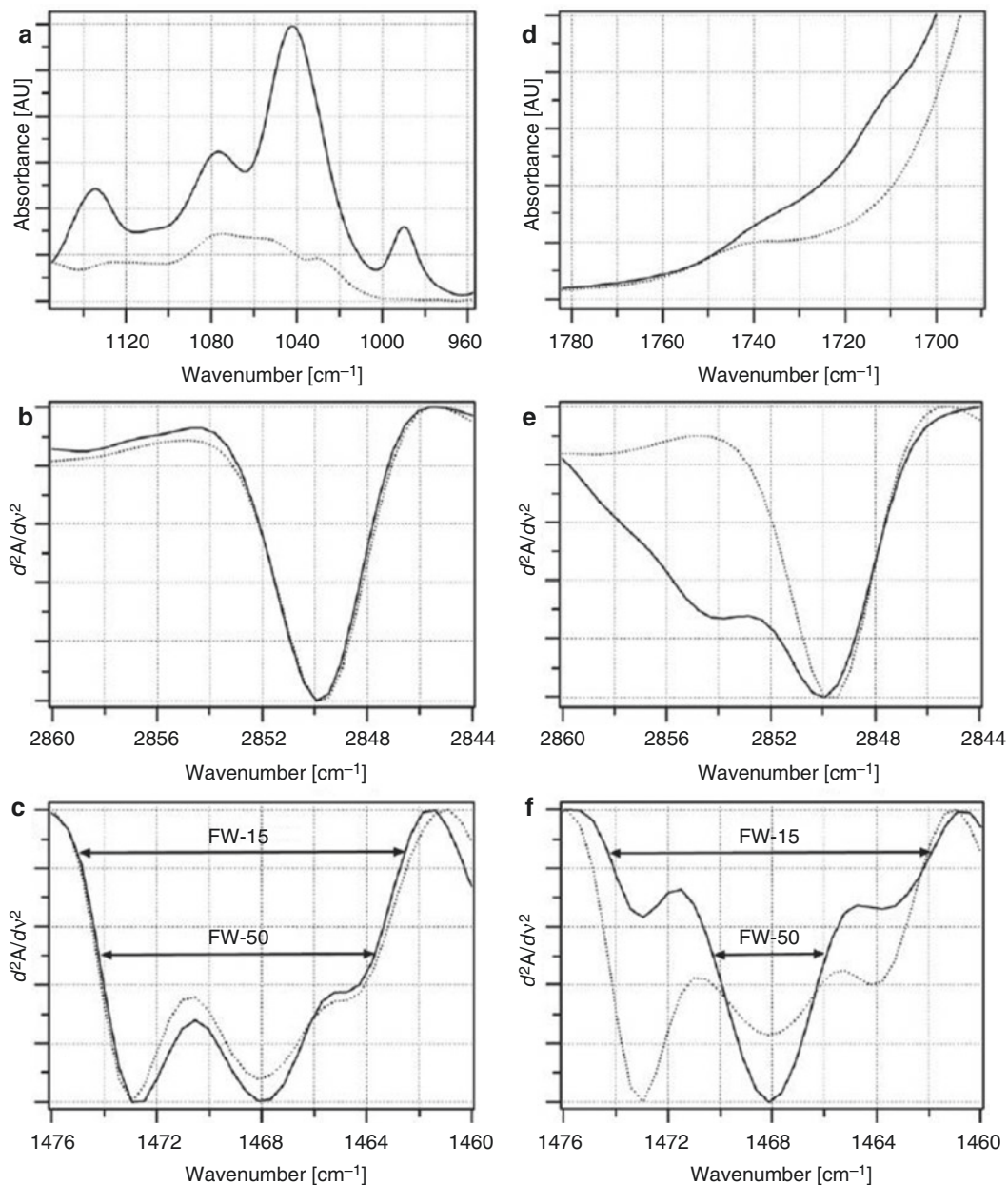


**Fig. 13.4** Influence of propylene glycol (a–c) and oleic acid (d–f) on the molecular organization of the lipids in human SC. Absorbance and second-derivative spectra collected at 32 °C from excised human skin after treat-

ment with propylene glycol (a–c) and oleic acid (d–f). Dotted lines were acquired with control skin samples (From Boncheva et al. (2008), with permission)

an increase of the intensity to 1468  $\text{cm}^{-1}$ , showing the formation of a new fluid phase (Fig. 13.4f).

In a previous study, Anigbogu et al. (1995) also showed using Raman spectroscopy that DMSO penetrated the SC and altered both the

keratin conformation from  $\alpha$ -helix to  $\beta$ -sheets and the lipid bilayer from a crystalline phase with alkyl chains of lipid molecules in their all-*trans* conformation (called “gel”) to a liquid crystalline phase where the alkyl chains of lipids undergo

equilibrium between *gauche* and *trans* conformations. After the immersion of the SC obtained from human abdominal skin into aqueous solutions of DMSO or deuterated DMSO-*d6* for 1 h, CRM was performed and spectra showed an alteration of the keratin conformation:  $\alpha$ -helix progressively converted into  $\beta$ -sheets as the concentration of DMSO increased. A plateau was reached at a concentration of DMSO above 60% for which the protein conformation was approximately 50%  $\alpha$ -helix and 50%  $\beta$ -sheets. Lipid bilayer organization was only altered at high DMSO concentrations (70% to 100%). This behavior can be related to the penetration enhancement power of DMSO, which is generally significant when used at concentrations above 60% (Williams and Barry 2004).

Saar et al. (2010) used SRS to follow *trans*-retinol skin penetration by tuning the excitation wavelength to the vibration of *trans*-retinol (C = C stretch at  $1596\text{ cm}^{-1}$ ). Images showed that penetration of *trans*-retinol occurred through the hair shaft. SRS was also used to image human skin *in vivo* up to a depth of  $50\text{ }\mu\text{m}$  showing the localization of *trans*-retinol around the hair and in the top of the sebaceous gland.

#### 13.4.2 Penetration Enhancement of Various Drugs Followed by Confocal Raman Microscopy

Tfayli et al. (2007) studied the penetration of metronidazole, a drug used in the treatment of rosacea, on excised human skin samples. The drug was applied on the skin as a solution in transcutol (diethylene glycol monoethyl, Gattefossé, France), a penetration enhancer. They first determined specific vibrations which can be detected in the skin in the Raman spectrum of metronidazole dissolved in transcutol: two vibration bands were selected at  $1191$  and  $1369\text{ cm}^{-1}$ . Metronidazole was applied at the concentration of  $18\text{ }\mu\text{g}\cdot\text{mL}^{-1}$  in transcutol, and Raman spectra were acquired at several depths in the skin after, respectively, 1 and 2 h diffusion time. Metronidazole was detected down

to  $23\text{--}24\text{ }\mu\text{m}$  in the skin after 1 h diffusion and between  $15$  and  $40\text{ }\mu\text{m}$  after 2 h. These results were confirmed by Raman images obtained on thin slices which were cut in the skin samples at the end of the experiment. Spectral images were reconstructed by integration of the metronidazole vibration ( $1191\text{ cm}^{-1}$ ) intensity. They showed that metronidazole was present in the hair follicles at  $40\text{--}45\text{ }\mu\text{m}$  and at  $25\text{ }\mu\text{m}$  in the SC. Furthermore, the authors used CRM to study the effect of metronidazole-transcutol solution on skin structure. A decrease in the intensity of the  $1084\text{ cm}^{-1}$  peak was observed after applying the metronidazole-transcutol solution, corresponding to a decrease of the lipid chains' organization. This fluidization of the lipid chains in the skin can be related to the drug or the transcutol penetration (Tfayli et al. 2007).

The same team applied their methodology to follow caffeine penetration in human skin samples. Caffeine is widely used in cosmetics as an active substance; it is also one of the most frequently used compounds in transdermal delivery studies. Due to its low  $\log P$ , caffeine highly penetrates through the skin and generates high fluxes (Bolzinger et al. 2008). Raman analysis of caffeine is a challenge due to its rapid penetration and low storage in the SC. Tfayli et al. (2013) applied solutions of caffeine at two concentrations,  $2.57 \times 10^{-1}\text{ mg}\cdot\text{mL}^{-1}$  and  $5.15 \times 10^{-2}\text{ mg}\cdot\text{mL}^{-1}$  on human skin samples. Raman spectra were collected every half hour in the skin samples from the surface to  $50\text{ }\mu\text{m}$  depth by  $6\text{ }\mu\text{m}$  increments. The total duration was 4 h after caffeine solution application. Raman analysis was not possible with the most concentrated solution due to the crystallization of caffeine on the skin surface, caffeine crystals generating high intensity signals which hide the Raman skin signal. The diluted solution allowed to monitor the caffeine in the skin, using two vibration bands at  $555\text{ cm}^{-1}$  ( $\delta\text{ C}=\text{O-N}$ ) and  $1360\text{ cm}^{-1}$  ( $\nu\text{ CN}$ ). The maximum of caffeine signal intensity at  $12\text{ }\mu\text{m}$  under the skin surface was recorded after 2 h35 after exposure. After 4 h, caffeine was no more detected in the skin by Raman analysis. Several causes were proposed by the authors: a too low concentration in the skin due to caffeine diffu-



sion, a heterogeneity of the diffusion which may result in the absence of caffeine in the analyzed volume, and a too low penetration depth (50  $\mu\text{m}$ ) enabled by the Raman analysis.

Saar et al. (2011) used SRS to study the penetration of two nonsteroidal anti-inflammatory drugs, ketoprofen and ibuprofen, applied as solutions in propylene glycol on skin samples. 3D images of the skin during drug penetration and drug concentration profiles in the skin depth were obtained as a function of time. Ketoprofen presents a specific vibration band at 1599  $\text{cm}^{-1}$  corresponding to the aromatic CH bond stretching, whereas no specific bands could be detected for ibuprofen and propylene glycol. These two molecules were used in deuterated form to create a specific vibration band around 2120  $\text{cm}^{-1}$  corresponding to the  $\text{CD}_2$  bond stretching. The incident laser wavelength was tuned either to 1599  $\text{cm}^{-1}$  to observe ketoprofen penetration or to 2120  $\text{cm}^{-1}$  in order to image ibuprofen and propylene glycol in the skin. First ketoprofen in deuterated propylene glycol solution was applied on skin samples. Raman analysis at the skin surface and at 12  $\mu\text{m}$  and 15  $\mu\text{m}$  in the SC revealed the penetration of ketoprofen and propylene glycol, signal intensities increasing with time until 158 min after solution application. Integration of the signals obtained at each position in the skin allowed drawing depth profiles of propylene glycol and ketoprofen concentration at each measurement time. The results showed that propylene glycol penetrates the skin more rapidly and more efficiently than ketoprofen. Furthermore, it was shown that propylene glycol concentration at 15  $\mu\text{m}$  under the skin surface increased continuously with time until reaching its surface value after 120 min. Focusing on a hair shaft area, the authors showed that the propylene glycol concentration was the same throughout the experiment time (158 min), whereas it increased continuously in another area of the SC. This was explained by a rapid penetration of propylene glycol in the hair shaft which was saturated before the first measurement time. Finally, the authors applied a solution of deuterated ibuprofen in “normal” propylene glycol (i.e., nondeuterated). They observed the formation of

ibuprofen crystal at the skin surface before the first measurement, less than 30 min after application. This was explained by a rapid penetration of propylene glycol which increased the ibuprofen concentration at the skin surface above its solubility, leading to its crystallization.

The penetration of  $\beta$ -carotene, a lipophilic molecule dissolved in DMSO, was studied by Ashtikara (2013). Three main bands were used to identify  $\beta$ -carotene in the skin, the C = C bond stretching at 1510 and 1153  $\text{cm}^{-1}$  and the C- $\text{CH}_3$  bond rocking at 1004  $\text{cm}^{-1}$ . Raman analysis showed that  $\beta$ -carotene hardly penetrated the skin; it was essentially found in the first 10  $\mu\text{m}$  of the SC and presented a heterogeneous distribution. This result was quite expected with such a lipophilic molecule which possesses poor skin permeability (Ashkitara 2013). DMSO may have enhanced the penetration of  $\beta$ -carotene, but this was not proved by the authors.

All these studies showed the potential of CRM for imaging the skin with regards to its composition (lipids, proteins, water), for identification and localization of drug and/or excipients such as penetration enhancers in the SC and epidermis in order to improve the knowledge on penetration mechanism.

## Conclusion

CRM is a very promising tool for the investigation of the penetration enhancement mechanisms and the effect of penetration enhancers on the SC structure, lipid chain organization, and protein conformation. However, there are still few studies reporting such investigations. Development of such a technique for evaluation of penetration enhancers requires that Raman microscopy techniques pass from the academic research laboratory to the routine analysis. The current skin absorption method based on extraction and HPLC analysis is well established and described in Organization for Economic and Cooperation Development (OECD) guidelines. In contrast to conventional methods used for the determination of the drug distribution in skin layers, which require separation of various skin layers (tape-stripping) and extraction by solvents, CRM

may bring about a definite improvement because it allows measurement of depth concentration profiles without separation of skin layers. Additionally, CRM gives access to information on skin lipids and proteins that the classical methods do not provide. The methodology has to be further improved for *in vivo* analysis for which there is no standard technique available. Raman techniques are also very promising for academic research because these methods allow for the first time the nondestructive and simultaneous evaluation (in the same experiment) of the skin penetration of several molecules and their effect on the *stratum corneum* lipid organization and interactions with proteins. The penetration of drugs and other ingredients in the skin from a formulation can be measured and their respective contribution to the percutaneous process can be evaluated. The new SRS microscopy allows the investigation of the diffusion pathways in the skin with high sensitivity.

## References

- Anigbogu ANC, Williams AC, Barry BW, Edwards HGM (1995) Fourier transform Raman spectroscopy of interactions between the penetration enhancer dimethyl sulfoxide and human stratum corneum. *Int J Pharm* 125:265–282
- Aqil M, Ahad A, Sultana Y, Ali A (2007) Status of terpenes as skin penetration enhancers. *Drug Discov Today* 12:1061–1067
- Ashtikara M (2013) Matthäus, Schmitt M, Krafft C, Fahr a, Popp J. Non-invasive depth profile imaging of the stratum corneum using confocal Raman microscopy: first insights into the method. *Eur J Pharm Sci* 50:601–608
- Babita K, Kumar V, Rana V, Jain S, Tiwary AK (2006) Thermotropic and spectroscopic behavior of skin: relationship with percutaneous permeation enhancement. *Curr Drug Deliv* 3:95–113
- Barry BW, Edwards H, Williams A (1992) Fourier transform Raman and infrared vibrational study of human skin: assignment of spectral bands. *J Raman Spectrosc* 23:641–645
- Benson HAE (2005) Transdermal drug delivery: penetration enhancement techniques. *Curr Drug Deliv* 2:23–33
- Bolzinger MA, Briançon S, Pelletier J, Fessi H, Chevalier Y (2008) Percutaneous release of caffeine from microemulsion, emulsion and gel dosage forms. *Eur J Pharm Biopharm* 68:446–451
- Bolzinger MA, Briançon S, Pelletier J, Chevalier Y (2012) Penetration of drugs through skin, a complex rate-controlling membrane. *Curr Opin Colloid Interface Sci* 17:156–165
- Boncheva M, Damien F, Normand V (2008) Molecular organization of the lipid matrix in intact *Stratum corneum* using ATR-FTIR spectroscopy. *Biochim Biophys Acta* 1778:1344–1355
- Bouwstra JA, Ponc M (2006) The skin barrier in healthy and diseased state. *Biochim Biophys Acta* 1758:2080–2095
- Bouwstra JA, Gooris GS, van der Spek JA, Bras W (1991) Structural investigations of human stratum corneum by small angle X-ray scattering. *J Invest Dermatol* 97:1005–1012
- Bouwstra JA, Cheng K, Gooris GS, Weerheim A, Ponc M (1996) Phase behavior of isolated skin lipids. *Biochim Biophys Acta* 1300:177–186
- Bouwstra JA, Honeywell-Nguyen PL, Gooris GS, Ponc M (2003) Structure of the skin barrier and its modulation by vesicular formulations. *Prog Lipid Res* 42:1–36
- Bouwstra JA, Gooris GS, Ponc M (2007) Skin lipid organization, composition and barrier function. *IFSCC Magazine* 10:297–307
- Bronaugh RL, Maibach HI (1999) Percutaneous absorption. *Drugs – cosmetics – mechanisms – methodology*, 3rd edn. Marcel Dekker, New York
- Cappel MJ, Kreuter J (1991) Effect of nonionic surfactants on transdermal drug delivery: I. Polysorbates. *Int J Pharm* 69:143–153
- Caspers P, Lucassen G, Bruining H, Puppels G (2000) Automated depth-scanning confocal Raman microspectrometer for rapid *in vivo* determination of water concentration profiles in human skin. *J Raman Spectrosc* 31:813–818
- Caspers PJ, Lucassen GW, Carter EA, Bruining HA, Puppels GJ (2001) *In vivo* confocal Raman microspectroscopy of the skin: noninvasive determination of molecular concentration profiles. *J Invest Dermatol* 116:434–442
- Caspers PJ, Williams AC, Carter EA, Edwards HG, Barry BW, Bruining HA, Puppels GJ (2002) Monitoring the penetration enhancer dimethyl sulfoxide in human stratum corneum *in vivo* by confocal Raman spectroscopy. *Pharm Res* 19:1577–1580
- Caspers PJ, Lucassen GW, Puppels GJ (2003) Combined *in vivo* confocal Raman spectroscopy and confocal microscopy of human skin. *Biophys J* 85:572–580
- Chandrasekharan SK, Campbell PS, Michaels AS (1977) Effect of dimethylsulfoxide on drug permeation through human skin. *AICHE J* 23:810–815
- Ciampi E, van Ginkel M, McDonald PJ, Pitts S, Bonnist EYM, Singleton S, Williamson A-M (2011) Dynamic *in vivo* mapping of model moisturiser ingress into human skin by GARfield MRI. *NMR Biomed* 24:135–144
- Crowther JM, Sieg A, Blenkiron P, Marcott C, Matts PJ, Kaczvinsky JR, Rawlings AV (2008) Measuring the

- effects of topical moisturizers on changes in stratum corneum thickness, water gradients and hydration in vivo. *Br J Dermatol* 159:567–577
- Damien F, Boncheva M (2010) The extent of orthorhombic lipid phases in the stratum corneum determines the barrier efficiency of human skin in vivo. *J Invest Dermatol* 130:611–614
- Darlenski R, Sassning S, Tsankov N, Fluhr JW (2009) Non-invasive in vivo methods for investigation of the skin barrier physical properties. *Eur J Pharm Biopharm* 72:295–303
- Downes A, Elfick A (2010) Raman spectroscopy and related techniques in biomedicine. *Sensors* 10:1871–1889
- Egawa M, Kajikawa T (2009) Changes in the depth profile of water in the stratum corneum treated with water. *Skin Res Technol* 15:242–249
- Egawa M, Hirao T, Takahashi M (2007) In vivo estimation of stratum corneum thickness from water concentration profiles obtained with Raman spectroscopy. *Acta Derm Venereol* 87:4–8
- Evans CL, Xie XS (2008) Coherent anti-stokes Raman scattering microscopy: chemical imaging for biology and medicine. *Annu Rev Anal Chem* 1:883–909
- Failloux N, Bonnet I, Perrier E, Baron M-H (2004) Effects of light, oxygen and concentration on vitamin A<sub>1</sub>. *J Raman Spectrosc* 2:140–147
- Förster M, Bolzinger MA, Montagnac G, Briçon S (2011a) Confocal Raman microspectroscopy of the skin. *Eur J Dermatol* 21:851–863
- Förster M, Bolzinger MA, Ach D, Montagnac G, Briçon S (2011b) Ingredients tracking of cosmetic formulations in the skin: a confocal Raman microscopy investigation. *Pharm Res* 28:858–872
- Francoeur ML, Golden GM, Potts RO (1990) Oleic acid: its effects on stratum corneum in relation to (trans)dermal drug delivery. *Pharm Res* 7:621–627
- Freudiger CW, Min W, Saar BG, Lu S, Holtom GR, He C, Tsai JC, Kang JX, Xie XS (2008) Label-free biomedical imaging with high sensitivity by stimulated Raman scattering microscopy. *Science* 322:1857–1861
- Fu D, Lu F-K, Zhang X, Freudiger C, Pernik DR, Holtom G, Xie XS (2012) Quantitative chemical imaging with multiplex stimulated Raman scattering microscopy. *J Am Chem Soc* 134:3623–3626
- Gay CL, Guy RH, Golden GM, Mak VHW, Francoeur ML (1994) Characterization of low temperature (i.e., < 65 degrees C) lipid transitions in human stratum corneum. *J Invest Dermatol* 103:233–239
- Groen D, Poole DS, Gooris GS, Bouwstra JA (2011) Is an orthorhombic lateral packing and a proper lamellar organization important for the skin barrier function? *Biochim Biophys Acta - Biomembranes* 1808:1529–1537
- Hancewicz TM, Xiao C, Weissman J, Foy V, Zhang S, Misra M (2012) A consensus modeling approach for the determination of stratum corneum thickness using in-vivo confocal Raman spectroscopy. *J Cosmet Dermatol Sci Appl* 2:241–251
- Herkenne C, Alberti I, Naik A, Kalia YN, Mathy F-X, Pr at V, Guy RH (2008) *In vivo* methods for the assessment of topical drug bioavailability. *Pharm Res* 25:87–103
- Kaushik D, Batheja P, Kilfoyle B, Rai V, Michniak-Kohn B (2008) Percutaneous permeation modifiers: enhancement versus retardation. *Expert Opin Drug Deliv* 5:517–529
- Li L, Wang H, Cheng J-X (2005) Quantitative coherent anti-stokes Raman scattering imaging of lipid distribution in coexisting domains. *Biophys J* 89:3480–3490
- Lu F-K, Ji M, Fu D, Ni X, Freudiger CW, Holtom G, Xie XS (2012) Multicolor stimulated Raman scattering microscopy. *Mol Phys* 110:1927–1932
- M lot M, Pudney PDA, Williamson AM, Caspers PJ, Van Der Pol A, Puppels GJ (2009) Studying the effectiveness of penetration enhancers to deliver retinol through the stratum corneum by in vivo confocal Raman spectroscopy. *J Control Release* 138:32–39
- Min W, Freudiger CW, Lu S, Xie XS (2011) Coherent nonlinear optical imaging: beyond fluorescence microscopy. *Annu Rev Phys Chem* 62:507–530
- Montes LF, Day JL, Wand CJ (1967) Kennedy L. Ultrastructural changes in the horny layer following local application of DMSO to Guinea pig skin. *J Invest Dermatol* 48:184–189
- Naik A, Pechtold LARM, Potts RO, Guy RH (1995) Mechanism of oleic acid-induced skin penetration in vivo in humans. *J Control Release* 37:299–306
- Nandakumar P, Kovalev A, Volkmer A (2009) Vibrational imaging based on stimulated Raman scattering microscopy. *New J Phys* 11:033026
- Norl n L (2001) Skin barrier structure and function: the single gel phase model. *J Invest Dermatol* 117:830–836
- Ongpipattanakul B, Burnette RR, Potts RO, Francoeur ML (1991) Evidence that oleic acid exists in a separate phase within stratum corneum lipids. *Pharm Res* 8:350–354
- Pilgram GSK, Engelsma-van Pelt AM, Bouwstra JA, Koerten HK (1999) Electron diffraction provides new information on human stratum corneum lipid organisation studied in relation to depth and temperature. *J Invest Dermatol* 113:403–409
- Pudney PDA, M lot M, Caspers PJ, Van Der Pol A, Puppels GJ (2007) An *in vivo* confocal Raman study of the delivery of trans-retinol to the skin. *Appl Spectrosc* 61:804–811
- Saar BG, Freudiger CW, Reichman J, Stanley CM, Holtom GR, Xie XS (2010) Video-rate molecular imaging in vivo with stimulated Raman scattering. *Science* 330:1368–1370
- Saar BG, Contreras-Rojas LR, Xie XS, Guy RH (2011) Imaging drug delivery to skin with stimulated Raman scattering microscopy. *Mol Pharm* 8:969–975
- Slipchenko MN, Chen H, Ely DR, Jung Y, Carvajal MT, Cheng J-X (2010) Vibrational imaging of tablets by epi-detected stimulated Raman scattering microscopy. *Analyst* 135:2613–2619

- Song Y, Xiao C, Mendelsohn R, Zheng T, Strekowski L, Michniak B (2005) Investigation of iminosulfuranes as novel transdermal penetration enhancers: enhancement activity and cytotoxicity. *Pharm Res* 22:1918–1925
- Stoughton RB, McClure WO (1983) Azone – a new non-toxic enhancer of cutaneous penetration. *Drug Dev Ind Pharm* 9:725–744
- Tfaily S, Gobinet C, Josse G, Angiboust JF, Baillet A, Manfait M, Piot O (2013) Vibrational spectroscopies for the analysis of cutaneous permeation: experimental limiting factors identified in the case of caffeine penetration. *Anal Bioanal Chem* 405:1325–1332
- Tfaily A, Piot O, Pitre F, Manfait M (2007) Follow-up of drug permeation through excised human skin with confocal Raman microspectroscopy. *Eur J Biophys* 36:1049–1058
- Tfaily A, Piot O, Manfait M (2008) Confocal Raman microspectroscopy on excised human skin: uncertainties in depth profiling and mathematical correction applied to dermatological drug permeation. *J Biophoton* 1:140–153
- Tfaily A, Guillard E, Manfait M, Baillet-Guffroy A (2010) Thermal dependence of Raman descriptors of ceramides. Part I: effect of double bonds in hydrocarbon chains. *Anal Bioanal Chem* 397:1281–1296
- Tfaily S, Josse G, Gobinet C, Angiboust JF, Manfait M, Piot O (2012a) Shedding light on the laser wavelength effect in Raman analysis of skin epidermises. *Analyst* 137:4241–4246
- Tfaily S, Gobinet C, Josse G, Angiboust JF, Manfait M, Piot O (2012b) Confocal Raman microspectroscopy for skin characterization: a comparative study between human skin and pig skin. *Analyst* 137:3673–3682
- Tfaily A, Guillard E, Manfait M, Baillet-Guffroy A (2012c) Molecular interactions of penetration enhancers within ceramides organization: a Raman spectroscopy approach. *Analyst* 137:5002–5010
- Tfaily A, Guillard E, Manfait M, Baillet-Guffroy A (2012d) Raman spectroscopy: feasibility of in vivo survey of stratum corneum lipids, effect of natural aging. *Eur J Dermatol* 22:36–41
- Touitou E, Meidan VM, Horwitz E (1998) Methods for quantitative determination of drug localized in the skin. *J Control Release* 56:7–21
- Walker RB, Smith EW (1996) The role of percutaneous penetration enhancers. *Adv Drug Deliv Rev* 18:295–301
- van Hal DA, Jeremiase E, Junginger HE, Spies F, Bouwstra JA (1996) Structure of fully hydrated human stratum corneum: a freeze-fracture electron microscopy study. *J Invest Dermatol* 106:89–95
- van der Pol A, de Sterke J, Caspers PJ (2007) Modeling and interpretation of water concentration gradients in the stratum corneum as measured by confocal Raman microspectroscopy. *Int J Cosmet Sci* 29:235
- Williams AC, Barry BW (2004) Penetration enhancers. *Adv Drug Deliv Rev* 56:603–618
- Windheuser JJ, Haslam JL, Caldwell L, Shaffer RD (1982) The use of *N,N*-diethyl-*m*-toluamide to enhance dermal and transdermal delivery of drugs. *J Pharm Sci* 71:1211–1213
- Wu J, Polefka TG (2008) Confocal Raman microspectroscopy of stratum corneum: a pre-clinical validation study. *Int J Cosmet Sci* 30:47–56
- Xiao C, Flach CR, Marcott C, Mendelsohn R (2004) Uncertainties in depth determination and comparison of multivariate with univariate analysis in confocal Raman studies of a laminated polymer and skin. *Appl Spectrosc* 58:382–389
- Yu B, Kim KH, So PTC, Blankschtein D, Langer R (2003) Visualization of oleic acid induced transdermal diffusion pathways using two photon fluorescence microscopy. *J Invest Dermatol* 120:448–455
- Zhang G, Flach CR, Mendelsohn R (2007a) Tracking the dephosphorylation of resveratrol triphosphate in skin by confocal Raman microscopy. *J Control Release* 123:141–147
- Zhang G, Moore DJ, Flach CR, Mendelsohn R (2007b) Vibrational microscopy and imaging of skin: from single cells to intact tissue. *Anal Bioanal Chem* 387:1591–1599

# ATR-FTIR Spectroscopy and the Skin Barrier: Evaluation of Penetration-Enhancement Effects

# 14

Julia Covi-Schwarz, Victoria Klang,  
and Claudia Valenta

## Contents

14.1	<b>Introduction and Theoretical Background</b> .....	247
14.2	<b>ATR-FTIR Spectroscopy and Dermal Drug Delivery</b> .....	248
14.2.1	Characterisation of the Stratum Corneum by ATR-FTIR Spectroscopy.....	248
14.2.2	Influence of Selected Penetration Enhancers and Vehicles on the Skin Barrier .....	250
	<b>Conclusion</b> .....	252
	<b>References</b> .....	252

## 14.1 Introduction and Theoretical Background

A prerequisite for dermal and transdermal drug delivery is to overcome the skin barrier. To this end, a thorough knowledge of the skin, its complex organisation and its barrier properties is essential. A plethora of biophysical methods have been employed to study the skin's main barrier, the stratum corneum. Among them, Fourier transform infrared (FTIR) spectroscopy was found to be a particularly promising approach. FTIR spectroscopy is a highly sensitive method to analyse molecule vibrations after excitation with the radiation of the infrared range. The functional principle of this technique is well known and described in the respective literature (Markovich and Pidgeon 1991; Naik and Guy 1997; Guenzler and Gremlich 2003). In contrast to traditional infrared spectrometers, FTIR instruments feature a Michelson interferometer and offer several distinct advantages (Perkins 1987). The signal-to-noise ratio is improved when compared to traditional IR devices, and thus higher sensitivity can be achieved (Hesse et al. 2012). Moreover, due to the exact definition of the mirror position, wavenumbers can be determined more precisely. Last but not least, the simultaneous recording of all frequencies renders FTIR spectroscopy a time-saving and convenient technique (Guenzler and Gremlich 2003). A further modification of this method is attenuated total

---

J. Covi-Schwarz  
University of Vienna, Research Platform  
'Characterisation of Drug Delivery Systems on Skin  
and Investigation of Involved Mechanisms,  
Althanstraße 14, 1090 Vienna, Austria  
e-mail: [julia.schwarz@univie.ac.at](mailto:julia.schwarz@univie.ac.at)

V. Klang • C. Valenta (✉)  
University of Vienna, Research Platform  
'Characterisation of Drug Delivery Systems on Skin  
and Investigation of Involved Mechanisms,  
Althanstraße 14, 1090 Vienna, Austria

University of Vienna, Department of Pharmaceutical  
Technology and Biopharmaceutics,  
Althanstraße 14, 1090 Vienna, Austria  
e-mail: [victoria.klang.vie@gmail.com](mailto:victoria.klang.vie@gmail.com);  
[claudia.valenta@univie.ac.at](mailto:claudia.valenta@univie.ac.at)

reflection (ATR)-FTIR spectroscopy, which is a non-invasive technique to characterise organic samples rapidly and with high sensitivity (Yadav et al. 2009; Obata et al. 2010). Furthermore, in vivo sampling is possible with this internal technique (Naik and Guy 1997). A crystal that consists of material with a higher refractive index than the sample is required, such as zinc selenide or diamond. The gaseous, liquid, or solid sample is placed directly on the crystal during analysis. A beam of infrared light is sent through the crystal and is repeatedly reflected (Guenzler and Gremlich 2003); thus, the beam can penetrate the sample up to a depth of about 1  $\mu\text{m}$ . This penetration depth corresponds to approximately 1–1.5 cell layers of the stratum corneum. Therefore, recorded spectra contain information about the surface of the sample. In order to characterise skin samples, the stratum corneum may remain on the intact skin; it is not necessary to separate it from underlying tissue (Rodriguez et al. 2010). Conveniently, the non-invasive nature of this technique offers the possibility to perform further experiments such as tape-stripping on the same skin sample (Caussin et al. 2009; Klang et al. 2012a). By correlating the peak intensity at a defined frequency with the concentration of an applied substance, even quantitative IR analysis is possible. In this case, the use of deuterated drugs and excipients is advantageous for a precise distinction from endogenous substances (Cotte et al. 2004; Dias et al. 2008; Schwarz et al. 2013).

Having summarised the basic principles of FTIR spectroscopy and the possibilities offered by this technique, the next section will provide an overview of experimental findings that elucidate the characteristic skin barrier properties through FTIR analysis. In this context, typical skin bands in ATR-FTIR spectra are discussed. Furthermore, the influence of selected permeation enhancers and dermal delivery systems on the respective skin bands as demonstrated in many studies is discussed. The importance of ATR-FTIR spectroscopy in skin science is well documented by the large number of recent publications using this technique to gather new information on the molecular level. This article represents a non-

exhaustive overview of recent findings of interest in the field; selected data are presented, and the conclusions obtained in the respective contributions are discussed.

---

## 14.2 ATR-FTIR Spectroscopy and Dermal Drug Delivery

### 14.2.1 Characterisation of the Stratum Corneum by ATR-FTIR Spectroscopy

ATR-FTIR experiments have been widely employed to characterise human skin samples in vivo (Puttnam and Baxter 1962; Sakuyama et al. 2010; Gorcea et al. 2012) and in vitro (Boncheva et al. 2008; Hasanovic et al. 2011). Obtaining human skin samples for such experiments often involves significant organisational and legislative issues. Therefore, animal models such as the bovine udder skin model (Heise et al. 2002) are frequently employed as a substitute for human skin. Other types of skin that have been investigated by ATR-FTIR include porcine skin (Hasanovic et al. 2011), rat skin (Obata et al. 2010), guinea pig skin (Bello et al. 2006) and snake skin (Wonglertnirant et al. 2012). Minor differences held aside, the porcine ear skin model represents a highly adequate in vitro substitute for human skin (Jacobi et al. 2007; Hasanovic et al. 2011; Klang et al. 2012b). Figure 14.1 shows a typical ATR-FTIR spectrum of porcine ear skin with its characteristic skin bands. The latter will be discussed in the following section. These skin bands can be determined by ATR-FTIR with high reproducibility.

Although it represents a very basic and simplified model of the human skin barrier, the bricks and mortar model by Elias is still a valid approach to depict the skin structure (Elias and Friend 1975). While the bricks represent the stratum corneum proteins, that is, the cornified cells termed corneocytes, the mortar depicts the intercellular lipid matrix within the stratum corneum. The molecular organisation of the stratum corneum lipids is essential for the barrier function of the skin (Boncheva et al. 2008). The lipids are

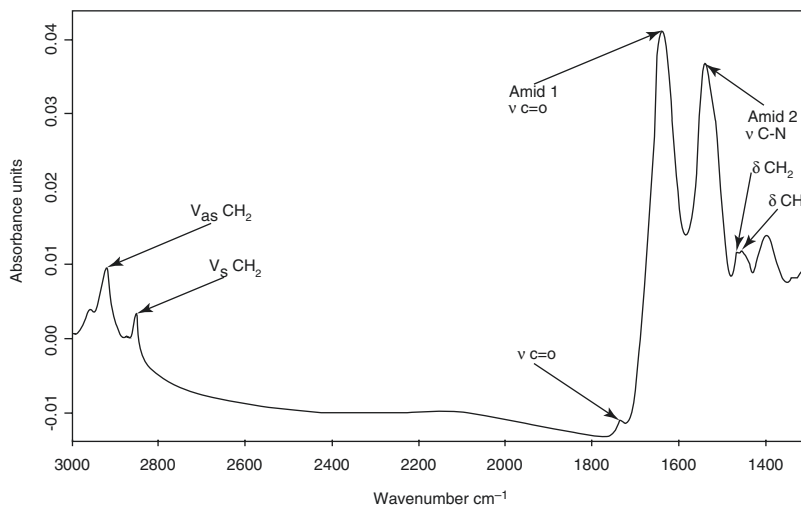


**Fig. 14.1** ATR-FTIR spectrum of porcine ear skin recorded at 32 °C, showing the typical skin bands

arranged in two suborganisational patterns: the lamellar organisation, that is, the arrangement in layers parallel to the skin surface, and the lateral organisation, which describes the lipid arrangement in the lipid lamellae themselves. Regarding the lamellar organisation, long-periodicity phases and short-periodicity phases are present (Caussin et al. 2009; Obata et al. 2010; Groen et al. 2011). Recent findings suggest that the long-periodicity phase is essential for the skin barrier function (Caussin et al. 2009; Groen et al. 2011). Regarding the lateral lipid organisation, the domain mosaic model is consistent with most experimental data. This model proposes that the lipids are organised in ordered domains and connected by lipids in a disordered phase (Forslind 1994). The ordered domains, also referred to as gel phase, contain lipids in the orthorhombic or hexagonal phase. The disordered domain consists of lipids in the liquid-crystalline phase (Boncheva et al. 2008; Rodriguez et al. 2010; de Sousa Neto et al. 2011). Lipids in the orthorhombic phase are tightly packed, and the alkyl chains are organised in an all-trans conformation. The packing in the hexagonal phase is less tight, and the lipids have more rotational freedom. The lipids in the liquid-crystalline phase have the greatest freedom of movement and their alkyl chains exhibit a high percentage of gauche conformation (Bouwstra and Ponc 2006; Boncheva

et al. 2008; Rodriguez et al. 2009). The lipid organisation is an important factor to determine skin permeability (Boncheva et al. 2008; de Sousa Neto et al. 2011). In addition to lipid composition, temperature and skin hydration, solvents or penetration enhancers can likewise influence the lateral packing of the stratum corneum lipids and thus the skin barrier (Naik and Guy 1997).

Regarding the stratum corneum, the most informative lipid absorbances in the IR spectrum originate from the hydrophobic alkyl chains (Potts and Francoeur 1993). In particular, the carbon–hydrogen stretching vibrations with peaks at 2850 and 2920  $\text{cm}^{-1}$ , that is, the asymmetric and symmetric stretching modes, provide information about the conformational order of the hydrocarbon lipid chains of the horny layer (Naik and Guy 1997; Babita et al. 2006; Hathout et al. 2011). Although both bands describe the three-dimensional arrangement of the lipids, the symmetric stretching mode is more susceptible to changes (Moore et al. 1997; Gooris and Bouwstra 2007; Rodriguez et al. 2010). The peak width as well as its wavenumber allow a classification of the lipids. The symmetric stretching band  $\nu_s$  appears at a wavenumber of about 2849–2850  $\text{cm}^{-1}$  if the majority of the lipids are arranged in an orthorhombic pattern. During the transformation to a more fluid structure and a

mainly hexagonal lipid arrangement, the peak width increases and is shifted to higher wavenumbers (2851–2852  $\text{cm}^{-1}$ ). When most lipids are arranged in the liquid-crystalline phase, the symmetric stretching peak appears at a wavenumber of about 2853–2854  $\text{cm}^{-1}$  (Boncheva et al. 2008; Caussin et al. 2008).

In addition, the  $\text{CH}_2$ -scissoring band at about 1460  $\text{cm}^{-1}$  characterises the lateral packing of the lipid chains in the stratum corneum. Depending on the arrangement of the lipid domain, either one or two peaks are visible in the skin spectrum (Moore et al. 1997; Boncheva et al. 2008; Rodriguez et al. 2010). When two separate bands appear in the spectrum with a distance of approximately 10 wavenumbers, the orthorhombic phase dominates. These two separate peaks are caused by the interaction between closely packed lipid chains, and appear between 1460 and 1470  $\text{cm}^{-1}$  (Hasanovic et al. 2011). Moreover, as shown by Boncheva and coworkers, the scissoring bandwidth, especially when consulting second derivative spectra, provides a suitable measure for the presence and extent of the orthorhombic and hexagonal phases (Boncheva et al. 2008). The more lipids pass into the hexagonal phase, the more the distance between the two peaks decreases, until they merge (Caussin et al. 2008). The  $\text{C}=\text{O}$ -stretching band represents the lipid ester carbonyl and is mainly indicative of the presence of sebum in and on the SC (Machado et al. 2010).

While around 1650  $\text{cm}^{-1}$ , the stretching band of the  $\text{C}=\text{O}$  group of keratin (amide 1) is present in the spectrum, the stretching band of the  $\text{C}-\text{N}$  bond of the amino group of keratin appears at around 1550  $\text{cm}^{-1}$  (amide 2) (Moore et al. 1997; Babita et al. 2006; Rodriguez et al. 2009; He et al. 2009). The amide 1 band describes the secondary structure of keratin (He et al. 2009). Wavenumbers 1615–1638  $\text{cm}^{-1}$  suggest a  $\beta$ -sheet arrangement, 1638–1645  $\text{cm}^{-1}$  a random coil structure, 1645–1662  $\text{cm}^{-1}$   $\alpha$ -helix arrangement and 1662–1695  $\text{cm}^{-1}$   $\beta$ -turning structure (He et al. 2009). Excipients or penetration enhancers can affect the secondary structure of keratin. They may induce a larger degree of freedom and may thus enhance the penetration of co-applied

drugs (He et al. 2009). Moreover, it is possible to analyse the absorption of water within the stratum corneum by analysing the amide 1 and 2 bands. While the intensity of the amide 2 peak remains stable, the intensity of the amide 1 band increases upon water absorption. By calculating the ratio of these intensities, the water content in the skin can be determined (Prasch et al. 2000; He et al. 2009).

#### 14.2.2 Influence of Selected Penetration Enhancers and Vehicles on the Skin Barrier

The characterisation of the skin barrier by biophysical methods is constantly exploring new levels as sophisticated methods of analysis are continuously evolved and refined. Among other methods, ATR-FTIR spectroscopy has successfully been employed to determine the influence of substances such as solvents, penetration enhancers, excipients, or even of complex drug delivery systems on the stratum corneum (Babita et al. 2006). With this method, the enhancer efficacy can be evaluated, while the mode of action can be elucidated as well (Naik and Guy 1997). In the following section, examples of recent ATR-FTIR studies of interest are discussed in which the penetration enhancement effect and mechanism of certain excipients and vehicles were investigated.

Regarding the stratum corneum lipids, there are two main effects that can be observed when the skin is treated with penetration enhancers. Some enhancers combine both modes of action, while others only make use of one of them. On the one hand, a fluidisation of the stratum corneum lipids can be induced and observed most prominently on the  $\text{CH}_2$ -stretching peaks in the spectra. In this case, the lateral packing of the lipids becomes less tight, and substances can penetrate the stratum corneum more easily. On the other hand, penetration enhancers can also cause a lipid extraction. Due to the lower amount of lipids in the stratum corneum, the barrier is weakened (Naik and Guy 1997). Furthermore, penetration enhancers may also affect the skin



barrier by changing the secondary structure of keratin. This leads to a loose accumulation of stratum corneum proteins with a larger degree of carbon movement (He et al. 2009).

The effect of ethanol, one of the most prominent permeation enhancers and a simple vehicle, on the skin barrier has been investigated by numerous groups (Kurihara-Bergstrom et al. 1990; Bommannan et al. 1991; Krill et al. 1992; Panchagnula et al. 2001). An *in vitro* study on human skin showed that ethanol induced lipid extraction and could thereby enhance the flux of salicylate (Kurihara-Bergstrom et al. 1990). These results were confirmed *in vivo* (Bommannan et al. 1991). Interestingly, in this study as well as in another study employing the stratum corneum of hairless mouse skin, a shift of the symmetric  $\text{CH}_2$ -stretching band to lower wavenumbers was observed. These findings indicate an increase in lipid order after treatment with ethanol, which represents a rather surprising observation. Based on these findings, ethanol seems to enhance drug penetration by stratum corneum lipid extraction and does not, even at high concentrations, fluidise the lipids (Babita et al. 2006).

Fatty acids are natural constituents of the stratum corneum lipids. Therefore, compounds of this group, such as oleic acid, have a natural ability to intercalate within the lipid bilayer and thus modulate the barrier function (Babita et al. 2006). Oleic acid is a penetration enhancer that is widely used in the field of transdermal drug delivery. Regarding its mode of action, it is assumed that the molecules create a highly permeable, fluid-like phase that coexists with the endogenous stratum corneum lipids, but disrupts their tight packing (Ongpipattanakul et al. 1991; Babita et al. 2006; Boncheva et al. 2008). This hypothesis was supported by experimental data which showed a shift of the symmetric  $\text{CH}_2$ -stretching vibration to higher wavenumbers (Mak et al. 1990; Boncheva et al. 2008). Moreover, the scissoring bandwidth confirmed that oleic acid forms a separate phase within the stratum corneum lipids (Boncheva et al. 2008).

Propylene glycol, a vehicle for penetration enhancers and a cosolvent in many dermal drug delivery systems, interacts mostly with keratin

and does not alter the stratum corneum lipid organisation (Mak et al. 1990). It does not show an effect on the symmetric  $\text{CH}_2$ -stretching band, which indicates a preservation of the conformational order of the lipids (Panchagnula et al. 2001; Boncheva et al. 2008, 42). However, a decrease in height and area of the  $\text{CH}_2$ -stretching peak suggests a mild extraction of stratum corneum lipids (Babita et al. 2006).

Dimethyl sulfoxide (DMSO) is a well-known, but rather aggressive, penetration enhancer. Results of ATR-FTIR studies suggested lipid extraction, protein denaturation and lipid fluidisation to be among the enhancer's mode of action (Naik and Guy 1997; Babita et al. 2006). DMSO effectively enhances the skin permeation of both hydrophilic and lipophilic drugs, but concentrations of more than 60% w/w are required for this effect. However, such high concentrations lead to erythema on skin, and thus DMSO is rarely used nowadays (Babita et al. 2006). In lower concentration, DMSO may be employed as a drug solubiliser in the stratum corneum (Remane et al. 2006).

The analysis of the effect of dermal or transdermal drug delivery systems on the skin barrier properties is a rather complex task. Where possible, employing deuterated compounds is advantageous to distinguish the skin bands from the formulation peaks in the spectra (Naik and Guy 1997). Otherwise, very careful data interpretation is necessary. However, reliable results can be obtained, especially if control spectra are recorded. For instance, the influence of natural sucrose esters on the stratum corneum was analysed by ATR-FTIR. Sucrose oleate and laurate showed no effect on the skin bands or drug permeation when applied in aqueous solutions (Ayala-Bravo et al. 2003). However, a permeation-enhancing effect could be determined when the sucrose esters were dissolved in Transcutol. Especially sucrose laurate induced a decreased absorbance and a frequency shift to higher wavenumbers of the  $\text{CH}_2$ -stretching bands (Ayala-Bravo et al. 2003). Another group investigated the effect of sucrose laurate on the permeation of ibuprofen from a hydrogel (Csizmazia et al. 2012). Besides an increase in drug permeation and a more pronounced skin-hydrating effect as shown

by the amide bands, the sucrose laurate-loaded hydrogel resulted in the same slight lipid extraction and fluidisation as the control hydrogel. The latter effects were reversible, and thus, sucrose laurate may be used as a mild penetration and hydration enhancer (Csizmazia et al. 2012). In another study, microemulsions based on natural surfactants, namely sucrose laurate, lecithin and alkylpolyglucoside, were investigated (Schwarz et al. 2012a). In skin diffusion experiments, lecithin showed the strongest skin-enhancing properties for the model drugs flufenamic acid and fluconazole. Accordingly, the  $\text{CH}_2$ -stretching indicated that the stratum corneum lipids had undergone a phase transition to liquid-crystalline organisation. Also, the  $\text{CH}_2$ -scissoring and the amide bands suggested a more permeable skin structure (Schwarz et al. 2012a). In contrast, the application of solid lipid nanoparticles and nanostructured lipid carriers based on alkylpolyglucosides seemed to exert a barrier-strengthening effect on the stratum corneum (Schwarz et al. 2012b). Both the  $\text{CH}_2$ -stretching and  $\text{CH}_2$ -scissoring bands indicated a strictly orthorhombic organisation of the lipid chains.

### Conclusion

In summary, ATR-FTIR spectroscopy provides an excellent tool for *in vivo* and *in vitro* characterisations of penetration-enhancement effects on the stratum corneum. Besides its high sensitivity, the non-destructive nature of this technique as well as the short duration of the experiments are convenient and advantageous features of this method. As the knowledge about the barrier function of the skin is continuously being expanded, more accurate predictions about penetration-enhancement properties of substances as well as their skin-irritation potential will become possible.

### References

- Ayala-Bravo HA, Quintanar-Guerrero D, Naik A, Kalia YN, Cornejo-Bravo JM, Ganem-Quintanar A (2003) Effects of sucrose oleate and sucrose laureate on *in vivo* human stratum corneum permeability. *Pharm Res* 20:1267–1273
- Babita K, Kumar V, Rana V, Jain S, Tiwary AK (2006) Thermotropic and spectroscopic behaviour of skin: relationship with percutaneous permeation enhancement. *Curr Drug Deliv* 3:95–113
- Bello D, Smith TJ, Woskie SR, Streicher RP, Boeniger MF, Redlich CA, Liu Y (2006) An FTIR investigation of isocyanate skin absorption using *in vitro* guinea pig skin. *J Environ Monit* 8:523–529
- Bommannan D, Potts RO, Guy RH (1991) Examination of the effect of ethanol on human stratum corneum *in vivo* using infrared spectroscopy. *J Control Release* 16:299–304
- Boncheva M, Damien F, Normand V (2008) Molecular organization of the lipid matrix in intact Stratum corneum using ATR-FTIR spectroscopy. *Biochim Biophys Acta* 1778:1344–1355
- Bouwstra J, Ponc M (2006) The skin barrier in healthy and diseased state. *Biochim Biophys Acta* 1758:2080–2095
- Caussin J, Gooris GS, Janssens M, Bouwstra JA (2008) Lipid organization in human and porcine stratum corneum differs widely, while lipid mixtures with porcine ceramides model human stratum corneum lipid organization very closely. *Biochim Biophys Acta* 1778:1472–1482
- Caussin J, Rozema E, Gooris GS, Wiechers JW, Pavel S, Bouwstra JA (2009) Hydrophilic and lipophilic moisturizers have similar penetration profiles but different effects on SC water distribution *in vivo*. *Exp Dermatol* 18:954–961
- Cotte M, Dumas P, Besnard M, Tchoreloff P, Walter P (2004) Synchrotron FT-IR microscopic study of chemical enhancers in transdermal drug delivery: example of fatty acids. *J Control Release* 97:269–281
- Csizmazia E, Eros G, Berkesi O, Berkó S, Szabó-Révész P, Csányi E (2012) Ibuprofen penetration enhance by sucrose ester examined by ATR-FTIR *in vivo*. *Pharm Dev Technol* 17:125–128
- de Sousa Neto D, Gooris G, Bouwstra J (2011) Effect of the omega-acylceramides on the lipid organization of stratum corneum model membranes evaluated by X-ray diffraction and FTIR studies (Part I). *Chem Phys Lipids* 164:184–195
- Dias M, Naik A, Guy RH, Hadgraft J, Lane ME (2008) *In vivo* infrared spectroscopy studies of alkanol effects on human skin. *Eur J Pharm Biopharm* 69:1171–1175
- Elias PM, Friend DS (1975) The permeability barrier in mammalian epidermis. *J Cell Biol* 65:180–191
- Forslind B (1994) A domain mosaic model of the skin barrier. *Acta Derm Venereol* 74:1–6
- Gooris G, Bouwstra J (2007) Infrared spectroscopic study of stratum corneum model membranes prepared from human ceramides, cholesterol, and fatty acids. *Biophys J* 92:2785–2795
- Gorcea M, Hadgraft J, Moore DJ, Lane ME (2012) Fourier transform infrared spectroscopy studies of lipid domain formation in normal and ceramide deficient stratum corneum lipid models. *Int J Pharm* 435:63–68

- Groen D, Poole DS, Gooris GS, Bouwstra JA (2011) Is an orthorhombic lateral packing and a proper lamellar organization important for the skin barrier function? *Biochim Biophys Acta* 1808:1529–1537
- Guenzler H, Gremlich HU (2003) IR-Spektroskopie, 4th edn. Wiley-VCH GmbH & Co. KGaA, Weinheim
- Hasanovic A, Winkler R, Resch GP, Valenta C (2011) Modification of the conformational skin structure by treatment with liposomal formulations and its correlation to the penetration depth of aciclovir. *Eur J Pharm Biopharm* 79:76–81
- Hathout RM, Mansour S, Geneidi AS, Mortada ND (2011) Visualization, dermatopharmacokinetic analysis and monitoring the conformational effects of a microemulsion formulation in the skin stratum corneum. *J Colloid Interface Sci* 354:124–130
- He W, Guo X, Xiao L, Feng M (2009) Study on the mechanisms of chitosan and its derivatives used as transdermal penetration enhancers. *Int J Pharm* 382:234–243
- Heise HM, Kuepper L, Pittermann W, Kietzmann M (2002) Epidermal in vivo and in vitro studies by attenuated total reflection spectroscopy using a novel mid-infrared fibre probe. In: Marks R, Levêque JL, Voegeli R (eds) *The essential stratum corneum*. Martin Dunitz Ltd, London, p 257
- Hesse M, Meier H, Zeeh B (2012) *Spektroskopische Methoden in der organischen Chemie*, 8th edn. Georg Thieme Verlag KG, Stuttgart
- Jacobi U, Kaiser M, Toll R, Mangelsdorf S, Audring H, Otberg N, Sterry W, Lademann J (2007) Porcine ear skin: an in vitro model for human skin. *Skin Res Technol* 13:19–24
- Klang V, Schwarz JC, Haberfeld S, Xiao P, Wirth M, Valenta C (2012a) Skin integrity testing and monitoring of in vitro tape stripping by capacitance-based sensor imaging. *Skin Res Technol*. doi:10.1111/j.1600-0846.2012.00637.x
- Klang V, Schwarz JC, Lenobel B, Nadj M, Auböck J, Wolzt M et al (2012b) In vitro vs in vivo tape stripping: validation of the porcine ear model and penetration assessment of novel sucrose stearate emulsions. *Eur J Pharm Biopharm* 80:604–614
- Krill SL, Knutson K, Higuchi WI (1992) Ethanol effects on the stratum corneum lipid phase behaviour. *Biochim Biophys Acta* 112:273–280
- Kurihara-Bergstrom T, Knutson K, DeNoble LJ, Goates CY (1990) Percutaneous absorption enhancement of an ionic molecule by ethanol–water systems in human skin. *Pharm Res* 7:762–766
- Machado M, Hadgraft J, Lane ME (2010) Assessment of the variation of skin barrier function with anatomic site, age, gender and ethnicity. *Int J Cosmet Sci* 32(6):397–409. doi:10.1111/j.1468-2494.2010.00587.x
- Mak VHW, Potts RO, Guy RH (1990) Oleic acid concentration and effect in human stratum corneum: non-invasive determination by attenuated total reflectance infrared spectroscopy in vivo. *J Control Release* 12:67–75
- Markovich RJ, Pidgeon C (1991) Introduction to Fourier transform infrared spectroscopy and applications in the pharmaceutical sciences. *Pharm Res* 8:663–675
- Moore D, Rerek M, Mendelsohn R (1997) FTIR spectroscopy studies of the conformational order and phase behavior of ceramides. *J Phys Chem B* 101:8933–8940
- Naik A, Guy RH (1997) Infrared spectroscopic and differential scanning calorimetric investigations of the stratum corneum barrier function. In: Potts RO, Guy RH (eds) *Mechanisms of transdermal drug delivery*. Marcel Dekker Inc, New York, pp 87–162
- Obata Y, Utsumi S, Watanabe H, Suda M, Tokudome Y, Otsuka M, Takayama K (2010) Infrared spectroscopic study of lipid interaction in stratum corneum treated with transdermal absorption enhancers. *Int J Pharm* 389:18–23
- Ongpipattanakul B, Burnette RR, Potts RO, Francoeur ML (1991) Evidence that oleic acid exists in a separate phase within stratum corneum lipids. *Pharm Res* 8:350–354
- Panchagnula R, Salve PS, Thomas NS, Jain AK, Ramarao P (2001) Transdermal delivery of naloxone: effect of water, propylene glycol, ethanol and their binary combinations on permeation through rat skin. *Int J Pharm* 219:95–105
- Perkins WD (1987) Fourier transform-infrared spectroscopy part II. *Adv of FT-IR J Chem Edu* 64:A269–A271
- Potts RO, Francoeur ML (1993) Infrared spectroscopy of stratum corneum lipids. In: Walters KA, Hadgraft J (eds) *Pharmaceutical skin penetration enhancement*. Marcel Dekker Inc, New York
- Prasch T, Knübel G, Schmidt-Fonk K, Ortanderl S, Nieveler S, Förster T (2000) Infrared spectroscopy of the skin: influencing the stratum corneum with cosmetic products. *Int J Cosmet Sci* 22:371–383
- Puttnam NA, Baxter BH (1962) Spectroscopic studies of skin in situ by attenuated total reflectance. *J Soc Cosmet Chem* 18:469–472
- Remane Y, Leopold CS, Maibach HI (2006) Percutaneous penetration of methyl nicotinate from ointments using the laser Doppler technique: bioequivalence and enhancer effects. *J Pharmacokinetic Pharmacodyn* 33:719–735
- Rodriguez G, Barbosa-Barros L, Rubio L, Cocera M, Diez A, Estelrich J, Pons R, Caelles J, De la Maza A, Lopez O (2009) Conformational changes in stratum corneum lipids by effect of bicellar systems. *Langmuir* 25:10595–10603
- Rodriguez G, Rubio L, Cocera M, Estelrich J, Pons R, De la Maza A, Lopez O (2010) Application of bicellar systems on skin: diffusion and molecular organization effects. *Langmuir* 26:10578–10584
- Sakuyama S, Hirabayashi C, Hasegawa J, Yoshida S (2010) Analysis of human face skin surface molecules in situ by Fourier-transform infrared spectroscopy. *Skin Res Technol* 16:151–160
- Schwarz JC, Klang V, Hoppel M, Mahrhauser D, Valenta C (2012a) Natural microemulsions: formulation design and skin interaction. *Eur J Pharm Biopharm* 81:557–562
- Schwarz JC, Weixelbaum A, Pagitsch E, Löw M, Resch GP, Valenta C (2012b) Nanocarriers for dermal drug

- delivery: influence of preparation method, carrier type and rheological properties. *Int J Pharm* 437: 83–88
- Schwarz JC, Pagitsch E, Valenta C (2013) Comparison of ATR-FTIR spectra of porcine vaginal and buccal mucosa with ear skin and penetration analysis of drug and vehicle components into pig ear. *Eur J Pharm Sci* 50(5):595–600
- Wonglertnirant N, Ngawhirunpat T, Kumpugdee-Vollrath M (2012) Evaluation of the mechanism of skin enhancing surfactants on the biomembrane of shed snake skin. *Biol Pharm Bull* 35:523–531
- Yadav S, Wickett RR, Pinto NG, Kasting GB, Thiel SW (2009) Comparative thermodynamic and spectroscopic properties of water interaction with human stratum corneum. *Skin Res Technol* 15:172–179

# Confocal Microscopy for Visualization of Skin Penetration

# 15

Mukul A. Ashtikar, Daya D. Verma, and Alfred Fahr

## Contents

15.1	<b>Introduction</b> .....	255
15.2	<b>Confocal Laser Scanning Microscope</b> ....	256
15.2.1	Principle of CLSM .....	257
15.2.2	Major Advantages of CLSM .....	259
15.2.3	Major Disadvantages of CLSM .....	259
15.2.4	CLSM Used for Tracking Liposomal Formulations in the Skin .....	260
15.2.5	Tracking the Penetration of Fluorescence Labels into Hair Follicles .....	266
15.2.6	The Efficacy of Dermaroller® to Enhance Penetration into the Skin .....	267
15.3	<b>Two-Photon Fluorescence Microscopy</b> ...	268
15.3.1	Principle of Two-Photon Fluorescence Microscopy .....	268
15.3.2	Application of Two-Photon Microscopy in Skin Penetration Experiments .....	270
15.4	<b>Confocal Raman Microscopy</b> .....	272
15.4.1	Principles of Raman Microscopy .....	272
15.4.2	Confocal Raman Microscopy for Skin Penetration Experiments .....	273
15.5	<b>Coherent Raman Microscopy</b> .....	275
	<b>Conclusion</b> .....	277
	<b>References</b> .....	278

M.A. Ashtikar  
Lehrstuhl für Pharmazeutische Technologie,  
Friedrich-Schiller-Universität Jena, Jena, Germany  
e-mail: [Mukul-arun.ashtikar@uni-jena.de](mailto:Mukul-arun.ashtikar@uni-jena.de)

D.D. Verma  
Novartis Pharmaceutical Corp., East Hanover, NJ, USA  
e-mail: [ddverma@yahoo.com](mailto:ddverma@yahoo.com)

A. Fahr (✉)  
Friedrich-Schiller-Universität Jena, Institut für  
Pharmazie, Lehrstuhl für Pharmazeutische  
Technologie, Lessingstraße 8, 07743 Jena, Germany  
e-mail: [alfred.fahr@uni-jena.de](mailto:alfred.fahr@uni-jena.de)

## 15.1 Introduction

Over the years, various methods such as diffusion experiments (Addicks et al. 1987; du Plessis et al. 1994), microdialysis (Benfeldt 1999; Fang et al. 1999; Murakami et al. 1998; Schnetz and Fartasch 2001), visualization by microscopic techniques like conventional fluorescence microscopy (Kriwet and Müller-Goymann 1995; Yarosh et al. 1994), electron microscopy (Bouwstra and Honeywell-Nguyen 2002; Hashimoto et al. 1991; Hofland et al. 1995; Kanerva 1990; Schreiner et al. 2000; van den Bergh et al. 1999), confocal laser scanning microscopy (Betz et al. 2001; Kirjavainen et al. 1996; Schatzlein and Cevc 1998; van Kuijk-Meuwissen et al. 1998a, b; Vardaxis et al. 1997; Veiro and Cummins 1994), etc., have been exploited by researchers for studying percutaneous penetration and to gain a better understanding of the skin barrier. Tape stripping and microdialysis experiments, though extensively used to measure the amount and rate of penetration of the model compound, are lacking in providing information about the effect of the model drug on cells and lipid organization or particular pathways for the penetration of the model drug. These techniques also do not give much information about spatial distribution of the model drug inside the tissue or comment on the mechanism of penetration and more importantly, these are destructive methods where tissue has to be carefully removed or homogenized to quantify the amount of drug.

Electron microscopy has been extremely useful in understanding the structure of the stratum corneum (SC) and intercellular lipid organization. Bouwstra and coworkers have made important contributions to the understanding of the interactions between vesicles and human skin (Hofland et al. 1994, 1995; Schreiner et al. 2000). They employed freeze fracture electron microscopy and small angle X-ray scattering to study the effects of vesicular formulations on the SC. Their results indicated increased diffusion of the drug due to adsorption and fusion of drug-loaded vesicles to the surface of the skin. They also reported perturbations in the ultrastructure of the SC intercellular lipid domains due to mixing of liposomal components with SC lipids, which could have also enhanced penetration of the model drug. Although freeze fracture electron microscopy provides rather useful information about the effect of liposomal vesicles on the ultrastructure of the skin barrier, it lacks in providing information of penetration pathways and depth up to which the model drug has penetrated.

Another widely appreciated technique is the conventional fluorescence microscopy. Evaluation of skin treated with fluorescently labeled liposomes by fluorescence microscopy has demonstrated that the fluorescent marker remained in the SC (Kriwet and Müller-Goymann 1995) or penetrated deeper in the epidermis mainly along the hair shaft (Yarosh et al. 1994). However, during the sample preparation the tissue needs to be (cryo-) fixed which might lead to the alteration of the original specimen by the change in skin lipid organization, redistribution of the marker, etc.

Confocal microscopy has evolved over the last five to six decades and today it is an essential tool for a life-sciences laboratory; it has emerged as a sophisticated tool for tracking and studying transport phenomena of different compounds with a high degree of precision. Confocal microscopy offers significant advantages over other microscopic techniques in evaluation of thick specimens due to their inherent ability to distinguish photons generated from different focal planes of the specimen. This ability is mainly achieved in two ways, either by introducing a

pinhole aperture in front of the detector which limits the out of focus light or by utilizing a non-linear technique such as 2-photon fluorescence, which excites the specimen only in a very small focal plane at a time. Confocal microscopes create quite sharp images compared to conventional microscopes where light coming from different planes of the specimen is not differentiated, resulting in blurry and low resolution images. Confocal microscopy on a broad basis can be classified as an imaging and spectroscopic technique. Confocal techniques that are discussed in this chapter are confocal laser scanning microscopy (CLSM), two-photon microscopy, and Raman microspectroscopic techniques. Although these techniques are based on different principles, they all have something in common and that is confocality, ability to image one small focal volume at a time to construct a high-resolution image. Thanks to the modern electronics and optics, we are able to image deeper into a thick biological specimen like skin at high resolution, high speed, and in-vitro as well as in-vivo conditions. Sophisticated lasers and detection systems have enabled us to exploit nonlinear excitation phenomena such as 2-photon fluorescence, coherent anti-stokes Raman scattering, stimulated Raman scattering, etc. The following chapter reviews these techniques and discusses some of the results obtained pertaining to dermal delivery.

---

## 15.2 Confocal Laser Scanning Microscope

In the last two decades, CLSM has been extensively used as a tool to visualize the fluorescent model compounds in the skin. CLSM examination revealed valuable additional morphological information of porcine skin in wound healing studies which was not obtained by conventional microscopy (Vardaxis et al. 1997). CLSM was also used to understand the mechanism by which nanoparticulate systems facilitate skin transport. The surface images revealed that (a) polystyrene nanoparticles accumulated preferentially in the follicular openings, (b) this distribution increased

in a time-dependent manner, and (c) the follicular localization was favored by particles of smaller size (Alvarez-Roman et al. 2004). Simonetti et al. visualized diffusion pathways across the SC of native and in vitro reconstructed epidermis by using CLSM (Simonetti et al. 1995).

Many researchers used CLSM to evaluate the penetration of liposomes into human or animal skin using a fluorescent compound or a fluorescent model drug. It was demonstrated that flexible liposomes penetrated deeper into the skin in non-occlusive conditions than after occlusive application (van Kuijk-Meuwissen et al. 1998a) as measured by a fluorescent liposome marker. Touitou and coworkers examined the penetration of fluorescent probes into fibroblasts and nude mice skin by CLSM and showed that ethosomes facilitated the penetration of all probes into the cells, as evident from the high-intensity fluorescence as compared to the hydroethanolic solution or conventional liposomes (Touitou et al. 2001).

Many research groups examined different lipid combinations for their potential to influence the skin. Zellmer et al. used CLSM to demonstrate that vesicles made of native human SC lipids interact rapidly with phosphatidylserine liposomes, weakly with human SC lipid liposomes and do not interact with phosphatidylcholine (PC) liposomes (Zellmer et al. 1998). Kirjavainen et al. reported that lipophilic fluorescent marker, *L*- $\alpha$ -phosphatidylethanolamine-*N*-lissamine rhodamine B sulfonyl (N-Rh-PE) was able to penetrate deeper into the SC from liposomal vesicles containing dioleylphosphatidylethanolamine (DOPE) than from liposomes without DOPE. A pretreatment of the skin with unlabeled liposomes containing DOPE or lyso-phosphatidylcholine (lyso-PC) enhanced the subsequent penetration of the fluorescent markers, N-Rh-PE, and sulforhodamine B into the skin, suggesting a possible penetration enhancing activity (Kirjavainen et al. 1996).

Procedures like iontophoresis which enhance the percutaneous flux of model drugs like calcein (Turner and Guy 1998) and mannitol (Kirjavainen et al. 2000) were also examined by CLSM in animal models. Grams et al. used CLSM to visualize

time resolved diffusion of a lipophilic dye into the hair follicle of fresh and unfixed piece of human scalp skin. The authors claimed that this technique was able to visualize the diffusion of a dye into the upper hair follicle at different time points (Grams et al. 2004). In another study, they also report that follicular accumulation of lipophilic dyes increased when applied in combination of surfactant-propylene glycol (Grams et al. 2003).

### 15.2.1 Principle of CLSM

Confocality is achieved in CLSM by using a point illumination and point detection. Marvin Minsky constructed the first confocal microscope in 1957 at Harvard (Semwogerere and Weeks 2008). He used a zirconium arc lamp and two pinholes, one in front of the lamp and another in front of the detector to achieve the confocality, while the sample was scanned through the light beam to generate the image. Today's confocal microscopes although different are based on the same principle of point illumination and detection, and their ability to image thick samples with high resolution have enabled their use in studying skin penetration of various molecules and delivery systems.

A CLSM can create a very sharp and high-resolution image of a specimen compared to a conventional microscope. This ability arises from the fact that CLSM is able to filter light coming from parts of the specimen that are not in focus, and in the process as much as 95% of the light coming from the specimen can be blocked to generate an image. As a result, very few photons actually make it to the detector therefore a very high intensity light source in the form of laser is used in modern CLSMs. One disadvantage of this is that more than one laser might be required in order to have multiple excitation wavelengths.

The principle of confocality is explained in the schematic diagram in Fig. 15.1a where light coming from the specimen is focused on the detector with the help of two lenses. Due to the pinhole in front of the detector only the light coming from a very small focal point reaches the detector and light from out of focus regions of the

specimen is blocked by the pinhole. The second pinhole is employed in front of the light source, which limits the amount of specimen that is illuminated at any time, and as a result reduces the background scatter from out of focus region of the specimen. Two pinholes of the confocal microscope are able to significantly reduce the background blur and produce very high-resolution images (Hollricher and Ibach 2011; Nwaneshiudu et al. 2012).

Schematic representation of a CLSM is provided in Fig. 15.1b. In a modern CLSM, a beam of

light is provided by a laser which passes through a pinhole onto a dichroic mirror which directs the light to a scanning mirror assembly and onto the specimen through the microscope objective. The scanning mirrors scan the laser across the specimen in order to generate the image. Light reflected from the specimen is de-scanned at the scanning mirrors and passes to the photo-multiplier tube (PMT) detectors through the dichroic mirror (Semwogerere and Weeks 2008). Light coming from out of focus regions of the specimen is blocked at the detector by a pinhole. The image

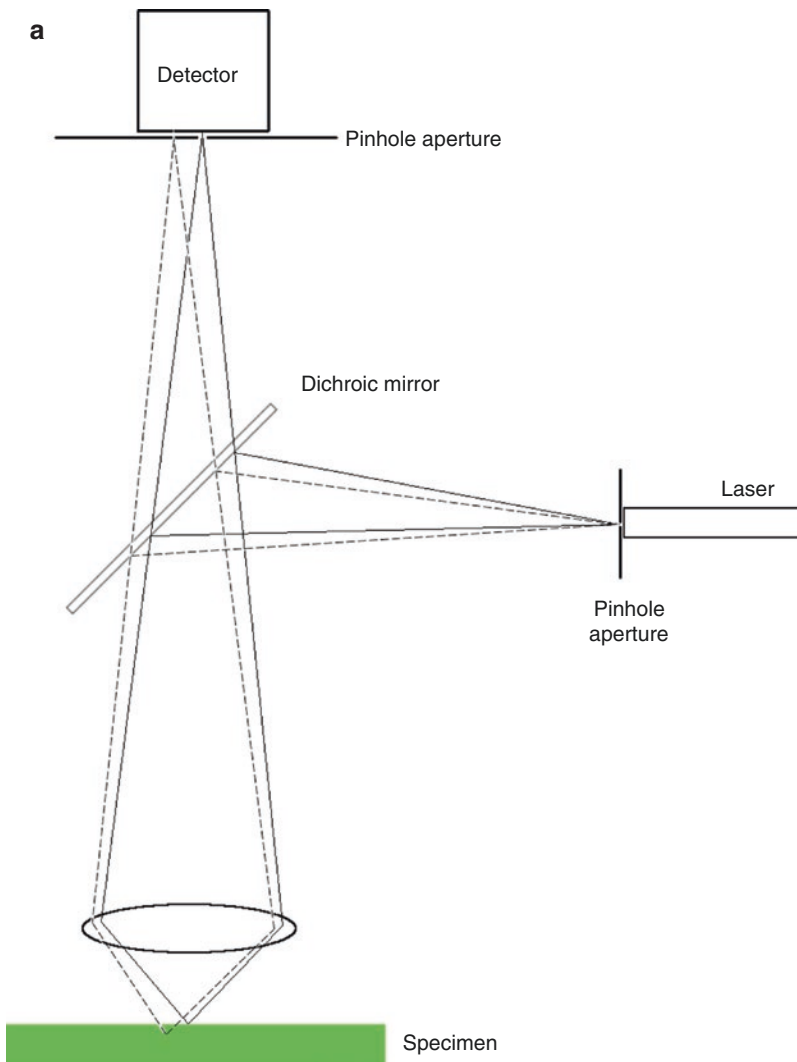


**Fig. 15.1** (a) Pinhole in front of the detector rejects light emerging from out of focus regions. (b) Schematic representation of CLSM optics (Semwogerere and Weeks 2008)



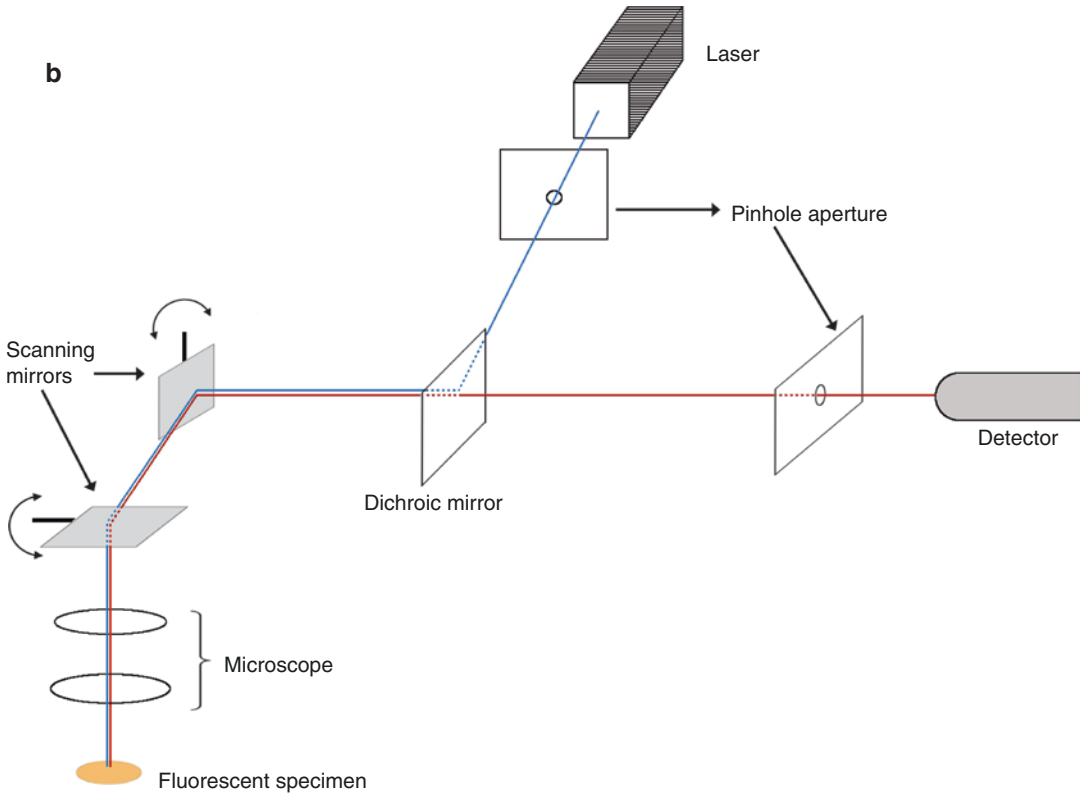


**Fig. 15.1** (continued)

of the specimen is reconstructed by a computer from the spatial coordinates and corresponding light intensity at the detector.

### 15.2.2 Major Advantages of CLSM

Blurring effect observed in the conventional microscope is either eliminated or reduced to a great extent in CLSM, and as a result, images generated are very sharp, have a high contrast and a higher resolution. In practice a CLSM can have at best a horizontal resolution of  $0.2\ \mu\text{m}$  and at best a vertical resolution of  $0.5\ \mu\text{m}$ . Further, a 3D sectioning or optical sectioning of the sample is possible as a very small focal point is imaged at a time which also gives possibility to image thicker specimens using a confocal microscope. Using multiple lasers, it is possible to excite different fluorophores simultaneously.

### 15.2.3 Major Disadvantages of CLSM

CLSM has an inherent resolution limitation of about  $0.2\ \mu\text{m}$  and is dependent on the wavelength of excitation. Due to the high intensity light source, photo bleaching and photo-damage in the illuminated region of the specimen is possible and repeated scans with high-energy light beam greatly reduce the viability of biological tissues and thereby the available time for studying a given specimen. For a high quality image, CLSM usually needs long scan times and as a result, CLSM is not suitable for imaging rapid physiological events in a cell or a tissue. In addition, because lasers emit light only at certain narrow bandwidths, in order to be able to excite a large range of fluorophores, multiple lasers need to be employed which along with the complex electronics, scanning mirrors, and sophisticated data acquisition system raise the cost.

## 15.2.4 CLSM Used for Tracking Liposomal Formulations in the Skin

Liposomes have been extensively studied and suggested as a vehicle for topical drug delivery (Chen et al. 2010, 2011; Dragicevic-Curic et al. 2008, 2009; Ntimenou et al. 2012). However, the mechanism of penetration of liposomes as drug carriers into the intact skin is not fully understood. In this section, we will discuss the interactions between liposomes, containing hydrophilic and lipophilic fluorescent probes, and human as well as rat skin using CLSM.

### 15.2.4.1 Tracking Skin Penetration of Liposomally Entrapped or Un-entrapped Hydrophilic Fluorescent Model Drug

The mechanism of action of liposomes as penetrable drug carriers in topical delivery is not completely understood. In order to evaluate if liposomes are able to increase skin penetration of only entrapped hydrophilic drugs or also of un-entrapped hydrophilic drugs, three different liposomal formulations using carboxyfluorescein (CF) as a fluorescent hydrophilic model drug were prepared: 'CF<sub>in-out</sub>' (non-entrapped CF was not removed), 'CF<sub>in</sub>' (non-entrapped CF was removed), and 'CF<sub>out</sub>' (a pre-calculated amount of CF was added to empty liposomes). All the liposomal formulations had a similar size of liposomes and the concentration of CF was the same in all formulations (Verma et al. 2003b). After 6 h incubation of the skin with different formulations, the skin was cryofixed and 7  $\mu\text{m}$  thick sections were cut using a cryo-microtome. These cross-sections were investigated using CLSM for the skin penetration of CF.

The penetration studies and CLSM images showed that liposomes CF<sub>in-out</sub> exhibited maximum deposition of CF in the SC, whereas liposomes CF<sub>in</sub> showed higher penetration of CF into the deeper skin layers such as the viable epidermis (Fig. 15.2), and through the skin to the acceptor compartment of the Franz diffusion cell. These results were comparable to the data obtained from tape stripping experiments. This

study confirmed the assumption that liposomes CF<sub>in-out</sub> were not under osmotic stress and will, therefore, transfer themselves more easily into the SC. The results indicated further that phospholipid vesicles not only carry the entrapped hydrophilic substance, but also the non-encapsulated hydrophilic substance into the SC and possibly to the deeper layers of the skin. Although CLSM served as a useful tool to estimate skin penetration, CLSM images do not provide the visualization of single liposomes, so the exact mechanism of penetration of liposomes still remains an unsolved question.

### 15.2.4.2 Effect of Vesicle Diameter on Skin Penetration of Liposomally Entrapped Drugs

The influence of vesicle size on the penetration of fluorescently labeled liposomes into the human skin was investigated using lipophilic fluorescent label, 1,1'-dioctadecyl-3,3,3',3'-tetramethylindocarbocyanine perchlorate (DiI) (Verma et al. 2003a). In all CLSM images (Fig. 15.3) very high fluorescence was observed in the SC, which was expected due to the lipophilic nature of the fluorescent label, DiI. This study indicated that large vesicles with a size  $\geq 600$  nm were not able to deliver their contents into the deeper layers of the skin. These liposomes probably stayed in/on the SC and after drying they formed a layer of lipid, which would have further strengthened the barrier properties of the SC. The liposomes with size  $\leq 300$  nm were able to deliver their contents to some extent into the deeper layers of the skin. However, the liposomes with size  $\leq 70$  nm were most promising for dermal drug delivery into the deeper skin layers as they showed maximum fluorescence both in viable epidermis, as well as in dermis.

### 15.2.4.3 Synergistic Penetration Enhancement Effect of Ethanol and Phospholipids on Topical Drug Delivery

It was observed that the composition of liposomal formulation had an appreciable effect on the penetration of compounds into and through the

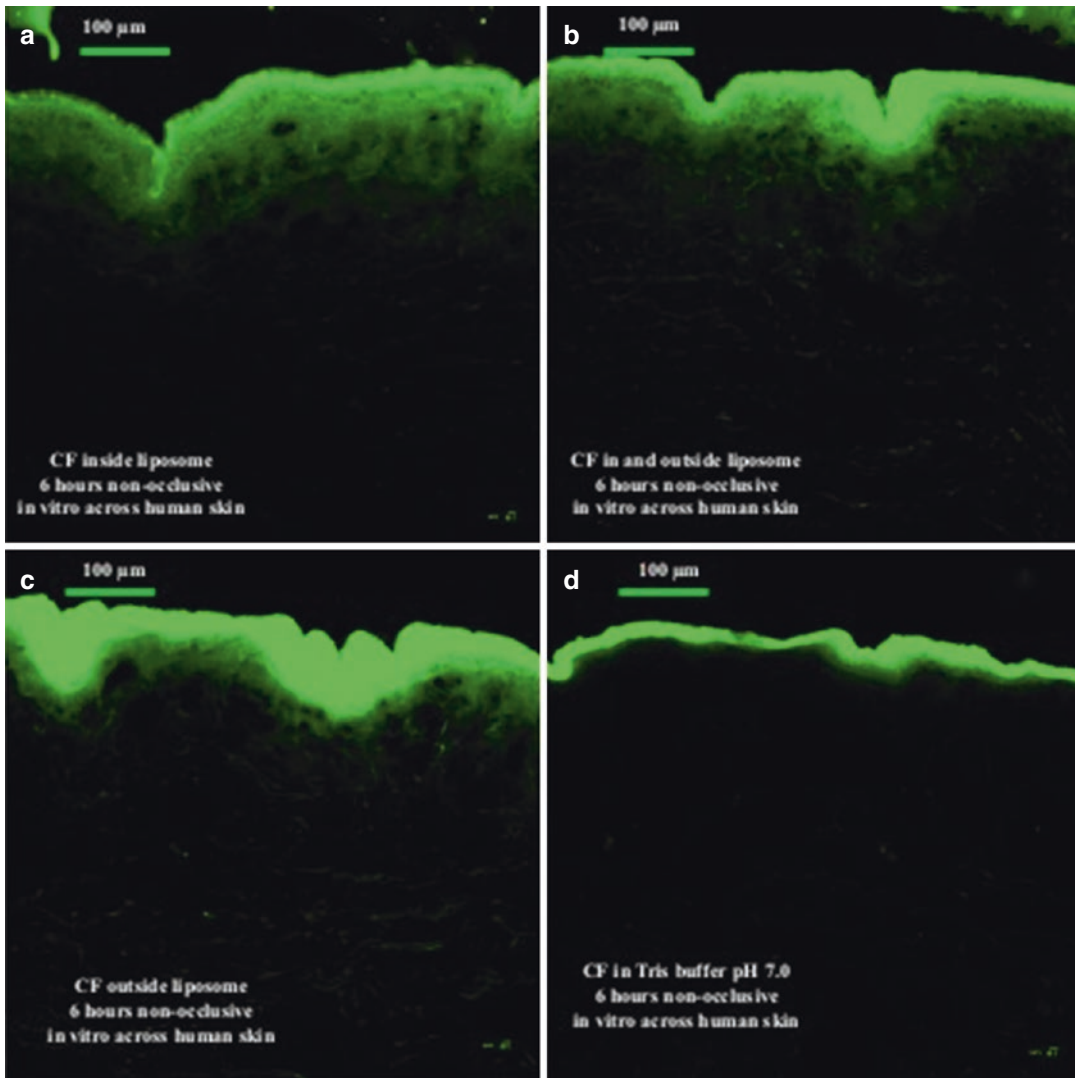


**Fig. 15.2** Fluorescence micrographs of cross-sections of human abdominal skin incubated on Franz diffusion cells with different formulations containing CF. Formulations were applied without occlusion for 6 h. (a) Liposomes

CF<sub>in</sub>; (b) liposomes CF<sub>in-out</sub>; (c) liposomes CF<sub>out</sub>, CF outside liposomes; and (d) CF dissolved in Tris buffer. Scale bar represents 100 μm (Reprinted from Verma et al. (2003b) with permission from Elsevier)

skin (Hofland et al. 1994; Jimbo et al. 1983; Loftsson et al. 1989; Tenjarla et al. 1999). Hence, the effect of lipid vesicular systems embodying ethanol in relatively high concentrations on the percutaneous penetration of cyclosporin A (CyA) was investigated using a standardized skin stripping technique and CLSM (Verma and Fahr 2004). Ethanol has been widely reported as an efficient skin penetration enhancer in the concentration of 5–100% (Bhatia and Singh 1999;

Kobayashi et al. 1994; Simonetti et al. 1995). In a preliminary study, we have seen that not only are the amount and the type of phospholipids important for skin penetration enhancement, but also the amount of ethanol has a significant role in delivering the fluorescent model compounds into the skin (Fig. 15.4) (Verma 2002). We hypothesized that ethanol and phospholipids might have synergistic skin penetration enhancing effect.

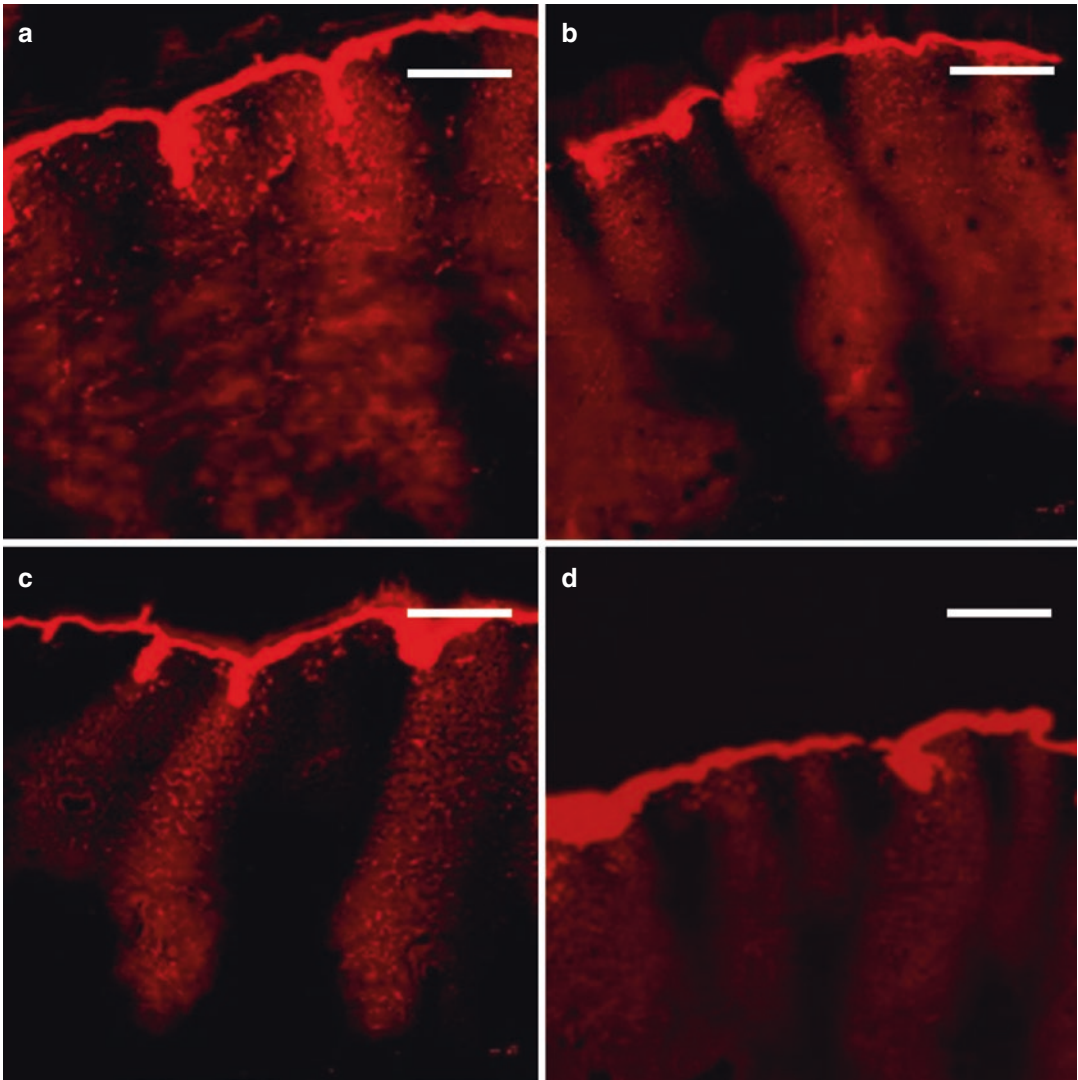


**Fig. 15.3** Fluorescence micrographs of cross-sections of human abdominal skin incubated on Franz diffusion cells with different formulations containing DiI. The vesicles were applied non-occlusively for 12 h. (a) Ethanolic solu-

tion of DiI; (b) NAT8539/ethanol (10/3.3); (c) NAT8539/ethanol (10/10); (d) NAT8539/ethanol (10/20). Scale bar represents 50  $\mu\text{m}$  (Reprinted from Verma et al. (2003a) with permission from Elsevier)

In order to evaluate synergistic effect of the ethanol and phospholipids on penetration of DiI, vesicles with composition of 10% (w/v) phospholipid mixture NAT 8539 (Lipoid, Germany) and ethanol at different concentrations ranging from 0 to 20% w/v were prepared. The results of the CLSM studies are represented in Fig. 15.5. Ethanolic solution of the DiI dye was able to deliver only weak fluorescence into the SC, and

no fluorescence was noticeable in the viable epidermis and dermis (Fig. 15.5a). Formulation, NAT 8539/ethanol (10/3.3), produced a homogeneous bright fluorescence throughout the SC, but no fluorescence was observed in the viable epidermis and dermis (Fig. 15.5b). Formulation, NAT 8539/ethanol (10/10), produced a bright fluorescence throughout the SC with very weak to weak fluorescence observed in the viable

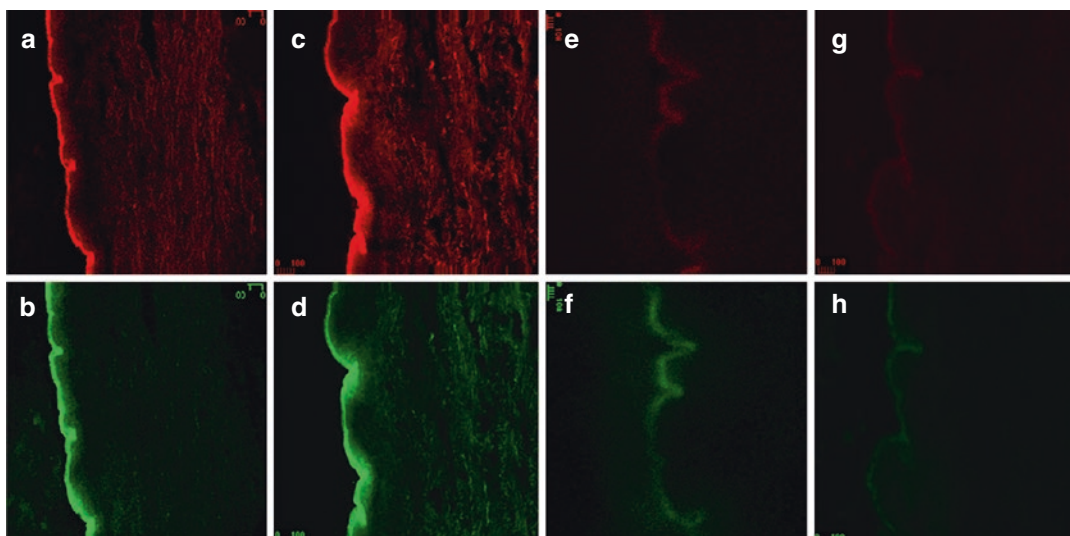


**Fig. 15.4** Fluorescence micrographs of cross-sections of human skin incubated with vesicles with different lipid content for 12 h. (a, b) Ethanolic solution of N-Rh-PE (a) and CF (b). (c, d) Flexible liposomes with N-Rh-PE (c)

and CF (d). (e, f) PL 90H-liposomes with N-Rh-PE (e) and CF (f); (g, h) PL25 liposomes with N-Rh-PE (g) and CF (h)

epidermis and dermis (Fig. 15.5c). Formulation NAT 8539/ethanol (10/20) produced a homogeneous bright fluorescence throughout the SC and very a weak fluorescence was noticeable in the viable epidermis and dermis (Fig. 15.5d). CLSM experiments have shown that the ethanolic solution of DiI was not even able to deliver the fluorescent label into the SC. In contrast, all the formulations with NAT 8539 and ethanol produced a bright fluorescence homogeneously throughout the SC. Formulations prepared with NAT 8539 containing 10 and 20% ethanol were also able to show very weak fluorescence in the viable epidermis and dermis. The results above were confirmed by in vitro penetration studies followed by tape stripping and extraction of the radioactively labeled CyA from various layers of the skin. Ethanol, together with NAT 8539 had synergistic effects on the delivery of the CyA into the skin, and the enhancement effect of ethanol was concentration dependent. Although CLSM images do not provide pure quantitative data regarding the skin penetration, they are, however, extremely useful as a comparative tool and give useful information about the distribution of the drug within the skin.

#### 15.2.4.4 Terpenes as Penetration Enhancers in Liposomes

In this study, CLSM was used to investigate if incorporation of penetration enhancers (terpenes) into liposomal formulations had an effect on their percutaneous penetration enhancing ability in human and rat skin (Verma 2002). Fluorescent derivative of CyA, D-Ala-8-CS-beta-aminebenzofurazan (FI-CyA) and DiI, were used as lipophilic markers while Alexa Fluor-488<sup>®</sup> (Life Technologies GmbH, Germany) was used as a hydrophilic fluorescent marker. Vesicles with and without terpenes were compared with ethanolic and hydro-alcoholic solutions of the fluorescent labels. Double-labeled vesicles, vesicles containing both DiI and Alexa Fluor-488<sup>®</sup>, were applied to skin for 6 and 12 h. Penetration of the fluorescent labels was visualized by CLSM both in terms of depth and intensities of the fluorescence. Fluorescent intensities of the CLSM images were semi-quantitatively scored ranging from no fluorescence to bright fluorescence. Further details regarding imaging and formulations can be found elsewhere (Verma 2002).

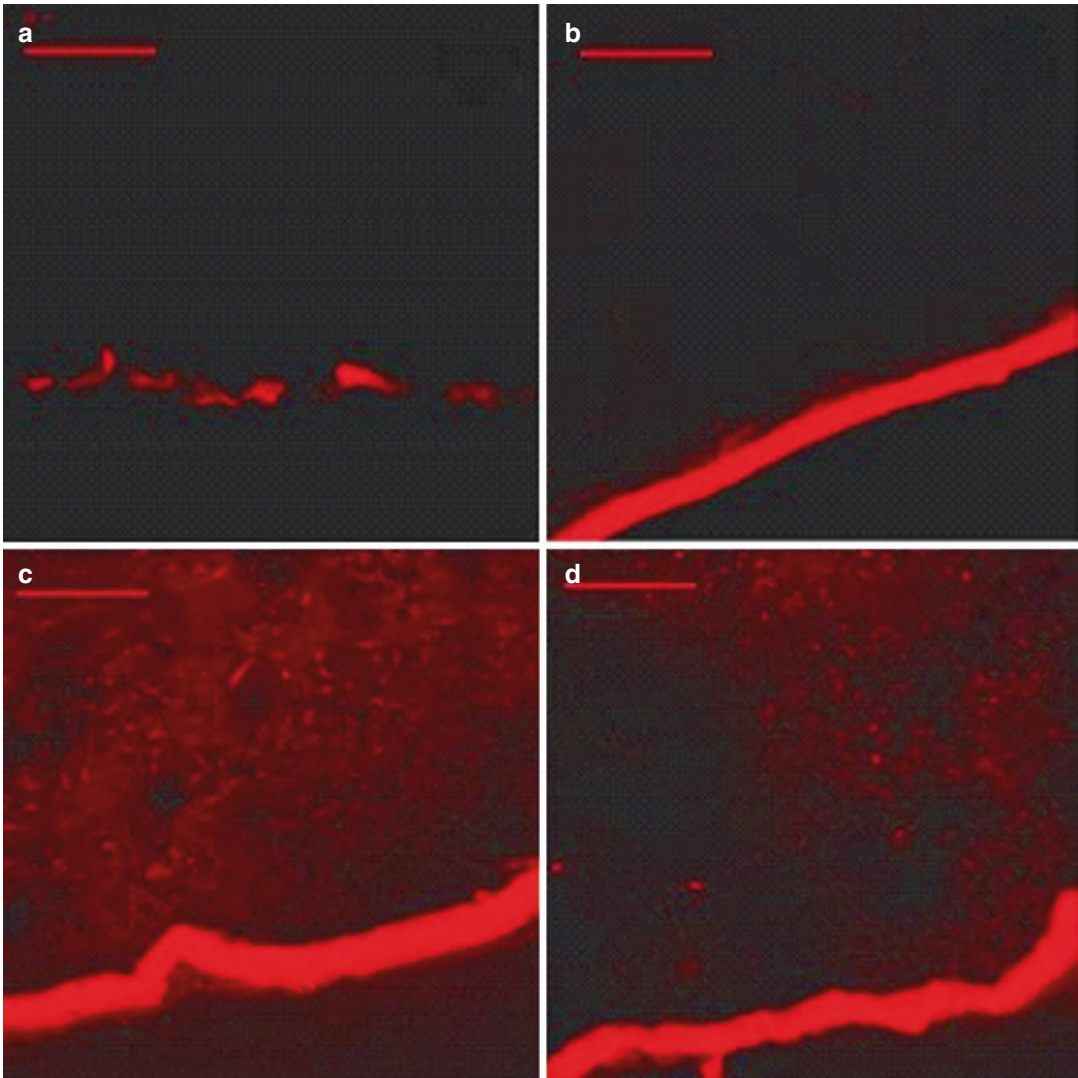


**Fig. 15.5** Fluorescence micrographs of cross-sections of human abdominal skin incubated on Franz diffusion cells with different formulations containing DiI. The vesicles were applied without occlusion for 12 h. (a) Ethanolic

solution of DiI; (b) NAT8539/ethanol (10/3.3); (c) NAT8539/ethanol (10/10); (d) NAT8539/ethanol (10/20). Scale bar represents 50  $\mu\text{m}$  (Reprinted from Verma and Fahr (2004) with permission from Elsevier)

CLSM images of cross-sections of rat skin incubated for 6 h with FI-CyA liposomes prepared with and without terpenes are compared in Fig. 15.6. A bright fluorescence was observed in the SC (Fig. 15.6b) for skin treated with FI-CyA liposomes without terpenes, but only a negligible or no fluorescence was observed in the viable epidermis and dermis. The skin treated with FI-CyA liposomes containing 1% terpenes showed a relatively higher fluorescence in the SC

and weak fluorescence in the epidermis, suggesting diffusion of the FI-CyA from SC to the epidermis (Fig. 15.6c). Ethanolic solution of FI-CyA showed a very weak fluorescence in the SC and no fluorescence was observed in the viable epidermis and dermis (Fig. 15.6a). Based on the fluorescence scores obtained from CLSM images, results indicate that penetration enhancers do play an important role in the penetration of fluorescent labels into the skin.

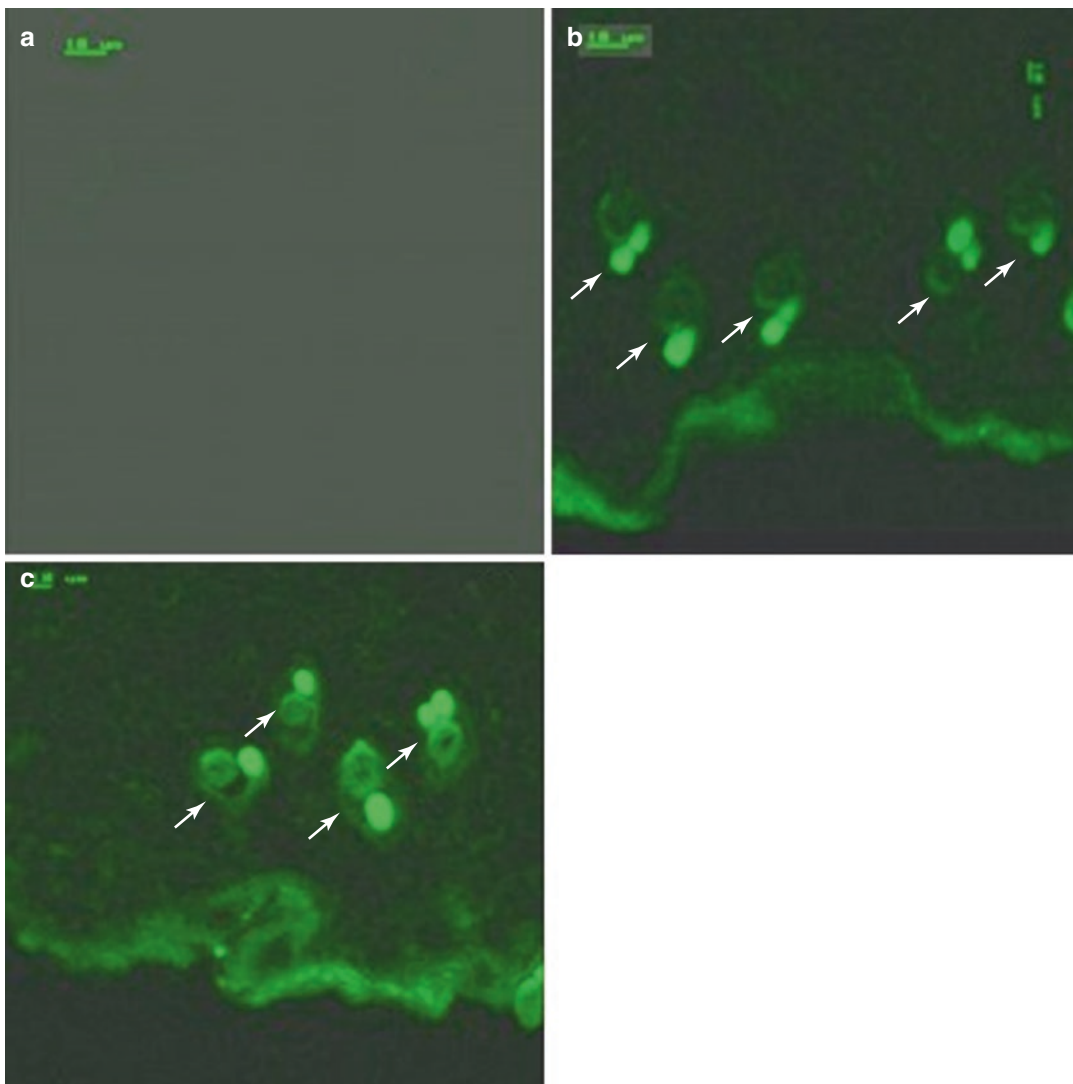


**Fig. 15.6** Cross-sections of rat skin incubated with different formulations containing FI-CyA. The vesicles were applied non-occlusively for 6 h on rat skin. (a) Ethanolic solution of FI-CyA, (b) FI-CyA liposomes without ter-

penes, and (c) liposomes containing 1% terpenes. The length bar represents 10  $\mu\text{m}$ . *Arrows* represent hair follicles in the dermis

Cross-sections of human skin treated with double-labeled (DiI and Alexa Fluor 488<sup>®</sup>) liposomes with and without terpenes are represented in Fig. 15.7. Incubation period of formulation with the skin was 6 h (Fig. 15.7a–c) and 12 h (Fig. 15.7d–f). Control was provided by skin samples treated with hydro-alcoholic solution containing both dyes mentioned above. In all the samples, the fluorescence was restricted mainly to the SC and to a smaller or larger extent, to the

viable epidermis. Samples treated with hydro-alcoholic solutions of the dyes exhibited fluorescence for both DiI and Alexa Fluor-488<sup>®</sup> only in the SC. Increasing the incubation period from 6 h to 12 h only increased the fluorescence intensities for both the labels (Fig. 15.7a, d). In samples treated with dual labeled liposomes without terpenes, fluorescent markers after 6 h diffusion are restricted to the SC only. DiI penetrated up to deeper layers of the SC however no fluorescence

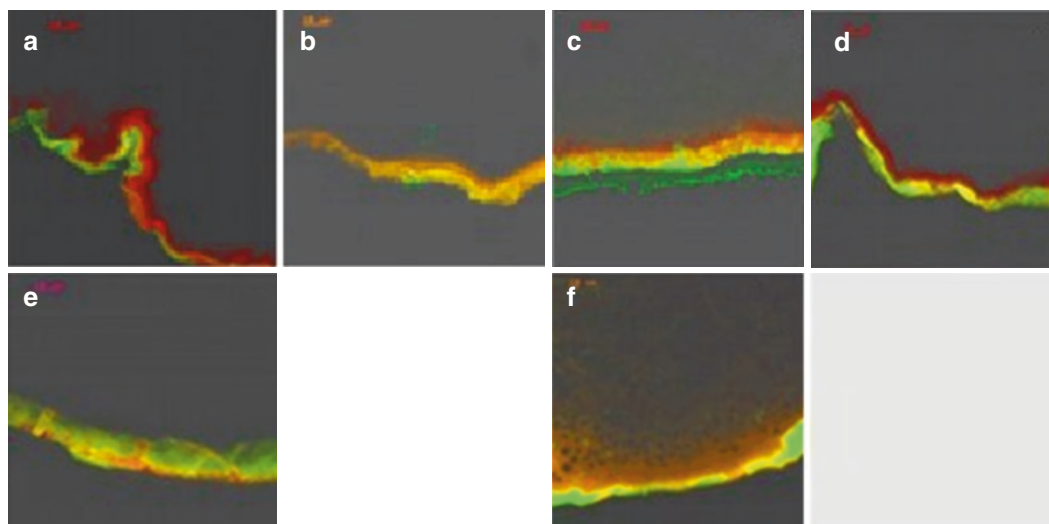


**Fig. 15.7** Cross-sections of human abdominal skin treated with formulations containing two fluorescent markers, DiI and Alexa Fluor 488<sup>®</sup>. The formulations were applied without occlusion for 6 h (a–c) and 12 h

(d–f). (a, c) Hydro-alcoholic solution of DiI and Alexa Fluor 488, (b, e): double-labeled liposomes without terpenes (c, f): double-labeled vesicles containing 1% terpenes. The bar represents 10  $\mu$ m

was observed in the viable epidermis and dermis (Fig. 15.7b). Increasing the incubation period to 12 h did not have marked improvement in penetration depths. CLSM images (Fig. 15.7e) show higher intensities and slightly higher penetration up to viable epidermis achieved for both the dyes. Although distribution of Alexa Fluor-488<sup>®</sup> appears uniform for both 6 and 12 h diffusion samples, distribution of lipophilic dye DiI was not uniform for 12 h samples. For skin treated with liposomal formulations containing 1% terpenes, much higher intensities were observed for both the fluorescent dyes in the SC (Fig. 15.7c, f). For sample with 6 h incubation, very weak fluorescence for Alexa Fluor-488<sup>®</sup> while weak fluorescence for DiI was observed in the viable epidermis. For 12 h incubation samples, fluorescence intensity scores were bright-fluorescence at SC for both the dyes and moderate fluorescence intensities were observed in the viable epidermis. Surprisingly, the reddish fluorescence continued from the epidermis toward the dermis, indicating a diffusion of the lipophilic marker. It was observed that liposomal formulations containing terpenes as penetration enhancers were

able to deliver relatively higher amounts of fluorescent labels into the SC, epidermis, and to a small extent the dermis. In this study, we clearly demonstrated the ability of CLSM to simultaneously image two fluorescent dyes.

## 15.2.5 Tracking the Penetration of Fluorescence Labels into Hair Follicles

### 15.2.5.1 Tracking of Fluorescently Labeled Cyclosporin A into Rat Hair Follicles

CLSM has been successfully used to track the follicular penetration of drugs. Topical application of the CF-loaded liposomes has been reported to significantly increase the accumulation of CF in the pilosebaceous units compared to other non-liposomal formulations (Lieb et al. 1992). Using CLSM, Patzelt et al. demonstrated that follicular penetration for nanoparticles was size dependent (Patzelt et al. 2011).

The effect of terpenes as penetration enhancers in liposomes for targeting hair follicles was



investigated using FI-CyA vesicles (as mentioned above), with and without terpenes, in rat skin. Figure 15.6 also depicts the role of the pilosebaceous unit in the penetration of drugs into the skin. A bright fluorescence was observed in the pilosebaceous units (bright green fluorescent regions in dermis in Fig. 15.6b, c identified as the hair shaft, a part of the pilosebaceous unit) for both formulations, with and without PE. The fluorescence was also visualized in the outer root sheath of the hair shaft (Figs. 15.6b–c and 15.8) (Verma 2002). The images presented here demonstrate that the liposomal vesicles can enter the pilosebaceous unit and deliver their content to the hair follicle and possibly to the hair bulb. The importance of this was stressed upon by the fact that ethanolic solution of FI-CyA failed to deliver any fluorescence into the skin. These CLSM results were supported by *in vivo* studies with Dundee Experimental Bald Rats model (Verma et al. 2004) and other published reports (Agarwal et al. 2000; Bohm and Luger 1998; Lieb et al. 1992; Niemiec et al. 1995). The CLSM investigations enabled us to visualize the accumulation of fluorescent label in the pilosebaceous units, which is not possible with tape stripping.

### 15.2.5.2 Accumulation of CF and N-Rho-PE Loaded Liposomes in the Human Hair Follicles

In this study, liposomal formulations containing CF and N-Rh-PE were prepared (Verma 2002). Liposomal formulations were able to deliver both the hydrophilic and lipophilic fluorescent labels to the human hair follicles as seen in Fig. 15.9a, b. Studies represented in Figs. 15.6, 15.8, and 15.9 demonstrated that the presence of hair follicles plays a significant role in the skin penetration of drugs, as well as that the presence of penetration enhancers helps the formulation in enhancing the follicle delivery of drugs.

### 15.2.6 The Efficacy of Dermaroller® to Enhance Penetration into the Skin

CLSM was also used to investigate the efficacy of the micro-perforation devices, Dermaroller® (Horst Liebl ETS, France), in increasing the skin penetration of a fluorescent lipophilic model compound DiI encapsulated in liposomes (Verma 2002). Three types of Dermarollers® were tested in this study, namely, Dermaroller® C8 0.13–15°,

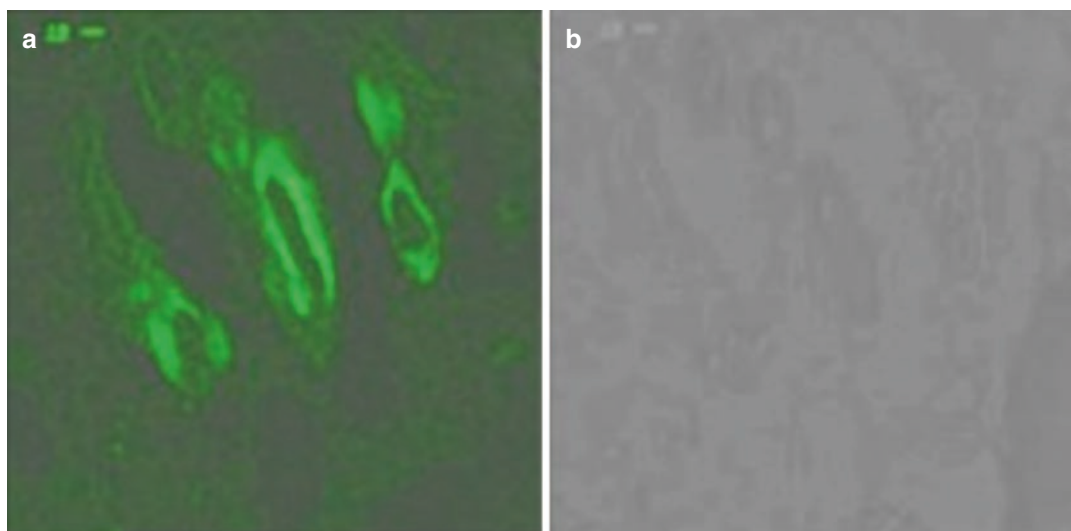


**Fig. 15.8** FI-CyA liposomes treated rat skin cross-section demonstrating the role of pilosebaceous units in the penetration of substance into the skin. The bar represents

10 µm. (a) Fluorescence micrograph and (b) transmission-mode image of the cross-section

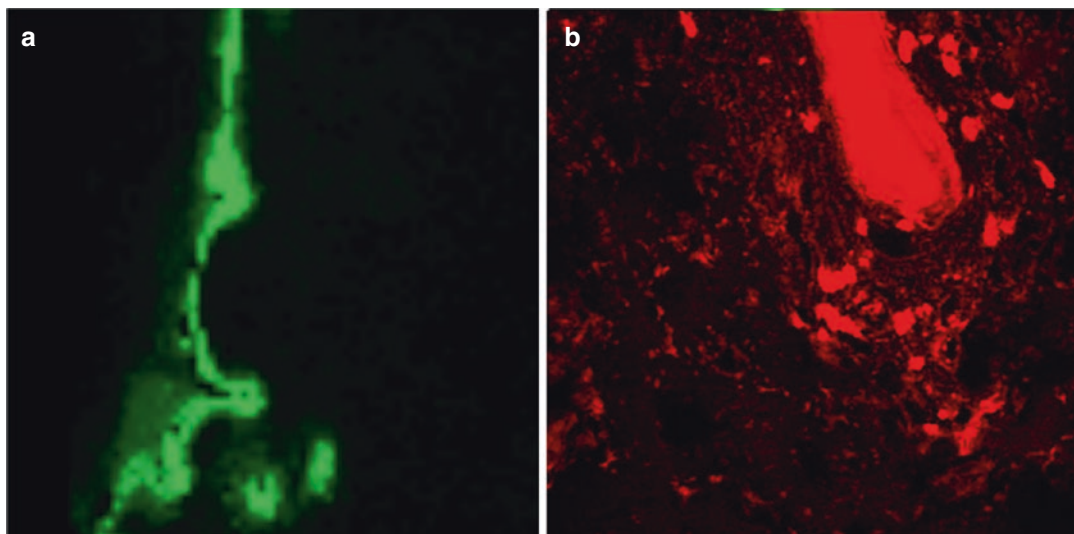


**Fig. 15.9** Fluorescence micrographs showing (a) CF delivery to hair follicles and (b) high-resolution micrograph showing rhodamine delivery to hair follicle following topical application of fluorescent liposomes

M8 1.5–15°, and M8 1.5–30°. Control was provided by the skin not treated with Dermarollers®.

Bright intensity of fluorescence was observed in SC for all samples treated with Dermaroller and for control (Fig. 15.10). For control samples, however, fluorescence intensities in the viable epidermis and dermis were very low. For Dermaroller® C8 0.13–15°, highest fluorescence was observed in the SC and fluorescence intensities rapidly decreased in the viable epidermis and dermis (Fig. 15.10b). Dermaroller® C8 0.13–15° was intended for delivering drugs to the SC whereas Dermaroller® M8 1.5–15° and M8 1.5–30° were optimized for delivering drugs to the deeper regions of skin. Both M8 Dermarollers® did show very high fluorescence intensities in the dermis region (Fig. 15.10c, d). We observed that samples treated with both M8 Dermarollers® showed only a weak fluorescence in the viable epidermis region and showed weak lateral diffusion of the fluorescent label from the pores. This might be because Dermaroller® was able to deliver the liposomes into the deeper layers quickly during application of the Dermaroller but after the application, liposomes probably were not able to diffuse to a great extent from the surface of the skin to the deeper layers in the skin. In this study, we emphasized on the spatial distribution of the fluorescent label which helped us to

get a better understanding of the mode of action of the micro-perforation device, Dermaroller®.

### 15.3 Two-Photon Fluorescence Microscopy

#### 15.3.1 Principle of Two-Photon Fluorescence Microscopy

As seen from aforementioned studies, CLSM is a very good technique for the imaging of biological samples; however, it suffers from some disadvantages. One of the most important limitations of the CLSM is that because only a small fraction of the incident light reaches the detector, relatively high intensities of light are required to achieve high signal to noise ratios. This results in high total energy transfer to the specimen during imaging. Also, the laser beam excites the fluorophores in the specimen above and below the focal plane that is under investigation and this can cause severe photo bleaching, photo damage, and even dehydration of the biological specimen. Many fluorophores generate free radicals or singlet oxygen when excited which can be toxic if imaging living cells or tissue. CLSM also suffers from low axial resolution especially when imaging deep within a thick

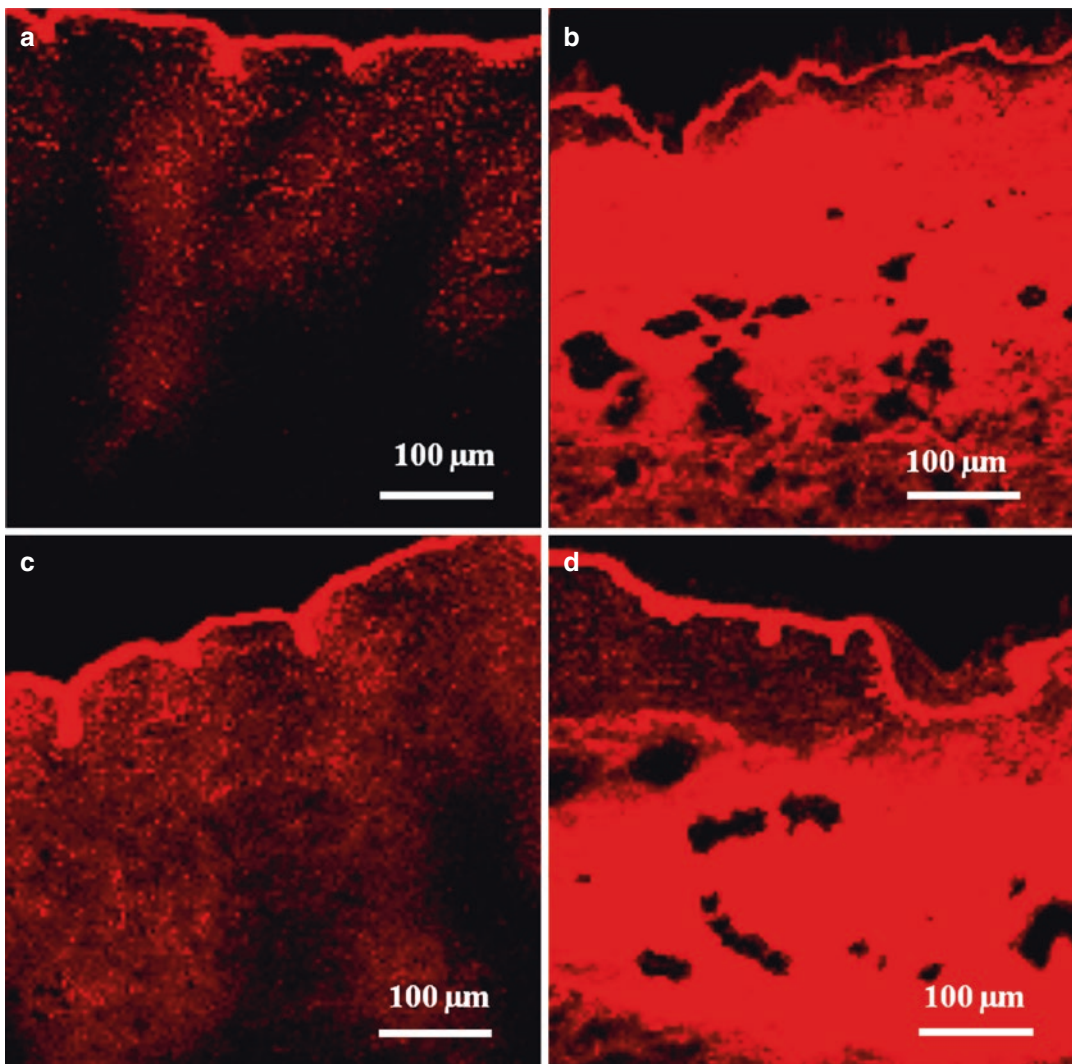


**Fig. 15.10** Fluorescent micrographs of cross-sections of human abdominal skin pretreated with Dermalroller® and incubated on a Franz diffusion cell with liposomes containing lipophilic fluorescent label DiI. The liposomes

were applied without occlusion for 3 h. (a) Control; (b) Model C 8 0.13–15°; (c) Model M 8 1.5–15°; (d) Model M 8 1.5–30°

tissue. The poor axial resolution results from the scattering of light by the specimen itself, which can lead to detection of light that is not generated from the observed focal plane. Also CLSM employs short wavelength excitation sources and shorter wavelengths are scattered stronger (scattering intensity is inversely proportional to fourth power of the wavelength) hence these excitation sources are not very efficient at deep tissue imaging.

Due to limitations in deep tissue imaging, when adopting a CLSM for imaging skin, the sample must be cryo-sectioned and this is not always possible and desirable.

Multiphoton excitation phenomenon was proposed in 1931; however, Kaiser and Garret were able to validate it only in 1961 after the development of lasers which were sufficiently powerful to generate the high photon flux required for two-photon excitation. Figure 15.11a explains the

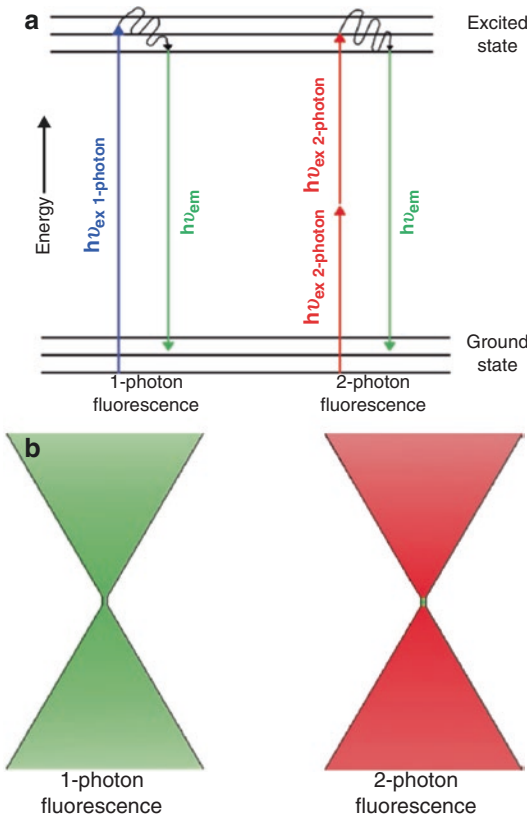


**Fig. 15.11** (a) Jablonski diagram elucidating the differences between single photon fluorescence and two photon fluorescence phenomenon. (b) Excitation volume in one-photon and two-photon fluorescence phenomena

energy transfer during one-photon and two-photon excitation. In single-photon fluorescence, the fluorescence photon is generated when a high energy photon is incident on the fluorophore, which results in raising the energy level of one of the electrons to an excited state. In two-photon excitation, if two low energy photons arrive together within  $10^{-18}$  s of one another, the combined energy transfer of the two low energy photons is sufficient to raise the same electron to a higher energy level (Dunn and Young 2006). A low energy photon is too weak to illicit the two-photon fluorescence phenomenon in the fluorophore. Hence, in order to increase the probability of simultaneous incidence of photons a laser with very high photon flux is required. Setup of a two-photon microscope is quite similar to that of a

confocal scanning microscope with two major differences. One is the light source, two-photon microscopes use a tunable Ti-sapphire high frequency pulsed laser which has a pulse length of approximately a few hundred femtoseconds. The second important difference is the lack of any pinholes in front of the detector to avoid detecting scattered light from out of focus plane.

One of the important advantages of 2-PFM is that total energy delivered to the specimen is much lower as compared to a CLSM. Also the two-photon excitation phenomenon occurs only at a very small focal volume (Fig. 15.11b) and as a result fluorophores in a very small volume of the specimen are excited, which reduces the probability of photo-bleaching, photo-damage. In addition, no confocal pinhole aperture is required to block the scattered light from out of focus planes. The near-infrared (NIR) light source used in a 2-PFM is very efficient at imaging deeper regions of the biological samples, as it is least scattered and absorbed by the biological samples. These advantages mean that the skin samples can be studied without cryofixing and cutting.

Disadvantages of a two-photon microscope include a relatively high price of the ultra-short pulsed Ti-sapphire lasers and the fact that they require an elaborate cooling system. Also, 2-PFM has lower lateral resolution compared to CLSM, but in practice the difference in their resolution is not significant.

### 15.3.2 Application of Two-Photon Microscopy in Skin Penetration Experiments

Carrer et al. used 2-PFM to study the architecture and physical properties of the pig skin epidermis and permeability of different liposomal formulations in the pig skin (Carrer et al. 2008). In this study, authors were able to easily distinguish different layers of the pig epidermis based on their morphological differences without any significant sample preparation. To study the hydration/polarity of different layers of the

epidermis they used Laurdan generalized polarization (Laurdan-GP) values as an indicator of polarity. As expected, the Laurdan-GP values were highest for SC and decreased for deeper layers of the skin indicating an increase in fluidity or hydration. The authors report an interesting observation in the intercluster region (canyons or wrinkles as in human skin), the Laurdan-GP values in the canyons were quite high, comparable to that of SC, and they did not change with depth (from surface of SC to dermis), indicating that canyons might show environment similar to SC. To study the penetration of liposomal formulations, Lissamine rhodamine B 1,2-dihexadecanoyl-*sn*-glycero-3-phosphoethanolamine was incorporated in the liposomal membrane. After 16-h diffusion, image stacks were collected and penetration was measured in the form of ratio of fluorescence intensity of rhodamine and autofluorescence of the skin. Authors report that the liposomes with lower lipid content (10 mg/ml) were able to deliver more fluorescent label to the lower parts of viable epidermis compared to the formulations with higher lipid content (25 and 50 mg/ml).

van den Bergh et al. elucidated the mechanism of interactions of elastic and rigid liposomal vesicles with human skin (van den Bergh et al. 1999). Using 2-PFM and different electron microscopic techniques they studied interactions between skin and various elastic liposomal formulations to understand the modulation of the skin barrier. They observed that fluorescently labeled elastic vesicles primarily affected the intercellular lipid lamellae of the SC, while the underlying layers of the viable epidermis remained relatively unchanged. This effect was visualized using 2-PFM, in the form of small penetration pathways that were confined to the SC only. Authors also reported that the penetration enhancing ability of elastic vesicles was dependent on whether vesicles were applied with or without occlusion.

Oleic acid is a good penetration enhancer and has been found to increase transdermal penetration of both hydrophilic and hydrophobic drugs by modulating the intercellular lipid domains in

the SC. Yu et al. used a high-speed two-photon microscope with dual channels capable of simultaneous monitoring of autofluorescence of skin and fluorescence from rhodamine as a model drug (Yu et al. 2003). Treatment of human skin with oleic acid as a penetration enhancer was found to induce increased intra-corneocyte diffusion of the hydrophilic model drug (sulforhodamine-B), while causing localization of the hydrophobic model drug (Rhodamine-B hexyl ester) to the intercellular region. Hence, Yu et al. provided evidence that for chemical penetration enhancers, intra-corneocyte diffusion is an important enhancement mechanism along with fluidization of intercellular lipid domains, and physicochemical properties of the drug would determine which pathway predominates in the penetration enhancement.

In 2002, Jenlab GmbH introduced a dual-channeled noninvasive multi-photon tomograph capable of *in vivo* optical biopsies with subcellular spatial resolution based on near-IR femtosecond pulsed laser. König et al. reported the potential of this microscope to acquire high-resolution images from deep within the skin *in vitro* and *in vivo* (König et al. 2006; Schenke-Layland et al. 2006). The microscope utilized the second harmonic generation (SHG) signal to monitor the position of the microscope in the skin, while the fluorescence channel was used to detect either autofluorescence from the NAD(P)H, flavins, melanin, etc., or to detect exogenous fluorophores. *In vivo* imaging capabilities of 2-PFM promises great advances in cancer diagnostics and skin diseases, as well as in understanding the mechanisms involved in dermal drug delivery.

2-PFM is, as already mentioned, a relatively young technology. Bio-Rad Laboratories (USA) introduced the first commercial two-photon microscope in 1996 and since then this technology has seen exponential growth in its use and applications. Its ability to take high-resolution optical biopsies of the intact skin or even do live imaging *in vivo* holds a great potential to unlock the secrets that were kept in the dark by nature.

## 15.4 Confocal Raman Microscopy

### 15.4.1 Principles of Raman Microscopy

Fluorescence microscopy has seen a lot of evolution in the last couple of decades and modern microscopic techniques, like CLSM, multi-photon microscopy, and various imaging modes such as fluorescence life-time imaging, Förster resonance energy transfer, etc., have increased the applications and flexibility of the fluorescence imaging. However, fluorescence microscopy still has certain disadvantages; mainly, fluorescence microscopy still utilizes exogenous dyes to label the drug or formulation. These labels are often toxic or could cause perturbations in the cells or other physiological processes. The biggest limitation for studying skin penetration is that often the fluorescent label and the formulation or the drug do not travel together and consequently fluorescence imaging could give incorrect interpretation of the observations.

Due to the disadvantages of fluorescent labeling to monitor the penetration depth in the skin, label-free vibrational spectroscopic techniques have gained importance. Vibrational spectroscopy is an identification technique based on the principle that it is possible to interfere with the vibrational state of a molecule by irradiating it with light of certain frequencies. Such interactions can be recorded in the form of spectra which are representative of the bonds present in the molecule. Because each molecule has its unique atomic structure and as a result a characteristic vibrational state, the vibrational spectra can provide a host of information about the structure of the molecule. Vibrational spectroscopy involves different techniques such as mid infrared (IR) spectroscopy, NIR spectroscopy, Raman spectroscopy, etc., but for this chapter we shall only review the Raman spectroscopic techniques. In addition, because water content in the biological specimen interferes strongly with IR spectroscopy, Raman techniques are more suitable for studying the drug penetration into the skin.

When a monochromatic beam of light is incident on the sample, most of the light is scat-

tered by the sample such that the scattered light has the same wavelength as the incident light; this phenomenon is known as elastic scattering or Rayleigh scattering. However, a small fraction of photons do interact with the molecules of the sample and as a result, scattered photons have a different energy compared to the incident photons which manifests in the form of a shift in the wavelength of the scattered photons. This phenomenon is known as inelastic scattering or Raman scattering. Raman effect was first observed by C.V. Raman in 1928 (Raman and Krishnan 1928). It is a very weak phenomenon, about one photon undergoes Raman scattering in a million Rayleigh scattered photons. Due to low signal to noise ratio, Raman spectroscopic techniques were not very practical as they needed an intense source of light and a sophisticated detection system. After the discovery of lasers and charged coupled detectors (CCD), however, Raman spectroscopy has seen tremendous increase in its application (Hollricher 2011).

To understand the Raman effect, we shall first have a look at the Rayleigh scatter. According to the classical theory, when photons are incident on the sample, they are absorbed by the molecules of the sample and are excited to a virtual state. When molecules relax back, if they relax to the same energy level as they started in, the emitted photons have the same energy as the incident photons and this type of scattering is called Rayleigh scattering. This effect is explained schematically in Fig. 15.12. In Raman scattering, a molecule relaxes back to a higher energy level after absorbing a photon, and as a result the emitted photon has lower energy by an amount required to vibrationally excite the molecule. Reemitted photon exhibits red shift and hence this effect is also called 'Stokes Raman scattering'. If after absorbing the photon the molecule loses a fraction of vibrational energy, i.e., if the molecule relaxes back to a lower energy state compared to its energy state before absorbing the photon, then the emitted photon has higher energy compared to the incident photon. This phenomenon is called the 'anti-stokes Raman scattering'. Raman spectrum is a plot of

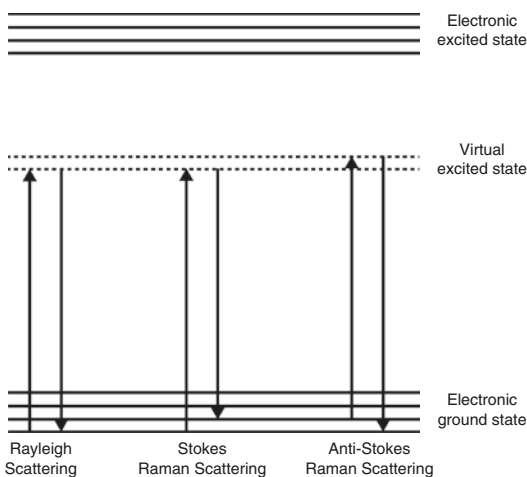


**Fig. 15.12** Jablonski diagram representation of Rayleigh and Raman scattering

wavenumber shifts observed between Raman radiation and excitation radiation. Raman effect and fluorescence are distinct phenomena, in the latter, incident photons are absorbed and molecules transition from ground state to an electronic excited state due to the resonance between the vibrational frequency of the molecule and incident photons. As a result for a given molecule, fluorescence can be observed only at a certain fixed frequency range. However, Raman effect is not a resonant effect and can take place for a wider range of excitation wavelengths. In addition, fluorescence phenomenon lasts much longer in terms of few nanoseconds, while Raman scattering is much short lived, i.e., less than a picosecond.

In modern Raman microscopes, the light source is provided by a laser and is focused onto the sample with the help of an objective with high numerical aperture. Scattered light is collected by the same objective and passed through a dichroic mirror then to a spectrometer to resolve the Raman shifts, which are detected by a sensitive CCD camera. The Raman map of the sample is usually generated by scanning the sample with the help of a piezo driven stage through the laser beam. In order to improve the signal to noise ratio, most microscopes employ a confocal detection to reduce the scattered light from out of focus planes. Raman scattering intensity is pro-

portional to the fourth power of the frequency of incident photons. Hence, excitation at 400 nm would give a 16 times more intense Raman signal compared to excitation at 800 nm (Hollricher 2011). However, skin has a very strong autofluorescence in the range of 400–700 nm and hence lower wavelengths are not ideal for Raman mapping of the skin. Although Longer wavelengths are useful for imaging thick specimen, in a diffraction-limited system they are also associated with lower spatial resolution. As a result, selecting the right wavelength of excitation is very important in order to maintain a good balance between resolution and signal quality. For collecting Raman spectra from skin, usually lasers with wavelength of 633, 660, or 785 nm are preferred.

#### 15.4.2 Confocal Raman Microscopy for Skin Penetration Experiments

There are several studies which report application of confocal Raman microscopy (CRM) in determining the penetration of various ingredients into the skin, such as retinol (Failloux et al. 2004; Forster et al. 2011; Mélot et al. 2009), dimethyl sulfoxide (Caspers et al. 2002), water (Caspers et al. 2000), urea (Wascotte et al. 2007), 5-fluorouracil (Zhang et al. 2007), etc. Xiao et al. demonstrated the ability of CRM to study and understand the penetration mechanism of phospholipids from liposomal formulations, in pig skin (Xiao et al. 2005). Penetration of two liposomal formulations was tested, liposomes in gel crystalline state were prepared from 1,2-dipalmitoyl (d62)-sn-glycero-3-phosphocholine (DPPC-d62), while liposomes in liquid crystalline state were prepared from 1-palmitoyl(d31)-2-oleoyl-sn-glycero-3-phosphocholine (P-d<sub>31</sub>OPC). After the application of liposomes to pig skin, Raman spectra were obtained using a CRM employing laser at 785 nm and spectra were recorded in the region of 100 – 3450 cm<sup>-1</sup>. Exogenous phospholipids were monitored by observing the CD<sub>2</sub> and CD<sub>3</sub> stretching vibration bands at 2080 and 2220 cm<sup>-1</sup>, respectively, while the skin was moni-

tored using the Phenylalanine-ring breathing mode at  $1004\text{ cm}^{-1}$  and the amide-I band at  $1652\text{ cm}^{-1}$ . The results indicated that the liquid state phospholipid P-d<sub>31</sub>OPC penetrated 40–48  $\mu\text{m}$  deep into the skin as compared to the gel state phospholipid DPPC-d<sub>62</sub>, which was found to penetrate only 10–15  $\mu\text{m}$  deep.

We reported a method for recording depth profiles using CRM in excised human skin biopsies to study diffusion patterns of drugs and components of the formulation system (Ashtikar et al. 2012). Figure 15.13 shows a XZ-penetration profile, where every pixel represents intensity of Raman signal obtained from intact human skin treated with deuterated invasomes (P-d<sub>31</sub>OPC). The depth profile scans (XZ-scans) were collected using WITec Alpha 300R CRM. Excitation was provided by 785 nm laser and step size for collecting the depth profiles was 1  $\mu\text{m}$  with illumination time of 0.5s/spectra. In Fig. 15.13b, the penetration profile of deuterated phospholipid is plotted as a gradient from red to yellow, where the red color corresponds to the highest concentration of P-d<sub>31</sub>OPC. The protein distribution of the skin is plotted in blue. Spectra corresponding to the invasomes and stratum corneum are represented in Fig. 15.13c. The penetration profile was constructed using spectral un-mixing algorithm,

vertex component analysis, which decomposes a given dataset into fractions of most dissimilar spectral information and reconstructs the image by plotting their individual abundances (Du et al. 2008; Winter 1999). P-d<sub>31</sub>OPC penetrated to a depth of  $\sim 10\text{--}15\text{ }\mu\text{m}$  after application of flexible invasomes; also it was interesting to note that the penetration profile of the phospholipid was not uniform throughout the stratum corneum.

Retinol is a common ingredient of the anti-aging creams, which is highly lipophilic and does not penetrate the skin very well. Raman microscopy is widely employed for studying penetration profiles of retinol as it has a characteristic Raman peak at  $1594\text{ cm}^{-1}$ , which can easily be traced through the various layers of the skin. In vitro penetration profile of retinol in human skin biopsies was studied by Failloux et al. using CRM. They have reported that retinol penetrated the SC faster when it was applied in the form of microspheres as compared to an oil in water emulsion (Failloux et al. 2004). Förster et al. studied the penetration of retinol from various emulsions and also monitored penetration of oil and aqueous components of the emulsion by using D(26)-n-dodecane and deuterated water, respectively. Their results show that retinol penetration from an emulsion depends on the nature

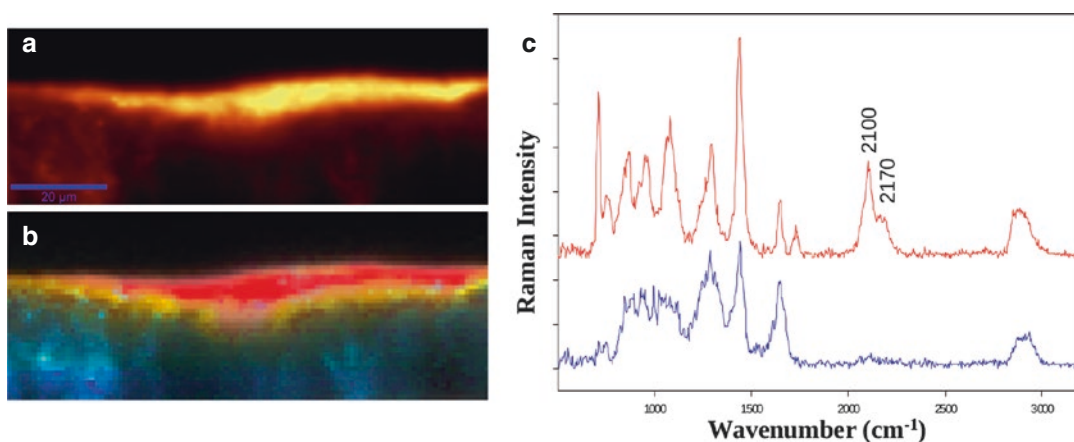


**Fig. 15.13** XZ-profiles recorded on a full thickness human skin treated with deuterated invasomes. (a) Raman map generated by integrating C-H stretching intensities from 2800 to  $3100\text{ cm}^{-1}$ . (b) False color image showing dissimilar spectral mixing. Red color represents highest

C-D signal and while-blue represents signal from endogenous skin tissue. (c) The red spectra on the right are representative of the applied P-d<sub>31</sub>OPC while blue spectra are representative of the skin. Peaks at 2100 and  $2170\text{ cm}^{-1}$  represent C-D stretching vibrations



of the surfactant used and that an emulsified retinol can penetrate deeper in the skin, while micellar retinol is localized in the SC (Forster et al. 2011). Mélot et al. studied the effect of penetration enhancers to deliver retinol into human skin *in vivo*. The *in vivo* measurements were carried out using an inverted Raman microscope customized for fast *in vivo* spectral acquisition from volar forearm. Formulations containing penetration enhancers like oleic acid, polyethylene glycol showed to have improved penetration of retinol into SC after 6 h of application time (Mélot et al. 2009).

Caspers et al. used CRM to study the interactions between human skin and dimethyl sulfoxide (DMSO) *in vivo* (Caspers et al. 2002). DMSO shows strong C-S-C symmetric and asymmetric vibration modes at 671 and 702  $\text{cm}^{-1}$ , while the position of the microscope in the skin was determined using the natural moisturizing factor to protein ratio (NMF, 885 & 1415  $\text{cm}^{-1}$ ). Authors reported that DMSO penetrated the SC within 20 min, however traces of DMSO could be found in the SC even after 72 h. Caspers et al. also reported the use of CRM for monitoring *in vivo* water profiles in the SC. Water content at various depths was determined by calculating the ratio of the water intensities (3350–3550  $\text{cm}^{-1}$ ) and protein intensities ( $\text{CH}_3$  stretching mode 2910–2965  $\text{cm}^{-1}$ ). Chrit et al. also reported application of CRM for *in vitro* and *in vivo* measurement of water in human skin, and they were able to demonstrate the hydration efficiency of a cosmetic product containing hydrating polymers in microcapsules (Chrit et al. 2007).

CRM was used to follow the penetration of metronidazole dissolved in diethylene glycol monoethyl (Transcutol®, Gattefossé, France) in human skin (Tfayli et al. 2007). Metronidazole was tracked in the skin by monitoring ( $\nu$  C-N) stretching vibrations at 1191 and 1369  $\text{cm}^{-1}$ , while the skin proteins were tracked from the amide-I, amide-III, Phenylalanine-ring breathing mode and other weaker spectral features. Spectra were collected from full thickness skin 1 and 2 h after the application of metronidazole solution at different *z*-planes with 4  $\mu\text{m}$  steps. Maximum penetration depth achieved for metronidazole

was  $\sim 25 \mu\text{m}$  in the SC. Several changes were noted in the Raman shifts for C-H vibration bands associated with skin endogenous proteins and lipids. Zhang et al. took advantage of differences in the Raman spectra of 5-fluorouracil (5-FU) and the prodrug of 5-FU (1-ethoxycarbonyl-5-fluorouracil) to determine the spatial distribution and the transformation of prodrug to 5-FU in skin (Zhang et al. 2007).

---

## 15.5 Coherent Raman Microscopy

In spontaneous Raman microscopy, images are recorded using the mapping mode where Raman spectra from each point on the sample are collected. Due to the inherent weak nature of the Raman scattering, acquisition of such images can take several hours. This is a problem for biological samples as they can undergo dehydration or photo damage due to high exposure to the intense laser radiation. Today several variants of Raman microscopy are available, such as coherent anti-Stokes Raman scattering microscopy (CARS), stimulated Raman scattering microscopy (SRS), surface-enhanced Raman scattering (SERS), etc., which have an advantage of higher S/N ratio. In this part, we would like to introduce CARS and SRS in brief with some examples of their application in transdermal delivery research, but it is out of scope of this book to go in depth into the principles and instrumentation of these techniques; further references can be found elsewhere (Chabay et al. 1976; Cheng 2007; Eesley 1981; Nandakumar et al. 2009; Scholten and Scholten 1989; Scholten et al. 1989).

CARS and SRS are nonlinear enhancement techniques, which enhance the weak Raman signal and as a result reduce the imaging duration to a few minutes or even seconds (Hanson and Bardeen 2009). In both techniques the molecular vibrations are excited by using a Stokes and pump laser beams. CARS is a complex process in which three laser beams Stokes ( $\omega_s$ ), pump ( $\omega_p$ ), and probe ( $\omega_{pr}$ ) interact with the sample to generate anti-stokes emission. When difference in the  $\omega_s$  and  $\omega_p$  frequencies approach the vibrational frequency of a molecular bond ( $\omega_v$ ), such that

$\omega_v = \omega_p - \omega_s$ , the electrons in the electron cloud around the molecular bond are in the virtual excited vibrational state. Such vibrational excitations only take place in small focal volume where both Stokes and pump beams are coherently in phase. To probe the virtual excitations, a third beam ( $\omega_{pr}$ ) is applied, which gets scattered off and generates anti-Stokes radiation ( $\omega_{as}$ ) modulated at difference frequency such that  $\omega_{as} = \omega_{pr} + (\omega_p - \omega_s)$  (Min et al. 2011). The emitted photon is blue shifted and as a result can be easily separated from the incident laser beams. Due to the nature of the excitation source of CARS microscope, it also generates 2-photon fluorescence and second harmonic generation (SHG) signal, and a multimodal detection system could be employed to detect these signals (Le et al. 2007; Potma et al. 2001; Wang et al. 2008).

The capability to identify endogenous and exogenous components by a multimodal-imaging mode is demonstrated in Fig. 15.14, which shows CARS, SHG, and 2-photon fluorescence signals collected from a human skin cross-section (Heuke et al. 2012). Figure 15.14a shows the anti-stokes Raman shifts recorded for C-H

stretching mode at  $2850\text{ cm}^{-1}$ , which are mainly generated by the intercellular lipids and adipocytes. Figure 15.14b shows the SHG signal, which is generated mainly from the collagen fibers of the dermis. Figure 15.14c shows 2-photon fluorescence detected at 435–485 nm, and Fig. 15.14d shows a false color image generated by overlapping all the signals, where CARS signal is represented as green, SHG as white, and two-photon fluorescence as red.

In vivo real-time video-rate epi-CARS (back-scattered CARS) imaging was demonstrated by Evans et al. on anesthetized female mice (Evans et al. 2005). The excitation source was tuned in order to excite the  $\text{CH}_2$  stretching vibrations and anti-Stokes photons were detected with the help of a sensitive PMT detector. The microscope had lateral resolution of  $0.3\ \mu\text{m}$  and axial resolution of  $1.5\ \mu\text{m}$ . Authors were able to image the mouse skin at various depth up to  $100\ \mu\text{m}$  and identified lipid rich structures such as sebaceous glands and adipocytes. Real time diffusion of the topically applied mineral oil was also observed in the mouse skin. The mineral oil penetrated the SC within 20 min, however it remained confined to

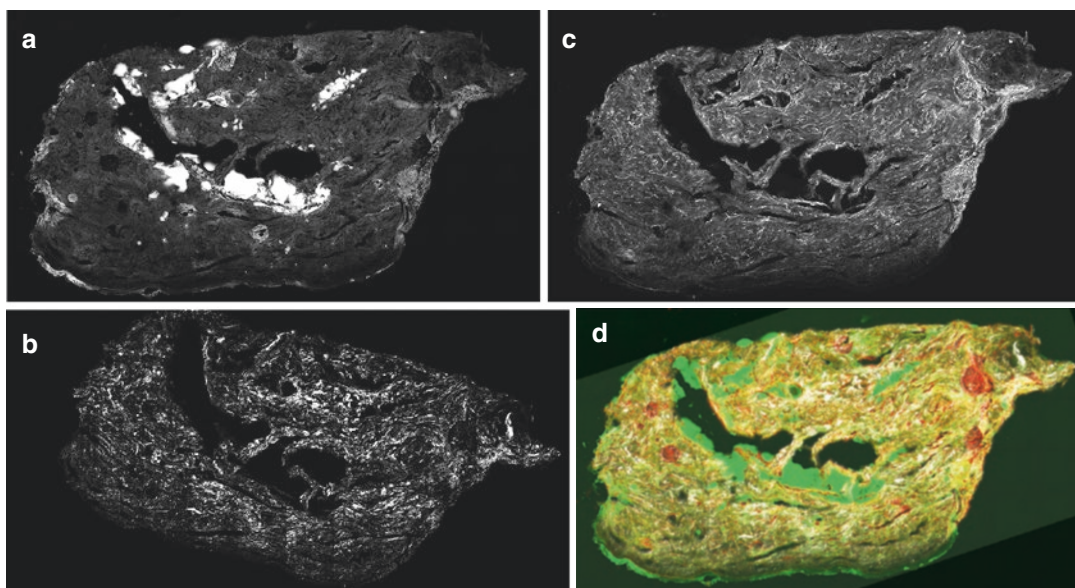


**Fig. 15.14** Multimodal CARS image of an untreated skin cross-section to demonstrate the scope of multimodal microscopy. (a) CARS map for  $\text{CH}_2$  symmetrical stretching vibrations, (b) SHG image, and (c) two-photon fluo-

rescence image. (d) False color image showing overlap of CARS (green), SHG (white), and two-photon fluorescence (red) signals

the viable epidermis and was not able to penetrate the dermis. Zimmerley et al. used CARS microscopy to generate quantitative concentration maps of deuterated water and d-glycine in human hair (Zimmerley et al. 2009), while Breunig et al. demonstrated application of in vivo multimodal CARS microscopy in healthy and diseased human skin (Breunig et al. 2012). In healthy human skin, they were able to follow a topically applied emulsion cream, while in skin affected with psoriasis they were able to identify differences in the SC intercellular lipid domains compared to the healthy skin.

CARS microscopy is more sensitive than spontaneous Raman microscopy; however, it has some drawbacks such as the presence of non-resonant background and more importantly anti-Stokes shifts are slightly different from Stokes Raman shifts, which makes spectral interpretation more complicated. In SRS, pump beam and Stokes beam coincide the sample such that difference in the frequencies between Stokes and pump-beams matches a molecular vibration. This results in an increase in the rate of molecular vibrations. The energy required for this excitation is taken up from the pump laser field and as a result pump beam experiences loss in intensity (stimulated Raman loss). Stokes beam experiences a gain in intensity due to the emission of Stokes photons as the molecular vibrations return to ground state (stimulated Raman gain). In SRS microscopy, either stimulated Raman loss or gain can be used as a contrast mechanism (Min et al. 2011; Nandakumar et al. 2009). Using SRS microscopy, Saar et al. were able to determine penetration profiles of ibuprofen and ketoprofen from solutions in propylene glycol applied topically onto mouse skin (Saar et al. 2011). Ketoprofen was tracked in the skin by following the aromatic C-H stretching vibrations at  $1599\text{ cm}^{-1}$ , ibuprofen and propylene glycol were deuterated and were monitored at  $2120\text{ cm}^{-1}$ , while skin lipid architecture was imaged from  $\text{CH}_2$  stretching vibrations at  $2845\text{ cm}^{-1}$ . Ketoprofen and propylene glycol penetrated the SC mainly via intercellular lipid pathways and through hair follicles. From time resolved images at various depths, the authors showed that propylene glycol penetrated deeper

and faster than ketoprofen into the skin. In addition, penetration of propylene glycol via hair follicle was much faster and reached a steady state in less than 30 min compared to  $\sim 2\text{ h}$  via intercellular lipid penetration in the SC to reach similar levels. Penetration profiles of ibuprofen were similar to that of ketoprofen. Ibuprofen crystals on the surface of the SC during penetration also indicated faster penetration of the solvent propylene glycol compared to ibuprofen. Freudiger et al. reported application of SRS microscopy to construct three-dimensional diffusion profiles of DMSO and retinoic acid in mouse skin. From the diffusional profiles they were able to show that DMSO mainly penetrated the SC via the protein phase while retinoic acid penetrated mainly via the lipid rich intercellular spaces (Freudiger et al. 2008).

Coherent Raman microscopy is a label-free and more sensitive approach of tapping into the advantages of Raman effect compared to the spontaneous Raman microscopy. Due to the enhancement of the Raman effect, the image acquisition is much faster and hence more suitable for biological samples compared to spontaneous Raman microscopy. Also the nonlinear excitation approach in the generation of CARS and SRS signal is limited to a very small focal volume, which increases the resolution of these techniques without using the confocal detection setup. CARS and SRS microscopic techniques are relatively young compared to other techniques discussed here. Today these microscopes are mainly confined to the photonics labs; however, both the techniques hold a great promise for mainstream applications.

## Conclusion

Microscopic techniques are very important in understanding the mechanisms involved in skin penetration as they enable spatial visualization of the drug in the skin. In this chapter, we report almost 50 years of development in the microscopic techniques and at least today, no technique holds superiority in all the aspects of imaging such as resolution, signal quality, specificity, speed, sample preparation, sample stability, etc. These are rather complementary

techniques, which are able to provide a host of information according to the requirements and objectives of the experiments. For skin penetration experiments, 2-PFM was first to set high standards owing to its ability to acquire high-resolution optical biopsies, *in vitro* as well as *in vivo*. Raman microscopic techniques provide a unique opportunity for label-free imaging. With development of modern Raman variants like CARS and SRS microscopy, the signal to noise ratio has been greatly improved and high speed, label free, 3D imaging is now possible however the complex nature of these microscopes and expensive optics have limited their widespread application.

**Acknowledgment** Authors would like to acknowledge Prof. Dr. Benjamin Dietzek and Prof. Dr. Jürgen Popp from Institut für Photonische Technologien, Jena, Germany, for their cooperation in acquiring multimodal CARS images on the human skin cross-sections.

## References

- Addicks WJ, Flynn GL, Weiner N (1987) Validation of a flow-through diffusion cell for use in transdermal research. *Pharm Res* 4(4):337–341
- Agarwal R, Katare OP, Vyas SP (2000) The pilosebaceous unit: a pivotal route for topical drug delivery. *Methods Find Exp Clin Pharmacol* 22(2):129–133
- Alvarez-Roman R, Naik A, Kalia YN, Guy RH, Fessi H (2004) Skin penetration and distribution of polymeric nanoparticles. *J Control Release* 99(1):53–62. doi:10.1016/j.jconrel.2004.06.015
- Ashtikar M, Matthäus C, Krafft C, Popp J, Fahr A (2012) Non-invasive imaging of transdermal drug penetration profiles using Raman microscopy. 9th International conference and workshop on Biological Barriers – *in vitro* and *in silico* tools for drug delivery and nanosafety research, Saarland University, Saarbrücken, 29 Feb–9 Mar 2012
- Benfeldt E (1999) *In vivo* microdialysis for the investigation of drug levels in the dermis and the effect of barrier perturbation on cutaneous drug penetration. *Studies in hairless rats and human subjects. Acta Derm Venereol Suppl (Stockh)* 206:1–59
- Betz G, Imboden R, Imanidis G (2001) Interaction of liposome formulations with human skin *in vitro*. *Int J Pharm* 229(1–2):117–129
- Bhatia KS, Singh J (1999) Effect of linolenic acid/ethanol or limonene/ethanol and iontophoresis on the *in vitro* percutaneous absorption of LHRH and ultrastructure of human epidermis. *Int J Pharm* 180(2):235–250
- Bohm M, Luger TA (1998) The pilosebaceous unit is part of the skin immune system. *Dermatology* 196(1):75–79
- Bouwstra JA, Honeywell-Nguyen PL (2002) Skin structure and mode of action of vesicles. *Adv Drug Deliv Rev* 54(Suppl 1):S41–S55
- Breunig HG, Buckle R, Kellner-Hofer M, Weinigel M, Lademann J, Sterry W et al (2012) Combined *in vivo* multiphoton and CARS imaging of healthy and disease-affected human skin. *Microsc Res Tech* 75(4):492–498. doi:10.1002/jemt.21082
- Carrer DC, Vermehren C, Bagatolli LA (2008) Pig skin structure and transdermal delivery of liposomes: a two photon microscopy study. *J Control Release* 132(1):12–20. doi:10.1016/j.jconrel.2008.08.006
- Caspers PJ, Lucassen GW, Bruining HA, Puppels GJ (2000) Automated depth-scanning confocal Raman microspectrometer for rapid *in vivo* determination of water concentration profiles in human skin. *J Raman Spectrosc* 31(8–9):813–818. doi:10.1002/1097-4555(200008/09)31:8/9<813::AID-JRS573>3.0.CO;2-7
- Caspers PJ, Williams AC, Carter EA, Edwards HG, Barry BW, Bruining HA et al (2002) Monitoring the penetration enhancer dimethyl sulfoxide in human stratum corneum *in vivo* by confocal Raman spectroscopy. *Pharm Res* 19(10):1577–1580
- Chabay I, Klauminzer GK, Hudson BS (1976) Coherent anti-Stokes Raman spectroscopy (CARS): Improved experimental design and observation of new higher-order processes. *Appl Phys Lett* 28(1):27–29
- Chen M, Liu X, Fahr A (2010) Skin delivery of ferulic acid from different vesicular systems. *J Biomed Nanotechnol* 6(5):577–585
- Chen M, Liu X, Fahr A (2011) Skin penetration and deposition of carboxyfluorescein and temoporfin from different lipid vesicular systems: *in vitro* study with finite and infinite dosage application. *Int J Pharm* 408(1–2):223–234. doi:10.1016/j.ijpharm.2011.02.006
- Cheng JX (2007) Coherent anti-Stokes Raman scattering microscopy. *Appl Spectrosc* 61(9):197–208
- Chrit L, Bastien P, Biatry B, Simonnet JT, Potter A, Minondo AM et al (2007) *In vitro* and *in vivo* confocal Raman study of human skin hydration: assessment of a new moisturizing agent, pMPC. *Biopolymers* 85(4):359–369. doi:10.1002/bip.20644
- Dragicevic-Curic N, Grafe S, Albrecht V, Fahr A (2008) Topical application of temoporfin-loaded invasomes for photodynamic therapy of subcutaneously implanted tumours in mice: a pilot study. *J Photochem Photobiol B* 91(1):41–50. doi:10.1016/j.jphotobiol.2008.01.009
- Dragicevic-Curic N, Scheglmann D, Albrecht V, Fahr A (2009) Development of different temoporfin-loaded invasomes—novel nanocarriers of temoporfin: characterization, stability and *in vitro* skin penetration studies. *Colloids Surf B Biointerfaces* 70(2):198–206. doi:10.1016/j.colsurfb.2008.12.030
- du Plessis J, Ramachandran C, Weiner N, Müller DG (1994) The influence of particle size of liposomes on

- the deposition of drug into skin. *Int J Pharm* 103(3):277–282. doi:10.1016/0378-5173(94)90178-3
- Du Q, Raksuntorn N, Younan NH, King RL (2008) End-member extraction for hyperspectral image analysis. *Appl Opt* 47(28):F77–F84
- Dunn KW, Young PA (2006) Principles of multiphoton microscopy. *Nephron Exp Nephrol* 103(2):e33–e40
- Eesley GL (1981) Coherent Raman spectroscopy, GL Eesley (ed). Pergamon Press, Oxford/New York
- Evans CL, Potma EO, Puoris'haag M, Cote D, Lin CP, Xie XS (2005) Chemical imaging of tissue in vivo with video-rate coherent anti-Stokes Raman scattering microscopy. *Proc Natl Acad Sci U S A* 102(46):16807–16812. doi:10.1073/pnas.0508282102
- Failloux N, Baron MH, Abdul-Malak N, Perrier E (2004) Contribution of encapsulation on the biodisponibility of retinol. *Int J Cosmet Sci* 26(2):71–77. doi:10.1111/j.0412-5463.2004.00206.x
- Fang JY, Hsu LR, Huang YB, Tsai YH (1999) Evaluation of transdermal iontophoresis of enoxacin from polymer formulations: in vitro skin permeation and in vivo microdialysis using Wistar rat as an animal model. *Int J Pharm* 180(2):137–149
- Forster M, Bolzinger MA, Ach D, Montagnac G, Briancon S (2011) Ingredients tracking of cosmetic formulations in the skin: a confocal Raman microscopy investigation. *Pharm Res* 28(4):858–872. doi:10.1007/s11095-010-0342-0
- Freudiger CW, Min W, Saar BG, Lu S, Holtom GR, He C et al (2008) Label-free biomedical imaging with high sensitivity by stimulated Raman scattering microscopy. *Science* 322(5909):1857–1861. doi:10.1126/science.1165758
- Grams YY, Alaruiikka S, Lashley L, Caussin J, Whitehead L, Bouwstra JA (2003) Permeant lipophilicity and vehicle composition influence accumulation of dyes in hair follicles of human skin. *Eur J Pharm Sci* 18(5):329–336
- Grams YY, Whitehead L, Cornwell P, Bouwstra JA (2004) Time and depth resolved visualisation of the diffusion of a lipophilic dye into the hair follicle of fresh unfixed human scalp skin. *J Control Release* 98(3):367–378. doi:10.1016/j.jconrel.2004.05.010
- Hanson KM, Bardeen CJ (2009) Application of nonlinear optical microscopy for imaging skin. *Photochem Photobiol* 85(1):33–44. doi:10.1111/j.1751-1097.2008.00508.x
- Hashimoto K, Kagetsu N, Taniguchi Y, Weintraub R, Chapman-Winokur RL, Kasiborski A (1991) Immunohistochemistry and electron microscopy in Langerhans cell histiocytosis confined to the skin. *J Am Acad Dermatol* 25(6 Pt 1):1044–1053
- Heuke S, Ashtikar M, Matthäus C, Fahr A, Dietzek B, Popp J (2012) Coherent anti-stokes Raman scattering microscopy of human skin (Unpublished data)
- Hofland HE, van der Geest R, Bodde HE, Junginger HE, Bouwstra JA (1994) Estradiol permeation from non-ionic surfactant vesicles through human stratum corneum in vitro. *Pharm Res* 11(5):659–664
- Hofland HE, Bouwstra JA, Bodde HE, Spies F, Junginger HE (1995) Interactions between liposomes and human stratum corneum in vitro: freeze fracture electron microscopical visualization and small angle X-ray scattering studies. *Br J Dermatol* 132(6):853–866
- Hollricher O (2011) Raman instrumentation for confocal Raman microscopy. In: Dieing T, Hollricher O, Toporski J (eds) *Confocal Raman microscopy*, Springer Series in Optical Sciences. 158. Springer, Berlin/Heidelberg, pp 43–60
- Hollricher O, Ibach W (2011) High-resolution optical and confocal microscopy. In: Dieing T, Hollricher O, Toporski J (eds) *Confocal Raman microscopy*, Springer Series in Optical Sciences. 158. Springer, Berlin/Heidelberg, pp 1–20
- Jimbo Y, Ishihara M, Osamura H, Takano M, Ohara M (1983) Influence of vehicles on penetration through human epidermis of benzyl alcohol, isoeugenol and methyl isoeugenol. *J Dermatol* 10(3):241–250
- Kanerva L (1990) Electron microscopy of the effects of dithranol on healthy and on psoriatic skin. *Am J Dermatopathol* 12(1):51–62
- Kirjavainen M, Urtti A, Jaaskelainen I, Suhonen TM, Paronen P, Valjakka-Koskela R et al (1996) Interaction of liposomes with human skin in vitro--the influence of lipid composition and structure. *Biochim Biophys Acta* 1304(3):179–189
- Kirjavainen M, Urtti A, Monkkonen J, Hirvonen J (2000) Influence of lipids on the mannitol flux during transdermal iontophoresis in vitro. *Eur J Pharm Sci* 10(2):97–102
- Kobayashi D, Matsuzawa T, Sugibayashi K, Morimoto Y, Kimura M (1994) Analysis of the combined effect of 1-menthol and ethanol as skin permeation enhancers based on a two-layer skin model. *Pharm Res* 11(1):96–103
- Konig K, Ehlers A, Stracke F, Riemann I (2006) In vivo drug screening in human skin using femtosecond laser multiphoton tomography. *Skin Pharmacol Physiol* 19(2):78–88. doi:10.1159/000091974
- Kriwet K, Müller-Goymann CC (1995) Diclofenac release from phospholipid drug systems and permeation through excised human stratum corneum. *Int J Pharm* 125(2):231–242. doi:10.1016/0378-5173(95)00130-B
- Le TT, Langohr IM, Locker MJ, Sturek M, Cheng JX (2007) Label-free molecular imaging of atherosclerotic lesions using multimodal nonlinear optical microscopy. *J Biomed Opt* 12(5):054007. doi:10.1117/1.2795437
- Lieb LM, Ramachandran C, Egbaria K, Weiner N (1992) Topical delivery enhancement with multilamellar liposomes into pilosebaceous units: I. In vitro evaluation using fluorescent techniques with the hamster ear model. *J Invest Dermatol* 99(1):108–113
- Loftsson T, Somogyi G, Bodor N (1989) Effect of choline esters and oleic acid on the penetration of acyclovir, estradiol, hydrocortisone, nitroglycerin, retinoic acid and trifluorothymidine across hairless mouse skin in vitro. *Acta Pharm Nord* 1(5):279–286

- Mélot M, Pudney PDA, Williamson A-M, Caspers PJ, Van Der Pol A, Puppels GJ (2009) Studying the effectiveness of penetration enhancers to deliver retinol through the stratum corneum in vivo confocal Raman spectroscopy. *J Control Release* 138(1):32–39. doi:[10.1016/j.jconrel.2009.04.023](https://doi.org/10.1016/j.jconrel.2009.04.023)
- Min W, Freudiger CW, Lu S, Xie XS (2011) Coherent nonlinear optical imaging: beyond fluorescence microscopy. *Annu Rev Phys Chem* 62:507–530. doi:[10.1146/annurev.physchem.012809.103512](https://doi.org/10.1146/annurev.physchem.012809.103512)
- Murakami T, Yoshioka M, Yumoto R, Higashi Y, Shigeki S, Ikuta Y et al (1998) Topical delivery of keloid therapeutic drug, tranilast, by combined use of oleic acid and propylene glycol as a penetration enhancer: evaluation by skin microdialysis in rats. *J Pharm Pharmacol* 50(1):49–54
- Nandakumar P, Kovalev A, Volkmer A (2009) Vibrational imaging based on stimulated Raman scattering microscopy. *New J Phys* 11(3):033026
- Niemiec SM, Ramachandran C, Weiner N (1995) Influence of nonionic liposomal composition on topical delivery of peptide drugs into pilosebaceous units: an in vivo study using the hamster ear model. *Pharm Res* 12(8):1184–1188
- Ntimenou V, Fahr A, Antimisiaris SG (2012) Elastic vesicles for transdermal drug delivery of hydrophilic drugs: a comparison of important physicochemical characteristics of different vesicle types. *J Biomed Nanotechnol* 8(4):613–623
- Nwaneshiudu A, Kuschal C, Sakamoto FH, Anderson RR, Schwarzenberger K, Young RC (2012) Introduction to confocal microscopy. *J Invest Dermatol* 132(12), e3. doi:[10.1038/jid.2012.429](https://doi.org/10.1038/jid.2012.429)
- Patzelt A, Richter H, Knorr F, Schäfer U, Lehr C-M, Dähne L et al (2011) Selective follicular targeting by modification of the particle sizes. *J Control Release* 150(1):45–48. doi:<http://dx.doi.org/10.1016/j.jconrel.2010.11.015>
- Potma EO, de Boei WP, van Haastert PJM, Wiersma DA (2001) Real-time visualization of intracellular hydrodynamics in single living cells. *Proc Natl Acad Sci* 98(4):1577–1582. doi:[10.1073/pnas.98.4.1577](https://doi.org/10.1073/pnas.98.4.1577)
- Raman C, Krishnan K (1928) A new type of secondary radiation. *Nature* 121(3048):501–502. doi:[10.1038/121501c0](https://doi.org/10.1038/121501c0)
- Saar BG, Contreras-Rojas LR, Xie XS, Guy RH (2011) Imaging drug delivery to skin with stimulated Raman scattering microscopy. *Mol Pharm* 8(3):969–975. doi:[10.1021/mp200122w](https://doi.org/10.1021/mp200122w)
- Schatzlein A, Cevc G (1998) Non-uniform cellular packing of the stratum corneum and permeability barrier function of intact skin: a high-resolution confocal laser scanning microscopy study using highly deformable vesicles (Transfersomes). *Br J Dermatol* 138(4):583–592
- Schenke-Layland K, Riemann I, Damour O, Stock UA, König K (2006) Two-photon microscopes and in vivo multiphoton tomographs—powerful diagnostic tools for tissue engineering and drug delivery. *Adv Drug Deliv Rev* 58(7):878–896. doi:[10.1016/j.addr.2006.07.004](https://doi.org/10.1016/j.addr.2006.07.004)
- Schnetz E, Fartasch M (2001) Microdialysis for the evaluation of penetration through the human skin barrier - a promising tool for future research? *Eur J Pharm Sci* 12(3):165–174
- Scholten T, Scholten TAHM (1989) Coherent Anti-stokes Raman Scattering (CARS): technique and application to biophysical studies; the potentials of CARS microscopy
- Scholten TA, Lucassen GW, De Mul FF, Greve J (1989) Nonresonant background suppression in CARS spectra of dispersive media using phase mismatching. *Appl Opt* 28(7):1387–1400. doi:[10.1364/ao.28.001387](https://doi.org/10.1364/ao.28.001387)
- Schreiner V, Gooris GS, Pfeiffer S, Lanzendorfer G, Wenck H, Diembeck W et al (2000) Barrier characteristics of different human skin types investigated with X-ray diffraction, lipid analysis, and electron microscopy imaging. *J Invest Dermatol* 114(4):654–660. doi:[10.1046/j.1523-1747.2000.00941.x](https://doi.org/10.1046/j.1523-1747.2000.00941.x)
- Semwogerere D, Weeks ER (2008) Confocal microscopy. In: *Encyclopedia of biomaterials and biomedical engineering*. Informa Healthcare, New York, pp 705–714
- Simonetti O, Hoogstraate AJ, Bialik W, Kempenaar JA, Schrijvers AH, Bodde HE et al (1995) Visualization of diffusion pathways across the stratum corneum of native and in-vitro-reconstructed epidermis by confocal laser scanning microscopy. *Arch Dermatol Res* 287(5):465–473
- Tenjarla SN, Kasina R, Puranajoti P, Omar MS, Harris WT (1999) Synthesis and evaluation of N-acetylprolinate esters – novel skin penetration enhancers. *Int J Pharm* 192(2):147–158
- Tfayli A, Piot O, Pitre F, Manfait M (2007) Follow-up of drug permeation through excised human skin with confocal Raman microspectroscopy. *Eur Biophys J* 36(8):1049–1058. doi:[10.1007/s00249-007-0191-x](https://doi.org/10.1007/s00249-007-0191-x)
- Toutitou E, Godin B, Dayan N, Weiss C, Piliponsky A, Levi-Schaffer F (2001) Intracellular delivery mediated by an ethosomal carrier. *Biomaterials* 22(22):3053–3059
- Turner NG, Guy RH (1998) Visualization and quantitation of iontophoretic pathways using confocal microscopy. *J Invest Dermatol Symp Proc* 3(2):136–142
- van den Bergh BA, Vroom J, Gerritsen H, Junginger HE, Bouwstra JA (1999) Interactions of elastic and rigid vesicles with human skin in vitro: electron microscopy and two-photon excitation microscopy. *Biochim Biophys Acta* 1461(1):155–173
- van Kuijk-Meuwissen ME, Junginger HE, Bouwstra JA (1998a) Interactions between liposomes and human skin in vitro, a confocal laser scanning microscopy study. *Biochim Biophys Acta* 1371(1):31–39
- van Kuijk-Meuwissen ME, Mouglin L, Junginger HE, Bouwstra JA (1998b) Application of vesicles to rat skin in vivo: a confocal laser scanning microscopy study. *J Control Release* 56(1–3):189–196
- Vardaxis NJ, Brans TA, Boon ME, Kreis RW, Marres LM (1997) Confocal laser scanning microscopy of porcine skin: implications for human wound healing studies. *J Anat* 190(Pt 4):601–611

- Veiro JA, Cummins PG (1994) Imaging of skin epidermis from various origins using confocal laser scanning microscopy. *Dermatology* 189(1):16–22
- Verma D (2002) Thesis title: invasomes – novel vesicular carriers for enhanced topical delivery: characterization and skin penetration properties. Philipps-Universität Marburg, Marburg
- Verma DD, Fahr A (2004) Synergistic penetration enhancement effect of ethanol and phospholipids on the topical delivery of cyclosporin A. *J Control Release* 97(1):55–66. doi:[10.1016/j.jconrel.2004.02.028](https://doi.org/10.1016/j.jconrel.2004.02.028)
- Verma DD, Verma S, Blume G, Fahr A (2003a) Particle size of liposomes influences dermal delivery of substances into skin. *Int J Pharm* 258(1–2):141–151
- Verma DD, Verma S, Blume G, Fahr A (2003b) Liposomes increase skin penetration of entrapped and non-entrapped hydrophilic substances into human skin: a skin penetration and confocal laser scanning microscopy study. *Eur J Pharm Biopharm* 55(3):271–277
- Verma DD, Verma S, McElwee KJ, Freyschmidt-Paul P, Hoffmann R, Fahr A (2004) Treatment of alopecia areata in the DEBR model using cyclosporin A lipid vesicles. *Euro J Dermatol* 14(5):1–7
- Wang HW, Le TT, Cheng JX (2008) Label-free imaging of arterial cells and extracellular matrix using a multimodal CARS microscope. *Opt Commun* 281(7):1813–1822. doi:[10.1016/j.optcom.2007.07.067](https://doi.org/10.1016/j.optcom.2007.07.067)
- Wascotte V, Caspers P, de Sterke J, Jadoul M, Guy RH, Preat V (2007) Assessment of the “skin reservoir” of urea by confocal Raman microspectroscopy and reverse iontophoresis in vivo. *Pharm Res* 24(10):1897–1901. doi:[10.1007/s11095-007-9314-4](https://doi.org/10.1007/s11095-007-9314-4)
- Winter ME (1999) N-FINDR: an algorithm for fast autonomous spectral end-member determination in hyperspectral data. *Proc SPIE*. 266–75. doi:[10.1117/12.366289](https://doi.org/10.1117/12.366289).
- Xiao C, Moore DJ, Rerek ME, Flach CR, Mendelsohn R (2005) Feasibility of tracking phospholipid permeation into skin using infrared and Raman microscopic imaging. *J Invest Dermatol* 124(3):622–632. doi:[10.1111/j.0022-202X.2004.23608.x](https://doi.org/10.1111/j.0022-202X.2004.23608.x)
- Yarosh D, Bucana C, Cox P, Alas L, Kibitel J, Kripke M (1994) Localization of liposomes containing a DNA repair enzyme in murine skin. *J Invest Dermatol* 103(4):461–468
- Yu B, Kim KH, So PT, Blankschtein D, Langer R (2003) Visualization of oleic acid-induced transdermal diffusion pathways using two-photon fluorescence microscopy. *J Invest Dermatol* 120(3):448–455. doi:[10.1046/j.1523-1747.2003.12061.x](https://doi.org/10.1046/j.1523-1747.2003.12061.x)
- Zellmer S, Reissig D, Lasch J (1998) Reconstructed human skin as model for liposome-skin interaction. *J Control Release* 55(2–3):271–279
- Zhang G, Moore DJ, Sloan KB, Flach CR, Mendelsohn R (2007) Imaging the prodrug-to-drug transformation of a 5-fluorouracil derivative in skin by confocal Raman microscopy. *J Invest Dermatol* 127(5):1205–1209. doi:[10.1038/sj.jid.5700690](https://doi.org/10.1038/sj.jid.5700690)
- Zimmerley M, Lin C-Y, Oertel DC, Marsh JM, Ward JL, Potma EO (2009) Quantitative detection of chemical compounds in human hair with coherent anti-Stokes Raman scattering microscopy. *J Biomed Opt* 14(4):044019. doi:[10.1117/1.3184444](https://doi.org/10.1117/1.3184444)

# Clinical Cutaneous Drug Delivery Assessment Using Single and Multiphoton Microscopy

# 16

Anthony P. Raphael and Tarl W. Prow

## Contents

16.1	<b>Introduction</b> .....	283
16.2	<b>Cutaneous Applications of Single Photon Microscopy</b> .....	284
16.2.1	Characterization of Percutaneous Drug Delivery.....	284
16.2.2	Reflectance Microscopy for the Assessment of Therapeutic Changes in the Skin.....	287
16.3	<b>Applications of Multiphoton Microscopy</b> .....	290
16.3.1	Assessment of the Cutaneous Delivery of Nanoparticle Compounds Using Multiphoton Microscopy.....	292
16.3.2	Analysing the Skin's Metabolic Response to Drugs Using Multiphoton Microscopy Fluorescence Lifetime Imaging.....	295
16.4	<b>Advancements in Non-invasive Analysis of Drug Delivery to the Skin Using Multimodal Imaging</b> .....	298
	<b>Conclusion</b> .....	299
	<b>References</b> .....	300

## 16.1 Introduction

Due to the relative complexity of confocal microscope instrumentation, the techniques are more suited for drug delivery *ex vivo* and within small animal models. In particular, single photon microscopy-based techniques such as confocal laser scanning microscopy (CLSM) have been used to characterize enhanced percutaneous drug delivery (e.g. iontophoresis (Tomoda et al. 2012), biolistic particle delivery (Xia et al. 2011), microneedles (Prow et al. 2010), etc.). CLSM has also been used in a range of *in vivo* and *ex vivo* animal models including mice (Prow et al. 2010; Fernando et al. 2010; Chen et al. 2012; Raphael et al. 2010), rats (Ito et al. 2012) and pigs (Dubey and Kalia 2010; Lopez et al. 2011). Multiphoton microscopy (MPM) is an additional technique that results in high-resolution imaging within biological tissues at greater depths than single photon systems. MPM combined with fluorescence lifetime imaging (FLIM) (multimodal imaging) results in information on the progression of disease and metabolic changes within the skin. The combination of MPM-FLIM to visualize and assess specific drug–cell/tissue interactions is a powerful technique. Further, combinatorial technologies are being developed with a range of non-invasive techniques being integrated with current single and multiphoton microscopes (e.g. optical coherence tomography (OCT), photoacoustic spectroscopy and Raman spectroscopy).

A.P. Raphael • T.W. Prow (✉)  
Dermatology Research Centre, School of Medicine,  
The University of Queensland, Princess Alexandra  
Hospital, Translational Research Institute,  
Brisbane, QLD 4102, Australia  
e-mail: [t.prow@uq.edu.au](mailto:t.prow@uq.edu.au)



Although single and multiphoton microscopies have been well characterized within *ex vivo* and *in vivo* animal models, their use is yet to be established within clinical studies. The lack of clinical microscopy is due partly to ethical considerations such as the inability to apply for ethics (studies require clinician involvement) and shortage of volunteers. Even though many of the microscope systems being developed can be modified for *in vivo* work, it does not make them clinically suitable. Investigators are required to use independent microscope systems – one being for animal work and the other for human work. Another limitation to confocal microscopy is that the techniques often require fluorescent dyes that when conjugated to a drug change the drug's physical and chemical properties.

Even with the issues limiting the clinical analysis of percutaneous enhancers, there is much interest in the area. With advancement in microscopy and multimodal imaging techniques, it is expected that the clinical assessment of percutaneous drug delivery will become standard practice and important in determining the effectiveness of novel percutaneous drug delivery systems. This chapter focuses on single photon and multiphoton approaches that have been utilized *in vivo* within human skin addressing their advantages and limitations as potential techniques for the analysis of percutaneous penetration enhancers.

---

## 16.2 Cutaneous Applications of Single Photon Microscopy

The most relevant technique in relation to percutaneous penetration is the use of CLSM for *in vitro*, *ex vivo* and *in vivo* models. CLSM has the ability to restrict out-of-focus light, collecting only fluorescence signal from a single optical plane. Each plane is then processed computationally to construct three-dimensional images of the fluorescent signal. In particular, CLSM is extremely useful for observing spatial properties of molecules within cells and/or tissues, which is relevant to the field of pharmaceutical science and drug delivery (Agarwal et al. 2008; White and Errington 2005). However, the availability of

current *in vivo* CLSM systems are limited with the two major instruments being the Optiscan Stratum™, Optiscan Ltd., Australia (designed for fluorescence imaging), and the Vivascope® 1500 and 3000 series from Lucid Inc., USA, designed for reflectance imaging but also with fluorescence capabilities (Fig. 16.1). What distinguishes these clinical microscopes from those used in the laboratory for *ex vivo* and *in vitro* analysis are their small size and portability (both companies have hand-held scanning systems). Although the microscope size limits the room available for complex optics (i.e. the excitation and collection ability), it is expected that the continual development of compact optics and lasers will result in greater functionality and downstream use of such CLSMs.

### 16.2.1 Characterization of Percutaneous Drug Delivery

Percutaneous drug delivery encompasses many approaches from the simple passive diffusion of small compounds through to the active delivery of much larger macromolecules. The need for enhanced percutaneous penetration has been well-established, with a range of chemical and physical techniques being developed. CLSM has played and is continuing to play an important role in validating these techniques – visualizing the delivery and distribution within the skin (Prow et al. 2010; Fernando et al. 2010). For example, in Fig. 16.2 we show the difference in delivery profiles between topical and microneedle enhanced delivery of sodium fluorescein within volunteers. By averaging the signal intensity per optical section we were able to 'map' the delivery profiles in a cross-sectional manner. This is a powerful technique because it clearly shows the influence of enhanced percutaneous delivery giving insight into distribution and penetration of the payload.

Lademann et al. (2003) investigated the use of a hand-held CLSM designed for dermatology applications (Optiscan Stratum™, Optiscan Ltd., Australia) (Lademann et al. 2003). The device was designed to be relatively simple and portable

**Fig. 16.1** Volunteer being imaged with a hand-held in vivo reflectance confocal microscope (Vivascope 3000<sup>®</sup>, Lucid Inc., USA)



for ease-of-use within a clinical setting. The excitation source consisted of an argon ion laser with a wavelength of 488 nm specific for in vivo dyes curcumin or fluorescein. The two dyes were applied to male and female volunteers in either ethanol or sunscreen emulsion. Fluorescein application resulted in visualization of the different skin layers – stratum corneum, stratum granulosum, stratum basale and although of low resolution, the papillary dermis (Fig. 16.3). Lademann et al. hypothesized that using their CLSM system in conjunction with the fluorescein/ethanol solution, different skin layers could be distinguished between a healthy or diseased state (Lademann et al. 2003).

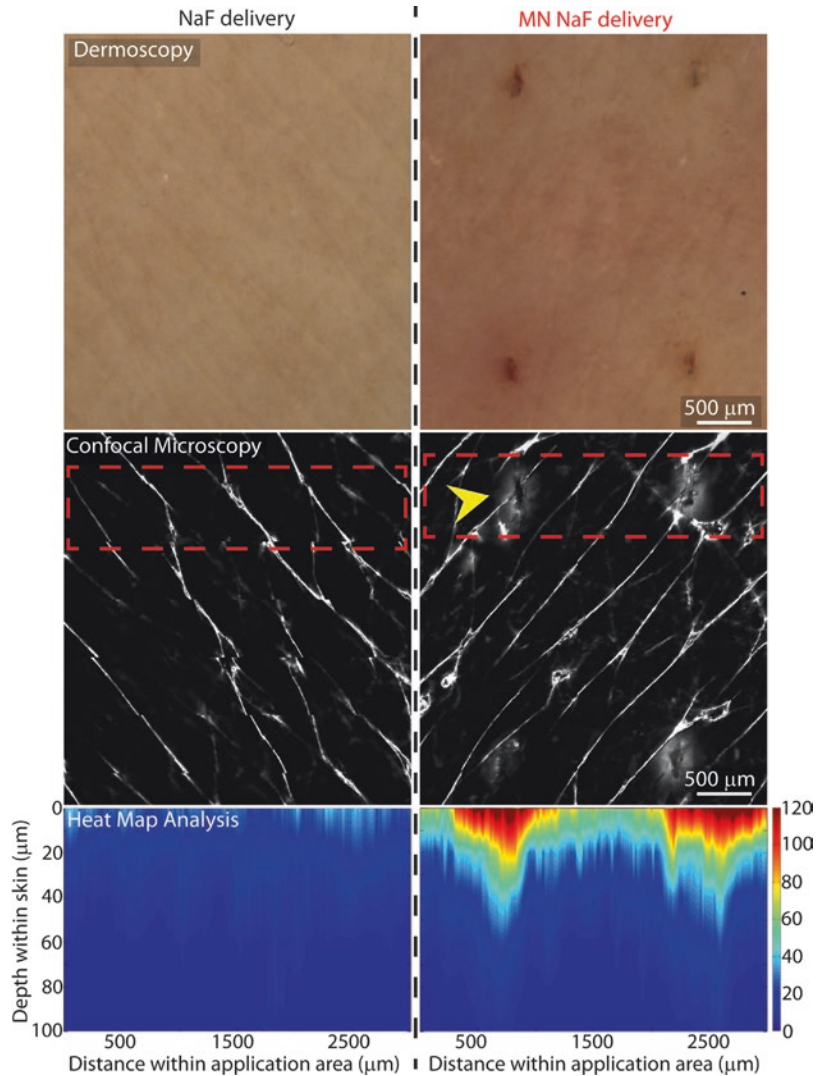
The curcumin/sunscreen emulsion was used to investigate potential penetration pathways and distribution of sunscreens within the skin. It was determined that the sunscreens accumulated around the edges of the corneocytes. Initially only the skin surface could be detected, however over time (20 min) three cell layers of the stratum corneum became visible. Additionally, the curcumin solution accumulated around the hair follicles and within the sweat glands. Interestingly, Lademann et al. were able to distinguish between active and passive sweat glands based on the distribution of the dye in or around the gland (Lademann et al. 2003). This study demonstrated that hand-held CLSMs have the potential for non-invasive clinical imaging.

The Optiscan Stratum<sup>TM</sup> has also been used as a validation tool assessing the penetration of

microneedles within volunteers (Mukerjee et al. 2004; Bal et al. 2010a, b). Mukerjee et al. developed hollow and solid microneedles up to 200  $\mu\text{m}$  in length with various diameters (Mukerjee et al. 2004). Solid microneedles were applied to the skin, near the first knuckle of the thumb followed by application of a 0.1% sodium fluorescein solution. The application of the sodium fluorescein solution without microneedles resulted in no dye solution penetrating through the stratum corneum. CLSM assessment of microneedle application resulted in the visualization of successful microneedle penetration to a depth of 160  $\mu\text{m}$ . Although no investigation was done on dye distribution and diffusion within the skin, the study showed that the application of Optiscan Stratum<sup>TM</sup> was a suitable technique for investigating the microneedle enhanced delivery of fluorescein.

In 2010, Bal et al. conducted a more in-depth microneedle study in volunteers using the delivery of fluorescein as a visual guide for characterizing the microneedle conduits and their closure over time (Bal et al. 2010a). Bal et al. also used the Optiscan Stratum<sup>TM</sup>. The microneedle array consisted of 5 microneedles, 300  $\mu\text{m}$  in length, 120  $\mu\text{m}$  in diameter and a spacing of 2 mm. Bal et al. investigated the two techniques of fluorescein – microneedle application by either applying the dye to the skin prior to or after microneedle administration. After each application CLSM was used to characterize the microneedle conduit. Dye application post microneedle piercing resulted in

**Fig. 16.2** Images showing the in vivo human delivery of sodium fluorescein (*NaF*) with and without microneedles (*MN*) using dermoscopy (*top panels*) and confocal laser scanning microscopy (*middle panels*). The bottom panels are a cross-sectional heat map representation of the average delivery profile (represented by *rectangular box*). *Arrow* indicates a microneedle deposition site



significantly higher signal than dye application prior to microneedles. Bal et al. concluded that the conduits closed within 10–15 min after microneedle application and that a depth of 150  $\mu\text{m}$  was achieved (suitable for macromolecules to reach the viable epidermis (Fig. 16.4a, b)).

More recently, Vergou et al. compared the use of transepidermal water loss (TEWL) and CLSM for the in vivo characterization of the stratum corneum barrier in volunteers (Vergou et al. 2012). Once again, this study was done using the Optiscan Stratum<sup>TM</sup>. TEWL is a relatively standard technique used to characterize the integrity of the epidermal barrier following disruption with percutaneous penetration enhancers.

However, TEWL measurements can be influenced by internal and external factors such as humidity, temperature and air convection. Additionally, TEWL is not reliable post drug application where the drug or chemical enhancer solution is still on the skin's surface. Vergou et al. assessed the barrier integrity prior to and post treatment of dry skin (without disease) with gel and oil products (Valeo Holundergel and Valeo Dehnungspflegeoel, L'estetic GmbH, Germany) designed to rehydrate the skin following radiotherapy treatment (Vergou et al. 2012). The gel was designed to penetrate the skin – increasing hydration – followed by the oil which formed a protective layer on the skin's surface to maintain

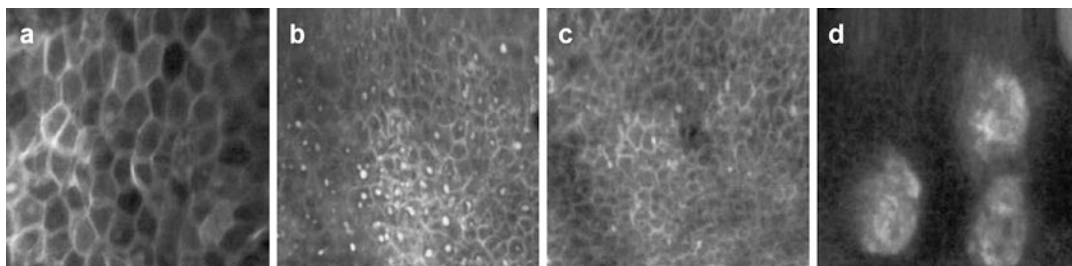


**Fig. 16.3** Confocal laser scanning microscopy of sodium fluorescein within the different layers of volunteer skin: (a) stratum corneum, (b) stratum granulosum, (c) stratum

basale, and (d) papillary dermis (Adapted from Lademann et al. (2003))

hydration. The products were applied twice daily on the volar forearm over a 4-week period. No treatment was done to the other arm.

Assessment was done prior, 2 weeks after and 4 weeks after application. The initial TEWL values were standardized to 100% between volunteers and it was determined that for all volunteers the TEWL for untreated skin remained constant ( $99 \pm 17\%$ ). The TEWL reading for the treated arm increased by  $21 \pm 27\%$  suggesting disruption of the epidermal barrier. However, stratum corneum hydration and elasticity experiments resulted in an average increase of 20% and 10%, respectively, indicating improved integrity of the epidermal barrier. CLSM showed a similar trend to the hydration and elasticity studies, where a distinct improvement in the integrity of the stratum corneum was observed. Prior to treatment the corneocytes showed an ‘irregular mountainous structure’. After the 4-week treatment, the corneocytes formed a flat honey-comb pattern surrounded by intact lipid layers. Vergou et al. hypothesized that even though TEWL is non-invasive, when placed on the skin surface it disrupted the protective oil layer resulting from the treatment. Accumulated water from the gel treatment was then detected by TEWL (Vergou et al. 2012). This resulted in higher TEWL readings, which inferred a greater disruption of the stratum corneum, when in reality visual microscopic inspection showed that the stratum corneum was intact.

Overall Vergou et al. and others have shown the utility and importance of visual methods when characterizing topically applied formulations *in vivo*. The application and instrumentation of the described *in vivo* fluorescence microscopes are relatively simple to use and

result in information relating to drug distribution within skin and insight into their mechanism of action. A benefit of using the Optiscan Stratum™ in relation to the investigation of percutaneous enhanced penetration is that tissue and cellular disruption can be visualized. Understanding the change in skin integrity is important for characterizing the chemical and/or physical methods used to deliver drugs. However, the limitation of the current technique is that a fluorescent solution is required to visualize the skin layers (in the previous cases, sodium fluorescein). Depending on the depth required, the fluorescent solution is injected into the skin or topically applied, potentially influencing the drug of interest.

### 16.2.2 Reflectance Microscopy for the Assessment of Therapeutic Changes in the Skin

Reflectance confocal microscopy (RCM) is an alternate approach to fluorescence-based CLSMs. RCM can especially be useful to characterize skin integrity and disruption as well as the change in disease state of the skin following therapeutic treatment (Ardigo et al. 2010; Segura et al. 2011; Ulrich et al. 2009). Various studies have been published characterizing the morphological changes seen in the skin over time, including studies looking at wound healing.

RCM utilizes a near-infrared diode laser as a monochromatic and coherent light source. The light source is reflected (backscattered) off the sample and passes through a pinhole aperture to

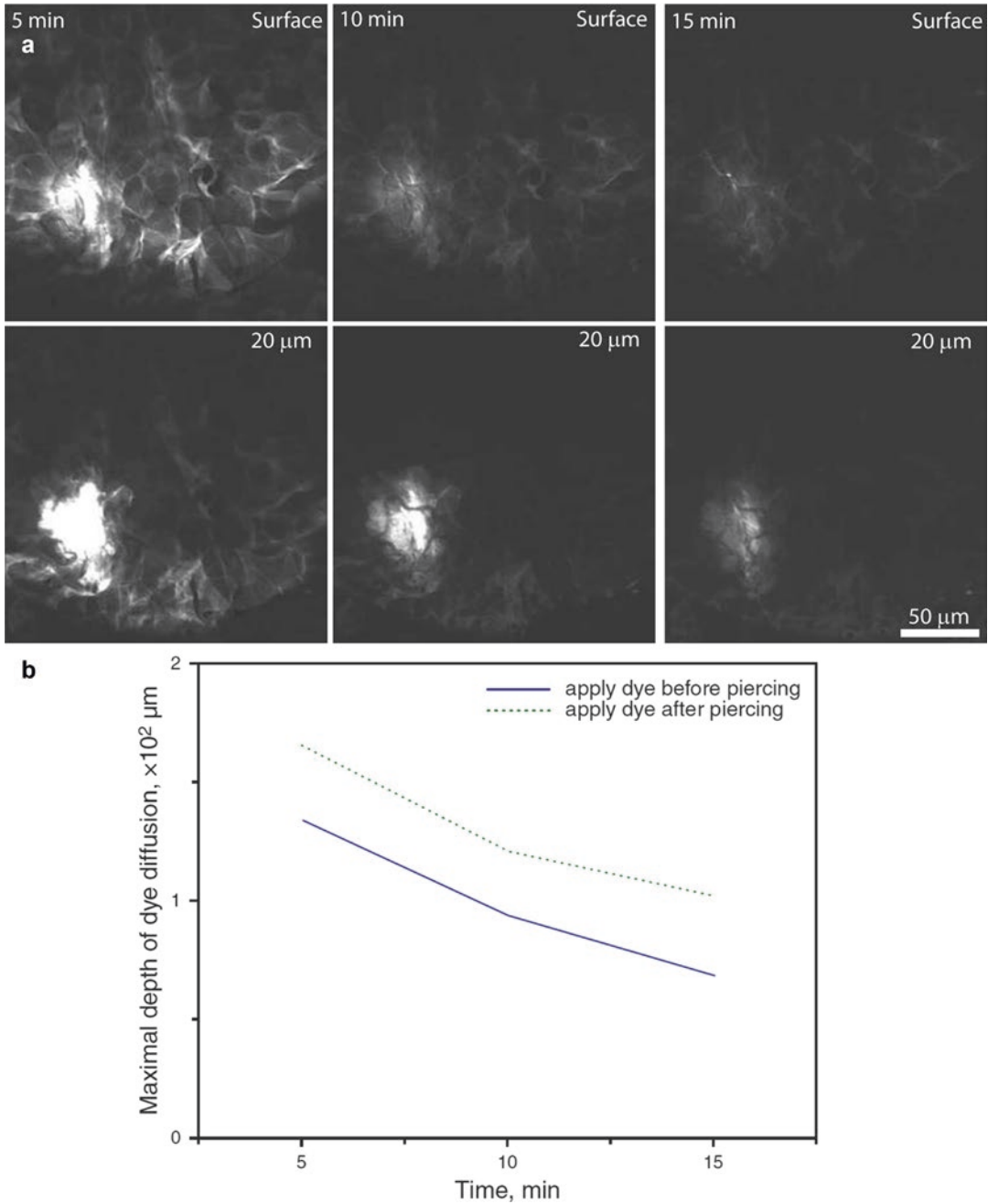


**Fig. 16.4** Microneedle-enhanced delivery of sodium fluorescein in volunteers. (a) Confocal laser scanning microscopy of microneedle delivery 5, 10 and 15 min post application at two depths (surface and 20 μm below the

surface). (b) Comparison maximum depth of dye diffusion over time between sodium fluorescein application before or after microneedle insertion (Adapted from Bal et al. (2010a))

the detector. RCM results in quasi-histological resolution because backscattering occurs at the edges of two biological materials with different refraction indexes – thus distinguishing cellular

structures. RCM can be used for assessing structural changes within the skin in addition to serial imaging of the same site over time (Wurm et al. 2012). Furthermore, the use of near-infrared

laser sources results in relatively deep imaging down to the dermo-epidermal junction. The high cellular and structural resolution images obtained from RCM make it a valuable tool when assessing percutaneous penetration enhancers. RCM has the potential of providing information on the change in skin integrity post chemical and/or physical enhancement and unlike the previous fluorescence-based technique described it does not require a dye solution.

RCM is also used as a qualitative and quantitative technique where differences can be observed relating to the cellular and extracellular structures within skin. For example, we have investigated in the Prow group, the differences in skin from two age groups, 20–30 years and 50–60 years, respectively, using RCM (Fig. 16.5). The RCM images in Fig. 16.5b–d, f–h correspond to three distinct skin layers of interest (stratum corneum, stratum spinosum and dermo-epidermal junction). We have reported in detail and scored the RCM features associated with photo-ageing on the forearm of the two age groups (Wurm et al. 2012). We concluded that 15 statistically significant RCM features, such as furrow width/shape, keratinocyte irregularity/disarray and dermal papillae morphology could be used to quantify photo-ageing in forearm skin (Wurm et al. 2012).

One particular area that has seen much attention using RCM is the characterization and pre- and post-topical treatment of pre-cancerous and cancerous skin lesions (actinic keratosis [AK], basale cell carcinoma [BCC], squamous cell carcinoma [SCC] and melanoma). Segura et al. investigated the efficacy of photodynamic therapy (PDT) using methyl-aminolevulinic acid (MAL) on the treatment of BCCs (Segura et al. 2011). Six patients were treated with 1–3 cycles of MAL-PDT with each cycle consisting of two sessions of MAL-PDT 7 days apart. To enhance MAL penetration into the skin, debridement of the BCC surface was done with a curette followed by a 3 h application of MAL. The patients were assessed 1 week and 3 months post treatment using RCM with consecutive follow-ups (without RCM) every 6 months for 3 years. The RCM used was a commercially available instrument designed specifically for in vivo applications (Vivascope 1500®, Lucid Inc., USA). The system consists of

a 830 nm diode laser and a 30× water immersion lens facilitating a horizontal optical resolution of 2 μm and vertical resolution of 5 μm. It was determined that RCM analysis was suitable for characterizing whether lesions underwent partial or complete remission. In these cases not all treated lesions underwent complete remission. However, those that did were characterized by the presence of normal dermal papilla and collagen fibres (Fig. 16.6).

Torres et al. published a similar study treating basale cell carcinomas (BCCs) with 5% imiquimod (Torres et al. 2004). Patients applied imiquimod 5 times daily for 2, 4 or 6 weeks, with RCM analysis at the 6-week follow-up. Torres et al. also used a Lucid Inc., USA, based RCM system designed for in vivo investigations. Whereas Segura et al. characterized the BCCs based on the skin morphology within the dermo-epidermal junction and dermis, Torres et al. focused on the keratinocyte structure and cytoplasm-to-nucleus ratio within the epidermis (Torres et al. 2004). BCCs were characterized as having elongated keratinocytes with a high cytoplasm-to-nucleus ratio compared to normal skin, which consisted of a lower ratio and regular honey-comb pattern of the cells (Fig. 16.7). Even though in this study, RCM was seen as a useful technique evaluating tumour regression in vivo without the need of surgery, there were still some limitations. The investigators felt that the technique was time-consuming (although far quicker than an invasive surgery approach). There were also technical difficulties due to movement of the relatively large scanning head, skin contact angle and maintaining contact with the skin during imaging. These limitations can be overcome with practice, however it does prevent implantation of such in vivo systems especially in laboratories that are familiar primarily with in vitro and ex vivo investigations. However, it should be noted that the RCM used was a much earlier model available from Lucid Inc. (Vivascope 1000®) and since then Lucid Inc. have developed small hand-held systems with greater ease-of-use and flexibility (Fig. 16.1).

In summary, CLSM systems are increasing in their use as non-invasive techniques for percutaneous drug delivery. Although fluorescence-based systems are limited mainly to in vitro and

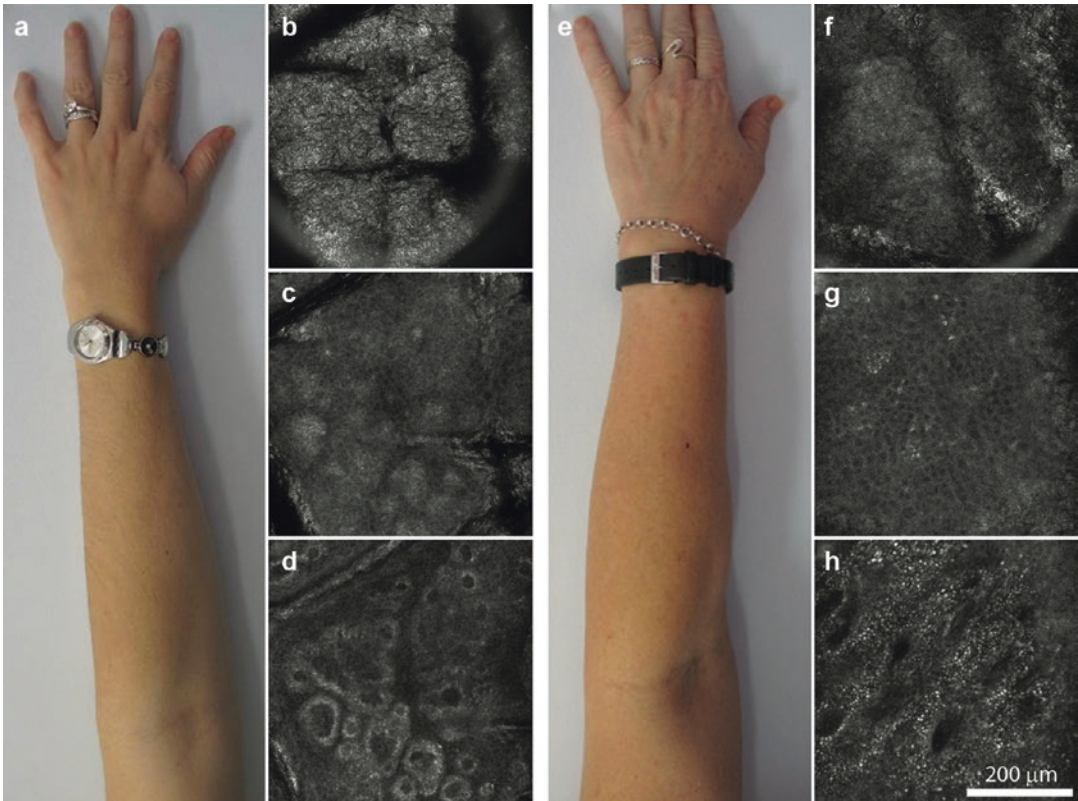


**Fig. 16.5** Clinical photographs and their corresponding reflectance confocal microscopy (RCM) images. (a) and (e) show representative clinical photographs of volunteers from the two age groups, 20–30 years and 50–60 years, respectively. (b–d) and (f–h) show the corresponding

RCM images of volunteers (a) and (e), respectively. (b) and (f) – stratum corneum, (c) and (g) – stratum spinosum, (d) and (h) – dermo-epidermal junction (Prow, Raphael and AR Soyer, unpublished 2012)

ex vivo applications, RCM is being utilized clinically much more due to its ability to resolve cellular and structural morphology within the skin pre and post drug application. With an increase in biocompatible fluorophores, user-friendly equipment and cost-effective instruments, it is expected that in vivo CLSM systems will continue to be incorporated into pharmaceutical and percutaneous research.

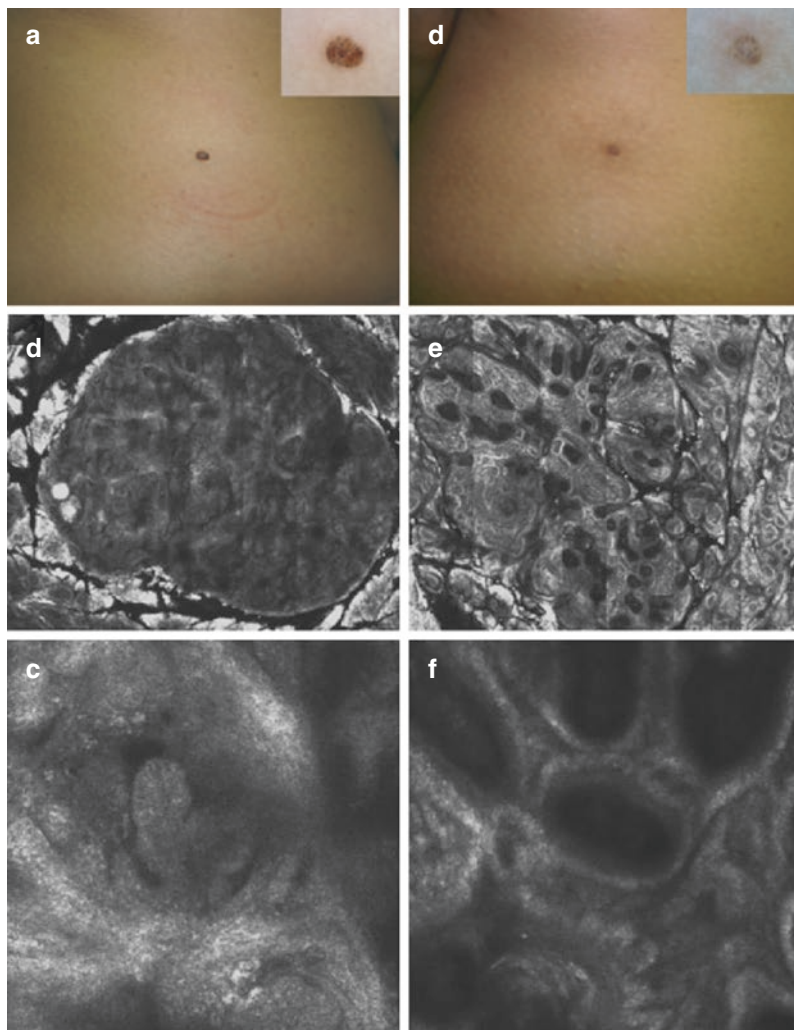
### 16.3 Applications of Multiphoton Microscopy

Multiphoton microscopy (MPM) is a deep tissue imaging technique that is predominantly used for non-linear two-photon excitation of fluorophores.

MPM can additionally be used for three-photon excitation as well as second and third harmonic generation of biological structures. These features, combined with the fact that MPM can result in single photon sensitivity with submicron resolution has led it to being an important microscopic technique with the highest resolution in the area of non-invasive clinical imaging (Fig. 16.8) (Konig et al. 2006; JenLab GmbH).

Two-photon excitation works on the theoretical principal developed by Maria Göppert-Mayer, where two photons of similar energy interact with a molecule (fluorophore) resulting in excitation equivalent to the absorption of a single photon with twice the energy (Fig. 16.9) (Zipfel et al. 2003; Prow 2012). The probability of successful two-photon interaction (absorption) can be measured

**Fig. 16.6** Clinical, dermoscopy and RCM images of a 4 mm pigmented basal cell carcinoma on the abdomen of a 25-year-old woman. **(a)** Clinical and dermoscopy (*inset*) images of the lesion before photodynamic therapy. **(b)** A 4 × 4 mm reflectance confocal microscopy image (RCM) of the lesion prior to treatment. **(c)** Magnified image (0.5 × 0.5 mm) of the lesion at the dermo-epidermal junction. **(d)** Clinical and dermoscopy (*inset*) images of the lesion after two cycles of photodynamic therapy. **(e)** A 4 × 4 mm RCM image of the lesion after treatment showing reduction in tumour size. **(f)** Magnified image (0.5 × 0.5 mm) of the lesion after treatment at the dermo-epidermal junction showing the presence of normal dermal papilla (Adapted from Segura et al. (2011))



quantitatively by the two-photon cross-section ( $\sigma_{2p}$ ). The two-photon cross-section is referred to as Göppert-Mayer (GM) where 1 GM is equivalent to  $10^{-50}$  cm<sup>4</sup>s. Instead of measuring  $\sigma_{2p}$ , which is quite complex, the product of the fluorescence quantum yield ( $\varphi_F$ ) and absolute two-photon cross-section is calculated, which is the two-photon 'action' cross-section ( $\varphi_F \sigma_{2p}$ ) (Zipfel et al. 2003). To determine the optimal wavelength for two-photon excitation, it is useful to have an understanding of the change in  $\varphi_F \sigma_{2p}$  values with wavelength (two-photon excitation spectra). This is because a molecule's maximum single photon excitation does not always correspond to two photon excitation with similar energy (in particular symmetrical and intrinsic molecules). Therefore, when selecting fluorescent

tracers for analysis of percutaneous penetration with multiphoton microscopy it is important to have an understanding of  $\varphi_F \sigma_{2p}$ .

For successful excitation to occur, the photons need to interact with the molecule almost simultaneously (approx.  $10^{-16}$  s). Therefore, the probability of successful two-photon excitation is greatest within the beam area within the focal plane. Outside of the focal plane the probability drops significantly with negligible fluorescence emission. To further increase the probability of two-photon excitation and generate sufficient fluorescence for imaging, high laser powers are required. However, high laser powers are detrimental to biological samples. To address this problem, MPMs utilize a pulsed laser (most



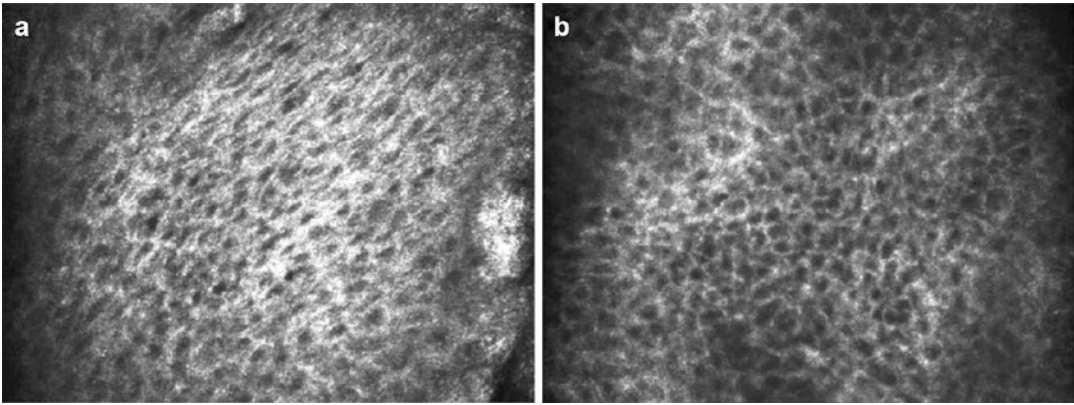


**Fig. 16.7** Reflectance confocal microscopy (RCM) images of a basal cell carcinoma (BCC) before and after treatment with imiquimod. **(a)** BCC morphology prior to treatment showing elongated cells with a high cytoplasm-

to-nucleus ratio (nucleus low signal, cytoplasm high signal). **(b)** BCC morphology 2 weeks after treatment showing regular honey-comb pattern and normal cytoplasm-to-nucleus ratio (Adapted from Torres et al. (2004))

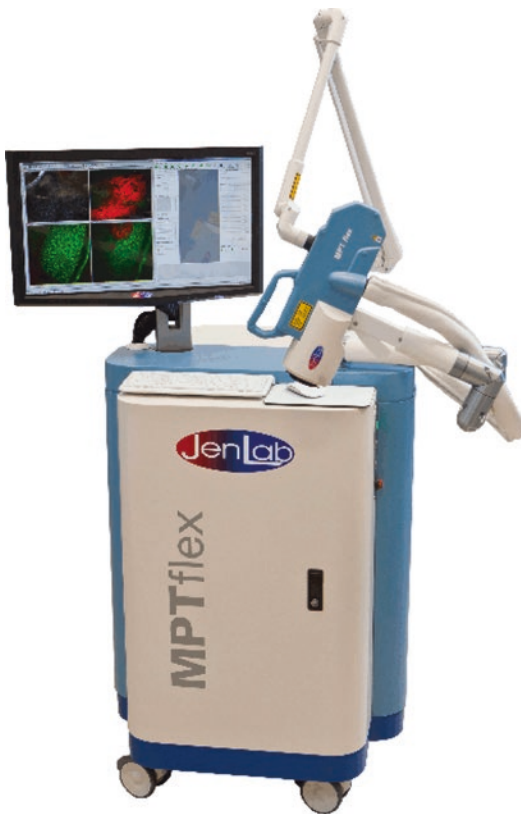


**Fig. 16.8** In vivo multiphoton microscopy system (MPTflex™, JenLab GmbH, Germany) (Reprinted from JenLab website (JenLab GmbH))

commonly being a mode-locked titanium sapphire laser), which produces approx. 80 million

pulses per second with a pulse duration of approx. 100 fs. The pulsed laser results in a significant increase in the probability of two photon excitation while keeping the average power relatively low. These laser power peaks contain enough dense photons to create fluorophore excitation and also retain the average power fairly low.

Seeing that molecules outside the focal plane have a low probability of successful two-photon excitation, fluorescence MPMs do not require a pinhole to reduce background noise. Absence of a collecting pinhole results in greater acquisition of emitted photons than single photon systems (Masters et al. 1997). These advantages in addition to the longer wavelengths used for MPM result in overall less scattering of the excitation beam and greater signal collection, allowing for deeper optical sectioning within specimens (approx. 2–3 times greater than what can be achieved with single photon microscopy).

### 16.3.1 Assessment of the Cutaneous Delivery of Nanoparticle Compounds Using Multiphoton Microscopy

Conventional imaging techniques for nanoparticle identification utilizes electron microscopy, in particular transmission electron microscopy (TEM) (Butler et al. 2012). Its high resolution (ability to

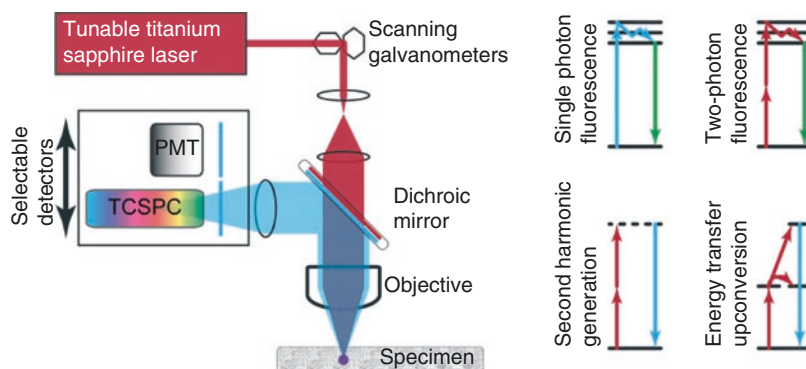


**Fig. 16.9** Simplified schematic of the optical layout for multiphoton microscopy and energy transfer diagrams. Tuneable 80 MHz titanium sapphire laser sources are most commonly used for MPM. The light source is then raster scanned over the imaging area using scanning galvanometers. The dichroic mirror and objective lens then pass the

excitation beam to the sample. The emission is collected and passed to one or more detectors. Photomultiplier tubes and time-correlated single-photon counting detectors can be used depending on application. Single, two-photon and second-harmonic generation Jablonski diagrams are shown on the right (Reprinted from Prow (2012))

visualize individual nanoparticles) and ability to distinguish nanoparticles extra/intra-cellularly makes it a powerful technique in relation to nanoparticle – cell co-localization (Prow et al. 2008). However, for samples to be imaged using TEM, they must be at a thickness that allows the electrons to transmit through the sample. This is a time-consuming highly technical process that requires sectioning and embedding of the sample within resin prior to imaging. Additionally, TEM is an ex vivo microscopy technique and therefore inherent to the limitations of using an ex vivo model system to describe what is occurring in vivo.

Single photon microscopy is another technique that has been used for nanoparticle imaging both ex vivo and in vivo (Prow et al. 2006, 2008, 2012). As discussed earlier, the major advantage of this technique is its ease of use and availability of relatively inexpensive equipment. However, for the nanoparticles to be detected they need to be intrinsically fluorescent or be fluorescently labelled.

Dromard et al. conducted a study investigating the use of in vivo corneocyte imaging using a customized fibered confocal fluorescence microscope technique (Dromard et al. 2007). Briefly, an optical fibre bundle was attached to a fluorescence microscope set-up and used to image the surface of the skin. Although not assessing the delivery of nanoparticles to the skin, Dromard

et al. applied fluorescein or 300 nm fluorescein embedded nanoparticles to the surface of the skin (Dromard et al. 2007). The nanoparticles accumulated preferentially around the edges of the corneocytes defining their boundaries. This approach provided a relatively simple and quick analysis of nanoparticle interaction with the surface of the skin.

MPM is one particular technique that is showing great promise as a tool for defining the risk of nanoparticle exposure (Fig. 16.10). In particular, MPM results in high-resolution deep tissue imaging within biological tissues (ex vivo or in vivo) with the ability to separate nanoparticle signals from endogenous fluorophores (although MPM is not able to resolve individual nanoparticles) (Fig. 16.10) (Prow 2012; Labouta et al. 2011; Liu et al. 2012). Furthermore, when coupled with fluorescence lifetime imaging (FLIM) and time-correlated single photon counting (TCSPC) detectors, MPM systems have the capability of distinguishing between the simultaneous excitation of nanoparticles and endogenous fluorescence within biological tissues without the need of fluorescent dyes (not possible with other techniques).

We utilized the advantages of MPM-FLIM to investigate the use of TCSPC for simultaneous monitoring of zinc oxide nanoparticles and the metabolic state of volunteer skin (without the use

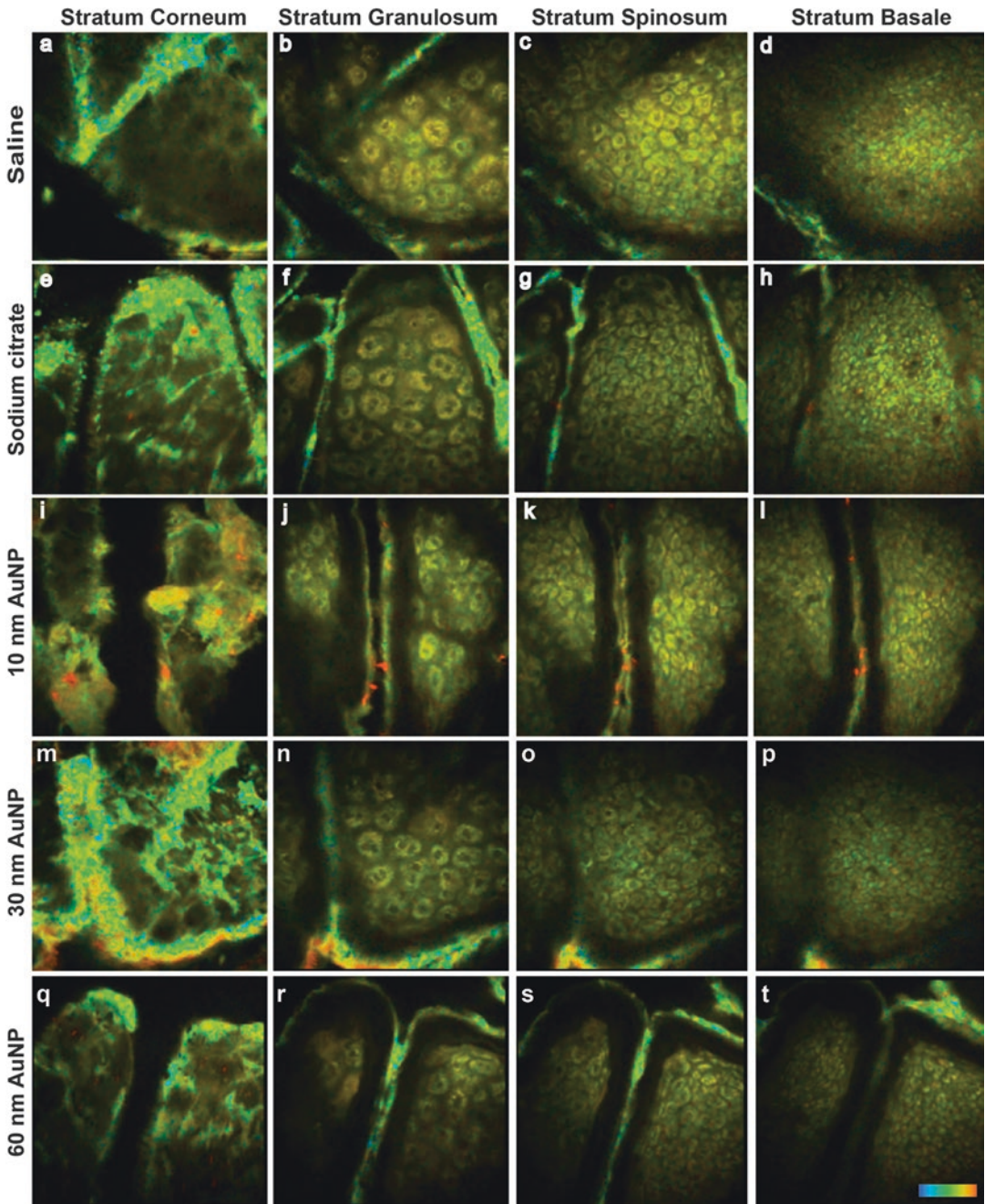


**Fig. 16.10** En face multiphoton microscopy fluorescence lifetime imaging (MPM-FLIM) showing the layers of freshly excised human skin after 24 h treatment with gold nanoparticles. Nanoparticles are pseudocoloured based on signal 95–100% (orange to red), skin autofluorescence is pseudocoloured based on signal 0–95% (blue/green to

yellow) (Adapted from Liu et al. (2012)) The samples consisted of a (a–d) saline control, (e–h) sodium citrate control, (i–l) 10 nm gold nanoparticle treated skin, (m–p) 30 nm gold nanoparticle treated skin and, (q–t) 60 nm gold nanoparticle treated skin.

of fluorescent dyes) (Lin et al. 2011) (Fig. 16.11). The study consisted of a single healthy volunteer and eight others with psoriasis or atopic dermatitis (five with active psoriasis lesions and three with atopic dermatitis). Zinc oxide nanoparticles were applied to the forearm of healthy, tape-stripped and lesional skin. The application time for the healthy and tape-stripped skin was 4 and 24 h, but for the lesional skin only 2 h. In vivo imaging was done using a DermaInspect® MPM (JenLab GmbH, Germany) with a pulse mode-locked 80 MHz titanium sapphire MaiTai® laser. The excitation wavelength was 740 nm and the emission was filtered through a band pass filter (350–450 nm) prior to the TCSPC 830 FLIM detector. The multiphoton-excited photoluminescence (derived from the fluorescence lifetime amplitude) was used to separate the zinc oxide nanoparticle signal from the endogenous nicotinamide adenine nucleotide (NADH), also expressed as NAD(P)H signal. The microscopy set up clearly showed the zinc oxide nanoparticle distribution within the different skin types and layers (Fig. 16.11).

Roberts et al. used a similar MPM set up analysing xenobiotic transport in vivo (fluorescein and zinc oxide nanoparticles within rat liver and human skin) (Roberts et al. 2008). It was also determined that zinc oxide nanoparticles do not penetrate the skin and this was further verified using scanning electron microscopy coupled with energy-dispersive x-ray (SEM-EDX) of treated ex vivo human skin. Zvyagin et al. resulted in similar conclusions using MPM and SEM-EDX of both zinc oxide and titanium dioxide nanoparticle penetration in ex vivo and in vivo human skin (Zvyagin et al. 2008).

König et al. conducted a study using MPM to investigate the delivery and distribution of poly(lactic-co-glycolic acid) (PLGA) nanoparticles (approx. diameter of 200 nm) loaded with the antirheumatic drug flufenamic acid (Konig et al. 2006). The drug was specifically chosen because it fluoresces at 420 nm. The excitation wavelength was tuned to 720 nm to distinguish between the loaded nanoparticles compared to the unloaded controls. It was determined that like the zinc oxide and titanium dioxide nanoparticles the PLGA nanoparticles remained on the surface of the skin.

Overall MPM provides an in vivo microscopy technique that is well suited for the high resolution and deep imaging or nanoparticles within the skin. The majority of the studies using these systems within humans have focused on zinc oxide and titanium dioxide nanoparticles. This is because these nanoparticles are clinically relevant being utilized in numerous daily lotions such as sunscreens and cosmetics. It is expected that with the continual increase in nanoparticles as a percutaneous delivery enhancer, MPM will play an important role in assessing nanoparticle penetration and distribution within skin potentially providing information aiding in their clinical approval and use.

### 16.3.2 Analysing the Skin's Metabolic Response to Drugs Using Multiphoton Microscopy Fluorescence Lifetime Imaging

The combination of MPM with FLIM provides an in vivo microscopy technique which could potentially provide information on the progression of disease and metabolic changes within skin post drug administration (Prow 2012; Labouta et al. 2011; Liu et al. 2012; Lin et al. 2011). MPM itself is useful because it provides detailed resolution on the morphological changes of the cells (in particular keratinocytes) and also any changes to the collagen network. However, one endogenous fluorophore of particular interest is NAD(P)H (i.e. NADH and NADPH). NAD(P)H is localized within living cells, either unbound in the cytoplasm or bound to mitochondrial enzymes, and plays an important role in cellular metabolism (Sanchez et al. 2010). Depending on the cellular microenvironment (i.e. cellular metabolism), the NAD(P)H fluorescence lifetime changes, which can be detected by FLIM. Simply put, an increase in oxidation within the skin may result in an increase in unbound NAD(P)H and a decrease in bound as well as their corresponding lifetimes (unbound has a short lifetime and bound has a longer lifetime).

As discussed in the previous section, we used MPM-FLIM for simultaneous monitoring of zinc oxide nanoparticles and the metabolic state of volunteer skin (Lin et al. 2011). It was determined that

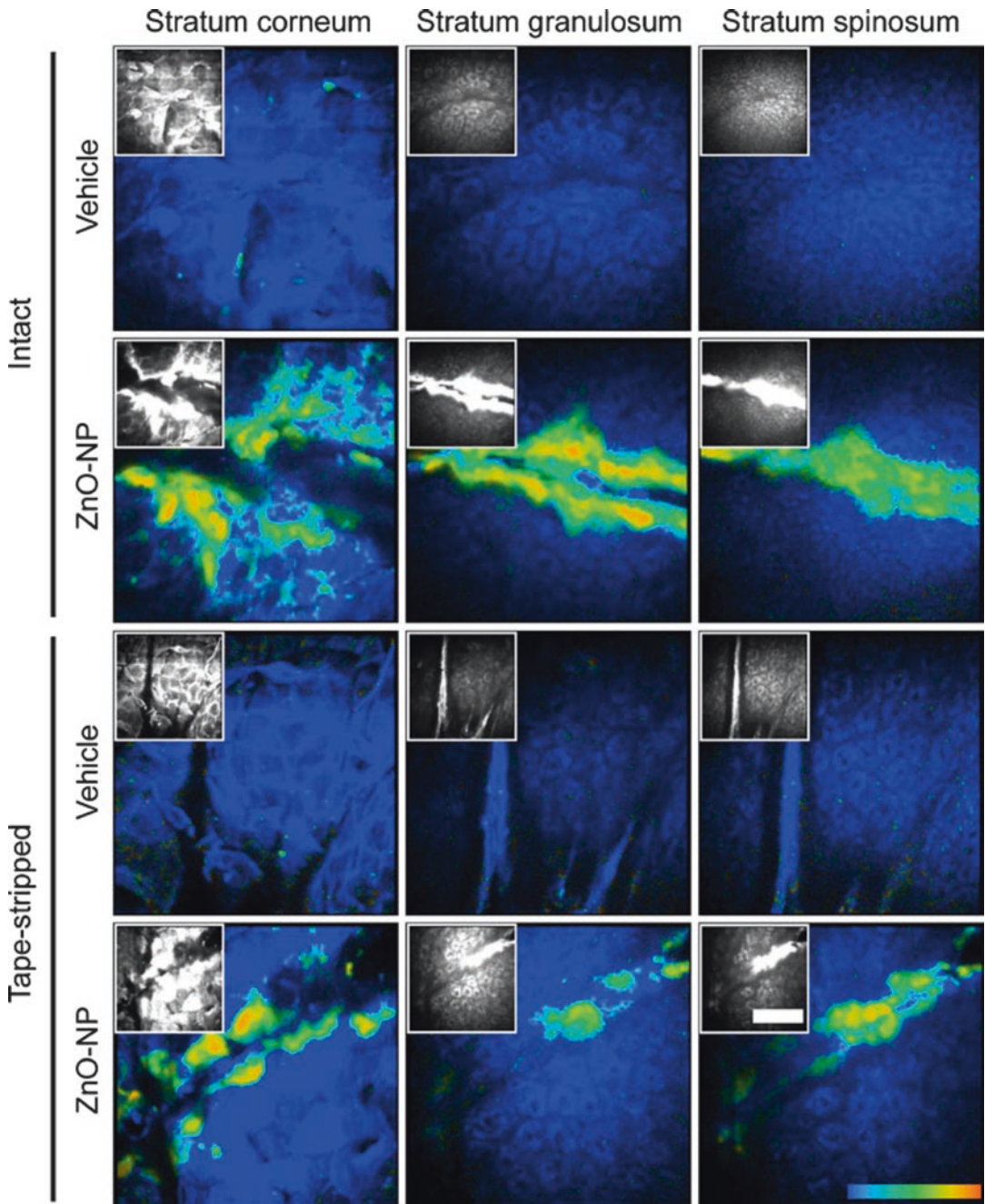


**Fig. 16.11** In vivo multiphoton microscopy (MPM) images of intact and tape-stripped skin at different layers within the skin after 24 h treatment with zinc oxide nanoparticles. Nanoparticles are pseudocoloured based on

signal 90–100% (green to red), skin autofluorescence is pseudocoloured based on signal 0–85% (blue). Grayscale insets show overall intensity only (Reprinted from Lin et al. (2011))

the free NAD(P)H signal increased significantly in tape-stripped skin treated for 4 h with zinc oxide nanoparticles compared to the control. However, no significant changes were detected for the

lesional skin (Fig. 16.12). This corresponded to what was reported by König et al. where the application of FLIM was found to be technically challenging in thicker stratum corneum (i.e. lesional

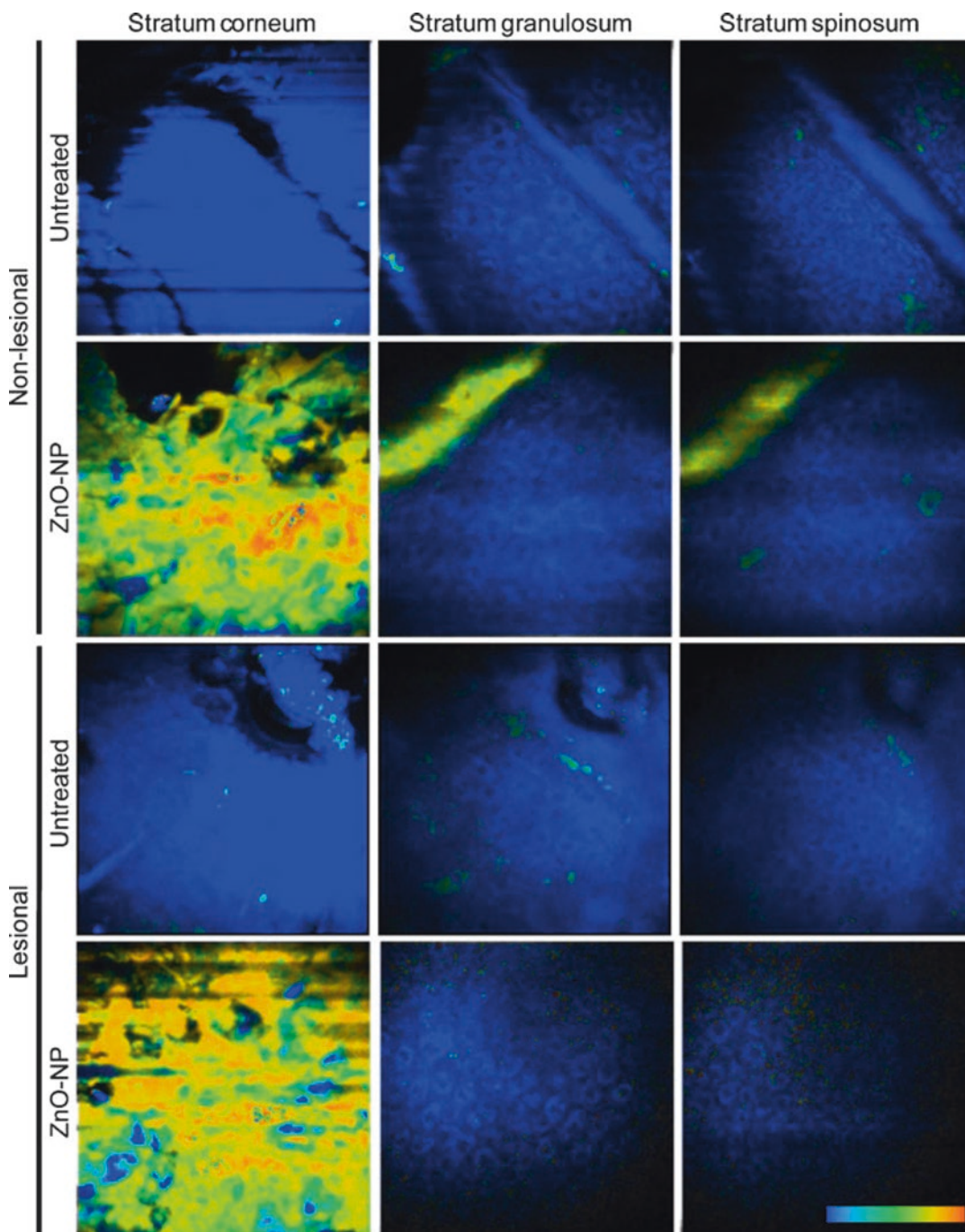


**Fig. 16.12** In vivo multiphoton microscopy (MPM) images of intact and tape-stripped skin at different layers within the skin after 2 h treatment with zinc oxide nanoparticles. Nanoparticles are pseudocoloured based on

signal 90–100% (green to red), skin autofluorescence is pseudocoloured based on signal 0–85% (blue) (Reprinted from Lin et al. (2011))

areas) (König et al. 2011). However, König et al. observed a greater variance in the amplitude of bound and unbound NAD(P)H lifetimes in lesional

skin compared to healthy skin. The lesional coefficient of variation was largest in the stratum spinosum, being 8.1 times greater than non-lesional

areas. It is proposed that these differences in FLIM output, combined with the high resolution visual images from MPM, can be used to assess therapeutic or toxic effects following topical exposure.

## 16.4 Advancements in Non-invasive Analysis of Drug Delivery to the Skin Using Multimodal Imaging

Non-invasive multimodal imaging is the combination of two or more imaging techniques used within a single examination. The origins of multimodal imaging can be largely attributed to the development of combined nuclear medicine, positron emission tomography and magnetic resonance imaging. These multimodal instruments were developed due to the need for more accurate and localized imaging of drug–cell/tissue interaction in relation to neurology and oncology, in particular the longitudinal assessment of tumour progression/regression after treatment.

There is much interest in the areas of pharmaceutical science and percutaneous drug delivery for the incorporation of multimodal imaging, resulting in the development and introduction of various multimodal *in vivo* skin imaging techniques (Konig et al. 2009, 2010; Graf and Boppart 2012; Zhang et al. 2011). One common technique as discussed in the previous section is the use of MPM-FLIM. The significance of MPM and FLIM is that the same area of skin can be imaged with MPM and analysed by FLIM concurrently providing information-specific drug–cell/tissue interactions. However, a major challenge when combining different imaging techniques for skin analysis is that each instrument often has a different field-of-view and optical sectioning ability. Additionally, the region-of-interest within skin studies is often quite small (being limited to the size of the objective lens) making it difficult to image the exact same area of skin with different techniques.

Although not technically multimodal, König et al. investigated the use of sequential optical coherence tomography (OCT) and MPM (Konig et al. 2009). OCT is a reflectance-based technique where optically sectioned images are

obtained by measuring the amplitude and the echo time delay of backscattered light. König et al. used two OCT systems (EX1301<sup>®</sup>, Michelson Diagnostics, UK and HSL-2000-10 MDL<sup>®</sup>, Santec Corp., Japan) in conjunction with the DermaInspect MPM<sup>®</sup> (JenLab GmbH, Germany) (Konig et al. 2009). To image the same area of skin between instruments, a custom metal O-ring and custom glass coverslip was developed to fit into the MPM, OCT and dermoscope (Fig. 16.13a–d). The locator was reversibly fixed to the skin using double-sided adhesive tape. The OCT provided fast low resolution wide-field cross-sectional images 5×2 mm<sup>2</sup> in size. This was a contrast to the high cellular resolution of the MPM images. However, MPM has a small acquisition volume approximately 0.3×0.3×0.2 mm<sup>3</sup>. It is their differences that make the two techniques complimentary, where OCT provides a wide-field image within a lesion showing potential areas of interest that can be further analysed at a much higher resolution using MPM. König et al. investigated three different skin states being hemangioma, Pemphigus vulgaris and melanocytic lesions using the combined MPM-OCT systems. It was observed that OCT was capable of identifying features of interest that when examined by MPM was shown to be significant. For example, optical biopsies of Pemphigus vulgaris resulted in regions of low signal or ‘black cavities’ within the skin using OCT (Fig. 16.13e). These cavities (blisters) were also observed in the MPM images showing regions absent of cells and signal (Fig. 16.13f).

The study by König et al. showed the significance of combining MPM and OCT analysis (Konig et al. 2009). However, the two systems were independent being two different instruments, limiting its utility and ease of use. Graf and Boppart addressed this issue by integrating the two systems into a single instrument (Graf and Boppart 2012). In addition, Graf and Boppart utilized optical coherence microscopy, which is a high resolution variation of OCT. The initial challenge faced when integrating the two systems was choice of laser. MPM most commonly utilizes a wave-length tuneable titanium sapphire laser with a narrow 10–20 nm optical bandwidth.

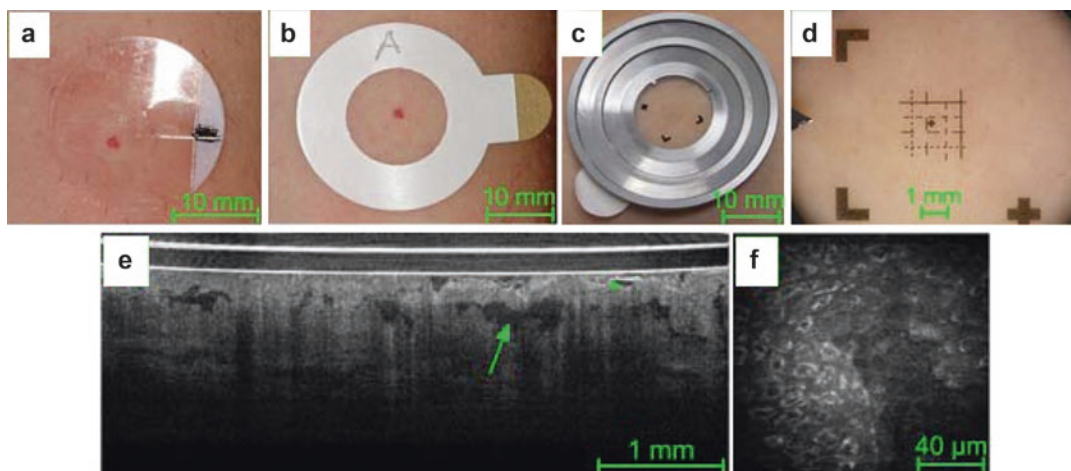


**Fig. 16.13** Images of interface for alignment of dermoscope, multiphoton microscopy (MPM) and optical coherence tomography (OCT) and representative images from MPM and OCT. Interface consisting of (a) cover lens, (b) double-sided adhesive, (c) metal O-ring, and (d) coverslip

with locator markings. (e) OCT image showing subcorneal (\*) and subepidermal (arrow) blistering, and (f) corresponding MPM optical section showing subcorneal blistering (Adapted from König et al. (2009))

This is in contrast to OCM, which utilizes a broad optical bandwidth (100–200 nm) laser source. Graf and Boppart achieved excitation using a commercially available titanium sapphire dual spectrum laser source based on supercontinuum generation. The laser was integrated into the MPM-OCM system and described in detail by Graf and Boppart (2012).

The next challenge was that MPM requires a high numerical aperture (NA) lens compared to OCM which relies on the coherence length and not the NA. By separating the laser source into two beams (one for MPM and the other for OCM) Graf and Boppart were able to independently control the effective NA for both the MPM and OCM while maintaining a single objective lens (Graf and Boppart 2012). Finally the reconstruction of the collected OCM data had to be reprocessed to compensate for the coherence gate curvature so as to utilize the full field of view and integrate with the MPM images. To validate the MPM-OCM system, multiple focal areas from the dorsal hand of a human volunteer was imaged. The system resulted in high cellular resolution within the skin attributed to the MPM in addition to wide area mosaics  $1 \times 1$  mm in size (Graf and Boppart 2012). The combined system provides data on both scattering and fluorescence-based

contrast providing complimentary information about the state of the skin.

The combination of MPM and OCT/OCM provided a novel imaging modality assessing the cellular and extracellular structure within skin. The multimodal MPM-OCM system benefited from the high-resolution capabilities of MPM in combination with the wide-field imaging of OCM. Such MPM-based multimodal imaging techniques have potential clinical cutaneous drug delivery applications, in particular the ability to resolve cellular and structural morphology within the skin pre and post nanoparticle drug application. The continual development of multimodal systems has the potential to provide novel in vivo analytical techniques resulting in information on drug distribution and interaction within cells and tissues.

## Conclusion

This chapter introduces and discusses the major imaging techniques used for the non-invasive in vivo analysis of percutaneous drug delivery. Single photon microscopy techniques to characterize percutaneous drug delivery have been well established within in vitro, ex vivo and in vivo animal models. With non-invasive clinical analysis of drug



distribution and diffusion being a major goal in the area of percutaneous drug delivery, CLSM systems are being developed to address this need, resulting in small portable fluorescence and reflectance microscopes for clinical use. Fluorescence CLSMs have the potential to provide information on drug pathways and skin barrier integrity post percutaneous enhancement. Not being restricted to fluorescence, reflectance CLSM utilizes backscattering of cellular structure within the skin to obtain structural images of tissue. RCM has been shown to be a clinically important technique – being able to resolve structural changes within skin before and after cutaneous drug delivery. The ability to assess the change in cellular morphology during treatment is an important tool, providing insight into drug/enhancer efficacy and the mechanism of action within the skin.

An alternate technique that has shown much promise in the area of non-invasive *in vivo* analysis is the use of multiphoton microscopy (MPM) for deep tissue imaging. A significant feature of MPM is that it can be used for second and third harmonic generation of biological structures (analysis of endogenous fluorophores within the skin). Additionally, MPM results in single photon sensitivity with submicron resolution making it one of the highest resolution techniques in the area of non-invasive clinical imaging. MPM is also unique because it has the ability to separate nanoparticle signals from the endogenous fluorophores *in vivo* (not possible with other systems). When combined with fluorescence lifetime imaging the technique increases its utility, being able to provide information on the progression of disease and metabolic changes within skin pre and post drug administration.

In the last decade, there has been an increase in multimodal imaging techniques (such as MPM-FLIM). The driving force behind the development of multimodal systems is to combine the advantages of individual imaging techniques potentially providing information on localization, extent and metabolic activity/

functional changes within the skin following cutaneous drug delivery. For example, investigations with MPM-OCT-based systems have benefited from MPM's resolution and OCT's wide-field and imaging depth providing detailed information on structural abnormalities within diseased skin. With advances in optics and lasers it is expected that the range of diverse multimodal systems will increase providing a powerful tool set for the *in vivo* analysis of percutaneous drug delivery.

Overall, visualization of percutaneous delivery is a significant experimental technique providing clear information on drug distribution and optimal delivery strategies. Downstream computational image analysis extends the qualitative visualization of drug delivery to a semi-quantitative and quantitative analytical method resulting in information on drug trafficking, concentration and diffusivity within tissues – all important factors in understanding percutaneous delivery of drugs.

---

## References

- Agarwal A, Tripathi PK, Tripathi S, Jain NK (2008) Fluorescence imaging: applications in drug delivery research. *Curr Drug Targets* 9:895–898
- Ardigo M, Cameli N, Berardesca E, Gonzalez S (2010) Characterization and evaluation of pigment distribution and response to therapy in melasma using *in vivo* reflectance confocal microscopy: a preliminary study. *J Eur Acad Dermatol Venereol* 24:1296–1303
- Bal S, Kruithof AC, Liebl H, Tomerius M, Bouwstra J, Lademann J et al (2010a) *In vivo* visualization of microneedle conduits in human skin using laser scanning microscopy. *Laser Phys Lett* 7(3):242–246
- Bal SM, Kruithof AC, Zwier R, Dietz E, Bouwstra JA, Lademann J et al (2010b) Influence of microneedle shape on the transport of a fluorescent dye into human skin *in vivo*. *J Control Release* 147:218–224
- Butler MK, Prow TW, Guo YN, Lin LL, Webb RI, Martin DJ (2012) High-pressure freezing/freeze substitution and transmission electron microscopy for characterization of metal oxide nanoparticles within sunscreens. *Nanomedicine* 7(4):541–551. doi:10.2217/nmm.11.149
- Chen X, Fernando GJP, Raphael AP, Yukiko SR, Fairmaid EJ, Primiero CA et al (2012) Rapid kinetics to peak serum antibodies is achieved following influenza vaccination by dry-coated densely packed microprojections to skin. *J Control Release* 158(1):78–84

- Dromard T, Ravaine V, Ravaine S, Leveque JL, Sojic N (2007) Remote in vivo imaging of human skin corneocytes by means of an optical fiber bundle. *Rev Sci Instrum* 78(5):053709. doi:10.1063/1.2736346
- Dubey S, Kalia YN (2010) Non-invasive iontophoretic delivery of enzymatically active ribonuclease A (13.6 kDa) across intact porcine and human skins. *J Control Release* 145(3):203–209
- Fernando GJP, Chen X, Prow TW, Crichton ML, Fairmaid EJ, Roberts MS et al (2010) Potent immunity to low doses of influenza vaccine by probabilistic guided micro-targeted skin delivery in a mouse model. *PLoS One* 5(4):e10266
- Graf BW, Boppart SA (2012) Multimodal in vivo skin imaging with integrated optical coherence and multiphoton microscopy. *IEEE J Sel Top Quantum Electron* 18(4):1280–1286
- Ito Y, Hirono M, Fukushima K, Sugioka N, Takada K (2012) Two-layered dissolving microneedles formulated with intermediate-acting insulin. *Int J Pharm* 436(1–2):387–393
- JenLab GmbH. *MPTflex Multiphoton Laser Tomography*. <http://www.jenlab.de/MPTflex-TM.114.0.html>. 31 Oct 2012
- König K, Ehlers A, Stracke F, Riemann I (2006) In vivo drug screening in human skin using femtosecond laser multiphoton tomography. *Skin Pharmacol Physiol* 19(2):78–88. doi:10.1159/000091974
- König K, Raphael AP, Lin LL, Grice JE, Soyer HP, Breunig HG et al (2011) Applications of multiphoton tomographs and femtosecond laser nanoprocessing microscopes in drug delivery research. *Adv Drug Deliv Rev* 63(4–5):388–404
- König K, Speicher M, Buckle R, Reckfort J, McKenzie G, Welzel J et al (2009) Clinical optical coherence tomography combined with multiphoton tomography of patients with skin diseases. *J Biophotonics* 2(6–7):389–397. doi:10.1002/jbio.200910013
- König K, Speicher M, Kohler MJ, Scharenberg R, Kaatz M (2010) Clinical application of multiphoton tomography in combination with high-frequency ultrasound for evaluation of skin diseases. *J Biophotonics* 3(12):759–773. doi:10.1002/jbio.201000074
- Labouta HI, Liu DC, Lin LL, Butler MK, Grice JE, Raphael AP et al (2011) Gold nanoparticle penetration and reduced metabolism in human skin by toluene. *Pharm Res* 28(11):2931–2944
- Lademann J, Richter H, Otberg N, Lawrenz F, Blume-Peytavi U, Sterry W (2003) Application of a dermatological laser scanning confocal microscope for investigation in skin physiology. *Laser Phys* 13(5):756–760
- Lin LL, Grice JE, Butler M, Zvyagin AV, Becker W, Robertson TA et al (2011) Time-correlated single photon counting for simultaneous monitoring of zinc oxide nanoparticles and NAD(P)H in intact and barrier-disrupted volunteer skin. *Pharm Res* 28(11):2920–2930
- Liu DC, Raphael AP, Sundh D, Grice JE, Soyer HP, Roberts MS et al (2012) The human stratum corneum prevents small gold nanoparticle penetration and their potential toxic metabolic consequences. *J Nanomater* Article ID 721706
- Lopez RFV, Seto JE, Blankschtein D, Langer R (2011) Enhancing the transdermal delivery of rigid nanoparticles using the simultaneous application of ultrasound and sodium lauryl sulfate. *Biomaterials* 32(3):933–941
- Masters BR, So PT, Gratton E (1997) Multiphoton excitation fluorescence microscopy and spectroscopy of in vivo human skin. *Biophys J* 72(6):2405–2412. doi:10.1016/S0006-3495(97)78886-6, S0006-3495(97)78886-6 [pii]
- Mukerjee EV, Collins SD, Isseroff RR, Smith RL (2004) Microneedle array for transdermal biological fluid extraction and in situ analysis. *Sensors Actuators A* 114:267–275
- Prow T, Grebe R, Merges C, Smith JN, McLeod DS, Leary JF et al (2006) Nanoparticle tethered antioxidant response element as a biosensor for oxygen induced toxicity in retinal endothelial cells. *Mol Vis* 12:616–625
- Prow TW (2012) Multiphoton microscopy applications in nanodermatology. *Wiley Interdiscip Rev Nanomed Nanobiotechnol* 4(6):680–690. doi:10.1002/wnan.1189
- Prow TW, Bhutto I, Kim SY, Grebe R, Merges C, McLeod DS et al (2008) Ocular nanoparticle toxicity and transfection of the retina and retinal pigment epithelium. *Nanomedicine* 4(4):340–349. doi:10.1016/j.nano.2008.06.003
- Prow TW, Chen X, Prow NA, Fernando GJP, Tan CSE, Raphael AP et al (2010) Nanopatch-targeted skin vaccination against West Nile virus and Chikungunya virus in mice. *Small* 6(16):1776–1784
- Prow TW, Monteiro-Riviere NA, Inman AO, Grice JE, Chen X, Zhao X et al (2012) Quantum dot penetration into viable human skin. *Nanotoxicology* 6(2):173–185. doi:10.3109/17435390.2011.569092
- Raphael AP, Prow TW, Crichton ML, Chen X, Fernando GJP, Kendall MAF (2010) Targeted, needle-free vaccinations in skin using multilayered, densely-packed dissolving microprojection arrays. *Small* 6(16):1785–1793
- Roberts MS, Roberts MJ, Robertson TA, Sanchez W, Thorling C, Zou Y et al (2008) In vitro and in vivo imaging of xenobiotic transport in human skin and in the rat liver. *J Biophotonics* 1(6):478–493. doi:10.1002/jbio.200810058
- Sanchez WY, Prow TW, Sanchez WH, Grice JE, Roberts MS (2010) Analysis of the metabolic deterioration of ex vivo skin from ischemic necrosis through the imaging of intracellular NAD(P)H by multiphoton tomography and fluorescence lifetime imaging microscopy. *J Biomed Opt* 15(4):046008
- Segura S, Puig S, Carrera C, Lecha M, Borges V, Malvehy J (2011) Non-invasive management of non-melanoma skin cancer in patients with cancer predisposition genodermatosis: a role for confocal microscopy and photodynamic therapy. *J Eur Acad Dermatol Venereol* 25:819–827
- Tomoda K, Terashima H, Suzuki K, Inagi T, Terada H, Makino K (2012) Enhanced transdermal delivery

- of indomethacin using combination of PLGA nanoparticles and iontophoresis in vivo. *Colloids Surf B Biointerfaces* 92(1):50–54
- Torres A, Niemeyer A, Berkes B, Marra D, Schanbacher C, Gonzalez S et al (2004) 5% imiquimod cream and reflectance-mode confocal microscopy as adjunct modalities to Mohs micrographic surgery for treatment of basal cell carcinoma. *Dermatol Surg* 30 (12 Pt 1):1462–1469. doi:[10.1111/j.1524-4725.2004.30504.x](https://doi.org/10.1111/j.1524-4725.2004.30504.x)
- Ulrich M, Krueger-Corcoran D, Roewert-Huber J, Sterry W, Stockfleth E, Astner S (2009) Reflectance confocal microscopy for noninvasive monitoring of therapy and detection of subclinical actinic keratoses. *Dermatology* 220:15–24
- Vergou T, Schanzer S, Richter H, Pels R, Thiede G, Patzelt A et al (2012) Comparison between TEWL and laser scanning microscopy measurements for the in vivo characterization of the human epidermal barrier. *J Biophotonics* 5(2):152–158
- White NS, Errington RJ (2005) Fluorescence techniques for drug delivery research: theory and practice. *Adv Drug Deliv Rev* 57:17–42
- Wurm EMT, Longo C, Curchin C, Soyer HP, Prow TW, Pellacani G (2012) In vivo assessment of chronological ageing and photoageing in forearm skin using reflectance confocal microscopy. *Br J Dermatol* 167(2): 270–279
- Xia J, Martinez A, Daniell H, Ebert SN (2011) Evaluation of biolistic gene transfer methods in vivo using non-invasive bioluminescent imaging techniques. *BMC Biotechnol* 11:62
- Zhang EZ, Povazay B, Laufer J, Alex A, Hofer B, Pedley B et al (2011) Multimodal photoacoustic and optical coherence tomography scanner using an all optical detection scheme for 3D morphological skin imaging. *Biomed Opt Express* 2(8):2202–2215. doi:[10.1364/BOE.2.002202](https://doi.org/10.1364/BOE.2.002202)
- Zipfel WR, Williams RM, Webb WW (2003) Nonlinear magic: multiphoton microscopy in the biosciences. *Nat Biotechnol* 21(11):1369–1377. doi:[10.1038/nbt899](https://doi.org/10.1038/nbt899)
- Zvyagin AV, Zhao X, Gierden A, Sanchez W, Ross JA, Roberts MS (2008) Imaging of zinc oxide nanoparticle penetration in human skin in vitro and in vivo. *J Biomed Opt* 13(6):064031. doi:[10.1117/1.3041492](https://doi.org/10.1117/1.3041492)

Claudine Piérard-Franchimont,  
Trinh Hermanns-Lê, and Gérald E. Piérard

## Contents

17.1	Introduction .....	303
17.2	SPBF Modulation and Corneoxenometry .....	304
17.3	Dose-Response Corneoxenometry with Chemical Penetration Enhancers ...	305
17.4	Corneoxenometry and Organic Solvents .....	305
	Conclusion .....	306
	References .....	306

## 17.1 Introduction

One of the outmost functions of the epidermis is to guarantee a continuous permeability barrier preventing the body from the ingress of potentially noxious xenobiotics. The toxic, irritant and caustic compounds are various. The skin permeability barrier function (SPBF) is therefore essential for maintaining a regulated and constant internal milieu. In recent decades, much research was undertaken to modulate or keep intact the SPBF (Notman et al. 2013) which is located in the stratum corneum (SC). The concerns are multifaceted. On the one hand, some formulations are designed for protecting or restoring the SPBF (Xhaufaire-Uhoda et al. 2008a). On the other hand, chemical penetration enhancers, also named absorption enhancers or accelerants, are offered for overcoming the genuine SPBF in order to increase specific drug penetration through the SC. In fact, penetration enhancers act in a number of distinct ways to induce a temporary and reversible failure in the SPBF (Woodford and Barry 1986; Hadgraft and Walters 1994; Keerthi et al. 2012; Seto et al. 2012). Some of these compounds alter or disrupt the epidermal lipids in their solubility properties and ordered structure (Notman et al. 2013). Other penetration enhancers impede the corneocyte's cohesiveness and the tidy SC structure.

The desirable attributes for penetration enhancers are varied (Woodford and Barry 1986;

---

C. Piérard-Franchimont • T. Hermanns-Lê  
G.E. Piérard, MD, PhD (✉)  
Laboratory of Skin Bioengineering and Imaging,  
Liège University Hospital, CHU Sart Tilman,  
BE-4000, Liège, Belgium  
e-mail: [Gerald.Pierard@ulg.ac.be](mailto:Gerald.Pierard@ulg.ac.be)

Hadgraft and Walters 1994). The compounds must be pharmacologically inert without any activity at cell receptor sites. In addition, the penetration enhancer must be compatible, both chemically and physically, with the drugs and vehicles in the relevant dosages. Its onset of action has to be rapid with a predictable duration of activity. The effects are expected to be completely and rapidly reversible upon removal of the material or formulation from the skin. Furthermore, the effects should ideally be unidirectional, allowing only the ingress of specific xenobiotics without any loss of endogenous compounds from the internal tissues. Penetration enhancers should be cosmetically acceptable, odorless, inexpensive, tasteless, colorless and spreading smoothly over the skin with a suitable “feel”. The risk for irritation, allergy and systemic toxicity must be minimal or absent. Despite the diversity of penetration enhancers, none of them combines all of the desirable above-mentioned attributes.

Some penetration enhancers are chemicals specifically designed for this purpose. An example is given by the 1-dodecylazacycloheptan-2-one (laurocapram, Azone®). Other compounds, such as surfactants and solvents, are more regular constituents of any topical formulation (Som et al. 2012). The efficacy of penetration enhancers toward various drugs were thoroughly explored and compared (Williams and Barry 1992). Synergistic effects were reached after combining different classes of penetration enhancers such as solvents and lipid fluidizers (Wotton et al. 1985; Ward and Du Reau 1991). Some binary and ternary mixtures were reported to be more active than single penetration enhancers (Rojas et al. 1991). In complex formulations, each component possibly acts in many different ways, precluding the determination of the actual operative interactions.

---

## 17.2 SPBF Modulation and Corneoxenometry

There is a need for accurate assessments of the alterations in the SPBF because any effect quantification of penetration enhancers should allow to design safe, reliable and effective formulations (Diembeck et al. 1999). SPBF is hardly explored

with confidence on most in vitro models using reconstructed epidermis or whole skin. Usage of excised human skin is subject to ethical concerns and necessitates both a surgical setting and an experienced laboratory. Skin of animals is often irrelevant due to prominent interspecies differences.

In vivo testing with penetration enhancers was claimed to be performed safely by some investigators in contrast to others who reported severe cell damage in the epidermis and even skin necrosis (Lavrijsen et al. 1994). Such potential hazards call for ex vivo predictive bioassays on human SC (Abrams et al. 1993; Goffin et al. 1997a; Welss et al. 2004; Kandárovà et al. 2009; Macfarlane et al. 2009; Engelbrecht et al. 2012; Kojima et al. 2012; Ochalek et al. 2012). This chapter focuses on the value of corneoxenometry and corneosurfametry in predicting the value of chemical penetration enhancers. The corneoxenometry bioassay named after corneocyte, xenobiotic and metry was introduced as a convenient and simple approach to explore the effect of some xenobiotics on human SC (Goffin et al. 1997a). It is a variant of corneosurfametry which was specifically designed for testing neat or diluted surfactants (Piérard et al. 1994; Goffin et al. 1995, 1996; Piérard and Piérard-Franchimont 1996; Uhoda et al. 2003).

Corneoxenometry is used for investigating the effects of chemicals potentially harmful to the SC (Goffin et al. 1997a, b, 1998, 2000; Xhaufaire-Uhoda et al. 2008b). The bioassay entails a collection of cyanoacrylate skin surface strippings (CSSS) from normal human skin. The harvested SC sheet which is uniform in thickness is subjected to the ex vivo action of the selected xenobiotics. CSSS covered in excess with each chemical are kept for 2 h at room temperature in a close environment in order to limit any evaporation from the test solution. Samples are thereafter thoroughly rinsed under running tap water, air dried and stained for 3 min with a toluidine blue-basic fuchsine solution at pH 3.45. Any lipid disruption and protein denaturation is responsible for an increased dye binding on corneocytes (Fig. 17.1). Harsh compounds to the skin considerably increase the staining intensity of the CSSS (Goffin et al. 1997a, b, 1998, 2000; Uhoda et al.

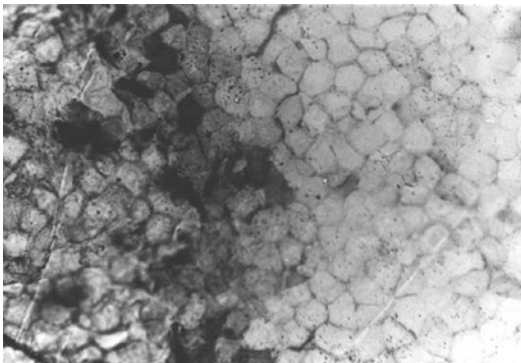


**Fig. 17.1** Corneoxenometry. Aspect of a cyanoacrylate skin surface stripping stained by a toluidine blue-basic fuchsine after contact with a penetration enhancer. The staining of corneocytes is uneven and indicates where the damages take place

2003; Welss et al. 2004; Kandàrovà et al. 2009; Macfarlane et al. 2009; Engelbrecht et al. 2012). After placing the samples on a white reference tile, reflectance colorimetry (Chroma Meter CR400 Minolta, Osaka, Japan) is used to derive the  $L^*$  and Chroma  $C^*$  values. Colorimetry is used to quantify the corneoxenometry reactivity. The colorimetric index of mildness (CIM) is calculated (Abrams et al. 1993; Goffin et al. 1996, 1997b; Piérard and Piérard-Franchimont 1996; Uhoda et al. 2003) as follows:  $CIM = L^* - \text{Chroma } C^*$ . The relative index of irritancy (RII) is calculated as follows:  $[RII = 1 - [(CIM \text{ product}) / (CIM \text{ water})^{-1}]$ . Obviously, RII is not a direct measure of any SPBF breaching. However, it correlates with clinical signs of irritancy, and with increased transepidermal water loss (Piérard et al. 1995). In fact, the bioassay explores the combined effects of (a) lipid removal and disorganization, and (b) protein denaturation as well. Hence, any RII increase is a clue for SC damage responsible for SPBF impairment.

### 17.3 Dose-Response Corneoxenometry with Chemical Penetration Enhancers

Data from both corneoxenometry and corneoxenometry are reproducible and sensitive enough to frequently disclose significant CIM and RII

differences between formulations (Piérard et al. 1995). A dose-response effect was searched for ethanol and laurocapram using the corneoxenometry bioassay (Goffin et al. 2000). In the same study, other assessments were performed using a gel formulation (propylene carbonate, hydroxypropyl cellulose, butylhydroxytoluene, ethanol, glycerol) containing 10% propylene glycol and a combination of three other enhancers, namely, N-acetyl-L-cysteine (NAC), urea and salicylic acid (SA). The three latter penetration enhancers were present in various proportions with keeping their global concentrations at the 20% level.

Both the nature and concentration of the respective penetration enhancers affected the RII values. For each formulation, the interindividual variability was reasonably low. Linear dose-effect responses were obtained with ethanol in the range 0–100%, and laurocapram in the range 0–5%. The 10% propylene glycol-based gel exhibited a wide range in RII values when supplemented with NAC, urea and SA. In the bioassay, NAC exhibited a moderate effect on the SC. RII values raised with increasing amounts of urea replacing NAC. The RII worsening was more striking with SA supplementation replacing urea. The combination of SA and urea always proved to be more active than SA alone.

### 17.4 Corneoxenometry and Organic Solvents

The effects of organic solvents were studied on many occasions (Peck et al. 1994; Garcia et al. 2000). In particular, they were compared using corneoxenometry (Ochalek et al. 2012). Series of CSSS were immersed for 1, 5, 10, 30, 60 or 120 min in vials containing deionized water or an organic solvent including chloroform, ethanol, hexane, methanol, chloroform:methanol (2:1, v/v), hexane:ethanol (2:3, v/v) and hexane:methanol (2:3, v/v). After contact with the selected solvent(s) for the predetermined time, CSSS were thoroughly rinsed for 20 s under running tap water, air-dried and stained for 3 min with toluidine blue-basic fuchsine dyes.

The CIM ranking from the least to the most aggressive product was as follows: hexane

(40.7), ethanol (26.5), methanol (23.5), hexane-ethanol (23.3), chloroform (20.8), chloroform-methanol (15.5) and hexane-methanol (7.8). CIM values showed that the effect of hexane-methanol on SC was significantly higher ( $p < 0.01$ ) than those of all other solvents with the exception of chloroform-methanol. There was no significant difference between ethanol, methanol and hexane-ethanol, but each of them was significantly ( $p < 0.05$ ) more aggressive than hexane.

The influence of exposure time of solvents with the SC showed some inter-product differences. However, all correlations reached significance ( $p < 0.01$ ) and best fitted as logarithmic relationships. For each solvent, most of the CIM changes were reached within 10 min.

The organic solvents under consideration are known to extract lipids (Bligh and Dyer 1959; Scheuplein and Ross 1970; Deffond et al. 1986; Imokawa et al. 1986; Abrams et al. 1993; Lavrijsen et al. 1994). In addition, SC alterations other than lipid extraction are likely (Abrams et al. 1993). Large interindividual CIM differences were found for each solvent or mixture (Goffin et al. 1997b) reflecting the variability in the overall lipid extraction by these solvents (Diembeck et al. 1999). The induced alterations on normal human SC by solvents (corneoxenometry bioassay) were indeed reported to be more variable than those induced by diluted surfactants (corneourfamestry bioassay) (Goffin et al. 1998; Xhaufaire-Uhoda et al. 2008b). Despite interindividual inconsistencies in corneocyte alterations, significant differences were reported among solvents using the corneoxenometry bioassay (Goffin et al. 1997b). Hexane-methanol and chloroform-methanol were the mixtures strongly altering the SC structure. Chloroform-methanol is indeed considered to be the most potent extraction mixture for lipids in biologic samples. However, it did not reach the top ranking at the corneoxenometry bioassay (Goffin et al. 1997b). Such a finding further illustrated the fact that organic solvents alter other biologic components (Diembeck et al. 1999), which in turn affect the corneoxenometry data.

The corneoxenometry bioassay allows to assess the influence of the contact time between

solvents and the SC. In previous studies (Goffin et al. 1997b), the time range between 1 and 120 min was selected following available information about the kinetics of lipid extraction from human SC [13]. The corneoxenometry data were in line with previous experiments using other methodological approaches (Deffond et al. 1986; Imokawa et al. 1986; Abrams et al. 1993; Lavrijsen et al. 1994). However, it does not explore the effects of solvents on the living epidermis and on the nature and intensity of inflammation that is present in irritant dermatitis.

### Conclusion

Corneoxenometry appears as a relevant and predictive bioassay for assessing the overall effect of single and combined penetration enhancers. It is cheap, rapid, minimally invasive and relevant to human skin. In addition, the reproducibility, specificity and sensibility are reasonably high. Corneoxenometry is therefore a valuable screening test proposed as an alternative to animal and in vitro testings.

### References

- Abrams K et al (1993) Effect of organic solvents on in vitro human skin water barrier function. *J Invest Dermatol* 101:609–613
- Bligh EG, Dyer WJ (1959) A rapid method of total lipid extraction and purification. *Can J Biochem Physiol* 37:911–917
- Deffond D et al (1986) In vivo measurements of epidermal lipids in man. *Bioeng Skin* 2:71–85
- Diembeck W et al (1999) Test guidelines for in vitro assessment of dermal absorption and percutaneous penetration of cosmetic ingredients. *Food Chem Toxicol* 37:191–205
- Engelbrecht TN et al (2012) Study of the influence of the penetration enhancer isopropyl myristate on the nanostructure of stratum corneum lipid model membranes using neutron diffraction and deuterium labelling. *Skin Pharmacol Physiol* 25:200–217
- Garcia N et al (2000) Use of reconstructed human epidermis cultures to assess the disrupting effect of organic solvent on the barrier function of excised human skin. *In Vitro Mol Toxicol* 13:159–171
- Goffin V et al (2000) Penetration enhancers assessed by corneoxenometry. *Skin Pharmacol Appl Skin Physiol* 13:280–284
- Goffin V et al (1997a) Sodium hypochlorite, bleaching agents and the stratum corneum. *Ecotoxicol Environ Safe* 37:199–202

- Goffin V, Letawe C, Piérard GE (1997b) Effect of organic solvents on normal human stratum corneum. Evaluation by the corneoxenometry bioassay. *Dermatology* 195:321–324
- Goffin V, Paye M, Piérard GE (1995) Comparison of in vitro predictive tests for irritation induced by anionic surfactants. *Contact Dermatitis* 33:38–41
- Goffin V, Piérard-Franchimont C, Piérard GE (1996) Sensitive skin and stratum corneum reactivity to household cleaning products. *Contact Dermatitis* 34:81–85
- Goffin V, Piérard-Franchimont C, Piérard GE (1998) Shielded corneoxenometry and corneoxenometry: novel bioassays for the assessment of skin barrier products. *Dermatology* 196:434–437
- Hadgraft J, Walters KA (1994) Skin penetration enhancement. *J Dermatol Treat* 5:43–47
- Imokawa G et al (1986) Selective recovery of deranged water-holding properties by stratum corneum lipids. *J Invest Dermatol* 87:758–761
- Kandárovà H et al (2009) In vitro skin irritation testing: improving the sensitivity of the EpiDerm skin irritation test protocol. *Altern Lab Anim* 37:671–689
- Keerthi H, Panakanti PK, Yamsani MR (2012) Design and characterization of Atenolol transdermal therapeutic systems: enhancement of permeability via iontophoresis. *PDA J Pharm Sci Technol* 66:318–332
- Kojima H et al (2012) Validation study of the in vitro skin irritation test with the LabCyte EPI-MODEL24. *Altern Lab Anim* 40:33–50
- Lavrijsen APM et al (1994) Validation of an in vivo extraction method for human stratum corneum ceramides. *Arch Dermatol Res* 286:495–503
- Macfarlane M et al (2009) A tiered approach to the use of alternatives to animal testing for the safety assessment of cosmetics: skin irritation. *Regul Toxicol Pharmacol* 54:188–196
- Notman R et al (2013) Breaching the skin barrier – Insightsbarrier-insights from molecularsimulation molecular stimulation of model membranes. *Adv Drug Deliv Rev* 65:237–250, Epub March 3, 2012
- Ochalek M et al (2012) SC lipid model membranes designed for studying impact of ceramide species on drug diffusion and permeation. Part III: influence of penetration enhancer on diffusion and permeation of model drugs. *Int J Pharm* 436:206–213, Epub Jul 4, 2012
- Peck KD, Ghanem AH, Higuchi WI (1994) Hindered diffusion of polar molecules through and effective pore radii estimates of intact and ethanol treated human epidermal membrane. *Pharm Res* 11:1306–1314
- Piérard GE et al (1995) Surfactant induced dermatitis. A comparison of corneoxenometry with predictive testing on human and reconstructed skin. *J Am Acad Dermatol* 33:462–469
- Piérard GE, Goffin V, Piérard-Franchimont C (1994) Squamometry and corneoxenometry in rating interactions of cleansing products with stratum corneum. *J Soc Cosmet Chem* 45:269–277
- Piérard GE, Piérard-Franchimont C (1996) Drug and cosmetic evaluations with skin stripping. In: Maibach HI (ed) *Dermatologic research techniques*. CRC Press, Boca Raton, pp 133–149
- Rojas J et al (1991) Optimization of binary and ternary solvent systems in the percutaneous absorption of morphine base. *STP Pharmacol Sci* 1:70–75
- Scheuplein R, Ross L (1970) Effect of surfactants and solvents on the permeability of epidermis. *J Soc Cosmet Chem* 21:853–873
- Seto JE et al (2012) Fluorescent penetration enhancers for transdermal applications. *J Control Release* 158:85–92
- Som I, Bhatia K, Yasir M (2012) Status of surfactants as penetration enhancers in transdermal drug delivery. *J Pharm Bioallied Sci* 4:2–9
- Uhoda E, Goffin V, Piérard GE (2003) Responsive corneoxenometry following in vivo preconditioning. *Contact Dermatitis* 49:292–296
- Ward AJI, Du Reau C (1991) The essential role of lipid bilayers in the determination of stratum corneum permeability. *Int J Pharm* 74:137–146
- Welss T, Basketter DA, Schröder KR (2004) In vitro skin irritation: facts and future. State of the art review of mechanisms and models. *Toxicol In Vitro* 18:231–243
- Williams AC, Barry BW (1992) Skin absorption enhancers. *Critic Rev Ther Drug Carrier Syst* 9:305
- Woodford R, Barry BW (1986) Penetration enhancers and the percutaneous absorption of drugs: an update. *J Toxicol Cut Occular Toxicol* 5:165
- Wotton PK et al (1985) A Vehicle effect on topical drug delivery Effect of azone on the cutaneous penetration of metronidazole and propylene glycol. *Int J Pharmacol* 24:19–26
- Xhaufflaire-Uhoda E et al (2008a) Skin protection creams in medical settings: successful or evil? *J Occup Med Toxicol* 3:15–20
- Xhaufflaire-Uhoda E et al (2008b) Effect of various concentrations of glycolic acid at the corneoxenometry and collagenometry bioassays. *J Cosmet Dermatol* 7:294–298



---

## **Part III**

# **The Retardation of Percutaneous Drug Penetration**

Katharina Bohnenblust-Woertz  
and Christian Surber

## Contents

18.1	Introduction .....	311
18.2	Cyclodextrins and Photostability .....	312
18.3	Transcutol® .....	312
18.4	Encapsulation Structures .....	313
18.5	Physical Properties of Organic Particulate UV Absorbers .....	315
18.6	Inorganic Materials .....	315
18.7	Penetration Retarders .....	316
18.8	Vehicle Effects .....	317
	Conclusions .....	317
	References .....	318

## 18.1 Introduction

There is overwhelming evidence indicating that human skin is damaged in different ways by exposure to sunlight. Of the solar radiation reaching the earth's surface, the ultraviolet (UV) component (290–400 nm) is a major factor leading to skin pathologies that range in severity from inflammatory responses, cutaneous photoaging, dendritic keratitis to various types of skin cancer (Pathak 1991; Ziegler et al. 1994; Hochberg and Enk 1999; Surber et al. 2012). The increasing knowledge of the deleterious effects of sunlight has promoted the widespread use of topical sunscreen preparations (Hayden et al. 1998; Green et al. 1991), which contain chemicals that absorb, reflect, or scatter UV radiation (Patel et al. 1992) and are thereby highly effective skin protectants. Organic sunscreen agents are compounds that decrease the intensity of UV light reaching the epidermal strata by absorbing radiation (typical electron promotion from a lower- to a higher-energy molecular orbital). The activated sunscreen molecule dissipates the excess energy in the form of heat, by fluorescence, phosphorescence, interaction with neighboring molecules, or by undergoing photochemical modifications (Broadbent et al. 1996). Particulate sunscreens present a physical barrier between the incident radiation and the epidermis, scattering or reflecting the radiation. However, to be effective, these agents must remain on or in the outermost layers of the skin, the stratum corneum

K. Bohnenblust-Woertz  
Galderma Spirig, Egerkingen, Switzerland

C. Surber (✉)  
University Hospital Zürich, Department of  
Dermatology, Zürich, Switzerland

University Hospital Basel, Department of  
Dermatology, Petersgraben 4,  
CH-4031 Basel, Switzerland  
e-mail: [christian.surber@unibas.ch](mailto:christian.surber@unibas.ch)

(SC). One major drawback of current sunscreen formulations is that they are constantly lost from the skin surface by abrasion from clothing, sweating, or swimming, requiring frequent reapplication for continued effectiveness. Moreover, several of the chemical sunscreens currently on the market exhibit irritancy and sensitization reactions after absorption into the dermal strata in predisposed individuals, often causing immunological problems (Deflandre and Lang 1998; Dromgoole and Maibach 1990; Mariani et al. 1998). A significant improvement in sunscreen technology would be the development of systems that retard the penetration of the chemical into the skin and bind the agent in the stratum corneum so that minimal loss occurs by diffusion or abrasion. The degree of sunscreen penetration depends strongly on the physicochemical properties of the active compound and of the nature of the vehicle in which the sunscreen is applied, that is, polarity of the ingredients that form the vehicle and the filters particle size (Benech-Kieffer et al. 2000). Therefore, the development of suitable formulations that prevent penetration of the sunscreen into the skin is a challenge for developers. Some of the few vehicular penetration retardation strategies being researched for sunscreens are reviewed below.

---

## 18.2 Cyclodextrins and Photostability

Cyclodextrins are cyclic, toroidal-shaped oligosaccharides with a hydrophilic external surface and a hydrophobic central core. They are capable of incorporating appropriately sized, nonpolar compounds or some lipophilic moiety of a molecule into their apolar cavities, forming non-covalent inclusion complexes (Rajewski and Stella 1996; Loftsson and Brewster 1996). This type of molecular encapsulation can lead to changes in some of the physical and chemical properties of the included substance, such as the enhancement of stability to air and light and apparent aqueous solubility (Rajewski and Stella 1996; Loftsson and Brewster 1996; Uekama et al. 2003). Moreover, cyclodextrin complexation can affect the topical availability of applied drugs, either increasing or

decreasing their penetration into or permeation through the skin (Rajewski and Stella 1996; Loftsson and Masson 2001). Butylmethoxydibenzoylmethane (BM-DBM) is a widely used filter that provides protection against UVA radiation in the 320–400 nm range. However, BM-DBM experiences marked photodegradation (Schwack and Rudolph 1995; Scalia et al. 1998; Tarras-Wahlberg et al. 1999; Chatelain and Gabard 2001; Damiani et al. 1999; Scalia et al. 2002), forming highly reactive photolytic products that are exposed to the living tissues of the epidermis and dermis following percutaneous permeation. Scalia et al. (1998, 2002) have demonstrated that the degree of decomposition and free radical formation upon exposure of BM-DBM to simulated sunlight were reduced by complexation with hydroxypropyl-13-cyclodextrin (HP-13-CD). The effects of HP-13-CD and sulfobutylether-13-cyclodextrin (SBE7-13-CD) on *in vitro* human skin penetration and retention of the sunscreen agent BM-DBM were investigated by Simeoni et al. (2004). They reported that approximately 14–16% of the applied dose of BM-DBM penetrated into the skin tissue; however, no sunscreen was detected in the dermis and in the receptor phase. The greater proportion (84.6–95.5%) of the absorbed UV filter was localized in the SC with no significant differences between uncomplexed and complexed BM-DBM. Notable levels (2.3% of the applied dose) of the sunscreen agent accumulated in the epidermis from the preparation containing free BM-DBM. The epidermal concentration of the UV filter was markedly reduced (0.7% of the applied dose) by complexation with SBE7-13-CD, whereas HP-13-CD had no effect. The results demonstrated that complexation of BM-DBM with SBE7-13-CD attained high sunscreen levels at the skin surface where its action is most desirable and produced lower concentrations of the active in the epidermis.

---

## 18.3 Transcutol®

Ethoxydiglycol (Transcutol® CG, Gattefosse, France) is a hygroscopic liquid that is freely miscible with both polar and nonpolar solvents.

Transcutol® has been recognized as a potential transdermal permeation enhancer due to its non-toxicity, biocompatibility with skin, and excellent solubilizing properties (Godwin et al. 2002). However, Transcutol® has also been reported to increase the skin accumulation of topically applied compounds without a concomitant increase in transdermal permeation (Ritschel et al. 1991; Panchagnula and Ritschel 1991). It is theorized that this depot effect is created by a swelling of stratum corneum intercellular lipids, without alteration of their multiple bilayer structure. The expanded lipid domain is then able to retain drugs (especially lipophilic compounds) to form the depot, with a simultaneous decrease in transdermal permeation.

Godwin et al. (2002) studied the influence of Transcutol® CG concentrations in sunscreen formulations on the transdermal permeation and skin accumulation of the UV absorbers 2-hydroxy-4-methoxybenzophenone (oxybenzone) and 2-octyl-4-methoxycinnamate (cinnamate).

When formulated alone, both these lipophilic sunscreens have been shown to permeate through the skin and enter the systemic circulation (Treffel and Gabard 1996). In their study, the concentration of the UV absorber was held constant at 6% (w/w) for all vehicle systems while the concentration of Transcutol® CG was varied from 0 to 50% (w/w). The data demonstrated that both UV absorbers exhibited an increase in skin *accumulation* with increasing concentrations of Transcutol® CG. Skin accumulation of oxybenzone was significantly ( $P < 0.05$ ) greater than that of cinnamate for all formulations investigated. However, no significant differences were found in the transdermal *permeation* of oxybenzone or cinnamate for any of the formulations tested. The results of this study demonstrate that the inclusion of Transcutol® CG in sunscreen formulations appears to increase the skin accumulation of the UV absorbers oxybenzone and cinnamate, without a concomitant increase in transdermal permeation. Their data support the theory of the formation of an intracutaneous depot for both oxybenzone and cinnamate when formulated with Transcutol® CG. These observations have to be confirmed in vivo. As the accumulation occurs

not only in the epidermis but also in deeper layers of the skin the potential bioavailability remains unknown.

---

## 18.4 Encapsulation Structures

Colloidal drug carriers, including submicron emulsions, nanospheres, nanocapsules, liposomes, and lipid complexes, have been attracting increasing interest as drug delivery vehicles. These encapsulation systems have been evaluated for the intravenous administration of lipophilic drugs, as improved parenteral formulations, and as systems for site-specific drug delivery such as tumors (Allemann et al. 1993). In general, two techniques have been used for the preparation of nanocapsules based on biodegradable polymers: the emulsification-diffusion technique (Quintanar-Guerrero et al. 1996) and the solvent displacement procedure (Fessi et al. 1988; Al Khouri Fallouh 1986). The ideal medium in which an active ingredient is incorporated must provide not only the necessary solubility but also maintain contact between the active ingredient and the skin. The nature of the colloidal carrier and the effects of size and surface charge influence penetration and permeation of UV filters into the skin (Zeevi et al. 1994; Treffel and Gabard 1996; Gupta et al. 1999).

Alvarez-Roman et al. (2001) investigated the optimization of a solvent displacement method for poly( $\epsilon$ -caprolactone) nanocapsules, using the lipophilic UV filter, octyl methoxycinnamate (OMC) as the oil core. In addition, these researchers evaluated the influence of polysorbate 85 (Tween 85) and poloxamer 188 (Pluronic F 68) as filter-stabilizing agents, the OMC loading capacity, and the photoprotective potential of the formulations. The OMC-nanocapsule-gel preparation resulted in a significantly better ( $P < 0.05$ ) protection against UV-induced erythema than a simple OMC gel. Sunscreen effectiveness implies that the sunscreens adhere to the skin more efficiently as a protective film. These results suggest that the nanoparticles are able to cover more efficiently the skin surface due to their high specific surface area. Sunscreen

nano-capsules, therefore, show good potential as improved skin retention vehicles.

Liposomes and emulsions are formulated from biocompatible excipients and can easily be produced on a large scale. Compared to liposomes and emulsions, solid particles afford protection of incorporated active compounds against chemical degradation and allow more flexibility in modulating the release of the compound. The advantages of solid particles, emulsions, and liposomes were, therefore, combined by the development of solid lipid nanoparticles (SLNs) (Müller et al. 2002), produced by simply exchanging the liquid lipid (oil) of the emulsions by a solid lipid.

Wissing and Müller (2002a) compared an SLN and a conventional o/w emulsion carrier system for the sunscreen oxybenzone, by studying the in vitro rate of release with a membrane-free model and static Franz diffusion cells. They reported that the release rate could be decreased by up to 50% with the SLN formulation. Penetration of oxybenzone into stratum corneum on the forearm in vivo was also investigated by a tape stripping method. In congruity with the in vitro data, it was shown that the active release rate could be decreased by 30–60% with SLN formulations. In all test models, oxybenzone penetrated into the skin less rapidly and to a lesser extent than from conventional emulsions. The authors concluded that using SLN as a carrier system offers two main advantages. SLNs act as physical sunscreens on their own; therefore, the concentration of molecular sunscreen agents can be decreased while maintaining the formulation sun protection factor. Moreover, SLNs are able to provide a sustained release carrier system, enabling the sunscreen to remain longer at its site of action on the surface of the skin.

Similar results were obtained by Wissing et al. (2002b) when they compared the efficacy of a conventional o/w emulsion and crystalline lipid nanoparticles (CLN) incorporating the sunscreen benzophenone-3. This in vitro study based on the Transpore™ test (3M, USA) (Diffey and Parr 1996) showed that the amount of molecular sunscreen can be decreased by up to 50% while maintaining the UV protection efficacy, simply because of the particulate nature of the CLN structures.

Nanocapsules (NC) have been introduced as a new generation of carriers for cosmetics and UV blockers for use on human skin and hair. Jimenez et al. (2004) compared the porcine skin permeation of a lipophilic sunscreen, OMC, from different emulsions and encapsulated sunscreen-poly( $\epsilon$ -caprolactone) nanocapsules. Their results showed that the use of NC emulsions decreases the permeation of OMC through pig skin when compared with equivalent w/o and o/w emulsions. NC emulsions are, therefore, novel vehicle-type dispersion systems and can be used advantageously as sunscreen carriers to lower permeation of the active through the skin.

A very promising approach is to entrap the organic UV absorbers in a sol-gel silica glass shell. The product is commercialized under the trade name of Eusolex® UV Pearls™ (Merck, Germany) and is promoted under the slogan *Sunglasses for the Skin™*. The UV absorber, which is usually an oil or oil soluble compound, constitutes about 80% of the capsule weight. The products are manufactured as an aqueous dispersion, containing 35% (by weight) UV absorber(s). The particle size is about 1 micron on average and they do not tend to agglomerate; therefore, they give a “pleasant skin feeling”. The refraction index of the particles is small enough that they appear transparent when applied topically. The glass microcapsules were shown to effectively retain the encapsulated UV absorbers in a series of stress experiments. These include temperature, drying, pressure (e.g., spraying), and incubation with emollients, tensides, and other raw materials, which could have the potential to extract the capsules content. All experiments clearly demonstrated the stability of the capsules. Additionally, different skin penetration experiments showed the maintenance of sunscreen actives on or near the surface of the skin compared to non-encapsulated material.

The encapsulated sunscreens obtained through the Sol-Gel glass-making technology is currently the most promising technology for significantly improved product characteristics. The direct contact between the sunscreen filters and the body tissues is suppressed – the filter is no longer bio-available. Products with UV Pearls are therefore suited for products for sensitive skin. In addition,

the UV Pearls give the product a pleasant sensory feel (Pflücker et al. 2002).

---

### 18.5 Physical Properties of Organic Particulate UV Absorbers

Most of the UV filters in use are oil-soluble and, consequently, are incorporated into the oil phase of sunscreen emulsions; however, even solubility in the oil may be problematic. UV absorbers that are poorly soluble in oils and relatively insoluble in water may be micronized to form aqueous dispersions of ultrasmall particle size. The protective performance of these particles depends on size, as both absorption and scattering play a role in the attenuation of UV light. To this end, it is desirable to achieve particle sizes in the submicrometer range.

Herzog et al. (2004a) generated microparticles of a benzotriazole derivative in the 0.16–40  $\mu\text{m}$  range by milling particles in the presence of a dispersing agent. The UV absorption increases with a decrease in particle size, while the light scattering shows a maximum at a certain particle size. These researchers investigated the UV-attenuating properties of particulate organic absorbers as a function of particle size, with special emphasis on the differentiation between absorption and scattering functionalities of the particles (Herzog et al. 2004b). The efficiency of the UV extinction of the dispersion increases with decreasing particle size down to a maximum extinction at a particle size of 80 nm, and the UV extinction decreases for particles smaller than 80 nm indicating an optimum at 80 nm. It was found from reflection spectroscopic measurements that scattering accounts for about 10%, and absorption 90%, of the UV-attenuating effect of the particles.

---

### 18.6 Inorganic Materials

Micronized  $\text{TiO}_2$  particles with a diameter of about 15 nm are used in sunscreens as physical UV filters. These particles are suspected to be absorbed through the stratum corneum into the epidermis or dermis via intercellular channels,

hair follicles, and sweat glands. This penetration is undesirable because of the risk of damage to DNA and RNA by the photocatalytic effects of the  $\text{TiO}_2$  after absorption of UV light (Dunford et al. 1997). Furthermore, the particles can activate the immune system and accumulations of these particles in the skin can decrease the threshold for allergies (Granum et al. 2001). The function of the stratum corneum as a barrier against dermal uptake of ultrafine particles was the subject of several investigations, which came to different conclusions concerning the penetration depth of the particles (Pflücker et al. 2001; Tan et al. 1996). Researchers have investigated a number of other ultrafine, inorganic particles, including ceria ( $\text{CeO}_2$ ) (Yabe and Sato 2003) and zinc oxide, for efficacy as UV-protectants. Most of these agents are ideal for cosmetic applications because they are relatively transparent to visible light, but have excellent ultraviolet radiation absorption properties, and appear transparent on the skin. However, many of these chemicals exhibit high photocatalytic potential after UV activation (Cai et al. 1991). This reactivity can be lowered by coating of the particles (with amorphous silica for example) or by doping with a metal ion possessing lower valence and larger ionic size.

Menzel et al. (2004) investigated the percutaneous penetration of coated  $\text{TiO}_2$  through pig skin and observed a penetration of particles through the stratum corneum into the underlying stratum granulosum via the intercellular spaces, but the  $\text{TiO}_2$  particle concentration in the stratum spinosum was negligible. Hair follicles did not seem to be major penetration pathways as  $\text{TiO}_2$  was not detected inside these appendages. These findings show the importance of coating the  $\text{TiO}_2$  particles as a mechanism to reduce genetic damage in the skin. Alternatively, any formulation mechanism that would retard the penetration of the particles below the outermost SC layers would be highly advantageous. One possible mechanism to achieve this may be the chemical sequestration of the organic active. To minimize absorption of sunscreen agents through the skin, organic materials may be incorporated in the nanospaces of inorganic materials, thereby avoiding direct exposure to the stratum corneum's bio-

chemical environment. Layered double hydroxides (LDHs) consist of hydrotalcite-like layers and exchangeable interlayer anions (Taylor 1984; Sato et al. 1993; Cavani et al. 1991; Lakraimi et al. 2000). The unique anion exchange capability of LDH enables the encapsulation of UV absorbents with a negative charge. However, organic UV absorbents are often de-intercalated by an anion exchange reaction with carbonate ions, since the selectivity of ion exchange of carbonate is higher. This problem may also be minimized by silica coating of the entire composite (El-Toni et al. 2005).

## 18.7 Penetration Retarders

Transdermal penetration enhancers have been synthesized and tested for their ability to increase the amount of co-administered drug in a topical formulation that can be delivered through the skin. The uniform, parallel arrangement of molecules in the lipid bilayer is disrupted by the presence of the enhancer, causing convolution of the bilayer molecules and, subsequently, decreasing the ability of these structures to act as a barrier to the passive diffusion of chemicals applied to the skin surface. The net result is a reversible reduction in the barrier properties of the skin, and higher concentrations of drug reaching the dermal circulation. *Conversely*, it should be possible to chemically bind the molecules of the lipid bilayers more closely and rigidly together, thereby increasing the barrier potential of this intercellular domain. This has been the premise of the very limited research that has been carried out in the field of penetration retarders.

Hadgraft et al. (1996) reported the existence of compounds of a similar structure to *N-Dodecylcaprolactam* (Azone<sup>®</sup>) (sulfur analogue of Azone) which acted as drug retardants rather than enhancers. Such agents would have applications in formulations that contain sunscreens, pesticides, or drugs with specific local-skin targeting. These authors tested Azone<sup>®</sup> and five of its analogues using in vitro diffusion-cell methodology and human cadaver skin. In addition, the compounds were tested for their ability

to reduce the phase-transition temperature of dipalmitoyl phosphatidylcholine (DPPC). The two drugs used for the evaluation were metronidazole and diethyl m-toluamide (DEET), and all experiments were performed for 40 h. The compounds were placed in the donor chambers of Franz diffusion cells in a 1 % ethanolic solution and left for 2 h. This pretreatment was followed by the application of a finite dose of metronidazole or DEET in the ethanolic solution (5 μmol/ml). Based on the reduction of the phase-transition temperature of DPPC, the analogues of Azone were ranked: N-0539 > N-0721 > N-0253 = N-0131 > N-0915. Therefore, N-0915 increased the phase transition temperature, suggesting that it enters the bilayer of the liposome and increases the carbon side-chain rigidity. This may imply that N-0539 would be a retarder rather than an enhancer. All compounds, except N-0915, showed some degree of enhancement activity. In contrast, N-0915 produced an enhancement ratio at 40 h of only 0.2, compared with the control; a significant retardation rather than an enhancement. Experiments with DEET showed a similar trend in activity with all six compounds tested.

More recently Michniak-Kohn (Kaushik et al. 2010) and her group investigated the enhancement/retardation of percutaneous permeation of diethyl-m-toluamide (DEET) in the presence of five percutaneous penetration modifiers (laurocapram, 3-dodecanoyloxazolidin-2-one (N-0915), S,S-dimethyl-N-(4-bromobenzoyl) iminosulfurane (DMBIS), S,S-dimethyl-N-(2-methoxycarbonylbenzenesulfonyl) iminosulfurane (DMMCB), and tert-butyl 1-dodecyl-2-oxoazepan-3-yl-carbamate (TBDOC)). These permeation modifiers were formulated in either water, propylene glycol (PG), ethanol, or polyethylene glycol 400 (PEG 400). The permeation studies indicated that laurocapram enhanced DEET permeation in PG, but retarded in PEG 400. Likewise, N-0915 acted as a retardant with ethanol and PEG 400, but not with water. DMBIS decreased the permeation with ethanol as compared to permeation with water, PEG 400 or PG. Similarly, DMMCB acted as a retardant with ethanol and PEG 400, but not with water or PG. TBDOC formulations revealed

its activity as a retardant with ethanol, but behaved as enhancer with water, PG and PEG 400.

The investigations of Hadgraft and Michniak-Kohn are significant since they underline the role of pharmaceutical formulations and show that ingredients termed as enhancers can become a retardant or vice versa depending upon the vehicle in which they are applied to the skin.

Very obvious is the penetration retarding effect produced by the lipophilicity and the high molecular weight of filters. An illustrative example is the design and development of Bis-Ethylhexyloxyphenol Methoxyphenyl Triazine (Tinosorb® S, BASF, Germany) with a molar mass of 627.81 g/mol and a log partition coefficient n-octanol/water: >5.5 at 20 °C, a molecular feature that predicts no permeation into deeper parts of the skin (Bos and Meinardi 2000).

---

## 18.8 Vehicle Effects

Similarly, there are relatively few studies examining the effect of vehicle viscosity on cutaneous penetration following the application of finite or small “in use” doses of topical drug formulations. Cross et al. (2001) compared the effect of viscosity on the *in vitro* penetration of benzophenone from four different types of emulsion formulations. The researchers maintained the same thermodynamic activity in all test modes, using both epidermal and high density polyethylene (HDPE) membranes, and allowed for control of any possible vehicle-skin interactions. In addition, the change in percutaneous absorption and retention kinetics of benzophenone from the emulsions following infinite and finite dose application was determined in an attempt to define the effects of viscosity on actual “in use” conditions. In the latter situation, factors such as formulation evaporation (estimated from the rate of vehicle water loss) would be expected to make a significant contribution to release kinetics (metamorphosis of the vehicle) (Surber and Smith 2005). The results from the human epidermal permeation flux data indicate that while the flux of benzophenone decreased with formulation viscosity for the infinite dosed formulation, the flux was increased

with increasing viscosity for the finite dosed formulation (simulating “in use” situation). The epidermal membrane retention of benzophenone also decreases with viscosity for the infinite dose. In contrast, the epidermal membrane retention for the finite dose appears to be unaffected by the viscosity of the formulation used. The absorption and retention profiles with viscosity are similar for HDPE membranes to that observed for human epidermal membranes. However, even the concepts of “finite” and “infinite” dose have been open to wide interpretation by researchers (Surber and Davis 2002).

The discrepancy in the infinite and finite dosing results is likely to arise from the differing diffusion of benzophenone in the formulations, and skin hydration arising in the two situations. Slower water evaporation is likely to result in a higher water content in the residual vehicle film and an increase in skin penetration due to a higher diffusivity in a more hydrated membrane (Roberts and Walker 1993). It is unlikely that the formulations have affected drug partitioning into the skin as epidermal retention for the four vehicles was similar. Hence, the flux of benzophenone-3 through both human epidermal and HDPE membranes decreases with increasing formulation viscosity. The clinical implications from the study is that caution should be exercised in assuming that more viscous formulations applied to the skin may retard the penetration of topically applied sunscreens. Viscous formulations impede the skin penetration of benzophenone under infinite dosing conditions, but appear to cause faster skin penetration using finite dosed “in use” formulations. The interesting aspect from a formulation viewpoint is that it may be possible to modulate absorption by simple changes in the vehicle matrix, a conclusion that corroborates early findings of Haigh et al. (1992).

---

### Conclusions

A number of strategies have been individually evaluated to limit the absorption of sunscreens after topical application. It would be interesting to judiciously combine these scientific concepts that have been investigated individually, into an integrated topical delivery system of



chemical composition, formulation microstructure and specific penetration retarder such that the delivered sunscreen chemical is held in a bound reservoir in the layers of the stratum corneum, preventing penetration into the lower strata and dermis, and minimizing surface loss. In this manner, the sun-protecting agent would be held at its optimal site of action – the uppermost layer of the skin – for a prolonged period, and would induce minimal sensitizing or irritancy activity because of exposure to the systemic circulation. The design and the development of the Eusolex® UV Pearls™ and Bis-Ethylhexyloxyphenol Methoxyphenyl Triazine (Tinosorb® S) – a high molecular lipophilic, photostable, broad-spectrum UV absorber efficiently covering both the UVA and UVB range – impressively demonstrate retardation strategies for sunscreen agents. Perhaps the addition of a specific keratin-binding agent may extend the longevity of the sunscreen even further. Clearly sunscreen optimization technology is still in its infancy in terms of maintaining the active protectant at its site of action. Hopefully, formulation research will soon enable the development of optimized sun-induced skin cancer protection vehicles.

## References

- Al Khouri Fallouh N, Roblot-Treupel L, Fessi H, Devissaguet JP, Puisieux F (1986) Development of a new process for the manufacture of polyisobutylcyanoacrylate nanocapsules. *Int J Pharm* 28:125–132
- Allemann E, Gurny R, Doelker E (1993) Drug-loaded nanoparticles – preparation methods and drug targeting issues. *Eur J Pharm Biopharm* 39:173–191
- Alvarez-Roman R, Barre G, Guy RH, Fessi H (2001) Biodegradable polymer nanocapsules containing a sunscreen agent: preparation and photoprotection. *Eur J Pharm Biopharm* 52:191–195
- Benech-Kieffer F, Wegrich P, Schwarzenbach R, Klecak G, Weber T, Leclaire J et al (2000) Percutaneous absorption of sunscreens in vitro: interspecies comparison, skin models and reproducibility aspects. *Skin Pharmacol Appl Skin Physiol* 13:324–335
- Bos JD, Meinardi MM (2000) The 500 Dalton rule for the skin penetration of chemical compounds and drugs. *Exp Dermatol* 9(3):165–169
- Broadbent JK, Martincigh BS, Raynor MW, Salter LF, Moulder R, Sjoberg P et al (1996) Capillary supercritical fluid chromatography combined with atmospheric pressure chemical ionisation mass spectrometry for the investigation of photoproduct formation in the sunscreen absorber 2-ethylhexyl-p-methoxycinnamate. *J Chromatography* 732:101–110
- Cai R, Hashimoto K, Itoh K, Kubota Y, Fujishima A (1991) Photokilling of malignant cells with ultrafine TiO<sub>2</sub> powder. *Bull Chem Soc Jap* 64:1268–1273
- Cavani F, Trifiro F, Vaccari A (1991) Hydrotalcite-type anionic clays: preparation, properties and applications. *Catalysis Today* 11:173–301
- Chatelain E, Gabard B (2001) Photostabilization of butyl methoxydibenzoylmethane (Avobenzone) and ethylhexyl methoxycinnamate by bis-ethylhexyloxyphenol methoxyphenyl triazine (Tinosorb S), a new IN broad-band filter. *Photochem Photobiol* 74:401–406
- Cross SE, Jiang R, Benson HAE, Roberts MS (2001) Can increasing the viscosity of formulations be used to reduce the human skin penetration of the sunscreen oxybenzone? *J Invest Dermatol* 117:147–150
- Damiani E, Greci L, Parsons R, Knowland J (1999) Nitroxide radicals protect DNA from damage when illuminated in vitro in the presence of dibenzoylmethane and a common sunscreen ingredient. *Free Radical Biol Med* 26:809–816
- Deflandre A, Lang G (1998) Photostability assessment of sunscreens. Benzylidene camphor and dibenzoylmethane derivatives. *Int J Cos Sci* 10:53–62
- Diffey BL, Parr PM (1996) Sunscreen protection against UVB, UVA and blue light: an in vivo and in vitro comparison. *Brit J Dermatol* 124:258–263
- Dromgoole SH, Maibach HI (1990) Sunscreening agent intolerance: contact and photocontact sensitization and contact urticaria. *J Am Acad Dermatol* 22:1068–1078
- Dunford R, Salinaro A, Cai L, Serpone N, Horikoshi S, Hidaka H, Knowland J (1997) Chemical oxidation and DNA damage catalysed by inorganic sunscreen ingredients. *FEES Lett* 418:87–90
- El-Toni AM, Yin S, Sato T (2005) Silica coating of Zn2Al/ 4-hydroxy-3-methoxybenzoic acid nanocomposites via seeded polymerization technique. *Mat Chem Phys* 89:154–158
- Fessi H, Devissaguet JP, Puisieux F, Thies C (1988) Procédé de préparation de systèmes colloïdaux dispersibles d'une substance, sous forme de nanoparticules. *French Pat* 2:608–988
- Godwin DA, Kim NH, Felton LA (2002) Influence of transcutol CG on the skin accumulation and transdermal permeation of ultraviolet absorbers. *Eur J Pharm Biopharm* 53:3–27
- Granum B, Gaarder PI, Groeng EC, Leikvold RB, Namork E, Lovik M (2001) Fine particles of widely different composition have an adjuvant effect on the production of allergenspecific antibodies. *Toxicol Lett* 118:171–181
- Green A, Williams G, Neale R, Hart V, Leslie D, Parsons P et al (1991) Daily sunscreen application and betacarotene supplementation in prevention of basal-cell and squamous-cell carcinomas of the skin: a randomised controlled trial. *Lancet* 354:723–729

- Gupta VK, Zatz JL, Rerek M (1999) Percutaneous absorption of sunscreens through micro-Yucatan pig skin in vitro. *Pharm Res* 16:1602–1607
- Hadgraft J, Peck J, Williams DG, Pugh WJ, Allan G (1996) Mechanisms of action of skin penetration enhancers/retarders: Azone and analogues. *Int J Pharm* 141:17–25
- Haigh JM, Smith EW, Meyer E, Fassihi R (1992) Influence of the oil phase dispersion in a cream base on the in vivo release of betamethasone 17-valerate. *S.T.P. Pharm Sci* 2:259–264
- Hayden CG, Roberts MS, Benson HA (1998) Sunscreens: are Australians getting the good oil. *Australian New Zealand J Med* 28:639–646
- Herzog B, Katzenstein A, Quass K, Stehlin A, Luther H (2004a) Physical properties of organic particulate UV-absorbers used in sunscreens: I. Determination of particle size with fiber-optic quasi-elastic light scattering (FOQELS), disc centrifugation, and laser diffractometry. *J Colloid Interface Sci* 271:136–144
- Herzog B, Quass K, Schmidt E, Muller S, Luther H (2004b) Physical properties of organic particulate UV absorbers used in sunscreens: II. UV-attenuating efficiency as function of particle size. *J Colloid Interface Sci* 276:354–363
- Hochberg M, Enk D (1999) Partial protection against epidermal IL-10 transcription and Langerhans cell depletion by sunscreens after exposure of human skin to UVB. *Photochem Photobiol* 70:766–772
- Jimenez MM, Pelletier J, Bobin MF (2004) Influence of encapsulation on the in vitro percutaneous absorption of octyl methoxycinnamate. *Int J Pharm* 272:45–55
- Kaushik D, Costache A, Michniak-Kohn B (2010) Percutaneous penetration modifiers and formulation effects. *Int J Pharm* 386(1–2):42–51. doi:10.1016/j.ijpharm.2009.10.052
- Lakrainsi M, Legrouri A, Barroug A, De Ray A, Besse J (2000) Preparation of a new stable hybrid material by chloride-2,4-dichlorophenoxyacetate ion exchange into the zinaluminum-chloride layered double hydroxide. *J Mat Chem* 10:1007–1011
- Loftsson T, Brewster ME (1996) Pharmaceutical applications of cyclodextrins. 1. Drug solubilization and stabilization. *J Pharm Sci* 85:1017–1025
- Loftsson T, Masson M (2001) Cyclodextrins in topical drug formulations: theory and practice. *Int J Pharm* 225:15–30
- Mariani E, Neuhoﬀ C, Bargagna A, Bonina F, Giacchi M, De Guidi G et al (1998) Synthesis, in vitro percutaneous absorption and phototoxicity of new benzylidene derivatives of 1,3,3-trimethyl-2-oxabicyclo[2.2.2]octan-6-one as potential sunscreens. *Int J Pharm* 161:65–73
- Menzel F, Reinert T, Vogt J, Butz T (2004) Investigations of percutaneous uptake of ultrafine TiO<sub>2</sub> particles at the high energy ion nanoprobe LIPSION. *Nucl Instr Method Phys Res Sec B Beam Interact Mater Atoms* 219–220:82–86
- Müller RH, Radtke M, Wissing SA (2002) Solid lipid nanoparticles (SLN) and nanostructured lipid carriers (NLC) in cosmetic and dermatological preparations. *Adv Drug Delivery Rev* 54:S131–S155
- Panchagnula R, Ritschel WA (1991) Development and evaluation of an intracutaneous depot formulation of corticosteroids using Transcutol as a cosolvent: in-vitro, ex-vivo, and in vivo rat studies. *Skin Pharmacol* 43:609–614
- Patel NP, Highton A, Moy RL (1992) Properties of topical sunscreen formulations. A review. *J Dermatol Surg Oncol* 18:316–320
- Pathak MA (1991) Ultraviolet radiation and the development of non-melanoma and melanoma skin cancer: clinical and experimental evidence. *Skin Pharmacol* 4:85–94
- Pflücker F, Wendel V, Hohenberg H, Gartner E, Will T, Pfeiffer S, Wepf R (2001) The human stratum corneum layer: an effective barrier against dermal uptake of different forms of topically applied micronised titanium dioxide. *Skin Pharmacol Appl Skin Physiol* 14(Suppl 1):92–97
- Pflücker F, Guinard H, Lapidot N, Chaudhuri R, Marchio F, Driller H (2002) Sunglasses for the skin: Reduction of dermal UV filter uptake by encapsulation. *SÖFW Journal* 128(6):24–28
- Quintanar-Guerrero D, Fessi H, Allemann E, Doelker E (1996) Influence of stabilizing agents and preparative variables on the formation of poly(-lactic acid) nanoparticles by an emulsification-diffusion technique. *Int J Pharm* 143:133–141
- Rajewski RA, Stella VJ (1996) Pharmaceutical applications of cyclodextrins. 2. In vivo drug delivery. *J Pharm Sci* 85:42–69
- Ritschel WA, Panchagnula R, Stemmer K, Ashraf M (1991) Development of an intracutaneous depot for drugs. Binding, drug accumulation and retention studies, and mechanism of depot. *Skin Pharmacol* 4:235–245
- Roberts M, Walker M (1993) Water – the most natural skin penetration enhancer. In: Waiters K, Hadgraft J (eds) *Skin penetration enhancement*. Marcel Dekker, New York, pp 1–30
- Sato T, Onai S, Yoshioka T, Okuwaki A (1993) Causticization of sodium carbonate with rock-salt type magnesium aluminium oxide formed by the thermal decomposition of hydrotalcite-like layered double hydroxide. *J Chem Technol Biotechnol* 57:137–140
- Scalia S, Villani S, Scatturin A, Vandelli MA, Forni F (1998) Complexation of the sunscreen agent, butyl-methoxydibenzoylmethane, with hydroxypropyl- $\beta$ -cyclodextrin. *Int J Pharm* 175:205–213
- Scalia S, Casolari A, Iaconinoto A, Simeoni S (2002) Comparative studies of the influence of cyclodextrins on the stability of the sunscreen agent, 2-ethylhexyl-p-methoxycinnamate. *J Pharm Biomed Anal* 30:1181–1189
- Schwack W, Rudolph T (1995) Photochemistry of dibenzoyl methane INA filters Part 1. *J Photochem Photobiol/Biol* 28:229–234
- Simeoni S, Scalia S, Benson HAE (2004) Influence of cyclodextrins on in vitro human skin absorption of the

- sunscreens, butyl-methoxydibenzoylmethane. *Int J Pharm* 280:163–171
- Surber C, Davis AF (2002) Bioavailability and bioequivalence of dermatological formulations. In: Waiters KA (ed) *Dermatological and transdermal formulations*. Marcel Dekker, Inc., New York/Basel, pp 401–498
- Surber C, Smith EW (2005) The mystical effects of dermatological vehicles. *Dermatology* 210:157–168
- Surber C, Ulrich C, Hinrichs B, Stockfleth E (2012) Photoprotection in immunocompetent and immunocompromised people. *Br J Dermatol* 167(Suppl 2):85–93
- Tan MH, Commens CA, Burnett L, Snitch PJ (1996) A pilot study on the percutaneous of micro fine titanium dioxide from sunscreens. *Australasian J Dermatol* 37:185–187
- Tarras-Wahlberg N, Stenhagen G, Larko O, Rosen A, Wennberg AM, Wennerstrom O (1999) Changes in ultraviolet absorption of sunscreens after ultraviolet irradiation. *J Invest Dermatol* 113:547–553
- Taylor RM (1984) The rapid formation of crystalline double hydroxy salts and other compounds by controlled hydrolysis. *Clay Minerals* 19:591–603
- Treffel P, Gabard B (1996) Skin penetration and sun protection factor of ultra-violet filters from two vehicles. *Pharm Res* 13:770–774
- Uekama K, Hirayama F, Irie T (2003) Cyclodextrin drug carrier systems. *Chem Rev* 98:2045–2076
- Wissing SA, Müller RH (2002a) Solid lipid nanoparticles as carrier for sunscreens: in vitro release and in vivo skin penetration. *J Control Release* 81: 225–233
- Wissing SA, Müller RH (2002b) The development of an improved carrier system for sunscreen formulations based on crystalline lipid nanoparticles. *Int J Pharm* 242:373–375
- Yabe S, Sato T (2003) Cerium oxide for sunscreen cosmetics. *J Solid State Chem* 171:7–11
- Zeevi A, Klang S, Alard V, Brossard F, Benita S (1994) The design and characterization of a positively charged submicron emulsion containing a sunscreen agent. *Int J Pharm* 108:57–68
- Ziegler A, Jonason AS, Leffell DJ, Simon JA, Sharma HW, Kimmelman J et al (1994) Sunburn and p53 in the onset of skin cancer. *Nature* 372:773–776

Dominique Jasmin Lunter and Rolf Daniels

## Contents

19.1	<b>Introduction</b> .....	321
19.2	<b>Manufacture and Characterization of Film Forming Emulsions</b> .....	323
19.3	<b>Main Characteristics of Emulsion Films</b> .....	324
19.4	<b>In Vitro Performance of Film Forming Emulsions</b> .....	329
19.4.1	In Vitro Skin Permeation.....	329
19.4.2	In Vitro Skin Penetration.....	331
	<b>Conclusion</b> .....	332
	<b>References</b> .....	332

## 19.1 Introduction

The therapy of chronic skin diseases, such as atopic dermatitis or psoriasis, requires treatment of the affected areas of skin over several weeks or months. Patients need to apply topical formulations every day, in some cases even several times per day. This makes therapy inconvenient and negatively affects patients' compliance which is mandatory for an effective treatment (Anand and Bley 2011). As it is known that compliance to a treatment increases with a decreasing number of intakes/applications of medicines, several attempts have been made to develop dermal formulations that allow sustained release or permeation of the active pharmaceutical ingredient (api) from an appropriate reservoir.

In principle, there are two formulation options which can be used to provide sustained dermal therapy: semisolids and patches (Fig. 19.1). A simple approach to control release from semisolids and partitioning into the skin is to change the solubility of the drug in the vehicle, e.g., by altering the lipophilicity of the vehicle. A more hydrophilic vehicle may lead to fast displacement of a lipophilic drug from the vehicle and the build-up of a reservoir in the outermost layers of the skin from which the api permeates slowly into the viable skin. On the other hand, the employment of a more lipophilic vehicle may lead to sustained release of a lipophilic api from the formulation to the skin. Although reasonable formulated semi-

---

D.J. Lunter • R. Daniels (✉)  
Department of Pharmaceutical Technology, Eberhard  
Karls University, Auf der Morgenstelle 8, 72076  
Tuebingen, Germany  
e-mail: [dominique.lunter@uni-tuebingen.de](mailto:dominique.lunter@uni-tuebingen.de);  
[rolf.daniels@uni-tuebingen.de](mailto:rolf.daniels@uni-tuebingen.de)

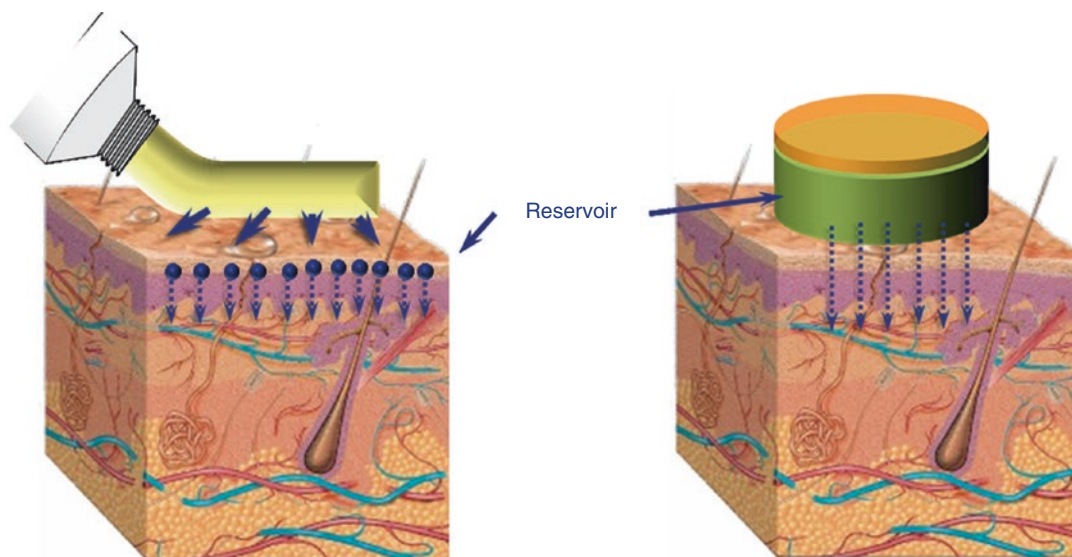


**Fig. 19.1** Formulations for sustained dermal therapy; left: rapid release of the api from a semisolid formulation and build-up of a reservoir in stratum corneum; right:

patch which exhibits a reservoir for the api (e.g., estrogen, opioids, scopolamine)

solids allow sustained release or permeation of the api, about 90% of the semisolid formulation is usually withdrawn from the skin by clothing or contact to other surfaces. Therefore, semisolids are unlikely to show the required substantivity which is pivotal to ensure adequate contact to the skin for an extended treatment interval. Patches provide an alternative. The prolonged contact time to the skin is a clear advantage but the size of the patch limits the area that can be treated. Furthermore, most patches are not flexible enough to allow for unlimited movement of the patients' skin. Therefore, patches may lead to an uncomfortable feeling of tension on the skin.

All these disadvantages give rise to a need for a formulation concept which combines the advantages of both formulation principles: sustained release, high substantivity and the possibility to conveniently treat larger areas of affected skin. We thus developed film forming emulsions, which are easy to spread and therefore allow convenient treatment of larger areas of affected skin. These oil-in-water (O/W) emulsions form a water insoluble film on the skin which ensures adequate substantivity and sustains permeation of the api (Lunter and Daniels 2012a, b). Table 19.1

**Table 19.1** Formulation principles of dermal sustained release formulations

Type of formulation	Advantages	Disadvantages
Semisolid formulation	Convenient spreadability Possibility to treat large areas of skin	Insufficient substantivity High application frequency
Patch	High substantivity Low application frequency	Limited area Insufficient flexibility leading to a feeling of tension on the skin
Film forming emulsion	Convenient spreadability Possibility to treat large areas of skin High substantivity Low application frequency	

compares characteristics of semisolid, patches and film forming emulsions.

Important prerequisites for film forming emulsions allowing sustained dermal therapy are:

- Sustained permeation of the api from the formulation at an adequate permeation rate

- Delivery of an effective amount of the api to the tissue of interest
- Film formation of the aqueous polymer dispersion which is incorporated in the aqueous phase of the emulsions at skin surface temperature
- Strong adhesion to skin to ensure prolonged contact time of the formulation and the drug to the skin
- Sufficient flexibility to prevent rupture upon movement of the patient
- Compatibility of all components within the formulation
- Adequate storage stability of the emulsions

Nonivamide was used as a model drug in our studies. It is a synthetic analogue of capsaicin which may be used in the treatment of chronic pruritus (Anand and Bley 2011; Ikoma 2010; Ständer and Luger 2010), a symptom that accompanies various skin diseases, like atopic dermatitis or psoriasis. Conventional formulations containing capsaicinoids need to be applied several times a day. This has to be performed very carefully every time to avoid any unintended contact with the drug, which can induce an intense burning sensation. This makes therapy inconvenient and negatively affects patient compliance, which is mandatory for effective treatment (Anand and Bley 2011). Therefore, capsaicinoids are a good example where sustained release formulations could contribute to an improvement in patient compliance and thereby ensure therapeutic success.

---

## 19.2 Manufacture and Characterization of Film Forming Emulsions

Film forming emulsions consist of an O/W emulsion with the api dissolved in the dispersed oil phase. The emulsions are stabilized by a water soluble polymer (polyvinyl alcohol) which also acts as a polymeric emulsifier. To allow the formation of a water insoluble film on skin the dispersions of sustained release polymers, namely, Ethyl Acrylate and Methyl Methacrylate Copolymer Dispersion (Eudragit® NE 30D (NE),

Evonik Röhm GmbH, Germany) and Ammonio Methacrylate Copolymer Dispersion, Type B (Eudragit® RS 30D (RS), Evonik Röhm GmbH, Germany) are added to the aqueous phase. Therefore, the preparation of film forming emulsions poses a number of challenges to the producer. First, the drug needs to be incorporated into the inner oil-phase. Second, polymer dispersions are sensible to shear stress, the dispersions may only be added to the emulsion after homogenization. Third, the dispersions (NE and RS) are not compatible with each other unless pH is adjusted to pH 5–6 and polysorbate 80 is added to both dispersions prior to mixing (Lehmann and Dreher 1986). Fourth, the glass transition temperature of the polymers needs to be lowered to <20 °C by the addition of a plasticizer (Triethyl citrate, Sigma-Aldrich Chemie GmbH, Germany) to ensure complete film formation on the skin. Therefore, a three-step manufacturing process needed to be applied. First, the emulsion itself was made by homogenizing the drug solution in oil and the aqueous polymer solution. Second, the pH of the dispersions (NE and RS) was adjusted to pH 5–6 by addition of hydrochloric acid and the dispersions were plasticized. For that purpose, triethyl citrate was added to RS and the dispersion was stirred. Subsequently, polysorbate 80 was added to the plasticized RS and the dispersion was again stirred. Similarly, polysorbate 80 was added to NE and the dispersion was stirred. No triethyl citrate was added to NE. Third, the dispersions were added to the emulsion in order to obtain the final film forming emulsion. Figure 19.2 gives a scheme of the preparation of film forming emulsions. Compositions of film forming emulsions are given in Table 19.2.

Film forming emulsions were characterized by laser diffraction to verify absence of flocculation. The data show that droplet sizes of emulsions before and after addition of Eudragit® were similar (Fig. 19.3). The addition of the dispersion of Eudragit® resulted in a supplementary peak at approx. 120 nm which corresponds to polymer particles of the Eudragit® dispersions. No additional peaks were detected. This indicates that no flocculation occurred and stable emulsions containing a combination of NE and RS were formed.

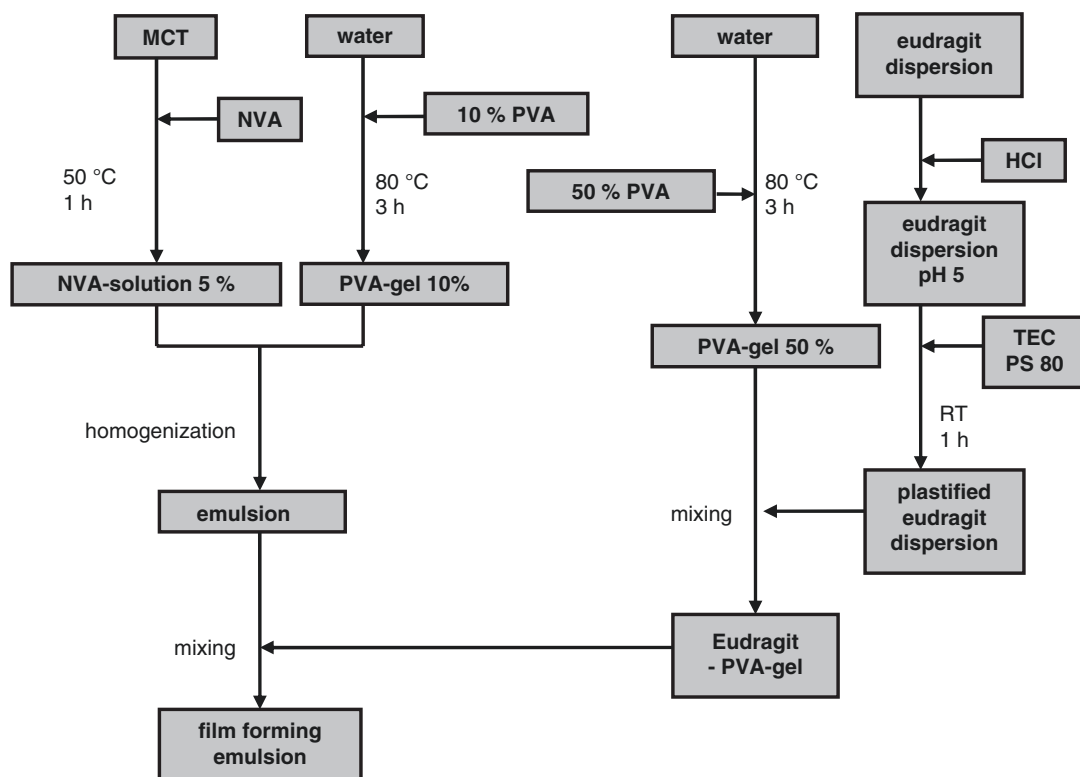


**Fig. 19.2** Preparation scheme for film forming emulsions. *HCl* hydrochloric acid, *MCT* medium chain triglycerides, *NVA* nonivamide, *PS 80* polysorbate 80, *PVA* polyvinyl alcohol, *TEC* triethyl citrate

### 19.3 Main Characteristics of Emulsion Films

Film forming emulsions form a film on skin. In this film, the oil droplets are encapsulated in a dry polymeric matrix. The api which is dissolved in the oil phase needs to diffuse through this matrix in order to reach the skin. As this is a slow process, drug release is sustained. Even more important than the sustained release characteristics is an adequate substantivity which the emulsion films need to ensure in order to allow prolonged contact of the api to the skin. To achieve the required substantivity, complete film formation needs to occur at skin surface temperature (30–32 °C), the film needs to adhere strongly to the skin and needs to show sufficient elasticity to be able to follow the movements of the skin. The emulsion films were therefore examined concerning glass transition tempera-

ture ( $T_g$ ), built-up, adherence and elongation to identify promising candidates for in vitro release testing. Compositions of the tested emulsions are given in Table 19.1.

The  $T_g$  of pure RS is well above 20 °C and triethyl citrate was used to lower  $T_g$  to a sufficient extent. Polysorbate 80, which had to be added to the Eudragit® dispersions to prevent flocculation exhibits, a plasticizing effect similar to that of triethyl citrate (Grützmann and Wagner 2005) and polyvinyl alcohol may also contribute to changes in  $T_g$ . Therefore, measurements of  $T_g$  were taken out on films obtained from mixtures containing all excipients of the aqueous phase in the composition used in the preparation of film forming emulsions. Results are shown in Fig. 19.4.

Glass transition temperatures of all polymer blends are well below 20 °C. The data clearly show that  $T_g$  decreases with increasing NE content. This is due to the low  $T_g$  of NE itself (12 °C,

**Table 19.2** Composition of film forming emulsions and which tests they are used in

Retard polymer composition	NE (%)	RS (%)	PVA (g)	Water (g)	RS (g)	NE (g)	TEC (g)	PS 80 (g)	MCT (g)	Used in testing of:			
										Mechanical properties	Permeation infinite dose	Permeation finite dose	Penetration
0/100	8	8	50.5	15.9	0	4.0	1.6	20	+	-	-	-	
25/75	8	8	51.2	11.9	4.3	3.0	1.6	20	+	-	-	-	
40/60	8	8	51.6	9.5	6.8	2.4	1.6	20	+	+	+	+	
50/50	8	8	51.9	7.9	8.5	2.0	1.6	20	+	-	-	-	
60/40	8	8	52.1	6.4	10.2	1.6	1.6	20	+	-	-	-	
0/100	8	8	53.2	0	17.0	0	1.6	20	+	-	-	-	

PVA polyvinyl alcohol, NE Eudragit® NE, RS Eudragit® RS, TEC triethyl citrate, PS 80 polysorbate 80, MCT medium chain triglycerides



**Fig. 19.3** Droplet size distribution of (■) Eudragit®-dispersion, (▲) pure emulsion, (○) film forming emulsion containing RS, (◇) film forming emulsion containing NE and RS, and (□) film forming emulsion containing NE; average of 3 measurements; lines are a guide to the eye

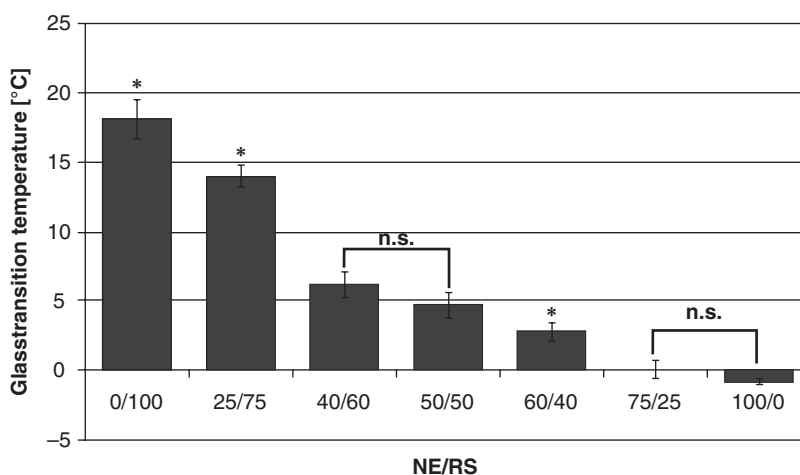
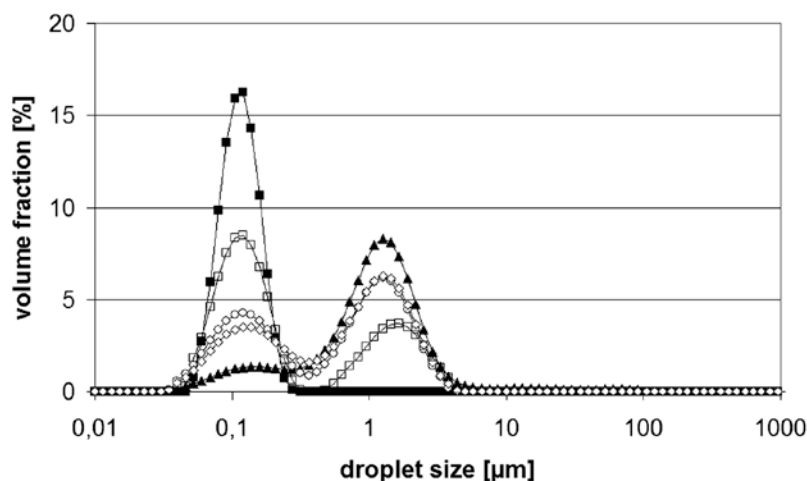


**Fig. 19.4** Glass transition temperature of mixtures of Eudragit®NE 30D+polysorbate 80+polyvinyl alcohol and RS 30D+triethyl citrate+polysorbate 80+polyvinyl

alcohol; mean  $\pm$  SD;  $n=3$ ; "\*" statistically different data; "n. s." not statistically different data

according to our measurements), which is further reduced due to the addition of polysorbate 80.

With regard to  $T_g$ , all formulations fulfilled the requirements and were therefore used in further experiments.

In general, complete film formation is achieved when  $T_g$  is lowered to a value approximately 10 °C beyond process temperature. Therefore, the decrease of  $T_g$  to <20 °C allows film formation at skin surface temperature (30–32 °C). Upon drying, the polymers which are located in the continuous aqueous phase form a polymeric matrix which encapsulates the oil

droplets and thereby preserves the dispersed character in the dry state. The built-up of these emulsion films was studied by confocal Raman microscopy (CRM). Figure 19.5 shows color-coded CRM images of dried emulsion films. It can be seen that the oil droplets are completely embedded in a polymeric matrix of either polyvinyl alcohol and RS or polyvinyl alcohol, NE and RS, or polyvinyl alcohol and NE. This indicates that the coalescence of the oil droplets upon drying was successfully prevented and the dispersed character is maintained in the emulsion films. Retardation of drug release from the oil solution

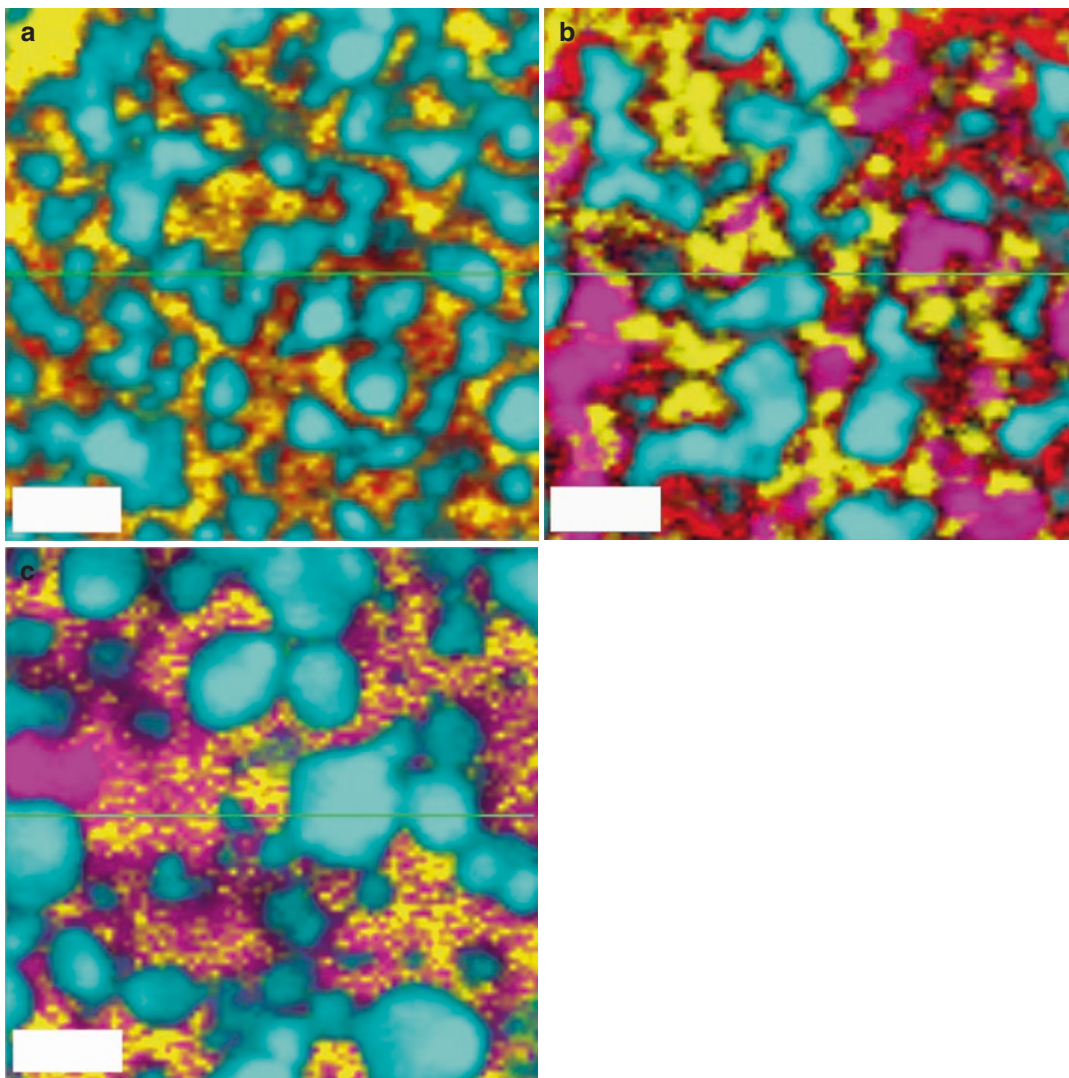


**Fig. 19.5** Raman microscopic color-coded images of dry emulsion films. (a) Film forming emulsion containing RS, (b) film forming emulsion containing NE and RS, and (c)

film forming emulsion containing NE; (■) MCT, (■) PVA; (■) Eudragit® NE, (■) Eudragit® RS; scale bar: 3  $\mu$ m

by diffusion through the polymeric matrix is therefore rendered possible.

To allow substantivity, adequate adhesion to skin needs to be assured. Adhesion was tested using glass as a surrogate for skin (Fig. 19.6). Polycarbonate was used as a control. Adhesion to polycarbonate was found to be significantly higher than adhesion to glass. Emulsion films containing NE (no RS) adhered weakly to glass whereas films containing RS (no NE) adhered weakly to polycarbonate. Adhesion of films con-

taining a mixture of NE and RS is stronger compared to adhesion of films that contain only one of the sustained release polymers and is independent of NE/RS ratio.

Adhesion to polycarbonate is generally higher as both polymers (NE and RS) consist mainly of non-polar monomers. These non-polar monomers interact stronger with non-polar polycarbonate. One might have expected that adhesion of emulsion films which contain mixtures of NE and RS might be influenced by NE/RS ratio. The

fact that this is not the case may be explained by a possible segregation of the components during the drying process and, possibly, the built-up of the same structures at the bottom of the film, independent of NE/RS ratio in the native film forming emulsions. However, films containing both sustained release polymers show higher adhesion than films that contain only one of the polymers and are therefore regarded as superior.

Concerning elasticity, the results of research on the extensibility of human skin indicate that a reasonable value of elongation that the emulsion films should exhibit is approximately 30% (Langer 1978; Sumino et al. 2009). Figure 19.7

shows that the elongation of emulsion films is largely influenced by NE content as NE itself is more elastic than RS and polyvinyl alcohol. The more NE the films contain, the more elastic they are. However, the relationship between NE fraction and elongation is not linear. Films containing >40 parts NE show an elasticity of >30% and are therefore regarded as adequate with regard to an application onto skin.

These results indicate that emulsion films are capable of (i) encapsulating the dispersed oil phase upon drying, (ii) adhering strongly to skin, and (iii) following the normal movements of skin. Adequate substantivity could thus be assumed.

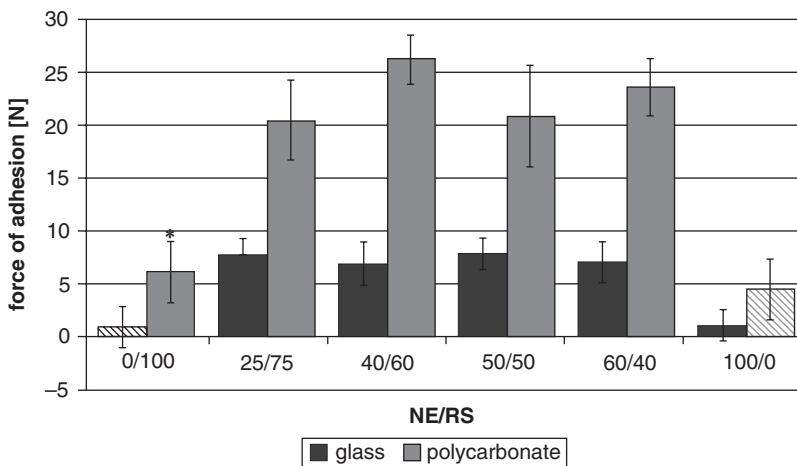


**Fig. 19.6** Comparison of force of adhesion of free films from emulsions containing varying amounts of Eudragit® NE30D and RS30D to (a) glass and (b) polycarbonate;

mean ± SD; n = 5; “\*” statistically different data; “n. s.” not statistically different data

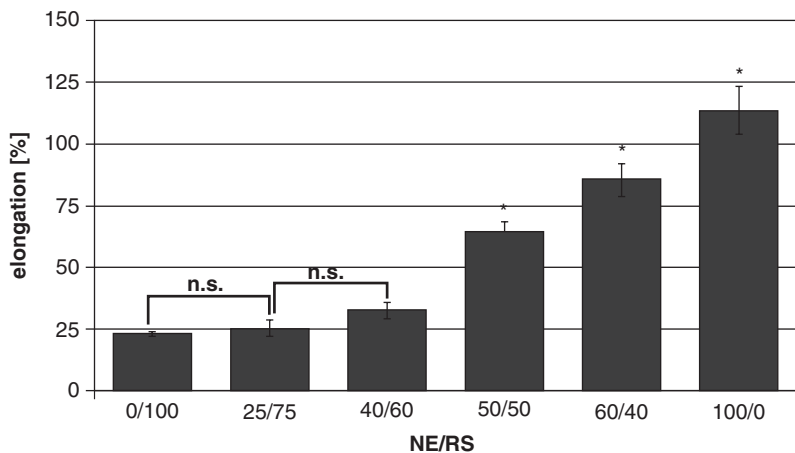


**Fig. 19.7** Comparison of elongation at break of free films from emulsions containing varying amounts of Eudragit® NE30D and RS30D; mean ± SD; n = 5; “\*” statistically different data; “n. s.” not statistically different data

## 19.4 In Vitro Performance of Film Forming Emulsions

Emulsion films containing 40 parts NE (60 parts RS, respectively) were used in in vitro permeation and penetration experiments, as they show a  $T_g < 20^\circ\text{C}$  encapsulate the oil droplets in the dried emulsion film, adhere strongly to glass and show an elongation of approximately 30%. To investigate the influence of the sustained release polymers on permeation from emulsion films, formulations containing only RS were also used in in vitro permeation experiments.

### 19.4.1 In Vitro Skin Permeation

To prove that emulsion films slow down and sustain dermal permeation of nonivamide, permeation of nonivamide from dried emulsion films was compared to permeation from "Hydrophilic Nonivamide Cream" (HNC), which releases nonivamide rapidly (Neues Rezeptur Formularium 2010). To investigate nonivamide permeation from film forming emulsions, formulations containing 1% nonivamide and HNC containing nonivamide in concentrations used in the therapy of chronic pain or pruritus were employed (see Table 19.3 for composition of HNCs).

An infinite dose set-up was used to be able to calculate steady-state flux and allow parametrical comparison of permeation from different formulations. In this study, nonivamide permeation from emulsion films was compared to nonivamide permeation from HNC in order to explore the capability of emulsion films to allow permeation rates suitable for therapy. Additionally, finite dose experiments were performed to elucidate the ability of emulsion films to sustain nonivamide delivery to the skin.

Results of infinite dose permeation experiments are shown in Fig. 19.8a, b and Table 19.4.

It can be observed that after a lag time of 20 h nonivamide permeates the skin. The data clearly show that permeation rates from HNC increase linearly with increasing nonivamide content whereas permeation coefficients remain constant. Permeation from emulsion films is linear with the

square root of time and permeation rate is equivalent to that from HNC 0.05%. The permeation coefficient from the emulsion films is 23 times smaller compared to that from HNC 0.05%. From emulsion films approx. 1% of nonivamide permeated the skin after 48 h, whereas from HNC approx. 30% permeated. Permeation rate and overall permeated amount from the emulsion films containing 40 parts NE are slightly higher than the respective parameters of the emulsion films containing only RS. However, the differences are not statistically significant.

The fact that the permeation coefficients of nonivamide from HNC are independent of nonivamide content clearly shows that enhanced permeation rates solely depend on higher thermodynamic activity of the api in more concentrated formulations (Hadgraft 2001). The distinctly lower permeation coefficient, lower cumulative amounts permeated and smaller proportion permeated from the emulsion films as well as the correlation of cumulative amounts permeated to the square root of time prove that diffusion through the polymeric matrix instead of diffusion through skin is the rate limiting step in drug delivery from emulsion films (Higuchi 1961, 1962). The permeation rates of nonivamide from emulsion films can be assumed to be appropriate for therapy because they are equivalent to those of the hydrophilic creams which are frequently used in the therapy of chronic pruritus. Permeation rates and coefficients of nonivamide from both emulsion films are of the same magnitude. Thus, it can be concluded that the nature of polymer does not largely affect permeation. Nevertheless, polymer composition does influence mechanical properties of emulsion films. Emulsion films containing 40 parts NE exhibit superior properties with regard to adhesion and elongation and were therefore chosen for use in finite dose experiments.

Results of permeation experiments under a finite dose regime show that nonivamide permeates from HNC 0.05% for 6–9 h only (Fig. 19.9). In contrast, permeation from the optimized emulsion films lasts for 24 h and a constant permeation rate is maintained throughout the observation period. In contrast to the results of

**Table 19.3** Composition of HNCs

	water	GMS	Cetyl alcohol	White soft paraffin	MCT	PEG-20-GMS	PG	Ethanol 90%	NVA
HNC 1%	50.0	2.0	3.0	12.8	3.8	3.6	15.0	9.0	1.0
HNC 0.1%	50.0	2.0	3.0	12.8	3.8	3.6	15.0	9.90	0.1
HNC 0.05%	50.0	2.0	3.0	12.8	3.8	3.6	15.0	9.95	0.05
HNC 0.025%	50.0	2.0	3.0	12.8	3.8	3.6	15.0	9.975	0.025

GMS glycerol monostearate, MCT medium chain triglycerides, PEG-20-GMS polyethylene glycol-20-glycerol mono-stearate, PG propylene glycol, NVA nonivamide, HNC hydrophilic nonivamide cream

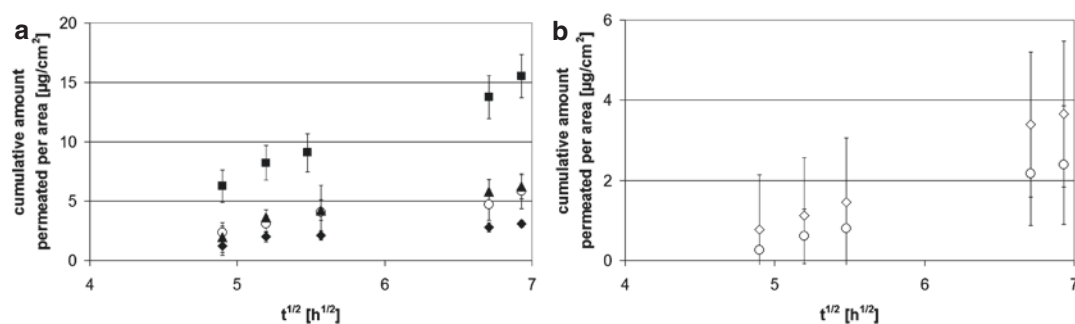


**Fig. 19.8** In vitro skin permeation profiles of nonivamide under infinite dose conditions: (a) comparison of (■) HNC 0.01%, (▲) HNC 0.05%, (◆) HNC 0.025%, (○) film forming emulsion containing RS and (b) comparison

of (○) film forming emulsion containing RS and (◇) film forming emulsion containing NE and RS; n=5; average ± standard deviation

**Table 19.4** Permeation characteristics; n=5; mean ± standard deviation; “\*” statistically different data; HNC=hydrophilic nonivamide cream

	Permeation rate [ $\mu\text{g}/\text{cm}^2\text{h}^{1/2}$ ]	Permeation coefficient [ $\text{mL}/\text{cm}^2\text{h}^{1/2}$ ]	Cumulative amount permeated after 48 h [ $\mu\text{g}/\text{cm}^2$ ]	Percentage permeated after 48 h [%]
Film forming emulsion containing Eudragit® RS	1.5 ± 0.5	1.5 ± 0.5*	5.8 ± 1.5	1.2 ± 0.3*
HNC 0.1%	4.2 ± 0.3*	42.3 ± 2.8	15.5 ± 1.8*	32.6 ± 3.8
HNC 0.05%	1.8 ± 0.6	35.8 ± 11.8	6.2 ± 1.0	26.1 ± 4.2
HNC 0.025%	0.9 ± 0.2	38.0 ± 7.1	3.1 ± 0.3	26.1 ± 2.5
Film forming emulsion containing Eudragit RS	1.2 ± 0.7	1.2 ± 0.7	2.4 ± 0.8	0.5 ± 0.2
Film forming emulsion containing Eudragit® NE and RS	1.5 ± 0.2	1.5 ± 0.2	3.7 ± 0.8	0.8 ± 0.2
HNC 0.1%	3.5 ± 1.1*	34.5 ± 11.4*	7.1 ± 0.4*	12.0 ± 5.1*

infinite dose experiments, the amount permeated from the emulsion films is higher than the amount permeated from HNC 0.05 % at any time point. The cumulative amount permeated from the emulsion films is therefore five times higher than that from HNC 0.05 %. From the emulsion films, constant flux is achieved over a period of 24 h. After 48 h merely  $8.0 \pm 3.5$  % of the applied dose permeated through skin. This indicates that the amount of nonivamide in the formulation does still suffice to maintain a constant flux. Extension

of treatment intervals to 12 or even 24 h by utilization of emulsion films may therefore be possible.

### 19.4.2 In Vitro Skin Penetration

As the target structures of capsaicinoids are located within the viable epidermis (Anand and Bley 2011; Ikoma 2010; Ständer and Luger 2010), it was of great importance to examine the nonivamide concentration in the skin to ensure that effective drug levels are obtained. As no distinct values of effective nonivamide concentrations in skin exist, we decided to compare nonivamide concentrations in skin achieved with film forming emulsions to those obtained with HNC 0.05 %, because the effectiveness of this formulation is proven clinically. Thus, we concluded that film forming emulsions would also be effective if they were able to produce drug levels similar to those obtained with HNC 0.05 %.

Results of penetration experiments (Fig. 19.10a, b) reveal that nonivamide content in the stratum corneum is higher than in the viable skin, independent of formulation and incubation

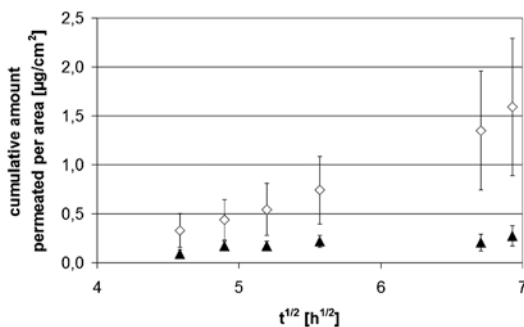


**Fig. 19.9** In vitro skin permeation profiles of nonivamide under finite dose conditions comparison of (▲) HNC 0.05 % and (◇) film forming emulsion containing NE and RS; n = 5; average  $\pm$  standard deviation

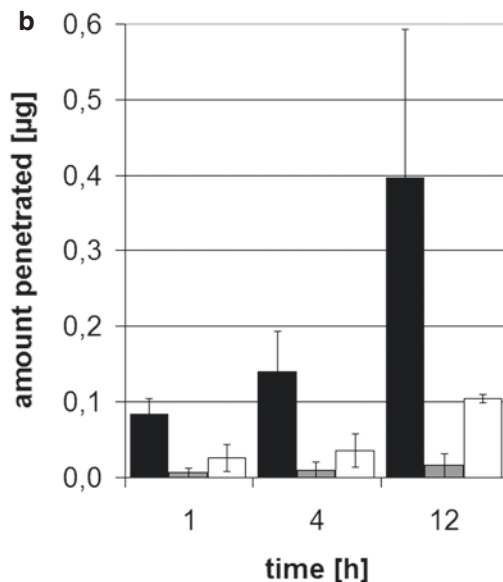
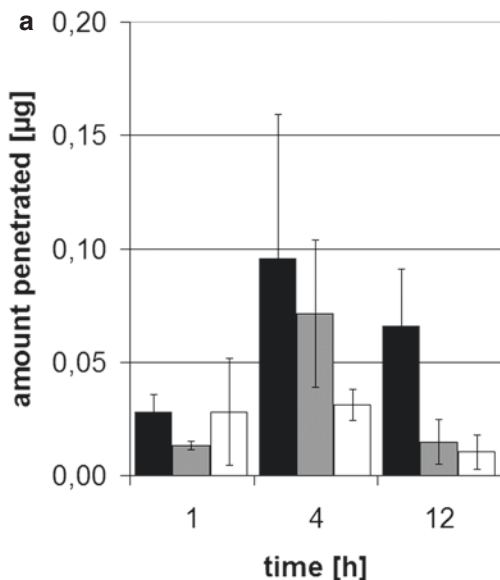


**Fig. 19.10** In vitro skin penetration profiles of nonivamide under finite dose conditions comparison of (a) HNC 0.05 % and (b) film forming emulsion containing

NE and RS; drug amounts in (■) stratum corneum, (■) epidermis, (□) dermis; n = 3; average  $\pm$  standard deviation

time. HNC 0.05 % delivers only low amounts of nonivamide to the skin within 1 h. A maximum concentration in all parts of the skin is apparent after 4 h. Although concentration in stratum corneum is still high after 12 h, the amount in viable skin decreases to a level similar to that obtained after 1 h. The nonivamide amount that penetrated into viable skin from the emulsion films after 1 h is as small as for HNC 0.05 %, but the amount present in stratum corneum is already 25 times higher. It increases substantially after 4 and 12 h. Nonivamide concentrations in the viable skin are equivalent or even higher than those obtained with HNC 0.05 %.

Substantially higher drug contents in stratum corneum may be associated with the high lipophilicity of nonivamide ( $\log P_{O/W}$ : 3.74), which results in its accumulation in lipid rich tissue (Kasting 2001; Schlupp et al. 2010). The presence of a maximum nonivamide concentration in skin after 4 h incubation with HNC 0.05 % is in accordance with the clinical experience, i.e., HNC has to be applied at least 4 times a day. Results of penetration experiments employing the optimized emulsion films clearly indicate that nonivamide concentrations achieved in epidermis and dermis are of the same magnitude as those observed with HNC 0.05 %. In contrast to HNC 0.05 %, the emulsion films maintain drug concentration in skin over a period of 12 h. These findings suggest that therapy of chronic pain or pruritus may be facilitated by film forming emulsions as the treatment interval may be extended substantially.

### Conclusion

The results of this work elucidate the possibility of formulating sustained release semi-solid formulations with the innovative concept of film forming emulsions. We were able to formulate stable emulsions which form a film on skin that encapsulates the dispersed oil phase. It is shown that the rate of permeation of the active substance from its oily solution is determined by diffusion through the polymeric matrix in which the droplets are embedded. Thereby, constant permeation

rates and efficient api concentrations in skin can be maintained for a period of 12 h. This is a clear advantage over conventional semi-solid formulations as application intervals can be extended. This results in enhanced compliance and ensures therapeutic success.

Furthermore, employment of film forming emulsions is possible for a multitude of lipophilic substances using film forming emulsions as a drug delivery system which may be tailored to specific needs of patients and will thereby allow sustained dermal therapy of various diseases.

**Acknowledgments** The authors would like to thank Martin Schenk and his team from the Department of Experimental Medicine at the University of Tuebingen for the supply of pig ears and Evonik Industries for the donation of Eudragit® dispersions.

### References

- Anand P, Bley K (2011) Topical capsaicin for pain management: therapeutic potential and mechanisms of action of the new high-concentration capsaicin 8% patch. *Br J Anaesth* 107:490–502
- Grützmann R, Wagner KG (2005) Quantification of the leaching of triethyl citrate/polysorbate 80 mixtures from Eudragit RS films by differential scanning calorimetry. *Eur J Pharm Biopharm* 60:159–162
- Hadgraft J (2001) Skin, the final frontier. *Int J Pharm* 224:1–18
- Higuchi T (1961) Rate of release of medicaments from ointment bases containing drugs in suspension. *J Pharm Sci* 50:874–875
- Higuchi WI (1962) Analysis of data on the medicament release from ointments. *J Pharm Sci* 51:802–804
- Ikoma A (2010) Neuroanatomy of itch. In: Misery L, Ständer S (eds) *Pruritus*. Springer, New York, pp 3–6
- Kasting GB (2001) Kinetics of finite dose absorption through skin 1. Vanillynonanamide *J Pharm Sci* 90:202–212
- Langer K (1978) On the anatomy and physiology of the skin III. The elasticity of the cutis. *Br J Plast Surg* 31:185–199
- Lehmann K, Dreher D (1986) *Mischbarkeit wässriger Poly(meth)acrylat-Dispersionen für Arzneimittelüberzüge*. *Pharm Ind* 48:1182–1183
- Lunter DJ, Daniels R (2012a) New film forming emulsions containing Eudragit® NE and/or RS 30D for sustained dermal delivery of nonivamide. *Eur J Pharm Biopharm* 82:291–298

- Lunter DJ, Daniels R (2012b) In-vitro skin permeation and penetration of nonivamide from novel film forming emulsions
- Neues Rezeptur Formularium (2010) Hydrophile Capsaicinoid Creme 0,025 %/0,05 %/0,1 % (NRF 11.125). Govi Verlag, D-Eschborn
- Schlupp P, Blaschke T, Kramer KD, Höltje H-D, Mehnert W, Schäfer-Korting M (2010) Drug release and skin penetration from solid lipid nanoparticles and a cream base: a systematic approach from a comparison of three glucocorticoides. *Skin Pharmacol Physiol* 24:199–209
- Ständer S, Luger TA (2010) Neuroreceptors and neuromediators. In: Misery L, Ständer S (eds) *Pruritus*. Springer, New York, pp 7–16
- Sumino H, Ichikawa S, Kasama S, Takahashi T, Kumakura H, Takayama Y, Kanda T, Murakami M, Kurabayashi M (2009) Effects of raloxifene and hormone replacement therapy on forearm skin elasticity in postmenopausal women. *Maturitas* 62:53–57



---

## **Part IV**

# **Current Status of Dermal and Transdermal Drug Delivery**

# Penetration-Enhancement Strategies for Dermal and Transdermal Drug Delivery: An Overview of Recent Research Studies and Patents

Syed Sarim Imam and Mohammed Aqil

## Contents

20.1	<b>Introduction</b> .....	337
20.2	<b>Skin Penetration Enhancement Techniques</b> .....	338
20.2.1	Microneedles .....	338
20.2.2	Sonophoresis .....	342
20.2.3	Electroporation .....	342
20.2.4	Magnetophoresis .....	343
20.2.5	Thermal Ablation .....	343
20.2.6	Photomechanical Waves .....	344
20.2.7	Inclusion Complex .....	344
20.2.8	Solid Lipid Nanoparticles (SLN) .....	344
20.2.9	Microemulsion .....	345
20.2.10	Dendrimers .....	345
20.2.11	Vesicles .....	345
20.3	<b>Synergistic Use of Enhancement Techniques</b> .....	349
	<b>Conclusion</b> .....	350
	<b>References</b> .....	350

## 20.1 Introduction

The skin, the largest organ of the body, is composed of several layers: the stratum corneum (SC) which is the uppermost layer, the viable epidermis, the dermis, and the lower layers of adipose tissue (Schaefer and Redelmeier 1996; Carlos et al. 1999). Nevertheless, the SC is a remarkably efficient barrier, thus causing difficulties for the transdermal delivery of therapeutic agents. The skin is a multilayered organ composed of many histological layers generally described in terms of tissue layers, that is, the epidermis and the dermis (Lai-Cheong and McGrath 2009). Epidermis, composed of keratinocytes (95 % cells bearing keratin), has been used to conceptualize the barrier property of the skin. The second layer beneath the epidermal layer is the dermis, which is much thicker than the epidermis (usually 1–4 mm). The main components of the dermis are collagen and elastic fibers. Compared to the epidermis, there are fewer cells and much more fibers in the dermis (Igarashi et al. 2007). The components of transdermal drug delivery systems (TDDS) are liners, adherents, drug reservoirs, drug release membranes, etc. (Wokovich et al. 2006) that play an imperative role in the release of the drug from the TDDS and in the drug permeation through the skin. It is considered that a well-designed TDDS can supply the drug at a rate to sustain the required therapeutic plasma concentration without much fluctuation that may cause basic mani-

S.S. Imam  
Department of Pharmaceutics, Glocal School of Pharmacy, The Glocal University, Saharanpur 247121, Uttar Pradesh, India  
e-mail: [sarimimam@gmail.com](mailto:sarimimam@gmail.com)

M. Aqil (✉)  
Department of Pharmaceutics, Faculty of Pharmacy, Hamdard University, M.B. Road, New Delhi 110062, India  
e-mail: [aqilmalik@yahoo.com](mailto:aqilmalik@yahoo.com)

festation or therapeutic inefficacy (Thomas and Finnin 2004). Lag times to reach steady-state fluxes are in hours, as the transport of most drugs across the skin is very slow. Attainment of a therapeutically effective drug level is, therefore, difficult without enhancing skin permeation (Kai et al. 1990). A number of techniques have been developed to enhance and control transport across the skin, and enlarge the range of drugs delivered. These involve chemical and physical methods, based on two strategies: increasing skin permeability and/or providing the driving force acting on the drug (Foldvari 2000). There have been many ingenious technologies developed to enhance percutaneous transport for therapeutic and diagnostic purposes, ranging from chemical enhancers to iontophoresis, electroporation, and pressure waves generated by ultrasound effects or the synergistic mixtures of two or more methods (Ahad et al. 2010). To enhance transdermal absorption, different methodologies have been investigated and developed, including the use of drug derivatives, drug-saturated systems, physical approaches, and chemical penetration enhancers (sorption promoters) that facilitate the diffusion of drugs through the SC (Ahad et al. 2009; Asbill and Michniak 2000). The transdermal product has a promising future because of its noteworthy upward trend (Paudel et al. 2010). The fate of effectiveness of a TDDS lies on the drug's ability to invade the skin barrier and how it reaches the targeted site (Prausnitz et al. 2004b). The molecules permeate across the SC by intercellular, intracellular (transcellular), or follicular (appendageal) pathways. Transdermal drug delivery has been a subject of increasing research interest since the introduction of the first transdermal product TransdermScop<sup>®</sup> patch developed by Alza Corp., USA, for delivery of scopolamine, in 1981 (Santus and Baker 1993). The patent literature is often a rich source of information that is unobtainable and is an under-used resource mainly due to legal style of writing. The result of the search of patents concerning transdermal skin penetration techniques shows to provide much useful information. Several transport techniques have been demonstrated to bypass or modulate

the barrier function of the skin to allow easier passage of drugs into the dermal microcirculation, as summarized in Table 20.1 (Bogner and Wilkosz 2003; Rizwan et al. 2009b).

---

## 20.2 Skin Penetration Enhancement Techniques

An attempt was made to provide an overall overview of information about transdermal patents and to summarize the different major penetration-enhancement techniques used in cutaneous drug delivery systems (Table 20.2).

### 20.2.1 Microneedles

Microneedles (MN) technology for enhanced transdermal drug delivery was first reported by Henry et al (1998). Since then, there has been an increasing interest in this technology. Increased skin permeability by using the microneedle technology involves creating larger transport pathways (of micron dimensions) in the skin using arrays of microscopic needles. MN can penetrate the skin to create micron-sized pores that are big enough to permit the transport of macromolecules and even microparticles (Prausnitz 2004a). Safety studies performed with MN ranging in length between 500 and 1500  $\mu\text{m}$  showed that the pain induced by the MN is significantly lower when compared to hypodermic needles (Gill and Prausnitz 2007). Most drug delivery studies have emphasized solid MN, which have been shown to increase skin permeability to a broad range of molecules. MN-mediated drug delivery has been extensively investigated for transdermal delivery of drug-loaded nanocarriers (Donnelly et al. 2010; Gomaa et al. 2014). MN technology has been disclosed in Patent No. 5879326 to Godshall and Anderson (1999) and Patent No. 5250023 to Lee and Shin (1993). The use of micron-scale needles in increasing skin permeability has been proposed and shown to dramatically increase transdermal drug delivery, especially of macromolecules, such as insulin, proteins, oligonucleotides, and vaccines (Henry et al. 1998; Prausnitz

**Table 20.1** Transdermal drug delivery technologies and available commercial products

S. No	Enhancement method	Technology	Manufacturer	Drug
1	Iontophoresis	E-Trans®	Alza	Fentanyl
2	Iontophoresis	Iontophoretic drug delivery system	Iomed®	Lidocaine and epinephrine
3	Microporation	Microstructured transdermal system	3 M	Hydrophilic molecules, large molecules
4	Microporation	Macroflux®	ZosanoPharma, Inc.	Therapeutic protein
5	Needleless injector	PowderJect®	PowderJect Pharmaceuticals	Insulin
6	Needleless injector	IntraJect®	Weston Medical	Vaccines
7	Microparticulate delivery	SMP (solvent microparticle system)	Atrix Labs	Dapsone
8	Thermal ablation	Heat-aided drug delivery system	Zars, Inc.	Lidocaine and tetracaine
9	Phonophoresis	SonoPrep®	Echo Therapeutics, Inc	Peptides, other large molecules

et al. 2004a). Eppstein (2003) described a noninvasive method for increasing the permeability of the skin, mucosal membrane through thermal microporation. Another approach that has been investigated more recently is an integrated delivery system comprising a hypodermic needle and a transdermal patch (Coulman et al. 2006a). Transdermal delivery of insulin *in vivo* was studied using solid MN, and it was demonstrated that MN increased insulin delivery and thereby decreased blood glucose levels in diabetic hairless rats (Martanto et al. 2003). Patent of King and Walters (2003) claimed delivery of macromolecules into cells without employing a pressurized fluid injection step. The macromolecules in the electrode coating having a polynucleotide vaccine (deoxyribonucleic acid vaccine and/or ribonucleic acid vaccine) or a protein-based vaccine are administered using MN. Rosenberg (2003) provides a reliable way to deliver individual and multiple pharmaceutical agents in small doses by an intradermal device (MN). The multiple chambers of the delivery device enable the administration of multiple vaccines, adjuvants, and pharmaceutical agents simultaneously without prior reformulation or combination of pharmaceutical agents. A hollow microneedle of the conical shaped body with beveled, noncoring tip that is able to pierce tissue with broad base for transcutaneously conveying fluid was developed

by Cho (2005). The base of microneedle was broad relative to height to minimize breakage during insertion. The microneedle device has few disadvantages, such as requiring a direct pushing motion against the skin and less efficient, compelling of drug fluid due to tiny openings. Gartstein and Sherman (2006) suggested a microstructured device (MN) for delivering the drug, which can provide efficient flow for some types of fluid compounds through the SC. The microstructured device could penetrate the outer skin layers by sliding or rubbing motions parallel to the skin surface, rather than perpendicular to the skin surface. Wilkinson and Hwang (2006) patented an invention entitled “valved intradermal delivery device and method of intradermally delivering a substance to a patient.” They explained in their patent about controlled flow of pharmaceutical agents, such as a drug or vaccine, through the device for the delivery into or below the SC to a depth sufficient for the pharmaceutical agent to be absorbed and utilized by the body. US Patent No. 5,457,041 of Ginaven and Facciotti (1995) reported MN made up of silicon, which carry a biologically active substance and are pierced into the target cells within the skin tissue. Thus, the biological substance is transferred from the tip portion and deposited within the target cells of the skin tissue. Gertsek et al. (2003) disclosed that MN have advantages of delivering a

**Table 20.2** Different penetration enhancement techniques

S. No.	Technique	Patent information	Invention/Description	Application/Claim
1	Iontophoresis	US6119036 Allen Jr (2000)	Aqueous suspension or hydrophilic gel reservoir was replaced with silicone matrix	Problems with existing reservoir, like drug instability, electroosmotic (EEO) flow, dryness of reservoir are solved, and thus the life span of the device is improved
2	Iontophoresis	US6248349 Suzuki et al. (2001)	Consists of peptides in a porous matrix	Reduces skin irritation
3	Microneedle	US7184826 Cormier et al. (2007)	Device consisting of a sheet having plurality of microblades has been unveiled for piercing and anchoring to the skin	Increased transdermal flux of polypeptide or protein and improved attachment of device to the skin with minimal to no skin irritation
4	Microneedle	US6230051 Cormier et al. (2001)	Consists of plurality of microblades for piercing the skin	Particular microblade geometry allows better penetration of the skin with less "push-down" (i.e., penetration and insertion) force required by the user
5	Microneedle	US 8,911,749 Ghartey-Tagoe et al (2014)	Microneedle array comprises a vaccine and a polymeric material	Insertion into the skin of a patient with an array of microprojections which comprises a vaccine for that disease
6	Microneedle	US20130245601A1 Pettis et al (2014)	The methods employ small gauge needles, especially microneedles, placed in the intradermal space to deliver the substance to the intradermal space as a bolus or by infusion	Delivery devices which place the needle outlet at an appropriate depth in the intradermal space and control the volume and rate of fluid delivery provide accurate delivery of the substance to the desired location without leakage
7	Microemulsion	US5688761 Owen et al. (1997)	Convertible or phase-reversible microemulsion, capable of being changed from w/o to o/w system by the addition of water to the former has been disclosed for delivering protein systemically	System was particularly useful for storing proteins for long periods of time at room temperature and above until they are ready for use

8	Ethosome	US5540934 Touitou (1996); US20060182766A1 Modi (2006)	System composed of phospholipids (0.5–10%), ethanol (20–50%), propylene glycol (0–20%), and at least 20% water	Enhanced transdermal delivery of various pharmaceutical agents
9	Vesicle	US 8,865,208 Akatsuka et al. (2014)	Vesicle composed of glycerin fatty acid ester, a polyglycerin fatty acid ester, and a pyroglutamic acid glycerin fatty acid ester	Vesicle can be contained in an external preparation for use onto the <i>skin</i>
10	Transfersome	US6165500 Cevc (2000)	Transfersomes composed of phospholipids/glycerophospholipids and other lipids with added surfactants	Highly deformable vesicles which enhance insulin penetration, and are effective for prolonged drug delivery
11	Transfersomes	CN102949341 (A) Lin et al. (2013)	Tacrolimus transfersome prepared with phospholipid (2–10%), penetration enhancer (3–8%), surface-active agent (0.8–3%), antioxidant (0.005–0.2%), and water	Tacrolimus transfersomes have the advantages of relatively high drug-loading capacity, strong skin permeation, being capable of targeting deep skin
12	Transfersome	CN102846546 (A) Chen et al. (2013)	Two phospholipid materials with different phase-change temperatures, which are dipalmitoylphosphatidyl choline and soybean lecithin, are adopted as a composite phospholipid material	Phospholipid transfersome which promotes propranolol percutaneous absorption
13	Inclusion complex	US5817332 (A) Uritti et al. (1998)	Cyclized polysaccharide	Capable of improving the solubility of the therapeutic agent in the buffer solution by forming an inclusion complex with the therapeutic agent

reconstituted pharmaceutical agent, where the dried substance is reconstituted by the dispensing diluent from the bladder within the device. MN with suction pump (vacuum generator) were developed to provide painless, precised insertion, controlled depth penetration, and variable, programmable delivery of active principles (Angel et al. 2006). A vacuum generator was attached to MN, which creates suction at the site of application to penetrate the surface of the skin (Angel et al. 2006; Angel and Hunter 2008). This modified device could be attached to the skin more effectively than prior devices and can be made with an extremely reproducible size and shape. Increased transdermal flux of polypeptides or proteins and improved attachment of the device to the skin with minimal to no skin irritation have been achieved by developing a device consisting of microblades (Cormier et al. 2007). These studies suggest that MN may provide a powerful new approach for transdermal drug delivery of macromolecules, especially for the delivery of proteins, DNA, and vaccines.

### 20.2.2 Sonophoresis

In 1990s, sonophoresis received a great attention from researchers for the delivery of macromolecules through the skin (Rizwan et al. 2009b). It uses low-frequency ultrasound ( $f < 100$  kHz) that enables the penetration of the drug. Commonly used frequencies for sonophoresis are generally separated into two: (i) low-frequency sonophoresis (LFS) (range of 20–100 kHz), and (ii) high-frequency sonophoresis (HFS), which includes frequencies in the range of 0.7–16 MHz (Mitragotri et al. 1995). The systemic absorption of drugs through the transdermal route depends upon the treatment duration, intensity, and frequency of ultrasound (Rizwan et al. 2009b). Mitragotri and associates reported in their two patents (US Patent No. 6,002,961 (1999) and U.S. Patent No. 6,018,678 (2000)) about applications of low-frequency (20 KHz) ultrasound for enhanced transdermal delivery of high-molecular weight proteins. Their findings indicated that permeation enhancement is dependent on the energy dose and

length of ultrasound pulse which is consistent with a cavitation-based mechanism. Mitragotri et al. (1998) used low-frequency (20 KHz) ultrasound of intensity between 12.5 and 225 mW/cm<sup>2</sup> for enhanced transdermal delivery of high-molecular weight proteins. The application of ultrasound significantly enhances permeation through human cadaver skin, that is, by 3.3, 8, and 9.8 times for insulin, gamma interferon, and erythropoietin, respectively. Therefore, it was possible to deliver an insulin dose of about 13 U/h from a patch having an area of 100 cm<sup>2</sup> and providing an insulin flux of 100 mU/cm<sup>2</sup>/h. Weaver et al. (2012) disclosed in their patent that this method provides rapid, controlled, and higher drug transdermal fluxes, and allows drug delivery or analyte extraction at lower ultrasound intensities ( $f < 100$  kHz) than when ultrasound is applied in the absence of an electric field. Shimada and Shapland (1993) invented the use of multiple frequency sonophoresis for enhancing the diffusion of substance to or through the SC layer of the skin. This invention used two different frequencies, that is, 1 and 3 MHz. The method has many advantages such as decreased required time to administer substances and increase in blood perfusion at the treated area, which promote penetration of diffused substances across the skin membrane. Weimann (2007) reported a device consisting of a suspension of encapsulated drug as microparticulate system in place of drug solution. The radiation frequency was applied for a short period of time at a distance from the skin area, effective to generate cavitation bubbles. The penetration studies showed that microparticles of up to 25  $\mu$ m penetrated into the skin under the conditions tested, whereas particles larger than about 40  $\mu$ m did not penetrate.

### 20.2.3 Electroporation

This permeation enhancement technique involves the application of high-voltage pulse for a very short duration of time (<1 s). The high-voltage pulse forms aqueous pathway across the lipid bilayer of the skin (Prausnitz 1999; Rizwan et al. 2009b). The use of electroporation in transdermal delivery of macromolecules and

physostigmine is documented in literature for organophosphate poisoning (Vanbever et al. 1997; Rowland and Chilcott 2000). US Patent No. 5,318,514 of Hofmann (1994) disclosed an apparatus including plurality of needle electrodes which can penetrate into the skin of the patient. To overcome the barrier, a novel, nonviral approach, involving the basic concept of electroporation to introduce genes and other therapeutic agents into the epidermis was provided by Zhang and Rabussay (2005). Rabussay (US US6266560 (B1)) (2001) disclosed a noninvasive method for treating erectile dysfunction using electroporation for enhanced delivery of a vasoactive or androgenic drug composition. It is applied to the penis which affords an alternative treatment for patients affected by erectile dysfunction.

### 20.2.4 Magnetophoresis

Magnetophoresis is a kind of a penetration-enhancement technique, in which flux enhancement is achieved by applying magnetic fields inducing mechanical forces to charged particles in such a way to force them into the skin (Giammarusti 2004). The skin barrier exposed to a magnetic field also might show structural alterations that could attribute to an increase in permeability (Murthy and Hiremath 2001). Ostrow et al. (2003) developed a system to provide an unencumbered self-powered transdermal patch for large-molecule drugs, which delivers the drug in an efficient manner directly to the affected area. The transdermal patch consists of a membrane composed of an inert biochemical substance. When an electric charge is passed through the membrane, it becomes electro-osmotic, which enhances the drug solution to pass through the skin surface to create an electroporative effect. The galvanic and electromagnetic current drivers can be utilized to propel permeant drugs through means of iontophoresis, magnetophoresis, or combined electromagnetophoresis. By this technique, the multiple patches could be configured as a linked patch unit for the user with a flexible cuff apparatus to provide circumferential treatment of a body part.

### 20.2.5 Thermal Ablation

In the transdermal thermal ablation technique, the skin surface is heated to vaporize tissue, which can locally remove the stratum corneum at the site(s) of heating. It is a noninvasive technique to remove small portions of the stratum corneum and thereby to increase skin permeability through micron-scale channels in the skin (Jeong et al. 2011). The major advantage of this technique is that the micropores are surrounded by healthy tissue, which facilitates skin recovery; typically, only 5–15 % of the skin surface is removed (Gold 2007; Trelles et al. 2009). Due to short exposure of the skin to ablation, the temperature gradient across the stratum corneum can be steep enough, so that the skin surface is extremely hot, while the viable epidermis and deeper skin tissues do not experience a significant temperature rise. Park et al. (2008) reported only a few-fold increase in skin permeability to a hydrophilic tracer compound after heating human cadaver skin to 150 °C, while after heating the skin to 300 °C, a 1000-fold increase in skin permeability was observed. A novel microfabricated device P.L.E.A.S.E.<sup>®</sup> (Precise Laser Epidermal System; Pantec Biosolutions, AG) is used to convert electrical energy into thermal and mechanical energy by ejecting a jet of superheated steam at the skin on a timescale on the order of 100 μs (Bachhav et al. 2011). The excitation and evaporation of stratum corneum lead to the formation of micropores, structures with a diameter of 100–150 μm by fractional ablation, which serve as transport conduits across the epidermis. The depth of each micropore is determined by the laser fluence (energy applied per unit area) used to create the pore and can be modulated to ensure either selective removal of the stratum corneum or to reach progressively further into the epidermis down to the dermal–epidermal junction. In a few seconds, this P.L.E.A.S.E.<sup>®</sup> device can create an array of several hundred micropores with a given depth, which lead to significant increase in molecular transport rates through the skin (Zech et al. 2011; Bachhav et al. 2010).



## 20.2.6 Photomechanical Waves

Photomechanical waves (PW) are pressure waves that can act by intense laser radiation, which lead to enhance skin permeation (Ogura et al. 2002). These waves act for a range of few nanoseconds to microseconds, while the amplitude is in hundreds of atmospheres (bar). The pressure waves interact with cells and tissues in ways that are different from those of ultrasound (Doukas and Kollias 2004). The application of PW for transdermal delivery has a number of advantages, such as the substantial penetration depth as well as the large size of molecules (proteins and genes) that can be delivered. These waves do not cause pain or discomfort and injury to the viable skin (Lee et al. 1999). They further reported that when a drug solution is placed on the skin and covered by a black polystyrene, and irradiated with a laser pulse, the photomechanical waves are responsible for stressing the horny layer and enhancing the permeation of drug solution. The drugs delivered via the epidermis can enter the vasculature and produce a systemic effect. PW can thus be applied for rapid delivery of human  $\sigma$ -aminolevulinic acid (ALA) allergen (Nethercott 1990) and insulin (Lee et al. 1998). Lee et al. (1998) have shown that 40 kDa dextran could be delivered 400 mm deep into the skin in vivo in an animal model using PW.

## 20.2.7 Inclusion Complex

The most extensively studied agents to form inclusion complexes are cyclodextrins (Pankaj and Samir 2009). The cyclodextrin drug complex has been used to enhance the solubility and permeability of a drug by encapsulation of an active drug molecule in its core. Inclusion complex contains a lipophilic core in which appropriately sized insoluble molecules can form noncovalent inclusion complexes which lead to increased aqueous solubility and chemical stability (Loftsson and Brewster 1996). Cyclodextrins have been reported to varyingly increase skin penetration, alone or in combination with other permeation enhancers (Legendre et al. 1995).

Cyclodextrins can complex with enhancers like quaternary ammonium salts and reduce their toxic side effects on the skin, while still maintaining their skin permeabilization capacity, thereby showing a synergy between safety and potency (Martini et al. 1996). The skin penetration enhancement has also been attributed to extraction of stratum corneum lipids by cyclodextrins (Bentley et al. 1997).

## 20.2.8 Solid Lipid Nanoparticles (SLN)

Solid lipid nanoparticles (SLN) were developed at the beginning of the 1990s as an alternative carrier system to emulsions, liposomes, and polymeric nanoparticles (Muller et al. 2000). The research activities on SLN during the last decade focused almost exclusively on pharmaceutical applications. However, topical application of SLN was also studied, for both pharmaceutical and cosmetic products containing SLN. Major ingredients of SLN include solid lipids, emulsifiers, and water. The lipids include triglycerides, partial glycerides, fatty acids such as stearic acid, steroids like cholesterol, and waxes. SLNs have been used recently as carriers for transdermal drug administration. The encapsulated drug may penetrate across the skin and then expel drug from the SLN matrix as a consequence of polymorphic transitions occurring in the solid lipid (Shah et al. 2007). The active compound of cosmetic products must be retained in the skin, that is, it should penetrate sufficiently deep, but not too deep into the skin, which would lead to systemic availability (Muller et al. 2002). SLNs have been reported to deliver many macromolecules into the skin, including antibodies, hormones, RNA, and DNA (Chen et al. 2008; Westesen and Siekmann 2001). They exhibit high physical stability, potential of epidermal targeting, protection of incorporated labile actives against degradation, and excellent in vivo tolerability (Muller et al. 2000; Herzog. 2006). SLN composed of oil-soluble UV absorbers (1–40%), solid lipids (20–98.9%), emulsifiers (0.1–20%), and liquid lipids (0–40%) have been formulated, and skin protection

efficiency was evaluated. The developed formulation showed improved effectiveness in skin protection by reduced absorption of UV absorbers (Herzog, 2006). The patent of Constantinides et al. (2006) describes SLN suspensions for mucosal and parenteral administration. However, the developed formulation could also be administered transdermally in the form of creams, ointments, etc. Muller and Olbrich (2004) described SLN in their US patent No. 6,770,299 entitled "Lipid matrix-drug conjugates particle for controlled release of active ingredient." The SLN was prepared by high-pressure homogenization in order to obtain particles of submicron size. Westesen and Siekmann (2001) used the emulsifying process to prepare SLN and reported about nonspherical particles showing controlled release of poorly water-soluble drugs, primarily applied by i.v. and also by other administration routes including the dermal route.

### 20.2.9 Microemulsion

Microemulsions (ME) are lipid-based drug delivery systems, which have been used to enhance the transdermal permeation and bioavailability of poorly soluble drugs (Rizwan et al. 2009a). The permeation enhancement largely depends on the relative composition and concentration of the used oil, surfactant, and co-surfactant. Kreilgaard et al (2000) studied the ME system loaded with lipophilic (lidocaine) and hydrophilic (prilocaine hydrochloride) drug molecules and compared the drug flux to the flux obtained with conventional vehicles. The transdermal flux of both drugs was increased up to four and ten times, respectively, as compared to a conventional formulation. However, researchers also demonstrated the enhancing effect of different individual constituents, such as oil and surfactant present in ME. US Patent No. 6,426,078 (Bauer et al 2002) described oil-in water ME for lipophilic vitamins composed of diethylene glycol monoethyl ether or propylene glycol as co-emulsifier. The co-surfactant provided a considerable effect on the penetration of vitamins through the skin. The suitable combination of surfactants has also influenced the flux

across the skin. The transdermal administration of oligonucleotides and nucleic acids offers promise of simpler, easier, and less injurious administration without need for sterile procedures and their concomitant expenses.

### 20.2.10 Dendrimers

The PAMAM dendrimers are widely used as transdermal carriers for drugs (Sonke 2009). These were proven to pass the cell membrane barrier, and therefore they were used as transdermal carriers to transport several water-insoluble drugs into the cell membrane (Venuganti and Perumal 2009; Borowska et al. 2010). They are three-dimensional nanosized (1–100 nm), highly branched monodispersed macromolecules, obtained by chemical reaction and producing a unique structure (Tomalia et al. 1985). They contain a dendritic core, which can accommodate hydrophilic and hydrophobic drug molecules, and they have been reported to release drugs in a controlled manner (Umesh et al. 2006). The PAMAM dendrimers themselves are biodegradable and nontoxic (Hans and Lowman 2002). Filipowicz and Wołowicz (2011) prepared riboflavin-loaded PAMAM dendrimers and concluded that the transdermal diffusion of dendrimer complexes, both through PVDF (polyvinylidene difluoride) and PES (polyethersulfone) membranes was enhanced two to three times compared to control. The water-soluble PAMAM dendrimers can be successfully used in cosmetic and dermatological emulsions (Wollensak et al. 2003).

### 20.2.11 Vesicles

The most recent trend in dermal and transdermal drug delivery is the use of vesicle formulations as delivery systems. Many vesicular carriers have been reported in the literature which include liposomes (Mezei and Gulasekharan 1980), niosomes (Niemiec et al. 1995), Transfersomes® (Idea AG, Germany) (Cevc and Blume 1992), and invasomes (Dragicevic-Curic et al. 2008). These

formulations have been reported to solubilize insoluble drugs by which the bioavailability of drugs increased. The walls of lipid vesicles are made up of amphiphilic molecules in a bilayer conformation. In an excess of water, these amphiphilic molecules can form unilamellar or multilamellar vesicles (Gregoriadis and Florence 1993). The internal aqueous compartment of vesicles can entrap hydrophilic drugs, whereas lipophilic and amphiphilic drugs can be attached to the vesicle by hydrophobic and/or electrostatic interactions (Martin and Lloyd 1992). They can improve drug deposition within the skin at the site of action where the goal is to reduce systemic absorption (to provide a localizing effect) and thus minimize side effects. They can provide targeted delivery to skin appendages in addition to their potential for transdermal delivery (El Maghraby et al. 2006). Naturally, all molecules pass through by a combination of all three routes (intercellular, transcellular, and appendageous), the relative importance of which will vary depending on the molecule's physicochemical characteristics. Skin delivery of drugs by vesicles has gained attention after the commercialization of the dermal therapeutic system containing the antimycotic agent, econazole (Elsayed et al. 2007).

### 20.2.11.1 Liposomes

Liposomes are microscopic vesicles (size ranges from 50 nm to several hundred nm) containing phospholipid bilayers with enclosed aqueous spaces. They are generally classified as unilamellar lipid vesicles (ULV) and multilamellar lipid vesicles (MLV), and are composed of mainly phospholipids along with or without other additives, like cholesterol. The stability and permeability across the skin can be altered by changing the phospholipid composition (Bal et al. 2010). Studies have shown that liposomal systems deliver increased amounts of drugs to the skin as compared to conventional gel dosage forms. Mezei and Gulasekharam (1980) described the use of liposomes for triamcinolone acetonide in both a lotion and a gel for dermal delivery. Further, Mezei (1985) showed that triamcinolone acetonide concentrations in the skin were observed to be fourfold to fivefold higher when delivered from

liposomes as compared to conventional formulations. Depending upon their solubility and partitioning characteristics, the drug molecules are located differently in the liposomal environment and exhibit varying entrapment and release properties. The lipophilic drugs are entrapped almost completely in the lipid bilayers, whereas the hydrophilic drugs may be entrapped in the aqueous core of liposomes. The entrapment of hydrophilic drugs in liposomes depends on the liposome bilayer composition and method of preparation (Fang 2006). The systemic absorption is increased by releasing the drug from liposomes at the target site in skin appendages (El Maghraby et al. 2008). Thierry (2000) described in his patent, liposomes which are composed of cationic lipopolyamine (spermine-5-carboxy-glycinediiododecylamide) and neutral lipid (dioleoylphosphatidyl ethanolamine) and contain biologically active agents like nucleic acids or proteins. Mezei et al (1999) described liposomes containing selegilin, which provided high selegilin blood level, decreased drug metabolism, prolonged therapeutic effect, and showed stability for a long time. High blood level for 72 h was achieved by liposome with a low number of lamellae, whereas the multilamellar liposomes ensured a measurable blood level even after 168 h. Kirjavainen et al. (1996) studied the skin penetration of liposomes and showed that liposomes initially penetrate the SC, then destabilize SC lipids and fuse with the lipid matrix. Yang et al. (2007) studied paclitaxel liposomes containing 3 % (v/v) Tween 80 obtained by freeze-drying with sucrose as a lyoprotectant. The PEGylated liposomes showed greater tumor growth inhibition effect in *in vivo* studies compared to the solution of paclitaxel.

### 20.2.11.2 Niosomes

Niosomes are unilamellar or multilamellar vesicles made up of phospholipids and nonionic surfactants with or without incorporation of cholesterol or other lipids. Transdermal delivery of the active compound incorporated into niosomes results in its enhanced delivery through the SC (Torchilin 2007). Ming et al. (2013) prepared hyaluronic acid (HA)-based niosomes for tumor therapy, and the results of the study

revealed that incorporation of HA significantly promoted the endocytosed amount of HA-loaded nanocarrier by tumor cells. Varaporn et al. (2012) prepared niosomal formulations of ellagic acid prepared with a mixture of Span 60<sup>®</sup> and Tween 60<sup>®</sup> and reported in their study that EA-loaded niosomes delivered a higher amount of EA into the deeper layer of the skin as compared to EA solution. The permeation experiments revealed that the penetration of EA from niosomes depended on the vesicle size.

Imam et al. (2015) formulated risperidone niosomes formulation and reported in their result that niosomes showed significantly higher skin permeation in comparison to conventional liposomes. The pharmacokinetic study in rats indicated that bioavailability was 1.31 times higher than that of oral dosage form. Luteolin and ursolic acid loaded niosomes (Abidin et al. 2014; Jamal et al. 2015) were prepared using different nonionic surfactants and characterized for in vitro and in vivo antiarthritic activity. The result of the study showed that niosomes provide both improved encapsulation and enhanced transdermal flux value across rat skin. The in vivo data revealed that analgesic effect of drug-loaded niosomes was comparable to that of standard gel.

Qumbar et al. (2014) prepared lacidipine-loaded niosomes and reported that the overall mean value of  $AUC_{0-t}$  by transdermal delivery was 2.56 times higher than that by oral route, and the difference was found to be statistically significant ( $p < 0.05$ ), demonstrating improved bioavailability of lacidipine from niosomes. Pioglitazone niosomes were developed and were optimized using quality by design (QbD) approach and evaluated for particle size, percentage entrapment, and transdermal flux. The permeation enhancement of pioglitazone niosome was 3.16 times higher than that from control formulation (ethanol buffer formulation, 3:7), and further significant increase in bioavailability (2.26 times) was achieved vis-a-vis tablet formulation (Prasad et al. 2014).

### 20.2.11.3 Transfersomes

Cevc and Blume (1992) invented a new class of deformable, ultraflexible vesicles termed Transfersomes<sup>™</sup> (Idea AG, Germany). They are

composed of phospholipids, such as phosphatidylcholine and surfactants (Trotta et al 2004; Cevc 1996). The surfactant acts as an edge activator that destabilizes the lipid bilayers and increases the deformability of the vesicles (Honeywell-Nguyen et al. 2004; Bouwstra et al. 2003). Due to the high flexibility of Transfersomes, they are able to squeeze through one-tenth the size of their own diameter and penetrate deeper across SC (Cevc 1996). Cevc and Blume (1992) have suggested that the driving force for vesicles' penetration into the skin is the osmotic gradient that is caused by the difference in water content between the relatively dehydrated skin surface (~20% water) and the aqueous viable epidermis. Transfersomes squeeze through the SC lipid lamellar regions penetrating deeper to follow the osmotic gradient. Cevc (2000) patented insulin transfersomes for enhanced and prolonged delivery of insulin by the transdermal route. The distribution and biological activity of the corticosteroid Transfersomes have also been reported following topical administration of commercially available lotion and cream products (Cevc 2003). Later, Cevc (2007) developed transfersomes comprising of phosphatidylcholine, nonionic surfactant along with consistency builder, antioxidant, microbiocide, and corticosteroid, capable of penetrating into the skin. Transfersomes were found to be ten times more effective, as compared to conventional products during in vivo studies in humans. Ahad et al. (2012) developed and statistically optimized nanotransfersomes for enhanced transdermal delivery of valsartan by conventional rotary evaporation method. Nanotransfersomes proved significantly superior in terms of the amount of drug permeated in the skin, with an enhancement ratio of  $33.97 \pm 1.25$  when compared to rigid liposomes. Chaudhary et al. (2013) formulated transdermal drug delivery named nanotransfersomes (deformable vesicular system) of Diclofenac diethylamine (DDEA) and Curcumin (CRM). The optimized formulation provided a large surface area with higher penetration potential of 1.39-fold and 1.43-fold for DDEA and CRM, respectively. In another study, the same research group reported nanotransfersomes achieving

higher absorption of DDEA and CRM with relative bioavailability of 398.54 and 2456.90%, respectively (Chaudhary et al. 2014)

#### 20.2.11.4 Ethosomes

Ethosomes are vesicles composed of water, high content of ethanol (up to 45%), and phospholipids (Touitou et al. 2000; Pankaj and Samir 2009). The high concentration of ethanol provides soft, flexible vesicles, which easily penetrate into the deeper skin layers enabling enhanced drug delivery. The mechanism of drug penetration across the skin was found to be similar to that of liposomes. Briefly, the vesicles enter the SC carrying drug molecules into the skin and also act as penetration enhancers by modifying the intercellular lipid lamellae of the SC (Dubey et al. 2007b). Researchers suggested that ethanol present in ethosomal formulations fluidizes both vesicular lipid bilayers and SC lipids and thus provides greater malleability to vesicles and increases skin permeability. Dubey et al. (2007a) evaluated methotrexate (MTX)-loaded ethosomes as carriers for transdermal delivery. The vesicles showed high entrapment and thus enhanced transdermal flux and decreased lag time across the human cadaver skin. Ethosomes show the enhanced permeation effect due to the synergistic action of high concentrations of ethanol and phospholipids contained in the vesicles on the skin lipids. The release of the drug could be the result of fusion of ethosomes with skin lipids and drug release at various points along the penetration pathway (Touitou et al. 2000). Recently, Ahad et al. (2013) reported valsartan ethosomes for transdermal delivery and found that ethosomes proved to be superior in terms of the amount of drug permeated through the skin, with an enhancement ratio of  $43.38 \pm 1.37$  in comparison to conventional liposomes. Recently, Ahmed et al. (2015) formulated tramadol-loaded ethosome and evaluated for flux when compared with liposome (control). The result showed significant enhancement in flux and bioavailability (7.51 times) compared with oral tramadol. The overall results suggest that the developed formulation is an efficient carrier for transdermal delivery of tramadol.

#### 20.2.11.5 Invasomes

Invasomes are a novel lipid vesicular drug delivery system having a size  $<150$  nm. They are composed of phosphatidylcholine, ethanol, and terpenes alone or a combination of terpenes (Verma and Fahr 2004; Dragicevic-Curic et al. 2008). In invasomes, terpenes are used as important constituents, which act as potent penetration enhancers, and they have been shown to enhance the percutaneous absorption of many drugs. These phenomena, that is, an increased deformability of vesicles and a disorganized SC bilayer structure induced by the action of invasomes constituents on the skin lipids, are thought to facilitate the penetration of invasomes. Invasomes may follow the transepidermal osmotic gradient into and through the SC, and such vesicles are hence able to squeeze themselves through the intracellular regions of the SC due to their highly elastic membranes and due to the transepidermal water gradient. Thus, compared to more rigid conventional liquid-state vesicles, elastic vesicles might further increase the drug transport across the skin. The differential scanning calorimetry and X-ray diffraction revealed that terpenes increase drug permeation by disrupting lipid packaging of the SC and/or disturbing the stacking of the bilayers (Cornwell et al. 1996).

Quadry et al. prepared isradipine invasomes with ameliorated flux, reasonable entrapment efficiency, and more effectiveness for transdermal delivery. The invasomes delivery systems may be a promising carrier for transdermal delivery of isradipine for the management of hypertension.

In another study, nano-invasomes of olmesartan with beta-citronellene as a potential permeation enhancer were developed and optimized using Box–Behnken design. The confocal laser microscopy of rat skin showed that invasome formulation was evenly distributed and permeated deep into the skin. Further, the pharmacokinetic result showed that transdermal nano-invasomes formulation showed 1.15 times improvement in bioavailability of olmesartan with respect to the control formulation in wistar rats (Kamran et al. 2016).

### 20.3 Synergistic Use of Enhancement Techniques

A number of synergistic techniques have been used successfully to enhance transdermal drug transport, and their combinations have been hypothesized to be more effective in comparison to a single treatment (Table 20.3). Many researchers reported the use of binary combination techniques; however, others used multiple techniques simultaneously, including iontophoresis combined with chemical penetration enhancers; ultrasound combined with chemical penetration enhancers; iontophoresis combined with ultrasound; multiple combinational techniques to achieve penetration enhancement of drugs (Henley 1995; Mitragotri et al. 1998; Rowe et al. 2001; Giammarusti 2004). Iontophoresis has been synergistically used with chemical permeation enhancers, ultrasound, and liposomes, to further improve the drug penetration through the skin (Kost et al. 2000; Francoeur and Potts 1991; Bommannan et al. 1992).

The combination of iontophoresis and chemical penetration enhancers has been reported by Francoeur and Potts (1991). They

reported that enhancers such as oleic acid and 1-dodecylazacycloheptan-2-one (0.01–5% w/v) in combination with iontophoresis provided higher flux compared to the use of oleic acid or iontophoresis alone. The use of liquid permeation enhancers in an iontophoretic device is generally limited by the occurrence of adverse interactions between the enhancer and drug, body surface, or device components. Henley (1995) reported in his patent about the synergistic use of iontophoresis and ultrasonic transdermal delivery devices, which can achieve greater skin penetration of drugs and even larger peptide molecules such as insulin for a prolonged period of time. Such device can be used to deliver cholecystokinin, nicotine, valium and naloxone, heparin (peptide), fentanyl, and other therapeutic agents.

Seward (2006) and Kwiatkowski (2008) employed iontophoresis/electroporation and an array of microneedles for enhanced delivery of macromolecules. These combined systems have the ability to deliver drugs in a controlled manner for a prolonged period. Kwiatkowski (2008) developed a transdermal patch for therapeutic agents that include two arrays of electrically conductive microprojections, and two reservoirs for

**Table 20.3** Combination of penetration enhancement techniques

S. No	Patent number	Technique	Application
1	US5814599 Mitragotri et al. (1998)	Uses low-frequency ultrasound and liposomes or microparticles	Insulin, erythropoietin, and interferon were administered through the skin
2	US5736580 Huntington and Cormier (1998)	Iontophoretic device with enhancers for electrotransport delivery of drugs	Improves shelf life and reduces interactions
3	US7127284 Seward (2006)	Electroporation with microneedle	Enhances the intracellular delivery of genes, nucleic acids, proteins, and other large molecules
4	US6009345 (A) Hofmann (1999)	Electroporation with iontophoresis	Sufficient migration of molecules through pores in the stratum corneum is achieved
5	US5947921 (A) Kost et al. (1999)	Sonophoresis with chemical enhancers	Provides higher drug fluxes, allows rapid control, and allows drug delivery at lower ultrasound intensities
6	TW200534866 (A) Liu et al. (2005).	Niosomes with inclusion complex	Produces the enhanced transdermal permeation as well as its application

the same or different drugs. The microprojections are adapted to provide a perforation of the epidermis to the depth of between about 50 and 150  $\mu\text{m}$ . Rowe et al. (2001) disclosed a two-step noninvasive method which involves the application of ultrasound to increase skin permeability followed by the application of a chemical enhancer (alcohol, fatty acid, DMSO, and others) to further increase the transdermal drug transport.

A technique to enhance the flux rate of bioactive molecules by the synergistic application of microporation with different enhancement methods has also been reported (Ben-Amoz 1989; Eppstein 2003; Giammarusti 2004). The low-frequency ultrasound was used to enhance the transdermal delivery of high-molecular weight proteins which was further enhanced and controlled by the use of drug carriers, such as liposomes or microparticles (Mitragotri et al. 1998; Eppstein 1998). The enhancement achieved by the combination of techniques is higher than the sum of enhancements persuaded by the separate application of one of the technique individually. These combinations offer many advantages over application of a single technique for enhanced transdermal drug delivery.

### Conclusion

This chapter gives an exhaustive review on patents and research papers published over the years in the area of dermal and transdermal penetration-enhancement techniques. It embodies reports that exemplify novel permeation techniques and the ones which form the basis of our current knowledge base. There are many permeation enhancement techniques which come in and out of favor, and this is reflected in the text above. In recent years, the use of a number of combination techniques has aided in our understanding of the nature of the skin barrier and the way in which chemicals interact with and influence the skin structure.

### References

- Abidin L, Mujeeb M, Imam SS, Aqil M, Khurana D (2014) Enhanced transdermal delivery of Luteolin via non-ionic surfactant based vesicle: quality evaluation and antiarthritic assessment. *Drug Del Early Online* 1–6. doi:10.3109/10717544.2014.945130
- Ahad A, Aqil M, Kanchan K, Hema C, Yasmin S, Mujeeb M, Sushama T (2009) Chemical penetration enhancers: a patent review. *Expert Opin Ther Pat* 19(7):969–988
- Ahad A, Aqil M, Kohli K, Sultana Y, Mujeeb M, Ali A (2012) Formulation and optimization of nano-transfersomes using experimental design technique for accentuated transdermal delivery of valsartan. *Nanomedicine* 8(2):237–249
- Ahad A, Aqil M, Kohli K, Sultana Y, Mujeeb M, Ali A (2010) Transdermal drug delivery: the inherent challenges and technological advancements. *Asian J Pharm Sci* 5:276–288
- Ahad A, Aqil M, Kohli K, Sultana Y, Mujeeb M (2013) Enhanced transdermal delivery of an anti-hypertensive agent via nanoethosomes: Statistical optimization, characterization and pharmacokinetic assessment. *Int J Pharm* 443:26–38
- Ahmed S, Imam SS, Zafar A, Ali A, Aqil M, Gul A (2015) Invitro and preclinical assessment of factorial design based nanoethosomes transgel formulation of an opioid analgesic. *Art Cells Nanomed Biotech*. doi: 10.3109/21691401.2015.1102742
- Akatsuka H, Imamura H, Ishihara Y (2014) US 8865208
- Allen Jr LV (2000) US6119036
- Angel AB, Hunter IW, Hansen P (2006) US20067066922
- Angel AB, Hunter IW (2008) US20087364568
- Asbill CS, Michniak BB (2000) Percutaneous penetration enhancers: local versus transdermal activity. *Pharm Sci Technol Today* 3:36–41
- Bachhav YG, Heinrich A, Kalia YN (2011) Using laser microporation to improve transdermal delivery of diclofenac: increasing bioavailability and the range of therapeutic applications. *Eur J Pharm Biopharm* 78(3): 408–414
- Bachhav YG, Summer S, Heinrich A, Bragagna T, Bohler C, Kalia YN (2010) Effect of controlled laser microporation on drug transport kinetics into and across the skin. *J Control Rel* 146(1):31–36
- Bal SM, Ding Z, Evan R, Jiskoot W, Bouwstra JA (2010) Advances in transcutaneous vaccine delivery: do all ways lead to Rome? *J Control Rel* 148:266–282
- Bauer K, Neuber C, Schmid A, Volker KM (2002) US6426078
- Ben-Amoz D (1989) US4866050
- Bentley MV, Vianna RF, Wilson S, Collett JH (1997) *J Pharm Pharmacol* 49:397–402
- Bogner RH, Wilkosz MF (2003) Transdermal drug delivery part 2: upcoming developments. *US Pharmacist* 28:05
- Bommannan D, Okuyama H, Guy RH, Stauffer P, Flynn GL (1992) US5115805
- Borowska K, Laskowska B, Magon A, Mysliwiec B, Pyda M, Wołowicz S (2010) PAMAM dendrimers as solubilizers and hosts for 8-methoxypsoralene enabling transdermal diffusion of the guest. *Int J Pharm* 398:185–189
- Bouwstra JA, Honeywell-Nguyen PL, Gooris GS, Ponc M (2003) Structure of the skin barrier and its modulation by vesicular formulations. *Prog Lipid Res* 42(1):1–36

- Carlos S, Scott KF, Robert GJ (1999) Non-steroidal anti-inflammatory drug formulations for topical application to the skin. CA2299288
- Cevc G (2003) Transdermal drug delivery of insulin with ultradeformable carriers. *Clin Pharmacokinet* 42(5):461–474
- Cevc G, Blume G (1992) Lipid vesicles penetrate into intact skin owing to the transdermal osmotic gradients and hydration force. *Biochim Biophys Acta* 1104(1):226–232
- Cevc G (1996) Transfersomes, liposomes and other lipid suspensions on the skin: permeation enhancement, vesicle penetration, and transdermal drug delivery. *Crit Rev Ther Drug Carrier Syst* 13(3–4):257–388
- Cevc G (2000) US20006165500
- Cevc G (2007) US20077175850
- Chen J, Cai B, Gu W, Xiao H, Li J (2013) CN102846546 (A)
- Chen T, Vargeese C, Vagle K, Wang W, Zhang Y (2008) US20087404969
- Cho ST (2005) US20056980855
- Constantinides P, Patil RT, Liang L (2006) US20060078618
- Cormier MJN, Nat AS, Neukermans AP, Block B (2001) US20016230051
- Cormier MJN, Neukermans AP, Block B, Theeuwes FT, Amkraut AA (2007) US20077184826
- Cornwell PA, Barry BW, Bouwstra JA, Gooris GS (1996) Modes of action of terpene penetration enhancers in human skin; differential scanning calorimetry, small angle X-ray diffraction and enhancer uptake studies. *Int J Pharm* 127:9–26
- Coulman S, Allender C, Birchall J (2006) Microneedles and other physical methods for overcoming the stratum corneum barrier for cutaneous gene therapy. *Crit Rev Ther Drug Carrier Syst* 23:205–258
- Donnelly RF, Morrow DI, Fay F, Scott CJ, Abdelghany S, Singh RR, Garland MJ, Woolfson AD (2010) Microneedle-mediated intradermal nanoparticle delivery: potential for enhanced local administration of hydrophobic pre formed photosensitisers. *Photodiag Photodyn Ther* 7:222–231
- Doukas AG, Kollias N (2004) Transdermal drug delivery with a pressure wave. *Adv Drug Deliv Rev* 56:559–579
- Dragicevic-Curic N, Scheglmann D, Albrecht V, Fahr A (2008) Temoporfin-loaded invasomes: development, characterization and in vitro skin penetration studies. *J Cont Rel* 127:59–69
- Dubey V, Mishra D, Dutta T, Nahar M, Saraf DK, Jain NK (2007a) Dermal and transdermal delivery of an antipsoriatic agent via ethanolic liposomes. *J Cont Rel* 123:148–155
- Dubey V, Mishra D, Jain NK (2007b) Melatonin loaded ethanolic liposomes: physicochemical characterization and enhanced transdermal delivery. *Eur J Pharm Biopharm* 67:398–405
- El Maghraby GM, Barry BW, Williams AC (2008) Liposomes and skin: from drug delivery to model membranes. *Eur J Pharm Sci* 34:203–222
- EL Maghraby GM, Williams AC, Barry BW (2006) Can drug-bearing liposomes penetrate intact skin? *J Pharm Pharmacol* 58(4):415–429
- Elsayed MMA, Abdullah OY, Naggat VF, Khalafallah NM (2007) Lipid vesicles for skin delivery of drugs: reviewing three decades of research. *Int J Pharm* 332:1–16
- Eppstein JA (2003) US20036527716
- Eppstein JA (1998) US5722397
- Fang JY (2006) Nano- or submicron-sized liposomes as carriers for drug delivery. *Forum Chang Gung Med J* 29(4):358–362
- Filipowicz A, Wołowiec S (2011) Solubility and in vitro transdermal diffusion of riboflavin assisted by PAMAM dendrimers. *Int J Pharm* 408:152–156
- Foldvari M (2000) Non-invasive administration of drugs through the skin: challenges in delivery system design. *Pharm Sci Technol Today* 3:417–425
- Francoeur ML, Potts RO (1991) US5023085
- Gartstein V, Sherman FF (2006) US20067108681
- Gertsek M, Wilkinson BM, Pettis RJ (2003) US20036656147
- Ghartey-Tagoe E, Wendorf J, Williams S, Singh P, Worsham RW, Trautman JC, Bayramov D, Bowers DL, Klemm AK, Steven R, Chen G (2014) United States Patent, 8911749
- Giammarusti P (2004) US20046795727
- Gill HS, Prausnitz MR (2007) Coated microneedles for transdermal delivery. *J Cont Rel* 117:227–237
- Ginaven RO, Facciotti D (1995) US5457041
- Godshall NA, Anderson RR (1999) US5879326
- Gold MH (2007) Fractional technology: a review and clinical approaches. *J Drugs Dermatol* 6:849–852
- Gomaa AY, Martin JG, Fiona JM, Ryan FD, Labiba KE, Clive GW (2014) Microneedle/nanoencapsulation mediated transdermal delivery: mechanistic insights. *Eur J Pharm Biopharm* 86(2):145–155
- Gregoriadis G, Florence AT (1993) Liposomes in drug delivery. *Clinical, diagnostics and ophthalmic potential*. *Drugs* 45:15–28
- Hans ML, Lowman AM (2002) Biodegradable nanoparticles for drug delivery and targeting. *Curr Opin Solid State Mater Sci* 6:319–327
- Chaudhary H, Kohli K, Kumar K (2013) Nano-transfersomes as a novel carrier for transdermal delivery. *Int J Pharm* 454:367–380
- Chaudhary H, Kohli K, Kumar K (2014) A novel nano-carrier transdermal gel against inflammation. *Int J Pharm* 465(1–2):175–186
- Henley JL (1995) US5415629
- Henry S, McAllister D, Allen MG, Prausnitz MR (1998) Micro fabricated microneedles: a novel method to increase transdermal drug delivery. *J Pharm Sci* 87:922–925
- Herzog B (2006) US20067147841
- Hofmann GA (1994) US5318514
- Hofmann GA (1999) US6009345 (A)
- Honeywell-Nguyen PL, Gooris GS, Bouwstra JA (2004) Quantitative assessment of the transport of elastic and rigid vesicle components and a model drug from these vesicle formulations into human skin in vivo. *J Invest Dermatol* 123(5):902–910
- Huntington JA, Cormier M (1998) US5736580



- Igarashi T, Nishino K, Nayar SK (2007) The appearance of human skin: a survey, found, Trends. Comput Graph Vis 3:1–95
- Imam SS, Aqil M, Akhtar M, Sultana Y, Ali A (2015) Formulation by design-based proniosome for accentuated transdermal delivery of risperidone: in vitro characterization and in vivo pharmacokinetic study. Drug Del 22(8):1059–1070
- Jamal M, Imam SS, Aqil M, Amir M, Mir SR, Mujeeb M (2015) Transdermal potential and anti-arthritis efficacy of ursolic acid from niosomal gel systems. Int Immunopharm 29:361–369
- Jeong WL, Priya G, Jung-Hwan P, Mark GA, Mark RP (2011) Microsecond thermal ablation of skin for transdermal drug delivery. J Cont Rel 154:58–68
- Kai T, Mak VHW, Potts RO, Guy RH (1990) Mechanism of percutaneous penetration enhancement: effect of n-alkanols on the permeability barrier of hairless mouse skin. J Control Rel 12:103–112
- Kamran M, Ahad A, Aqil A, Imam SS, Sultana Y, Ali A (2016) Design, formulation and optimization of novel soft nano-carriers for transdermal olmesartan medoxomil delivery: in vitro characterization and in vivo pharmacokinetic assessment. Int J Pharm 505(1–2):147–158
- King AD, Walters RE (2003) US20036603998
- Kirjavainen M, Urtti A, Jaaskelainen I (1996) Interaction of liposomes with human skin in vitro – the influence of lipid composition and structure. Biochim Biophys Acta 1304:179–189
- Kost J, Pishko M, Langer RS, Blankschtein D, Mitragotri SS, Johnson ME (1999) US5947921 (A)
- Kost J, Pliquett U, Mitragotri SS, Langer RS, Weaver JC (2000) US20006041253
- Kreilgaard M, Pedersen EJ, Jaroszewski JW (2000) NMR characterization and transdermal drug delivery potential of microemulsion systems. J Cont Rel 69:421–433
- Kwiatkowski M (2008) US20087345163
- Lai-Cheong JE, McGrath JA (2009) Structure and function of skin, hair and nails. Medicine 37:223–226
- Lee HB, Shin BC (1993) US5250023
- Lee S, Kollias N, McAuliffe DJ, Flotte TJ, Doukas AG (1999) Topical delivery in humans with a single photomechanical wave. Pharm Res 16:1717–1721
- Lee S, McAuliffe DJ, Flotte TJ, Kollias N, Doukas AG (1998) Photomechanical transcutaneous delivery of macromolecules. J Invest Derm 111:925–929
- Legendre JY, Rault I, Petit A, Luijten W, Demuyneck I, Horvath S, Ginot YM, Cuine A (1995) Effects of beta-cyclodextrins on skin: implications for the transdermal delivery of pibredil and a novel cognition enhancing-drug, S-9977. Eur J Pharm Sci 3:311–322
- Lin H, Yu C, Lei W, Lin D (2013) CN102949341 (A)
- Liu CC, Lee YC, Yang CC (2005) TW200534866 (A)
- Loftsson T, Brewster ME (1996) Pharmaceutical applications of cyclodextrins. Drug solubilization and stabilization. J Pharm Sci 85:1017–1025
- Martanto W, Davis S, Holiday N, Wang J, Gill H, Prausnitz M (2003) Transdermal delivery of insulin using microneedles *in vivo*. Proc Int Symp Control Rel Bioactive Mater 666
- Martin GP, Lloyd AW (1992) Basic principles of liposomes for drug use. In: Braun-Falco O et al. (eds) Liposome dermatics. Springer Berlin, pp 20–26
- Martini A, Artico R, Civaroli P, Muggetti L, De Ponti R (1996) Critical micellar concentration shifting as a simple tool for evaluating cyclodextrin/enhancer interactions. Int J Pharm 127(2):239–244
- Mezei M, Gaal J, Szekacs G, Szebeni G, Marmarosi K, Magyar K, Lengyel J, Szatmari I, Turi A (1999) US5888536
- Mezei M, Gulasekharan V (1980) Liposomes- a selective drug delivery system for topical route of administration. 1. Lotion dosage form. Life Sci 26:1473–1477
- Mezei M (1985) Liposomes as a skin drug delivery system. In: Speiser DD (ed) Topics in pharmaceutical sciences. Elsevier, Amsterdam, pp 345–358
- Ming K, Hyunjin P, Chao F, Lin H, Xiaojie C, Xiguang C (2013) Construction of hyaluronic acid noisome as functional transdermal nanocarrier for tumor therapy. Carb Pol 94:634–641
- Mitragotri S, Blankschtein D, Langer R (1995) Ultrasound mediated transdermal protein delivery. Science 269: 850–853
- Mitragotri SS, Blankschtein D, Langer RS (2000) US6018678
- Mitragotri SS, Blankschtein D, Langer RS (1998) US5814599
- Mitragotri SS, Blankschtein D, Langer RS (1999) US6002961
- Modi P (2006) US20060182766A1
- Muller RH, Karsten M, Sven G (2000) Solid lipid nanoparticles (SLN) for controlled drug delivery-a review of the state of the art. Eur J Pharm Biopharm 50:161–177
- Muller RH, Olbrich C (2004) US6770299
- Muller RH, Radtke M, Wissing SA (2002) Solid lipid nanoparticles (SLN) and nanostructured lipid carriers (NLC) in cosmetic and dermatological preparations. Adv Drug Deliv Rev 54:S131–S155
- Murthy SN, Hiremath SRR (2001) Physical and chemical permeation enhancers in transdermal delivery of terbutaline sulphate. AAPS Pharm Sci Tech 2:1–5
- Nethercott JR (1990) Practical problems in the use of patch testing in the evaluation of patients with contact dermatitis. Current Problems in Dermatology 2(4):97–123
- Niemiec SM, Ramachandran C, Weiner N (1995) Influence of non-ionic liposomal composition on topical delivery of peptide drugs into pilosebaceous units: an in vivo study using the hamster ear model. Pharm Res 12:1184–1188
- Ogura M, Sato S, Kuroki M (2002) Transdermal delivery of photosensitizer by the laser-induced stress waves in combination with skin heating. Jpn J Appl Phys 41:L814–L816
- Ostrow A, Koops GH, Tannenbaum J (2003) US20036564093
- Owen AJ, Yiv SH, Sarkahian AB (1997) US5688761
- Pankaj K, Samir M (2009) Enhancement of transdermal drug delivery via synergistic action of chemicals. Biochim Biophys Acta 1788:2362–2373

- Park JH, Lee JW, Kim YC, Prausnitz MR (2008) The effect of heat on skin permeability. *Int J Pharma* 359(1–2):94–103
- Paudel KS, Milewski M, Swadley CL, Brogden NK, Ghosh P, Stinchcomb AL (2010) Challenges and opportunities in dermal/transdermal delivery. *Ther Deliv* 1:109–131
- Pettis RJ, Down JA, Harvey NG (2014) United States Patent, 20130245601 A1
- Prasad PS, Imam SS, Aqil M, Sultana Y, Ali A (2014) QbD based carbopoltransgel formulation: characterization, pharmacokinetic assessment and therapeutic efficacy in diabetes. *Drug Delivery, Early Online* 1–10. doi:[10.3109/10717544.2014.936536](https://doi.org/10.3109/10717544.2014.936536)
- Prausnitz MR (1999) A practical assessment of transdermal drug delivery by skin electroporation. *Adv Drug Deliv Rev* 35:61–76
- Prausnitz MR (2004a) Microneedles for transdermal drug delivery. *Adv Drug Deliv Rev* 56:581–587
- Prausnitz MR, Mitragotri S, Langer R (2004b) Current status and future potential of transdermal drug delivery. *Nat Rev Drug Discov* 3:115–124
- Qadri GR et al (2015) Invasomes of isradipine for enhanced transdermal delivery against hypertension: formulation, characterization and in vivo pharmacodynamic study. *Art Cells Nanomed Biotech*. doi:[10.3109/21691401.2016.1138486](https://doi.org/10.3109/21691401.2016.1138486)
- Qumbar M, Ameenuzzafar AJ, Imam SS, Fazil M, Ali A (2014) DOE-based stability indicating RP-HPLC method for determination of lacidipine in niosomal gel in rat: pharmacokinetic determination. *Pharm Anal Acta* 5:8
- Rabussay D, Hofmann GA, Zhang L (2001) US6266560 (B1)
- Rizwan M, Aqil M, Azeem A, Talegaonkar S, Sultana Y, Ali A (2009a) Enhanced transdermal delivery of carvedilol using nanoemulsion as a vehicle. *J Exp Nanosci* 5(5):390–411
- Rizwan M, Azeem A, Aqil M, Talegaonkar S, Sultana Y, Ali A (2009b) Enhanced transdermal drug delivery techniques: an extensive review of patents. *Rec Pat Drug Del Form* 3:105–124
- Rosenberg ZB (2003) US20036623457
- Rowe S, Kost J, Mitragotri SS, Pishko M, Davis M (2001) US20016234990
- Rowland CA, Chilcott RP (2000) The electrostability and electrically assisted delivery of an organophosphate pretreatment (physostigmine) across human skin *in vitro*. *J Cont Rel* 68:157–166
- Santus GC, Baker RW (1993) Transdermal enhancer patent literature. *J Control Rel* 25:1–20
- Schaefer H, Redelmeier TE (1996) Structure and dynamics of the skin barrier. In: Schaefer H, Redelmeier TE (eds) *Skin barrier*. Karger, Tokyo, pp 1–33
- Seward KP (2006) US20067127284
- Shah KA, Date AA, Joshi MD, Patravale VB (2007) Solid lipid nanoparticles (SLN) of tretinoin: Potential in topical delivery. *Int J Pharm* 345:163–171
- Shimada J, Shapland JE (1993) US5267985
- Sonke S (2009) Dendrimers as versatile platform in drug delivery applications. *Eur J Pharm Biopharm* 71:445–462
- Suzuki Y, Iga K, Matsumoto Y (2001) US6248349
- Thierry AR (2000) US6110490
- Thomas BJ, Finin BC (2004) The transdermal revolution. *Drug Discov Today* 9:697–703
- Tomalia DA, Baker H, Dewald J, Hall M, Kallos G, Martin S (1985) A new class of polymers: starburst-dendritic macromolecules. *Polym J* 17:117–132
- Torchilin VP (2007) Targeted pharmaceutical nanocarriers for cancer therapy and imaging. *AAPS J* 9(2):128–147
- Toutou E, Godin B, Weiss C (2000) Enhanced delivery of drugs into and across the skin by ethosomal carriers. *Drug Dev Res* 50:406–415
- Toutou E (1996) US5540934
- Trelles MA, Mordon S VM, Urdiales F, Levy JL (2009) Results of fractional ablative facial skin resurfacing with the erbium:yttrium–aluminium–garnet laser 1 week and 2 months after one single treatment in 30 patients. *Lasers Med Sci* 24:186–194
- Trotta M, Peira E, Carlotti ME, Gallarate M (2004) Deformable liposomes for dermal administration of methotrexate. *Int J Pharm* 270(1–2):119–125
- Umesh G, Hrushikesh BA, Abhay A, Narendra KJ (2006) A review of in vitro–in vivo investigations on dendrimers: the novel nanoscopic drug carriers. *Nanomedicine* 2:66–73
- Uritti, AO, Sutinen MR, Paronen TP. US5817332 (A) 1998
- Vanbever R, Prausnitz MR, Preat V (1997) Macromolecules as novel transdermal transport enhancers for skin electroporation. *Pharm Res* 14:638–644
- Varaporn BJ, Pratyawadee S, Jiraphong S, Doungdaw C (2012) Physicochemical properties and skin permeation of Span 60/Tween 60 niosomes of ellagic acid. *Int J Pharm* 423:303–311
- Venuganti VV, Perumal OP (2009) Poly(amidoamine) dendrimers as skin penetration enhancers: influence of charge, generation and concentration. *J Pharm Sci* 98: 2345–2356
- Verma DD, Fahr A (2004) Synergistic penetration enhancement effect of ethanol and phospholipids on the topical delivery of cyclosporine A. *J Cont Rel* 97: 55–66
- Weaver JC, Langer RS, Mitragotri SS, Pliquett U, Kost J (2012) RS20110241 (A2)
- Weimann LJ (2007) US20077232431
- Westesen K, Siekmann B (2001) US6207178
- Wilkinson BM, Hwang CG (2006) US20067047070
- Wokovich AM, Prodduturi S, Doub WH, Hussain AS, Buhse LF (2006) Transdermal drug delivery system (TDDS) adhesion as a critical safety, efficacy and quality attribute. *Eur J Pharm Biopharm* 64:1–8
- Wollensak G, Spoerl E, Seiler T (2003) Riboflavin/ultraviolet-A-induced collagen crosslinking for the treatment of keratoconus. *Ophthalmology* 110: 1031–1040
- Yang T, Fu-De C, Min-Koo C, Jei-Won C, Suk-Jae C, Chang-Koo S, Dae-Duk K (2007) Enhanced solubility and stability of PEGylated liposomal paclitaxel: *in vitro* and *in vivo* evaluation. *Int J Pharm* 338:317–326
- Zech NH, Murtinger M, Uher P (2011) Pregnancy after ovarian superovulation by transdermal delivery of follicle-stimulating hormone. *Fertil Steril* 95(8):2784–2785
- Zhang L, Rabussay DP (2005) US6972013

Marianna Foldvari and P. Kumar

## Contents

21.1 Introduction .....	355
References .....	357

---

## 21.1 Introduction

Topical application of drugs can be performed for two distinct purposes, either as a localised treatment for dermatological or deeper tissue conditions (dermal) or for systemic delivery (transdermal). There are distinct set of development strategies for both of these two applications, although the first hurdle in both cases is to cross the stratum corneum barrier (Elsabahy and Foldvari 2013). In healthy, uncompromised skin, the physical barrier properties of the skin prevail and prevent most external substances to permeate into the body. The properties of most drugs fall outside the optimum range of permeability (Bos and Meinardi 2000) and hence require some type of an enhancer to be therapeutically useful. The suggested size limit of molecules for passive delivery through the skin is below 500 Da (Bos and Meinardi 2000). Unassisted penetration of molecules above this molecular weight through intact skin is extremely low.

In the past decade, the discovery of new dermal and transdermal technologies with the simultaneous understanding of the physiological pathways in skin layers in much greater detail resulted in the increasing use of the dermal route for delivering not only small drug molecules but also proteins, nucleic acids and vaccine antigens.

Most of the topical or transdermal products on the market were developed for small and lipophilic molecules, resulting in about 30 transdermal prod-

---

M. Foldvari (✉)  
School of Pharmacy, University of Waterloo,  
200 University Avenue West, Waterloo, ON  
N2L 3G1, Canada  
e-mail: [foldvari@uwaterloo.ca](mailto:foldvari@uwaterloo.ca)

P. Kumar  
Helix BioPharma Inc.,  
#109-111 Research Drive, Saskatoon, SK S7N 3R2,  
Canada

ucts including those intended for local tissue treatment (e.g. clonidine, estradiol, fentanyl, nitroglycerine, nicotine, testosterone, lidocaine, diclofenac sodium).

However, the delivery of most biopharmaceuticals is limited to parenteral administration through IV, IM or SC injections. With increased number of macromolecules (DNA and recombinant proteins) as drugs being discovered and approved, new drug delivery technologies are being explored to deliver these molecules through the skin (Prausnitz and Langer 2008).

One important area of progress involves protein pharmaceuticals. In the past several years, therapeutic opportunities were greatly expanded by using biopharmaceuticals, such as proteins and peptides. Important classes of biopharmaceutical compounds (biodrugs) include interferons and cytokines, blood/clotting factors (erythropoietin), growth hormones/factors, hormones (insulin), enzymes, monoclonal antibodies (mAbs) and vaccines (McCrudden et al. 2013). Biodrugs (new biological entities or NBE) are becoming the most demanded medicines. Evaluate Pharma, for example, shows that seven of the top ten drugs are biopharmaceuticals in 2016. The PhRMA 2013 Annual Report (<http://www.phrma.org/>) lists over 900 biologics, including mAbs, vaccines, recombinant proteins, cell therapy, gene therapy and antisense in development from Phase I to III trials and submitted to the US Food and Drug Administration (FDA) for more than 100 diseases. In addition to innovator biodrugs, the 'generic' versions, so-called biosimilars (FDA recognises biosimilar and interchangeable biosimilar products) or 'follow-on biologics' or 'bio-betters' (a biologic with a structural modification compared to the original and better performance) are also emerging as important part of the biodrug pipeline. The global market size for biosimilars was \$2.5B in 2011, which is expected to grow by 8% between 2012 and 2016. Currently, more than 40 therapeutic mAbs are approved by EU and FDA, and many more are under review. The market for these is estimated at \$58B by 2016 (BCC Research). IMS Health estimated that by 2020, most biologics that make up \$64B of global sales will be off patent.

The combination of scientific and commercial factors contributes to the timeliness to introduce improvements in the delivery of biologics, which was previously not opportune.

So far, the only topically applied dermal or transdermal delivery systems available commercially is Regranex® (becaplermin, recombinant human platelet-derived growth factor, 25 kDa) for lower extremity diabetic ulcers (OMJ Pharmaceuticals/Ortho-McNeil), which is applied on broken skin; hence, localisation of the protein is the main function of the delivery system, and permeability enhancement is not a factor in its efficacy.

Another developing area is gene therapy. Topical delivery of genetic material appears to be promising, in that such delivery could be non-invasive and provide a more continuous supply of the protein within the skin. This approach could have further advantages over the delivery of protein drugs: (i) the DNA is a more stable molecule than the protein, (ii) the continuous expression of protein within the skin after topical administration limits systemic exposure and (iii) topical treatment can be self-administered by the patient. However, these advantages are contingent upon successful delivery of the DNA into the skin.

Current delivery and functional responses after topical application of DNA are only possible on pretreated or damaged skin (use of depilatory lotion, scraping or stripping (Shi et al. 1999; Yu et al. 1999; Watabe et al. 2001)) to remove the stratum corneum, the main permeability barrier layer of the skin. For example, DermaVir, a DNA vaccine by Genetic Immunity, utilises a novel nanoparticle technology, consisting of mannosylated polyethyleneimine-plasmid complex, for topical HIV vaccination, which is applied on the skin after dermabrasion (Liszewicz et al. 2012). Certain lipid-based delivery systems facilitate DNA uptake into intact skin, both in vitro and in vivo (Birchall et al. 2000; Delepine et al. 2000; Xu et al. 1999), but the efficiency of these systems is still too low to produce therapeutic levels of protein. In the design of effective in vivo systems, the optimum in vitro properties obtained in transfection experiments need to be extended to also include optimum percutaneous permeation-enhancer properties.

Currently, the most effective penetration into and permeation through the skin could be achieved by physical methods (e.g. microneedles (Escobar-Chavez et al. 2011), thermal ablation (Lee et al. 2011)) and electrical methods (e.g. electroporation (Charoo et al. 2010), iontophoresis (Gratieri et al. 2011)). Although the use of physical and electrical methods to enhance the drug permeation through the skin has shown some success in enhancing the delivery of both small and large molecules, there are still significant hurdles to overcome before approval.

Several non-invasive delivery vehicles, mostly lipid- or peptide-based (Baca-Estrada et al. 2000a), have been evaluated for macromolecule delivery, such as liposomes (Schuetz et al. 2005; Barry 2001), transfersomes (Benson 2006; Cevc et al. 1998), niosomes (Schreief and Bouwstrab 1994; Shilpa et al. 2011) and solid lipid nanoparticles (Puglia and Bonina 2012). Peptide-targeting ligands (Glogau et al. 2012) and biphasic vesicles (Biphaxis™) (Foldvari 2000; Foldvari et al. 2010; King et al. 2002) developed in our laboratory were demonstrated to be effective in delivering several therapeutic proteins and vaccine antigens (Baca-Estrada et al. 2000b; Foldvari 2010).

These delivery systems represent a trend towards potential protein and DNA delivery by completely non-invasive techniques using some form of sophisticated carrier system made from a structurally and chemically synergistic mixture of chemical permeation enhancers and pharmaceutical excipients.

## References

- Baca-Estrada ME, Foldvari M, Babiuk SL, Babiuk LA (2000a) Vaccine delivery: lipid-based delivery systems. *J Biotechnol* 83:91–104
- Baca-Estrada ME, Foldvari M, Ewen C, Badea I, Babiuk LA (2000b) Effects of IL-12 on immune responses induced by transcutaneous immunization with antigens formulated in a novel lipid-based biphasic delivery system. *Vaccine* 18:1847–1854
- Barry BW (2001) Novel mechanisms and devices to enable successful transdermal drug delivery. *Eur J Pharm Sci* 14:101–114
- Benson HA (2006) Transfersomes for transdermal drug delivery. *Expert Opin Drug Deliv* 3:727–737
- Birchall JC, Marichal C, Campbell L, Alwan A, Hadgraft J, Gumbleton M (2000) Gene expression in an intact ex-vivo skin tissue model following percutaneous delivery of cationic liposome-plasmid DNA complexes. *Int J Pharm* 197:233–238
- Bos JD, Meinardi MM (2000) The 500 Dalton rule for the skin penetration of chemical compounds and drugs. *Exp Dermatol* 9:165–169
- Cevc G, Gebauer D, Stieber J, Schatzlein A, Blume G (1998) Ultraflexible vesicles, Transfersomes, have an extremely low pore penetration resistance and transport therapeutic amounts of insulin across the intact mammalian skin. *Biochim Biophys Acta* 1368: 201–215
- Charoo NA, Rahman Z, Repka MA, Murthy SN (2010) Electroporation: an avenue for transdermal drug delivery. *Curr Drug Deliv* 7:125–136
- Delepine P, Guillaume C, Floch V, Loisel S, Yaouanc J, Clement J, Des Abbayes H, Ferec C (2000) Cationic phospholipids as nonviral vectors: in vitro and in vivo applications. *J Pharm Sci* 89:629–638
- Elsabahy M, Foldvari M (2013) Needle-free gene delivery through the skin: an overview of recent strategies. *Curr Pharm Des* 19(41):7301–7315
- Escobar-Chavez JJ, Bonilla-Martinez D, Villegas-Gonzalez MA, Molina-Trinidad E, Casas-Alancaster N, Revilla-Vazquez AL (2011) Microneedles: a valuable physical enhancer to increase transdermal drug delivery. *J Clin Pharmacol* 51:964–977
- Foldvari M (2000) Non-invasive administration of drugs through the skin: challenges in delivery system design. *Pharm Sci Technol Today* 3:417–425
- Foldvari M (2010) Biphasic vesicles: a novel topical drug delivery system. *J Biomed Nanotechnol* 6:543–557
- Foldvari M, Badea I, Wettig S, Baboolal D, Kumar P, Creagh AL, Haynes CA (2010) Topical delivery of interferon alpha by biphasic vesicles: evidence for a novel nanopathway across the stratum corneum. *Mol Pharm* 7:751–762
- Glogau R, Blitzer A, Brandt F, Kane M, Monheit GD, Waugh JM (2012) Results of a randomized, double-blind, placebo-controlled study to evaluate the efficacy and safety of a botulinum toxin type A topical gel for the treatment of moderate-to-severe lateral canthal lines. *J Drugs Dermatol* 11:38–45
- Gratieri T, Kalaria D, Kalia YN (2011) Non-invasive iontophoretic delivery of peptides and proteins across the skin. *Expert Opin Drug Deliv* 8:645–663
- King MJ, Badea I, Solomon J, Kumar P, Gaspar KJ, Foldvari M (2002) Transdermal delivery of insulin from a novel biphasic lipid system in diabetic rats. *Diabetes Technol Ther* 4:479–488
- Lee JW, Gadiraju P, Park JH, Allen MG, Prausnitz MR (2011) Microsecond thermal ablation of skin for transdermal drug delivery. *J Control Release* 154(1):58–68. doi:10.1016/j.jconrel.2011.05.003
- Lisziewicz J, Bakare N, Calarota SA, Banhegyi D, Szlavik J, Ujhelyi E, Toke ER, Molnar L, Lisziewicz Z, Autran B, Lori F (2012) Single DermaVir immunization: dose-dependent expansion of precursor/memory T

- cells against All HIV antigens in HIV-1 infected individuals. *PLoS One* 7, e35416
- McCrudden MT, Singh TR, Migalska K, Donnelly RF (2013) Strategies for enhanced peptide and protein delivery. *Ther Deliv* 4:593–614
- Prausnitz MR, Langer R (2008) Transdermal drug delivery. *Nat Biotechnol* 26:1261–1268
- Puglia C, Bonina F (2012) Lipid nanoparticles as novel delivery systems for cosmetics and dermal pharmaceuticals. *Expert Opin Drug Deliv* 9:429–441
- Schreief H, Bouwstrab J (1994) Liposomes and niosomes as topical drug carriers: dermal and transdermal drug delivery. *J Control Release* 30:1–15
- Schuetz YB, Naik A, Guy RH, Kalia YN (2005) Emerging strategies for the transdermal delivery of peptide and protein drugs. *Expert Opin Drug Deliv* 2:533–548
- Shi Z, Curiel DT, Tang DC (1999) DNA-based non-invasive vaccination onto the skin. *Vaccine* 17:2136–2141
- Shilpa S, Srinivasan BP, Chauhan M (2011) Niosomes as vesicular carriers for delivery of proteins and biologicals. *Int J Drug Deliv* 3:14–24
- Watabe S, Xin KQ, Ihata A, Liu LJ, Honsho A, Aoki I, Hamajima K, Wahren B, Okuda K (2001) Protection against influenza virus challenge by topical application of influenza DNA vaccine. *Vaccine* 19:4434–4444
- Xu Y, Hui SW, Frederik P, Szoka FC Jr (1999) Physicochemical characterization and purification of cationic lipoplexes. *Biophys J* 77:341–353
- Yu WH, Kashani-Sabet M, Liggitt D, Moore D, Heath TD, Debs RJ (1999) Topical gene delivery to murine skin. *J Invest Dermatol* 112:370–375

---

# Active Enhancement Methods in Transdermal Drug Delivery: Current Status and Future Perspectives

# 22

Ryan F. Donnelly

## Contents

22.1	Introduction .....	359
22.2	Active Enhancement Strategies .....	360
22.3	Moving Forwards .....	360
	Conclusion .....	364
	References .....	365

---

## 22.1 Introduction

Transdermal drug delivery has many advantages, including:

- Controlled delivery, achieving a steady-state profile, thus reducing the likelihood of peak-associated side effects and ensuring that drug levels are above the minimal therapeutic concentration
- Reduced dosing frequency, with one transdermal patch delivering drug from typically 24–72 h
- Avoidance of first-pass metabolism
- Non-invasive means of drug delivery, putting the patient in control (dosage form can be easily removed in the event of an adverse reaction)
- Less susceptible to bioavailability issues compared to the oral route
- Provides an alternative route when the patient is unable to take drugs orally

However, the use of the route is severely limited by the restrictions imposed by the lipophilic *stratum corneum* barrier, such that only lipophilic drugs of relatively low molecular weight and reasonable potency (low dose) are suitable candidates for conventional transdermal delivery (Williams 2003). Modulation of formulation excipients and addition of chemical enhancers can increase drug flux, but often not sufficiently

---

R.F. Donnelly  
School of Pharmacy, Queens University Belfast,  
Medical Biology Centre,  
97 Lisburn Road, Belfast BT9 7BL, UK  
e-mail: [r.donnelly@qub.ac.uk](mailto:r.donnelly@qub.ac.uk)

to ensure delivery of pharmacologically effective doses of drugs not possessing the specific physicochemical properties outlined above. Therefore, several active rate-controlled transdermal drug delivery technologies (electrical-based, structure-based, velocity-based, etc.) have been developed for the transdermal delivery of 'difficult' drugs. This is particularly so, given the high economic value of the transdermal delivery market, despite the relatively small number of actives (currently around 20) that can be delivered by this route. Broadly, facilitated delivery falls into two categories: technological, of which microneedles, electroporation, jet injectors, etc. are all good examples, and formulation approaches, most notably the focus on nanoscale delivery systems. The latter is discussed elsewhere in this book. Here, we will concentrate on the current state of play in active enhancement technologies used to enhance transdermal drug delivery, possible future developments and key milestones that must be achieved before patient benefit and commercial return on investment can be realised.

---

## 22.2 Active Enhancement Strategies

One of the most exciting developments currently ongoing in the transdermal drug delivery field is the use of active delivery devices. Such devices are minimally invasive in nature and can enhance the permeability of a biological membrane by targeting the shunt route (hair follicles and sweat glands) and creating transient aqueous transport pathways of micron dimensions across that membrane. In transdermal drug delivery, these devices force molecules across hair follicles and sweat glands or create micropore pathways in the skin's *stratum corneum* barrier which, in turn, enables delivery of a wide range of drug molecules. Often hydrophilic small molecules, as well as macromolecules of biological origin (e.g. insulin, vaccines), are investigated for delivery using such strategies. Recently, such 'active' devices, namely, iontophoresis, laser, thermal ablation, electroporation, radiofrequency, ultrasound, high-pressure jets and microneedle technology,

have all gained immense attention for their promising applications, both in the pharmaceutical and cosmeceutical industries. The ability of such strategies to achieve therapeutically useful plasma concentrations of hydrophilic drugs and macromolecules and enhance vaccine efficacy whilst reducing dose is beyond doubt. However, cost, safety and ease-of-use by patients remain concerns.

---

## 22.3 Moving Forwards

Given the ever-increasing evidence available within the academic and patent literature that a wide variety of active enhancement strategies are capable of achieving successful intradermal and transdermal delivery of conventional drugs, biopharmaceuticals, vaccines and active cosmeceutical ingredients, it is envisaged that the already-concerted industrial effort into development of such devices will now intensify. Furthermore, ever-more novel applications of active enhancement technologies are likely to come to the forefront. The ability of such devices to extract bodily fluids for drug and/or endogenous analyte monitoring is particularly interesting. For example, the use of microneedle-based devices to both deliver and extract molecules across the skin in a minimally invasive manner opens up the possibility for the development of a closed-loop responsive device, with a microneedle-based delivery component delivering a therapeutic molecule in response to information provided by a microneedle-based monitoring component. As technological advances continue, active enhancement devices may well become the pharmaceutical dosage forms and monitoring devices of the near future. However, there are a number of barriers that will first need to be addressed in order for the various technologies in this field to progress.

The ultimate commercial success of active enhancement delivery and monitoring devices will depend upon not only the ability of these devices to perform their intended function, but also their overall acceptability by both health care professionals (e.g. doctors, nurses and pharma-



cists) and patients. Accordingly, efforts to ascertain the views of these end-users will be essential moving forward. A study by the Birchall Group in this regard on microneedle-based drug delivery systems was highly informative (Birchall et al. 2011). The majority of health care professionals and members of the public recruited into this focus group-centred study were able to appreciate the potential advantage of using microneedles, including reduced pain, tissue damage, risk of transmitting infections and needle-stick injuries, feasibility for self-administration and use in children, needlephobes and/or diabetics. However, some concerns regarding effectiveness, means to confirm successful drug delivery (such as a visual dose indicator), delayed onset of action, cost of the delivery system, possible accidental use, misuse or abuse were also raised. Health care professionals were also concerned about interindividual variation in skin thickness, problems associated with injecting small volumes and risk of infection. Several other possible issues (accidental or errors based) and interesting doubts regarding microneedle use were discussed in this study. Overall, the group reported that 100% of the public participants and 74% of the health care professional participants were optimistic about the future of microneedle technology. Such studies, when appropriately planned to capture the necessary demographics, will undoubtedly aid industry in taking necessary action to address concerns and develop informative labelling and patient counselling strategies to ensure safe and effective use of microporation-based devices. Marketing strategies will, obviously, also be vitally important in achieving maximum market shares relative to existing and widely used conventional delivery systems.

Of the most commonly investigated active enhancement strategies, iontophoresis is the only one that does not create transient aqueous micropores in the skin, but rather uses an electrical potential difference to force charged, polar or neutral hydrophilic molecules of a wide range of sizes (up to about 12,000 daltons) across the low resistance shunt route in the stratum corneum, consisting of hair follicles and sweat glands. Iontophoresis induces a sensation of tingling or

itching, depending on the density of the applied current. Besides these uncomfortable but harmless effects, skin irritation is the most common local adverse effect of cutaneous iontophoresis (Roustit et al. 2014). It occurs at both the anode and the cathode. Erythema is the most frequently described adverse effect, with a variable frequency according to the iontophoresis protocols. Skin irritation spontaneously and rapidly resolves, does not lead to permanent skin damage and does not disturb the barrier function of the skin. Although rare, burns have been observed, mainly due to operator error and the incorrect choice of electrodes/formulation composition. Indeed, the electrochemistry at bare metal or graphite electrodes involves electrolysis of water, which induces changes in the pH of the skin by generating  $H^+$  and  $OH^-$  at the positive and negative electrodes, respectively. Variations in pH beyond the buffer capacities of the skin may lead to burns. High current density or prolonged application, as well as positioning of the electrodes over skin defects, increases the risk of burns. Burns are generally more serious under the cathode, due to involvement of  $OH^-$  and rise in pH. Indeed, an alkaline phase erodes the epidermis and reduces skin resistance, making skin erosion worse. Therefore, an appropriate choice of buffer concentration in the formulation is needed to reduce the risk of burns (Roustit et al. 2014). A better solution is to use Ag–AgCl rather than bare metal or carbon-active electrodes, because they function at a lower potential and do not operate by water electrolysis. Several simple recommendations can decrease the risk of skin injury, such as avoiding pressure on the electrodes (not tapping, binding or compressing either electrode) and ensuring that the electrode is uniformly wetted. Indeed, most commercially available electrodes are made of small sponges in contact with the skin. After dampening the sponge with the drug solution, it conducts the current. Therefore, heterogeneity in sponge dampening locally increases current density and may lead to skin injury. In the same way, the adhesive seal should adhere uniformly to the skin to avoid leaks. Moreover, cleansing the skin with alcohol and avoiding skin defects and contact between metal components

and the skin are also recommended. Finally, current intensity should be  $<0.5 \text{ mA cm}^{-2}$ .

Material defects are actually the main cause of skin injuries, such as burns, usually resulting from direct contact between metal components and the skin. Another consequence of material defects can be overdose, which is potentially harmful when drugs are delivered for a systemic action and have a narrow therapeutic index. The most striking recent example was the iontophoretic delivery of fentanyl (Ionsys®). After receiving marketing authorisation for the European Union in 2006, corrosion of a component within the system was found in one batch. Although no case of fentanyl overdose was reported, this defect could have resulted in fentanyl release without activation by the patient. This could have exposed patients to fentanyl overdose, with a risk of severe respiratory depression. Ionsys® has not been marketed in Europe since October 2008, and the marketing authorisation holder did not apply for renewal of authorisation. Ionsys® has recently been acquired by another pharmaceutical company (Incline Therapeutics Inc., Redwood City CA, USA), currently developing new features into the system in order to obtain regulatory approval (Roustit et al. 2014).

In most cases, iontophoretic devices are more expensive than conventional topical and transdermal formulations. Although there are limited data about the cost effectiveness of iontophoresis, in some cases, it has been shown to be in favour of iontophoresis compared with other formulations. Among the drugs in the pipeline which could lead to new marketing applications soon, agonists of the 5-HT<sub>1</sub> family receptors used as antimigraine agents (triptans) have raised interest. Indeed, subcutaneous (s.c.) administration of sumatriptan leads to a rapid but transient effect, whereas oral or nasal administration suffers from poor bioavailability. The pharmacokinetics of iontophoretically delivered sumatriptan (4 mA for 1 h followed by 2 mA for 3 h) in healthy subjects showed comparable concentration over time areas under the curve (AUC) to the s.c. route (Siegel et al. 2007; Marbury et al. 2009), but the maximal concentration was about 30% of that by the s.c. route, whereas time to maximum plasma concentration

was 5.6- to 8.3-fold that of the s.c. route (Marbury et al. 2009). Given that it avoids patient exposure to a rapid increase and high plasma concentrations of sumatriptan in comparison to s.c. administration, iontophoresis may reduce typical triptan-related adverse events (i.e. chest tightness, chest heaviness, paresthesias and sedation/fatigue/malaise) (Rapoport et al. 2010). A new drug application for an iontophoretic device containing sumatriptan (Zecuity®, formerly Zelrix®; NuPathe Inc., Conshohocken, PA, USA) has now been approved by the US Food and Drug Administration (FDA) (Nupathe 2015). Other iontophoretically delivered 5-HT<sub>1</sub> agonists, such as zolmitriptan or almotriptan, have been studied recently; to date, only preclinical data are available and suggest that these molecules are appropriate candidates for iontophoresis (Patel et al. 2009; Calatayud-Pascual et al. 2011).

Assessing the biological effects of ultrasound on tissues and cells has been investigated thoroughly. It has been commonly believed for decades that ultrasound effects on tissues and cells are mainly through three mechanisms: cavitation (mainly inertial cavitation), thermal and acoustic streaming (Azagury et al. 2014). Recently a new, non-thermal and non-cavitation mechanism for ultrasound effects on biological tissues has been proposed. There are innumerable devices in development that use sonophoresis technology. Indeed, portable, pocket-size sonicators for drug injection and analyte monitoring are now available commercially (Azagury et al. 2014). In future applications, ultrasound-based systems show promise for immunisation with vaccines and in topical gene therapy. Some current applications consist of drug delivery, administration of targeted therapeutic and diagnostic agents, detection and determination of analyte, termination of cancer tissues, fatty tissues or kidney and gall bladder stones (Azagury et al. 2014). Inovio's electroporation (high voltage, short duration) device also creates transient aqueous pores in the *stratum corneum* and is currently under development for vaccine delivery (Inovio 2015).

In order to gain acceptance from health care professionals, patients and, importantly, regulatory authorities (e.g. the US FDA and the EMA in

Europe), it appears a strong possibility that current safety concerns will need to be addressed. From a regulatory point of view, currently little is known about the safety aspects that would be involved with long-term usage of active enhancement devices. In particular, studies will need to be conducted to assess the effect that repeated microporation or application of electrical energy or ultrasound has upon skin barrier function. However, given the minimally invasive nature of the micropores created within the skin by microneedles or laser or thermal ablation, especially in comparison to the use of a hypodermic needle, and the fact that statistically it is highly unlikely that micropores would be created at exactly the same sites more than once in a patient's lifetime, it is envisaged that microporation technologies will be shown to have a favourable safety profile. Indeed, skin barrier function is known to completely recover within a few hours of microneedle removal, for example, regardless of how long the microneedles were in place (Banks et al. 2010; Goma et al. 2010; Kalluri et al. 2011). Local irritation or erythema (reddening) of the skin may be an issue for some patients. Since the skin is a potent immunostimulatory organ, it would be interesting to know whether repeated use of microporation devices to deliver biomolecules intradermally would ever cause an immune reaction to the drug, especially considering the abundance of immune-presenting cells in this compartment (Al-Zahrani et al. 2012), and whether such an effect would be so significant as to cause problems for patients.

Infection is an issue that has long been discussed in relation to use of microporation devices, since they, by necessity, puncture the skin's protective *stratum corneum* barrier. However, as we and others have shown (Donnelly et al. 2009, 2013; Wei-Ze et al. 2010), microbial penetration through microneedle-induced holes is minimal. Indeed, there have never been any reports of microneedles or other microporation devices causing skin or systemic infections. This may be because of the above-mentioned immune component of the skin, or the skin's inherent non-immune, enzyme-based, defences. Alternatively, since the micropores are aqueous in nature, microorganisms

may be more inclined to remain on the more hydrophobic *stratum corneum*. Whether skin-cleansing before microporation is necessary remains to be seen and is a vital question. Ideally, this would not have to be done, so as to avoid unnecessarily inconveniencing patients and making the use of these products in the domiciliary setting appear more akin to a self-administered injection than application of a conventional transdermal patch. Regulators will ultimately make the key decisions based on the weight of available evidence. Depending upon the application (e.g. drug/vaccine/active cosmeceutical ingredient delivery or minimally invasive monitoring), microporation-based devices may be classed as drug delivery stems, consumer products or medical devices. From a delivery perspective, it will be important if microporation devices, such as microneedles or jet injectors are considered as injections rather than topical/transdermal/intradermal delivery systems, since this will determine whether the final product will need to be sterilised, prepared under aseptic conditions or simply host a low bioburden. Any contained microorganisms may need to be identified and quantified, as may the pyrogen content. Should sterilisation be required, then the method chosen will be crucial, since the most commonly employed approaches (moist heat, gamma or microwave radiation, ethylene oxide) may adversely affect polymeric microneedles or electronic components of electroporation devices and/or any contained active ingredient (e.g. biomolecules).

Sterilisation and/or aseptic production will add considerably to costs for manufacturers. Indeed, the practicalities involved in the large-scale production of microporation devices for commercial applications will need to be carefully considered. Currently, microporation devices are made by a wide variety of techniques, often in processes that are completely different to those used in the production of conventional dosage forms. Often, multiple manufacturing steps are required, particularly for coated microneedles, for example, and those micromoulded from silicon or metal masters. Silicon microneedles typically require clean room processing. As such, it would appear that any pharmaceutical or medical

devices firm wishing to commercialise microporation technology would need to make a significant capital investment in order to design, develop and optimise a cost-effective, reproducible, method for mass production. Adaptation of standard quality control procedures will also be required. Ultimately, the regulatory specifications applied to the first generations of microporation products that reach the market may set the bar for all those that follow. Packaging of such devices will also be important, especially during transport and storage. Patient handling may only be controlled to a limited extent by effective product labelling and pharmacist-led counselling. Packaging should be sufficiently robust to prevent damage, contamination or accidental release of active ingredients during storage.

Whilst a wide variety of microneedle applicator designs have been disclosed within the patient literature, only a few, relatively crude, designs based upon high impact/velocity insertion, or rotary devices have been described (Thakur et al. 2011). Our own previous work has shown that application force has a significant role to play in microneedle insertion depth (Donnelly et al. 2010). Clearly, patients cannot 'calibrate' their hands and, so, will apply microneedles with different forces. However, we have recently carried out a pilot clinical study showing consistent depths of microneedle insertion into skin *in vivo* when applied by hand by human volunteers counselled by a pharmacist and in receipt of a patient information leaflet (Donnelly et al. 2014). One of the key findings of this work was that patients would like a level of assurance that the microneedle device has actually been inserted properly into their skin. This would be especially true in cases of global pandemics or bioterrorism incidents, where self-administration of microneedle-based vaccines becomes a necessity. Accordingly, a suitable means of confirming that skin puncture has taken place may need to be included within an applicator device or the microneedle product itself. Microneedle-based products are currently being pursued by a number of companies, including Löhmann Therapie

Systeme AG, 3M, Theraject, Corium, Vaxxas and Zosano Pharma; yet, no true microneedle array-based product has been marketed for drug delivery. Jet injectors, such as Bepak's SQ-Pen® (Bepak 2015) and pellet-based skin delivery devices like Glide Pharma's SDI® device (Glide Pharma 2015) already provide patients with a level of assurance that they have been used appropriately, and similar means of dosage confirmation could easily be built into radiofrequency, iontophoresis, electroporation, sonophoresis, laser or thermal microporation devices. Some of these devices are, understandably, easier to use by patients than others.

### Conclusion

A wide variety of microporation strategies and devices have been shown to be effective for the transdermal delivery of a diverse range of molecules, both *in vitro* and *in vivo*. The potential now exists to greatly expand the range of types of drugs that can be delivered effectively across the skin. This will significantly enhance the value of the transdermal delivery market and will be increasingly important over the coming years, as the number of new drugs of biological origin continues to increase. Small-scale clinical trials have highlighted the minimally invasive nature of microporation-based systems, causing no pain, minimal irritation if any and complete skin recovery within a few hours. Vaccine-loaded microneedle arrays, for example, have been shown to elicit a greater immune response in comparison to conventional injections and have a number of key advantages over the use of hypodermic needles. The ability of microorganisms to traverse induced skin pores within the skin has been found to be minimal and with a lower incidence for occurrence when compared to the skin damage caused through hypodermic needle skin puncture. Microporation devices also have the potential for use in non-invasive therapeutic drug/analyte monitoring, and the possibility for

closed-loop delivery systems may become important moving forward. Focus group studies have identified key areas that need to be addressed by the microneedles community in order for the technology to progress. These include a means to ensure reproducible microneedle application in every patient every time and confirmation of successful device insertion. Similar studies are clearly warranted for other microporation devices. A significant number of small and large industry players are presently engaged in clinical trials with the aim of commercialisation of their respective microporation-based devices. Future studies will be needed to address potential regulatory concerns over the use of such devices, as well as focussing on the design and development of processes to enable a low-cost, efficient means for mass production.

Overall, the future for the transdermal active delivery sector appears to be very bright, with rapid expansion in fundamental new knowledge feeding industrial development. In due course, it is hoped that microporation-based technological advancements will lead to enhanced disease prevention, diagnosis and control, with concomitant improvement in health-related quality of life for patients worldwide. Of the active delivery strategies currently available, microneedles appear the most promising, in this author's opinion. They are closest to conventional transdermal patches in design and application, particularly if mechanical applicator devices are ultimately proven to be unnecessary. Other devices, while technologically more advanced in some ways, may suffer from a perceived closeness to conventional injections (e.g. jet injectors), higher cost or patient confusion due to complex design and instructions (e.g. iontophoresis, sonophoresis, electroporation or laser-based devices). Ultimately, the market will decide which microporation technology proves to be most successful. Whichever strategy or strategies

are favoured most by patients, health care professionals and regulators will be the one(s) that benefit patients and industry in the long term.

---

## References

- Al-Zahrani S, Zaric M, McCrudden C, Scott C, Kissenpfennig A, Donnelly RF (2012) Microneedle-mediated vaccine delivery: harnessing cutaneous immunobiology to improve efficacy. *Expert Opin Drug Deliv* 9:541–550
- Azagury A, Khoury L, Enden G, Kost J (2014) Ultrasound mediated transdermal drug delivery. *Adv Drug Deliv Rev* 72:127–143
- Banks SL, Pinninti RR, Gill HS, Paudel KS, Crooks PA, Brogden NK, Prausnitz MR, Stinchcomb AL (2010) Transdermal delivery of naltrexol and skin permeability lifetime after microneedle treatment in hairless guinea pigs. *Pharm Sci* 99:3072–3080
- Birchall J, Clemo R, Anstey A, John D (2011) Microneedles in clinical practice – an explanatory study into the views and opinions of healthcare professionals and the public. *Pharm Res* 28:95–106
- Calatayud-Pascual MA, Balaguer-Fernandez C, Serna-Jimenez CE, Del Rio-Sancho S, Femenia-Font A, Merino V, Lopez-Castellano A (2011) Effect of iontophoresis on *in vitro* transdermal absorption of almotriptan. *Int J Pharm* 416:189–194
- Donnelly RF, Thakur RRS, Tunney MM, Morrow DIJ, McCarron PA, O'Mahony C, Woolfson AD (2009) Microneedle arrays allow lower microbial penetration than hypodermic needles *in vitro*. *Pharm Res* 26:2513–2522
- Donnelly RF, Garland MJ, Morrow DIJ, Migalska K, Thakur RRS, Majithiya R, Woolfson AD (2010) Optical coherence tomography is a valuable tool in the study of the effects of microneedle geometry on skin penetration characteristics and in-skin dissolution. *J Cont Rel* 147:333–341
- Donnelly RF, Singh TR, Alkilani AZ, McCrudden MT, O'Neill S, O'Mahony C, Armstrong K, McLoone N, Kole P, Woolfson AD (2013) Hydrogel-forming microneedle arrays exhibit antimicrobial properties: potential for enhanced patient safety. *Int J Pharm* 451:76–91
- Donnelly RF, Moffatt K, Zaid-Alkilani A, Vicente-Perez EM, Barry J, McCrudden MTC, Woolfson AD (2014) Hydrogel-forming microneedle arrays can be effectively inserted in skin by self-application: a pilot study centred on pharmacist intervention and a patient information leaflet. *Pharm Res* 31:1989–1999
- Gomaa YA, Morrow DIJ, Garland MJ, Donnelly RF, El-Khordagui LK, Meidan VM (2010) Effects of microneedle length, density, insertion time and

- multiple applications on human skin barrier function: assessments by transepidermal water loss. *Toxicol In Vitro* 24:1971–1978
- Kalluri H, Kolli CS, Banga AK (2011) Characterization of microchannels created by metal microneedles: formation and closure. *AAPS J* 13:473–481
- Marbury PM, O’Neill T, Siegel C, Du S, Sebree W (2009) Zelrix: a novel transdermal formulation of sumatriptan. *Headache* 49:817–825
- Patel SR, Zhong H, Sharma A, Kalia YN (2009) Controlled non-invasive transdermal iontophoretic delivery of zolmitriptan hydrochloride in vitro and *in vivo*. *Eur J Pharm Biopharm* 72:304–309
- Rapoport AM, Freitag F, Pearlman SH (2010) Innovative delivery systems for migraine: the clinical utility of a transdermal patch for the acute treatment of migraine. *CNS Drugs* 24:929–940
- Roustit M, Blaise S, Cracowski JL (2014) Trials and tribulations of skin iontophoresis in therapeutics. *Br J Clin Pharmacol* 77:63–71
- Siegel SJ, O’Neill C, Dube LM, Kaldeway P, Morris R, Jackson D, Sebree T (2007) A unique iontophoretic patch for optimal transdermal delivery of sumatriptan. *Pharm Res* 24:1919–1926
- Thakur RRS, Dunne NJ, Cunningham E, Donnelly RF (2011) Review of patents on microneedle applicators. *Recent Pat Drug Deliv Formul* 5:11–23
- Wei-Ze L, Mei-Ronga H, Jian-Pinga Z (2010) Super-short solid silicon microneedles for transdermal drug delivery applications. *Int J Pharm* 389:122–129
- Williams AC (2003) *Transdermal and topical drug delivery*. Pharmaceutical Press, London
- [www.bespak.com/NeedlefreejetInjectors](http://www.bespak.com/NeedlefreejetInjectors). Accessed 10 Apr 2015
- [www.glidepharma.com](http://www.glidepharma.com). Accessed 8 Apr 2015
- [www.inovio.com](http://www.inovio.com). Accessed 7 Apr 2015
- [www.ir.nupathe.com/press-releases/nupathe-s-zecuity-approved-by-the-fdafor-the-acut-nasdaq-path-975802](http://www.ir.nupathe.com/press-releases/nupathe-s-zecuity-approved-by-the-fdafor-the-acut-nasdaq-path-975802). Accessed 11 Apr 2015

---

**Part V**

**Safety Issues and Ethics in Studies on  
Dermal and Transdermal Delivery**

# Efficacy, Safety and Targets in Topical and Transdermal Active and Excipient Delivery

# 23

Yousuf H. Mohammed, Hamid R. Moghimi,  
Shereen A. Yousef, Navin C. Chandrasekaran,  
Césa R. Bibi, Sinduja C. Sukumar, Jeffrey E. Grice,  
Wedad Sakran, and Michael S. Roberts

## Contents

23.1	<b>Role of Efficacy/Active Potency in Topical and Transdermal Delivery</b> .....	369
23.1.1	Safety and Efficacy-Based Selection of Medication .....	370
23.1.2	Systemic Concentration of Solutes and Their Effect on Active Performance ....	373
23.1.3	Enhancing Efficacy by Increasing Fractional Solubility of an Active in the Formulation .....	374
23.2	<b>Role of Intended Targets on Topical and Transdermal Delivery</b> .....	377
23.2.1	Topical Delivery .....	377
23.2.2	Targeting of Keratinocytes .....	378
23.2.3	Targeting of Melanocytes .....	379
23.2.4	Targeting of Langerhans Cells .....	380
23.2.5	Targeting of Fibroblasts .....	381
23.2.6	Intradermal and Systemic Targeting .....	381
23.3	<b>Role of Safety and Active Toxicity in Transdermal Formulation</b> .....	382
23.3.1	Mechanisms of Contact and Photo Allergies and Irritations .....	382
23.3.2	Testing of Dermatologics, Cosmetics and Their Safety Evaluation .....	383
23.3.3	In Vitro Skin Irritancy Tests: A Need for Triangulation .....	383
	<b>Conclusion</b> .....	386
	<b>References</b> .....	386

Y.H. Mohammed • S.A. Yousef  
N.C. Chandrasekaran • C.R. Bibi • S.C. Sukumar  
J.E. Grice  
Therapeutics Research Centre, School of Medicine,  
University of Queensland, Princess Alexandra  
Hospital, Woolloongabba, QLD 4102, Australia

H.R. Moghimi  
Therapeutics Research Centre, School of Pharmacy  
and Medical Sciences, University of South Australia,  
Adelaide, SA 5000, Australia

School of Pharmacy, Shahid Beheshti University of  
Medical Sciences, Tehran, Iran

W. Sakran  
School of Pharmacy, Helwan University,  
Helwan, Egypt

M.S. Roberts (✉)  
Therapeutics Research Centre, School of Medicine,  
University of Queensland, Princess Alexandra  
Hospital, Woolloongabba, QLD 4102, Australia

Therapeutics Research Centre, School of Pharmacy  
and Medical Sciences, University of South Australia,  
Adelaide, SA 5000, Australia  
e-mail: [michael.roberts@unisa.edu.au](mailto:michael.roberts@unisa.edu.au)

## 23.1 Role of Efficacy/Active Potency in Topical and Transdermal Delivery

Formulating a suitable topical or transdermal product can often be challenging because the product must be optimized for an appropriate combination of product efficacy, consumer aesthetic acceptance, safety, stability, ease of production and cost. Much of the focus on overcoming the skin barrier to achieve measurable skin penetration therefore has an implicit assumption that the resulting active or excipient will be efficacious or safe, respectively (Roberts 2013). However, it is possible for the barrier



properties of the skin to be completely destroyed, allowing most actives to be delivered in high concentrations. This, in turn, may allow the ingress of previously innocuous excipients and external agents which can then lead to skin irritation and allergic responses. Accordingly, the key question that should be asked is: “Is the transdermal route suitable and required for the proposed therapeutic agent?” Obviously, an active such as acetaminophen, with an oral dose in the hundreds of milligrams, can never be delivered at a sufficient percutaneous flux to achieve efficacy. Alternatively, the skin provides for a regulated, constant delivery rate and much lower first pass metabolism than oral delivery and so may be the best route of delivery for certain actives. However, many actives for which transdermal delivery could be the only viable option are yet to be formulated effectively. This is largely because their physicochemical properties make them unsuitable candidates for skin permeation (Barry 2001).

Having an appropriate efficacy and potency for a therapeutic agent is a key pre-formulation consideration and will govern the selection of a transdermal delivery technology strategy. Such a strategy must also take into account the various factors affecting skin penetration, such as the condition of the skin to be treated (for example, whether it is healthy or diseased), the physicochemical properties of the penetrating molecule, the formulation in which the penetrating molecule is applied and the required dosing conditions (Wiechers 1989). An overriding consideration is also the aesthetic or sensorial properties of the product, as perceived by the user – its appearance, feel, odour, residue, stability, etc. Accordingly, we support Johann Wiechers’ proposed percutaneous product goal: “Both dermal and transdermal delivery aim to achieve one goal summarized in the four R’s of delivery: to deliver the right chemical at the right concentration to the right site in (dermal delivery) or beyond (transdermal delivery) the skin for the correct period of time” (Wiechers et al. 2004). However, we also suggest the inclusion of a fifth R: “...with the right sensorial feel to the consumer”.

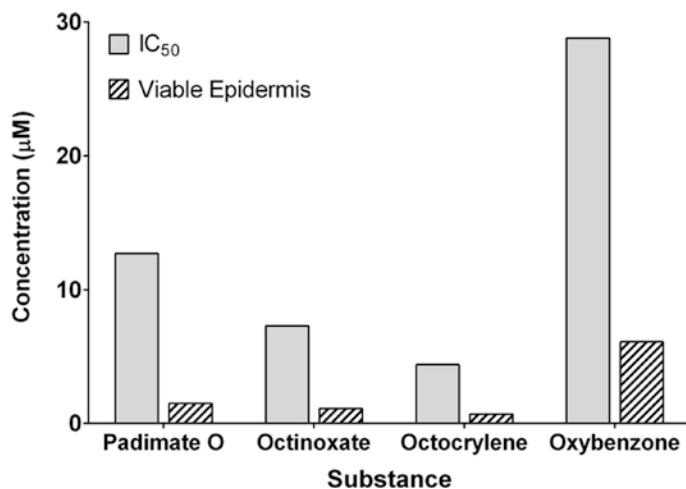
### 23.1.1 Safety and Efficacy-Based Selection of Medication

The formulation of a topical product should start with the choice of an appropriate active. The two considerations here are safety and efficacy. Hayden et al. (2005) assessed the safety of five sunscreens by determining their in vitro toxicity to human keratinocytes in culture then estimated the equivalent concentration to inhibit 50% of cells in viable epidermis, after adjustment for the differences in protein binding in the two media (Fig. 23.1). It is evident that the observed viable epidermal concentrations after topical application are somewhat less than either the observed  $IC_{50}$  in cultured keratinocytes or the equivalent estimated  $IC_{50}$  for viable epidermis, based on adjustments for differences in sunscreen binding in culture and in the viable epidermis. Although oxybenzone has an estimated unbound viable epidermal concentration of >50 times or more than those of the other sunscreens, this is still only 20% of the  $IC_{50}$  determined in keratinocyte culture.

These findings can be summarized by defining a *cutaneous margin of safety* after topical application as the ratio of concentration of active and excipient associated with toxicity (e.g.  $IC_{50}$ ) to the viable epidermal concentration of the active or excipient. A desirable margin of safety based on human models should be at least 10 to account for inter-subject variability. Toxicities, such as irritancy, photosensitization and corrosivity, are likely to be better defined by the probability of an event occurring in a given patient after a particular exposure and are dependent on patient susceptibility and the nature and conditions of the product used.

The second safety measure of interest is the *systemic margin of safety* which arises when an active applied to the skin for local cutaneous effect enters the systemic circulation and causes systemic side effects. This concept is most highly developed for topically applied corticosteroids and, in this case, is quantified by the extent of suppression of the adrenal gland in the hypothalamic–pituitary–adrenal axis. A systematic literature review of the risk of adrenal axis suppression

**Fig. 23.1** Keratinocyte culture  $IC_{50}$  and estimated unbound epidermal concentrations after human epidermal membrane penetration of sunscreens from a 1 % mineral oil solution (Adapted from Hayden et al. (2005))



and skin atrophy after application of topical corticosteroids in plaque psoriasis for the period 1980 to January 2011 found morning cortisol was reduced in 0–48% of patients in 11 short-term studies (Castela et al. 2012). Thong et al. (2007) have listed a range of topical drugs and chemicals known to cause systemic effects. The agents include anti-infectives, antihistamines, minoxidil, insecticides, solvents and steroids.

The corollary measure to safety is *cutaneous efficacy* and, in general, the more potent the topical product used, the less skin flux required to achieve a desired local cutaneous effect after topical application. A commonly used approach, analogous to that described earlier for toxicity, is to estimate the free drug concentration at the local target site ( $C^*$ ), which, for antivirals, is assumed to be the epidermal basal cell layer (Patel et al. 1996). Afouna et al. (1998) analysed the receptor solutions for full thickness hairless mouse skin mounted in Franz diffusion cells. Assuming that receptor sink conditions applied,  $C^*$  was estimated as the ratio of the steady state penetration flux ( $J_s$ ) to in vivo dermis permeability coefficient ( $k_{p,d}$ ):

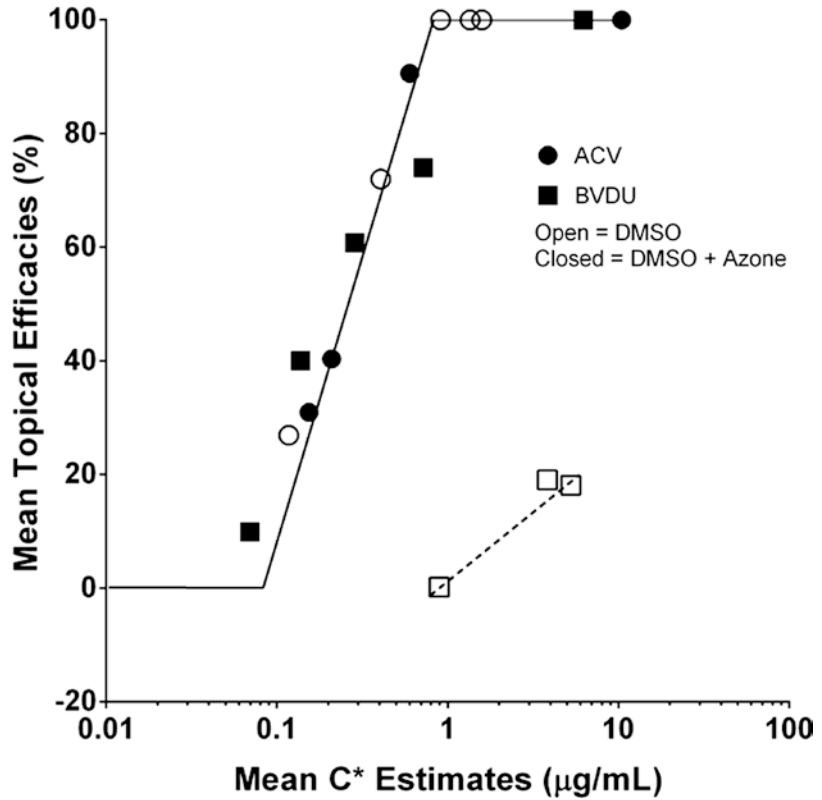
$$C^* = \frac{J_s}{k_{p,d}} \quad (23.1)$$

These  $C^*$  values derived for various formulations of bromovinyldeoxyuridine (BVDU) and acyclovir (ACV) were then compared with the in vivo efficacy of the formulations against cutaneous her-

pes simplex virus type 1 infections in hairless mice. Figure 23.2 shows a composite graph of their findings. It is evident that a similar concentration response relationship exists for the 95% dimethyl sulfoxide (DMSO)+5% Azone for both BVDU and ACV and for the 95% DMSO only formulation for ACV, whereas much higher BVDU  $C^*$  values are needed for the BVDU in 95% DMSO only formulation. They surmise that Azone could have two effects. Firstly, it may either enhance penetration of the active. This is evident from the 6.5 times higher  $C^*$  for 5% ACV in 95% DMSO +5% Azone than in the 95% DMSO only formulation. The effect is less for BVDU, where the  $C^*$  for 5% BVDU in 95% DMSO +5% Azone is 1.65 times that of 95% DMSO only formulation. Secondly, Azone may have a synergistic effect with the antiviral agents on viral kill, evident in the shift towards higher potencies of  $C^*$  for BVDU but not for ACV (Fig. 23.2).

A key assumption made in this analysis is that the dermal permeability coefficient (which is normally expressed in the pharmacokinetic literature as a dermal clearance ( $Cl_d$ ) (Siddiqui et al. 1989) (i.e.  $k_{p,d} = Cl_d / A$ , where  $A$  is the surface area of application) can be estimated by the ACV skin penetration flux that yields 50% topical efficacy ( $J_{50}$ ) divided by the free plasma levels of ACV that inhibit 50% of cutaneous lesions treated systemically with ACV ( $C^*_{50}$ ), i.e.  $k_{p,d} = J_{50} / C^*_{50}$ . It is also evident that systemic efficacy of various formulations is much less than

**Fig. 23.2** Correlation of estimated values of  $C^*$  from in vivo–in vitro experiments with observed in vivo efficacies for 9 acyclovir (ACV) formulations and 8 bromovinyldeoxyuridine (BVDU) formulations. *Open symbols:* formulations in DMSO without azone; *closed symbols:* formulations in DMSO with 5% azone (Adapted from Afouna et al. (1998))



when applied topically, showing the enhanced response that can be achieved by targeted topical application.

Davis has recast the free drug concentration approach described above in Eq. (23.2), which describes the efficacy of the active in terms of both potency of the active and how much penetrates to a target site (Davis 2008; Jepps et al. 2013):

$$\text{Efficacy} = \text{Potency} \times \text{Delivery} \quad (23.2)$$

A major issue not fully recognized in the work of Cordero and Davis (Cordero et al. 2001; Davis 2008) is that the fraction of active bound in the in vitro system used to determine potency may differ from that present in skin penetration studies and in vivo. In order to simplify the present description and be consistent with the work reported by Cordero and Davis, this important correction will not be included in the following discussion. Hence, if a cutaneous concentration for a desired effect is defined as  $C_{\text{eff}}$  and that observed after topical application as  $C_{\text{ve}}$ , the efficacy is given by the ratio  $C_{\text{ve}}/C_{\text{eff}}$ .  $C_{\text{ve}}$  is defined by

the penetration flux divided by the clearance from the viable epidermis. Cordero et al. assumed that this clearance, in turn, was related to the in vitro dermis diffusion and thickness. In reality, as discussed earlier in referring to the work of Afouna et al (1998), this should be in vivo clearance. Our own work supports this, suggesting that, firstly, uptake by the blood in the dermal capillaries located just below the viable epidermis is likely to be the rate limiting determinant of clearance in vivo (Cross and Roberts 2006) and secondly, carriage of topical non-steroidal anti-inflammatory drugs (NSAIDs) to deeper tissues below that application site is also dependent on blood flow for highly plasma protein-bound drugs (Dancik et al. 2013a, b). Accordingly, we have, for illustrative purposes, assumed both constant binding and clearance and expressed efficacy simply as a ratio of flux divided by the in vitro minimum inhibitory concentration (MIC), as originally proposed by Mertin and Lippold (Mertin and Lippold 1997).

Thus, a greater efficacy is provided by an active with either a higher flux or a greater potency (a

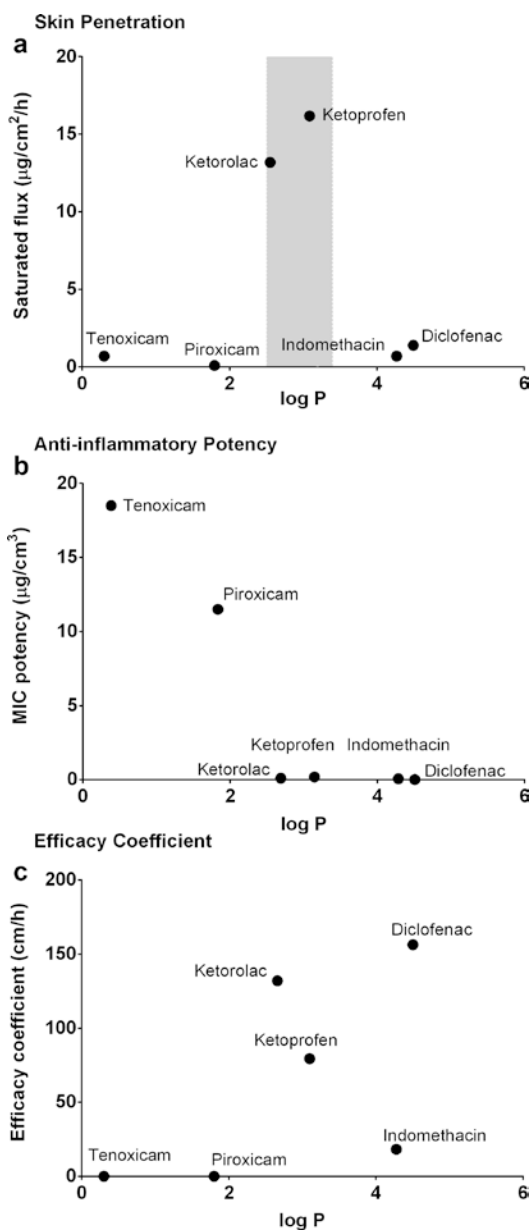


**Fig. 23.3** (a) Saturated skin flux, (b) in vitro anti-inflammatory activity (MIC) and (c) likely clinical efficacy of various non-steroidal anti-inflammatory drugs, expressed as an efficacy coefficient, calculated as saturated flux/MIC potency for a range of non-steroidal anti-inflammatory drugs with varying values for logarithm octanol–water partition coefficient ( $\log P$ ). Flux and MIC data from Cordero et al. (2001) (closed symbols) (Adapted from Jepps et al. (2013))

lower dose for the same effect). These concepts are illustrated in Fig. 23.3, where data from Cordero et al. and others for saturated skin flux (Fig. 23.3a),

anti-inflammatory activity (Fig. 23.3b) and efficacy (Fig. 23.3c) for a range of non-steroidal anti-inflammatory drugs are shown (Mertin and Lippold 1997; Wenkers and Lippold 2000; Cordero et al. 2001; Jepps et al. 2013).

In Fig. 23.3a, the shaded area indicates the region of optimal skin penetration occurring at a  $\log P$  of around 3 (Yano et al. 1986; Zhang et al. 2009). Ketorolac and ketoprofen, in this range, consequently have the greatest saturated flux. The more lipophilic actives also have a greater in vitro performance index of anti-inflammatory activity (i.e. lower MIC), and so these two compounds also have high efficacy coefficients. Diclofenac, although having a less favourable  $\log P$  of  $>4$ , still has the highest predicted efficacy coefficient as a consequence of having the lowest MIC. On the other hand, piroxicam has the least saturated flux of all these actives, as well as a relatively high MIC, and consequently has the lowest efficacy coefficient of these non-steroidal anti-inflammatory drugs (NSAIDs). Apart from a comparatively higher molecular weight and melting point, hydrogen bonding seems to be playing a pivotal role in the lower flux of piroxicam (Anrade and Costa 1999).

Adrian Davis (Davis 2007) also presented efficacy and systemic toxicity indices for topical immunosuppressive agents used in treating atopic dermatitis, extracted from Trotter's PhD thesis (Trotter 2004) at the SCI meeting in 2007 (see Fig. 23.4). The corresponding margins of safety for cyclosporin A, tacrolimus and pimecrolimus, calculated as the ratio of the systemic safety indices and the efficacy indices, were 2400, 47 and 457, respectively.

### 23.1.2 Systemic Concentration of Solutes and Their Effect on Active Performance

The *systemic efficacy* of many actives, such as anticonvulsants, anti-infective and cardiac drugs, can be defined by plasma concentrations after dosing by a particular route of administration. As shown in Fig. 23.5, in transdermal delivery occurring from a constant rate transdermal passive delivery patch, there is a lag prior to reaching

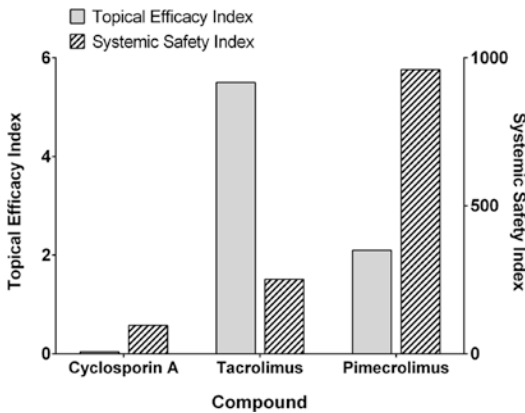


**Fig. 23.4** Comparison of topical efficacy and systemic safety indices for topical immunosuppressive agents, cyclosporin A, tacrolimus and pimecrolimus treatment in atopic dermatitis. The corresponding margins of safety are 2400, 46 and 457, respectively (Adapted from Davis (2008))

maximal levels and in returning to baseline on patch removal (Roberts and Walters 2007). Further, after reaching a maximum, the serum levels slowly decline with time, consistent with a reduction in flux due to a gradual depletion in the amount of active in the patch.

Topical products, especially transdermal patches, are often required to provide constant therapeutically effective plasma concentrations,  $C_{ss}$ . The penetration flux  $J_s$  ideally needed to reach such concentrations is given by Eq. (23.3), where  $Cl_{body}$  is the body clearance and  $F_s$  is the availability

$$J_s = \frac{C_{ss} Cl_{body}}{F_s} \quad (23.3)$$

Table 23.1 shows some estimated transdermal fluxes required for the topical administration of a number of pharmaceuticals used in transdermal systems, by substituting desired plasma concentrations and body clearances into Eq. (23.3).

### 23.1.3 Enhancing Efficacy by Increasing Fractional Solubility of an Active in the Formulation

A key goal in formulating an active in a transdermal product is to obtain a desired steady state skin penetration flux (amount penetrated over a

period of time) of the active.  $J_s$  is defined by Eq. (23.4) (Reeve et al. 2013), where  $J_{sat}$  is the flux from a saturated solution (often referred as maximum flux (Magnusson et al. 2004)),  $C_v$  is concentration of the active in a given formulation and  $S_v$  is the solubility of the active in the formulation.  $f_v$  represents the fractional solubility of the active in that formulation,  $\frac{C_v}{S_v}$ .

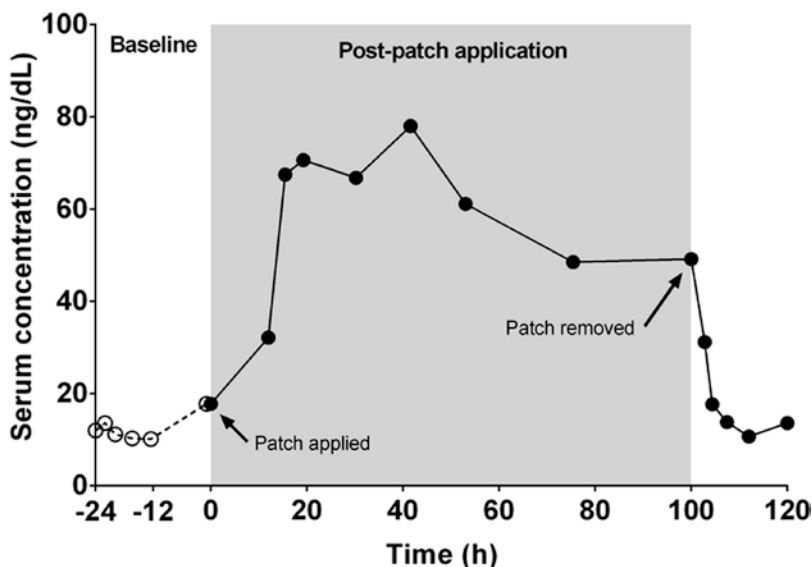
$$J_s = J_{sat} \frac{C_v}{S_v} = J_{sat} f_v \quad (23.4)$$

As is evident from Eq. (23.4), one way to maximize skin penetration is to use a fractional solubility approaching unity. Poulsen led a range of studies that showed maximal skin penetration will occur when an active is at saturation in a formulation (Poulsen et al. 1978).

As discussed in depth by Davis (2008), if an active is used at a concentration below its solubility in the vehicle, the product will normally have a lower efficacy than if the product was used at saturation. Consequently, products may be formulated to contain more active than will actually be needed for an adequate effect, as is the case with transdermal fentanyl patches, which have led to numerous deaths. The danger inherent to fentanyl is its potency (greater than 50–100 times that of morphine) and rapidity of action (Jumbelic 2010). An optimal dosing strategy demands that the rate of active penetration into the skin will achieve and sustain biologically active free levels at the target site within the specified limits. Also, ideally, these conditions should be independent of skin site and skin condition. This is a considerable challenge, given that there is wide variability in skin permeation, depending on the anatomical site (Rougier et al. 1988) and the condition of the skin, such as in particular disease states (Elias and Feingold 1992) or levels of hydration (Roberts and Walker 1993).

As discussed in other chapters in this book, another strategy to increase efficacy is to use a saturated active solution in the vehicle and to further increase either the stratum corneum solubility  $S_{sc}$  and/or its diffusivity  $D_{sc}$  using co-solvents and

**Fig. 23.5** Mean total testosterone concentrations in serum over time, following application of a single 28 cm<sup>2</sup> patch for 96 h, systemically delivering testosterone at a rate of approximately 300 µg/day (Adapted from Roberts and Walters (2008))



enhancers, in accordance with Eq. (23.5), where  $h_{sc}$  is the stratum corneum thickness:

$$J_{sat} = S_{sc} \cdot D_{sc} / h_{sc} \quad (23.5)$$

However, care has to be applied in representing such saturated fluxes as maximum fluxes because increasingly, formulations are being designed to include a volatile component that may result in enhanced skin penetration due to the generation of a transient supersaturated state. Many researchers have now promoted the use of supersaturated solutions (Coldman et al. 1969), with several showing that these can lead to even higher fluxes than those achieved with saturated solutions (Lippold 1992; Morgan et al. 1998; Iervolino et al. 2001; Timothy et al. 2002; Santos et al. 2012). More recently, there is an increasing tendency to either stabilize supersaturated products by using polymers (Raghavan et al. 2003) or to generate supersaturation on application to the skin as a consequence of the evaporation of the volatile components in the product (Hadgraft and Lane 2011). Supersaturated systems may be obtained either by design or via solvent evaporation or by mixing of co-solvents. The stability of supersaturated solutions is an important issue, and it would be useful to develop supersaturated systems that are stable throughout the product shelf life. Santos et al. (2011) investigated the permeation of fentanyl from supersaturated for-

mulations across silicone membranes. Supersaturated formulations containing either propylene glycol (PG)/water or PG/ethanol were prepared with varying degrees of saturation (DS) of fentanyl. Both PG/water and PG/ethanol formulations showed good correlation between the flux and DS. The enhancement observed for PG/ethanol formulations confirmed that enhanced active thermodynamic activity was induced due to ethanol evaporation. In further studies, tape-stripping was used to show that supersaturation of the active is maintained in the outer layers.

However, if the active lacks potency, a penetrating active will still prove to be inefficacious.

Obviously, an improved evaluation of product efficacy and safety will contribute to better therapeutic outcomes. Whereas the determination of bioequivalence for two solid oral dosage forms is based on a comparison of active and/or its metabolite concentrations in blood or urine after dosing from a generic product or that of an innovator in healthy volunteers, such considerations are really only appropriate for transdermal products meant for systemic effect. For most topically acting actives, such an approach is not appropriate as the site of action is local, not systemic. Hence, generic dermatological products are only required to demonstrate bioequivalence in clinical trials, including the vasoconstrictor test used to assess the efficacy of topical corticosteroids (Shah et al.

**Table 23.1** Transdermal delivery

Solute	Indication	Molecular weight	Melting point (°C)	$\log K_{\text{oct}}$	$t_{1/2}$	Plasma level ( $\mu\text{g/h}$ )	$F_s$	$\text{CL}_{\text{body}}$ L/h/70 kg	Estimated $J_{\text{sa}}$ required ( $\mu\text{g/h}$ )
Buprenorphine	Pain relief	468	209	3.44	4	0.1–0.52	0.5	76	15–80
Clonidine	Hypertension	230	140	1.77	6–20	0.2–2.0	1.0	13	2.7–28
Estradiol	Female hormone replacement	272	176	2.69	1	0.04–0.15	0.16	4–7 (CL/F)	1–6
Ethinyl estradiol	Female contraception	296	143	4.52	17	0.011–0.137	1	28	0.31–3.8
Fentanyl	Chronic pain	337	83	4.37	17	1	1	25–75	25–75
Isosorbide dinitrate	Angina	236	68	1.31	105	22	1	1.22	28
Methyl phenidate	ADHD	233	74.5	2.55	3–5	20–46	1	60 L/h/30 kg in children	720–2160
Nicotine	Smoking cessation	162	~80	1.17	2	10–30	1	72	900–2630
Nitroglycerin	Angina	227	13.5	1.62	0.04	1.2–11	1	13.5	16.2–148.5
Norelgestromin	Contraception	327	131	4.40	28				56–420
Norethindrone acetate	Contraception	340	162	3.99	9	2–15	1	28 (CL/F=25 L/h)	
Oxybutynin	Enuresis	357	130	5.19	2	3–4	1	25–34	75–135
Rivastigmine	Alzheimer's disease	250	124	2.14	1–4	2–10	1	130	260–1300
Rotigotine	Parkinson's disease	315	141	4.97	5–7	0.2–0.6	1	630	126–378
Scopolamine	Motion sickness	303	59	1.23	1.2–2.9	0.04	1	67–205	2.6–8.1
Selegiline	Depression	187	138	2.95	2	2	1		
Testosterone	Hypogonadism	288	153	3.31	2.3	60–100	1	3–5	180–500
Timolol	Hypertension	316	72	2.46	4.1	5–15	0.76	38	250–750
Triprolidine	Antihistamine	278	60	4.22	2–6	5–15	1	43.7	218–655

Adapted from Roberts and Walters (2008)

Examples of solutes on the market and their indications, effective plasma levels, body clearances ( $\text{CL}_{\text{body}}$ ), availability ( $F_s$ ), elimination half-life ( $t_{1/2}$ ) and physicochemical data used to estimate required solute transdermal Flux ( $J_s$ ) [from Eq. (23.3)] for passive topical delivery systems

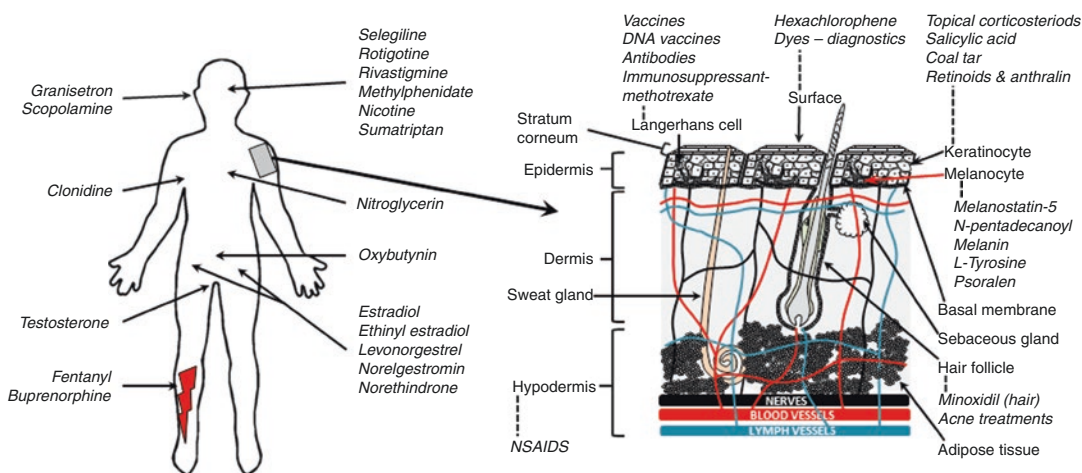


**Fig. 23.6** Target organs and sites for some common topically and transdermally delivered substances, highlighting the skin structure and various points of entry

1998). Franz et al. (2009) suggested that a substitute for clinical bioequivalence testing is to define the penetration fluxes of an active through excised human skin. Their evaluation, based on glucocorticosteroids and generic tretinoin gels, indicated that the in vitro model had greater sensitivity than the clinical method in detecting small differences between two products (Franz et al. 2009). It is unclear, however, how this approach can overcome the well-known wide variability in excised human skin permeability. More recently, Lehman and Franz have assessed the bioequivalence of topical retinoid products using pharmacodynamic assays (Lehman and Franz 2012).

## 23.2 Role of Intended Targets on Topical and Transdermal Delivery

There is a range of skin and systemic sites often targeted by topical and transdermal delivery, summarized in Fig. 23.6. In this section, we illustrate some of the actives and their formulations used to achieve appropriate targeted delivery by topical or transdermal delivery.

### 23.2.1 Topical Delivery

The skin is the site of application of numerous cosmetics and cosmeceutical preparations. In this section, we will discuss the importance of targets

on active delivery choices. Testing for safety of cosmetic preparations will be discussed in the following sections.

A chemist's role in overcoming an active's physicochemical properties to make it suitable for topical and transdermal delivery is a complicated task. Formulators have made use of physicochemical characteristics like molecular weight to stop an active from penetrating through the skin. One such example is a high molecular weight (>500 Da) UVA and UVB absorber Tinosorb<sup>®</sup> M (bisotrizole, INCI: methylene bis-benzotriazolyl tetramethylbutylphenol (and) aqua (and) decyl glucoside (and) propylene glycol (and) xanthan gum) developed by Ciba Chemicals (now part of BASF, Ludwigshafen, Germany). Similarly L'Oréal's sunscreen with Uvinul<sup>®</sup> N539 (2-ethylhexyl 2-cyano-3,3-diphenyl-2-propenoate, INCI: octocrylene), Parsol<sup>®</sup> 1789 (avobenzene; INCI: butyl methoxydibenzoylmethane) and Mexoryl<sup>®</sup> SX (MW-563; ecamsule, INCI: terephthalylidene dicamphor sulfon) was formulated to reduce solar-UV-induced skin damage (Seité et al. 2000). Sunscreens containing ecamsule (Mexoryl<sup>®</sup> SX) are exclusive to L'Oréal and its brands.

Chlorhexidine is another example of a molecule which binds extensively to the skin surface due to its cationic nature (Judd et al. 2013). This ensures that it does not penetrate into the skin and rather provides for a sustained antimicrobial action when used topically (Karpanen et al. 2008). Insect repellents are another good example of actives that



are not intended to penetrate. Penetration retardants and modifiers have been used for this purpose (Kaushik et al. 2010). On the other hand, terbinafine, a highly lipophilic but equally potent antifungal active, with a log  $P$  of 5.5, needs a different approach. When formulated as a micro-emulsion to enhance its stratum corneum solubility using a mixture of surfactant, co-surfactant and oil, terbinafine exhibited enhanced permeation parameters. Microbiological studies of the micro-emulsion showed better antifungal activity against *Candida albicans* and *Aspergillus flavus* compared to marketed products (Baboota et al. 2007). Retinol, with a high molecular weight and lipophilicity, is another active that is used for topical treatment of acne. These unfavourable properties were overcome by delivering Retinol using solid lipid nanoparticles (SLN). The suitability of the SLNs was compared to a nanoemulsion of the same size, with respect to the ability to influence active penetration and distribution within the skin. In both formulations, 500  $\mu\text{g}$  retinol was applied to porcine skin. Following the SLN dispersion for 6 h, a high retinol concentration was found in the stratum corneum and upper epidermis (approximately 3400 ng or 0.68 % in the top layer). The nanoemulsion, however, only transported 2500 ng (0.5 %) into the upper skin strata (Jenning et al. 2000).

For specific disease, conditions where the surface of the skin itself is the target of therapy, formulation and delivery strategy are of greatest importance. Creams, lotions, emulsions and other topical delivery vehicles have been used effectively for this. The challenge here is to modify the formulation according to the active characteristics and skin condition. Being the largest organ, skin is exposed to the damaging effects of UVA and UVB radiation, often leading to erythema. Antioxidants such as Vitamin A, Vitamin E and Vitamin C have shown beneficial effects in reducing oxidative damage to critical cellular components (Trevithick et al. 1993; Stamford 2012). While the photoprotective effect of topical antioxidants applied before UV exposure is well recognized, the beneficial effect of these compounds when administered after irradiation is less obvious (Wu et al. 2012). Only Vitamin A has been proven to be benefi-

cial in treating long-term photoaged and photo-damaged skin (Cho et al. 2005). The stratum corneum is a major barrier to the penetration of lipophilic Vitamin E (Cassano et al. 2009), and hydrophilic Vitamin C is prone to excessive oxidation. Oxidation of Vitamin C is triggered by its ionization in aqueous solution (Stamford 2012). Another example where erythema and papular oedema lesions are seen is *Herpes labialis*. In a recent study, iontophoretic application of 5 % acyclovir cream was tested in a placebo-controlled trial for treatment of herpes, among 200 patients with an incipient cold sore outbreak at the erythema or papular oedema lesion stage. A 20 min iontophoretic treatment cycle shortened the median classic lesion healing time by 35 h in the active group when compared to the control (Morrel et al. 2006). Steroids have also been popularly used in the treatment of erythema and other inflammatory skin conditions (Perry and Trafeli 2009; Paller 2012). Numerous studies have examined various factors controlling percutaneous absorption rates and dermal clearances of steroids (Siddiqui et al. 1989). The lipophilicity of steroids has been associated with their tissue accumulation and toxic effects. However, Magnusson et al. showed that the tissue accumulation of steroids was not linearly related to their lipophilicity, but the binding of steroids to tissue components led to their accumulation (Magnusson et al. 2006). Long-term corticosteroid usage has been associated with skin deterioration, abnormal skin aging and cutaneous mast cell depletion (Lavker and Schechter 1985; Gonzalez and Sethi 2012).

### 23.2.2 Targeting of Keratinocytes

One of the most widely explored aims of cellular targeting has been in the viable epidermis itself. Inflammatory conditions broadly known as dermatitis or eczema are largely reflected in epidermal involvement (Elias et al. 1999), including spongiosis, acantosis and parakeratosis, as well as some dermal involvement (Freeman-Anderson et al. 2008). The classical treatment for such conditions is the use of topical corticosteroids, which

can be classified on a four-point scale of potency (I–IV, mild, moderate, potent, very potent), based on their vasoconstrictor effects in humans. The body site to be treated determines the potency of the steroid to be used. For example, the face should be treated with mild corticosteroids only, such as hydrocortisone and hydrocortisone acetate. Care needs to be taken with the more potent steroids and in the treatment of chronic conditions. Intermittent dosing can be effective in these circumstances.

Salicylic acid has long been used for conditions such as psoriasis and ichthyosis that require keratolytic treatment. At lower concentrations, salicylic acid is known to have keratoplastic effects; however at higher concentrations, it is found to be keratolytic (Gloor and Beier 1984; Schwarb et al. 1999). Coal tar, retinoids and anthralin, as well as corticosteroids are some other commonly used treatments for psoriasis (Mitra and Wu 2010). Psoriatic skin is one such example where the “rigidization” of skin, ascribed to an increase in the levels of cholesterol and fall in the levels of ceramides and the lack of hydration, makes the topical route a big challenge (Wertz et al. 1989). The intricacies of topical delivery into psoriatic skin have lately been addressed by lipoidal carrier systems, such as liposomes. Recent work by Ward et al. describes the delivery of novel immunotherapy using a liposomal platform. Liposomes synthesized to incorporate clodronate were injected intradermally into KC-Tie2 mice. An elimination of the CD11c+, F4/80+ and CD11b+ cells was seen in the skin, and the CD8+ T-cell numbers returned to levels seen in control mice. Further, there was also a marked reduction in the levels of interleukin (IL)-1a, IL-6, IL-23 and tumour necrosis factor (TNF $\alpha$ ) (Ward et al. 2011). Peptides and proteins such as elafin and psoriasin are known to be highly upregulated in psoriatic skin (Madsen et al. 1991; Nonomura et al. 1994; Namjoshi et al. 2008). Peptide T analogue, DAPTA, was shown in clinical trials to clear psoriasis lesions and significantly inhibit the monocyte and lymphocyte chemotactic properties of RANTES (a beta chemokine found in increased amounts in psoriatic lesions). A better understanding of the

role of these peptides may provide new strategies for the treatment of diseases such as psoriasis (Harder and Schröder 2002).

### 23.2.3 Targeting of Melanocytes

The synthesis and distribution of melanin contribute to skin and hair colour. However, melanin and pigmentation-associated skin cancers are a major problem, while there is also interest in cosmetic skin whitening treatments where increased epidermal melanin synthesis causes unwanted darkening of the skin. Accurate determination of cutaneous melanin in normal skin and in disease conditions requires the collection of skin biopsies. However, our recent work has used multiphoton tomography and fluorescence lifetime imaging to non-invasively measure levels of epidermal melanin, which can be related to the visible skin colour (Dancik et al. 2013a, b). The use of these techniques has implications for lesion diagnosis and assessment of therapeutic progress.

Proteins and peptides play an important role in skin health as structural components of the skin as well as activators, regulators or inhibitors of certain biochemical processes occurring in the skin (Heidl 2009). Peptides as cosmeceuticals are a fast-growing segment of the personal care industry with an increasing trend towards the use of these agents in skin care regimens for protection from radiation and oxidant damage (Brandt et al. 2011). Peptides also play an important role in melanogenesis. Melanocyte-inhibiting factor (also known as Pro-Leu-Gly-NH $_2$ , Melanostatin, MSH release-inhibiting hormone or MIF-1) is an endogenous peptide fragment derived from oxytocin (Taleisnik 1971). Melanostatin is shown to inhibit melanin formation in *Streptomyces bikiniensis* NRRLB-1049 and B16 melanoma cells. A patent filed in 2010 describes a “one-step” process for production of esters and acetylated forms of peptides, describing melanostatin (MIF-1). This chemical modification approach improved metabolic properties leading to increased efficiency for therapeutic and cosmetic purposes including transdermal and topical administration (Skinner 2007). Melanocyte-stimulating hormone

analogues that function as melanocortin 1 receptor (MC1-R) agonists have been investigated as potential topical agents to prevent skin photocarcinogenesis. In cultured human melanocytes, tetrapeptide  $\alpha$ -MSH analogues, Ac-His-D-Phe-Arg-Trp-NH<sub>2</sub>, N-pentadecanoyl and 4-phenylbutyryl-His-d-Phe-Arg-Trp-NH<sub>2</sub> were more potent than  $\alpha$ -MSH in stimulating the activity of melanogenesis, reducing apoptosis and release of hydrogen peroxide and enhancing repair of deoxyribonucleic acid (DNA) photoproducts in melanocytes exposed to UV radiation (Abdel Malek 2006). Melanostatin-5 (Aqua-Dextran-Nonapeptide-1) is a new skin lightening biomimetic peptide. This peptide acts as a  $\alpha$ -MSH antagonist thus preventing and lightening hyperpigmentation (Dhatt 2006). Melanostatin-5 produces noticeable skin lightening by at least 33 % when formulated into a lightening product, and showed continued improvement over time.

### 23.2.4 Targeting of Langerhans Cells

Skin has evolved a highly competent immunological function, in Langerhans cells (LCs – estimated population 500–1000 cells mm<sup>-2</sup>) (Berman et al. 1983; Chen et al. 1985), which often serves as the first line of defence against many pathogens (Babiuk et al. 2000). The viable epidermis lacks the blood vessels and sensory nerve endings found in the dermis, which makes it an ideal site for pain-free delivery with minimal damage. There are many approaches for non-invasive targeting of viable epidermal cells and DNA vaccination against major diseases. There have been attempts at displaying foreign peptides and proteins on virus particles and insertion of mammalian cell-active expression cassettes in baculoviruses to express genes efficiently into many different mammalian cell types (Paul et al. 2013). Pearton et al. showed morphological changes in human LCs stimulated with influenza virus-like particulate vaccines delivered via intradermal injection. The LCs were more dispersed throughout the epidermis, often in close proximity to the basement membrane, and appeared vertically elongated, which provides essential evidence of host response (Pearton et al. 2010).

There are many physical approaches, both old and recent for targeting LCs; we will try to mention them in brief. The most well-known technique was: (a) Needle and Syringe: This is an inefficient and indirect way of targeting the dendritic cells with DNA. It has resulted in modest immune responses (Mumper and Ledebur 2001). Other disadvantages include risks due to needle stick injuries (Gill et al. 2009; Sullivan et al. 2010). (b) Liquid Jet Injector: This is a needle-free approach using high-speed liquid jet injectors (Furth et al. 1995) (Mark 2008). This technique has seen a recent resurgence, with liquid delivered around the LCs in gene transfer and DNA vaccination experiments (Furth et al. 1995). Current liquid jet injectors typically disrupt the skin in the epidermal and dermal layers to target LCs. Liquid jet injectors however have been reported to cause pain to the patients. (c) Microneedle Arrays: Unlike current liquid jet injectors, microneedles can accurately target the viable epidermis, are simple to use when built up as patches and are relatively pain free. McAllister et al. (2003) have shown that they can be made from a range of materials, including silicon, metal and other biodegradable polymers. This makes microneedles a cost-effective method for delivering oligonucleotides to epidermal cells for DNA vaccination (Kendall 2010). (d) Biolistic microparticle delivery: In this needle-free technique, pharmaceutical or immunomodulatory agents, formulated as particles, are accelerated in a supersonic gas jet to a sufficient momentum to penetrate the skin (or mucosal) layer and achieve a pharmacological effect. Sanford and Klein (Sanford et al. 1987) pioneered this innovation with systems designed to deliver DNA-coated metal particles (1  $\mu$ m diameter) into plant cells for genetic modification.

Follicular targeting has been approached as another way of targeting the LCs (Patzelt and Lademann 2013). Vogt et al. (2006) found a high density of LCs around hair follicles that were very susceptible to targeting with the use of nanoparticles. Nanoparticles of 40 nm diameter, but not larger particles in the micron size range, were delivered via the follicles and were able to diffuse through the follicular infundibulum to be taken up by the adjacent Langerhans cells.

### 23.2.5 Targeting of Fibroblasts

Triggered synovial fibroblasts, as part of a multi-part cellular complex, play an important role in the pathogenesis of rheumatoid arthritis (Pap et al. 2000; Seemayer et al. 2001). Diclofenac is a commonly used non-steroidal anti-inflammatory active for symptom control in osteoarthritis of the knee and soft tissue injuries (Bajaj et al. 2011). Although analgesics applied topically can provide a local enhanced active delivery for the superficial joint tissues by direct diffusion, they are unlikely to be effective for the deeper tissue synovial fluid (Xi et al. 2013). Recently, fibroblasts have been targeted using diclofenac in vesicles containing various penetration enhancers (Manca et al. 2013).

Fibroblasts also play an important role in development of hypertrophic scars, which result from an overgrowth of fibrous tissue at the site of an injury. The development of a hypertrophic scar is a complex interplay between fibroblasts and cytokines (Tredget et al. 1997). Zhao et al. recently delivered small interfering ribonucleic acid (siRNA) – transforming growth factor beta 1 (TGF $\beta$ 1)-337 from hydrogel pressure-sensitive adhesive patches in mice and demonstrated a down-regulation in collagen and reduction in scar size. The scar fibroblasts were shown to have significantly reduced by undergoing apoptosis (Zhao et al. 2013).

### 23.2.6 Intradermal and Systemic Targeting

The skin is an ideal route for targeted delivery of steroidal and non-steroidal anti-inflammatory agents and other analgesics for pain and inflammation. This has been achieved with many techniques. Topical NSAIDs and related solutes are often applied to the skin to target tissues directly below the application site. In a 1999 study, Roberts et al. used biopsy and microdialysis techniques to show that most solutes penetrate below dermal capillaries into the subcutaneous and deeper tissues of both rats and human subjects. The selectivity of local penetration is time related, and the concentrations of the NSAIDs in the

underlying tissues at longer times are often defined by recirculation from the systemic blood supply (Roberts and Cross 1999). Increased depths of penetration may be achieved by the use of vasoactive agents (Singh and Roberts 1994). On the other hand, steroids have been shown to accumulate in the skin to a greater extent. Magnusson et al. showed a slower penetration and a higher rate of accumulation of progesterone in the viable epidermis of full-thickness skin. These findings were consistent with dermal penetration limitation effects associated with high lipophilicity of the steroids (Magnusson et al. 2006). Previously, Pelchrzim et al. also showed a similar reservoir effect of the stratum corneum on corticosteroid penetration, although they considered this to be formulation dependent (Pelchrzim et al. 2004). Ketorolac has been successfully delivered by iontophoresis to human volunteers using silver electrodes with a current of 2 mA for five treatment sessions of 20 min every day in order to avoid the well-known gastrointestinal side effects of its oral delivery (Saggini et al. 1996).

Transdermal delivery has been successfully used to achieve systemic targeting, by exploiting the rich blood perfusion of the dermis. Fentanyl, a widely used opioid, has potency approximately 100–500-fold greater than morphine. Its physico-chemical and pharmacological properties, together with its pharmacokinetics (short half-life; high first pass effect), make it an ideal candidate to be delivered systemically through the skin. Fentanyl has been delivered transdermally using two different techniques. Firstly, it is formulated in transdermal patches to be passively delivered for the treatment of chronic pain. However, this technique cannot provide a rapid bolus active input for the relief of acute pain (Chelly et al. 2004). Iontophoresis has also been investigated for systemic Fentanyl delivery; for example, as a patient controlled system that could be activated for symptomatic relief (Ashburn et al. 1995). The skin also provides a potential route for the non-invasive delivery of peptides and proteins which are in danger of inactivation when delivered orally, due to chemical and enzymatic degradation, although there are significant challenges involved in achieving this (Benson and Namjoshi 2008).

### 23.3 Role of Safety and Active Toxicity in Transdermal Formulation

Cosmetics and pharmaceuticals must be formulated not only for efficacy, but also for patient or consumer acceptance. This is influenced by a perception of safety or lack of toxicity. Regarding safety and toxicity, it must be understood that for a topically applied active to have either therapeutic or toxic effects, it must first be absorbed through the skin. The toxic effects caused if the chemicals are absorbed can include acute irritation, corrosion and skin sensitization (Grice et al. 2010). Chemicals applied to the skin can also have direct effects on the stratum corneum, resulting in an alteration in its permeability. This concept has been effectively applied in the development of penetration enhancers. However, the harmful effects of excipients on the skin have been evaluated under increasing scrutiny by regulatory authorities. Regulatory considerations will be discussed later in this chapter.

Topically applied actives causing adverse effects can be classified as either allergens or irritants (Zweiman 1990). These allergens and irritants not only affect the skin but can also affect other body sites. Cutaneous active reactions can be classified into three types of contact dermatitis: (a) Allergic contact dermatitis, (b) irritant contact dermatitis and (c) photo contact dermatitis. The role and mechanism of irritation caused by various chemical penetration enhancers has been studied extensively.

#### 23.3.1 Mechanisms of Contact and Photo Allergies and Irritations

Allergic contact dermatitis (ACD) results from an adaptive immune response to the penetration of allergens into the skin. ACD progresses in two phases: (a) in the initial sensitization phase, the host is immunized to the allergen, and (b) in the elicitation phase, a rapid secondary immune

response is mounted following re-exposure to the allergen which manifests as ACD (Alenius et al. 2008). Cutaneous photosensitivity can be evoked by both systemic and topical exogenous photosensitizers leading to active photosensitivity and photo contact dermatitis, respectively. Photoallergenicity is a well-organized immunological reaction. The current understanding of ordinary contact dermatitis and active hypersensitivity is based on the hapten hypothesis: molecules bind covalently to proteins, and the resulting conjugates can be recognized as immunogenic determinants. Likewise, photosensitive chemicals have a haptenic moiety.

Although the terms structure–activity relationship (SAR) and quantitative structure–activity relationship (QSAR) are widely used, for skin sensitization, it is more meaningful to describe the relationship as being between chemistry and activity. Skin sensitization induction is a multi-stage process (Jowsey et al. 2006): *Stage 1*, Translocation of the sensitizer from the skin surface to the epidermal site of action. This depends on the dose given and duration of exposure; *Stage 2*, Covalent reaction of the sensitizer with skin protein. This is strongly dependent on the chemical nature of the sensitizer, in particular electrophilic reactivity and hydrophobicity. The nature of the skin proteins involved in this process is not established. Possibilities range from any protein encountered in the skin to highly nucleophilic proteins, “purpose-designed” by evolution, associated with epidermal Langerhans cell membranes; *Stage 3*, Response of epidermal Langerhans cells to the modified protein, resulting in migration to the lymph node and presentation of antigen, leading to antigen recognition by naïve T-lymphocytes resulting in clonal expansion. Regulators classify chemicals as being hazardous after an acute dermal contact if they lead to mortality (owing to absorption), cause acute irritation or corrosion and cause skin sensitization on multiple contacts. In the EU, evaluation of skin irritation/corrosion is mandatory for all products likely to be associated with skin exposure. The section below discusses testing protocols and requirements in the EU.

### 23.3.2 Testing of Dermatologics, Cosmetics and Their Safety Evaluation

The European Commission Scientific Committee on Consumer Safety (SCCP) adopted its most recent guidelines “The SCCS’s notes of guidance for the testing of cosmetic substances and their safety evaluation, 8th Revision” in December 2012 (SCCP 2012). These set out procedures for the safety evaluation of cosmetic substances (single ingredients or defined mixtures) and finished cosmetic products. In the guidelines, a cosmetic ingredient is defined as “any chemical substance or mixture of synthetic or natural origin, used in the formulation of cosmetic products.” A cosmetic ingredient may be:

1. A chemically well-defined single substance with a molecular and structural formula
2. A complex mixture, requiring a clear definition and often corresponding to a mixture of substances of unknown or variable composition and biological nature
3. A mixture of 1 and 2, used in the formulation of a finished cosmetic product

A finished cosmetic product is defined as “Any substance or mixture intended to be placed in contact with the external parts of the human body (epidermis, hair system, nails, lips and external genital organs) or with the teeth and the mucous membranes of the oral cavity with a view exclusively or mainly to cleaning them, perfuming them, changing their appearance, protecting them, keeping them in good condition or correcting body odours”.

Table 23.2 illustrates the SCCP requirements for testing of chemical and physical properties and the relevant toxicity studies for cosmetic substances.

Other requirements for SCCP evaluation of cosmetic substances are included under the general headings listed in Table 23.3.

The SCCP guidelines cover the evaluation of safety and microbiological quality of finished cosmetic products under the headings listed in Table 23.4.

**Table 23.2** SCCP requirements for testing of chemical and physical properties of cosmetic substances, and the associated toxicity studies (SCCP 2012)

Chemical and physical specifications	Relevant toxicity studies
Chemical identity	Acute toxicity
Physical form	Corrosivity and irritation
Molecular weight	Skin sensitization
Characterization and purity of the chemical	Dermal/percutaneous absorption
Characterization of the impurities or accompanying contaminants	Repeated dose toxicity
Solubility	Reproductive toxicity
Partition coefficient (log $P_{ow}$ )	Mutagenicity, genotoxicity
Additional relevant physical and chemical specifications	Carcinogenicity
Homogeneity and stability	Toxicokinetic studies
UV–VIS absorption spectrum	Photo-induced toxicity
Isomer composition	Human data
Functions and uses	

SCCP recognizes the increasing use of synthetic and semisynthetic ingredients, in addition to the ingredients derived from natural products that have been traditionally used in cosmetics. In addition, their requirements for evaluating the safety requirements for cosmetic products are increasingly being brought into line with those for therapeutic products.

### 23.3.3 In Vitro Skin Irritancy Tests: A Need for Triangulation

While dermal toxicity to exogenous materials is seldom associated with mortality, it may involve significant morbidity. Ethical concerns have brought about a paradigm shift in the way the skin irritancy of a cosmetic ingredient is evaluated. Prior to its phasing out and eventual ban by the European Commission, the scientific community has traditionally used in vivo animal testing methods to evaluate the safety of a topically

**Table 23.3** Safety evaluation procedure of cosmetic substances as applied by the SCCP: Further requirements for cosmetic ingredients (SCCP 2012)

Toxicological requirements for inclusion of a substance in one of the Annexes to Regulation (EC) No 1223/2009 (to be evaluated by the SCCP)Dir. 76/768/EEC
Basic requirements for cosmetic substances present in finished cosmetic substances (which are to be evaluated by individual safety assessors)
General principles for the calculation of the Margin of Safety and lifetime cancer risk for a cosmetic substance
The specific assessment of hair dyes and hair dye components
The Threshold of Toxicological Concern (TTC)
Aspects to consider with respect to the risk assessment for the inhalation route
Human biomonitoring

**Table 23.4** SCCP evaluation of finished cosmetic products: Safety and microbiological quality (SCCP 2012)

Toxicological profile of the substances
Stability and physical and chemical characteristics of the finished cosmetic product
Evaluation of the safety of the finished product
Microbiological quality: quantitative and qualitative limits
Challenge testing
Good manufacturing practice

applied product. There are many in vitro testing models that have been developed and commercialized to provide an alternative to animal testing. Models such as EpiSkin® (EpiSkin SNC, Lyon, France), SkinEthic® (SkinEthic laboratories (Nice, France) and EpiDerm® (Mat-Tek Inc., Ashland, USA) have reasonable similarities to human tissue in terms of morphology, lipid composition and biochemical markers (Netzlaff et al. 2005). Numerous reviews and research articles have been written comparing the different skin models to each other and to human skin (Lotte et al. 2002; Netzlaff et al. 2005; Schafer-Korting et al. 2006, 2008; Neis et al. 2010; Gotz et al. 2012; Brinkmann et al. 2013). Lotte et al. (2002) studied the permeation of lauric acid, caffeine and mannitol in EpiSkin®, SkinEthic® and EpiDerm® and observed that although there was huge variability in permeation data among the

skin models, the order of permeation was in line with that observed in ex vivo skin. Enzymatic equivalence and gene expression were also compared (Hu et al. 2010; Neis et al. 2010). In microarray analysis, Hu et al. (2010) found that the expression of a large percentage of the genes was consistent between EpiDerm® and human skin indicating the presence of similar metabolic pathways. In a 2005 review, Netzlaff et al. evaluated the morphology of commercially available skin models and compared their suitability for testing phototoxicity, irritancy, corrosivity and active transport (Netzlaff et al. 2005). They tabulated comparative morphological features and test results for these parameters. They commented that currently the models come close to reproducing human skin, but only in certain aspects. These skin models are useful in toxicity testing, including phototoxicity testing, and to an extent for drug transport studies. The variability in transport can be attributed to the incompletely developed barrier.

Before the enforcement of the EU chemicals policy REACH (Registration, Evaluation and Authorization of Chemicals) in 2009, Basketter et al. (2007) published report and recommendations of European Centre for the Validation of Alternative Methods (ECVAM's) Workshop 59<sup>a</sup>. This workshop was part of a concerted effort in recognizing the role of percutaneous/dermal absorption process in sensitization. They defined epidermal *disposition* as the specific location and stressed the quantification of chemicals in the epidermal compartment, which are relevant to local toxicity endpoints/skin sensitization. OECD Test Guideline (TG) 428 (OECD 2004), for in vitro skin absorption, provides general rules on how to measure systemic availability and concentrations of chemicals that permeate through all layers of the skin and the overall kinetics of skin absorption but does not allow for separate evaluation of epidermal disposition to be derived for local skin toxicity endpoints, such as skin sensitization. Hence, this report emphasizes the need to relate the in vivo dosimetry of sensitizers that penetrate into the viable epidermis via the stratum corneum of human skin to the concentrations used in in vitro applications. This requires the need to

estimate both the applied concentration of chemical onto the skin surface for given finite dose exposure conditions and to relate it to what is applied to cells *in vitro* as being representative of the target dose of chemical in human skin.

The models proposed by the SCCP for skin safety tests have been validated against *in vivo* Draize tests (SCCP 2012). However, these stand-alone methods rely heavily on quantification of optical density and colorimetry, which lead to a one-dimensional analysis. Moreover, since results obtained from previously conducted human tests studies on model compounds are necessary as reference values for *in vitro* assays, attention should also be paid to the generation of *in vivo* data and standardization of *in vivo* test protocols (Ponec 2002).

In the last decade, numerous committees and taskforces have been set up to constantly review the performance of *in vitro* irritancy and genotoxicity assays (Fentem et al. 1998; Eskes et al. 2012; Pfuhler et al. 2014). *In vitro* assays have shown a very high rate of positive genotoxicity results that do not correlate with *in vivo* genotoxicity or carcinogenicity (Kirkland et al. 2007). Due to the inability to follow up the *in vitro* tests with *in vivo* assays, many potential new products have been de-selected. The Cosmetics Europe (formerly COLIPA) Genotoxicity Task Force has driven and funded projects to help address the high rate of misleading positives in *in vitro* genotoxicity tests (Pfuhler et al. 2014). The ongoing “3D skin model” project is now validating the use of human reconstructed skin (RS) models in combination with the micronucleus (MN) and Comet assays. Non-testing methods like [quantitative] structure–activity relationships ([Q]SARs) or *in silico* methods are also a valuable way of gaining more toxicological information. Formation of chemical categories facilitates the application of read across between similar chemicals based on the assumption that their behaviour will be consistent for their class (Adler et al. 2011).

Even from before the complete ban on animal testing, alternative techniques to test dermal irritancy and immunogenicity caused by pharmaceutical and cosmetic products were being developed. Responses to irritants have been stud-

ied in cell culture for a significant period (Deleo et al. 1996). There are other approaches that can be used to complement the validated *in vitro* methods and satisfy the need for triangulation in safety evaluation. Human *ex vivo* skin is often used as a realistic model for *in vivo* human skin in transdermal active delivery. The study of detailed cellular and sub-cellular processes in the skin was previously not possible using conventional light microscopic methods, such as wide-field and confocal microscopy. Although these tools work reliably in cell cultures and thin tissue sections, their application in thick biological samples such as skin is greatly limited due to light-scattering and absorbing properties of biological tissues. However, this is being addressed with the increasing use of multiphoton or two photon microscopy (MPM/TPM). Understanding of the process of epidermal and transdermal transports of xenobiotics is important for rational design of topical active delivery and to avoid exposure to toxic and allergenic compounds. MPM allows 3D visualization of penetration and distribution with minimal sample preparation. Sanchez et al. have used cellular autofluorescence to show that *ex vivo* skin viability, including metabolic activity, can be preserved up to 7 days at 4 °C (Sanchez et al. 2010). MPM has also been used to demonstrate the importance of stratum corneum, in the sensitization phase of contact allergy (Samuelsson et al. 2009). One of the present drawbacks of MPM is that it tends to be qualitative rather than quantitative; however, the use of fluorescence lifetime imaging (FLIM) holds promise for quantitative analysis in tissue samples (Benati et al. 2011; Koenig et al. 2011). Excised skin obtained from elective abdominoplasties is a convenient resource, which when used within its viability provides an excellent model. However, not all research facilities have access to freshly excised skin. Skin from elective surgery is donated in goodwill to assist scientific research, and there are ethical constraints on its use for commercial testing. The EU prohibits financial gain through the use of human tissue (Netzlaff et al. 2005). Progress is ongoing in the development of advanced skin equivalents with immune and inflammatory equivalency.



Better culture media to maintain the viability of *ex vivo* skin and skin biopsies are also under development.

Chau et al. (2013) recently described an advanced static 3D skin equivalent which combines human keratinocytes, human dendritic cell and fibroblasts combined into a three-layer CellGrown™ tissue culture insert comprising keratinocyte and fibroblast layers at a thickness of 100 µm and 30 µm, respectively. Dinitrochlorobenzene (DNCB), an established skin sensitizer, was used topically to stimulate this skin model and showed extensive cell response with up-regulation of the cell surface antigens CD86 (cluster of differentiation 86) and HLA-DR (an MHC Class II antigen expressed mainly on antigen-presenting cells) on the dendritic cells. Another approach to emulate the human skin composition of both somatic and immune cell populations is the use of skin biopsies for *in vitro* cultures. Skin biopsies contain all the immune cell types relevant for the donor at the place of biopsy extraction (Giese and Marx 2014). A biopsy from the skin sample can then be used to test for the presence of inflammation-related human genes using real-time quantitative polymerase chain reaction (RQ-PCR). The *de novo* construction of full skin equivalents and the use of skin biopsies are two complementary and scientifically grounded approaches to model human skin immunity *in vitro* (Giese and Marx 2014).

### Conclusions

In this chapter, we have discussed some of the major issues facing the formulator: efficacy, safety, toxicity and skin targets. Efficacy, defined as the product of potency of the active and the amount delivered to its site of action, and formulation dictate the dosage of a given active. The formulator must be guided by the physicochemical properties of the particular active and knowledge of skin physiology to create a delivery system to target particular skin regions or cell populations. For all topically applied actives and cosmetics, safety and irritancy testing is required. Suitable predictive methods of *in vitro* testing must be estab-

lished and validated to replace *in vivo* animal testing that can no longer be used. A triangulation approach is suggested to deal with the problem of false positives in the *in vitro* tests.

**Acknowledgements** The authors thank the National Health & Medical Research Council of Australia for support of this work.

### References

- Abdel Malek Z (2006) Melanoma prevention strategy based on using tetrapeptide alpha-MSH analogs that protect human melanocytes from UV-induced DNA damage and cytotoxicity. *FASEB J* 20(9):1561–1563
- Adler S, Basketter D, Creton S, Pelkonen O, Benthem J, Zuang V, Andersen K, Angers-Loustau A, Aptula A, Bal-Price A, Benfenati E, Bernauer U, Bessems J, Bois F, Boobis A, Brandon E, Bremer S, Broschard T, Casati S, Coecke S, Corvi R, Cronin M, Daston G, Dekant W, Felter S, Grignard E, Gundert-Remy U, Heinonen T, Kimber I, Kleinjans J, Komulainen H, Kreiling R, Kreysa J, Leite S, Loizou G, Maxwell G, Mazzatorta P, Munn S, Pfueller S, Phrakonkham P, Piersma A, Poth A, Prieto P, Repetto G, Rogiers V, Schoeters G, Schwarz M, Serafimova R, Tähti H, Testai E, Delft J, Loveren H, Vinken M, Worth A, Zaldivar J-M (2011) Alternative (non-animal) methods for cosmetics testing: current status and future prospects—2010. *Arch Toxicol* 85(5):367–485
- Afouna MI, Mehta SC, Ghanem AH, Higuchi WI, Kern ER, De Clercq E, El-Shattawy HH (1998) Assessment of correlation between skin target site free drug concentration and the *in vivo* topical antiviral efficacy in hairless mice for (E)-5-(2-bromovinyl)-2'-deoxyuridine and acyclovir formulations. *J Pharm Sci* 87(8):917–921
- Alenius H, Roberts DW, Tokura Y, Lauerma A, Patlewicz G, Roberts MS (2008) Skin, drug and chemical reactions. *Drug Discov Today Dis Mechanisms* 5(2):e211–e220
- Anrade SM, Costa SMB (1999) Hydrogen bonding effects in the photophysics of a drug, Piroxicam, in homogeneous media and dioxane–water mixtures. *Phys Chem Chem Phys* 1:4213–4218
- Ashburn MA, Streisand J, Zhang J, Love G (1995) The iontophoresis of fentanyl citrate in humans. *Anesthesiology* 82(5):1146–1153
- Babiuk S, Baca-Estrada M, Babiuk LA, Ewen C, Foldvari M (2000) Cutaneous vaccination: the skin as an immunologically active tissue and the challenge of antigen delivery. *J Control Release* 66(2–3):199–214
- Baboota S, Al-Azaki A, Kohli K, Ali J, Dixit N, Shakeel F (2007) Development and evaluation of a microemulsion formulation for transdermal delivery of terbinafine. *PDA J Pharmaceu Sci Technol* 61(4):276–285

- Bajaj S, Whiteman A, Brandner B (2011) Transdermal drug delivery in pain management. *Contin Educ Anaesth Crit Care Pain* 11(2):39–43
- Barry BW (2001) Is transdermal drug delivery research still important today? *Drug Discov Today* 6(19): 967–971
- Basketter D, Pease C, Kasting G, Kimber I, Casati S, Cronin M, Diembeck W, Gerberick F, Hadgraft J, Hartung T, Marty JP, Nikolaidis E, Patlewicz G, Roberts D, Roggen E, Rovida C, van de Sandt J (2007) Skin sensitisation and epidermal disposition: the relevance of epidermal disposition for sensitisation hazard identification and risk assessment. The report and recommendations of ECVAM workshop 59. *Altern Lab Anim* 35(1):137–154
- Benati E, Bellini V, Borsari S, Dunsby C, Ferrari C, French P, Guanti M, Guardoli D, Koenig K, Pellacani G, Ponti G, Schianchi S, Talbot C, Seidenari S (2011) Quantitative evaluation of healthy epidermis by means of multiphoton microscopy and fluorescence lifetime imaging microscopy. *Skin Res Technol* 17(3): 295–303
- Benson HA, Namjoshi S (2008) Proteins and peptides: strategies for delivery to and across the skin. *J Pharm Sci* 97(9):3591–3610
- Berman B, Chen VL, France DS, Dotz WI, Petroni G (1983) Anatomical mapping of epidermal Langerhans cell densities in adults. *Br J Dermatol* 109(5): 553–558
- Brandt FS, Cazzaniga A, Hann M (2011) Cosmeceuticals: current trends and market analysis. *Semin Cutan Med Surg* 30(3):141–143
- Brinkmann J, Stolpmann K, Trappe S, Otter T, Genkinger D, Bock U, Liebsch M, Henkler F, Hutzler C, Luch A (2013) Metabolically competent human skin models: activation and genotoxicity of benzo[a]pyrene. *Toxicol Sci* 131(2):351–359
- Cassano R, Trombino S, Muzzalupo R, Tavano L, Picci N (2009) A novel dextran hydrogel linking trans-ferulic acid for the stabilization and transdermal delivery of vitamin E. *Eur J Pharm Biopharm* 72(1):232–238
- Castela E, Archier E, Devaux S, Gallini A, Aractingi S, Cribier B, Jullien D, Aubin F, Bachelez H, Joly P, Le Maitre M, Misery L, Richard MA, Paul C, Ortonne JP (2012) Topical corticosteroids in plaque psoriasis: a systematic review of risk of adrenal axis suppression and skin atrophy. *J Eur Acad Dermatol Venerol* 26(Suppl 3):47–51
- Chau DY, Johnson C, MacNeil S, Haycock JW, Ghaemmaghami AM (2013) The development of a 3D immunocompetent model of human skin. *Biofabrication* 5(3):035011
- Chelly JE, Grass J, Houseman TW, Minkowitz H, Pue A (2004) The Safety and Efficacy of a Fentanyl Patient-Controlled Transdermal System for Acute Postoperative Analgesia: A Multicenter, Placebo-Controlled Trial. *Anesth Analg* 98(2):427–433
- Chen H, Yuan J, Wang Y, Silvers WK (1985) Distribution of ATPase-positive Langerhans cells in normal adult human skin. *Br J Dermatol* 113(6):707–711
- Cho S, Lowe L, Hamilton TA, Fisher GJ, Voorhees JJ, Kang S (2005) Long-term treatment of photoaged human skin with topical retinoic acid improves epidermal cell atypia and thickens the collagen band in papillary dermis. *J Am Acad Dermatol* 53(5):769–774
- Coldman MF, Poulsen BJ, Higuchi T (1969) Enhancement of percutaneous absorption by the use of volatile: nonvolatile systems as vehicles. *J Pharm Sci* 58(9): 1098–1102
- Cordero JA, Camacho M, Obach R, Domenech J, Vila L (2001) *In vitro* based index of topical anti-inflammatory activity to compare a series of NSAIDs. *Eur J Pharm Biopharm* 51(2):135–142
- Cross SE, Roberts MS (2006) Dermal blood flow, lymphatics, and binding as determinants of topical absorption, clearance, and distribution. Dermal absorption models in toxicology and pharmacology. Boca Raton, FL: CRC Press, Taylor and Francis Group; pp 251–281
- Dancik Y, Favre A, Loy CJ, Zvyagin AV, Roberts MS (2013a) Use of multiphoton tomography and fluorescence lifetime imaging to investigate skin pigmentation *in vivo*. *J Biomed Opt* 18(2):026022
- Dancik Y, Miller MA, Jaworska J, Kasting GB (2013b) Design and performance of a spreadsheet-based model for estimating bioavailability of chemicals from dermal exposure. *Adv Drug Deliv Rev* 65(2):221–236
- Davis A (2007) Formulation strategies to overcome the skin's defence. SCI Meeting, London
- Davis AF (2008) Getting the dose right in dermatological therapy. In: Dermatologic, cosmeceutic, and cosmetic development. Boca Raton, FL: CRC Press, Taylor and Francis Group; pp 197–213
- Deleo VA, Carver MP, Hong J, Fung K, Kong B, Desalva S (1996) Arachidonic acid release: an *in vitro* alternative for dermal irritancy testing. *Food Chem Toxicol* 34(2):167–176
- Dhatt S (2006) Rebuilding the dermal matrix with this new in-demand ingredient in skin care products. *Aesthetic Trends Technol* 17–20
- Elias PM, Feingold KR (1992) Lipids and the epidermal water barrier: metabolism, regulation, and pathophysiology. *Semin Dermatol* 11(2):176–182
- Elias PM, Wood LC, Feingold KR (1999) Epidermal pathogenesis of inflammatory dermatoses. *Am J Contact Dermatol* 10(3):119–126
- Eskes C, Detappe V, Koëter H, Kreysa J, Liebsch M, Zuang V, Amcoff P, Barroso J, Cotovio J, Guest R, Hermann M, Hoffmann S, Masson P, Alépée N, Arce LA, Brüschweiler B, Catone T, Cihak R, Clouzeau J, D'Abrosca F, Delveaux C, Derouette JP, Engelking O, Facchini D, Fröhlicher M, Hofmann M, Hopf N, Molinari J, Oberli A, Ott M, Peter R, Sá-Rocha VM, Schenk D, Tomicic C, Vanparys P, Verdon B, Wallenhorst T, Winkler GC, Depallens O (2012) Regulatory assessment of *in vitro* skin corrosion and irritation data within the European framework: Workshop recommendations. *Regul Toxicol Pharmacol* 62(2):393–403
- Fentem JH, Archer GEB, Balls M, Botham PA, Curren RD, Earl LK, Esdaile DJ, Holzhütter HG, Liebsch M

- (1998) The ECVAM international validation study on *In vitro* tests for skin corrosivity. 2. Results and evaluation by the management team. *Toxicol In Vitro* 12(4):483–524
- Franz TJ, Lehman PA, Raney SG (2009) Use of excised human skin to assess the bioequivalence of topical products. *Skin Pharmacol Physiol* 22(5):276–286
- Freeman-Anderson NE, Pickle TG, Netherland CD, Bales A, Buckley NE, Thewke DP (2008) Cannabinoid (CB2) receptor deficiency reduces the susceptibility of macrophages to oxidized LDL/oxysterol-induced apoptosis. *J Lipid Res* 49(11):2338–2346
- Furth P, Shamay A, Henninghausen L (1995) Gene transfer into mammalian cells by jet injection. *Hybridoma* 14(2):149–152
- Giese C, Marx U (2014) Human immunity *in vitro*—Solving immunogenicity and more. *Adv Drug Deliv Rev*
- Gill HS, Andrews SN, Sakthivel SK, Fedanov A, Williams IR, Garber DA, Priddy FH, Yellin S, Feinberg MB, Staprans SI, Prausnitz MR (2009) Selective removal of stratum corneum by microdermabrasion to increase skin permeability. *Eur J Pharm Sci* 38(2):95–103
- Gloor M, Beier B (1984) Keratoplastic effect of salicylic acid, sulfur and a tensio-active mixture. *Z Hautkr* 59(24):1657–1660
- Gonzalez T, Sethi A (2012) Curcumin (turmeric) and its evolving role in skin health. In: Preedy V (ed) *Handbook of diet, nutrition and the skin*, vol. 2. Wageningen Academic Publishers, pp 332–348
- Gotz C, Pfeiffer R, Tigges J, Blatz V, Jackh C, Freytag EM, Fabian E, Landsiedel R, Merk HF, Krutmann J, Edwards RJ, Pease C, Goebel C, Hewitt N, Fritsche E (2012) Xenobiotic metabolism capacities of human skin in comparison with a 3D epidermis model and keratinocyte-based cell culture as *in vitro* alternatives for chemical testing: activating enzymes (Phase I). *Exp Dermatol* 21(5):358–363
- Grice JE, Zhang Q, Roberts MS (2010) Chemical structure–Skin transport relationships. In: Monteiro-Riviere NA (ed) *Toxicology of the skin*. Informa Healthcare USA, Inc., New York, pp 55–68
- Hadgraft J, Lane ME (2011) Skin: the ultimate interface. *Phys Chem Chem Phys* 13(12):5215–5222
- Harder J, Schröder J-M (2002) RNase 7, a novel innate immune defense antimicrobial protein of healthy human skin. *J Biol Chem* 277(48):46779–46784
- Hayden CG, Cross SE, Anderson C, Saunders NA, Roberts MS (2005) Sunscreen penetration of human skin and related keratinocyte toxicity after topical application. *Skin Pharmacol Physiol* 18(4):170–174
- Heidl M (2009) Peptides for prolonging youth. *Adv Exp Med Biol* 611:263–264
- Hu T, Khambatta ZS, Hayden PJ, Bolmarcich J, Binder RL, Robinson MK, Carr GI, Tiesman JP, Jarrold BB, Osborne R, Reichling TD, Nemeth ST, Aardema MJ (2010) Xenobiotic metabolism gene expression in the EpiDerm *in vitro* 3D human epidermis model compared to human skin. *Toxicol In Vitro* 24(5):1450–1463
- Iervolino M, Cappello B, Raghavan SL, Hadgraft J (2001) Penetration enhancement of ibuprofen from supersaturated solutions through human skin. *Int J Pharm* 212(1):131–141
- Jenning V, Gysler A, Schäfer-Korting M, Gohla SH (2000) Vitamin A loaded solid lipid nanoparticles for topical use: occlusive properties and drug targeting to the upper skin. *Eur J Pharm Biopharm* 49(3):211–218
- Jepps OG, Dancik Y, Anissimov YG, Roberts MS (2013) Modeling the human skin barrier—towards a better understanding of dermal absorption. *Adv Drug Deliv Rev* 65(2):152–168
- Jowsey IR, Basketter DA, Westmoreland C, Kimber I (2006) A future approach to measuring relative skin sensitising potency: a proposal. *J Appl Toxicol* 26(4):341–350
- Judd A, Scurr D, Heylings J, Wan K-W, Moss G (2013) Distribution and visualisation of chlorhexidine within the skin using ToF-SIMS: a potential platform for the design of more efficacious skin antiseptic formulations. *Pharm Res* 30(7):1896–1905
- Jumbelic MI (2010) Deaths with transdermal fentanyl patches. *Am J Forensic Med Pathol* 31(1):18–21
- Karpanen TJ, Worthington T, Conway BR, Hilton AC, Elliott TS, Lambert PA (2008) Penetration of chlorhexidine into human skin. *Antimicrob Agents Chemother* 52(10):3633–3636
- Kaushik D, Costache A, Michniak-Kohn B (2010) Percutaneous penetration modifiers and formulation effects. *Int J Pharm* 386(1–2):42–51
- Kendall MA (2010) Needle-free vaccine injection. *Handb Exp Pharmacol* 197:193–219
- Kirkland D, Pfuhrer S, Tweats D, Aardema M, Corvi R, Darroudi F, Elhajouji A, Glatt H, Hastwell P, Hayashi M, Kasper P, Kirchner S, Lynch A, Marzin D, Maurici D, Meunier J-R, Müller L, Nohynek G, Parry J, Parry E, Thybaud V, Tice R, van Benthem J, Vanparys P, White P (2007) How to reduce false positive results when undertaking *in vitro* genotoxicity testing and thus avoid unnecessary follow-up animal tests: report of an ECVAM workshop. *Mutat Res/Genet Toxicol Environ Mutagen* 628(1):31–55
- Koenig K, Raphael AP, Lin L, Grice JE, Soyer HP, Breunig HG, Roberts MS, Prow TW (2011) Applications of multiphoton tomographs and femtosecond laser nanoprocesing microscopes in drug delivery research. *Adv Drug Deliv Rev* 63(4–5):388–404
- Lavker RM, Schechter NM (1985) Cutaneous mast cell depletion results from topical corticosteroid usage. *J Immunol* 135(4):2368–2373
- Lehman PA, Franz TJ (2012) Assessing the bioequivalence of topical retinoid products by pharmacodynamic assay. *Skin Pharmacol Physiol* 25(5):269–280
- Lippold BC (1992) How to optimize drug penetration through the skin. *Pharm Acta Helv* 67(11):294–300
- Lotte C, Patouillet C, Zanini M, Messenger A, Roguet R (2002) Permeation and skin absorption: reproducibility of various industrial reconstructed human skin models. *Skin Pharmacol Appl Skin Physiol* 15(Suppl 1):18–30

- Madsen P, Rasmussen HH, Leffers H, Honore B, Dejgaard K, Olsen E, Kiil J, Walbum E, Andersen AH, Basse B (1991) Molecular cloning, occurrence, and expression of a novel partially secreted protein "psoriasin" that is highly up-regulated in psoriatic skin. *J Invest Dermatol* 97(4):701–712
- Magnusson BM, Anissimov YG, Cross SE, Roberts MS (2004) Molecular size as the main determinant of solute maximum flux across the skin. *J Invest Dermatol* 122(4):993–999
- Magnusson BM, Cross SE, Winckle G, Roberts MS (2006) Percutaneous absorption of steroids: determination of *in vitro* permeability and tissue reservoir characteristics in human skin layers. *Skin Pharmacol Physiol* 19(6):336–342
- Manca ML, Manconi M, Falchi AM, Castangia I, Valenti D, Lampis S, Fadda AM (2013) Close-packed vesicles for diclofenac skin delivery and fibroblast targeting. *Colloids Surf B Biointerfaces* 111:609–617
- Mark AFK (2008) Biolistic and other needle-free delivery systems. In: Gene and cell therapy. In: Templeton NS (ed.) Gene and cell therapy. Boca Raton, FL: CRC Press, Taylor and Francis Group; pp 405–422
- McAllister DV, Wang PM, Davis SP, Park JH, Canatella PJ, Allen MG, Prausnitz MR (2003) Microfabricated needles for transdermal delivery of macromolecules and nanoparticles: fabrication methods and transport studies. *Proc Natl Acad Sci U S A* 100(24):13755–13760
- Mertin D, Lippold BC (1997) *In-vitro* permeability of the human nail and of a keratin membrane from bovine hooves: prediction of the penetration rate of antimicrobials through the nail plate and their efficacy. *J Pharm Pharmacol* 49(9):866–872
- Mitra A, Wu Y (2010) Topical delivery for the treatment of psoriasis. *Expert Opin Drug Deliv* 7(8):977–992
- Morgan TM, Reed BL, Finnin BC (1998) Enhanced skin permeation of sex hormones with novel topical spray vehicles. *J Pharm Sci* 87(10):1213–1218
- Morrel EM, Spruance SL, Goldberg DI, Iontophoretic Acyclovir Cold Sore Study Group (2006) Topical iontophoretic administration of acyclovir for the episodic treatment of herpes labialis: a randomized, double-blind, placebo-controlled, clinic-initiated trial. *Clin Infect Dis* 43(4):460–467
- Mumper RJ, Ledebur HC (2001) Dendritic cell delivery of plasmid DNA – applications for controlled genetic immunization. *Mol Biotechnol* 19(1):79–95
- Namjoshi S, Caccetta R, Benson HA (2008) Skin peptides: biological activity and therapeutic opportunities. *J Pharm Sci* 97(7):2524–2542
- Neis MM, Wendel A, Wiederholt T, Marquardt Y, Jousen S, Baron JM, Merk HF (2010) Expression and induction of cytochrome p450 isoenzymes in human skin equivalents. *Skin Pharmacol Physiol* 23(1):29–39
- Netzlaff F, Lehr CM, Wertz PW, Schaefer UF (2005) The human epidermis models EpiSkin, SkinEthic and EpiDerm: an evaluation of morphology and their suitability for testing phototoxicity, irritancy, corrosivity, and substance transport. *Eur J Pharm Biopharm* 60(2):167–178
- Nonomura K, Yamanish K, Yasuno H (1994) Upregulation of elafin/SKALP gene expression in psoriatic epidermis. *J Invest Dermatol* 103(1):88–91
- OECD (2004) Test No. 428: skin absorption: *in vitro* method. OECD Publishing, Paris. DOI: <http://dx.doi.org/10.1787/9789264071087-en>
- Paller AS (2012) Latest approaches to treating atopic dermatitis. *Chem Immunol Allergy* 96:132–140
- Pap T, Muller-Ladner U, Gay RE, Gay S (2000) Fibroblast biology. Role of synovial fibroblasts in the pathogenesis of rheumatoid arthritis. *Arthritis Res* 2(5):361–367
- Patel PJ, Ghanem AH, Higuchi WI, Srinivasan V, Kern ER (1996) Correlation of *in vivo* topical efficacies with *in vitro* predictions using acyclovir formulations in the treatment of cutaneous HSV-1 infections in hairless mice: an evaluation of the predictive value of the C\* concept. *Antiviral Res* 29(2–3):279–286
- Patzelt A, Lademann J (2013) Drug delivery to hair follicles. *Expert Opin Drug Deliv* 10(6):787–797
- Paul A, Elias CB, Shum-Tim D, Prakash S (2013) Bioactive baculovirus nanohybrids for stem based rapid vascular re-endothelialization. *Sci Rep* 3
- Pearson M, Kang SM, Song JM, Anstey AV, Ivory M, Compans RW, Birchall JC (2010) Changes in human Langerhans cells following intradermal injection of influenza virus-like particle vaccines. *PLoS One* 5(8), e12410
- Pelchrzim R, Weigmann HJ, Schaefer H, Hagemester T, Linscheid M, Shah VP, Sterry W, Lademann J (2004) Determination of the formation of the stratum corneum reservoir for two different corticosteroid formulations using tape stripping combined with UV/VIS spectroscopy. *J Dtsch Dermatol Ges* 2(11):914–919
- Perry AD, Trafletti JP (2009) Hand dermatitis: review of etiology, diagnosis, and treatment. *J Am Board Fam Med* 22(3):325–330
- Pfuhler S, Fautz R, Ouedraogo G, Latil A, Kenny J, Moore C, Diembeck W, Hewitt NJ, Reisinger K, Barroso J (2014) The Cosmetics Europe strategy for animal-free genotoxicity testing: project status update. *Toxicol In Vitro* 28(1):18–23
- Ponec M (2002) Skin constructs for replacement of skin tissues for *in vitro* testing. *Adv Drug Deliv Rev* 54(Suppl 1):S19–S30
- Poulsen BJ, Chowhan ZT, Pritchard R, Katz M (1978) The use of mixtures of topical corticosteroids as a mechanism for improving total drug bioavailability: a preliminary report. *Curr Probl Dermatol* 7:107–120
- Raghavan SL, Schuessel K, Davis A, Hadgraft J (2003) Formation and stabilisation of triclosan colloidal suspensions using supersaturated systems. *Int J Pharm* 261(1–2):153–158
- Reeve E, Wiese MD, Hendrix I, Roberts MS, Shakib S (2013) People's attitudes, beliefs, and experiences regarding polypharmacy and willingness to Deprescribe. *J Am Geriatr Soc* 61(9):1508–1514
- Roberts MS (2013) Skin delivery – to Scheuplein and beyond. Preface. *Skin Pharmacol Physiol* 26(4–6):179–180
- Roberts MS, Cross SE (1999) Percutaneous absorption of topically applied NSAIDs and other compounds: role

- of solute properties, skin physiology and delivery systems. *Inflammopharmacology* 7(4):339–350
- Roberts MS, Walker M (1993) Water – the most natural penetration enhancer. In KA Walters, J Hadgraft (eds.) *Skin penetration enhancement*. Marcel Dekker, New York, pp 1–30
- Roberts MS, Walters KA (2008) Human skin morphology and dermal absorption. In: Roberts MS, Walters KA (eds.) *Dermal absorption and toxicity assessment*, Informa Healthcare, Boca Raton, FL: CRC Press, Taylor and Francis Group, LLC; pp 1–15
- Rougier A, Lotte C, Corcuff P, Maibach HI (1988) Relationship between skin permeability and corneocyte size according to anatomic site, age, and sex in man. *J Soc Cosmet Chem* 39(1):15–26
- Saggini R, Zoppi M, Vecchiet F, Gatteschi L, Obletter G, Giamberardino MA (1996) Comparison of electromotive drug administration with ketorolac or with placebo in patients with pain from rheumatic disease: a double-masked study. *Clin Ther* 18(6):1169–1174
- Samuelsson K, Simonsson C, Jonsson CA, Westman G, Ericson MB, Karlberg A-T (2009) Accumulation of FITC near stratum corneum—visualizing epidermal distribution of a strong sensitizer using two-photon microscopy. *Contact Dermatitis* 61(2):91–100
- Sanchez WY, Prow TW, Sanchez WH, Grice JE, Roberts MS (2010) Analysis of the metabolic deterioration of *ex vivo* skin from ischemic necrosis through the imaging of intracellular NAD(P)H by multiphoton tomography and fluorescence lifetime imaging microscopy. *J Biomed Opt* 15(4):046008
- Sanford JC, Klein TM, Wolf ED, Allen N (1987) Delivery of substances into cells and tissues using a particle bombardment process. *Particul Sci Technol* 5(1):27–37
- Santos P, Watkinson AC, Hadgraft J, Lane ME (2011) Enhanced permeation of fentanyl from supersaturated solutions in a model membrane. *Int J Pharm* 407(1–2):72–77
- Santos P, Watkinson AC, Hadgraft J, Lane ME (2012) Influence of penetration enhancer on drug permeation from volatile formulations. *Int J Pharm* 439(1–2):260–268
- SCCP (2012) Notes of guidance for testing of cosmetic ingredients and their safety evaluation by the SCCS. Retrieved 26/01/14, from [http://ec.europa.eu/health/scientific\\_committees/consumer\\_safety/docs/sccs\\_s\\_006.pdf](http://ec.europa.eu/health/scientific_committees/consumer_safety/docs/sccs_s_006.pdf)
- Schafer-Korting M, Bock U, Gamer A, Haberland A, Haltner-Ukomadu E, Kaca M, Kamp H, Kietzmann M, Korting HC, Krachter HU, Lehr CM, Liebsch M, Mehling A, Netzlaff F, Niedorf F, Rubbelke MK, Schafer U, Schmidt E, Schreiber S, Schroder KR, Spielmann H, Vuia A (2006) Reconstructed human epidermis for skin absorption testing: results of the German prevalidation study. *Altern Lab Anim* 34(3):283–294
- Schafer-Korting M, Mahmoud A, Lombardi Borgia S, Bruggener B, Kleuser B, Schreiber S, Mehnert W (2008) Reconstructed epidermis and full-thickness skin for absorption testing: influence of the vehicles used on steroid permeation. *Altern Lab Anim* 36(4):441–452
- Schwarz FP, Gabard B, Rufli T, Surber C (1999) Percutaneous absorption of salicylic acid in man after topical administration of three different formulations. *Dermatology* 198(1):44–51
- Seemayer CA, Distler O, Kuchen S, Muller-Ladner U, Michel BA, Neidhart M, Gay RE, Gay S (2001) Rheumatoid arthritis: new developments in the pathogenesis with special reference to synovial fibroblasts. *Z Rheumatol* 60(5):309–318
- Seité S, Colige A, Piquemal-Vivenot P, Montastier C, Fourtanier A, Lapière C, Nusgens B (2000) A full-UV spectrum absorbing daily use cream protects human skin against biological changes occurring in photoaging. *Photodermatol Photoimmunol Photomed* 16(4):147–155
- Shah VP, Flynn GL, Yacobi A, Maibach HI, Bon C, Fleischer NM, Franz TJ, Kaplan SA, Kawamoto J, Lesko LJ, Marty JP, Pershing LK, Schaefer H, Sequeira JA, Shrivastava SP, Wilkin J, Williams RL (1998) Bioequivalence of topical dermatological dosage forms—methods of evaluation of bioequivalence. AAPS/FDA workshop on ‘Bioequivalence of Topical Dermatological Dosage Forms—Methods of Evaluating Bioequivalence’, September 4–6, 1996, Bethesda, MD. *Skin Pharmacol Appl Skin Physiol* 11(2):117–124
- Siddiqui O, Roberts MS, Polack AE (1989) Percutaneous absorption of steroids: relative contributions of epidermal penetration and dermal clearance. *J Pharmacokinet Biopharm* 17(4):405–424
- Singh P, Roberts MS (1994) Effects of vasoconstriction on dermal pharmacokinetics and local tissue distribution of compounds. *J Pharm Sci* 83(6):783–791
- Skinner K (2007) “Methods and compositions for improved uptake of biological molecules.” U.S. Patent Application No. 11/769,548.
- Stamford NPJ (2012) Stability, transdermal penetration, and cutaneous effects of ascorbic acid and its derivatives. *J Cosmet Dermatol* 11(4):310–317
- Sullivan SP, Koutsonanos DG, del Pilar Martin M, Lee JW, Zarnitsyn V, Choi S-O, Murthy N, Compans RW, Skountzou I, Prausnitz MR (2010) Dissolving polymer microneedle patches for influenza vaccination. *Nat Med* 16(8):915–920
- Taleisnik S (1971) Regulation of formation and proposed structure of the factor inhibiting the release of melanocyte-stimulating hormone. *Proc Natl Acad Sci U S A* 68(7):1428–1433
- Thong H-Y, Freeman S, Maibach HI (2007) Systemic toxicity caused by absorption of drugs and chemicals through skin. In: Roberts MS, Walters KA (eds.) *Dermal absorption and toxicity assessment*, Informa Healthcare, Boca Raton, FL: CRC Press, Taylor and Francis Group, LLC; pp 405–432
- Timothy MM; Barry LR, Barrie CF (2003) Metered-dose transdermal spray (MDTS). In: Michael JR, Hadgraft

- J, Michael SR, editors. *Modified-release Drug Delivery Technology*. New York: Marcel Dekker; pp 523–531
- Tredget EE, Nedelec B, Scott PG, Ghahary A (1997) Hypertrophic scars, keloids, and contractures: the cellular and molecular basis for therapy. *Surg Clin North Am* 77(3):701–730
- Trevithick JR, Shum DT, Redae S, Mitton KP, Norley C, Karlik SJ, Groom AC, Schmidt EE (1993) Reduction of sunburn damage to skin by topical application of Vitamin E acetate following exposure to ultraviolet B radiation: effect of delaying application or of reducing concentration of Vitamin E acetate applied. *Scanning Microsc* 7(4):1269–1281
- Trottet L (2004) *Topical pharmacokinetics for a rational and effective topical drug development process*. Thesis, University of Greenwich
- Vogt A, Combadiere B, Hadam S, Stieler KM, Lademann J, Schaefer H, Autran B, Sterry W, Blume-Peytavi U (2006) 40 nm, but not 750 or 1,500 nm, nanoparticles enter epidermal CD1a+ cells after transcutaneous application on human skin. *J Invest Dermatol* 126(6):1316–1322
- Ward NL, Loyd CM, Wolfram JA, Diaconu D, Michaels CM, McCormick TS (2011) Depletion of antigen-presenting cells by clodronate liposomes reverses the psoriatic skin phenotype in KC-Tie2 mice. *Br J Dermatol* 164(4):750–758
- Wenkers BP, Lippold BC (2000) Prediction of the efficacy of cutaneously applied nonsteroidal anti-inflammatory drugs from a lipophilic vehicle. *Arzneimittelforschung* 50(3):275–280
- Wertz PW, Madison KC, Downing DT (1989) Covalently bound lipids of human stratum corneum. *J Investig Dermatol* 92(1):109–111
- Wiechers JW (1989) The barrier function of the skin in relation to percutaneous absorption of drugs. *Pharm Weekbl Sci* 11(6):185–198
- Wiechers JW, Kelly CL, Blease TG, Dederen JC (2004) Formulating for efficacy. *Int J Cosmet Sci* 26(4):173–182
- Wu Y, Chen HD, Li YH, Gao XH, Preedy VR (2012) Antioxidants and skin: an overview. In: Preedy V (ed) *Handbook of diet, nutrition and the skin*, vol. 2. Wageningen Academic Publishers, pp 68–90
- Xi H, Cun D, Xiang R, Guan Y, Zhang Y, Li Y, Fang L (2013) Intra-articular drug delivery from an optimized topical patch containing teriflunomide and lornoxicam for rheumatoid arthritis treatment: does the topical patch really enhance a local treatment? *J Control Release* 169(1–2):73–81
- Yano T, Nakagawa A, Tsuji M, Noda K (1986) Skin permeability of various non-steroidal anti-inflammatory drugs in man. *Life Sci* 39(12):1043–1050
- Zhang Q, Grice JE, Li P, Jepps OG, Wang GJ, Roberts MS (2009) Skin solubility determines maximum trans-epidermal flux for similar size molecules. *Pharm Res* 26(8):1974–1985
- Zhao R, Yan Q, Huang H, Lv J, Ma W (2013) Transdermal siRNA-TGFβ1-337 patch for hypertrophic scar treatment. *Matrix Biol* 32(5):265–276
- Zweiman B (1990) Adverse reactions to drug formulation agents—a handbook of excipients. *J Aller Clin Immunol* 85(2):528

---

# Ethical Considerations in Research Involving Dermal and Transdermal Drug Delivery

# 24

Dusanka Krajnovic and Nina Dragicevic

---

## Contents

24.1	<b>Introduction</b> .....	393
24.2	<b>General Ethical Considerations in Research</b> .....	394
24.2.1	General Ethical Principles in Research Involving Human Beings.....	394
24.2.2	Ethical Issues in Animal Skin Testing.....	398
24.3	<b>Ethical Issues on Skin Absorption Studies</b> .....	398
24.3.1	Ethical Issues Related to In Vivo Techniques.....	399
24.3.2	Ethical Issues of In Vitro Techniques Involving Human Skins.....	400
24.3.3	Ethical Issues in Animal In Vitro Tests.....	400
	<b>Conclusion</b> .....	400
	<b>References</b> .....	401

---

## 24.1 Introduction

Ethics or in a more general context the science of bioethics is truly incorporated into the modern world of new technologies as an integral part of its social needs necessary to value the results of scientific research. High ethical standards and expectations are of great importance to science and technology development, because they promote research integrity and subsequently support public trust and societal uptake of new products, services or technology. Access to information and commitment to the research ethics are of great importance for the social impact of various research studies, but in the literature very few types of study activities have rarely been addressed within the realm of ethics. The need for proper analysis of legislative and ethical concerns has long been recognized but the models applicable through different research canals are still to be improved. Addressing ethical questions related to research studies a priori support the social recognition and uptake of the products or technology investigated or developed and add to the quality of research. In this chapter, many different kinds of ethical problems relevant to skin penetration studies will be outlined, and basic ethical principles in research involving dermal and transdermal drug delivery will be discussed in detail. Transdermal and dermal drug delivery systems provide opportunities for innovative, challenging and demanding research with patient

---

D. Krajnovic, PhD (✉)  
Department for Social Pharmacy and Pharmaceutical Legislation, Center for the Study of Bioethics, University of Belgrade Faculty of Pharmacy, 450 Vojvode Stepe, 11000 Belgrade, Serbia  
e-mail: [parojcic@pharmacy.bg.ac.rs](mailto:parojcic@pharmacy.bg.ac.rs)

N. Dragicevic, PhD  
Department of Manufacturing, Apoteka “Beograd”, Bojanska 16/IV, 11000 Belgrade, Serbia  
e-mail: [ninadragicevic@hotmail.com](mailto:ninadragicevic@hotmail.com),  
[nina.dragicevic@apotekabeograd.co.rs](mailto:nina.dragicevic@apotekabeograd.co.rs)

benefit worldwide. Transdermal drug delivery has been accepted as a potential non-invasive route of drug administration, because of its many advantages, such as avoidance of the first-pass metabolism by the liver, possible sustained drug release, minimization of pain, reduction of side effects and better patient compliance and adherence. However, as an innovative area of pharmaceutical science, drug delivery science is sometimes underestimated, when measured by the number of medicines with topical or transdermal routes of delivery compared with oral therapy (Barry 2001). As human skin inhibits drug permeation and limits daily dosage delivery, many approaches have been developed in the attempt to enhance transdermal drug delivery and achieve systemic therapeutic concentration (Barry 2001; El Maghraby et al. 2008). Techniques used to enhance dermal and transdermal drug delivery may include different approaches to increase drug permeation, such as physical enhancers (ultrasound, iontophoresis, electroporation, magnetophoresis, microneedles), chemical enhancers (sulphoxides, azones, glycols, alkanols, terpenes, etc.), particulate systems (liposomes, niosomes, transfersomes, invasomes, microemulsion, solid lipid nanoparticles) and others (Barry 2001; Dragicevic-Curic et al. 2008, 2009a, b, 2010; Erős et al. 2012).. The proper analysis of ethical and moral implications of these methods is needed before the researchers' protocols are approved, because of the diversity of the enhancers and methods themselves. In some studies, ethical issues can be extensive and could be related to the vulnerable subjects as participants, research protocols in poor-resources countries, cultural difficulties toward skin and animal testing, bioengineered skin surrogates or difficulties to obtain human skin samples (Barry 2001; Hikima et al. 2012).

---

## 24.2 General Ethical Considerations in Research

Although highly unethical research is not widespread, the history of biomedical research includes many cases of unethical research, some

of which are internationally known 'scandals', such as medical experimentation in Nazi Germany; the Tuskegee Syphilis Study and Milgram experiments. A clear appreciation of general ethical principles in research and specific ethical issues that each study method and design might request is equally important to the researcher generating experimental data as to the user of this data (e.g. patients, consumers, governmental agencies or community). Ethics of research involving human beings are related to a variety of scientific disciplines including biotechnology as well as biomedical, social and human life sciences.

### 24.2.1 General Ethical Principles in Research Involving Human Beings

Depending on the research settings, purpose(s) of the study, research objects (humans, animals, tissue samples or models) and using *in vivo/in vitro* techniques, some generally agreed ethical principles for good preclinical (research) and clinical practice must be followed. For clinical research involving human participants, including research using identifiable human materials and existing data, these principles are stated in some internationally accepted ethical normatives such as Declaration of Helsinki (ethical principles for medical research involving human subjects, the latest version since 2013, which replaces the original 1964 versions and all subsequent versions) and CIOMS Guidelines (International Ethical Guidelines for Biomedical Research Involving Human Subjects, the latest revised version since 2002). The Declaration of Helsinki inception in 1964 elaborated and clarified 10 principles stated in Nürnbeg Code and provided the ethical foundation for Proposed International Guidelines endorsed by Council for International Organizations of Medical Sciences in collaboration with World Health Organisation in 1982, focusing on research in developing countries. Both documents evolved to their current forms and are still considered to be the core of international normatives encouraging cultural sensitivity



in implementing same standards for research in developing and resource-rich countries. Although internationally accepted as ethical guidelines, these documents could not provide universal answers to all ethical issues, but clearly could guide the researchers to confront the challenging task to design, conduct, monitor, control and oversee human research project. Later in 1996 these documents influenced the development of the international guidelines proposed by International Conference of Harmonization (ICH): Good Clinical Practice Guidelines (ICH GCP/E6) as well as regional EU legal documents such as the European Clinical Trial Directive (2001/20/EC), the new Clinical Trials Regulation (CTR) EU No 536/2014 and Good Clinical Practice Directive (2005/28/EC). Subsequently, many ethical guidelines and recommendations for human studies as well as legal rules for human studies are developed based on national basis in resource-poor and resource-rich settings (see Table 24.1.) Table 24.1 summarizes some of national guidelines and recommendations for ethical conduct in research, selected in a convenient way to include some of the BRIC and ICH countries along with some transition countries and developing countries. All the listed guidelines could be found in extensor, from the sources included in the reference list.

These normatives established universally accepted principles in human research addressing privacy, confidentiality, autonomy, beneficence and non-maleficence, beneficiary, justice, intellectual property, information and consent, participation and voluntariness and scientific and ethical review of the research by ethics committee. Some of them will be discussed shortly in the following text of this section. The integrity of the principal investigator throughout the protocol development, research process and publication process of the study results, as well as clearly stated conflict of interest if there is any, are also ethical principles, generally required in all kinds of research.

*Vulnerable (research) participants* are not included in the research unless it is absolutely proven necessary. Vulnerable persons are those who are relatively (or absolutely) incapable of

protecting their own interests. More formally, they may have insufficient power, intelligence, education, resources, strength or other needed attributes to protect their own interests. Individuals whose willingness to volunteer in a research study may be unduly influenced by the expectation, whether justified or not, being of benefits associated with participation, or of a retaliatory response from senior members of a hierarchy in the case of refusal to participate may also be considered vulnerable or explored subjects. Examples are members of a group with a hierarchical structure, such as medical, pharmacy, dental, and nursing students, subordinate hospital and laboratory personnel, employees of the pharmaceutical industry, members of the armed forces and persons kept in detention. Other vulnerable persons include patients with incurable diseases, people in nursing homes, unemployed or impoverished people, patients in emergency situations, ethnic minority groups, homeless people, nomads, refugees, minors and those incapable of giving consent. This list may not be exhaustive as there may be circumstances in which other groups are considered vulnerable, women for example, in an orthodox patriarchal society or adult young men having to ask a chieftain (Marshall 2007; Benatar 2002, 2004; Nuffield 2002; CIOMS 2012; WMA 2013; ICH 1996).

*Research ethics committee (REC)* is an independent multidisciplinary board of individuals who undertake the review of research protocols for ethical considerations. It is also known in local, regional and international regulations under different names: ethical review board (ERB), ethical review committee (ERC) are the most common used in Europe whereas in USA, this committee is known as human research ethics committee [HREC], institutional review board [IRB] (EC 2001; Garrard and Dawson 2005; CIOMS 2002; WMA 2005, WMA 2013; Council of Europe 2005; ICH 1996). The EU Directive on Clinical Trials defines a research ethics committee as: *an independent body in a Member State, consisting of healthcare professionals and nonmedical members, whose responsibility it is to protect the rights, safety*

**Table 24.1** Summary of ethical guidelines and recommendations for human studies from 16 selected countries around the world. Documents are sorted alphabetically by country's origin regardless of document's title in English and the date of endorsement

Country	Year of endorsement	National guideline or recommendation (title in English)	References
Australia	2000, 2006	Note for Guidance on Good Clinical Practice (CPMP/ICH/135/95) The Australian Clinical Trial Handbook, 2006	Therapeutic Goods Administration (2000, 2006)
Bosnia	2010	Rules on clinical testing and medical devices	The Ministry of Civil Affairs of Bosnia and Herzegovina (2010)
Brazil	2010	Good Clinical Practices: Document of the Americas.	Pan American Health Organization (2010)
Canada	2006	Guidance for records related to clinical trials	Health Canada (2006)
Croatia	2010	Rules on clinical trials and good clinical practice	Ministry of Health and Welfare (2010)
France	2006	Good clinical practice for biomedical research on human subjects	Décision du 24 novembre (2006)
Germany	2012	Good clinical practice - Verordnung	(Verordnung über die Anwendung der Guten Klinischen Praxis bei der Durchführung von klinischen Prüfungen mit Arzneimitteln zur Anwendung am Menschen) (GCP-Verordnung – GCP-V)
Great Britain	2005	Practice Guidance on Pharmacy Services for Clinical Trials	
India	2011	Draft Guidance on Approval of Clinical Trials and New Drugs UK – consolidated version of the Medicines for Human Use (Clinical Trials) Regulations 2004 (SI 1031)with all amendments (2006, 2008, 2009, 2010)	
New Zealand	2000	Note for Guidance on Good Clinical Practice (CPMP/ICH/135/95)	Therapeutic Goods Administration (TGA): Note for Guidance on Good Clinical Practice (2000)
Nigeria	2009	Good Clinical Practice Regulations	National Agency for Food and Drug Administration and Control Nigeria (2009a, b)
Norway	2010	Guidelines on Notification for Clinical Investigation of Medical Devices in Norway	
Serbia	2011	Rules on the content of the request or the documentation for the approval of clinical trials of medicinal products and medical devices as well as the way to clinical trials and medical devices	Ministry of health Serbia (2011)
Singapore	2011	Guidelines for Clinical Practice	Ministry of health Singapore, 2011
South Africa	2006	South African Good Clinical Practice Guidelines	Department of Health: Pretoria, South Africa (2006)
USA	2011	Good Clinical Practice Resource Guide	DMID: Good Clinical Practice Resource Guide (2011)

and wellbeing of human subjects involved in a trial and to provide public assurance of that protection, by, among other things, expressing an opinion on the trial protocol, the suitability of the investigators and the adequacy of facili-

ties, and on the methods and documents to be used to inform trial subjects and obtain their informed consent (EC 2001). Most ECs review study protocols for a single institution, such as hospital, with or without academic affiliation,

while some are centralized, and review protocols from more than one institution/clinic, which is very useful for multi-centred studies. Unfortunately they do not exist in many developing and poor-resource countries where much research is conducted nowadays. In some countries, protocols for studies are reviewed by hospital and faculty ethics committees which serve as research ethics committees (investigational boards) as well.

*Informed consent* is a decision to participate in research, taken by a competent individual who has received the necessary information and has adequately understood the information, and who, after considering the information, has reached the decision without having been subjected to coercion, undue influence or inducement, or intimidation. Involvement of uncompetent subjects are rarely needed for skin research in general, and could be justified for dermal and transdermal drug delivery studies, only if acceptable risk-benefit balance is estimated and predictable risks and burdens are identified. In the case of some vulnerable subjects not legally competent, informed consent is obtained from the legal guardians or parents. In a case of subjects' literacy, when written consent is not possible to obtain, an eye witness oral informed consent is recommended (WMA 2013; CIOMS 2002; NAFDAC 2009a, b; Nuffield 2007). An informed or valid consent must address to three questions: (1) does the potential participant have the capacity to consent requiring consideration of such issues as age, maturity, cognitive ability; (2) is the consent voluntary (i.e. is the decision made free from coercion, inducement, or intimidation including pressure from a family member); and (3) has the potential participant received sufficient information on which to base a decision? The CIOMS guidelines also stress that consent is not an event, but a process in which potential participants need to have time to study information, think about them and ask additional questions before being asked to make a decision. It is of absolute importance that information should be available in appropriate languages and written in a style that is understandable by patients, taking into consideration relevant factors, and including cultural and sometimes religious differences.

Consent form should be easily understandable and in writing, that documents a potential participant's consent to be involved in research and which describes the rights of an enrolled research participant. This form, in a clear and respectful manner, should include the following: title of research; researchers involved; research time frame; purpose of research; description of research; potential harms and benefits; treatment alternatives; statement of confidentiality; information and data to be collected; how long the data will be kept, how it will be stored and who can access it; any conflicts of interest; a statement of the participant's right to withdraw from participation at any point without any circumstances; and declarative statement of understanding that a participant agrees to and signs. The consent form should be in a language that the potential participant understands and for those with limited literacy, the verbal communication of the consent document details should be provided along with proper documentation of consent, if it will be given (WMA 2013; CIOMS 2002; ICH 1996; DHHS 2012).

Ethics review and evaluation of the research must take into account at least three considerations: ethical challenges, the institutional requirements and the legal constraints. Applicable law and legal rules are not always consistent and they could differ greatly. Besides, adhering ethical principles to national regulations and translating and applying them to studies carried out in developing countries is sometimes difficult because of social and cultural environments. Marchall elaborated several recommendations for researchers in multinational studies conducted in developing countries. They are listed below:

1. *Respect the cultural traditions of studied populations and communities*
2. *Strengthen capacity for developing collaborative partnerships*
3. *Strengthen education in research ethics for investigators*
4. *Strengthen capacity for independent ethical review of protocols*
5. *Ethical challenges in study design and informed consent for health research in resource-poor settings*

6. *Develop culturally meaningful approaches to informed consent*
7. *Apply appropriate standards of care and provisions for medical treatment*
8. *Provide ongoing feedback to the studied participants and community*
9. *Develop plans for resolving conflicts surrounding research implementation* (Marshall 2007).

### 24.2.2 Ethical Issues in Animal Skin Testing

Animal test or animal research refers to the use of live animals, animal tissues and samples or animal models in different research and for various purposes. Animals used for preclinical research are after the experiment killed or euthanized and their skin, blood and excrement are analyzed. For many substances (drugs) over the years the rate of skin absorption is calculated. In the scientific world globally, live animal tests were for some time considered to be morally and economically unacceptable (PETA 2013). Besides, despite their years of use, animal-

based studies of skin absorption rate have never been properly validated to establish their relevance to people. Other disadvantages include the potential for biasing the results of the animal studies by the process of washing off the test chemical from the animal's skin, thus facilitating absorption of the test chemical. Alternatives to the use of animals in toxicity testing include replacing animal tests with non-animal methods, as well as modifying animal-based tests to reduce the number of animals used and to minimize pain and distress of animals. This ethical practice is accepted globally in many countries and is known as the three Rs principles. When carrying out animal testing, researchers should provide a detailed explanation what step they have taken to comply with the principles of reduction, replacement and refinement. Reduction refers to methods that enable the investigator to obtain comparable levels of information from fewer animals, or to obtain more information from the same number

of animals. Replacement refers to the preferred use of non-animal methods over animal methods whenever it is scientifically possible. Refinement refers to methods that alleviate and minimize potential pain, suffering or distress for the animals used. These guiding principles are widely acknowledged as good science at universities, pharmaceutical companies, commercial facilities that provide animal testing for the industry, animals laboratory and others (Pauwels 2007; PETA 2013). Non-animal tests are generally faster and less expensive than the animal tests they replace and improve upon and could include, for example, the use of human skin leftover from surgical procedures or donated cadavers to measure the rate at which an active substance is able to penetrate the skin. Also the research involving animals or animals' skin must conform to the generally accepted scientific principles, based on the relevant sources and scientific literature and conducted in an adequate laboratory conditions, taking into account the institutional requirements as well as applicable laws. The conduct of animal-based tests is governed by national regulations and legislation, whereas studies using humans, especially in vivo studies, are generally governed by the international guidelines. The legislative requirements may vary widely between the countries, and not just in scope but in enforcement as well (Wakefield and Chilcott 2008).

### 24.3 Ethical Issues on Skin Absorption Studies

General ethical considerations in human studies that are applicable for those using any kind of dermal and transdermal drug delivery techniques are associated with consent, vulnerable and non-competent subjects, privacy and confidentiality, justice in research and balancing harms and benefits for the study subjects (Nuffield 2007; NAFDAC 2009a, b; Council of Europe CoE 2005; Marshall 2007). In the armamentarium of skin absorption and penetration studies, many different models are possible to be used, and the

choice of the specific ethical considerations are possible, as well as financial constraints and problems with limited availability of models or facilities, especially in resource-poor settings (Marshall 2007). As methods for measuring skin penetration and dermal delivery could be divided into two categories: in vivo and in vitro method, several different ethical issues have to be taken into account, assuming an acceptable risk-benefit balance, addressing privacy, confidentiality, intellectual property, consistency with local legislative and regulatory requirements, appropriate training and qualifications of the investigations and proper data management during and after the research. There are two kinds of in vivo measurements of skin penetration studies: (1) animal studies and (2) human studies, and both need a proper analysis of their ethical implications. Which method to apply will depend on the research question to be answered, which is probably one of the reasons why the present OECD guideline for studies on percutaneous penetration accepts several methods (OECD 2004a, c). In vivo transdermal and dermal human studies are carried out to determine the flux, the amount of drug delivered to the skin, as well as the therapeutic effectiveness. A drug's dermal delivery rate is mainly of interest to regulatory agencies concerned with toxicity or chemical exposures in the workplace. As human skin has only limited availability, alternatives were necessary and during the last decade several experimental models (in vitro technique) related to transdermal penetration and percutaneous penetration have been standardized and validated. In general, the in vitro models have the advantage of avoiding almost all ethical aspects associated with in vivo skin penetration studies (Holmgaard and Bo Nielsen 2009). *Ethical considerations in skin penetration studies include an assessment of predictable risk, burdens and scientific importance of the study, but also sensitive privacy concerns, content of informed consent and the process of obtaining consent. The recruiting method and possible advertising for recruitment of participants are also of relevance and must be thoroughly addressed by ethics committee's evaluation. Following the Declaration of Helsinki and ICH*

Good Clinical Practice, research must confirm to generally accepted scientific principles meaning that it should be conducted in adequate settings (laboratory equipment and qualified research staff) and be based on thorough knowledge of the scientific literature and relevant source of information (adequate study design and materials) (WMA 2013; ICH 1996).

### 24.3.1 Ethical Issues Related to In Vivo Techniques

Much attention related to percutaneous penetration studies have been discussed and introduced recently, with the intention to assess the penetration characteristics of specific substances (test substance). The gold standard, in vivo technique when the test substance (drug) is applied to the skin of human volunteers and blood and/or urine is collected and analyzed, has been used before all other techniques were ever considered and is still used where there is no adverse risk to the human volunteers participating (Benech-Kieffer et al. 2003; Hueber-Becker et al. 2004, 2007; Lammers et al. 2005; Nohynek et al. 2004, 2006). The amount of test substance measured in the blood and/or urine gives a good indication of the amount of substance absorbed through the skin into the systemic circulation. In transdermal/dermal drug delivery research combined with therapy, the human volunteers are not healthy persons but patients, and rarely, even vulnerable participants. When knowledge of the drug (active substance) is limited or incomplete and research is intended to disclose different unknown characteristics, the risk assessment may not be completely explained, which would give rise to ethical concern and would limit the use of healthy volunteers or patients. In traditional in vivo human technique, many ethical issues are to be considered by the investigator and evaluated by the ethics committee before the research is even allowed, in order to protect life, health, dignity, integrity, right to self-determination, privacy and confidentiality of those who gave consent to voluntarily participate.

### 24.3.2 Ethical Issues of In Vitro Techniques Involving Human Skins

During the last decade research efforts have been directed towards standardization and validation of experimental models. Various tissue culture methods have been rigorously evaluated and accepted in Europe as total replacements for animal-based skin absorption studies (OECD 2004c; PETA 2013; Holmgaard and Bo Nielsen 2009). These methods use skin from a variety of sources to measure the passage of a test chemical into and across skin to a fluid reservoir. By using an in vitro model, the ethical topics are minimized since the use of human volunteers or animals are excluded and the donor skin samples would be sent to destruction anyway, or artificial models are used (Holmgaard and Bo Nielsen 2009). Other advantages of the in vitro model are the possibilities to replicate the experiment with samples from the same person. Also different species can be studied under identical laboratory conditions and enable comparisons within and between species. The reliability and relevance of in vitro skin absorption studies have been thoroughly established through a number of international expert reviews, and these methods have been codified and accepted as an official test guideline of the Organization for Economic Cooperation and Development (OECD 2004b, c; Lehman et al. 2011).

### 24.3.3 Ethical Issues in Animal In Vitro Tests

Animal in vitro tests included using different forms of animal skins, but having a number of scientific disadvantages over the non-animal tests. Due to widespread demands in skin absorption studies based on regulatory aspects on the one hand, and scientific and public empowerment to ending live animal tests on the other hand, the need to establish alternative models has been recognized. In addition, some researchers have ethical and cultural restraints to use human skin (Hikima et al. 2012). Animal skin forms from pig (ear, flank, abdomen, or back),

mouse, hairless rat, hamster (cheek pouch), snake (shed skin) and cow udder have been suggested as alternatives (Haigh and Smith 1994). However, in comparison to human skin, animal species have different permeability of skin, so various enhancement of animal skin's permeability was also investigated. In general, porcine skin, especially the ear which is also easily available, is reported to match human skin best, and there are references pointing also to the alternative of cow udder skin. Searching for other alternative methods as well as bioengineered skin surrogates (artificial human skin) in the future would be additionally fostered with the EU ban of tests on animals for cosmetic products and of the marketing of final cosmetic products/ingredients tested on animals, from September 2009 (Klein 2012; EC 2003, 2009).

### Conclusion

Transdermal and dermal drug delivery is one of the most promising routes of drug administration. There are in vitro as well as in vivo methods to investigate skin drug delivery through skin, and both have their own set of advantages, limitations and disadvantages. Which method will be used by researchers will depend on the research question(s), available resources and laboratory conditions, and scientific knowledge. Institutional requirements, applicable local and regional laws and regulations have to be correctly addressed for the research to be conducted, and sometimes specific cultural and moral-defined issues must be fulfilled as well. Several guiding ethical principles are widely acknowledged including risk-benefit balance, vulnerable and incapable participants, privacy concerns, informed consent, conflict of interest, confidentiality, scientific integrity and intellectual property.

**Acknowledgement** DK's work is down within the framework of a project financially supported by the Ministry of Science and Education of the Republic of Serbia (Project No. 41004). The funding agreement ensured the author's independence in designing the research, interpreting the data, writing and publishing the report.

DK wishes to thank her colleague Mrs Andrijana Milošević Georgiev for technical assistance with the final preparation of the text.

## References

- Barry WB (2001) Novel mechanism and devices to enable successful transdermal delivery. *Eur J Pharm Sci* 14:101–114
- Benatar S (2002) Reflections and recommendations in research ethics in developing countries. *Soc Sci Med* 54:1131–1141
- Benatar SR (2004) Linking moral progress to medical progress: New opportunities for the declaration of Helsinki. *World Med J* 50(1):11–13
- Benech-Kieffer F, Meuling WJ, Leclerc C, Roza L, Leclaire J, Nohynek G (2003) Percutaneous absorption of Mexoryl SX in human volunteers: comparison with in vitro data. *Skin Pharmacol Appl Skin Physiol* 16:343–355
- Council for International Organizations of Medical Sciences (CIOMS) (2002) International ethical guidelines for biomedical research involving human subjects. [http://www.cioms.ch/publications/layout\\_guide2002.pdf](http://www.cioms.ch/publications/layout_guide2002.pdf). Accessed 2 Feb 2013
- Council of Europe (CoE) (2005) Additional protocol to the convention on human rights and biomedicine, concerning biomedical research. <http://conventions.coe.int/treaty/EN/Treaties/Html/195>. Accessed 22 Jan 2013
- Décision du 24 novembre 2006 fixant les règles de bonnes pratiques cliniques pour les recherches biomédicales portant sur des médicaments à usage humain. *JORF n°277 du 30 novembre 2006*, page 18033, texte n° 64. <http://www.legifrance.gouv.fr/affichTexte.do?cidTexte=JORFTEXT000000819256>
- Department of Health (2006) South African good clinical practice guidelines. Department of Health, Pretoria. <http://www.kznhealth.gov.za/research/guideline2.pdf>. Accessed 2 Feb 2013
- Department of Health and Human Services (DHHS) (2012) Code of Federal Regulations; Protection of human subjects; Title 21, Part 50. <http://www.access-data.fda.gov/scripts/cdrh/cfdocs/cfcfr/CFRSearch.cfm?CFRPart=50>. Accessed 22 Jan 2013
- Division of Microbiology and Infectious Diseases (DMID): Good Clinical Practice Resource Guide (2011). <http://www.niaid.nih.gov/LabsAndResources/resources/DMIDClinRsrch/Documents/handbook.pdf>. Accessed 2 Feb 2013
- Dragicevic-Curic N, Scheglmann D, Albrecht V, Fahr A (2008) Temoporfin-loaded invasomes: development, characterization and in vitro skin penetration studies. *J Control Release* 127(1):59–69
- Dragicevic-Curic N, Scheglmann D, Albrecht V, Fahr A (2009a) Development of different temoporfin-loaded invasomes-novel nanocarriers of temoporfin: characterization, stability and in vitro skin penetration studies. *Colloids Surf B Biointerfaces* 70(2):198–206
- Dragicevic-Curic N, Scheglmann D, Albrecht V, Fahr A (2009b) Development of liposomes containing ethanol for skin delivery of temoporfin: characterization and in vitro penetration studies. *Colloids Surf B Biointerfaces* 74(1):114–122
- Dragicevic-Curic N, Gräfe S, Gitter B, Winter S, Fahr A (2010) Surface charged temoporfin-loaded flexible vesicles: in vitro skin penetration studies and stability. *Int J Pharm* 384(1–2):100–108
- El Maghraby GM, Barry BW, Williams AC (2008) Liposomes and skin: from drug delivery to model membranes. *Eur J Pharm Sci* 34(4–5):203–222. doi:10.1016/j.ejps.2008.05.002
- Erős G, Hartmann P, Berkó S, Csizmazia E, Csányi E, Sztojkov-Ivanov A, Németh I, Szabó-Révész P, Zupkó I, Kemény L (2012) A novel murine model for the in vivo study of transdermal drug penetration. *ScientificWorldJ*. doi:10.1100/2012/543536/
- Garrard E, Dawson A (2005) What is the role of the research ethics committee? Paternalism, inducements, and harm in research ethics. *J Med Ethics* 31(7):419–423. doi:10.1136/jme.2004.010447
- Haigh JM, Smith EW (1994) The selection and use of natural and synthetic membranes for in vitro diffusion experiments. *Eur J Pharm Sci* 2:311–330
- Health Canada (2006) Guidance for records related to clinical trials. [http://www.hc-sc.gc.ca/dhp-mps/alt\\_formats/hpfb-dgpsa/pdf/compli-conform/gui\\_68-eng.pdf](http://www.hc-sc.gc.ca/dhp-mps/alt_formats/hpfb-dgpsa/pdf/compli-conform/gui_68-eng.pdf). Accessed 2 Feb 2013
- Hikima T, Kaneda N, Matsuo K, Tojo K (2012) Prediction of percutaneous absorption in human using three-dimensional human cultured epidermis LabCyte EPI-MODEL. *Biol Pharm Bull* 35(3):362–368
- Holmgaard R, Bo Nielsen J (2009) Dermal absorption of pesticides – evaluation of variability and prevention. In: Pesticides Research No. 124. Danish Ministry of the Environment. <http://www2.mst.dk/udgiv/publications/2009/978-87-7052-980-8/pdf/978-87-7052-981-5.pdf>. Accessed 23 Feb 2013
- Hueber-Becker F, Nohynek GJ, Meuling WJ, Benech-Kieffer F, Toutain H (2004) Human systemic exposure to a [14C]-para-phenylenediamine-containing oxidative hair dye and correlation with in vitro percutaneous absorption in human or pig skin. *Food Chem Toxicol* 42(8):1227–36
- Hueber-Becker F, Nohynek GJ, Dufour EK, Meuling WJ, de Bie AT, Toutain H, Bolt HM (2007) Occupational exposure of hairdressers to [14C]-para-phenylenediamine-containing oxidative hair dyes: a mass balance study. *Food Chem Toxicol* 45(1):160–9
- International Conference of Charmonisation (ICH) (1996) Good clinical practice guidelines. [http://www.ich.org/fileadmin/Public\\_Web\\_Site/ICH\\_Products/Guidelines/Efficacy/E6\\_R1/Step4/E6\\_R1\\_Guideline.pdf](http://www.ich.org/fileadmin/Public_Web_Site/ICH_Products/Guidelines/Efficacy/E6_R1/Step4/E6_R1_Guideline.pdf). Accessed 12 Dec 2012
- Klein J (2012) EU cosmetics directive and the Ban on animal testing: compliance, challenges, and the GATT as a potential barrier to animal welfare. *Trans Law Contemp Probl* 21:251–275
- Lammers JHCM, Meuling WJ, Muijsers H, Freidig AP, Bessems JGM (2005) Neurobehavioural evaluation and kinetics of inhalation of constant or fluctuating toluene concentrations in human volunteers. *Environ Toxicol Pharmacol* 20:431–442

- Lehman PA, Raney SG, Franz TJ (2011) Percutaneous absorption in man: in vitro-in vivo correlation. *Skin Pharmacol Physiol* 24(4):224–230. doi:10.1159/000324884
- Marshall PA (2007) Ethical challenges in study design and informed consent for health research in resource-poor settings. World Health Organization, Geneva, [http://whqlibdoc.who.int/publications/2007/9789241563383\\_eng.pdf](http://whqlibdoc.who.int/publications/2007/9789241563383_eng.pdf). Accessed 12 Dec 2012
- Ministry of Health and Welfare (2010) Rules on clinical trials and good clinical practice. <http://narodne-novine.nn.hr/clanci/sluzbeni/329774.html>. Accessed 2 Feb 2013
- Ministry of Health Serbia (2011) Rules on the content of the request or the documentation for the approval of clinical trials of medicinal products and medical devices as well as the way to clinical trials and medical devices. <http://www.alims.gov.rs/ciril/files/2012/06/p-klinicka-64-2011.pdf>. Accessed 2 Feb 2013
- Ministry of Health Singapore (2011) Guidelines for clinical practice. [http://www.moh.gov.sg/content/moh\\_web/home/Publications/guidelines/cpg.html](http://www.moh.gov.sg/content/moh_web/home/Publications/guidelines/cpg.html). Accessed 2 Feb 2013
- National Agency for Food and Drug Administration and Control (NAFDAC) (2009) Good Clinical Practice Regulations. <http://apps.who.int/medicinedocs/documents/s17103e/s17103e.pdf>. Accessed 2 Feb 2013.
- National Agency for Food and Drug Administration and Control (NAFDAC) (2009) Documentation Guidelines for Clinical Trial in Nigeria. <https://www.google.rs/search?q=Documentation+Guidelines+for+Clinical+Trial+in+Nigeria&oq=Documentation+Guidelines+for+Clinical+Trial+in+Nigeria&aqs=chrome.0.57.710j0&sourceid=chrome&ie=UTF-8>. Accessed 2 Feb 2013
- Nohynek GJ, Skare JA, Meuling WJ, Hein DW, De Bie AT, Toutain H (2004) Urinary acetylated metabolites and N-acetyltransferase-2 genotype in human subjects treated with a para-phenylenediamine-containing oxidative hair dye. *Food Chem Toxicol* 42:1885–1891
- Nohynek GJ, Meuling WJ, Vaes WH, Lawrence RS, Shapiro S, Schulte S, Steiling W, Bausch J, Gerber E, Sasa H, Nau H (2006) Repeated topical treatment, in contrast to single oral doses, with Vitamin A-containing preparations does not affect plasma concentrations of retinol, retinyl esters or retinoic acids in female subjects of child-bearing age. *Toxicol Lett* 163: 65–76
- Nuffield Council on Bioethics (NCB) (2002) The ethics of research related to healthcare in developing countries. <http://www.nuffieldbioethics.org/sites/default/files/Ethics%20of%20research%20related%20to%20healthcare%20in%20developing%20countries%20I.pdf>. Accessed 5 Feb 2013
- Nuffield Council on Bioethics (NCB) (2007) Public health: ethical issues. <http://www.nuffieldbioethics.org/sites/default/files/Public%20health%20-%20ethical%20issues.pdf>. Accessed 17 Jan 2013
- Organisation for Economic Co-operation and Development (OECD) (2004a) Skin absorption: *in vivo* method. In: OECD Guideline for the testing of Chemicals. Organisation for Economic Co-operation and Development. <http://www.oecd-library.org/docserver/download/9742701e.pdf?expires=1372542736&id=id&accname=guest&checksum=ADC7492D661D414EAB7E00307E6FA41E>. Accessed 23 Feb 2013
- Organisation for Economic Co-operation and Development (OECD) (2004b) Skin absorption: in vitro method. In: OECD Guideline for the testing of chemicals. Organisation for Economic Co-operation and Development. <http://iccvam.niehs.nih.gov/SuppDocs/FedDocs/OECD/OECDtg428.pdf>. Accessed 23 Feb 2013
- Organisation for Economic Co-operation and Development (OECD) (2004c) Guidance document for the conduct of skin absorption studies. In: OECD Environmental Health and Safety Publications Series on Testing and Assessment No. 28. Environment Directorate Organisation for Economic Co-operation and Development.
- Pan American Health Organization (2010) Good Clinical Practices: Document of the Americas. [http://www.anvisa.gov.br/medicamentos/pesquisa/goodclinical-practices\\_english.pdf](http://www.anvisa.gov.br/medicamentos/pesquisa/goodclinical-practices_english.pdf). Accessed 2 Feb 2013
- Pauwels E (ed) (2007) Ethics for researchers – Facilitating Research Excellence in FP7. European Communities, Luxemburg
- People for the ethical treatment of animals (PETA): Skin absorption: animal test. <http://www.peta.org/issues/animals-used-for-experimentation/skin-absorption.aspx>. Accessed 23 Feb 2013
- The European Parliament and the Council of the European Union (EC) (2001) Directive 2001/20/EC of the European Parliament and of the Council of 4 April 2001 on the approximation of the laws, regulations and administrative provisions of the Member States relating to the implementation of good clinical practice in the conduct of clinical trials on medicinal products for human use. <http://eur-lex.europa.eu/LexUriServ/LexUriServ.do?uri=CELEX:32001L0020:EN:NOT>. Accessed 2 Feb 2013
- The European Parliament and the Council of the European Union (EC) (2003) Directive 2003/15/EC of the European Parliament and of the council of 27 February 2003 amending Council Directive 76/768/EEC on the approximation of the laws of the Member States relating to cosmetic products. <http://eur-lex.europa.eu/LexUriServ/LexUriServ.do?uri=OJ:L:2003:066:0026:0035:en:PDF>. Accessed 2 Feb 2013
- The European Parliament and the Council of the European Union (EC) (2009): Regulation EU No 1223/2009 of the European Parliament and of the Council of 30 November 2009 on cosmetic products. [http://ec.europa.eu/health/sites/health/files/endocrine\\_disruptors/docs/cosmetic\\_1223\\_2009\\_regulation\\_en.pdf](http://ec.europa.eu/health/sites/health/files/endocrine_disruptors/docs/cosmetic_1223_2009_regulation_en.pdf). Accessed 2 Feb 2013



- The Ministry of Civil Affairs of Bosnia and Herzegovina (2010) Rules on clinical testing and medical devices. [http://www.almbih.gov.ba/\\_doc/regulative/pravilnik\\_klinicka\\_bos.pdf](http://www.almbih.gov.ba/_doc/regulative/pravilnik_klinicka_bos.pdf). Accessed 2 Feb 2013
- Therapeutic Goods Administration (TGA) (2000) Note for Guidance on Good Clinical Practice (CPMP/ICH/135/95). <http://www.tga.gov.au/pdf/euguide/ich13595.pdf>. Accessed 2 Feb 2013
- Therapeutic Goods Administration (TGA) (2006) The Australian Clinical Trial Handbook. <http://www.tga.gov.au/pdf/clinical-trials-handbook.pdf>. Accessed 2 Feb 2013
- Verordnung über die Anwendung der Guten Klinischen Praxis bei der Durchführung von klinischen Prüfungen mit Arzneimitteln zur Anwendung am Menschen (GCP-Verordnung - GCP-V)
- Wakefield JC, Chilcott RP (2008) In vivo measurements of skin absorption. In: Chilcott RP, Price S (eds) Principles and practice of skin toxicology. Wiley, Chichester, pp 109–115
- World Medical Association (WMA) (2005) Medical ethics manual, 2nd edn. [http://www.wma.net/en/30publications/30ethicsmanual/pdf/ethics\\_manual\\_en.pdf](http://www.wma.net/en/30publications/30ethicsmanual/pdf/ethics_manual_en.pdf). Accessed 15 Feb 2013
- World Medical Association (WMA) (2013) Declaration of Helsinki: ethical principles for medical research involving human subjects as adopted by the WMA October 2013. <http://www.wma.net/en/30publications/10policies/b3/>. Accessed 2 Feb 2014

---

# Index

## A

- Ablation methods
  - artificial pores of skin, 237–238
  - gene delivery, 239
  - laser, 237
  - lipophilic drugs, 233
  - mechanisms, 476
  - peptide patch technologies, 239–240
  - physical, 233–234
  - preclinical applications to skin
    - nonthermal, 476
    - thermal, 476
  - radio-frequency electrical, 234–236
  - thermal, 236–237
  - vaccination and allergy treatment, 238–239
- Abrasion
  - mechanism, 475
  - preclinical and clinical applications, 475–476
- Acoustic cavitation, 6
- Actinic keratosis, 39
- Active microporation techniques
  - electroporation, 263
  - high-pressure gas or liquid, 259–261
  - laser microporation, 261–262
  - radio frequency, 261
  - thermal microporation, 261
  - ultrasound, 262–263
- Active pharmaceutical ingredient (API), 221
- Acute postoperative pain, 85
- Acyclovir (ACV), 72, 81–82
- Ag-coated stainless steel gauze anode, 150, 152–153
- Allergy treatment, by ablation methods, 238–239
- Alniditan, by electroporation, 117
- Altea's PassPort® system, 267–268
- Alzheimer's disease, 86
- Aminolevulinic acid, 333
- 5-Aminolevulinic acid, 44
- Amphotericin B, 44
- Anaesthetics, topical, 81
- Analytical methods, 391–392
  - experimental methods, 393
  - iontophoretic drug transport, 394
  - mathematical modeling, 392–393

- passive and chemically enhanced diffusion, 393–394
- Antibiotics, iontophoresis, 89
- Anticancer drugs, 39
- Antigen-presenting cells (APCs), 442
- Antineoplastic agents, 83
- Aquapuncture, 222
- Aspergillus parasiticus*, 165
- Atenolol, by electroporation, 117
- A-Wand systems, 47

## B

- Ballistic vaccination, 487–489
- Becton, Dickinson and Company (BD), 269
- Bevacizumab, 64, 89
- Biological effects, of microwaves
  - biological membranes, 165–166
  - non-thermal, 164–165
  - thermal, 164
- Biological fluid, 312
- Biological micro-device system, 344
- BioMEMS, 306
- Blood–brain barrier (BBB), 166
- Buprenorphine, by electroporation, 117

## C

- Caffeine, 45
- Calcein
  - electroporation, 117
  - sonophoresis, 41, 45
- Calcitonin
  - electroporation, 117
  - iontophoresis, 87
- Calcitonin gene-related peptide (CGRP), 84
- Calcium, 42, 45
- Caliper electrodes, 128
- Cardiotonics, 41
- Cavitation
  - acoustic, 6
  - inertial, 6–7
  - stable, 6
  - ultrasound-induced, 7

- Chemical enhancers  
 and electroporation  
   factors influencing drug delivery, 408  
   investigation, 407  
   synergistic enhancement effect, 408–415  
 and microneedles  
   concept of, 415  
   synergistic enhancement effect, 415–416  
 and sonophoresis  
   definition, 400  
   low-frequency, 401–402  
   mechanisms of action, 402  
   synergistic enhancement effect, 402–407  
   ultrasound, 400–401  
   uses, 401  
   ultrasound and, 50  
 Chemical penetration enhancers (CPEs), 392, 396, 445  
 Chemical permeation enhancers, 129  
 Cicatrizants, 41  
 Coat and poke, 275, 276  
 Coated microneedles (CMNs)  
   arrays (*see also* Microneedles (MNs) arrays)  
     dip-coating methods, 280, 281  
     disadvantage, 280  
     drug formulation, 280  
     follow-up study, 282–283  
     Macroflux<sup>®</sup>, 282  
     OVA, 282–283  
     PLA types, 283, 284  
     research groups, 281–282  
     versatility, 280  
   skin vaccination methods, 494  
 Confocal laser scanning microscopy (CLSM), 203  
 Conventional electroporation (ON-SKIN EP), 383–386  
 Conventional heating treatment, 162, 165  
 Corticosteroids, 40  
 Cosmetic applications, of iontophoresis, 90–92  
 Cutaneous DNA immunization, 441–442  
   hair follicles  
     after “cold” waxing-based plucking, 447  
     CSSS, 448–449  
     cycle, 446–447  
     delivery sites, 446  
     structure and biology, 446  
     “warm” waxing *vs.* “cold,” 448  
   microneedle-mediated  
     DNA-coated microprobes, 451  
     electroporation techniques, 451  
     FDA-approved smallpox vaccine, 452  
     gene gun, 451  
     influenza vaccines, 452  
     methods, 450–451  
     on nanoparticles, 455–456  
     nanopatch microprojections, 453  
     novel approach, 449–450  
     optimization, 454  
     PEM, 454  
   stratum corneum barrier  
     chemical techniques, 445  
     novel techniques, 445  
     physical techniques, 443–445  
 Cyanoacrylate skin surface stripping (CSSS), 448–449  
 Cyclodextrins, 414  
 Cyclosporin A  
   electroporation, 117  
   sonophoresis, 44  
 Cystic fibrosis, 81
- D**  
 Dendritic cells (DCs), 442  
 Dermaportation system, 198–199  
 Dermisonics, Inc. (USA), 46–47  
 Desmopressin (DDAVP), 289  
 Dexamethasone, 89  
 Dexamethasone sodium phosphate (DP), 44, 82  
 Diclofenac sodium, 43, 83  
 Digoxin, 44  
 Dipalmitoylphosphatidylcholine (DPPC), 183–185  
 Diphenylhexatriene (DPH), 184, 185  
 Diphtheria toxoid (DT), 278  
 Disposable-cartridge jet injectors (DCJIs), 224–225  
 Dissolving MNs (DMNs), 493–494  
 DNA immunization, cutaneous. *See* Cutaneous DNA immunization  
 Doxepin, 118, 132–133  
 Doxepin-loaded cyclodextrins, 132–133  
 Drug delivery. *See also specific types*  
   bioavailability, 238  
   chemical nature of, 237  
   dose response, 238  
   lack of reservoir, 238  
   molecular size, 237–238  
   PK profile, 238  
 Drug-membrane interactions, 71  
 Drug release, sonophoresis in, 34–35  
 Dual frequency, 375–376  
 Dyclonine, 332–333
- E**  
 Electrically assisted drug delivery, by iontophoresis  
   current density, 69–70  
   delivery system, 73–74  
   formulation, 70–73  
 Electrochemical transdermal device (ECTD)  
   advantages, 142  
   electrochemical mechanism, 143–145  
   electrode materials selection  
     Ag-coated stainless steel gauze anode, 150, 152–153  
     anode material influences, 149–151  
     electrolysis of water, 149  
     flux enhancement, 153  
     palladium-coated stainless steel cathode, 151–153  
     reverse current, 154  
   experimental setup, 141–142  
   hydrogel formulation development  
     chloride ions, 147  
     discoloration of anode, 147  
     fentanyl citrate, 148–149  
     gas formation, 147

- HPC concentration, 145
    - pressure-sensitive adhesive, 149, 150
    - sodium chloride effect, 147
    - sorbic acid influences, 146
  - US Patent 5 533 995, 142–143
  - in vivo testing to humans, 155–156
  - Electrolytes, 413–414
  - Electromagnetic radiations, by microwave, 162–163
  - Electromigration (EM), 62, 69
  - Electroosmosis (EO), 62, 355
  - Electroporation (EP)
    - biophysical changes due to, 113
    - chemical enhancers and
      - factors influencing drug delivery, 408
      - investigation, 407
      - synergistic enhancement effect, 408–415
    - clinical applications, 472
    - cutaneous DNA immunization, 444
    - diagnostic analytes, 135
    - electrical current for, 106
    - electrical parameters factors influencing penetration
      - electrode design, 109–111
      - pulses, 108–109
      - pulsing parameters, 109, 110
    - gene delivery, 116
    - histological changes due to, 113–115
    - iontophoresis, 356, 359–360
    - LHRH, 134
    - macroscopic barrier and skin irritation, 115
    - microporation, 263
    - molecular transport, 108
    - new pathways creation, 107
    - permeation enhancements methods, 129–130
    - physical methods, 381–382
    - physicochemical factors influencing
      - penetration
        - electrolytes, 112
        - molecular size, 111
        - permeant charge, 111
        - pH, 111
        - temperature, 112
    - preclinical applications, 469–470
      - cancer vaccines, 470–471
      - DNA vaccines, 470
      - gene expression studies, 470
      - metabolic disorders, 471
      - wound repair, 471
    - preexisting pathways expansion, 107
    - safety and tolerability, 124–126
    - skin electrodes development
      - non-penetrating electrodes, 468–469
      - penetrating electrodes, 468
    - synergic effect, 382–383
    - synergistic effect, 383–386
    - thermal effects, 108
    - transdermal and topical drug delivery, 105, 116
    - transdermal delivery
      - doxepin and doxepin-loaded cyclodextrins, 132–133
      - fentanyl, 130–131
      - heparin, 133–134
      - insulin, 131–132
      - ultrasound and, 370–372
      - vaccines and genes, 134
  - Electroporation devices
    - design considerations, 126–127
    - needle-free microelectrode array, 127–129
    - pulse generator, 127
  - Electrorepulsion, 355
    - iontophoresis, 78
  - EMLA®, 10
  - Enhanced permeation retention (EPR), 211
  - Epidermal powder immunization (EPI), 489–490
  - Erythropoietin (EPO), 288
  - Etching, 307–308
  - European Medicines Agency (EMA), 85
- F**
- Fabrication. *See* Microneedles (MNs)
  - Faraday's law, 69
  - Fast-acting topical hydrophilic drug delivery
    - biological micro-device system, 344
    - dose control, in peptide model, 346–347
    - harnessing, biological system for drug delivery, 344–345
    - kinetics of drug release, 345–346
    - principal approaches, 343–344
    - systemic delivery, 347–348
  - Fentanyl, 45
    - electroporation, 130–131
  - Fentanyl citrate, 148–149
  - Field in motion (FIM), 200, 202
  - Flufenamic acid, 43
  - 5-Fluorouracil (5-FU)
    - electroporation, 117
    - iontophoresis, 84
    - sonophoresis, 44
  - Fourier transform infrared spectroscopy (FTIR), 168, 170
  - Fully loaded SDMA (fSDMA), 288
- G**
- Ganciclovir, 44
  - Gene delivery
    - to inner skin through pores, 239
    - sonophoresis in, 35, 42
  - Gene transfer, 463–464
    - by active enhancers, 464
    - electroporation, 134
    - future prospects, 476
    - physical delivery devices
      - ablation, 476
      - abrasion, 475–476
      - for cancer vaccines, 466–468
      - design and gene expression, 464–465
      - of DNA vaccines against infectious agents, 465–466
      - electroporation, 468–472
      - magnetofection, 474–475
      - plasma delivery, 473–474
      - sonoporation, 472–473

**H**

- Hair follicles (HFs)
  - after “cold” waxing-based plucking, 447
  - CSSS, 448–449
  - cycle, 446–447
  - delivery sites, 446
  - structure and biology, 446
  - “warm” waxing vs. “cold,” 448
- Heparin, electroporation, 117, 133–134
- Herpes labialis, 81
- High-frequency ultrasound (HFU), 370, 372
- High-pressure gas or liquid microporation, 259–261
- Hollow microneedles (HMNs), 312, 329
  - arrays, 290–293 (*see also* Microneedles (MNs) arrays)
  - design and fabrication
    - ceramic-based, 311
    - coated, 311–312
    - metal-based, 310–311
    - silicon-based, 310
  - skin vaccination methods, 495
- Hormones, 41
- Human immunodeficiency virus, Kaposi sarcoma in, 84
- Hyaluronan, 45
- Hyaluronic acid delivery, 186–187
- Hydrocortisone acetate, 44
- Hydrocortisone, for polyarthritis, 4
- Hydrophilic compounds
  - kinetics of drug release, 345–346
  - nano-injection system, 345
  - peptide model, 346–347
  - systemic delivery, 347–348
- Hydrophilic drug delivery, fast-acting topical
  - biological micro-device system, 344
  - dose control, in peptide model, 346–347
  - harnessing, biological system for drug delivery, 344–345
  - kinetics of drug release, 345–346
  - principal approaches, 343–344
  - systemic delivery, 347–348
- Hydroxypropyl cellulose (HPC), 143, 145–146
- Hyperhidrosis, 39, 80

**I**

- Ibuprofen, 43
- ImaRx Therapeutics, Inc. (USA), 47–48
- Immunosuppressives, 39
- In-skin electroporation (IN-SKIN EP), 383–386
- Indomethacin, 43
- Inertial cavitation, 6–7
- Inflammation, soft tissue, 82
- Influenza, 335–336
- Injections, 370, 379
- Insulin, 40, 44, 334
  - electroporation, 117, 131–132
  - iontophoresis, 87
- Interstitial fluid monitoring (ISF), 313
- Intradermal injection, 486–487
- Intradermal vaccination, 278

- Intraepidermal delivery, 186–187
- Invasive electrodes, 110–111
- Iontophoresis
  - application sites, 63–64
  - chemical and physical enhancers, 358–359
  - chronology, 62–63
  - cosmetic applications, 90–92
  - CPE, 396
  - current density, 79
  - cutaneous DNA immunization, 443–444
  - dose delivered in, 80
  - drug administration, 77
  - drug transport, in analytical and numerical methods, 394
  - electrical mobility, 68
  - electrically assisted drug delivery
    - current density, 69–70
    - delivery system, 73–74
    - formulation, 70–73
  - electroporation, 356, 359–360
  - electrorepulsion, 78
  - local drug delivery, 80–84
  - microneedles, 358
  - nail, drug delivery to, 92–93
  - non-invasive sampling method, 93–96
  - ocular drug delivery, 88–90
  - passive diffusion, 77–78
  - pH, 72
  - physical enhancement
    - effective enhancement methods, 354–355
    - electroosmosis, 355
    - electrorepulsion, 355
    - transdermal delivery, 354
  - physical methods, 381–382
  - rationale and feasibility, 77–80
  - skin penetration, 354
  - steady-state plasma concentration, 79
  - synergic effect, 382–383
  - synergistic effect, 383–386
  - topical drug delivery, 78, 80–84
  - transdermal administration, 79
  - transdermal delivery, of peptides and proteins, 428–429
  - transdermal drug delivery, 77–78, 84–88
  - transient pores, 68
  - transport mechanism, 73
  - ultrasound, 356–358
  - ultrasound and, 50–51
  - vs. microneedles, 362–364
  - vs. sonophoresis, 360–362
- Iontophoretic device, 61–62
- Isoelectric point (pI), 62

**J**

- Jet injection, 259
- Jet injectors, 431–432, 490–492
  - liquid
    - applications, 224–225
    - design and operation, 222–223

- design parameters, 223–224
- documented research, 222
- mechanism of action, 223
- safety, 225
- powder
  - applications, 227
  - design and operation, 225–226
  - design parameters, 226–227
  - safety, 227–228
- Jet power, 223
  
- K**
- Kaposi sarcoma, 84
- Keratolytic molecules, 411–412
- Ketoprofen, 43, 83
- Ketorolac, 83
- Ketorolac tromethamine, 43
  
- L**
- Langerhans cells (LCs), 10, 442, 463
- Laser ablation, 237, 432
- Laser microporation, 261–262
- Laurocapram, 50
- Lercanidipine hydrochloride, 43
- Leuprolide, 87
- LHRH. *See* Luteinizing hormone releasing hormone (LHRH)
- Lidocaine, 5, 43, 332–333
- Lidocaine HCl, 118
- Light-to-pressure conversion, 176
  - efficiency, 178
  - maximization, 179
  - peak pressure, 179
  - power density, 180
  - practical development, 178
  - simulated laser pulses, 179–180
  - thermoelastic expansion mechanism, 178
- Light-to-pressure transducer polymer films, 182–183
- Lipid(s), 412–413
- Lipid dynamics
  - biophysical mechanism, 183
  - conformational studies, 184
  - dipalmitoylphosphatidylcholine, 183
  - DPH fluorescence anisotropy, 185
  - fluorescence anisotropy measurements, 184–185
  - fluorescent probes, 184
  - hypothesis, 184
- Liquid jet injectors
  - applications, 224–225
  - design
    - and operation, 222–223
    - parameters, 223–224
  - documented research, 222
  - mechanism of action, 223
  - safety, 225
- Local drug delivery, by iontophoresis, 80–84
- Local pain, 82
- Localized dissipation regions (LDRs), 108
- Localized transport regions (LTRs), 7–8, 402
- Low-frequency sonophoresis, 5, 357, 401–402
  - clinical studies, 10–11
  - macromolecular delivery, 9–11
  - mechanism, 6–7
  - parameters, 5–6
  - permeation pathways of, 7–9
  - pretreatment, 5
  - safety of, 11
  - simultaneous, 5
  - transdermal extraction of analytes, 11
- Low-molecular-weight heparin (LMWH), 8, 9
- Luciferase protein, 118
- Luteinizing hormone releasing hormone (LHRH), 87
  - electroporation, 117, 134
  
- M**
- Macroflux<sup>®</sup> transdermal microprojection delivery system, 358
- Macromolecules, 408, 411
- Magnetic energy, 195
- Magnetic film array, 200, 202
- Magnetofection (MF), 474–475
  - gene expression and preclinical application, 475
  - mechanism, 474–475
- Magnetophoresis
  - combination, 202–203
  - definition, 196
  - enhancement technologies, 202–204
  - field in motion, 200, 202
  - magnetic film array, 200, 202
  - mechanism of enhancement, 203–205
  - pulsed electromagnetic fields
    - Dermaportation system, 198–199
    - enhancement ratio, 199
    - MPM-FLIM, 200–201
    - small preliminary investigation, 199
  - static magnetic fields, 196, 198
  - summary of experimental data, 196, 197
- Mannitol, 4
  - electroporation, 117
- Metered dose transdermal spray (MDTS), 416
- Methotrexate
  - electroporation, 118
  - iontophoresis, 84, 89
- Methyl aminolevulinate, 333
- Methyl nicotinate, 44, 332
- Methyl prednisolone, 44
- Metoprolol, electroporation, 117
- Micro-device system, application, 348
- Microdermabrasion, 243, 373–374
  - biophysical and molecular effects
    - loss of skin barrier property, 249–250
    - molecular changes, 250
    - skin healing, 250
  - degree of stratum corneum, 244
  - device practicality and cost, 251, 253
  - drug delivery duration, 253–254
  - equipment manufacturers, 245, 246

- Microdermabrasion (*cont.*)  
 future directions, 254  
 mechanism, 244–245  
 operating parameters  
 flow rate, 247  
 masks, 248–249  
 pressure, 245–247  
 stationary vs. mobile hand tip, 247–248  
 reproducibility and standardization, 253  
 transdermal drug delivery with  
 stratum corneum role, 251  
 viable epidermis, 251  
 in vitro, 251, 252  
 in vivo, 251, 253
- Microdialysis, 82, 135
- Microelectromechanical systems (MEMS) fabrication  
 technology  
 etching, 307–308  
 photolithography, 306–308  
 thin film deposition, 306, 307
- Microfabrication  
 classification, 308  
 in-plane designs, 308, 309  
 out-of-plane designs, 308, 309  
 shape and geometry, 308, 309  
 solid/hollow, design and fabrication, 310–312  
 technology, 358
- Microneedles (MNs), 305  
 chemical enhancers and  
 concept of, 415  
 synergistic enhancement effect, 415–416  
 CMNs, 494  
 DMNs, 495  
 HMNs, 493–494  
 iontophoresis, 358, 362–364  
 MEMS, 306–308  
 microfabrication  
 classification, 308  
 in-plane designs, 308, 309  
 out-of-plane designs, 308, 309  
 shape and geometry, 308, 309  
 solid/hollow, design and fabrication, 310–312  
 microporation, 263  
 minimally invasive monitoring methods  
 differential strategies, for MN-based fluid  
 extraction, 316  
 female mosquito's proboscis, inspiration,  
 314–315  
 fluid flow, 313–314  
 hypodermic needles, 312  
 ISF, 313  
 little true progression, 312  
 MN-based integrated sample extraction and  
 monitoring devices, 317–319  
 SMNs, 493  
 transdermal delivery, of peptides and proteins,  
 425–428  
 ultrasound and, 51–52, 372–373
- Microneedles (MNs), in human studies  
 drug and vaccine delivery, 331–332  
 influenza, 335–336  
 peptides and proteins, 333–334  
 small molecules, 332–333
- patient and provider  
 concerns, 338  
 opinions, 337
- performance and safety  
 insertion, 326–327  
 liquid infusion via hollow, 327–328  
 pain, 328–329  
 safety, 329–331  
 skin resealing, 331
- skin needling studies, 336–337
- willingness  
 to self-administer, 337–338  
 to vaccinate with, 337
- Microneedles (MNs) arrays, 380  
 advantage, 275  
 coated  
 dip-coating methods, 280, 281  
 disadvantage, 280  
 drug formulation, 280  
 follow-up study, 282–283  
 Macroflux<sup>®</sup>, 282  
 OVA, 282–283  
 PLA types, 283, 284  
 research groups, 281–282  
 versatility, 280
- developments, 296–297  
 drug delivery strategies, 275–277  
 factors influencing skin penetration, 293–294  
 hollow, 290–293  
 polymeric, 275  
 aforementioned studies, 286  
 Banga's research group, 285  
 DDAVP, 289  
 drug-loaded, 284  
 EPO, 288  
 examples of, 284, 285  
 fabrication, 286–287  
 follow-up study, 285, 286  
 localise, 287, 288  
 mould-based techniques, 284  
*Nature Medicine*, 290  
 nifedipine hydrochloride, 285  
 rhGH, 289  
 SDMP fabrication technique, 287–288  
 silicon, 283, 284  
 water-soluble and biodegradable, 284
- progression to widespread clinical use, 297–299  
 safety and public perception, 294–296
- solid  
 cutaneous delivery, 278  
 fabrication, 277  
 insertion, 279  
 intradermal vaccination, 278  
 utility, 278
- super-short, 278, 279
- Microporation, 257  
 in clinical trial  
 Altea's PassPort<sup>®</sup> system, 267–268  
 Becton, Dickinson and Company, 269

- Pantec Biosolutions AG, 268
  - TransPharma Medical's implementation, 267
    - by different devices, 259
    - active microporation techniques, 259–263
    - physical microporation technique, 263
    - radio frequency, 261
  - micropore closure and recovery, 264–267
  - optical coherence topography, 258
  - passive method, 258
  - safety associated with, 263–264
  - of skin enhances, 258
  - transdermal drug delivery, 258
  - Microstructured transdermal system (MTS), 298
  - Microwaves
    - biological effects
      - biological membranes, 165–166
      - non-thermal, 164–165
      - thermal, 164
    - enhancement effects
      - intensity and exposure time, 167–168
      - stratum corneum lipid disruption, 168–171
    - and matter(objects and materials), 163
    - physics and applications, 162–163
    - thermal and non-thermal effects, 163–164
  - Migraine treatment, 86
  - Minimally invasive monitoring methods
    - differential strategies, for MN-based fluid extraction, 316
    - female mosquito's proboscis, inspiration, 314–315
    - fluid flow, in MN fabrication, 313–314
    - hypodermic needles, 312
    - ISF, 313
    - little true progression, 312
    - MN-based integrated sample extraction and monitoring devices, 317–319
  - Moxibustion pretreatment
    - heat, 209
    - history, 212
    - Na-SA
      - intravenous injection, 214–215
      - in vitro skin application, 212–214
      - in vivo skin application, 215
    - PassPort™ System, 210
    - skin temperature, 212, 213
    - tissue distribution, 215–216
    - typical model, 212
    - vein and enhanced permeation retention, 211
  - MPM-FLIM. *See* Multiphoton microscopy–fluorescence lifetime imaging microscopy (MPM–FLIM)
  - MRX-801, 48
  - Multi-use nozzle jet injectors (MUNJIs), 224–225
  - Multiphoton microscopy–fluorescence lifetime imaging microscopy (MPM–FLIM), 200–201
- N**
- N-trimethyl chitosan (TMC), 278
  - Na-SA. *See* Sodium salicylate (Na-SA)
  - Nail, drug delivery to
    - iontophoresis, 92–93
    - sonophoresis in, 35
  - Nail drug release, 42
  - Nalbuphine, electroporation, 117
  - Naltrexone, 332
  - Nanocarriers, ultrasound and, 52–53
  - Needle-free jet injection, 445
  - Needle-free microelectrode array, 127–129
  - Needle-type electrodes, 127
  - Nernst-Einstein equation, 67
  - Nernst-Planck equation, 67
  - Nicotinate, 4
  - Non-invasive sampling method, iontophoresis, 93–96
  - Non-steroidal anti-inflammatory drugs (NSAIDs), 82–83
  - Non-thermal effects, microwaves, 163–164
  - Noninvasive electrode, 110
  - Nuclear magnetic resonance (NMR), 170
  - Numerical methods, 391–392
    - experimental methods, 393
    - iontophoretic drug transport, 394
    - mathematical modeling, 392–393
    - passive and chemically enhanced diffusion, 393–394
- O**
- Octreotide, 86–87
  - Ocular drug delivery
    - iontophoresis, 88–90
    - sonophoresis in, 35
  - Ocular drug release, 42
  - Ohm's law, 64
  - Oligonucleotides, 41, 45
    - low-frequency ultrasound, 9–10
  - OnabotulinumtoxinA, 44
  - Onychomycosis, drugs for, 45
  - Optical coherence tomography (OCT), 327
  - Optical coherence topography (OCT), 258
  - Ovalbumin (OVA), 282–283
- P**
- Pain, local, 82
  - Painless Laser Epidermal System (P.L.E.A.S.E.®), 268, 432
  - Palladium-coated stainless steel cathode, 151–153
  - Palmoplantar hyperhidrosis, 80
  - Panax notoginseng, 42
  - Panax notoginseng*, 45
  - Pantec Biosolutions AG, 268
  - Parathyroid hormone, 333–334
  - Parkinson's disease, 86
  - Partially loaded SDMA (pSDMA), 288
  - Passive diffusion
    - analytical and numerical methods, 393–394
    - transient flux and cumulative amount, 395
  - PassPort™ System, 210, 236, 237
  - Patch-Cap, 46
  - Patient-controlled analgesia (PCA), 85–86
  - Penbutolol sulfate, 43
  - Penetration enhancement. *See also specific types*
    - iontophoresis, 67–68, 77–78
    - photoacoustic (PA) waves, 181–183



- Penetration pathways  
 through hair follicles, 19–20  
 through stratum corneum, 20–21  
 transcellular pathways, 21
- Peptide delivery  
 by iontophoresis, 86  
 low-frequency ultrasound, 9  
 transdermal delivery of (*see* Transdermal delivery, of peptides and proteins)
- Peptide model, 346–347
- Peptide patch technologies, 239–240
- Peptide transport, 274
- Peptides and proteins, transdermal delivery of. *See* Transdermal delivery, of peptides and proteins
- Permeation enhancement  
 high molecular weight compounds  
 to increase, 381–382  
 synergic effect, 382–383  
 synergistic effect, 383–386  
 by microwave  
 biological membranes, 165–166  
 non-thermal, 164–165  
 thermal, 164
- Permselectivity, 62
- pH  
 electroporation impact by, 111  
 iontophoresis impact by, 72
- Photoacoustic calorimetry (PAC), 181
- Photoacoustic (PA) waves, 175–176  
 ablation, 177  
 hyaluronic acid delivery, 186–187  
 intraepidermal delivery, 186–187  
 light-to-pressure conversion, 176  
 efficiency, 178  
 maximization, 179  
 peak pressure, 179  
 power density, 180  
 practical development, 178  
 simulated laser pulses, 179–180  
 thermoelastic expansion mechanism, 178
- lipid dynamics  
 biophysical mechanism, 183  
 conformational studies, 184  
 dipalmitoylphosphatidylcholine, 183  
 DPH fluorescence anisotropy, 185  
 fluorescence anisotropy measurements, 184–185  
 fluorescent probes, 184  
 hypothesis, 184
- piezophotonic materials, 180–181  
 shock wave, 177  
 thermoelastic processes, 177  
 transepidermal water loss, 186  
 typical, 176
- Photodynamic antimicrobial chemotherapy, 73
- Photodynamic therapy (PDT), 84
- Photolithography, 306–308
- Physical delivery devices  
 ablation, 476  
 abrasion, 475–476  
 for cancer vaccines, 466–468  
 design and gene expression, 464–465  
 of DNA vaccines against infectious agents, 465–466  
 electroporation, 468–472  
 magnetofection, 474–475  
 plasma delivery, 473–474  
 sonoporation, 472–473
- Physical enhancement techniques  
 combination strategies, 433  
 effective enhancement methods, 354–355  
 electroosmosis, 355  
 electroporation, 429–430  
 electrorepulsion, 355  
 future perspective, 434  
 iontophoresis, 428–429  
 jet injector, 431–432  
 laser ablation, 432  
 microneedles, 425–428  
 sonophoresis, 430–431  
 thermal and radio-frequency ablation, 432–433  
 transdermal delivery, 354
- Physical enhancers, 358–359, 374
- Physical microporation technique, 263
- Physostigmine, 4
- Piezophotonic materials, 180–181
- Piroxicam, 43, 83
- Pirprofen, 83
- Plasma delivery  
 design and gene delivery, 473–474  
 gene expression and vaccines, 474
- P.L.E.A.S.E.<sup>®</sup> (Painless Laser Epidermal System), 237
- Pockets, 280
- Poke with patch, 275, 276
- Polyelectrolyte multilayers films (PEM), 454
- Polymeric microneedles (MNs) arrays. *See also* Microneedles (MNs) arrays  
 aforementioned studies, 286  
 Banga's research group, 285  
 DDAVP, 289  
 drug-loaded, 284  
 EPO, 288  
 examples of, 284, 285  
 fabrication, 286–287  
 follow-up study, 285, 286  
 localise, 287, 288  
 mould-based techniques, 284  
*Nature Medicine*, 290  
 nicardipine hydrochloride, 285  
 rhGH, 289  
 SDMP fabrication technique, 287–288  
 silicon, 283, 284  
 water-soluble and biodegradable, 284
- Powder jet injectors  
 applications, 227  
 design  
 and operation, 225–226  
 parameters, 226–227  
 safety, 227–228
- Pressure-sensitive adhesives (PSA), 149, 150
- Pretreatment sonophoresis, 5
- Procaine hydrochloride, 43
- Protein delivery  
 by iontophoresis, 86

- low-frequency ultrasound, 9
- transdermal delivery of (*see* Transdermal delivery, of peptides and proteins)
- Protoporphyrin IX, 84
- Pulsed electromagnetic fields (PEMF)
  - Dermaportation system, 198–199
  - enhancement ratio, 199
  - MPM-FLIM, 200–201
  - small preliminary investigation, 199
- Pulsing parameters, 108
  
- R**
- Radio-frequency (RF) ablation, 432–433
- Radio frequency microporation, 261
- Reactive oxygen species (ROS), 165
- Recombinant DNA technology, 442
- Recombinant human growth hormone (rhGH), 289
- Reverse iontophoresis
  - efficiency of extraction, 95
  - fluxes of extraction, 95
  - influencing factors, 94
  - iontophoretic extraction, 94–95
  - iontophoretic sampling, 94
  - transport numbers of drugs, 94
- Rivastigmine, 43
  
- S**
- Salicylic acid (SA)
  - cathodal transport, 93
  - electroporation, 118
- Scopolamine, 348
- Self-dissolving micropile array (SDMA), 287–288
- Simultaneous sonophoresis, 5
- Skin abrasion, 444–445
- Skin barrier, loss of
  - electrical resistance, 249–250
  - transepidermal water loss, 249
- Skin cancer treatment, 83
- Skin electroporation. *See* Electroporation
- Skin permeability, 209
- Skin permeation enhancement. *See* Permeation enhancement
- Skin Permeation System, 49
- Skin vaccination methods
  - advanced tools, 486
  - ballistic vaccination, 487–489
  - epidermal powder immunization, 489–490
  - intra-dermal injection, 486–487
  - jet injector, 490–492
  - microneedles
    - CMNs, 494
    - DMNs, 495
    - HMNs, 493–494
    - SMNs, 493
  - tattoo vaccination, 492–493
- Sodium dodecyl sulfate (SDS), 406
- Sodium fluorescein, 35
- Sodium lauryl sulfate (SLS), 50, 405
- Sodium salicylate (Na-SA)
  - intravenous injection, 214–215
  - skin application
    - in vitro, 212–214
    - in vivo, 215
- Soft tissue inflammation, 82
- Solid microneedles (SMNs), 328–329
  - arrays (*see also* Microneedles (MNs))
    - cutaneous delivery, 278
    - fabrication, 277
    - insertion, 279
    - intra-dermal vaccination, 278
    - utility, 278
  - design and fabrication
    - ceramic-based, 311
    - coated, 311–312
    - metal-based, 310–311
    - silicon-based, 310
  - skin vaccination methods, 493
- Sonoderm technology, 47
- SonoLysis, 47–49
- Sonophoresis
  - categories, 356–358
  - chemical enhancers and
    - definition, 400
    - low-frequency, 401–402
    - mechanisms of action, 402
    - synergistic enhancement effect, 402–407
    - ultrasound, 400–401
    - uses, 401
  - cutaneous DNA immunization, 444
  - iontophoresis *vs.*, 360–362
  - low-frequency, 5
    - clinical studies, 10–11
    - macromolecular delivery, 9–11
    - mechanism, 6–7
    - parameters, 5–6
    - permeation pathways of, 7–9
    - safety of, 11
    - transdermal extraction of analytes, 11
  - therapeutic applications
    - drug release, 34–35
    - gene delivery, 35, 42
    - nail delivery, 35
    - ocular drug delivery, 35
    - topical/transdermal drug release by, 36–42
    - transdermal delivery, of peptides and proteins, 430–431
    - ultrasound and, 3–4
- Sonophoretic devices
  - A-Wand systems, 47
  - Patch-Cap, 46
  - Sonoderm technology, 47
  - SonoLysis, 47–49
  - SonoPrep®, 49
  - U-Strip, 46–47
  - U-Wand, 47
  - ultrasound and
    - chemical penetration enhancers, 50
    - iontophoresis, 50–51
    - microneedles, 51–52
    - nanocarriers, 52–53
- Sonophoretic enhanced microneedles array (SEMA)
  - method, 51

- Sonoporation, 472–473  
 mechanism, 472–473
- SonoPrep®, 10, 11, 49
- Sorbic acid, 146
- Specific absorption rate (SAR), 163, 164
- Square-wave pulse electroporators, 108
- Stable cavitation, 6
- Static magnetic fields, 196, 198
- steady-state plasma concentration, 79
- Stimulants, 41
- Stratum corneum (SC), 273–274  
 chemical techniques, 445  
 degree of, 244  
 electroporation, 106–107, 113  
 lipid disruption by microwaves, 168–171  
 novel techniques, 445  
 physical techniques, 443–445  
 role, 251
- Surfactants, 414
- Surfactant–sonophoresis synergism, 406
- Symphony tCGM System, 49
- Synergistic enhancement, 259
- T**
- Tattoo vaccination, 492–493
- Terazosin HCl, electroporation, 117
- Testosterone, 45
- Tetracaine, electroporation, 117
- Tetracycline, 44
- Therapeutic-frequency ultrasound, 357
- Thermal ablation, 236–237  
 transdermal delivery, of peptides and proteins, 432–433
- Thermal effects  
 ablation methods, 236–237  
 biological effects, of microwaves, 164  
 microwaves, 163–164
- Thermal microporation, 261
- Thermal poration, cutaneous DNA immunization, 444
- Thin film deposition, 306, 307
- Time constant, 393, 394
- Timolol, electroporation, 117
- Topical drug delivery. *See also* Fast-acting topical  
 hydrophilic drug delivery  
 iontophoresis, 78, 80–84
- Transcorneal iontophoresis, 88–89
- Transcutaneous immunization (TCI), 10
- Transdermal delivery, of peptides and proteins, 423–424  
 biopharmaceuticals, 424–426  
 physical enhancement techniques  
 combination strategies, 433  
 electroporation, 429–430  
 future perspective, 434  
 iontophoresis, 428–429  
 jet injector, 431–432  
 laser ablation, 432  
 microneedles, 425–428  
 sonophoresis, 430–431  
 thermal and radio-frequency ablation, 432–433
- Transdermal drug delivery, 274. *See also* Iontophoresis  
 fast-acting topical hydrophilic drug delivery, 343  
 iontophoresis, 77–78, 84–88  
 microporation, 258  
 sonophoresis, 21
- Transdermal extraction, of analytes, 11
- Transepidermal water loss (TEWL), 113, 186, 265, 327  
 electroporation, 124  
 loss of skin barrier property, 249
- TransPharma Medical's implementation, 267
- Transscleral iontophoresis, 88–89
- Triamcinolone acetoneide, 44
- TUCSON trial, 48
- Tweezertrodes, 128
- U**
- U-Strip, 46–47
- U-Wand, 47
- Ultrasound (US), 369–370. *See also* Sonoporation  
 absorption of ultrasonic energy, 31  
 classification, 400  
 cutaneous DNA immunization, 444  
 and electroporation, 370–372  
 frequencies, 374–376  
 gene expression and therapeutics, 473  
 and injections, 370  
 iontophoresis, 356–358  
 and microdermabrasion, 373–374  
 and microneedles, 372–373  
 microporation, 262–263  
 principal medical applications, 32  
 SC disruption process, 33  
 and sonophoretic devices  
 chemical penetration enhancers, 50  
 iontophoresis, 50–51  
 microneedles, 51–52  
 nanocarriers, 52–53  
 sound wave propagation, 32, 33  
 therapies, 32
- Ultrasound-mediated transdermal  
 low-frequency sonophoresis, 5  
 clinical studies, 10–11  
 macromolecular delivery, 9–11  
 mechanism, 6–7  
 parameters, 5–6  
 permeation pathways of, 7–9  
 safety of, 11  
 transdermal extraction of analytes, 11  
 and sonophoresis, 3–4
- US Patent 5 533 995, 142–143
- V**
- Vaccines  
 by ablation methods, 238–239  
 electroporation, 134  
 low-frequency ultrasound, 10
- Vacuum pressure, 245–247
- Vasoactive intestinal polypeptide (VIP), 84
- Vasodilators, 41
- ViaDerm™, 267
- ViaDor™, 234–235
- Visual analog scale, 11
- Vitamin C, by iontophoresis, 90